DEVELOPMENT OF HUMANIZED MOUSE MODELS FOR INFECTIOUS DISEASES AND CANCER

EDITED BY: Moriya Tsuji and Ramesh Akkina
PUBLISHED IN: Frontiers in Immunology

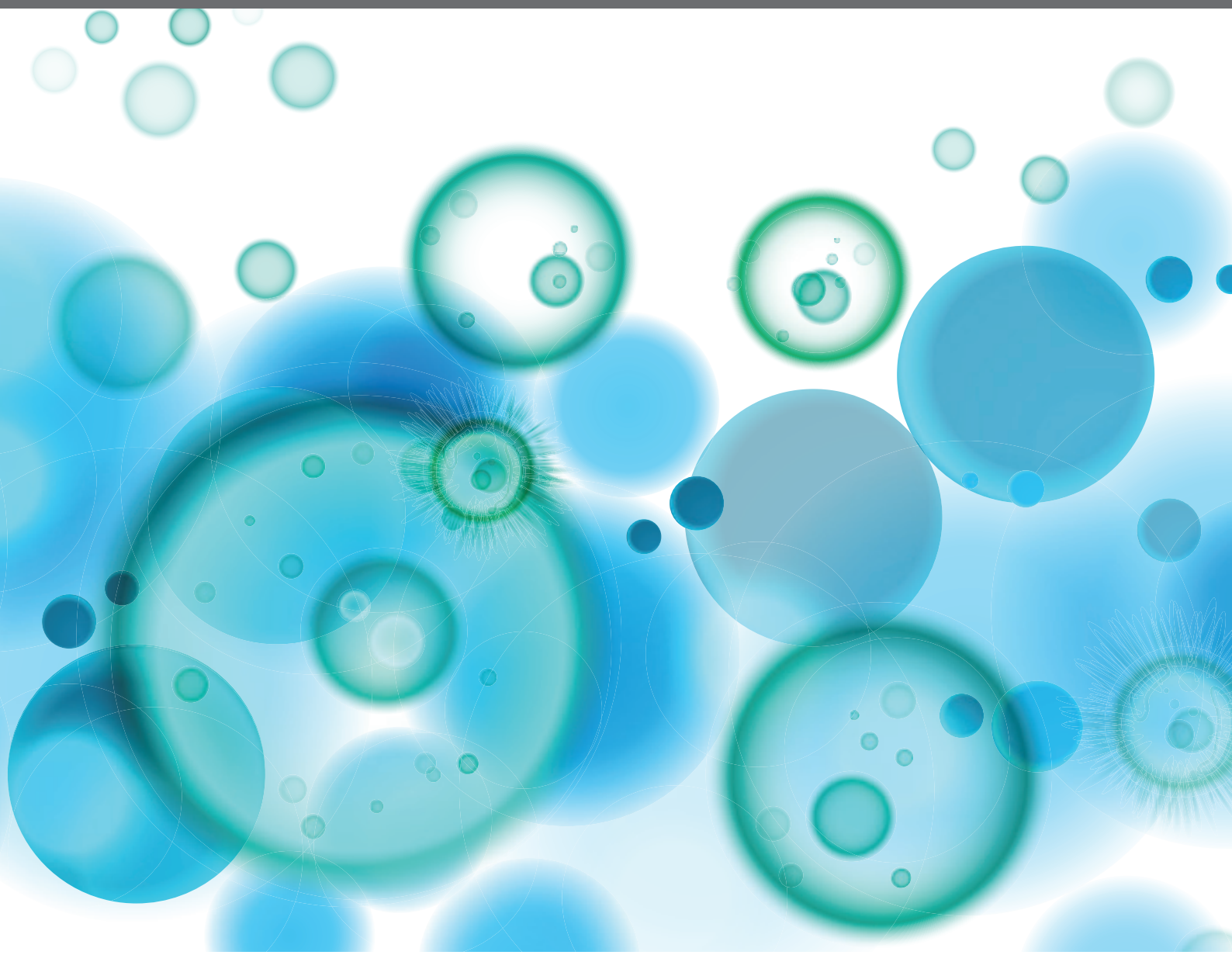

frontiers Research Topics

frontiers

ISSN 1664-8714
ISBN 978-2-88963-481-1
DOI 10.3389/978-2-88963-481-1

About Frontiers

Frontiers is more than just an open-access publisher of scholarly articles: it is a pioneering approach to the world of academia, radically improving the way scholarly research is managed. The grand vision of Frontiers is a world where all people have an equal opportunity to seek, share and generate knowledge. Frontiers provides immediate and permanent online open access to all its publications, but this alone is not enough to realize our grand goals.

Frontiers Journal Series

The Frontiers Journal Series is a multi-tier and interdisciplinary set of open-access, online journals, promising a paradigm shift from the current review, selection and dissemination processes in academic publishing. All Frontiers journals are driven by researchers for researchers; therefore, they constitute a service to the scholarly community. At the same time, the Frontiers Journal Series operates on a revolutionary invention, the tiered publishing system, initially addressing specific communities of scholars, and gradually climbing up to broader public understanding, thus serving the interests of the lay society, too.

Dedication to Quality

Each Frontiers article is a landmark of the highest quality, thanks to genuinely collaborative interactions between authors and review editors, who include some of the world's best academicians. Research must be certified by peers before entering a stream of knowledge that may eventually reach the public - and shape society; therefore, Frontiers only applies the most rigorous and unbiased reviews.
Frontiers revolutionizes research publishing by freely delivering the most outstanding research, evaluated with no bias from both the academic and social point of view. By applying the most advanced information technologies, Frontiers is catapulting scholarly publishing into a new generation.

What are Frontiers Research Topics?

Frontiers Research Topics are very popular trademarks of the Frontiers Journals Series: they are collections of at least ten articles, all centered on a particular subject. With their unique mix of varied contributions from Original Research to Review Articles, Frontiers Research Topics unify the most influential researchers, the latest key findings and historical advances in a hot research area! Find out more on how to host your own Frontiers Research Topic or contribute to one as an author by contacting the Frontiers Editorial Office: researchtopics@frontiersin.org

DEVELOPMENT OF HUMANIZED MOUSE MODELS FOR INFECTIOUS DISEASES AND CANCER

Topic Editors:
Moriya Tsuji, Columbia University Irving Medical Center, United States
Ramesh Akkina, Colorado State University, United States

Citation: Tsuji, M., Akkina, R., eds. (2020). Development of Humanized Mouse Models for Infectious Diseases and Cancer. Lausanne: Frontiers Media SA.
doi: 10.3389/978-2-88963-481-1

Table of Contents

05 ***Editorial: Development of Humanized Mouse Models for Infectious Diseases and Cancer***
Moriya Tsuji and Ramesh Akkina

08 ***Humanized Mouse Models of* Staphylococcus aureus *Infection***
Dane Parker

14 ***Exploring the Immunopathogenesis of Viral Hemorrhagic Fever in Mice With a Humanized Immune System***
Günther Schönrich and Martin J. Raftery

23 ***Tracking Human Immunodeficiency Virus-1 Infection in the Humanized DRAG Mouse Model***
Jiae Kim, Kristina K. Peachman, Ousman Jobe, Elaine B. Morrison, Atef Allam, Linda Jagodzinski, Sofia A. Casares and Mangala Rao

31 ***Multidimensional Analysis Integrating Human T-Cell Signatures in Lymphatic Tissues With Sex of Humanized Mice for Prediction of Responses After Dendritic Cell Immunization***
Valery Volk, Andreas I. Reppas, Philippe A. Robert, Loukia M. Spineli, Bala Sai Sundarasetty, Sebastian J. Theobald, Andreas Schneider, Laura Gerasch, Candida Deves Roth, Stephan Klöss, Ulrike Koehl, Constantin von Kaisenberg, Constanca Figueiredo, Haralampos Hatzikirou, Michael Meyer-Hermann and Renata Stripecke

50 ***Type I Interferon Responses by HIV-1 Infection: Association With Disease Progression and Control***
Andrew Soper, Izumi Kimura, Shumpei Nagaoka, Yoriyuki Konno, Keisuke Yamamoto, Yoshio Koyanagi and Kei Sato

61 ***Enhanced Antibody Responses in a Novel NOG Transgenic Mouse With Restored Lymph Node Organogenesis***
Takeshi Takahashi, Ikumi Katano, Ryoji Ito, Motohito Goto, Hayato Abe, Seiya Mizuno, Kenji Kawai, Fumihiro Sugiyama and Mamoru Ito

75 ***Modeling Human Antitumor Responses* In Vivo *Using Umbilical Cord Blood-Engrafted Mice***
Nicholas A. Zumwalde and Jenny E. Gumperz

82 ***Generation of Human Immunosuppressive Myeloid Cell Populations in Human Interleukin-6 Transgenic NOG Mice***
Asami Hanazawa, Ryoji Ito, Ikumi Katano, Kenji Kawai, Motohito Goto, Hiroshi Suemizu, Yutaka Kawakami, Mamoru Ito and Takeshi Takahashi

98 ***Human γ-Herpesvirus Infection, Tumorigenesis, and Immune Control in Mice With Reconstituted Human Immune System Components***
Christian Münz

104 ***Ultra-Sensitive HIV-1 Latency Viral Outgrowth Assays Using Humanized Mice***
Kimberly Schmitt and Ramesh Akkina

110 **Plasmodium falciparum** ***Liver Stage Infection and Transition to Stable Blood Stage Infection in Liver-Humanized and Blood-Humanized FRGN KO Mice Enables Testing of Blood Stage Inhibitory Antibodies (Reticulocyte-Binding Protein Homolog 5)*** **In Vivo**
Lander Foquet, Carola Schafer, Nana K. Minkah, Daniel G. W. Alanine, Erika L. Flannery, Ryan W. J. Steel, Brandon K. Sack, Nelly Camargo, Matthew Fishbaugher, Will Betz, Thao Nguyen, Zachary P. Billman, Elizabeth M. Wilson, John Bial, Sean C. Murphy, Simon J. Draper, Sebastian A. Mikolajczak and Stefan H. I. Kappe

118 ***Human Immune System Mice for the Study of Human Immunodeficiency Virus-Type 1 Infection of the Central Nervous System***
Teresa H. Evering and Moriya Tsuji

127 ***Humanized Mouse Models for the Study of Human Malaria Parasite Biology, Pathogenesis, and Immunity***
Nana K. Minkah, Carola Schafer and Stefan H. I. Kappe

137 ***Humanized Mice Engrafted With Human HSC Only or HSC and Thymus Support Comparable HIV-1 Replication, Immunopathology, and Responses to ART and Immune Therapy***
Liang Cheng, Jianping Ma, Guangming Li and Lishan Su

150 ***The Use of the Humanized Mouse Model in Gene Therapy and Immunotherapy for HIV and Cancer***
Mayra A. Carrillo, Anjie Zhen and Scott G. Kitchen

158 ***Dissemination of*** **Orientia tsutsugamushi*****, a Causative Agent of Scrub Typhus, and Immunological Responses in the Humanized DRAGA Mouse***
Le Jiang, Erin K. Morris, Rodrigo Aguilera-Olvera, Zhiwen Zhang, Teik-Chye Chan, Soumya Shashikumar, Chien-Chung Chao, Sofia A. Casares and Wei-Mei Ching

frontiers in Immunology

EDITORIAL
published: 10 January 2020
doi: 10.3389/fimmu.2019.03051

Editorial: Development of Humanized Mouse Models for Infectious Diseases and Cancer

Moriya Tsuji[1] *and Ramesh Akkina*[2]*

[1] Aaron Diamond AIDS Research Center, Affiliate of the Rockefeller University, New York, NY, United States, [2] Department of Microbiology, Immunology and Pathology, Colorado State University, Fort Collins, CO, United States

Keywords: humanized mice in infectious disease research, humanized mice in cancer research, new humanized mouse models, humanized mice for HIV, malaria, vaccines and therapeutics, improved humanized mouse models

Editorial on the Research Topic

Development of Humanized Mouse Models for Infectious Diseases and Cancer

Many knowledge gaps exist in translating research results from conventional animal models such as mice to the human, especially in the clinical context. *In vivo* systems incorporating human cells and tissues in a physiological setting will help bridge this gap. In this regard, humanized mice with engrafted human cells provide suitable tools to study human specific pathogens and cancer. With a transplanted human immune system, they also offer a dynamic setting for immune responses. Central to the preparation of new generation humanized mice is the availability of various strains of immunodeficient mice. Many new advances in this arena include derivation of mouse strains transgenic for human cytokines and HLA alleles, allowing improved human cell engraftment and immune responses. Transplantation of tissues such as human liver together with an autologous immune system paved the way for new studies not previously feasible. Human specific pathogens such as HIV, hepatitis viruses, and malaria parasites are being intensely studied in these systems and important data on pathogen life cycles, viral latency, and human specific immune responses are gathered. In the cancer field, patient derived xenograft models are facilitating testing of various chemo- and immunotherapies. Recent applications of these models expanded immensely to address host-parasite interactions involving more diverse agents and in studying viral-bacterial co-infections as well. Studies on novel gene, cellular and antibody therapies have also greatly expanded by the use of these mice.

The current Research Topic incorporates a number of original research papers and review articles addressing a wide range of topics that include new model development, viruses, bacteria, parasites, cancer, and vaccine studies demonstrating the ever increasing versatility of humanized mice in biomedical research.

Two humanized mouse models are widely used in HIV research, the simpler and less expensive hu-HSC mouse model and the BLT hu-mouse model requiring surgery to transplant human thymic tissue and hematopoietic stem cells (HSC). Cheng et al. compared immune reconstitution and HIV-1 infection between NRG-huHSC and NRG-Hu Thy/HSC models. Interestingly, both models were found to support comparable levels of virus replication, immunopathology, and therapeutic responses to ART and immunotherapy approaches suggesting that hu-HSC mice can be effectively used in many HIV experimental settings with reduced cost and labor. Soper et al. reviewed the impact of type I IFN (IFN-I) in HIV-1 infection *in vivo* utilizing hu-HSC mouse models. They found that the effects of IFN-I in the *in vivo* context were much more complicated than previously predicted from *in vitro* studies, thus underscoring the advantage of using humanized mouse models in assessing the nuances of IFN-I effects for/against viral infections.

OPEN ACCESS

Edited and reviewed by:
Denise Doolan, Australian Institute of Tropical Health and Medicine, Division of Tropical Health and Medicine, James Cook University, Australia

***Correspondence:**
Ramesh Akkina
akkina@colostate.edu

Specialty section:
This article was submitted to Vaccines and Molecular Therapeutics, a section of the journal Frontiers in Immunology

Received: *09 December 2019*
Accepted: *12 December 2019*
Published: *10 January 2020*

Citation:
Tsuji M and Akkina R (2020) Editorial: Development of Humanized Mouse Models for Infectious Diseases and Cancer. Front. Immunol. 10:3051. doi: 10.3389/fimmu.2019.03051

A major goal in the HIV/AIDS field is to achieve full viral eradication and a complete cure. However, this has been elusive due to the presence of minute levels of latently infected cells even in fully virus suppressed patients on long-term therapy. Ultra-sensitive assays are needed to verify when full HIV remission is achieved. Schmitt and Akkina reviewed the current status of HIV latency detection assays and discussed the higher sensitivity achieved utilizing humanized mouse-based viral outgrowth assays (hmVOA) vs. *in vitro* VOAs.

In the context of HIV-1 viral persistence, the central nervous system (CNS) has come into the limelight as a unique, immunologically privileged compartment supporting infection and consequent immune-mediated damage. Evering and Tsuji reviewed the current work on HIV-1 in the CNS using human immune system (HIS) mouse models with a focus on cells of myeloid lineage playing a major role. They predict that the new HIS mouse models in the current pipeline will further facilitate novel diagnostic, therapeutic, and viral eradication strategies in the CNS.

Lentiviral gene transduction of human hematopoietic cells including HSC opened up many avenues of gene and cellular therapies. Humanized mice played an ever increasing role in modeling these new strategies and providing important pre-clinical data. Carrillo et al. reviewed recent developments in CAR-T cell-based immunotherapies and their combination with antibody targeting of immune checkpoint inhibitors such as PD-1. Stem-cell based approaches using TCRs against HIV and cancer were discussed. Hyperimmune activation during HIV-1 infection appears to be driven by chronic IFN-I induction. Hu-mouse studies determined that blocking the IFN-I signaling by antibodies decreased immune activation and resulted in reversal of T cell exhaustion.

Kim et al. described the use of humanized DRAG mice (HLA class II DR4 transgenic) for HIV-1 transmission via intravaginal route. Superior human cell engraftment in mucosal sites was noted. Viral spread from the point of entry were studied in detail with the results supporting the utility of this improved model to study viral pathogenesis, tissue distribution, viral persistence and establishment of latent viral reservoirs. Volk et al. described a multidimensional analysis approach integrating human T cell signatures in lymphatic tissues with the sex of humanized mice as a predictor of responses after dendritic cell-based immunization. This new modality of multidimensional analysis can be potentially used as a framework for assessing predictive signatures of immune responses.

Viral hemorrhagic fevers (VHF) such as Ebola, Dengue, and Crimean-Congo hemorrhagic fever with high fatality rates constitute important public health concerns. While the natural hosts for these viruses in the wild are asymptomatic, humans are severely affected, incriminating a role for the human immune system in mediating severe pathology. Schönrich and Raftery reviewed the impact of humanized mice in VHF vaccines and therapeutics research, also emphasizing their role as surrogate models for the discovery of newly emerging zoonotic agents.

Hu-mice provide excellent models to study tumorigenesis and immune responses. Among the virus-related human cancers, EBV and KSHV account for 10% of morbidity. Their epidemiology varies drastically in different geographic regions. The review by Münz detailed the tumorigenesis by these viruses, interesting aspects of how KSHV infection is sustained longer during EBV coinfection in hu-mice, how the adaptive and innate immune responses play out and how this knowledge can be used to develop effective vaccines in the future. With regard to modeling anti-tumor responses *in vivo* in humanized mice, Zumwalde and Gumperz reviewed the use of humanized mice engrafted with human umbilical cord blood-derived HSC. They also discussed how T cells get suppressed during EBV tumorigenesis and how immunotherapy strategies can counteract this.

The tumor microenvironment contains unique immune cells, termed myeloid-derived suppressor cells (MDSC) and tumor-associated macrophages (TAM) that suppress host anti-tumor immunity and promote tumor angiogenesis and metastasis. Hanazawa et al. described the generation of a functional human TAM population in their novel humanized IL-6 transgenic mouse strain, NOG-hIL-6 Tg. Development of novel cancer immune therapies targeting immunoregulatory/immunosuppressive myeloid cells is now possible using this model. The same research group led by Takahashi et al. reported the derivation of a new transgenic mouse strain, NOG-pRORγt-γc, in which the γc gene was expressed in a lymph-tissue inducer (LTi) lineage by the endogenous promoter of RORγt. Lymph node development was greatly improved, a major deficiency with previous HIS mouse models. Increased numbers of IL-21–producing CD4+ T cells were seen in LNs and there was enhanced antigen specific IgG response thus providing a vastly improved HIS mouse model.

Two reports focused on bacterial studies. *Staphylococcus aureus* is an important human pathogen responsible for many disease conditions including fatal pneumonia and septicemia. While conventional mice have been useful to study these conditions to an extent, it has become clear that some virulence factors/toxins display higher specificity to the human cells/factors leading to more severe disease. Parker's review highlights the value of humanized mice in dissecting the role of *S. aureus* virulence factors in a human surrogate setting and in vaccine testing.

Over one million people worldwide are affected annually by Scrub typhus, a disease caused by an intracellular bacterium *Orientia tsutsugamushi*. Although standard mouse models provided a basic understanding, data is sparse on human immunopathogenesis and immune responses. Jiang et al. described the successful use of a humanized DRAGA (HLA-A2 and HLA-DR4-transgenic) mouse model capable of efficient human cellular and antibody responses. Footpad infection with *O. tsutsugamushi* resulted in disseminated lesions in various organs and invoked human immune responses including T cell activation, specific antibody and cytokine secretion mimicking human disease and responses. Vaccination with killed whole cell *O. tsutsugamushi* gave rise to both humoral and cellular responses thus providing a human relevant model for future vaccines and therapeutics testing.

Malaria continues to inflict high morbidity and mortality numbering in millions in many parts of the world. Transmitted

by mosquitoes, the parasite has a complex life cycle with many stages of development. Minkah et al. reviewed the current status of malaria animal models and point to the need to develop humanized mouse models that can support both the hepatic and blood stages of infection to study pathogenesis and enable therapeutic testing. With these criteria as a background, the report by Foquet et al. described establishment of a FRGN huHep/hRBC humanized mouse model. This animal model enabled human malaria parasites to successfully undergo the liver stages and culminate with the blood stages of infection *in vivo*. Imaging techniques used to test the efficacy of an inhibitory monoclonal antibody demonstrated the utility of the model in evaluating interventions that target one or both phases of the parasite life cycle.

In summary, this Research Topic highlights the recent advancements in biomedical research using different models of humanized mice. As can be seen, these models have been substantially improved over the past decade increasing their breadth in utility not only in studying the infection process of the pathogens but also allowed evaluation of host immune responses thus laying a foundation to build upon for future vaccine and therapeutic testing.

We thank all the authors of the manuscripts for their contributions to the humanized mouse field and reviewers for their constructive comments and input.

AUTHOR CONTRIBUTIONS

All authors listed have made a substantial, direct and intellectual contribution to the work, and approved it for publication.

FUNDING

Work done in the Akkina laboratory is supported by NIH grants, RO1 AI120021 and RO1 AI123234.

Conflict of Interest: The authors declare that the research was conducted in the absence of any commercial or financial relationships that could be construed as a potential conflict of interest.

frontiers in Immunology

MINI REVIEW
published: 04 May 2017
doi: 10.3389/fimmu.2017.00512

Humanized Mouse Models of *Staphylococcus aureus* Infection

*Dane Parker**

Department of Pediatrics, Columbia University, New York, NY, USA

Staphylococcus aureus is a successful human pathogen that has adapted itself in response to selection pressure by the human immune system. A commensal of the human skin and nose, it is a leading cause of several conditions: skin and soft tissue infection, pneumonia, septicemia, peritonitis, bacteremia, and endocarditis. Mice have been used extensively in all these conditions to identify virulence factors and host components important for pathogenesis. Although significant effort has gone toward development of an anti-staphylococcal vaccine, antibodies have proven ineffective in preventing infection in humans after successful studies in mice. These results have raised questions as to the utility of mice to predict patient outcome and suggest that humanized mice might prove useful in modeling infection. The development of humanized mouse models of *S. aureus* infection will allow us to assess the contribution of several human-specific virulence factors, in addition to exploring components of the human immune system in protection against *S. aureus* infection. Their use is discussed in light of several recently reported studies.

Keywords: *Staphylococcus aureus*, humanized mouse, pneumonia, lung, sepsis, skin, mouse model, infection

OPEN ACCESS

Edited by:
Ramesh Akkina,
Colorado State University, USA

Reviewed by:
Vijay Panchanathan,
Perdana University, Malaysia
Fabio Bagnoli,
GlaxoSmithKline, Italy

***Correspondence:**
Dane Parker
dp2375@columbia.edu

Specialty section:
This article was submitted to Vaccines and Molecular Therapeutics, a section of the journal Frontiers in Immunology

Received: *13 March 2017*
Accepted: *18 April 2017*
Published: *04 May 2017*

Citation:
Parker D (2017) Humanized Mouse Models of Staphylococcus aureus Infection. Front. Immunol. 8:512. doi: 10.3389/fimmu.2017.00512

Staphylococcus aureus

Staphylococcus aureus is a Gram-positive pathogen that can exist as a commensal on skin. It is a human pathogen and a leading cause of skin and soft tissue infections, pneumonia, endocarditis, and osteomyelitis (1, 2). In particular, methicillin-resistant *S. aureus* (MRSA) is a major problem not only in the hospital setting but also in the community causing significant economic burden (3–5). MRSA strains are twice as likely to kill and cost the US economy in excess of $4 billion/year (6–8). In contrast to hospital-acquired strains, community-acquired strains of *S. aureus* infect otherwise healthy individuals. The MRSA strain USA300 (4, 9, 10) infects healthy, hospitalized, and post-influenza patients in the context of pneumonia (11–14), is the dominant clone, and is epidemic in the United States. Secondary bacterial infection post-influenza is a leading cause of morbidity and mortality (15–17), which has been shown for history's major pandemics, and *S. aureus* is one of the most common pathogens (12, 18, 19). This is of increasing concern as the population ages, as they are at increased risk of influenza infection. Colonization of the nose with *S. aureus* is relatively common with up to 30% of the population being persistent carriers, while the proportion colonized with MRSA is increasing (20–23). Carriage increases the risk of infection (24, 25), and as a result of this, patients are often decolonized prior to surgery to prevent infection (26).

MOUSE MODELS OF INFECTION

Studies investigating the pathogenesis of *S. aureus* infection have relied heavily on the use of mouse models. Mice have been used to understand the role virulence factors play during infection as well

as the contribution of specific host pathways and factors in the response to *S. aureus*. Mouse models for several important clinical diseases have been developed, including: peritonitis (27, 28), pneumonia (29–31), sepsis (32), skin and soft tissue infection (33, 34), endocarditis (35, 36), abscesses (37, 38), osteomyelitis (39, 40), arthritis (41), and nasal colonization (42–44).

Mice possess a number of attributes that make them desirable in modeling infection. They are small in size, do not occupy significant space, are cheap, reproduce rapidly, and have similar immune, nervous, cardiovascular, and endocrine systems to humans (45–47). Another major advantage is their genetic tractability. In mice, genes can be readily inactivated "knocked out," genes inserted "knocked in," gene reporter fusions integrated into the genome, and tissue specific mutations developed. This genetic utility makes them attractive to study host immune factors important in infection. However, the use of mice is not without their limitations. Many features of mice are significantly different from humans, such as their small size, altered metabolic rate, fatty acid composition of cells, higher rates of reactive oxygen species generation and thus oxidative damage, different diet, microbiome, and typically being inbred (48). There has also been some controversy recently on how well mice correlate with human inflammatory stresses based on transcriptional profiling and pathway analyses (49–51).

WHY DO WE NEED HUMANIZED MICE FOR *S. aureus* INFECTION?

Although mice have proven extremely useful in determining the role of many *S. aureus* virulence factors and identifying host pathways that contribute to infection, they have been unable to predict success for vaccine candidates in humans (52, 53). This disconnect between the mouse model and efficacy in humans supports the conclusion that the mouse lacks all the necessary components to truly model *S. aureus* infection. It has also become increasingly apparent that *S. aureus* produces a number of virulence factors that have high species specificity toward the human molecular counterpart that they target.

One major group of proteins that possess human specificity are the bi-component toxins (54). Panton–Valentine leukocidin (PVL; LukSF), LukAB, and HlgCB, all preferentially target the human version of their receptor. PVL and HlgCB target the C5aR receptor, while LukAB targets CD11b (55). PVL does have some activity toward the rabbit version of the receptor; however, the other two toxins display only high specificity toward the human equivalent. The *S. aureus* superantigens/enterotoxins also show much greater affinity toward human cells, with vastly higher doses of protein required to invoke a response in mice (56, 57). *S. aureus* produces a large array of surface proteins required for its adherence to proteins encountered on the mucosal surface. Some of these surface proteins also display specificity toward their human counterpart, such as SdrG for human fibrinogen, Fnbp for fibronectin, and IsdB for hemoglobin (58). There are also likely to be several other yet-to-be-identified proteins that have human specificity based on the fact that *S. aureus* is a human-adapted pathogen. Thus, the development of a model that actually possesses the correct receptor targets and cells for these virulence factors to be investigated would be advantageous. The presence of an immune system to better model the human immune response would also no doubt prove useful in future vaccine development as well as gaining an improved understanding of the host–pathogen interaction in the context of *S. aureus* infection.

The host specificity of *S. aureus* toward human proteins has already been investigated in the context of superantigens and iron acquisition. It has been observed with the staphylococcal superantigens that HLA class II molecules control the superantigenic response and that this response is significantly reduced in non-human (including mice) models. A trend in this field has been to utilize knock-in mice expressing the appropriate HLA molecule for the superantigen (enterotoxin) under study. This has included HLA-DR3, HLA-DR4, and CD4 knock-in mice (59–63). Studies conducted using these mice have shown a significant increase in the immune response, indicative of the increased sensitivity of these cells to the superantigens. The preference for human hemoglobin over other mammal's hemoglobin has been observed and is dependent upon the staphylococcal hemoglobin receptor IsdB. *S. aureus* grows better in the presence of human hemoglobin when iron is limited and the expression of human hemoglobin in mice leads to increased susceptibility to *S. aureus* infection (64). Thus, evidence already exists that warrants humanizing mice would improve the capacity to model *S. aureus* infection.

HUMANIZED MICE

The use of humanized mice has only relatively recently become prevalent. Their use was accelerated through the development of the NSG mouse (non-obese diabetic/severe combined immunodeficient mouse with a null mutation in the IL2R common gamma chain) (65). These mice lack B, T, and NK cells, complement, and have defective myeloid cells (65, 66). The NSG mice have been observed to possess the most efficient engraftment rates and support human hemato-lymphopoiesis (66–68). The mice are typically generated through the transfer of human $CD34^+$ stem cells (69). Additionally, the implantation of human fetal liver/thymus tissue under the kidney capsule improves T cell development (70, 71). Humanized mice have been shown to evoke a human immune response to infection. The combinatorial diversity on their T cell receptors and IgG fully replicates the human samples that are used to populate the mice (72). Humanized mice have been utilized in the study of several viral pathogens such as EBV, HIV, and Dengue, as well as Malaria and *Salmonella* (73–76). Recently, a succession of studies has investigated the utility of these mice in the study of *S. aureus* pathogenesis.

RECENT DEVELOPMENTS WITH *S. aureus* AND HUMANIZED MICE

The first study to investigate the utility of humanized mice with *S. aureus* highlighted their increased susceptibility to infection.

Knop et al. (77) conducted intraperitoneal infections in humanized mice generated from irradiated NSG pups transferred with $CD34^+$ cells. Humanized mice displayed significantly increased mortality compared to their controls. While non-reconstituted NSG mice did display some residual toxicity from radiation, the addition of human cells was shown to confer the lethality seen with the humanized mice. Increased bacterial counts were also observed in several organs; lungs, spleen, kidneys, liver, brain, and the bone marrow. The T cells in the humanized mice showed evidence of activation (CD69 expression), Fas receptor expression, and increased apoptosis after infection. Analysis of the human cells indicated a large proportion of B cells, followed by T cells and myeloid cells. Levels of chimerism were highest in the spleen (60%) and bone marrow (50%), 30% in the peripheral blood and <20% in the peritoneal exudate. This study indicated that humanized mice could be useful in modeling *S. aureus* infection, and subsequent studies have built on this to investigate the role of human-specific virulence factors.

The second study to utilize humanized mice with *S. aureus* investigated their utility in the context of skin infection, also showing an increased susceptibility to infection (78). In a subcutaneous model of infection, 10- to 100-fold less organisms were required to cause analogous disease pathology in non-humanized mice. Tseng et al. (78) found no differences in bacterial clearance or cytokine production. The phenotype observed was pathological, indicating that cellular toxicity did not influence bacterial clearance. The size of the skin lesions also correlated to the levels of chimerism in the mice, larger lesions were observed in mice with a higher percentage of human $CD45^+$ cells. This model was then used to investigate the role of PVL in infection. PVL has a controversial role in infection. Conflicting epidemiological reports and animal studies exist, partly due to the fact many animal studies were performed prior to the identification of its receptor, C5aR, and its high preference for the human version of this receptor (79–87). The expression of PVL led to larger areas of dermonecrosis. This effect was due to its ability to target and kill neutrophils, as transfer of human neutrophils alone to NSG mice was able to recapitulate this phenotype. While the authors successfully showed a role for PVL in skin infection with molecular Koch's postulates, a PVL inhibitor *in vivo* was unable to reduce disease severity. Like the first study, this work also utilized stem cell transfer into neonate NSG mice and observed similar levels of engraftment in the spleen. This work proved the utility for the humanized mouse in delineating the functions of staphylococcal virulence factors as well as its usefulness as a model for skin infection.

The third and most recent humanized mouse study showcased the utility of these mice for respiratory infection (71). As in the previous studies, the humanized mice displayed a significant increase in susceptibility to infection. Compared to the standard mouse strains C57BL/6J, NOD and murinized controls (NSG mice transferred with murine bone marrow), the humanized mice contained bacterial burdens 40-fold higher. The role of PVL was also investigated in this pulmonary model and was shown to contribute to infection, using both bacterial mutants and neutralizing antibody (71). The presence of PVL led to increased bacterial burden, increased lung pathology and decreased cytokine production. The target of PVL appeared to be the macrophage, with increased numbers present in mice infected with the PVL-deficient strain. The NSG transgenic mouse with human *Il3* and *Csf2* knocked in has improved macrophage reconstitution compared to the standard NSG humanized mouse (88). Consistent with human macrophages conferring the increased susceptibility, the use of these additional knock-in mice had even higher levels of bacteria present in the airways and lung tissue. While a role for PVL in pulmonary infection was identified, this was not the case for another human-specific toxin LukAB, which displayed no phenotype in this model (71). This study differed from the previous two in its use of adult mice and the implantation of thymus tissue under the kidney capsule. This was apparent in the higher levels of T cells present among the human $CD45^+$ population, approximately 50% in the lung (71). What these three studies do show is that irrespective of the inoculation site the humanized mice had an increased susceptibility to infection, which will only improve as better humanized mouse models are generated.

FUTURE MODELS

The development of improved humanized mouse models will further increase the susceptibility and hence sensitivity of modeling *S. aureus* infections *in vivo*. This will be achieved through improved overall reconstitution of the human immune system, improved differentiation, and development of myeloid subsets, as well at the improved expression of neutrophils, an integral cell type particularly in pneumonia and skin infection models. Significant work has already been done in this area with the insertion of *Csf1*, *Csf2*, and *Il3* into mice, leading to improved differentiation of macrophages and alveolar macrophages, respectively (88, 89). The knocking in of *Csf2* and *Il3* was shown to increase the susceptibility of *S. aureus* in the context of acute pneumonia (71). Further studies have shown that the integration of thrombopoietin enhances maintenance and multilineage differentiation and insertion of signal-regulatory protein alpha prevents phagocytosis of the human cells by the remnant murine immune system (90, 91). Additional transgenics appropriate to *S. aureus* would include a combination of the aforementioned along with: human HLA types for the study of superantigens (92), insertion of human toll-like receptors for the innate immune response (75), as well as the incorporation of epithelial cells in the lung and skin for mucosal models (34, 93) and red blood cells for systemic studies (94, 95). These developments will facilitate adequate modeling of a broad range of *S. aureus* human-specific virulence factors.

CONCLUSION

Staphylococcus aureus is a significant human pathogen that has long been modeled in mice. Studies to-date in mice have delineated the roles of various bacterial and host factors important in infection; however, data on potential vaccine candidates identified in these models have not had similar success in human studies. Recent studies utilizing humanized mice have illuminated their utility in models of peritonitis, skin and soft tissue infection,

and pneumonia. Researchers have shown humanized mice have increased susceptibility to *S. aureus* and in skin and pneumonia models a role for PVL in infection has been identified. As the next generation of humanized mouse models are developed, the capacity for modeling *S. aureus* will only improve. Humanized mice will facilitate determining the role of virulence factors with human host specificity and hopefully provide a system whereby potential vaccine candidate translate efficacy to humans.

AUTHOR CONTRIBUTIONS

DP conceived and wrote the manuscript.

FUNDING

This work was supported by the American Lung Association (RG-310706) and NIH (R56HL12565).

REFERENCES

1. King MD, Humphrey BJ, Wang YF, Kourbatova EV, Ray SM, Blumberg HM. Emergence of community-acquired methicillin-resistant *Staphylococcus aureus* USA 300 clone as the predominant cause of skin and soft-tissue infections. *Ann Intern Med* (2006) 144(5):309–17. doi:10.7326/0003-4819-144-5-200603070-00005
2. Talan DA, Krishnadasan A, Gorwitz RJ, Fosheim GE, Limbago B, Albrecht V, et al. Comparison of *Staphylococcus aureus* from skin and soft-tissue infections in US emergency department patients, 2004 and 2008. *Clin Infect Dis* (2011) 53(2):144–9. doi:10.1093/cid/cir308
3. Mizgerd JP. Lung infection – a public health priority. *PLoS Med* (2006) 3(2):e76. doi:10.1371/journal.pmed.0030076
4. Klevens RM, Morrison MA, Nadle J, Petit S, Gershman K, Ray S, et al. Invasive methicillin-resistant *Staphylococcus aureus* infections in the United States. *JAMA* (2007) 298(15):1763–71. doi:10.1001/jama.298.15.1763
5. Mizgerd JP. Respiratory infection and the impact of pulmonary immunity on lung health and disease. *Am J Respir Crit Care Med* (2012) 186(9):824–9. doi:10.1164/rccm.201206-1063PP
6. Shorr AF, Tabak YP, Gupta V, Johannes RS, Liu LZ, Kollef MH. Morbidity and cost burden of methicillin-resistant *Staphylococcus aureus* in early onset ventilator-associated pneumonia. *Crit Care* (2006) 10(3):R97. doi:10.1186/cc4934
7. Klein E, Smith DL, Laxminarayan R. Hospitalizations and deaths caused by methicillin-resistant *Staphylococcus aureus*, United States, 1999-2005. *Emerg Infect Dis* (2007) 13(12):1840–6. doi:10.3201/eid1312.070629
8. Lee BY, Singh A, David MZ, Bartsch SM, Slayton RB, Huang SS, et al. The economic burden of community-associated methicillin-resistant *Staphylococcus aureus* (CA-MRSA). *Clin Microbiol Infect* (2013) 19(6):528–36. doi:10.1111/j.1469-0691.2012.03914.x
9. CDC. From the Centers for Disease Control and Prevention. Public health dispatch: outbreaks of community-associated methicillin-resistant *Staphylococcus aureus* skin infections – Los Angeles County, California, 2002-2003. *JAMA* (2003) 289(11):1377.
10. McDougal LK, Steward CD, Killgore GE, Chaitram JM, McAllister SK, Tenover FC. Pulsed-field gel electrophoresis typing of oxacillin-resistant *Staphylococcus aureus* isolates from the United States: establishing a national database. *J Clin Microbiol* (2003) 41(11):5113–20. doi:10.1128/JCM.41.11.5113-5120.2003
11. Francis JS, Doherty MC, Lopatin U, Johnston CP, Sinha G, Ross T, et al. Severe community-onset pneumonia in healthy adults caused by methicillin-resistant *Staphylococcus aureus* carrying the Panton-Valentine leukocidin genes. *Clin Infect Dis* (2005) 40(1):100–7. doi:10.1086/427148
12. Hageman JC, Uyeki TM, Francis JS, Jernigan DB, Wheeler JG, Bridges CB, et al. Severe community-acquired pneumonia due to *Staphylococcus aureus*, 2003-04 influenza season. *Emerg Infect Dis* (2006) 12(6):894–9. doi:10.3201/eid1206.051141
13. Centers for Disease Control and Prevention. Bacterial coinfections in lung tissue specimens from fatal cases of 2009 pandemic influenza A (H1N1) – United States, May-August 2009. *MMWR Morb Mortal Wkly Rep* (2009) 58(38):1071–4.
14. Tasher D, Stein M, Simoes EA, Shohat T, Bromberg M, Somekh E. Invasive bacterial infections in relation to influenza outbreaks, 2006-2010. *Clin Infect Dis* (2011) 53(12):1199–207. doi:10.1093/cid/cir726
15. Morens DM, Taubenberger JK, Fauci AS. Predominant role of bacterial pneumonia as a cause of death in pandemic influenza: implications for pandemic influenza preparedness. *J Infect Dis* (2008) 198(7):962–70. doi:10.1086/591708
16. Chertow DS, Memoli MJ. Bacterial coinfection in influenza: a grand rounds review. *JAMA* (2013) 309(3):275–82. doi:10.1001/jama.2012.194139
17. Papanicolaou G. Severe influenza and *S. aureus* pneumonia: for whom the bell tolls? *Virulence* (2013) 4(8):666–68. doi:10.4161/viru.26957
18. Louria DB, Blumenfeld HL, Ellis JT, Kilbourne ED, Rogers DE. Studies on influenza in the pandemic of 1957-1958. II. Pulmonary complications of influenza. *J Clin Invest* (1959) 38(1 Pt 2):213–65. doi:10.1172/JCI103791
19. Murray RJ, Robinson JO, White JN, Hughes F, Coombs GW, Pearson JC, et al. Community-acquired pneumonia due to pandemic A(H1N1)2009 influenza virus and methicillin resistant *Staphylococcus aureus* co-infection. *PLoS One* (2010) 5(1):e8705. doi:10.1371/journal.pone.0008705
20. Creech CB II, Kernodle DS, Alsentzer A, Wilson C, Edwards KM. Increasing rates of nasal carriage of methicillin-resistant *Staphylococcus aureus* in healthy children. *Pediatr Infect Dis J* (2005) 24(7):617–21. doi:10.1097/01.inf.0000168746.62226.a4
21. Finelli L, Fiore A, Dhara R, Brammer L, Shay DK, Kamimoto L, et al. Influenza-associated pediatric mortality in the United States: increase of *Staphylococcus aureus* coinfection. *Pediatrics* (2008) 122(4):805–11. doi:10.1542/peds.2008-1336
22. Gorwitz RJ, Kruszon-Moran D, McAllister SK, McQuillan G, McDougal LK, Fosheim GE, et al. Changes in the prevalence of nasal colonization with *Staphylococcus aureus* in the United States, 2001-2004. *J Infect Dis* (2008) 197(9):1226–34. doi:10.1086/533494
23. Rafee Y, Abdel-Haq N, Asmar B, Salimnia T, Pharm CV, Rybak Pharm MJ, et al. Increased prevalence of methicillin-resistant *Staphylococcus aureus* nasal colonization in household contacts of children with community acquired disease. *BMC Infect Dis* (2012) 12:45. doi:10.1186/1471-2334-12-45
24. Wertheim HF, Vos MC, Ott A, van Belkum A, Voss A, Kluytmans JA, et al. Risk and outcome of nosocomial *Staphylococcus aureus* bacteraemia in nasal carriers versus non-carriers. *Lancet* (2004) 364(9435):703–5. doi:10.1016/S0140-6736(04)16897-9
25. Stevens AM, Hennessy T, Baggett HC, Bruden D, Parks D, Klejka J. Methicillin-resistant *Staphylococcus aureus* carriage and risk factors for skin infections, Southwestern Alaska, USA. *Emerg Infect Dis* (2010) 16(5):797–803. doi:10.3201/eid1605.091851
26. Diller R, Sonntag AK, Mellmann A, Grevener K, Senninger N, Kipp F, et al. Evidence for cost reduction based on pre-admission MRSA screening in general surgery. *Int J Hyg Environ Health* (2008) 211(1–2):205–12. doi:10.1016/j.ijheh.2007.06.001
27. Sandberg A, Hessler JH, Skov RL, Blom J, Frimodt-Moller N. Intracellular activity of antibiotics against *Staphylococcus aureus* in a mouse peritonitis model. *Antimicrob Agents Chemother* (2009) 53(5):1874–83. doi:10.1128/AAC.01605-07
28. Rauch S, DeDent AC, Kim HK, Bubeck Wardenburg J, Missiakas DM, Schneewind O. Abscess formation and alpha-hemolysin induced toxicity in a mouse model of *Staphylococcus aureus* peritoneal infection. *Infect Immun* (2012) 80(10):3721–32. doi:10.1128/IAI.00442-12
29. Gomez MI, Lee A, Reddy B, Muir A, Soong G, Pitt A, et al. *Staphylococcus aureus* protein A induces airway epithelial inflammatory responses by activating TNFR1. *Nat Med* (2004) 10(8):842–8. doi:10.1038/nm1079
30. Bubeck Wardenburg J, Patel RJ, Schneewind O. Surface proteins and exotoxins are required for the pathogenesis of *Staphylococcus aureus* pneumonia. *Infect Immun* (2007) 75(2):1040–4. doi:10.1128/IAI.01313-06
31. Parker D, Prince A. *Staphylococcus aureus* induces type I IFN signaling in dendritic cells via TLR9. *J Immunol* (2012) 189(8):4040–6. doi:10.4049/jimmunol.1201055

32. Powers ME, Bubeck Wardenburg J. Igniting the fire: *Staphylococcus aureus* virulence factors in the pathogenesis of sepsis. *PLoS Pathog* (2014) 10(2): e1003871. doi:10.1371/journal.ppat.1003871
33. Miller LS, O'Connell RM, Gutierrez MA, Pietras EM, Shahangian A, Gross CE, et al. MyD88 mediates neutrophil recruitment initiated by IL-1R but not TLR2 activation in immunity against *Staphylococcus aureus*. *Immunity* (2006) 24(1):79–91. doi:10.1016/j.immuni.2005.11.011
34. Soong G, Paulino F, Wachtel S, Parker D, Wickersham M, Zhang D, et al. Methicillin-resistant *Staphylococcus aureus* adaptation to human keratinocytes. *MBio* (2015) 6(2):e00289-15. doi:10.1128/mBio.00289-15
35. Gibson GW, Kreuser SC, Riley JM, Rosebury-Smith WS, Courtney CL, Juneau PL, et al. Development of a mouse model of induced *Staphylococcus aureus* infective endocarditis. *Comp Med* (2007) 57(6):563–9.
36. Panizzi P, Nahrendorf M, Figueiredo JL, Panizzi J, Marinelli B, Iwamoto Y, et al. In vivo detection of *Staphylococcus aureus* endocarditis by targeting pathogen-specific prothrombin activation. *Nat Med* (2011) 17(9):1142–6. doi:10.1038/nm.2423
37. Cheng AG, Kim HK, Burts ML, Krausz T, Schneewind O, Missiakas DM. Genetic requirements for *Staphylococcus aureus* abscess formation and persistence in host tissues. *FASEB J* (2009) 23(10):3393–404. doi:10.1096/fj.09-135467
38. Cheng AG, McAdow M, Kim HK, Bae T, Missiakas DM, Schneewind O. Contribution of coagulases towards *Staphylococcus aureus* disease and protective immunity. *PLoS Pathog* (2010) 6(8):e1001036. doi:10.1371/journal.ppat.1001036
39. Horst SA, Hoerr V, Beineke A, Kreis C, Tuchscherr L, Kalinka J, et al. A novel mouse model of *Staphylococcus aureus* chronic osteomyelitis that closely mimics the human infection: an integrated view of disease pathogenesis. *Am J Pathol* (2012) 181(4):1206–14. doi:10.1016/j.ajpath.2012.07.005
40. Cassat JE, Hammer ND, Campbell JP, Benson MA, Perrien DS, Mrak LN, et al. A secreted bacterial protease tailors the *Staphylococcus aureus* virulence repertoire to modulate bone remodeling during osteomyelitis. *Cell Host Microbe* (2013) 13(6):759–72. doi:10.1016/j.chom.2013.05.003
41. Bremell T, Lange S, Yacoub A, Ryden C, Tarkowski A. Experimental *Staphylococcus aureus* arthritis in mice. *Infect Immun* (1991) 59(8): 2615–23.
42. Lijek RS, Luque SL, Liu Q, Parker D, Bae T, Weiser JN. Protection from the acquisition of *Staphylococcus aureus* nasal carriage by cross-reactive antibody to a pneumococcal dehydrogenase. *Proc Natl Acad Sci U S A* (2012) 109(34):13823–8. doi:10.1073/pnas.1208075109
43. Xu SX, Kasper KJ, Zeppa JJ, McCormick JK. Superantigens modulate bacterial density during *Staphylococcus aureus* nasal colonization. *Toxins (Basel)* (2015) 7(5):1821–36. doi:10.3390/toxins7051821
44. Planet PJ, Parker D, Cohen TS, Smith H, Leon JD, Ryan C, et al. Lambda interferon restructures the nasal microbiome and increases susceptibility to *Staphylococcus aureus* superinfection. *MBio* (2016) 7(1):e01939–15. doi:10.1128/mBio.01939-15
45. Buer J, Balling R. Mice, microbes and models of infection. *Nat Rev Genet* (2003) 4(3):195–205. doi:10.1038/nrg1019
46. Rosenthal N, Brown S. The mouse ascending: perspectives for human-disease models. *Nat Cell Biol* (2007) 9(9):993–9. doi:10.1038/ncb437
47. Perlman RL. Mouse models of human disease: an evolutionary perspective. *Evol Med Public Health* (2016) 2016(1):170–6. doi:10.1093/emph/eow014
48. Xiao L, Feng Q, Liang S, Sonne SB, Xia Z, Qiu X, et al. A catalog of the mouse gut metagenome. *Nat Biotechnol* (2015) 33(10):1103–8. doi:10.1038/nbt.3353
49. Seok J, Warren HS, Cuenca AG, Mindrinos MN, Baker HV, Xu W, et al. Genomic responses in mouse models poorly mimic human inflammatory diseases. *Proc Natl Acad Sci U S A* (2013) 110(9):3507–12. doi:10.1073/pnas.1222878110
50. Warren HS, Tompkins RG, Moldawer LL, Seok J, Xu W, Mindrinos MN, et al. Mice are not men. *Proc Natl Acad Sci U S A* (2014) 112(4):E345. doi:10.1073/pnas.1414857111
51. Takao K, Miyakawa T. Genomic responses in mouse models greatly mimic human inflammatory diseases. *Proc Natl Acad Sci U S A* (2015) 112(4):1167–72. doi:10.1073/pnas.1401965111
52. Bagnoli F, Bertholet S, Grandi G. Inferring reasons for the failure of *Staphylococcus aureus* vaccines in clinical trials. *Front Cell Infect Microbiol* (2012) 2:16. doi:10.3389/fcimb.2012.00016
53. Fowler VG, Allen KB, Moreira ED, Moustafa M, Isgro F, Boucher HW, et al. Effect of an investigational vaccine for preventing *Staphylococcus aureus* infections after cardiothoracic surgery: a randomized trial. *JAMA* (2013) 309(13):1368–78. doi:10.1001/jama.2013.3010
54. Alonzo F III, Torres VJ. Bacterial survival amidst an immune onslaught: the contribution of the *Staphylococcus aureus* leukotoxins. *PLoS Pathog* (2013) 9(2):e1003143. doi:10.1371/journal.ppat.1003143
55. DuMont AL, Yoong P, Day CJ, Alonzo F III, McDonald WH, Jennings MP, et al. *Staphylococcus aureus* LukAB cytotoxin kills human neutrophils by targeting the CD11b subunit of the integrin Mac-1. *Proc Natl Acad Sci U S A* (2013) 110(26):10794–9. doi:10.1073/pnas.1305121110
56. Lambris JD, Ricklin D, Geisbrecht BV. Complement evasion by human pathogens. *Nat Rev Microbiol* (2008) 6(2):132–42. doi:10.1038/nrmicro1824
57. Spaulding AR, Salgado-Pabon W, Kohler PL, Horswill AR, Leung DY, Schlievert PM. Staphylococcal and streptococcal superantigen exotoxins. *Clin Microbiol Rev* (2013) 26(3):422–47. doi:10.1128/CMR.00104-12
58. Foster TJ, Geoghegan JA, Ganesh VK, Hook M. Adhesion, invasion and evasion: the many functions of the surface proteins of *Staphylococcus aureus*. *Nat Rev Microbiol* (2014) 12(1):49–62. doi:10.1038/nrmicro3161
59. Yeung RS, Penninger JM, Kundig T, Khoo W, Ohashi PS, Kroemer G, et al. Human CD4 and human major histocompatibility complex class II (DQ6) transgenic mice: supersensitivity to superantigen-induced septic shock. *Eur J Immunol* (1996) 26(5):1074–82. doi:10.1002/eji.1830260518
60. Xu SX, Gilmore KJ, Szabo PA, Zeppa JJ, Baroja ML, Haeryfar SM, et al. Superantigens subvert the neutrophil response to promote abscess formation and enhance *Staphylococcus aureus* survival in vivo. *Infect Immun* (2014) 82(9):3588–98. doi:10.1128/IAI.02110-14
61. Karau MJ, Tilahun ME, Krogman A, Osborne BA, Goldsby RA, David CS, et al. Passive therapy with humanized anti-staphylococcal enterotoxin B antibodies attenuates systemic inflammatory response and protects from lethal pneumonia caused by staphylococcal enterotoxin B-producing *Staphylococcus aureus*. *Virulence* (2016):1–12. doi:10.1080/21505594.2016.1267894
62. Szabo PA, Goswami A, Memarnejadian A, Mallett CL, Foster PJ, McCormick JK, et al. Swift intrahepatic accumulation of granulocytic myeloid-derived suppressor cells in a humanized mouse model of toxic shock syndrome. *J Infect Dis* (2016) 213(12):1990–5. doi:10.1093/infdis/jiw050
63. Szabo PA, Rudak PT, Choi J, Xu SX, Schaub R, Singh B, et al. Invariant NKT cells are pathogenic in the HLA-DR4-transgenic humanized mouse model of toxic shock syndrome and can be targeted to reduce morbidity. *J Infect Dis* (2016) 215(5):824–29. doi:10.1093/infdis/jiw646
64. Pishchany G, McCoy AL, Torres VJ, Krause JC, Crowe JE Jr, Fabry ME, et al. Specificity for human hemoglobin enhances *Staphylococcus aureus* infection. *Cell Host Microbe* (2010) 8(6):544–50. doi:10.1016/j.chom.2010.11.002
65. Ishikawa F, Yasukawa M, Lyons B, Yoshida S, Miyamoto T, Yoshimoto G, et al. Development of functional human blood and immune systems in NOD/SCID/IL2 receptor {gamma} chain(null) mice. *Blood* (2005) 106(5):1565–73. doi:10.1182/blood-2005-02-0516
66. Shultz LD, Lyons BL, Burzenski LM, Gott B, Chen X, Chaleff S, et al. Human lymphoid and myeloid cell development in NOD/LtSz-scid IL2R gamma null mice engrafted with mobilized human hemopoietic stem cells. *J Immunol* (2005) 174(10):6477–89. doi:10.4049/jimmunol.174.10.6477
67. McDermott SP, Eppert K, Lechman ER, Doedens M, Dick JE. Comparison of human cord blood engraftment between immunocompromised mouse strains. *Blood* (2010) 116(2):193–200. doi:10.1182/blood-2010-02-271841
68. Tanaka S, Saito Y, Kunisawa J, Kurashima Y, Wake T, Suzuki N, et al. Development of mature and functional human myeloid subsets in hematopoietic stem cell-engrafted NOD/SCID/IL2rgammaKO mice. *J Immunol* (2012) 188(12):6145–55. doi:10.4049/jimmunol.1103660
69. Lan P, Tonomura N, Shimizu A, Wang S, Yang YG. Reconstitution of a functional human immune system in immunodeficient mice through combined human fetal thymus/liver and CD34+ cell transplantation. *Blood* (2006) 108(2):487–92. doi:10.1182/blood-2005-11-4388
70. Namikawa R, Weilbaecher KN, Kaneshima H, Yee EJ, McCune JM. Long-term human hematopoiesis in the SCID-hu mouse. *J Exp Med* (1990) 172(4): 1055–63. doi:10.1084/jem.172.4.1055
71. Prince A, Wang H, Kitur K, Parker D. Humanized mice exhibit increased susceptibility to *Staphylococcus aureus* pneumonia. *J Infect Dis* (2016). doi:10.1093/infdis/jiw425

72. Marodon G, Desjardins D, Mercey L, Baillou C, Parent P, Manuel M, et al. High diversity of the immune repertoire in humanized NOD.SCID. gamma c-/- mice. *Eur J Immunol* (2009) 39(8):2136–45. doi:10.1002/eji.200939480
73. Morosan S, Hez-Deroubaix S, Lunel F, Renia L, Giannini C, Van Rooijen N, et al. Liver-stage development of *Plasmodium falciparum*, in a humanized mouse model. *J Infect Dis* (2006) 193(7):996–1004. doi:10.1086/500840
74. Shultz LD, Brehm MA, Garcia-Martinez JV, Greiner DL. Humanized mice for immune system investigation: progress, promise and challenges. *Nat Rev Immunol* (2012) 12(11):786–98. doi:10.1038/nri3311
75. Brehm MA, Wiles MV, Greiner DL, Shultz LD. Generation of improved humanized mouse models for human infectious diseases. *J Immunol Methods* (2014) 410:3–17. doi:10.1016/j.jim.2014.02.011
76. Siu E, Ploss A. Modeling malaria in humanized mice: opportunities and challenges. *Ann N Y Acad Sci* (2015) 1342:29–36. doi:10.1111/nyas.12618
77. Knop J, Hanses F, Leist T, Archin NM, Buchholz S, Glasner J, et al. *Staphylococcus aureus* infection in humanized mice: a new model to study pathogenicity associated with human immune response. *J Infect Dis* (2015) 212(3):435–44. doi:10.1093/infdis/jiv073
78. Tseng CW, Biancotti JC, Berg BL, Gate D, Kolar SL, Muller S, et al. Increased susceptibility of humanized NSG mice to Panton-Valentine leukocidin and *Staphylococcus aureus* skin infection. *PLoS Pathog* (2015) 11(11):e1005292. doi:10.1371/journal.ppat.1005292
79. Lina G, Piemont Y, Godail-Gamot F, Bes M, Peter MO, Gauduchon V, et al. Involvement of Panton-Valentine leukocidin-producing *Staphylococcus aureus* in primary skin infections and pneumonia. *Clin Infect Dis* (1999) 29(5):1128–32. doi:10.1086/313461
80. Gillet Y, Issartel B, Vanhems P, Fournet JC, Lina G, Bes M, et al. Association between *Staphylococcus aureus* strains carrying gene for Panton-Valentine leukocidin and highly lethal necrotising pneumonia in young immunocompetent patients. *Lancet* (2002) 359(9308):753–9. doi:10.1016/S0140-6736(02)07877-7
81. Bubeck Wardenburg J, Bae T, Otto M, Deleo FR, Schneewind O. Poring over pores: alpha-hemolysin and Panton-Valentine leukocidin in *Staphylococcus aureus* pneumonia. *Nat Med* (2007) 13(12):1405–6. doi:10.1038/nm1207-1405
82. Labandeira-Rey M, Couzon F, Boisset S, Brown EL, Bes M, Benito Y, et al. *Staphylococcus aureus* Panton-Valentine leukocidin causes necrotizing pneumonia. *Science* (2007) 315(5815):1130–3. doi:10.1126/science.1137165
83. Villaruz AE, Bubeck Wardenburg J, Khan BA, Whitney AR, Sturdevant DE, Gardner DJ, et al. A point mutation in the agr locus rather than expression of the Panton-Valentine leukocidin caused previously reported phenotypes in *Staphylococcus aureus* pneumonia and gene regulation. *J Infect Dis* (2009) 200(5):724–34. doi:10.1086/604728
84. Diep BA, Chan L, Tattevin P, Kajikawa O, Martin TR, Basuino L, et al. Polymorphonuclear leukocytes mediate *Staphylococcus aureus* Panton-Valentine leukocidin-induced lung inflammation and injury. *Proc Natl Acad Sci U S A* (2010) 107(12):5587–92. doi:10.1073/pnas.0912403107
85. Shallcross LJ, Williams K, Hopkins S, Aldridge RW, Johnson AM, Hayward AC. Panton-Valentine leukocidin associated staphylococcal disease: a cross-sectional study at a London hospital, England. *Clin Microbiol Infect* (2010) 16(11):1644–8. doi:10.1111/j.1469-0691.2010.03153.x
86. Diep BA, Gillet Y, Etienne J, Lina G, Vandenesch F. Panton-Valentine leucocidin and pneumonia. *Lancet Infect Dis* (2013) 13(7):566. doi:10.1016/S1473-3099(13)70102-6
87. Shallcross LJ, Fragaszy E, Johnson AM, Hayward AC. The role of the Panton-Valentine leucocidin toxin in staphylococcal disease: a systematic review and meta-analysis. *Lancet Infect Dis* (2013) 13(1):43–54. doi:10.1016/S1473-3099(12)70238-4
88. Willinger T, Rongvaux A, Takizawa H, Yancopoulos GD, Valenzuela DM, Murphy AJ, et al. Human IL-3/GM-CSF knock-in mice support human alveolar macrophage development and human immune responses in the lung. *Proc Natl Acad Sci U S A* (2011) 108(6):2390–5. doi:10.1073/pnas.1019682108
89. Rathinam C, Poueymirou WT, Rojas J, Murphy AJ, Valenzuela DM, Yancopoulos GD, et al. Efficient differentiation and function of human macrophages in humanized CSF-1 mice. *Blood* (2011) 118(11):3119–28. doi:10.1182/blood-2010-12-326926
90. Strowig T, Rongvaux A, Rathinam C, Takizawa H, Borsotti C, Philbrick W, et al. Transgenic expression of human signal regulatory protein alpha in Rag2-/-gamma(c)-/- mice improves engraftment of human hematopoietic cells in humanized mice. *Proc Natl Acad Sci U S A* (2011) 108(32):13218–23. doi:10.1073/pnas.1109769108
91. Rongvaux A, Willinger T, Martinek J, Strowig T, Gearty SV, Teichmann LL, et al. Development and function of human innate immune cells in a humanized mouse model. *Nat Biotechnol* (2014) 32(4):364–72. doi:10.1038/nbt.2858
92. Akkina R. Human immune responses and potential for vaccine assessment in humanized mice. *Curr Opin Immunol* (2013) 25(3):403–9. doi:10.1016/j.coi.2013.03.009
93. Rosen C, Shezen E, Aronovich A, Klionsky YZ, Yaakov Y, Assayag M, et al. Preconditioning allows engraftment of mouse and human embryonic lung cells, enabling lung repair in mice. *Nat Med* (2015) 21(8):869–79. doi:10.1038/nm.3889
94. Arnold L, Tyagi RK, Meija P, Swetman C, Gleeson J, Perignon JL, et al. Further improvements of the *P. falciparum* humanized mouse model. *PLoS One* (2011) 6(3):e18045. doi:10.1371/journal.pone.0018045
95. Amaladoss A, Chen Q, Liu M, Dummler SK, Dao M, Suresh S, et al. De novo generated human red blood cells in humanized mice support *Plasmodium falciparum* infection. *PLoS One* (2015) 10(6):e0129825. doi:10.1371/journal.pone.0129825

Conflict of Interest Statement: The author declares that the research was conducted in the absence of any commercial or financial relationships that could be construed as a potential conflict of interest.

frontiers in Immunology

MINI REVIEW
published: 26 September 2017
doi: 10.3389/fimmu.2017.01202

Exploring the Immunopathogenesis of Viral Hemorrhagic Fever in Mice with a Humanized Immune System

Günther Schönrich and Martin J. Raftery*

Institute of Medical Virology, Charité – Universitätsmedizin Berlin, Berlin, Germany

Viral hemorrhagic fever (VHF) as a disease entity was first codified in the 1930s by soviet scientists investigating patients suffering from hantavirus infection. The group of hemorrhagic fever viruses (HFVs) has since expanded to include members from at least four different virus families: *Arenaviridae*, *Bunyaviridae*, *Filoviridae*, and *Flaviviridae*, all enveloped single-stranded RNA viruses. After infection, the natural hosts of HFVs do not develop symptoms, whereas humans can be severely affected. This observation and other evidence from experimental data suggest that the human immune system plays a crucial role in VHF pathogenesis. For this reason mice with a human immune system, referred to here as humanized mice (humice), are valuable tools that provide insight into disease mechanisms and allow for preclinical testing of novel vaccinations approaches as well as antiviral agents. In this article, we review the impact of humice in VHF research.

Keywords: viral hemorrhagic fever, humanized mice, mice with a humanized immune system, virus-induced immunopathogenesis, viruses

OPEN ACCESS

Edited by:
Ramesh Akkina,
Colorado State University,
United States

Reviewed by:
Vijay Panchanathan,
Perdana University, Malaysia
Axel T. Lehrer,
University of Hawaii at Manoa,
United States

****Correspondence:***
Günther Schönrich
guenther.schoenrich@charite.de

Specialty section:
This article was submitted to Vaccines and Molecular Therapeutics, a section of the journal Frontiers in Immunology

Received: *19 July 2017*
Accepted: *11 September 2017*
Published: *26 September 2017*

Citation:
Schönrich G and Raftery MJ (2017) Exploring the Immunopathogenesis of Viral Hemorrhagic Fever in Mice with a Humanized Immune System. Front. Immunol. 8:1202. doi: 10.3389/fimmu.2017.01202

INTRODUCTION

Emerging viral hemorrhagic fever (VHF) refers to a group of distinct but similar zoonotic diseases induced by different enveloped RNA viruses. They cause increased vascular permeability that affects one or more organ systems and finally may result in life-threatening shock (1). Thrombocytopenia, another key symptom of VHF, can be due to either increased platelet destruction or decreased platelet production by megakaryocytes (2). Hemorrhagic fever viruses (HFVs) belong to four separate virus families: *Flaviviridae*, *Bunyaviridae*, *Arenaviridae*, and *Filoviridae*. Small mammals such as rodents and bats are the natural hosts, which are chronically infected without developing obvious symptoms. Humans are dead-end hosts that usually clear the virus after incidental infection but may develop acute symptoms.

Suitable animal models that reproduce key symptoms of VHF are rare (3–5). Non-human primates (NHPs) are the gold standard for some VHF types such as Ebola virus disease (EVD) but cannot be used for others such as dengue fever (DF) (6, 7). In addition, ethical and economic considerations clearly restrict research with NHPs. Guinea pigs or hamsters show typical symptoms after infection with some HFVs (8–10). However, the lack of species-specific immunological reagents complicates experiments. Laboratory mice often do not support replication of HFV or require the adaption of virus isolates to the mouse, thereby reducing their value as a model of human infection (11, 12).

The advent of humanized mice (humice) has opened up a new avenue for VHF research. In the 1980s, experiments demonstrated successful engraftment of human hematopoietic stem cells

(HSCs) in immunodeficient mice (13). Today humice offer the opportunity to gain new and exciting insights into important human diseases such as cancer, allergies, and infections (14–17). Humice are an especially valuable test bed for HFVs. Firstly, HFVs specifically target human myeloid cells such as dendritic cells (DCs) (18–24). Secondly, evidence is accumulating that an inadequate immune response substantially contributes to VHF pathogenesis (25). This aspect is difficult to study in conventional animal models, as their immune system differs substantially due to evolution driven by exposure to different groups of pathogens over millions of years (26–28). For instance, there are major differences regarding the response of pattern recognition receptors to stimulation by invading pathogens. Although closely related to humans, even NHPs show interspecies immunological differences to humans (29, 30).

In this review, we summarize the novel insights gained from experiments with humice in VHF research.

CATEGORIES OF HUMICE USED IN VHF RESEARCH

The utility of immunodeficient mice as recipients of a human immune system has continuously increased. Efficient reconstitution with human hematopoietic cells was first described in non-obese diabetic (NOD)/severe combined immunodeficiency (SCID) mice (31, 32). The homozygous SCID mutation impairs murine T and B cell development, whereas the NOD background results in deficient natural killer (NK) cell function. The *Sirpa* gene polymorphism in the NOD background also curtails phagocytosis of engrafted human HSCs (33). NOD/SCID mice have subsequently been improved by truncation or deletion of the murine IL-2 receptor common gamma (IL-2Rγ) chain (34–36). This molecule represents an important component of the high-affinity receptors for several inflammatory cytokines. The NOD/SCID/IL-2Rγ$^{-/-}$ (NSG) mice are thus severely deficient in innate immunity and show augmented human HSC engraftment. The reconstitution with human HSCs in NSG mice is long lasting (37). In another approach, the IL-2Rγ$^{-/-}$ mutation was introduced into mice with a mutated recombination activating gene 2 (*Rag2*) on a BALB/c background (38). The *Rag2* mutation in these BALB/c Rag2$^{-/-}$/IL-2Rγ$^{-/-}$ (BRG) mice renders them completely free of murine T and B cell cells, whereas the SCID mutation is "leaky," meaning that some functional murine T and B cells develop (39).

The different types of humice differ with regard to efficiency of human HSC engraftment and the resulting composition of human hematopoietic cells (40–42). In VHF research, mainly HSC-engrafted humice and bone marrow/liver/thymus (BLT) humice are used. In the HSC-engrafted humice, human CD34^{+} HSCs from various sources (bone marrow, cord blood, peripheral blood or fetal liver) are inoculated into newborn immunodeficient mice and allowed to develop (**Figure 1**). A major disadvantage of HSC-engrafted humice is the lack of human T cell education due to the absence of a human thymus. This situation has been improved by generating transgenic NSG mice expressing human leukocyte antigen (HLA) molecules. Transgenic NSG mice expressing the HLA class I molecule HLA-A2 (hereafter referred to as NSG-A2 mice) facilitate the development of functional CD8 T cells after reconstitution with HLA-A2^{+} human HSCs (43–45). The expression of HLA class II molecules allows the development of both antibody-producing and class-switching human B cells (46–48).

The BLT humice enables human T cells to differentiate in an autologous human thymus (49, 50). BLT mice are generated by transplantation of human fetal liver and thymus tissue fragments under the kidney capsule of immunodeficient mice, e.g., NOD/SCID or NSG mice, followed by intravenous injection of autologous HSCs derived from fetal liver (**Figure 1**). The major advantage of BLT mice is their ability to mount a relatively effective human adaptive immune response due to the presence of a human thymic environment and the resultant HLA-restricted T cell repertoire. Caveats are the requirement of human fetal tissue and the relatively frequent development of graft-versus-host disease.

Elimination of human hematopoietic cells by murine phagocytic cells combined with defective human hematopoiesis in humice put a curb on human erythrocytes (51, 52), platelets (53), neutrophils (54–56), monocytes/macrophages (57), and NK cells (58, 59). An explanation for defective human hematopoiesis is the lack of binding of important murine growth factors and cytokines to receptors on human progenitor cells. An elegant solution of this problem is the generation of homozygous knock-in mice to replace murine with human cytokines (60–63). Germline-competent ES cells from NSG mice have been established to facilitate their genetic modification (64). Recently, transgenic NSG mice have been developed that constitutively express human "myeloid" cytokines: human stem cell factor, human granulocyte/macrophage colony-stimulating factor 2, and human IL-3. After reconstitution with human HSCs, these NSG-SGM3 mice allow better development of human myeloid cells, the key target cells of VHF viruses (65–68).

So far, four different HFVs from three virus families (*Flaviviridae*, *Filoviridae*, and *Bunyaviridae*) have been studied in humice.

FLAVIVIRUSES

Dengue viruses (DENVs) are the cause of the most important arthropod-borne viral disease in terms of global distribution and economic impact (69). The known DENV serotypes (DENV-1 to DENV-4) are members of the *Flaviviridae* family and carry a positive-sense single-stranded RNA genome. The *Aedes aegypti* mosquito, which is found in tropical and subtropical areas, functions as the main vector. Roughly 2.5 billion people, i.e., two fifths of mankind, live in endemic areas. An estimated 390 million people become infected per year. The most frequent clinical manifestation is DF, a self-limiting febrile disease with spontaneous recovery (70). However, some patients develop major complications such as plasma leakage leading to shock, respiratory distress, bleeding and organ impairment.

DF has been extensively studied in humice (**Table 1**). After DENV-2 infection, NOD/SCID mice and NSG mice develop fever, erythema, and human thrombocytopenia compatible to the human disease (71–73). The decrease in human

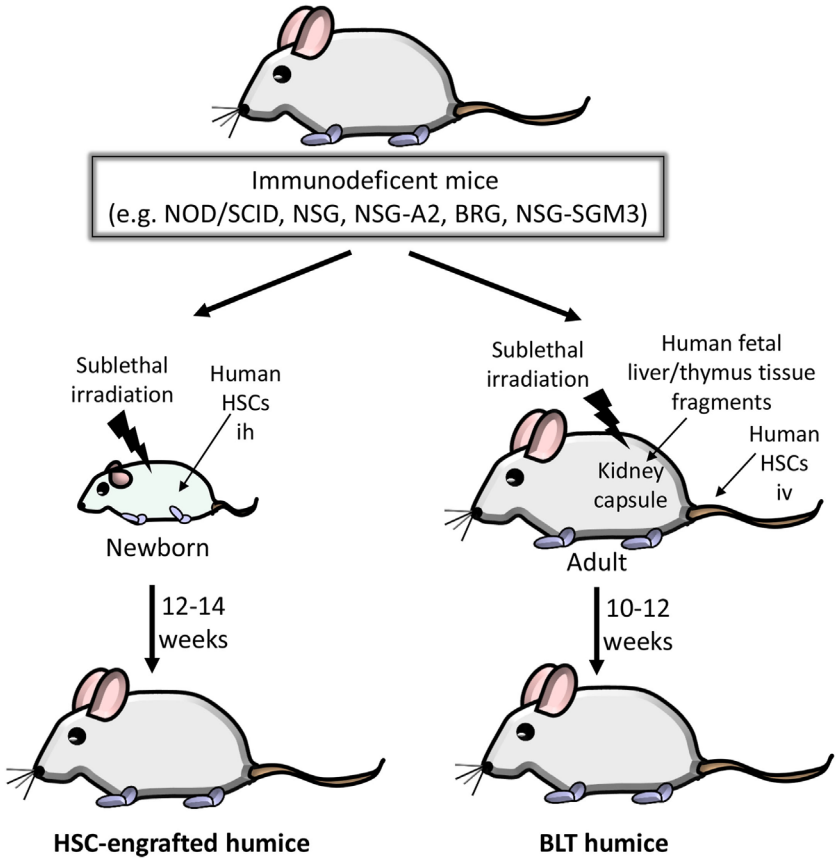

FIGURE 1 | Generation of humice in viral hemorrhagic fever research. Various immunodeficient mice can be used as a platform for generating mice with a human immune system. Non-obese diabetic (NOD)/severe combined immunodeficiency (SCID) mice show impaired murine T and B lymphocyte development due to the homozygous SCID mutation and are in addition deficient in natural killer (NK) cell function due to the NOD background. The *Sirpa* gene polymorphism in the NOD background also blunts phagocytosis of engrafted human hematopoietic stem cells (HSCs). The truncation or deletion of murine IL-2 receptor common gamma (IL-2Rγ) in NOD/SCID/IL-2Rγ$^{-/-}$ (NSG) mice further increases human HSC engraftment. NSG/A2 mice express human leukocyte antigen A2 to facilitate the development of functional CD8 T cells. In BALB/c Rag2$^{-/-}$/IL-2Rγ$^{-/-}$ (BRG) mice, the IL-2Rγ$^{-/-}$ mutation was introduced into BALB/c mice deficient in the recombination activating gene 2 (*Rag2*). Finally, NSG/SGM3 mice allow better development of human myeloid cells due to constitutive expression of human cytokines (stem cell factor, granulocyte/macrophage colony-stimulating factor 2, and IL-3). Left: HSC-engrafted humice. Human HSCs (derived from various sources such as bone marrow, cord blood, peripheral blood or fetal liver) are inoculated intrahepatically (ih) into sublethally irradiated newborn mice. Approximately 12–14 weeks after HSC inoculation, humice are monitored for engraftment of human HSCs by flow cytometric analysis. Right side: bone marrow/liver/thymus (BLT) humice. Human fetal liver and thymus are transplanted under the kidney capsule of sublethally irradiated 6- to 8-week-old mice and subsequently inoculated iv with autologous human fetal liver HSCs. The engraftment is verified 10–12 weeks later.

platelets is due to inhibition of human megakaryocyte development (74). DENV-2 could be detected in several human cell types in the bone marrow, spleen, and blood of these mice (73). In accordance, human cells isolated from the bone marrow of NSG mice were susceptible to DENV-2 infection *in vitro* (43). This cell tropism is in agreement with studies demonstrating DENV-derived protein in phagocytic cells in human autopsy tissue such as lymph nodes and spleen (75). Intriguingly, when infected *Aedes aegypti* transmitted DENV-2 to humice during feeding, more sustained and severe viremia, erythema and thrombocytopenia occurred compared to other modes of virus inoculation (76). This suggests that the mosquito bite itself and mosquito saliva contribute to dengue pathogenesis.

The immune system plays a crucial role in dengue pathogenesis (25, 77). Firstly, in humans, priming of the antiviral immune response with one DENV serotype often causes a more severe disease after infection with another DENV serotype at a later time point. Secondly, the most severe symptoms are observed at the peak of the human antiviral immune response. For these reasons the response of human immune cells has been studied in humice of DENV infection. Human anti-DENV IgM antibodies were detected 2 weeks after infection of BRG mice with DENV-2 followed by virus-reactive IgG at 6 weeks postinfection (78). In accordance, it was observed that NSG mice infected with DENV-2 through mosquito bite developed a virus-specific adaptive immune response (76). Moreover, human T cells from infected NSG-A2 mice secreted cytokines in response to known stimulatory HLA-A2-restricted DENV-2 peptides (43). Finally, NK cells are activated by contact with infected DCs before they control DENVs through IFN-γ secretion (79).

TABLE 1 | Humanized mouse models in viral hemorrhagic fever (VHF) research.

Disease	Virus/family	Platform	Key findings	Reference
DF	DENV-2/*Flaviviridae*	NOD/SCID, NSG	DF symptoms (fever, rash, and thrombocytopenia)	(71, 72)
DF	DENV-2/*Flaviviridae*	NSG	DENV-2 tropism as in human DF	(43, 73)
DF	DENV-2/*Flaviviridae*	NSG	Thrombocytopenia due to inhibition of megakaryocyte development	(74)
DF	DENV-2/*Flaviviridae*	NOD/SCID-BLT, NSG	Effective DF treatment with adenosine nucleoside inhibitor or therapeutic antibody	(84, 85)
DF	DENV-2/*Flaviviridae*	NSG/A2	Virus-specific HLA-A2-restricted human T cell response	(43)
DF	DENV-2/*Flaviviridae*	BRG, NSG, NSG/A2	Virus-specific huIgG and huIgM response	(43, 76, 78)
DF	DENV-2/*Flaviviridae*	BLT-NSG	Serotype-cross-reactive huIgM antibodies with poor neutralizing activity	(80, 81)
DF	DENV-2/*Flaviviridae*	NSG/SGM3-BLT	Higher levels of antigen-specific huIgM and huIgG compared to BLT-NSG	(82)
DF	DENV-2/*Flaviviridae*	NSG	Serum metabolomics similar to human DENV infections	(83)
EVD	EBOV/*Filoviridae*	NSG-A2	EVD symptoms (cell damage, liver steatosis, hemorrhage, high lethality)	(96)
EVD	EBOV/*Filoviridae*	NSG-BLT	Increased levels of pro-inflammatory cytokines and liver enzymes; histopathological findings typical for EVD	(94)
EVD	EBOV/*Filoviridae*	NSG-SGM3	Absence of characteristic EVD histopathology	(95)
CCHF	CCHFV/*Bunyaviridae*	NSG-SGM3	Lethal disease with severe neuropathology (gliosis, meningitis, meningoencephalitis)	(99)
HFRS	HTNV/*Bunyaviridae*	NSG, NSG-A2	Highest numbers of HTNV copies in the lung, humanized NSG-A2 mice develop faster and more severe symptoms such as thrombocytopenia	(112)

BLT, bone marrow/liver/thymus model; BRG, BALB/c Rag2$^{-/-}$ IL-2Rγ$^{-/-}$ mice; CCHF, Crimean–Congo hemorrhagic fever; CCHFV, Crimean-Congo hemorrhagic fever virus; DENV-2, dengue virus serotype 2; DF, dengue fever; EBOV, Ebola virus; EVD, Ebola virus disease; HFRS, hemorrhagic fever with renal syndrome; HTNV, hantaan virus; NOD, non-obese diabetic mice; NSG, NOD/SCID/IL-2Rγ$^{-/-}$ mice; NSG-A2, NSG mice constitutively expressing HLA-A2; NSG-SGM3, NSG mice constitutively expressing human stem cell factor, human granulocyte/macrophage colony-stimulating factor 2, and human IL-3; SCID, severe combined immunodeficiency mice; HLA, human leukocyte antigen.

The virus-specific immune response has also been studied in DENV-2-infected NSG-BLT mice (80, 81). Human T cells isolated from NSG-BLT mice during acute infection and in the convalescence phase secreted IFN-γ after stimulation with DENV-2 peptides (80). In addition, human B cells secreted DENV-2-reactive IgM antibodies (80). The majority of these antibodies were serotype cross-reactive, recognized epitopes on envelope proteins and intact virions, and neutralized poorly (81). The antibodies generated in the convalescence phase showed higher avidity compared to antibodies found in acute infection (81). Accordingly, NSG-BLT mice in the convalescence phase showed decreased virus titers after being challenged with a clinical DENV-2 strain. Furthermore, preincubation of DENV-2 virions with immune sera from immune NSG-BLT mice reduced viral replication after inoculation into naïve mice (81). In DENV-2-infected BLT mice generated from NSG-SGM3 mice, improved B cell development and higher levels of antigen-specific IgM and IgG were observed compared to DENV-2-infected NSG-BLT mice (82). The serum metabolomics of DENV-2-infected humice is similar to human DENV infections demonstrating the utility of humice for analyzing DENV-associated pathogenesis (83). In addition, a therapeutic antibody and an antiviral drug were successfully tested in DENV-2-infected humice (84, 85). These studies emphasize the value of humice in translational and preclinical VHF research.

FILOVIRUSES

The dramatic 2014 outbreak of EVD in West Africa underlines the need to better understand this deadly disease (86). Ebola virus (EBOV) and Marburg virus, a closely related HFVs, belong to the *Filoviridae* family in the order *Mononegavirales* (87). These large enveloped filamentous viruses are equipped with a negative-sense single-stranded RNA genome. Bats represent potential reservoirs for Marburg virus (88) and, more speculatively, perhaps also EBOV. They are persistently infected without showing symptoms and can spread the viruses to humans and NHPs. EVD has a high case fatality rate and affects many organs resulting in a variety of symptoms including gastrointestinal, respiratory, neurological, and vascular (89). Most impressive are the hemorrhagic manifestations such as petechiae, ecchymoses, and mucosal hemorrhages. The final and most severe stage of EBOV disease is characterized by shock, systemic impairment of coagulation and convulsions. The fatal outcome is most likely a consequence of both the direct effects of lytic EBOV replication and an inadequate immune response (90, 91). In EVD survivors, long-lasting activated CD8 T cells have been detected, suggesting that EBOV-derived stimulatory antigen persists at low levels within the organism (92).

Small animal models for analyzing filovirus pathogenesis have been generated using laboratory mice, guinea pigs, and the Syrian hamster (93). Recently, the potential of humice for modeling EBOV disease was explored in three different types of humice (**Table 1**) (6, 94–96). To this end, NSG-A2, NSG-SGM3, and NSG-BLT mice were infected with low-passage wild-type EBOV isolates. EBOV-infected NSG-A2 mice started to lose weight around day 7 postinfection and some hallmarks of human EBOV disease were observed including cell damage, liver steatosis, signs of hemorrhage, and high lethality (96). Intriguingly, there was a direct correlation between EBOV disease severity and the level of HSC engraftment. In contrast, unreconstituted NSG-A2 mice showed only mild symptoms with weight loss starting later in the third week postinfection and gradually continuing until the time of death around day 30 postinfection. NSG-A2 mice reconstituted with normal murine HSCs, another

important control, survived EBOV infection. These results emphasize the importance of human hematopoietic cells for EVD pathogenesis.

In EBOV-infected NSG-BLT mice, clinical illness depended on viral dose inoculated and donor tissue used for reconstitution (94). Moderate leukopenia and thrombocytopenia and histopathological alterations similar to those found in human victims were observed. Liver enzymes and key pro-inflammatory human cytokines associated with fatal EVD (e.g., TNF-α, IL-1, IL-6, and IL-10) were increased. In contrast, unreconstituted NSG control mice survived EBOV, underlining the role of human hematopoietic cells in EVD pathogenesis.

After EBOV infection of NSG-SGM3 mice, high virus titers were found in blood, liver, and spleen (95). Most of the mice died within 2 weeks of infection. In accordance with the concept that human myeloid cells spread VHF viruses within the organism, viral antigen was found in tissue-residing human macrophages and DCs and later in the course of infection also in murine parenchymal cells. In contrast to EBOV-infected NSG-A2 and NSG-BLT mice, the characteristic histopathology of severe human EBOV disease was not observed. This difference could be explained at least in part by the lack of HLA class I-restricted functional T cells in NSG-SGM3 mice. Thus, the lethal disease observed in these mice may be due to pathology directly induced by EBOV or due to innate immune responses.

BUNYAVIRUSES

A number of HFVs belong to the family *Bunyaviridae*. These are enveloped viruses that carry a genome consisting of three negative-sense single-stranded RNA segments (97). Recently, Crimean-Congo hemorrhagic fever virus (CCHFV) belonging to the genus *Nairovirus* and Hantaan virus (HTNV), the prototype member of the genus *Hantavirus*, have been analyzed in humice.

Crimean–Congo hemorrhagic fever (CCHF) represents the most relevant tick-borne viral disease in humans due to its wide distribution. Sporadic cases or outbreaks of CCHF are observed in a vast geographic area including western China, the Middle East, southern Europe, and most parts of Africa (98). CCHFV circulates in wild and domestic vertebrates that are transiently infected without showing symptoms. Humans become infected through tick bite or contact with body fluids from infected patients or animals. As with other VHFs, the spectrum of symptoms of Crimean-Congo hemorrhagic fever includes mild fever, vascular leakage resulting in multiorgan failure, and finally shock with coagulation defects. Case fatality rates of up to 30% have been reported. A recent study analyzed CCHFV-infected NSG-SGM3 mice (**Table 1**) (99). They showed lethal disease resembling CCHF in some respects. CCHFV was detected in many organs including liver, spleen, and brain, similar to CCHFV-infected mice deficient in type I IFN responses. Histopathological analysis revealed several features typically found in CCHF such as the presence of viral antigen within Kupffer cells, endothelial cells, and hepatocytes. Similar to human CCHF cases, vacuolar degeneration/steatosis and increased single cell necrosis were observed. CCHV-infected humice also developed CNS symptoms such as meningitis and meningoencephalitis. Intriguingly, a population of activated human CD8 T cells was identified that could contribute to immunopathology or virus elimination in a non-specific (HLA class I-independent) way (99).

Hantaviruses are globally emerging pathogens responsible for VHF in Africa, America, Asia, and Europe (100). Rodents, shrews, moles, and bats serve as natural hosts for hantaviruses. In contrast to all other pathogenic members of the family *Bunyaviridae*, hantaviruses are transmitted to humans *via* aerosols derived from rodent excreta. Depending on the geographic region, hemorrhagic fever with renal syndrome (HFRS) or hantavirus cardiopulmonary syndrome (HCPS) may develop (101). Both types of disease bear pathogenic similarities with increased vascular permeability and loss of platelets as leading symptoms (102). Hantavirus replicate in cell culture without causing obvious cytopathic phenomena, suggesting that immune mechanisms play a role in HFRS/HCPS (103, 104). In line with this view, the susceptibility to hantavirus infection and the clinical course of hantavirus-induced disease in humans are linked to polymorphisms of immune-related genes (105). Moreover, pathogenic hantaviruses infect human myeloid cells such as DCs and monocytes and interact with neutrophils, the most abundant immune cells (21, 23, 106–109). This tropism may help the pathogens to spread within the organism. In addition, this may also result in an inadequate immune response such as the excessive release of neutrophil extracellular traps that damages the endothelial barrier (110, 111).

Recently, hantaviral pathology was analyzed in HTNV-infected NSG mice and NSG-A2 (**Table 1**) (112). In both types of humice, hantaviral genomic RNA was detected in the kidney, liver, and spleen, but the highest viral copy numbers were found in the lung. Significant weight loss occurred earlier in NSG-A2 mice (day 10) than in NSG mice (day 15). HTNV-infected unreconstituted NSG mice that served as a control showed only a slight but not significant weight loss within the observation period. Inflammatory infiltrates in the lung of HTNV-infected NSG-A2 mice were stronger than in NSG mice. Similarly, the number of human platelets dropped significantly in NSG-A2 mice, whereas the observed reduction in NSG mice was not significant. Although hantaviruses infect human megakaryocytic cells, they do not cause alterations in cell survival or differentiation (113). Thus, it is likely that hantavirus-induced thrombocytopenia is due to increased platelet destruction (114). Taken together, these findings indicate that human hematopoietic cells including HLA-A2 restricted human T cells play a pivotal role in hantaviral pathogenesis.

CONCLUSION AND FUTURE DIRECTIONS

Humice are an extremely useful but still not optimal tool for elucidating the mechanisms of VHF immunopathogenesis, in particular, because of the very limited range of alternative research models. In addition, humice facilitate testing of vaccines and novel antiviral agents (115). Development of these

therapeutic agents is urgently needed for treatment and prevention of highly lethal VHFs. For example, humice can be used to generate human monoclonal antibodies for VHF prophylaxis (116). Finally, standardized humice allow the prospective testing of newly discovered HFVs or viruses suspected to be potentially HFVs and could form part of a zoonosis threat detection network. Future attempts have to improve the utility of humice as VHF models by further allowing better engraftment and differentiation of HSCs as well as the development of a fully functional lymphoid tissue architecture that efficiently supports human immune reactions.

AUTHOR CONTRIBUTIONS

Both authors contributed to the conception, writing, and critical revising of this review.

FUNDING

This work was supported by Deutsche Forschungsgemeinschaft (support code SCHO/9-1) and by the Bundesministerium für Bildung und Forschung (ERA-Net/GALHANT; support code 01DJ6022).

REFERENCES

1. Paessler S, Walker DH. Pathogenesis of the viral hemorrhagic fevers. *Annu Rev Pathol* (2013) 8:411–40. doi:10.1146/annurev-pathol-020712-164041
2. Schönrich G, Raftery MJ. Megakaryocytes and platelet production during viral infection. In: Schulze H, Italiano J, editors. *Molecular and Cellular Biology of Platelet Formation*. Switzerland: Springer (2016). p. 351–62.
3. Falzarano D, Bente DA. Animal models for viral haemorrhagic fever. *Clin Microbiol Infect* (2015). doi:10.1111/1469-0691.12630
4. Gowen BB, Holbrook MR. Animal models of highly pathogenic RNA viral infections: hemorrhagic fever viruses. *Antiviral Res* (2008) 78(1):79–90. doi:10.1016/j.antiviral.2007.10.002
5. Smith DR, Holbrook MR, Gowen BB. Animal models of viral hemorrhagic fever. *Antiviral Res* (2014) 112:59–79. doi:10.1016/j.antiviral.2014.10.001
6. Prescott J, Feldmann H. Humanized mice – a neoteric animal disease model for Ebola virus? *J Infect Dis* (2016) 213(5):691–3. doi:10.1093/infdis/jiv539
7. Zellweger RM, Shresta S. Mouse models to study dengue virus immunology and pathogenesis. *Front Immunol* (2014) 5:151. doi:10.3389/fimmu.2014.00151
8. Connolly BM, Steele KE, Davis KJ, Geisbert TW, Kell WM, Jaax NK, et al. Pathogenesis of experimental Ebola virus infection in guinea pigs. *J Infect Dis* (1999) 179(Suppl 1):S203–17. doi:10.1086/514305
9. Ebihara H, Zivcec M, Gardner D, Falzarano D, LaCasse R, Rosenke R, et al. A Syrian golden hamster model recapitulating ebola hemorrhagic fever. *J Infect Dis* (2013) 207(2):306–18. doi:10.1093/infdis/jis626
10. Hooper JW, Larsen T, Custer DM, Schmaljohn CS. A lethal disease model for hantavirus pulmonary syndrome. *Virology* (2001) 289(1):6–14. doi:10.1006/viro.2001.1133
11. Ebihara H, Takada A, Kobasa D, Jones S, Neumann G, Theriault S, et al. Molecular determinants of Ebola virus virulence in mice. *PLoS Pathog* (2006) 2(7):e73. doi:10.1371/journal.ppat.0020073
12. Valmas C, Basler CF. Marburg virus VP40 antagonizes interferon signaling in a species-specific manner. *J Virol* (2011) 85(9):4309–17. doi:10.1128/JVI.02575-10
13. Kamel-Reid S, Dick JE. Engraftment of immune-deficient mice with human hematopoietic stem cells. *Science* (1988) 242(4886):1706–9. doi:10.1126/science.2904703
14. Akkina R. New generation humanized mice for virus research: comparative aspects and future prospects. *Virology* (2013) 435(1):14–28. doi:10.1016/j.virol.2012.10.007
15. Ernst W. Humanized mice in infectious diseases. *Comp Immunol Microbiol Infect Dis* (2016) 49:29–38. doi:10.1016/j.cimid.2016.08.006
16. Fujiwara S. Humanized mice: a brief overview on their diverse applications in biomedical research. *J Cell Physiol* (2017). doi:10.1002/jcp.26022
17. Walsh NC, Kenney LL, Jangalwe S, Aryee KE, Greiner DL, Brehm MA, et al. Humanized mouse models of clinical disease. *Annu Rev Pathol* (2017) 12:187–215. doi:10.1146/annurev-pathol-052016-100332
18. Bosio CM, Aman MJ, Grogan C, Hogan R, Ruthel G, Negley D, et al. Ebola and Marburg viruses replicate in monocyte-derived dendritic cells without inducing the production of cytokines and full maturation. *J Infect Dis* (2003) 188(11):1630–8. doi:10.1086/379199
19. Geisbert TW, Hensley LE, Larsen T, Young HA, Reed DS, Geisbert JB, et al. Pathogenesis of Ebola hemorrhagic fever in cynomolgus macaques: evidence that dendritic cells are early and sustained targets of infection. *Am J Pathol* (2003) 163(6):2347–70. doi:10.1016/S0002-9440(10)63591-2
20. Mahanty S, Hutchinson K, Agarwal S, McRae M, Rollin PE, Pulendran B. Cutting edge: impairment of dendritic cells and adaptive immunity by Ebola and Lassa viruses. *J Immunol* (2003) 170(6):2797–801. doi:10.4049/jimmunol.170.6.2797
21. Marsac D, Garcia S, Fournet A, Aguirre A, Pino K, Ferres M, et al. Infection of human monocyte-derived dendritic cells by ANDES Hantavirus enhances pro-inflammatory state, the secretion of active MMP-9 and indirectly enhances endothelial permeability. *Virol J* (2011) 8:223. doi:10.1186/1743-422X-8-223
22. Negrotto S, Mena HA, Ure AE, Jaquenod De Giusti C, Bollati-Fogolin M, Vermeulen EM, et al. Human plasmacytoid dendritic cells elicited different responses after infection with pathogenic and nonpathogenic Junin virus strains. *J Virol* (2015) 89(14):7409–13. doi:10.1128/JVI.01014-15
23. Raftery MJ, Kraus AA, Ulrich R, Kruger DH, Schonrich G. Hantavirus infection of dendritic cells. *J Virol* (2002) 76(21):10724–33. doi:10.1128/JVI.76.21.10724-10733.2002
24. Wu SJ, Grouard-Vogel G, Sun W, Mascola JR, Brachtel E, Putvatana R, et al. Human skin Langerhans cells are targets of dengue virus infection. *Nat Med* (2000) 6(7):816–20. doi:10.1038/77553
25. Screaton G, Mongkolsapaya J, Yacoub S, Roberts C. New insights into the immunopathology and control of dengue virus infection. *Nat Rev Immunol* (2015) 15(12):745–59. doi:10.1038/nri3916
26. Barreiro LB, Quintana-Murci L. From evolutionary genetics to human immunology: how selection shapes host defence genes. *Nat Rev Genet* (2010) 11(1):17–30. doi:10.1038/nrg2698
27. Mestas J, Hughes CC. Of mice and not men: differences between mouse and human immunology. *J Immunol* (2004) 172(5):2731–8. doi:10.4049/jimmunol.172.5.2731
28. Zschaler J, Schlorke D, Arnhold J. Differences in innate immune response between man and mouse. *Crit Rev Immunol* (2014) 34(5):433–54. doi:10.1615/CritRevImmunol.2014011600
29. Barreiro LB, Marioni JC, Blekhman R, Stephens M, Gilad Y. Functional comparison of innate immune signaling pathways in primates. *PLoS Genet* (2010) 6(12):e1001249. doi:10.1371/journal.pgen.1001249
30. Magalhaes I, Vudattu NK, Ahmed RK, Kuhlmann-Berenzon S, Ngo Y, Sizemore DR, et al. High content cellular immune profiling reveals differences between rhesus monkeys and men. *Immunology* (2010) 131(1):128–40. doi:10.1111/j.1365-2567.2010.03284.x
31. Hesselton RM, Greiner DL, Mordes JP, Rajan TV, Sullivan JL, Shultz LD. High levels of human peripheral blood mononuclear cell engraftment and enhanced susceptibility to human immunodeficiency virus type 1 infection in NOD/LtSz-scid/scid mice. *J Infect Dis* (1995) 172(4):974–82. doi:10.1093/infdis/172.4.974
32. Shultz LD, Schweitzer PA, Christianson SW, Gott B, Schweitzer IB, Tennent B, et al. Multiple defects in innate and adaptive immunologic function in NOD/LtSz-scid mice. *J Immunol* (1995) 154(1):180–91.
33. Takenaka K, Prasolava TK, Wang JC, Mortin-Toth SM, Khalouei S, Gan OI, et al. Polymorphism in Sirpa modulates engraftment of human

hematopoietic stem cells. *Nat Immunol* (2007) 8(12):1313–23. doi:10.1038/ni1527
34. Ishikawa F, Yasukawa M, Lyons B, Yoshida S, Miyamoto T, Yoshimoto G, et al. Development of functional human blood and immune systems in NOD/SCID/IL2 receptor {gamma} chain(null) mice. *Blood* (2005) 106(5):1565–73. doi:10.1182/blood-2005-02-0516
35. Ito M, Hiramatsu H, Kobayashi K, Suzue K, Kawahata M, Hioki K, et al. NOD/SCID/gamma(c)(null) mouse: an excellent recipient mouse model for engraftment of human cells. *Blood* (2002) 100(9):3175–82. doi:10.1182/blood-2001-12-0207
36. Shultz LD, Lyons BL, Burzenski LM, Gott B, Chen X, Chaleff S, et al. Human lymphoid and myeloid cell development in NOD/LtSz-scid IL2R gamma null mice engrafted with mobilized human hemopoietic stem cells. *J Immunol* (2005) 174(10):6477–89. doi:10.4049/jimmunol.174.10.6477
37. Audige A, Rochat MA, Li D, Ivic S, Fahrny A, Muller CKS, et al. Long-term leukocyte reconstitution in NSG mice transplanted with human cord blood hematopoietic stem and progenitor cells. *BMC Immunol* (2017) 18(1):28. doi:10.1186/s12865-017-0209-9
38. Traggiai E, Chicha L, Mazzucchelli L, Bronz L, Piffaretti JC, Lanzavecchia A, et al. Development of a human adaptive immune system in cord blood cell-transplanted mice. *Science* (2004) 304(5667):104–7. doi:10.1126/science.1093933
39. Kotloff DB, Bosma MJ, Ruetsch NR. V(D)J recombination in peritoneal B cells of leaky scid mice. *J Exp Med* (1993) 178(6):1981–94. doi:10.1084/jem.178.6.1981
40. Garcia JV. In vivo platforms for analysis of HIV persistence and eradication. *J Clin Invest* (2016) 126(2):424–31. doi:10.1172/JCI80562
41. Rongvaux A, Takizawa H, Strowig T, Willinger T, Eynon EE, Flavell RA, et al. Human hemato-lymphoid system mice: current use and future potential for medicine. *Annu Rev Immunol* (2013) 31:635–74. doi:10.1146/annurev-immunol-032712-095921
42. Theocharides AP, Rongvaux A, Fritsch K, Flavell RA, Manz MG. Humanized hemato-lymphoid system mice. *Haematologica* (2016) 101(1):5–19. doi:10.3324/haematol.2014.115212
43. Jaiswal S, Pearson T, Friberg H, Shultz LD, Greiner DL, Rothman AL, et al. Dengue virus infection and virus-specific HLA-A2 restricted immune responses in humanized NOD-scid IL2rgammanull mice. *PLoS One* (2009) 4(10):e7251. doi:10.1371/journal.pone.0007251
44. Shultz LD, Saito Y, Najima Y, Tanaka S, Ochi T, Tomizawa M, et al. Generation of functional human T-cell subsets with HLA-restricted immune responses in HLA class I expressing NOD/SCID/IL2r gamma(null) humanized mice. *Proc Natl Acad Sci U S A* (2010) 107(29):13022–7. doi:10.1073/pnas.1000475107
45. Strowig T, Gurer C, Ploss A, Liu YF, Arrey F, Sashihara J, et al. Priming of protective T cell responses against virus-induced tumors in mice with human immune system components. *J Exp Med* (2009) 206(6):1423–34. doi:10.1084/jem.20081720
46. Danner R, Chaudhari SN, Rosenberger J, Surls J, Richie TL, Brumeanu TD, et al. Expression of HLA class II molecules in humanized NOD.Rag1KO.IL2RgcKO mice is critical for development and function of human T and B cells. *PLoS One* (2011) 6(5):e19826. doi:10.1371/journal.pone.0019826
47. Majji S, Wijayalath W, Shashikumar S, Pow-Sang L, Villasante E, Brumeanu TD, et al. Differential effect of HLA class-I versus class-II transgenes on human T and B cell reconstitution and function in NRG mice. *Sci Rep* (2016) 6:28093. doi:10.1038/srep28093
48. Suzuki M, Takahashi T, Katano I, Ito R, Ito M, Harigae H, et al. Induction of human humoral immune responses in a novel HLA-DR-expressing transgenic NOD/Shi-scid/gammacnull mouse. *Int Immunol* (2012) 24(4):243–52. doi:10.1093/intimm/dxs045
49. Lan P, Tonomura N, Shimizu A, Wang S, Yang YG. Reconstitution of a functional human immune system in immunodeficient mice through combined human fetal thymus/liver and CD34+ cell transplantation. *Blood* (2006) 108(2):487–92. doi:10.1182/blood-2005-11-4388
50. Melkus MW, Estes JD, Padgett-Thomas A, Gatlin J, Denton PW, Othieno FA, et al. Humanized mice mount specific adaptive and innate immune responses to EBV and TSST-1. *Nat Med* (2006) 12(11):1316–22. doi:10.1038/nm1431
51. Chen Q, Khoury M, Chen J. Expression of human cytokines dramatically improves reconstitution of specific human-blood lineage cells in humanized mice. *Proc Natl Acad Sci U S A* (2009) 106(51):21783–8. doi:10.1073/pnas.0912274106
52. Hu Z, Van Rooijen N, Yang YG. Macrophages prevent human red blood cell reconstitution in immunodeficient mice. *Blood* (2011) 118(22):5938–46. doi:10.1182/blood-2010-11-321414
53. Hu Z, Yang YG. Full reconstitution of human platelets in humanized mice after macrophage depletion. *Blood* (2012) 120(8):1713–6. doi:10.1182/blood-2012-01-407890
54. Coughlan AM, Freeley SJ, Robson MG. Humanised mice have functional human neutrophils. *J Immunol Methods* (2012) 385(1–2):96–104. doi:10.1016/j.jim.2012.08.005
55. Doshi M, Koyanagi M, Nakahara M, Saeki K, Saeki K, Yuo A. Identification of human neutrophils during experimentally induced inflammation in mice with transplanted CD34+ cells from human umbilical cord blood. *Int J Hematol* (2006) 84(3):231–7. doi:10.1532/IJH97.06040
56. Tanaka S, Saito Y, Kunisawa J, Kurashima Y, Wake T, Suzuki N, et al. Development of mature and functional human myeloid subsets in hematopoietic stem cell-engrafted NOD/SCID/IL2rgammaKO mice. *J Immunol* (2012) 188(12):6145–55. doi:10.4049/jimmunol.1103660
57. Gille C, Orlikowsky TW, Spring B, Hartwig UF, Wilhelm A, Wirth A, et al. Monocytes derived from humanized neonatal NOD/SCID/IL2Rgamma(null) mice are phenotypically immature and exhibit functional impairments. *Hum Immunol* (2012) 73(4):346–54. doi:10.1016/j.humimm.2012.01.006
58. Huntington ND, Legrand N, Alves NL, Jaron B, Weijer K, Plet A, et al. IL-15 trans-presentation promotes human NK cell development and differentiation in vivo. *J Exp Med* (2009) 206(1):25–34. doi:10.1084/jem.20082013
59. Strowig T, Chijioke O, Carrega P, Arrey F, Meixlsperger S, Ramer PC, et al. Human NK cells of mice with reconstituted human immune system components require preactivation to acquire functional competence. *Blood* (2010) 116(20):4158–67. doi:10.1182/blood-2010-02-270678
60. Rathinam C, Poueymirou WT, Rojas J, Murphy AJ, Valenzuela DM, Yancopoulos GD, et al. Efficient differentiation and function of human macrophages in humanized CSF-1 mice. *Blood* (2011) 118(11):3119–28. doi:10.1182/blood-2010-12-326926
61. Rongvaux A, Willinger T, Martinek J, Strowig T, Gearty SV, Teichmann LL, et al. Development and function of human innate immune cells in a humanized mouse model. *Nat Biotechnol* (2014) 32(4):364–72. doi:10.1038/nbt.2858
62. Rongvaux A, Willinger T, Takizawa H, Rathinam C, Auerbach W, Murphy AJ, et al. Human thrombopoietin knockin mice efficiently support human hematopoiesis in vivo. *Proc Natl Acad Sci U S A* (2011) 108(6):2378–83. doi:10.1073/pnas.1019524108
63. Willinger T, Rongvaux A, Takizawa H, Yancopoulos GD, Valenzuela DM, Murphy AJ, et al. Human IL-3/GM-CSF knock-in mice support human alveolar macrophage development and human immune responses in the lung. *Proc Natl Acad Sci U S A* (2011) 108(6):2390–5. doi:10.1073/pnas.1019682108
64. Landel CP, Dunlap J, Patton JB, Manser T. A germline-competent embryonic stem cell line from NOD.Cg-Prkdc (scid) Il2rg (tm1Wjl)/SzJ (NSG) mice. *Transgenic Res* (2013) 22(1):179–85. doi:10.1007/s11248-012-9629-8
65. Billerbeck E, Barry WT, Mu K, Dorner M, Rice CM, Ploss A. Development of human CD4+FoxP3+ regulatory T cells in human stem cell factor-, granulocyte-macrophage colony-stimulating factor-, and interleukin-3-expressing NOD-SCID IL2Rgamma(null) humanized mice. *Blood* (2011) 117(11):3076–86. doi:10.1182/blood-2010-08-301507
66. Brehm MA, Racki WJ, Leif J, Burzenski L, Hosur V, Wetmore A, et al. Engraftment of human HSCs in nonirradiated newborn NOD-scid IL2rgamma null mice is enhanced by transgenic expression of membrane-bound human SCF. *Blood* (2012) 119(12):2778–88. doi:10.1182/blood-2011-05-353243
67. Coughlan AM, Harmon C, Whelan S, O'Brien EC, O'Reilly VP, Crotty P, et al. Myeloid engraftment in humanized mice: impact of granulocyte-colony stimulating factor treatment and transgenic mouse strain. *Stem Cells Dev* (2016) 25(7):530–41. doi:10.1089/scd.2015.0289

68. Wunderlich M, Chou FS, Link KA, Mizukawa B, Perry RL, Carroll M, et al. AML xenograft efficiency is significantly improved in NOD/SCID-IL2RG mice constitutively expressing human SCF, GM-CSF and IL-3. *Leukemia* (2010) 24(10):1785–8. doi:10.1038/leu.2010.158
69. Bhatt S, Gething PW, Brady OJ, Messina JP, Farlow AW, Moyes CL, et al. The global distribution and burden of dengue. *Nature* (2013) 496 (7446):504–7. doi:10.1038/nature12060
70. Simmons CP, Farrar JJ, Nguyen V, Wills B. Dengue. *N Engl J Med* (2012) 366(15):1423–32. doi:10.1056/NEJMra1110265
71. Bente DA, Melkus MW, Garcia JV, Rico-Hesse R. Dengue fever in humanized NOD/SCID mice. *J Virol* (2005) 79(21):13797–9. doi:10.1128/JVI.79.21.13797-13799.2005
72. Mota J, Rico-Hesse R. Humanized mice show clinical signs of dengue fever according to infecting virus genotype. *J Virol* (2009) 83(17):8638–45. doi:10.1128/JVI.00581-09
73. Mota J, Rico-Hesse R. Dengue virus tropism in humanized mice recapitulates human dengue fever. *PLoS One* (2011) 6(6):e20762. doi:10.1371/journal.pone.0020762
74. Sridharan A, Chen Q, Tang KF, Ooi EE, Hibberd ML, Chen J. Inhibition of megakaryocyte development in the bone marrow underlies dengue virus-induced thrombocytopenia in humanized mice. *J Virol* (2013) 87(21):11648–58. doi:10.1128/JVI.01156-13
75. Balsitis SJ, Coloma J, Castro G, Alava A, Flores D, McKerrow JH, et al. Tropism of dengue virus in mice and humans defined by viral nonstructural protein 3-specific immunostaining. *Am J Trop Med Hyg* (2009) 80(3):416–24. doi:10.4269/ajtmh.2009.80.416
76. Cox J, Mota J, Sukupolvi-Petty S, Diamond MS, Rico-Hesse R. Mosquito bite delivery of dengue virus enhances immunogenicity and pathogenesis in humanized mice. *J Virol* (2012) 86(14):7637–49. doi:10.1128/JVI.00534-12
77. Malavige GN, Ogg GS. Pathogenesis of vascular leak in dengue virus infection. *Immunology* (2017) 151:261–9. doi:10.1111/imm.12748
78. Kuruvilla JG, Troyer RM, Devi S, Akkina R. Dengue virus infection and immune response in humanized RAG2(-/-)gamma(c)(-/-) (RAG-hu) mice. *Virology* (2007) 369(1):143–52. doi:10.1016/j.virol.2007.06.005
79. Costa VV, Ye W, Chen Q, Teixeira MM, Preiser P, Ooi EE, et al. Dengue virus-infected dendritic cells, but not monocytes, activate natural killer cells through a contact-dependent mechanism involving adhesion molecules. *mBio* (2017) 8(4):e741–717. doi:10.1128/mBio.00741-17
80. Jaiswal S, Pazoles P, Woda M, Shultz LD, Greiner DL, Brehm MA, et al. Enhanced humoral and HLA-A2-restricted dengue virus-specific T-cell responses in humanized BLT NSG mice. *Immunology* (2012) 136(3): 334–43. doi:10.1111/j.1365-2567.2012.03585.x
81. Jaiswal S, Smith K, Ramirez A, Woda M, Pazoles P, Shultz LD, et al. Dengue virus infection induces broadly cross-reactive human IgM antibodies that recognize intact virions in humanized BLT-NSG mice. *Exp Biol Med (Maywood)* (2015) 240(1):67–78. doi:10.1177/1535370214546273
82. Jangalwe S, Shultz LD, Mathew A, Brehm MA. Improved B cell development in humanized NOD-scid IL2Rgammanull mice transgenically expressing human stem cell factor, granulocyte-macrophage colony-stimulating factor and interleukin-3. *Immun Inflamm Dis* (2016) 4(4):427–40. doi:10.1002/iid3.124
83. Cui L, Hou J, Fang J, Lee YH, Costa VV, Wong LH, et al. Serum metabolomics investigation of humanized mouse model with dengue infection. *J Virol* (2017) 91:e00386-17. doi:10.1128/JVI.00386-17
84. Frias-Staheli N, Dorner M, Marukian S, Billerbeck E, Labitt RN, Rice CM, et al. Utility of humanized BLT mice for analysis of dengue virus infection and antiviral drug testing. *J Virol* (2014) 88(4):2205–18. doi:10.1128/JVI.03085-13
85. Robinson LN, Tharakaraman K, Rowley KJ, Costa VV, Chan KR, Wong YH, et al. Structure-guided design of an anti-dengue antibody directed to a non-immunodominant epitope. *Cell* (2015) 162(3):493–504. doi:10.1016/j.cell.2015.06.057
86. Baize S, Pannetier D, Oestereich L, Rieger T, Koivogui L, Magassouba N, et al. Emergence of Zaire Ebola virus disease in Guinea. *N Engl J Med* (2014) 371(15):1418–25. doi:10.1056/NEJMoa1404505
87. Rougeron V, Feldmann H, Grard G, Becker S, Leroy EM. Ebola and Marburg haemorrhagic fever. *J Clin Virol* (2015) 64:111–9. doi:10.1016/j.jcv.2015.01.014
88. Olival KJ, Hayman DT. Filoviruses in bats: current knowledge and future directions. *Viruses* (2014) 6(4):1759–88. doi:10.3390/v6041759
89. Feldmann H, Geisbert TW. Ebola haemorrhagic fever. *Lancet* (2011) 377(9768):849–62. doi:10.1016/S0140-6736(10)60667-8
90. Prescott JB, Marzi A, Safronetz D, Robertson SJ, Feldmann H, Best SM. Immunobiology of Ebola and Lassa virus infections. *Nat Rev Immunol* (2017) 17(3):195–207. doi:10.1038/nri.2016.138
91. Ruibal P, Oestereich L, Ludtke A, Becker-Ziaja B, Wozniak DM, Kerber R, et al. Unique human immune signature of Ebola virus disease in Guinea. *Nature* (2016) 533(7601):100–4. doi:10.1038/nature17949
92. Dahlke C, Lunemann S, Kasonta R, Kreuels B, Schmiedel S, Ly ML, et al. Comprehensive characterization of cellular immune responses following Ebola virus infection. *J Infect Dis* (2017) 215(2):287–92. doi:10.1093/infdis/jiw508
93. Yamaoka S, Banadyga L, Bray M, Ebihara H. Small animal models for studying filovirus pathogenesis. *Curr Top Microbiol Immunol* (2017). doi:10.1007/82_2017_9
94. Bird BH, Spengler JR, Chakrabarti AK, Khristova ML, Sealy TK, Coleman-McCray JD, et al. Humanized mouse model of Ebola virus disease mimics the immune responses in human disease. *J Infect Dis* (2016) 213(5):703–11. doi:10.1093/infdis/jiv538
95. Spengler JR, Lavender KJ, Martellaro C, Carmody A, Kurth A, Keck JG, et al. Ebola virus replication and disease without immunopathology in mice expressing transgenes to support human myeloid and lymphoid cell engraftment. *J Infect Dis* (2016) 214(Suppl 3):S308–18. doi:10.1093/infdis/jiw248
96. Ludtke A, Oestereich L, Ruibal P, Wurr S, Pallasch E, Bockholt S, et al. Ebola virus disease in mice with transplanted human hematopoietic stem cells. *J Virol* (2015) 89(8):4700–4. doi:10.1128/JVI.03546-14
97. Elliott RM, Schmaljohn CS. Bunyaviridae. In: Knipe DM, Howley PM, editors. *Fields Virology*. Philadelphia, USA: Lippincott Williams & Wilkins (2014). p. 1244–82.
98. Bente DA, Forrester NL, Watts DM, McAuley AJ, Whitehouse CA, Bray M. Crimean-Congo hemorrhagic fever: history, epidemiology, pathogenesis, clinical syndrome and genetic diversity. *Antiviral Res* (2013) 100(1):159–89. doi:10.1016/j.antiviral.2013.07.006
99. Spengler JR, Keating MK, McElroy AK, Zivcec M, Coleman-McCray JD, Harmon JR, et al. Crimean-Congo hemorrhagic fever in humanized mice reveals glial cells as primary targets of neurological infection. *J Infect Dis* (2017) jix215. doi:10.1093/infdis/jix215
100. Kruger DH, Figueiredo LT, Song JW, Klempa B. Hantaviruses – globally emerging pathogens. *J Clin Virol* (2015) 64:128–36. doi:10.1016/j.jcv.2014.08.033
101. Jonsson CB, Figueiredo LT, Vapalahti O. A global perspective on hantavirus ecology, epidemiology, and disease. *Clin Microbiol Rev* (2010) 23(2): 412–41. doi:10.1128/CMR.00062-09
102. Clement J, Maes P, Van Ranst M. Hemorrhagic fever with renal syndrome in the new, and hantavirus pulmonary syndrome in the old world: paradi(se)gm lost or regained? *Virus Res* (2014) 187:55–8. doi:10.1016/j.virusres.2013.12.036
103. Schonrich G, Rang A, Lutteke N, Raftery MJ, Charbonnel N, Ulrich RG. Hantavirus-induced immunity in rodent reservoirs and humans. *Immunol Rev* (2008) 225:163–89. doi:10.1111/j.1600-065X.2008.00694.x
104. Vaheri A, Strandin T, Hepojoki J, Sironen T, Henttonen H, Makela S, et al. Uncovering the mysteries of hantavirus infections. *Nat Rev Microbiol* (2013) 11(8):539–50. doi:10.1038/nrmicro3066
105. Charbonnel N, Pages M, Sironen T, Henttonen H, Vapalahti O, Mustonen J, et al. Immunogenetic factors affecting susceptibility of humans and rodents to hantaviruses and the clinical course of hantaviral disease in humans. *Viruses* (2014) 6(5):2214–41. doi:10.3390/v6052214
106. Koma T, Yoshimatsu K, Nagata N, Sato Y, Shimizu K, Yasuda SP, et al. Neutrophil depletion suppresses pulmonary vascular hyperpermeability and occurrence of pulmonary edema caused by hantavirus infection in C.B-17 SCID mice. *J Virol* (2014) 88(13):7178–88. doi:10.1128/JVI.00254-14
107. Lalwani P, Raftery MJ, Kobak L, Rang A, Giese T, Matthaei M, et al. Hantaviral mechanisms driving HLA class I antigen presentation require both RIG-I and TRIF. *Eur J Immunol* (2013) 43(10):2566–76. doi:10.1002/eji.201243066

108. Markotic A, Hensley L, Daddario K, Spik K, Anderson K, Schmaljohn C. Pathogenic hantaviruses elicit different immunoreactions in THP-1 cells and primary monocytes and induce differentiation of human monocytes to dendritic-like cells. *Coll Antropol* (2007) 31(4):1159–67. doi:10.0000/PMID18217475
109. Schonrich G, Kruger DH, Raftery MJ. Hantavirus-induced disruption of the endothelial barrier: neutrophils are on the payroll. *Front Microbiol* (2015) 6:222. doi:10.3389/fmicb.2015.00222
110. Raftery MJ, Lalwani P, Krautkrmer E, Peters T, Scharffetter-Kochanek K, Kruger R, et al. beta2 integrin mediates hantavirus-induced release of neutrophil extracellular traps. *J Exp Med* (2014) 211(7):1485–97. doi:10.1084/jem.20131092
111. Schonrich G, Raftery MJ. Neutrophil extracellular traps go viral. *Front Immunol* (2016) 7:366. doi:10.3389/fimmu.2016.00366
112. Kobak L, Raftery MJ, Voigt S, Kuhl AA, Kilic E, Kurth A, et al. Hantavirus-induced pathogenesis in mice with a humanized immune system. *J Gen Virol* (2015) 96(Pt 6):1258–63. doi:10.1099/vir.0.000087
113. Lutteke N, Raftery MJ, Lalwani P, Lee MH, Giese T, Voigt S, et al. Switch to high-level virus replication and HLA class I upregulation in differentiating megakaryocytic cells after infection with pathogenic hantavirus. *Virology* (2010) 405(1):70–80. doi:10.1016/j.virol.2010.05.028
114. Connolly-Andersen AM, Sundberg E, Ahlm C, Hultdin J, Baudin M, Larsson J, et al. Increased thrombopoiesis and platelet activation in hantavirus-infected patients. *J Infect Dis* (2015) 212(7):1061–9. doi:10.1093/infdis/jiv161
115. Akkina R. Human immune responses and potential for vaccine assessment in humanized mice. *Curr Opin Immunol* (2013) 25(3):403–9. doi:10.1016/j.coi.2013.03.009
116. Akkina R. Humanized mice for studying human immune responses and generating human monoclonal antibodies. *Microbiol Spectr* (2014) 2(2):1–12. doi:10.1128/microbiolspec.AID-0003-2012

Conflict of Interest Statement: The authors declare that the research was conducted in the absence of any commercial or financial relationships that could be construed as a potential conflict of interest.

frontiers in Immunology

ORIGINAL RESEARCH
published: 27 October 2017
doi: 10.3389/fimmu.2017.01405

Tracking Human Immunodeficiency Virus-1 Infection in the Humanized DRAG Mouse Model

*Jiae Kim[1,2], Kristina K. Peachman[1,2], Ousman Jobe[1,2], Elaine B. Morrison[2], Atef Allam[1,2†], Linda Jagodzinski[3], Sofia A. Casares[4] and Mangala Rao[2]**

[1] United States Military HIV Research Program, Henry M. Jackson Foundation for the Advancement of Military Medicine, Bethesda, MD, United States, [2] Laboratory of Adjuvant and Antigen Research, United States Military HIV Research Program, Walter Reed Army Institute of Research, Silver Spring, MD, United States, [3] United States Military HIV Research Program, Department of Laboratory Diagnostics and Monitoring, Walter Reed Army Institute of Research, Silver Spring, MD, United States, [4] United States Military Malaria Vaccine Program, Naval Medical Research Center, Silver Spring, MD, United States

OPEN ACCESS

Edited by:
Ramesh Akkina,
Colorado State University,
United States

Reviewed by:
Brent Palmer,
University of Colorado System,
United States
Johannes S. Gach,
University of California, Irvine,
United States

***Correspondence:**
Mangala Rao
mrao@hivresearch.org

†Present address:
Atef Allam,
Molecular Structure Section,
Laboratory of Viral Diseases, National Institute of Allergy and Infectious Diseases, National Institutes of Health, Bethesda, MD, United States

Specialty section:
This article was submitted to Vaccines and Molecular Therapeutics, a section of the journal Frontiers in Immunology

Received: 11 August 2017
Accepted: 11 October 2017
Published: 27 October 2017

Citation:
Kim J, Peachman KK, Jobe O, Morrison EB, Allam A, Jagodzinski L, Casares SA and Rao M (2017) Tracking Human Immunodeficiency Virus-1 Infection in the Humanized DRAG Mouse Model. Front. Immunol. 8:1405. doi: 10.3389/fimmu.2017.01405

Humanized mice are emerging as an alternative model system to well-established non-human primate (NHP) models for studying human immunodeficiency virus (HIV)-1 biology and pathogenesis. Although both NHP and humanized mice have their own strengths and could never truly reflect the complex human immune system and biology, there are several advantages of using the humanized mice in terms of using primary HIV-1 for infection instead of simian immunodeficiency virus or chimera simian/HIV. Several different types of humanized mice have been developed with varying levels of reconstitution of human CD45$^+$ cells. In this study, we utilized humanized Rag1KO. IL2Rγc^{KO}.NOD mice expressing HLA class II (DR4) molecule (DRAG mice) infused with HLA-matched hematopoietic stem cells from umbilical cord blood to study early events after HIV-1 infection, since the mucosal tissues of these mice are highly enriched for human lymphocytes and express the receptors and coreceptors needed for HIV-1 entry. We examined the various tissues on days 4, 7, 14, and 21 after an intravaginal administration of a single dose of purified primary HIV-1. Plasma HIV-1 RNA was detected as early as day 7, with 100% of the animals becoming plasma RNA positive by day 21 post-infection. Single cells were isolated from lymph nodes, bone marrow, spleen, gut, female reproductive tissue, and brain and analyzed for gag RNA and strong stop DNA by quantitative (RT)-PCR. Our data demonstrated the presence of HIV-1 viral RNA and DNA in all of the tissues examined and that the virus was replication competent and spread rapidly. Bone marrow, gut, and lymph nodes were viral RNA positive by day 4 post-infection, while other tissues and plasma became positive typically between 7 and 14 days post-infection. Interestingly, the brain was the last tissue to become HIV-1 viral RNA and DNA positive by day 21 post-infection. These data support the notion that humanized DRAG mice could serve as an excellent model for studying the trafficking of HIV-1 to the various tissues, identification of cells harboring the virus, and thus could serve as a model system for HIV-1 pathogenesis and reservoir studies.

Keywords: human immunodeficiency virus-1, human immunodeficiency virus vaginal transmission, humanized DRAG mouse, RNA, DNA, quantitative RT-PCR

INTRODUCTION

Human immunodeficiency virus-1 (HIV-1), the virus that causes acquired immunodeficiency disease is transmitted mainly through the sexual route (1). The early events that occur during HIV-1 sexual transmission and establishment of infection in humans are not completely understood. Insights into HIV-1 transmission in humans have been derived from extensive studies conducted in non-human primate (NHP) models with simian immunodeficiency virus (SIV) (2–4). These NHP studies have highlighted the very early establishment of small populations of founder virus in local areas of entry, early onset of CD4 depletion, and pathological processes in the local areas. These events are followed by an early and a late systemic phase of infection that exert their systemic effects slowly over months to years. Within 7–14 days, the infection became systemic with extensive viral replication and massive CD4 T-cell depletion in the lamina propria (5). An early capture HIV cohort study (RV217) of volunteers in East Africa and Thailand who were at high risk for HIV-1 infection demonstrated that the median peak viremia occurred 13 days after the first plasma sample was positive on nucleic acid testing (6). However, the early HIV events that occur before the plasma becomes HIV-1 RNA positive remain largely unknown.

A major obstacle for studying HIV-1 infection and pathogenesis is the lack of a good animal model. Although extensive studies have been performed in NHP models, these studies have utilized SIV or a chimera simian/HIV (SHIV), which are not the same as HIV-1 (7). Several human–mouse chimeras (humanized mice) have been generated to overcome the limited species tropism of HIV-1. The generation of a mouse with a reconstituted human immune system has enabled the use of humanized mice as a possible model for studying HIV-1 infection. At least 11 different types of humanized mice (8), each with unique characteristics are available. In this study, we utilized a more recently generated strain of humanized mice, the Rag1KO.IL2RγcKO.NOD mice expressing HLA class II-DR4 molecule (DRAG mice) (9–11). These mice were infused with HLA-matched human hematopoietic stem cells from umbilical cord blood and developed a high-reconstitution rate with long-lived functional B and T cells, all four classes of human immunoglobulins, and subclasses of IgG (9). In a previous study, our group has demonstrated that the humanized DRAG mouse model has some important features that correlate better with HIV-1 transmission in humans including high reconstitution of human $CD45^+$ cells in the gut and female reproductive tract (FRT) which includes the ovaries, fallopian tubes, uterus, cervix, and the vagina. This reconstitution of human $CD45^+$ cells is critical since the gut is an important venue for HIV-1 seeding and systemic spread. A majority of the $CD4^+$ T cells present in the DRAG mice also expressed the HIV-1 co-receptor, CCR5. In particular, the $CD4^+$ T follicular helper cells in the gut and FRT were highly permissive to HIV-1 infection (10). We also demonstrated that a single intravaginal infection (10,000 $TCID_{50}$; equivalent to 2.54 ng p24) of purified primary HIV-1 resulted in 100% infectivity of humanized DRAG mice (10). The use of primary virus is of increasing importance, especially in light of recent work that indicates that primary viruses behave differently from pseudoviruses and infectious molecular clones (12).

While no animal model can fully mimic the effects of HIV-1 in humans, because of some of the important features mentioned above, the humanized DRAG mouse model is suitable for investigating the early events after HIV-1 infection. Although the presence of SIV/SHIV in the FRT and gut of NHP following an intravaginal challenge are well established and in a separate study it was shown that low levels of viral RNA and DNA were present in distal tissues for several days following low-dose SHIV challenge (13, 14), the trafficking of the virus to the various tissues immediately after infection is still not completely understood. In the present study, we examined various tissues of the humanized DRAG mouse at different time points post-infection following an intravaginal infection with primary HIV-1. We determined how early HIV-1 RNA and DNA could be detected in the various organs post-infection compared with the appearance of the virus in the peripheral blood. Our results show that the earliest detection of viral RNA was in the gut and bone marrow and that the brain was the last organ to become HIV-1 RNA positive. Thus, the humanized DRAG mouse could serve as an excellent model for studying early HIV-1 pathogenesis and presumably also for HIV-1 reservoir studies.

MATERIALS AND METHODS

Mouse Strain

Humanized DRAG mice *[Rag1KO.IL2RγcKO.NOD ("NRG") strain]* with chimeric transgenes encoding for *HLA-DR*0401 [HLA-DRA/HLA-DRB1*0401])* fused to the *I-Ed MHC- II* molecule were generated as previously described (9). Four- to six-week-old DRAG mice were infused with *HLA-DR*0401*-positive human stem cells (9). Human cell reconstitution was periodically assessed in the peripheral blood samples. The generation of the humanized DRAG mouse is shown schematically in Figure S1 in Supplementary Material. Research was conducted under an approved animal use protocol in an AAALACi accredited facility in compliance with the Animal Welfare Act and other federal statutes and regulations relating to animals and experiments involving animals and adheres to principles stated in the Guide for the Care and Use of Laboratory Animals, NRC Publication, 2011 edition. Human cord blood samples were obtained from the New York Blood Center and were used to reconstitute the mice.

Intravaginal Infection of Humanized DRAG Mice with HIV-1

Fifty-four female humanized DRAG mice were injected subcutaneously with medroxyprogesterone (2.5 mg per 50 µL per mouse) (Greenstone LLC) 7 days prior to infection. Mice were anesthetized and administered intravaginally with purified primary HIV-1 BaL (10,000 $TCID_{50}$, ~2.54 ng p24) in a total volume of 20 µL as described previously (10). Tissues from 3 animals per time point were collected on days 4, 7, 14, and 21 post-infection for a total of 12 mice. Tissue from two control animals (non-infected) were also collected and processed for RNA and DNA. Plasma viral load over the course of up to 126 days was assessed in the remaining 42 mice. HIV-1 BaL was purified and quantified as described previously (12, 15). HIV-1 BaL was

used for infecting the humanized DRAG mice because of its high number of infectious units per milliliter of virus (1.4×10^6 I.U. per mL), as well as a high TCID 50/mL (2.47×10^6), which was necessary to deliver the virus in a small volume into the vaginal vault. In addition, during optimization of the vaginal infection in humanized DRAG mice, we observed a 100% infection rate.

Isolation of Single Cells from the Gut, FRT, Spleen, Bone Marrow, Brain, and Lymph Nodes

Prior to tissue collection, approximately 1 mL of blood was collected by cardiac puncture. This would be considered as a bleed out since the blood volume for a 25 g mouse is approximately 1.46 mL. A DRAG mouse weighs between 18 and 24 g. Bleed out before tissue collection prevented blood contamination of all the tissues and in particular the brain tissue. The following tissues were obtained from the humanized DRAG mice: gut, FRT, spleen, bone marrow, brain, and inguinal, popliteal, and mesenteric lymph nodes, and placed in 1× HBSS (Ca^{++} and Mg^{++} free), 1× HEPES, 5% FBS (vol/vol) wash buffer on ice. Single cells from the gut were isolated as previously described except collagenase II 1 U/mL (Sigma) was used instead of Collagenase VIII and DNase Type I. Also, the cells were not layered on a Percoll gradient. After centrifugation, the cells were subjected to $hCD45^+$ enrichment using anti-CD45 magnetic beads (StemCell Technologies). Cells not bound were removed while the bound cells were subjected to RNA and DNA isolation.

The FRT was processed in a similar manner to the intestinal tissue but was not enriched for hCD45. The fat from the lymph nodes and spleens were removed and single cells were isolated from the lymph nodes and the spleen by pushing them separately through a 70 μm cell strainer using the back of a syringe plunger. Cells were then centrifuged at 1,500 rpm at 4°C for 10 min and stored on ice or frozen until used for RNA and DNA isolation.

For isolation of bone marrow cells, the tips of the femur were cut off and the marrow was flushed into a 70 μm strainer with a syringe and pushed through the strainer using the back of a syringe plunger. After centrifugation, the cells were processed for the isolation of RNA and DNA. The brain tissue was diced into tiny pieces using razor blades and then incubated with collagenase IV (10 mg/100 mL; Life Tech Corp.) in 1× HBSS at 37°C for 90 min on a rotator. The supernatant from the collagenase treatment was placed on a 70 μm strainer and the cells were pushed through the strainer using the back of a syringe plunger. After centrifugation, the brain cells were enriched for $hCD45^+$ cells as described above.

Blood (approximately 1 mL) was collected in tubes containing 18 mM EDTA, centrifuged at 3,300 rpm at 4°C and then subjected to RNA and DNA isolation procedures.

Assessment of Viral Load in the Plasma

Blood samples (30 μL) were collected from humanized DRAG mice pre- and post-infection in tubes containing 18 mM EDTA solution. Following centrifugation at 3,300 rpm for 10 min at 4°C, plasma and the cell pellet were separately stored frozen at −20°C. The viral load in the plasma was determined using the Abbott RealTime HIV-1 Test (Abbott Molecular, Inc.) as previously described (10). The cell pellet was thawed, lysed, and HIV-1 RNA or DNA was extracted and quantified by quantitative real-time (qRT)-PCR. Student's *t*-test was used to determine if the decrease in viral load on day 42 was significant or not.

Assessment of HIV-1 Infection in Organs

RNA and DNA were extracted from at least 1×10^6 cells isolated from the harvested organs using the RNeasy Mini Kit and the DNeasy Blood and Tissue kit (Qiagen), respectively. The one-step RT-PCR assay was performed with a Viia7 (Applied Biosystems) using the TaqMan RNA-to-Ct kit (Applied Biosystems). DNA detection qPCR assay was performed using the TaqMan Universal Master Mix II (Applied Biosystems). Two primer/probe sets were used to detect and measure the viral RNA and a housekeeping gene for cellular RNA. The HIV RNA was detected using a primer/probe set for HIV-1 Gag forward: 5′-CATGTTTTCAGCATTATCAGAAGGA-3′, Gag reverse: 5′-TGCTTGATGTCCCCCCACT-3′, Gag probe: 5′-FAM-CCACCCCACAAGATTTAAACACCATGCTAA-BHQ-3′. The primer/probe set used for GAPDH–GAPDH forward: 5′- GAAGGTGAAGGTCGGAGTCAAC-3′, GAPDH reverse: 5′-CAGAGTTAAAAGCAGCCCTGGT-3′, GAPDH probe: 5′-HEX-TTTGGTCGTATTGGGCGCCT-BHQ-3′ (IDT). The reaction mixture (50 μL) contained the following amounts of reagents: 200 ng of total RNA, 1× final concentration of the TaqMan RT-PCR Mix and TaqMan RT Enzyme Mix, 0.2 μM Gag forward primer, 0.2 μM Gag reverse primer, 0.2 μM Gag probe, 0.2 μM GAPDH forward primer, 0.2 μM GAPDH reverse primer, and 0.2 μM GAPDH probe. The amplification reactions were performed using the following program: 48°C for 20 min, 95°C for 10 min (60 cycles of), 95°C for 15 s, and 59°C for 1 min.

Similar to the HIV-1 RNA measurement stated above, HIV-1 DNA was also measured using two primer/probe sets to detect and measure the viral DNA and cellular DNA. The HIV strong stop DNA was detected using the 5′R (5′-AACTAGGGAACCCACTGCTTAA), 3′U5 (5′ TGAGGG ATCTCTAGTTACCAGAGTCA), and R-probe (5′-FAM-CCTCAATAAAGCTTGCCTTGAGTGCTTCAA-BHQ 3′) and the cellular DNA was detected using the same GAPDH primer/probe set mentioned above. The 20 μL reactions contained 200 ng of total DNA, 1× final concentration of the Master Mix, 0.8 μM 5′R (strong stop forward) primer, 0.8 μM 3′U5 (strong stop reverse) primer, 0.25 μM R-probe, 0.8 μM GAPDH forward primer, 0.8 μM GAPDH reverse primer, and 0.25 μM GAPDH probe. The reactions were run using the following program: 95°C for 10 min (60 cycles of), 95°C for 15 s, and 60°C for 1 min. The calculations for determining the RNA or DNA copy number was performed as previously described (12), with the exception of the cell number. The calculated number of cells per reaction was determined and then adjusted using a calculation of 1 ng RNA = 1,000 cells (16). Assay acceptability was contingent on the linear regression R^2 value >0.95 for the viral and cellular RNA and DNA. Cells collected from uninfected control animals did not show any amplification of HIV-1 RNA or DNA positivity and served as negative controls in the study.

Statistical Analyses

All of the data were graphed and analyzed using GraphPad Prism, version 7.0 (GraphPad Software). Data are represented as mean ± SEM. Student's *t*-test was utilized to determine statistical significance.

RESULTS

Sexual transmission of HIV-1 is the most common route of HIV-1 infection. Therefore, humanized DRAG mice were infected vaginally with a single dose (10,000 $TCID_{50}$) of purified primary HIV-1 BaL (subtype B). This dose would be considered as a low to moderate dose based on previous studies where 200,000–700,000 $TCID_{50}$ (20–70-fold higher than our dose) was used (17, 18) for intravaginal infection of humanized mice. However, in two additional studies (19, 20) the intravaginal dose used was 156–3,000 $TCID_{50}$ (3–10-fold lower than our dose).

The plasma viral load in humanized DRAG mice was determined over a period of up to 126 days post-HIV-1 infection and the average of 54 mice is shown in **Figure 1**. Plasma viral loads for each individual humanized DRAG mouse is shown in Figure S2 in Supplementary Material. With a single infection, 89% of the mice became positive by day 14 and 100% of the mice ($n = 54$) became positive by day 21. RNA plasma positivity was detected in some animals as early as day 7 post-infection. Peak viremia was observed on day 21 (3 weeks post-infection), with plasma viral load of 5.0 log 10 copies per milliliter. There was a very slight but insignificant ($p = 0.29$) decrease in the viral load on day 42 with the viral load remaining steady with minimal changes up to day 126 (18 weeks) post-infection.

Single cell suspensions prepared from the bone marrow, spleen, and brain of uninfected humanized DRAG mice or from infected mice on days 4, 7, 14, and 21 post-HIV-1 BaL infection were analyzed for the presence of viral RNA (**Figure 2**) and DNA (**Figure 3**). Using qPCR, the number of viral RNA and DNA copies present per million cells was quantified using the appropriate standards and the data are presented in **Figures 2** and **3**. For blood samples, the EDTA-treated blood was centrifuged, the pelleted cells were lysed, and RNA and DNA were extracted and purified from the cells. As shown in **Figure 2**, viral RNA was detected as early as day 4 in the bone marrow of two out of three mice, however, no viral RNA was detected on day 7, although low

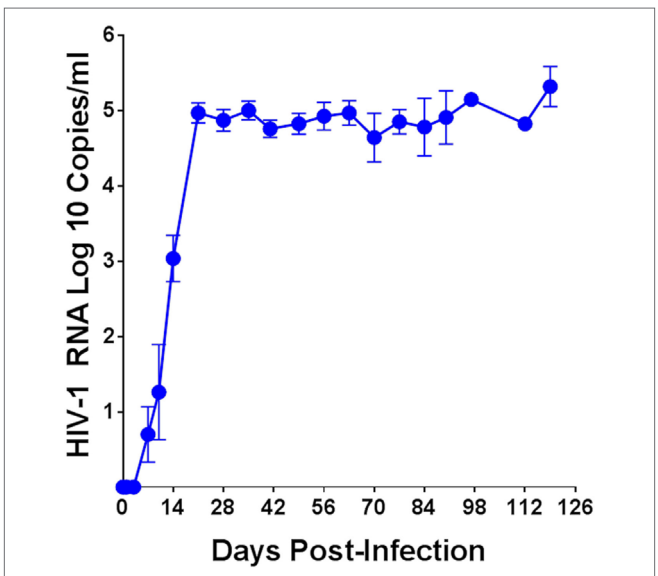

FIGURE 1 | Plasma human immunodeficiency virus (HIV)-1 viral load over time in humanized DRAG mice. Data are the mean ± SEM of 54 humanized DRAG mice infected intravaginally with a single dose of purified primary HIV-1 BaL (10,000 $TCID_{50}$, 2.54 ng p24).

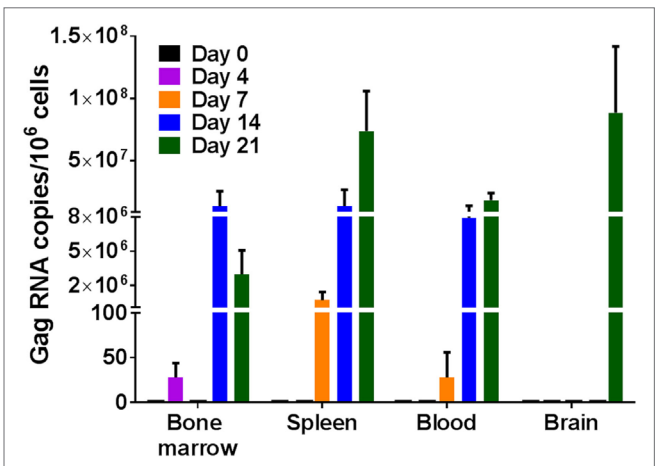

FIGURE 2 | Viral RNA detection in humanized DRAG mice tissues. RNA was isolated from single cell suspensions of bone marrow, spleen, blood, and brain. Viral RNA (gag) and cellular RNA (GAPDH) were detected using quantitative (q) real-time-PCR and quantified using appropriate RNA standards on days 0 ($n = 2$); 4 ($n = 3$); 7 ($n = 3$); 14 ($n = 3$); and 21 ($n = 3$). The data represent the average of triplicate samples ± SEM.

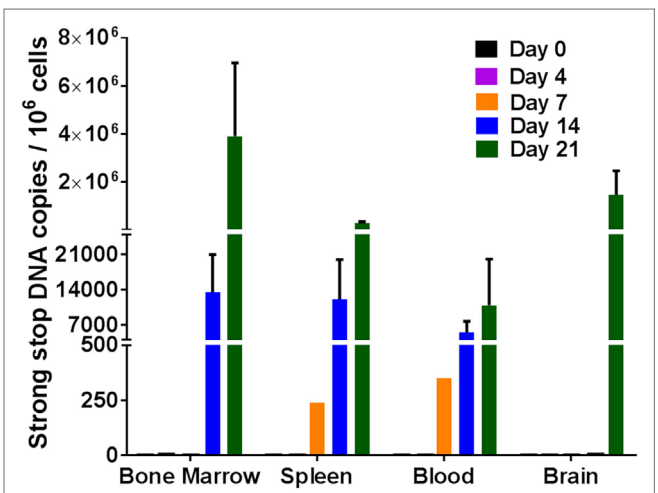

FIGURE 3 | Viral DNA detection in humanized DRAG mice tissues. DNA was isolated from single cell suspensions of bone marrow, spleen, blood, and brain. Viral DNA (strong stop) and cellular DNA (GAPDH) were detected using qPCR and quantified using appropriate DNA standards on days 0 ($n = 2$); 4 ($n = 3$); 7 ($n = 3$); 14 ($n = 3$); and 21 ($n = 3$). The data represent the average of triplicate samples ± SEM.

levels of viral RNA were detected in the spleen and blood cells in two out of three mice. By day 14 post-infection, bone marrows of all three mice, spleen cells from two out of three mice, and blood cells from all three mice averaged around eight million gag RNA copies/million cells. The gag RNA copies increased 10-fold in the spleen cells, averaging around 70 million gag RNA copies/million cells by day 21, indicating that the virus was replication competent and spreading to other tissues. In contrast, no viral RNA could be detected in the cells of the brain up to day 14, although the blood, spleen, and bone marrow cells contained actively replicating HIV-1. Unlike the earlier time point, at 21 days post-infection, two out of three mice were positive for the presence of viral RNA in the brain cells. These data demonstrate the prolific nature of the virus and that the brain is probably one of the last organs to become susceptible to HIV-1. It is possible that low levels of HIV-1 may be present at an earlier time point that is undetectable with our assay, which has a lower limit of detection of 10 copies/million. Even though it takes about 21 days to demonstrate the presence of replicating HIV-1 in the brain, in the time frame of infection, it is still relatively rapid.

To further solidify our results that the virus was indeed replicating, strong stop DNA was measured for the same tissue cells as described above for RNA. Similar results were obtained for viral DNA as was observed with viral RNA. Viral DNA was detected in the blood, spleen, and bone marrow cells on days 14 and 21 post-infection (**Figure 3**). By day 7, approximately 250–400 copies of viral DNA were detected in the spleen and blood tissues. There was an increase in the viral DNA copies by days 14 and 21 post-infection. Similar to the RNA data observed above, no viral DNA was detected in the cells from the brain in any of the mice 14 days post-infection. It was, however, present in two out of three mice at 21 days post-infection. The detection of the viral DNA indicates the presence of replicating virus at these different tissues after intravaginal infection.

Having established that the virus was present and actively replicating in the blood, spleen, bone marrow, and the brain of humanized DRAG mice within 21 days post-infection, we next focused on the FRT, gut, and the lymph nodes, which were of great interest since the gut and the FRT are important organs for seeding and spread of HIV-1 (21–25). Therefore, we examined the cells isolated from the gut, FRT, and lymph nodes at very early time points, on days 4 and 7 post-HIV-1 infection (**Table 1**). Generally, at this time point, not all of the humanized DRAG mice had detectable viral RNA copies in their plasma and the few that did, had levels that were fairly low.

TABLE 1 | Detection of human immunodeficiency virus (HIV)-1 RNA in various tissues.

	FRT	Gut	Lymph nodes
Day 4	0	1	1
Day 7	2	2	3

Humanized DRAG mice (n = 3) were infected intravaginally with a single dose of purified primary HIV-1 BAL (10,000 $TCID_{50}$, 2.54 ng p24). RNA was isolated from female reproductive tract (FRT), gut, and lymph nodes on days 4 and 7 post-infection. The number of mice that were positive for HIV-1 RNA on different days is shown.

On day 4 post-infection, viral RNA was present in the gut and lymph nodes of one out of three mice and no viral RNA could be detected in the FRT. By day 7 post-infection, viral RNA was detected in the cells of the gut and FRT in two out of three mice. Interestingly, all three mice were positive for viral RNA in cells isolated from the mesenteric and inguinal/popliteal lymph nodes. The presence of viral RNA in the lymph nodes of all three mice suggests that the virus is utilizing the lymphatic system for rapidly spreading to other areas. At day 7, only one mouse had a detectable viral load in the plasma and detectable viral DNA in the blood cell pellet (data not shown) and spleen, while a second mouse showed the presence of viral RNA in the spleen cells, despite an undetectable viral load in the plasma. These data suggest that the virus is probably trafficking to the spleen and bone marrow through the lymphatic system before appearing systemically.

DISCUSSION

Human immunodeficiency virus-1 replication is limited to only two species: humans and chimpanzees. Rodents cannot be used for HIV-1 vaccine efficacy or transmission studies as their cells lack proper receptor/co-receptor expression along with numerous HIV-1 translational and post-translational replication blocks (26). Thus, the limited species available for *in vivo* HIV-1 studies represents a significant challenge. Furthermore, access to primary human tissue is difficult and requires invasive techniques. NHP and humanized mice have therefore been the models of choice and used extensively to study SIV and HIV infection and pathogenesis. Despite the use of NHP and human tissue biopsies, the early events in SIV or HIV-1 infection are not completely understood (7, 27). In addition to using an appropriate animal model, it is equally important to use the appropriate primary virus. We have recently demonstrated differences in viral capture between primary viruses, pseudoviruses, and infectious molecular clones. Therefore, it is important to use primary HIV-1 propagated in human PBMCs for *in vitro* studies utilizing human tissue biopsies or for *in vivo* studies using humanized mice (12).

There are several models for humanized mice with different strains of mice and different engraftment methods that have been utilized to study HIV-1 infection, including the Hu-PBL-SCID, Hu-SRC-SCID, NSG, NRG, TKO-BLT, and BLT mice (8, 28, 29). In our studies, we have utilized DRAG mice, which has several advantages compared with other strains of humanized mice. Compared with NRG mice, DRAG mice express human HLA-DR4 molecules in cells from spleen, thymus, and bone marrow (9). Previous work has demonstrated that 93% of the humanized DRAG mice were able to reconstitute human T cells mice whereas in humanized NRG mice (RagKO.IL2RgcKO.NOD) which lack the expression of HLA-DR4 molecules, only 36% of the mice were able to reconstitute human T cells (9). This work also indicated that the numbers of human thymic precursors and peripheral human T cells in the T-cell reconstituted DRAG mice were significantly higher when compared with the T-cell reconstituted NRG mice (9). Although the humanized mice models have effective T-cell immune responses, the B-cell functions are not ideal for vaccination and immunization studies. Earlier work by our group has shown that the DRAG mice develop Peyer's

patches (10), while other humanized mice such as NRG, NSG, or BLT mice do not (30). The high level of reconstitution of human T and B cells in the humanized DRAG mice gut, FRT, and spleen, with the majority of $CD4^+$ T cells (79–96%) exhibiting a memory phenotype, the ability to generate all four human IgG subclasses, human IgA and IgE, and the ability to elicit specific IgG responses upon immunization makes the humanized DRAG mice an attractive model for pathogenesis and vaccine studies (8–11).

Our present study highlights the use of the humanized DRAG mouse model to determine the presence of HIV-1 in the various organs/tissues at early time points during acute infection following administration of purified primary subtype B HIV-1 (BaL) through the vaginal route. Previous work with humanized mice used infectious molecular clones or primary HIV-1 (19, 31–36). In several of these studies, the mice were injected with these viruses through the intraperitoneal or intravenous routes (31, 32, 34–37). We chose the intravaginal route to infect humanized DRAG mice since the major route of HIV-1 infection in humans is through the sexual route. Our data demonstrate that intravaginal administration of a single dose of purified primary HIV-1 BaL was sufficient for 100% of the mice ($n = 54$) to become HIV-1 RNA plasma positive within 21 days of infection; however, some of the mice became HIV-1 RNA plasma positive as early as 7 days post-infection. The 100% infectivity rate and the high reconstitution of human $CD45^+$ cells in the various organs and in particular in the gut and FRT (9, 10) encouraged us to examine the spread of the virus at early time points from the site of infection.

Our study demonstrated the following: (i) HIV-1 viral RNA and DNA with high-copy numbers in some cases, as measured by qRT-PCR, was present in all the tissues examined: bone marrow, spleen, blood, gut, lymph nodes, FRT, and brain; (ii) a progressive increase in the viral copy numbers for both RNA and DNA indicated that the virus was replication competent and spread rapidly; (iii) the earliest detection of HIV-1 RNA was on day 4 in the gut, lymph nodes, and bone marrow; (iv) the brain was the last tissue to become HIV-1 viral RNA positive by day 21.

Even though the brain was the last tissue to become RNA positive, it showed very high viral RNA copies (approximately 100 million) and approximately 2 million viral DNA copies, suggesting that the brain was highly susceptible to HIV-1. The high copy number could be due to a high quantity of HIV-1 trafficking to the brain or due to active HIV-1 replication in this tissue. The presence of HIV-1 in the brain was not due to contamination from the blood as the levels of RNA and DNA copies were 10-fold higher in the brain compared with the blood. Furthermore, while the blood was positive for HIV-1 by day 7, the brain tissue did not become positive for HIV-1 until day 21. Several groups have examined humanized NOD/SCID/IL2Rγ_c^{null} mouse brain tissue for the presence of HIV-1 after intraperitoneal injections of HIV-1_{ADA} or HIV-infected PHA blasts or after an intravenous infection with HIV-1_{MNp}. In the case of the HIV-1_{ADA} virus, DNA was analyzed at day 35 with only one out of the nine mice showing viral RNA in the brain (31). The brain viral RNA was at ~3,000 copies in the mouse with blood viral RNA ranging from 1,000 to 10,000,000 which is in a brain/blood ratio of 3- to 3,000-fold less than what we have observed. Using the intraperitoneal route with HIV-infected blast cells, Singh et al. (38) observed HIV-1-infected cells in the brain as early as 4 days after injection. This study did not determine viral RNA/DNA copies but does support transmission of HIV-1-infected cells into the brain. In the study that utilized HIV-$1MN_p$ infection through the intravenous route, viral DNA was analyzed at day 59, significantly later then our 21-day time point and the results showed a threefold higher DNA level in the blood than in the brain (39). The differences between our study and the other studies mentioned above could be due to the route of infection (intraperitoneal or intravenous vs. intravaginal), the virus used, or the time points examined.

The timing of infection in the DRAG mice as well as the trafficking of the virus from the FRT to other organs seem to be in good consensus to what has been reported previously in the NHP/SHIV model (14). After a single intravaginal dose of SHIV-SF162P3 (50,000 $TCID_{50}$), viral RNA was observed only in the vagina and cervix area starting at day 1 or 3 post-infection. At day 7, viral RNA was observed in various organs in the NHP including the mesenteric lymph node, bone marrow, spleen, and brain. By day 10 post-infection, the infection had become systemic with all organs of the three NHPs positive for viral RNA. The variability in DRAG mice on the presence of viral RNA in the various organs at 7 days post-infection was also observed with the NHP model. Although two out of five and four out of five NHPs were positive for viral RNA in the bone marrow and spleen, respectively, the plasma of these animals did not become positive until day 10 post-infection. Similarly, only one out of the five animals in each case was positive for viral DNA in the lymph nodes and spleen.

Our results indicate that HIV-1 infection in the humanized DRAG mouse was a very dynamic and rapid process. As early as day 4 post-infection, viral RNA was detected in the gut, lymph nodes, and bone marrow, although at this time point, the plasma was negative for viral RNA. This would suggest that the virus was utilizing the lymphatic system to spread to the other tissues. It is also important to point out that unlike the spleen and brain cells that contained the highest number of RNA viral copies, the bone marrow contained the highest number of viral DNA copies. This observation may be indicative of bone marrow harboring a viral reservoir at a higher rate than other tissues, although our assay does not distinguish between integrated and non-integrated DNA. This is an interesting observation nonetheless that requires further study. In support of our observation, it has been reported recently that the bone marrow of CD34-NSG humanized mouse was the major tissue site for HIV-1 infection with monocyte-macrophages and dendritic cells being the principal targets following an intraperitoneal infection with a macrophage-tropic virus (HIV-1_{ADA}) (31).

Our future work will be directed toward the identification of cells that harbor the virus in the various tissues as well as viral outgrowth assays to determine if the viral RNA negative organs are truly negative for HIV-1. In conclusion, our work demonstrates that the humanized DRAG mouse is an attractive model for studying HIV-1 pathogenesis and establishment of reservoirs because of the high level of reconstitution of human immune cells as well as viral persistence in diverse tissues such as the bone marrow, lymph nodes, and the brain, which could serve as a sanctuary site for HIV-1 to escape the host immune system.

ETHICS STATEMENT

Research was conducted under an approved animal use protocol in an AAALACi accredited facility in compliance with the Animal Welfare Act and other federal statutes and regulations relating to animals and experiments involving animals and adheres to principles stated in the Guide for the Care and Use of Laboratory Animals, NRC Publication, 2011 edition. The protocol was approved by the Institutional Animal Care and Use Committee.

AUTHOR CONTRIBUTIONS

MR and JK developed the hypothesis and designed experiments. SC provided humanized DRAG mice. KP and EM infected mice with HIV and collected organs. JK, KP, OJ, and AA isolated single cells from organs. JK performed all RNA and DNA isolation and qPCR. LJ performed plasma RNA viral loads. All authors contributed to the writing and editing of the manuscript.

ACKNOWLEDGMENTS

The authors thank Brett M. Pugliese, Michael F. Read, Robert Michael Edmondson, Ashley Williams, and Sayali Onkar for their assistance in processing the humanized mouse tissue; Holly Hack and Dominique Burt for performing the viral load determination in the plasma.

FUNDING

This work was supported through a Cooperative Agreement Award (W81XWH-11-0174) between the Henry M. Jackson Foundation for the Advancement of Military Medicine and the U.S. Army Medical Research and Materiel Command.

SUPPLEMENTARY MATERIAL

The Supplementary Material for this article can be found online at http://www.frontiersin.org/article/10.3389/fimmu.2017.01405/full#supplementary-material.

FIGURE S1 | Schematic representation of the generation of the human-immune-system DRAG mice. Procedure for generating the humanized DRAG mice as described in Danner et al. (9).

FIGURE S2 | Plasma HIV-1 viral loads over time in individual humanized DRAG mice. A total of 54 humanized DRAG mice were infected intravaginally with a single dose of purified primary HIV-1 BaL (10,000 $TCID_{50}$, 2.54 ng p24).

REFERENCES

1. Royce RA, Sena A, Cates W Jr, Cohen MS. Sexual transmission of HIV. *N Engl J Med* (1997) 336:1072–8. doi:10.1056/NEJM199704103361507
2. Miller CJ, Li Q, Abel K, Kim EY, Ma ZM, Wietgrefe S, et al. Propagation and dissemination of infection after vaginal transmission of simian immunodeficiency virus. *J Virol* (2005) 79:9217–27. doi:10.1128/JVI.79.14.9217-9227.2005
3. Haase AT. Targeting early infection to prevent HIV-1 mucosal transmission. *Nature* (2010) 464:217–23. doi:10.1038/nature08757
4. Haase AT. Early events in sexual transmission of HIV and SIV and opportunities for interventions. *Annu Rev Med* (2011) 62:127–39. doi:10.1146/annurev-med-080709-124959
5. Brenchley JM, Douek DC. HIV infection and the gastrointestinal immune system. *Mucosal Immunol* (2008) 1:23–30. doi:10.1038/mi.2007.1
6. Robb ML, Eller LA, Rolland M. Acute HIV-1 infection in adults in East Africa and Thailand. *N Engl J Med* (2016) 375:1195. doi:10.1056/NEJMc1609157
7. Garcia-Tellez T, Huot N, Ploquin MJ, Rascle P, Jacquelin B, Muller-Trutwin M. Non-human primates in HIV research: achievements, limits and alternatives. *Infect Genet Evol* (2016) 46:324–32. doi:10.1016/j.meegid.2016.07.012
8. Akkina R, Allam A, Balazs AB, Blankson JN, Burnett JC, Casares S, et al. Improvements and limitations of humanized mouse models for HIV research: NIH/NIAID "meet the experts" 2015 workshop summary. *AIDS Res Hum Retroviruses* (2016) 32:109–19. doi:10.1089/aid.2015.0258
9. Danner R, Chaudhari SN, Rosenberger J, Surls J, Richie TL, Brumeanu TD, et al. Expression of HLA class II molecules in humanized NOD.Rag1KO.IL2RgcKO mice is critical for development and function of human T and B cells. *PLoS One* (2011) 6:e19826. doi:10.1371/journal.pone.0019826
10. Allam A, Majji S, Peachman K, Jagodzinski L, Kim J, Ratto-Kim S, et al. TFH cells accumulate in mucosal tissues of humanized-DRAG mice and are highly permissive to HIV-1. *Sci Rep* (2015) 5:10443. doi:10.1038/srep10443
11. Wijayalath W, Majji S, Villasante EF, Brumeanu TD, Richie TL, Casares S. Humanized HLA-DR4.RagKO.IL2RgammacKO.NOD (DRAG) mice sustain the complex vertebrate life cycle of *Plasmodium falciparum* malaria. *Malar J* (2014) 13:386. doi:10.1186/1475-2875-13-386
12. Kim J, Jobe O, Peachman KK, Michael NL, Robb ML, Rao M, et al. Quantitative analyses reveal distinct sensitivities of the capture of HIV-1 primary viruses and pseudoviruses to broadly neutralizing antibodies. *Virology* (2017) 508:188–98. doi:10.1016/j.virol.2017.05.015
13. Shang L, Duan L, Perkey KE, Wietgrefe S, Zupancic M, Smith AJ, et al. Epithelium-innate immune cell axis in mucosal responses to SIV. *Mucosal Immunol* (2017) 10:508–19. doi:10.1038/mi.2016.62
14. Liu J, Ghneim K, Sok D, Bosche WJ, Li Y, Chipriano E, et al. Antibody-mediated protection against SHIV challenge includes systemic clearance of distal virus. *Science* (2016) 353:1045–9. doi:10.1126/science.aag0491
15. Jobe O, Peachman KK, Matyas GR, Asher LV, Alving CR, Rao M. An anti-phosphoinositide-specific monoclonal antibody that neutralizes HIV-1 infection of human monocyte-derived macrophages. *Virology* (2012) 430:110–9. doi:10.1016/j.virol.2012.04.017
16. Eriksson S, Graf EH, Dahl V, Strain MC, Yukl SA, Lysenko ES, et al. Comparative analysis of measures of viral reservoirs in HIV-1 eradication studies. *PLoS Pathog* (2013) 9:e1003174. doi:10.1371/journal.ppat.1003174
17. Deruaz M, Moldt B, Le KM, Power KA, Vrbanac VD, Tanno S, et al. Protection of humanized mice from repeated intravaginal HIV challenge by passive immunization: a model for studying the efficacy of neutralizing antibodies in vivo. *J Infect Dis* (2016) 214:612–6. doi:10.1093/infdis/jiw203
18. Council OD, Swanson MD, Spagnuolo RA, Wahl A, Garcia JV. Role of semen on vaginal HIV-1 transmission and maraviroc protection. *Antimicrob Agents Chemother* (2015) 59:7847–51. doi:10.1128/AAC.01496-15
19. Berges BK, Akkina SR, Folkvord JM, Connick E, Akkina R. Mucosal transmission of R5 and X4 tropic HIV-1 via vaginal and rectal routes in humanized Rag2-/- gammac -/- (RAG-hu) mice. *Virology* (2008) 373:342–51. doi:10.1016/j.virol.2007.11.020
20. Veselinovic M, Neff CP, Mulder LR, Akkina R. Topical gel formulation of broadly neutralizing anti-HIV-1 monoclonal antibody VRC01 confers protection against HIV-1 vaginal challenge in a humanized mouse model. *Virology* (2012) 432:505–10. doi:10.1016/j.virol.2012.06.025
21. Brenchley JM, Schacker TW, Ruff LE, Price DA, Taylor JH, Beilman GJ, et al. CD4+ T cell depletion during all stages of HIV disease occurs predominantly in the gastrointestinal tract. *J Exp Med* (2004) 200:749–59. doi:10.1084/jem.20040874
22. Ananworanich J, Schuetz A, Vandergeeten C, Sereti I, de Souza M, Rerknimitr R, et al. Impact of multi-targeted antiretroviral treatment on gut T cell depletion and HIV reservoir seeding during acute HIV infection. *PLoS One* (2012) 7:e33948. doi:10.1371/journal.pone.0033948
23. Shacklett BL. Cell-mediated immunity to HIV in the female reproductive tract. *J Reprod Immunol* (2009) 83:190–5. doi:10.1016/j.jri.2009.07.012

24. Howell AL, Asin SN, Yeaman GR, Wira CR. HIV-1 infection of the female reproductive tract. *Curr HIV/AIDS Rep* (2005) 2:35–8. doi:10.1007/s11904-996-0007-0
25. Takalani F, Mhlongo NN, Moonsamy S, Soliman MES. Review on the biological mechanisms associated with Depo-Provera and HIV-1 risk acquisition in women. *Cell Biochem Biophys* (2017). doi:10.1007/s12013-017-0806-5
26. Bieniasz PD, Cullen BR. Multiple blocks to human immunodeficiency virus type 1 replication in rodent cells. *J Virol* (2000) 74:9868–77. doi:10.1128/JVI.74.21.9868-9877.2000
27. Hessell AJ, Haigwood NL. Animal models in HIV-1 protection and therapy. *Curr Opin HIV AIDS* (2015) 10:170–6. doi:10.1097/COH.0000000000000152
28. Nixon CC, Mavigner M, Silvestri G, Garcia JV. In vivo models of human immunodeficiency virus persistence and cure strategies. *J Infect Dis* (2017) 215:S142–51. doi:10.1093/infdis/jiw637
29. Marsden MD, Zack JA. Humanized mouse models for human immunodeficiency virus infection. *Annu Rev Virol* (2017) 4(1):393–412. doi:10.1146/annurev-virology-101416-041703
30. Wahl A, Victor Garcia J. The use of BLT humanized mice to investigate the immune reconstitution of the gastrointestinal tract. *J Immunol Methods* (2014) 410:28–33. doi:10.1016/j.jim.2014.06.009
31. Arainga M, Su H, Poluektova LY, Gorantla S, Gendelman HE. HIV-1 cellular and tissue replication patterns in infected humanized mice. *Sci Rep* (2016) 6:23513. doi:10.1038/srep23513
32. Watanabe S, Terashima K, Ohta S, Horibata S, Yajima M, Shiozawa Y, et al. Hematopoietic stem cell-engrafted NOD/SCID/IL2Rgamma null mice develop human lymphoid systems and induce long-lasting HIV-1 infection with specific humoral immune responses. *Blood* (2007) 109:212–8. doi:10.1182/blood-2006-04-017681
33. Sun Z, Denton PW, Estes JD, Othieno FA, Wei BL, Wege AK, et al. Intrarectal transmission, systemic infection, and CD4+ T cell depletion in humanized mice infected with HIV-1. *J Exp Med* (2007) 204:705–14. doi:10.1084/jem.20062411
34. Berges BK, Wheat WH, Palmer BE, Connick E, Akkina R. HIV-1 infection and CD4 T cell depletion in the humanized Rag2-/-gamma c-/- (RAG-hu) mouse model. *Retrovirology* (2006) 3:76. doi:10.1186/1742-4690-3-S1-S73
35. Zhang L, Kovalev GI, Su L. HIV-1 infection and pathogenesis in a novel humanized mouse model. *Blood* (2007) 109:2978–81. doi:10.1182/blood-2006-07-033159
36. Gorantla S, Sneller H, Walters L, Sharp JG, Pirruccello SJ, West JT, et al. Human immunodeficiency virus type 1 pathobiology studied in humanized BALB/c-Rag2-/-gammac-/- mice. *J Virol* (2007) 81:2700–12. doi:10.1128/JVI.02010-06
37. Honeycutt JB, Wahl A, Baker C, Spagnuolo RA, Foster J, Zakharova O, et al. Macrophages sustain HIV replication in vivo independently of T cells. *J Clin Invest* (2016) 126:1353–66. doi:10.1172/JCI84456
38. Singh VB, Singh MV, Gorantla S, Poluektova LY, Maggirwar SB. Smoothened agonist reduces human immunodeficiency virus type-1-induced blood-brain barrier breakdown in humanized mice. *Sci Rep* (2016) 6:26876. doi:10.1038/srep26876
39. Watanabe S, Ohta S, Yajima M, Terashima K, Ito M, Mugishima H, et al. Humanized NOD/SCID/IL2Rgamma(null) mice transplanted with hematopoietic stem cells under nonmyeloablative conditions show prolonged life spans and allow detailed analysis of human immunodeficiency virus type 1 pathogenesis. *J Virol* (2007) 81:13259–64. doi:10.1128/JVI.01353-07

Disclaimer: The views expressed are those of the authors and should not be construed to represent the positions of the U.S. Army or the Department of Defense.

Conflict of Interest Statement: The authors declare that the research was conducted in the absence of any commercial or financial relationships that could be construed as a potential conflict of interest.

frontiers in Immunology

METHODS
published: 08 December 2017
doi: 10.3389/fimmu.2017.01709

Multidimensional Analysis Integrating Human T-Cell Signatures in Lymphatic Tissues with Sex of Humanized Mice for Prediction of Responses after Dendritic Cell Immunization

Valery Volk[1†], Andreas I. Reppas[2†], Philippe A. Robert[2], Loukia M. Spineli[3], Bala Sai Sundarasetty[1], Sebastian J. Theobald[1], Andreas Schneider[1], Laura Gerasch[1], Candida Deves Roth[1], Stephan Klöss[4], Ulrike Koehl[4], Constantin von Kaisenberg[5], Constanca Figueiredo[6], Haralampos Hatzikirou[2], Michael Meyer-Hermann[2]* and Renata Stripecke[1]*†*

[1] Department of Hematology, Hemostasis, Oncology and Stem Cell Transplantation, Hannover Medical School, Hannover, Germany, [2] Department of Systems Immunology, Braunschweig Integrated Centre of Systems Biology, Helmholtz Centre for Infection Research, Braunschweig, Germany, [3] Institute of Biostatistics, Hannover Medical School, Hannover, Germany, [4] Institute of Cellular Therapeutics and GMP Core Facility IFB-Tx, Hannover Medical School, Hannover, Germany, [5] Clinic of Gynecology and Obstetrics, Hannover Medical School, Hannover, Germany, [6] Department of Transfusion Medicine, Hannover Medical School, Hannover, Germany

Mice transplanted with human cord blood-derived hematopoietic stem cells (HSCs) became a powerful experimental tool for studying the heterogeneity of human immune reconstitution and immune responses *in vivo*. Yet, analyses of human T cell maturation in humanized models have been hampered by an overall low immune reactivity and lack of methods to define predictive markers of responsiveness. Long-lived human lentiviral induced dendritic cells expressing the cytomegalovirus pp65 protein (iDCpp65) promoted the development of pp65-specific human $CD8^+$ T cell responses in NOD.Cg-Rag1^{tm1Mom}-Il2rγ^{tm1Wj} humanized mice through the presentation of immune-dominant antigenic epitopes (signal 1), expression of co-stimulatory molecules (signal 2), and inflammatory cytokines (signal 3). We exploited this validated system to evaluate the effects of mouse sex in the dynamics of T cell homing and maturation status in thymus, blood, bone marrow, spleen, and lymph nodes. Statistical analyses of cell relative frequencies and absolute numbers demonstrated higher $CD8^+$ memory T cell reactivity in spleen and lymph nodes of immunized female mice. In order to understand to which extent the multidimensional relation between organ-specific markers predicted the immunization status, the immunophenotypic profiles of individual mice were used to train an artificial neural network designed to discriminate immunized and non-immunized mice. The highest accuracy of immune reactivity prediction could be obtained from lymph node markers of female mice (77.3%). Principal component analyses further identified clusters of markers best suited to describe the heterogeneity of immunization responses *in vivo*. A correlation analysis of these markers reflected a tissue-specific

OPEN ACCESS

Edited by:
Ramesh Akkina, Colorado State University, United States

Reviewed by:
Santhi Gorantla, University of Nebraska Medical Center, United States
Michael Schotsaert, Icahn School of Medicine at Mount Sinai, United States

***Correspondence:**
Haralampos Hatzikirou haralampos.hatzikirou@helmholtz-hzi.de;
Michael Meyer-Hermann mmh@theoretical-biology.de;
Renata Stripecke stripecke.renata@mh-hannover.de

†Shared first co-authorship.

Specialty section:
This article was submitted to Vaccines and Molecular Therapeutics, a section of the journal Frontiers in Immunology

Received: *24 August 2017*
Accepted: *20 November 2017*
Published: *08 December 2017*

Citation:
Volk V, Reppas AI, Robert PA, Spineli LM, Sundarasetty BS, Theobald SJ, Schneider A, Gerasch L, Deves Roth C, Klöss S, Koehl U, Kaisenberg Cv, Figueiredo C, Hatzikirou H, Meyer-Hermann M and Stripecke R (2017) Multidimensional Analysis Integrating Human T-Cell Signatures in Lymphatic Tissues with Sex of Humanized Mice for Prediction of Responses after Dendritic Cell Immunization. Front. Immunol. 8:1709. doi: 10.3389/fimmu.2017.01709

impact of immunization. This allowed for an organ-resolved characterization of the immunization status of individual mice based on the identified set of markers. This new modality of multidimensional analyses can be used as a framework for defining minimal but predictive signatures of human immune responses in mice and suggests critical markers to characterize responses to immunization after HSC transplantation.

Keywords: hematopoietic stem cell transplantation, cord blood, dendritic cell, T cell maturation, lymphatic, humanized mice, gender, artificial neural network

INTRODUCTION

Humanized mice transplanted with human hematopoietic stem cells (HSCs) became a broadly used experimental and preclinical platform to characterize the critical steps for the reconstitution of the human immune system (1–3). In this context, humanized mice are currently used to study human-specific infections and to test drugs, vaccines, and cell therapies (2, 3). Engraftment of human HSCs in the mouse bone marrow (BM) and subsequent early T cell development in thymus (Thy) could be conveniently studied in short-term models lasting 10–16 weeks (4). Yet, full maturation of T cells toward memory cells in HSC-transplanted humanized mice was shown to be considerably more heterogeneous and challenging and required periods of analyses of 20 weeks or longer (5, 6). Thus, this lymphopenia coincides with the delayed T cell immune reconstitution in patients after hematopoietic stem cell transplantation (HSCT) (5, 6). Multiple complementary approaches were tried to support the development of human cells in immune-deficient mice such as, for example, the administration of human cytokines (7) and the generation of new transgenic mouse strains expressing human cytokines (8) or human leukocyte antigens (HLA) molecules (9, 10). More complex and demanding strategies exploring co-transplantation with human fetal thymus and liver tissues (bone marrow, liver, thymus model) into mice showed an overall improved T cell development and maturation (11–14). Notably, since T cell responses depend on the strength of the signals delivered by the antigen/HLA to the T cell receptor (TCR) (signal 1), co-stimulation (signal 2), and pro-inflammatory cytokines (signal 3), studies demonstrating the presence of human dendritic cells (DCs) in humanized mice elucidated their role in activation of the cognate T cells (15). Thus, as potential alternative approaches for improving T cell reconstitution in humanized mice and ultimately in humans, adoptive autologous DCs, such as those explored clinically for cancer immunotherapy (16) and human immunodeficiency virus (17), or *in vivo* activated DCs, as previously shown to be effective in humanized mice (18), could represent valuable options. Likewise, we have previously described the preclinical testing of long-lived genetically engineered induced DC (iDCs) in humanized mice. These cells were generated after a fast overnight transduction of monocytes with lentiviral vectors encoding granulocyte-macrophage colony stimulating factor (GM-CSF), interferon-α (IFN-α), and the human cytomegalovirus (HCMV) phosphoprotein (pp) 65 (19, 20). iDCs expressing pp65 (iDCpp65) vaccines are currently in clinical development for protection of posttransplant patients (21), since pp65 has been long known to be a major immune-dominant $CD8^+$ cytotoxic T lymphocyte target antigen in healthy seropositive adults (22). Furthermore, non-exhausted, long-lived $CD8^+$ effector memory (EM) T cells are considered to be crucial to maintain lifelong protection from HCMV reactivation in posttransplant patients (23).

We previously demonstrated that multiple administrations of iDCpp65 into NOD.Cg-Rag1^{tm1Mom}-Il2rγ^{tm1Wj} (NRG) mice transplanted with human HSCs promoted a potent development of $CD8^+$ antigen-specific memory responses in short (16 weeks) (20) and long (20–36 weeks) models (19, 24). We have also demonstrated that another important factor to be considered regarding the analyses of human T cells in mice humanized with cord blood (CB)-HSCs is the gender of the recipient mouse. For the initial 10–15 weeks after HSCT, females showed a more robust T cell development and maturation, whereas male's T cells matched the female's T cell maturation status only 20 weeks posttransplant (25).

In this current work, we sought to evaluate whether humanized female and male mice would show differential patterns of T cell responses to iDCpp65. We characterized the $CD4^+$/$CD8^+$ T cells and their subsets [naïve (N), EM, central memory (CM), and terminal effector (TE)] in different lymphatic tissues and confirmed a distinct behavior between females and males, supported by statistical methods. In order to integrate the data obtained from different tissues and evaluate the immunization responsiveness among them, we adopted a classification machine learning algorithm based on an artificial neural network (ANN). A Principal Component Analysis (PCA) (26, 27) was further used to reduce the critical information required to predict responsiveness from the ANN (28). The markers pinpointed by the PCA revealed that the correlation structure of organ-specific markers is strongly impacted by immunization and, therefore,

Abbreviations: aAPC, artificial antigen-presenting cell; Ab, Antibody; ANN, artificial neural network; ANOVA, analysis of variance; B. D., below detection; BM, bone marrow; BLT, bone marrow, liver, thymus (mouse model); CB, cord blood; CM, central memory; CTL, cytotoxic lymphocytes; DN, double negative; DP, double positive; DC, dendritic cell; ELISPOT, enzyme-linked immuno spot assay; EM, effector memory; FBS, fetal bovine serum; HCMV, human cytomegalovirus; HIV, human immunodeficiency virus; HLA, human leukocyte antigen; HSCs, hematopoietic stem cells; HSCT, hematopoietic stem cell transplantation; iDCpp65, induced dendritic cells expressing pp65; IDLV-G2a-pp65, integration-deficient lentiviral vector co-expressing GM-CSF/IFN-α and the HCMV-pp65; IL, interleukin; MCP-1, monocyte chemoattractant protein 1; MLNs, mesenteric lymph nodes; N, naïve; NRG, NOD.Cg-Rag1^{tm1Mom}-Il2rγ^{tm1Wj}; PB, peripheral blood; PBS, phosphate-buffered saline; PCA, principal component analysis; Pp65, phosphoprotein 65; PLN, peripheral lymph nodes; SPL, spleen; TCRαβ, T cell receptor αβ; TE, terminal effector; Th1, T helper type 1; Thy, thymus; WT1, Wilms tumor 1 protein.

that these markers can be used as biomarkers to retrieve the information of the immunization status.

MATERIALS AND METHODS

Step 1: Generation of Humanized Mice Transplanted with Human CB-HSC

Study protocols were approved by the Ethics Committee of the Hannover Medical School for acquisition and banking of human HSCs obtained from umbilical cord tissues after informed consent from donors (mothers at term). The HSCs were labeled according to a numerical code that could not be traced back to the donor's personal information, thus keeping the donor's anonymity. All experiments involving mice were performed in accordance with the regulations and guidelines of the animal welfare of the State of Lower Saxony (Nds. Landesamt für Verbraucherschutz und Lebensmittelsicherheit, Dezernat 33/ Tierschutz). 5-week-old NRG mice were originally obtained from The Jackson Laboratory (JAX, Bar Harbor, ME, USA) and bred in-house under pathogen-free conditions. Prior to HSCT, mice were sublethally irradiated (450 cGy) using a [137^{Cs}] column irradiator (Gammacell 3000 Elan; Best Theratronics, Ottawa, ON, Canada). 4 h after irradiation, 1.5–2.0 × 10^5 human $CD34^+$ hematopoietic cells isolated from female donor umbilical CB were administrated to each mouse trough the tail vein as described (20, 24). We had previously shown that immune reconstitution in female mice recipients was faster than in males (25) and we, therefore, used female donors to avoid any putative immune responses against antigens expressed in the Y chromosome of male recipients. Stem cells from HLA*A02.01 positive (CB1, CB3) or negative (CB2) units were used to generate humanized mice (CB1: $n = 11$, CB2: $n = 10$, CB3: $n = 9$). Starting at week 10 posttransplantation, the human immune reconstitution in mouse peripheral blood (PB) was assessed by flow cytometry evaluating the frequency of human $CD45^+$ cells.

Step 2: Immunization of Mice with iDCs Expressing the pp65 Antigen

$CD14^+$ monocytes were isolated at high purity (from the same CB units used as source of $CD34^+$ HSCs) by immune-magnetic beads (Miltenyi Biotec, Bergisch Gladbach, Germany) and cryopreserved. $CD14^+$ cells were used for the generation of iDCpp65 after transduction with a tricistronic integrase-defective lentiviral vector co-expressing human cytokines GM-CSF/IFN-α and the HCMV-pp65 protein as described (IDLV-G2a-pp65) (20, 24). In short, monocytes were pre-conditioned with recombinant human GM-CSF and IL-4 (both 50 ng/ml; Cellgenix, Freiburg, Germany) for 8 h prior to lentiviral gene transfer. Transduction of monocytes with IDLV-G2a-pp65 was performed at a multiplicity of infection of 5 (2.5 mg/ml p24 equivalent) in the presence of 5 μg/ml protamine sulfate (Valeant, Duesseldorf, Germany) for 16 h. Afterward, cells were harvested by resuspension in phosphate-buffered saline (PBS), washed twice, and cryopreserved. For transduction quality assessment, a sample of frozen cells was thawed and maintained in the X-VIVO 15 medium (Lonza, Basel, Switzerland) for 7 days. Analyses of cell viability (by trypan blue exclusion), lentiviral copies per cell (by RT-q-PCR), and DC immunophenotype (by flow cytometry) were performed as previously described (20, 21, 24). For immunization, IDLV-transduced cells were thawed, washed twice with PBS, and re-suspended in PBS at concentration 5.0 × 10^6 cell/ml. Cells were kept on ice until injection. After CB-HSCT, mice were randomly distributed into two groups, a non-treated control and a group immunized with 5.0 × 10^5 iDCpp65 cells. Cells were administered subcutaneously in the left hind flank at weeks 6 and 10 and in right hind flank at weeks 7 and 11 posttransplantation (**Figure 1A**). Weekly weight and general health monitoring were performed until the end of the experiment at week 20 posttransplantation.

Step 3: Longitudinal Characterization of Human T Cell Development in PB

Samples of PB were collected from all mice at weeks 10, 16, and 20 after HSCT to evaluate the level of engraftment of human hematopoietic cells and expansion of T and B cells. Two rounds of lysis were performed to remove erythrocytes (0.83% ammonium chloride/20 mM HEPES, pH 7.2, for 5 min at room temperature, followed by stabilization with cold PBS and washing). Cells were labeled for flow cytometry analyses with the following antibodies as previously described (24): pacific blue anti-CD45, Alexa700 (AF700) anti-CD19, allophycocyanin (APC) anti-CD3, phycoerythrin-cyanine7 (PC7) anti-CD8 (BioLegend, Fell, Germany); allophycocyanin-H7 (APC-H7) anti-CD4, Phycoerythrin (PE) anti-CD14 (BD Biosciences, San Jose, CA, USA); and phycoerythrin-cyanine5 (PC5) anti-CD62L, fluorescein isothiocyanate (FITC) anti-CD45RA (Beckman Coulter, Krefeld, Germany) for 15 min at room temperature, washed, and analyzed by LSR II flow cytometer (BD Biosciences, Heidelberg, Germany).

Step 4: Evaluation of the Human T Cell Responses against pp65 in Immunized Mice

Three mice immunized with iDCpp65 and showing well-developed lymph nodes were used for obtaining human memory T cells in high purity as previously described (20, 24). Cryopreserved single cell suspensions generated from lymph nodes were thawed, pooled, and re-suspended in X-VIVO 15 medium. Activation of T cells was performed by MACS magnetic beads conjugated with anti-CD2/CD3/CD28 monoclonal antibodies (Miltenyi Biotec, Germany) in a bead-to-cell ratio of 1:2, in presence of 25 IU/ml of human IL-2, 5 ng/ml IL-7, and 5 ng/ml IL-15 (Cellgenix, Germany) for 48 h. Cytokines were refreshed every 2 days until the end of the homeostatic expansion (day 9 post-activation with magnetic beads). Activated cells were re-stimulated after coculture either with autologous iDC (for APC-mediated homeostatic stimulation but lacking antigens) or with iDCpp65 for 7 days using a T/DC cell ratio of 10:1. For intracellular IFN-γ detection, expanded T cells were first seeded in triplicates wells (3 × 10^5 cells/well) of a 96-well round-bottom plate and then, for 16 h, the cells were further activated with 10 μg/ml of

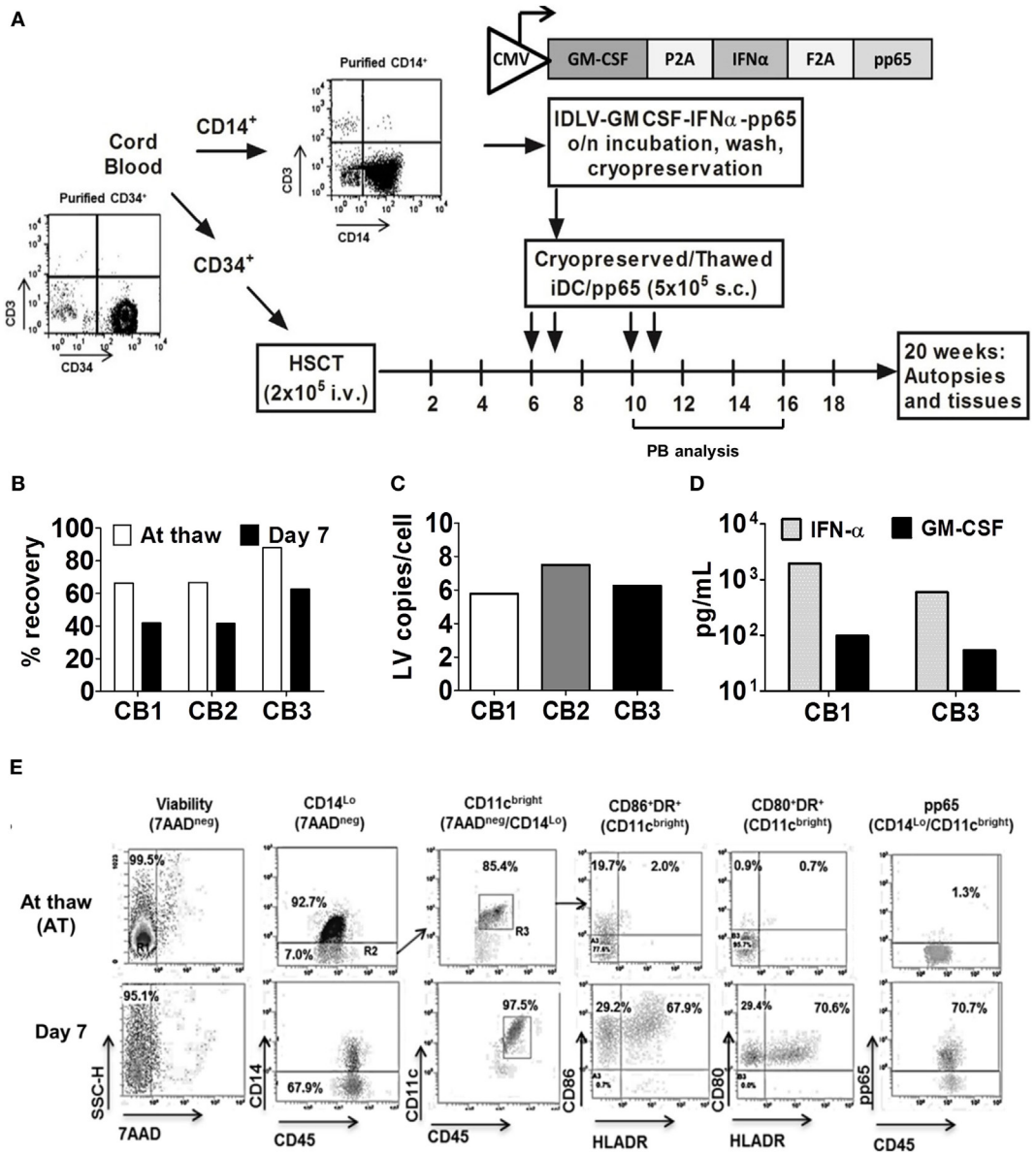

FIGURE 1 | Generation of induced dendritic cells expressing pp65 (iDCpp65) for immunization of humanized mice. **(A)** Scheme of experimental design. Purified CD34+ hematopoietic stem cells obtained from three cord blood (CB) units and devoid of contaminating T cells were used for transplantation of three mice cohorts. Purified CD14+ cells from the same CB were transduced with a tricistronic integrase-defective lentiviral vector co-expressing huGM-CSF, huIFN-α, and HCMV-pp65. Cryopreserved cells were thawed, analyzed for viability, identity, and potency characteristics *in vitro*, and used for prime/boost immunizations [at weeks 6, 7, 10, and 11 after hematopoietic stem cell transplantation (HSCT), $n = 17$]. Longitudinal analyses of peripheral blood were performed on weeks 10, 16, and 20 after HSCT. Mice were sacrificed at week 20 after HSCT and bone marrow, SPL, Thy, peripheral lymph node (PLN), and MLN were isolated and analyzed. Non-immunized humanized mice ($n = 11$) from the same corresponding CB units were used as controls. **(B)** Percentage of viable iDCpp65 cells after cryopreservation and thawing (white bars) and 7 days after the *in vitro* culture (black bars) for each CB unit. **(C)** iDCpp65 generated with CB 1 (white), 2 (gray), and 3 (black bars) were maintained for 7 days *in vitro* and the extracted DNA was analyzed by RT-q-PCR for LV copy number per cell. **(D)** Concentration of huIFN-α (gray bars) and huGM-CSF (black bars) determined for cell supernatants collected at day 7 of *in vitro* differentiation of iDCpp65 generated from CB donor 1 and 3 and measured by ELISA. **(E)** Representative dot plots of flow cytometry analyses of iDCpp65 (CB1) at thaw and at day 7 of differentiation *in vitro*, showing high viability (7AAD negative population), downregulation of CD14, upregulation of CD45 and CD11c (used as gates for further analyses), and upregulation of HLA-DR, CD80, CD86, and pp65 upon iDCpp65 differentiation.

CMV PepTivator (pp65 overlapping peptide pool, Miltenyi Biotec, Bergisch Gladbach, Germany) or 10 μg/ml of Wilms Tumor 1 (WT1) negative control overlapping peptide pool (Miltenyi Biotec, Germany). A protein transport inhibitor cocktail (eBioscience, Frankfurt, Germany) was added to the cells 2 h after peptide stimulation. At the end of stimulation, the surface staining with APC anti-CD3, APC-H7 anti-CD4, and PC7 anti-CD8 antibodies (BioLegend, Germany) was

performed. Subsequently, cells were permeabilized and fixated for intracellular staining with PE anti-IFN-γ antibodies (eBioscience, San Diego, CA, USA). Samples were acquired by LSR II flow cytometer and data were analyzed using FlowJo software version 7.6.4 (Tree Star Inc., Ashland, OR, USA). As targets for enzyme-linked immuno spot (ELISPOT) assays, K562 cells expressing HLA*A02.01 (also known as artificial antigen-presenting cells or "aAPCs") and aAPCs expressing pp65 endogenously (aAPC/pp65) were cultured in RPMI 1640 (Lonza, Switzerland) containing 10% fetal bovine serum. For IFN-γ detection by ELISPOT, MultiScreen HTS plates (Merk Millipore, Darmstadt, Germany) were coated with anti-IFN-γ antibodies (Mabtech, Nacka Strand, Sweden) at 4°C overnight. Then, 2.5×10^4 T cells were mixed with 7.5×10^4 aAPCs either not carrying an antigen, or with aAPCs pulsed with WT1 peptides (aAPC + WT1), or with aAPCs pulsed with pp65 peptides (aAPC + pp65) or expressing pp65 endogenously (aAPC/pp65). The T cell/aAPC cocultures were incubated overnight, washed, and incubated with biotin-conjugated anti-human IFN-γ monoclonal Ab, followed by incubation with alkaline phosphatase-conjugated streptavidin. Color development was performed using NBT/5-bromo-4-chloro-3-indolyl phosphate liquid substrate, and the plates were analyzed in an ELISPOT reader (AELVIS, Hannover, Germany). The mean ELISPOT counts for activation with iDC (4 replicate cultures) and iDCpp65 (6 replicate cultures) were obtained.

Step 5: Analyses of Human Cytokines in Mouse Plasma

At sacrifice, PB samples were collected by heart puncture and cells were subsequently sedimented by centrifugation. The supernatant containing plasma was stored at −80°C until the analysis. After thawing, plasma samples were centrifuged at 2,000*g* for 10 min at room temperature prior the analysis to remove remaining cell debris. 25 µl of plasma were used for analysis of each sample. The concentration in plasma of human GM-CSF, IFN-γ, monocyte chemoattractant protein (MCP-1), TNF-α, IL-1β, IL-2, IL-4, IL-5, IL-6, IL-7, IL-8, IL-10, and IL-12 (p70) was analyzed by a 14-plex Luminex kit (Milliplex Millipore, MA, USA) according to manufacturer's protocol.

Step 6: Characterization of the Terminal Human T Cell Responses in Lymphatic Tissues

Spleen (SPL), peripheral lymph nodes (PLN), mesenteric lymph nodes (MLNs), BM, and Thy cells were isolated after sacrifice and homogenized. For mice transplanted with CB1-3, cell suspensions generated with PLN and MLN were combined, whereas for CB2 and CB3, there was an additional cell suspension fraction of MLN analyzed separately. Cell suspensions were washed and re-suspended in PBS for subsequent staining with fluorochrome-conjugated monoclonal antibodies as described above for PB (24). Thymocytes were stained 15 min at room temperature with the following antibodies: pacific blue anti-CD45, AF700 anti-CD4, APC anti-CD3, PC7 anti-CD8, FITC anti-TCR αβ (BioLegend, Germany). After washing, cells were re-suspended in PBS containing 1% human serum and analyzed by an LSR II flow cytometer.

Step 7: Establishing the Database and Statistical Analyses

All variables consisting of cell phenotypes determined as relative frequency (PB and lymphatic tissues) and counts (lymphatic tissues) and cytokines concentrations (plasma) were organized in a PivotTable using Excel software 2010 (Microsoft, Redmond, WA, USA). Each sample was coded according to the CB unit (1, 2, or 3) cell type, tissue, time-point of analyses, intervention group (control or iDCpp65), and mouse gender (female "F" or male "M"). Beta regression analysis was employed to model the association between the intervention groups and the cell phenotypes measured as "relative frequency," which is expressed as odds ratio (i.e., the odds of event between iDCpp65 and control), whereas negative binomial regression was used to model the association between the intervention groups and the count cell phenotypes expressed as rate ratio (i.e., the incidence rate between iDCpp65 and control). Both models where implemented with and without stratification by gender. Parameter estimation was performed by least square means. The *p*-values calculated at significance levels 0.05 and 0.01 using the two-sided *z*-test statistic were considered significant. All analyses were implemented using the SAS 9.3 software (SAS, Cary, NC, USA). PROC GLIMMIX was used for Beta regression analysis, together with PROC GENMOD for the negative binomial regression analysis. A two-way analysis of variance was performed to analyze the results of the IFN-γ ELISPOT assay using GraphPad Prism version 5 software (GraphPad Software, Inc., La Jolla, CA, USA).

Step 8: ANN Classification Approach

The computational analysis was carried out in MatLab version 7.11.0, 2010 (MathWorks, Inc., Natick, MA, USA) using the Neural Network Pattern recognition application. The inputs (15 markers representing cell phenotypes for PB, SPL, PLN + MLN, or MLN, BM and 8 markers for Thy) and their corresponding outputs [immunization status of each mice, "yes" (1) or "no" (0)] were used for training the ANN. To find the appropriate number of neurons in the hidden layer, we performed a *k*-fold cross validation (29) (with *k* being equal to 3, 4, 5) resulting in 12 neurons (8 for Thy). The output layer consisted of two neurons. The classification accuracy (percentage of correct classifications) was estimated by averaging over 2000 ANN. For each of those ANN, the input dataset was randomly divided into training (70% samples/tissue), validation (15% samples) and testing (15% samples). The Levenberg–Marquardt back-propagation (trainlm) algorithm was used for the training step, as it is best suited for small networks (30). For the hidden layer, we used sigmoid transfer functions. The data were first standardized (i.e., each marker was normalized to 0 mean value and unit variance) in order all the markers to be at the same scale.

We also performed the same classification analysis of immunized (1) and non-immunized mice (0), but by dividing our

samples into male and female mice data sets. In this case, we used the same parameter setting for ANN as above and tested the classification accuracy for each subpopulation. In addition to the classification accuracy (defined as the fraction of correctly classified samples), we measured the sensitivity and specificity of the classification, applied inside each group. The *sensitivity*, defined as

$$\text{sensitivity} = \frac{\text{number of true positives}}{\text{number of true positives} + \text{number of false negatives}},$$

represents the probability of a sample classified as immunized (1) to belong to the immunized group.

The *specificity* provides the probability of a sample classified as non-immunized (0) to belong to the non-immunized group. Specificity is defined as

$$\text{specificity} = \frac{\text{number of true negatives}}{\text{number of true negatives} + \text{number of false positives}}.$$

The 15 markers correspond to the frequencies of human lymphocyte lineages analyzed per tissue (PB, BM, SPL, MLN + PLN, MLN) of each mouse included cells determined as frequencies of CD45, CD19/CD45, CD3/CD45, CD14/CD45 (in BM CD34/CD45 instead of CD14/CD45), CD4/CD45, CD8/CD45 and a frequency of other non-determined $CD45^+$ cells, frequencies of CD4 subtypes (N, CM, EM, and TE), and frequencies of CD8 subtypes (N, CM, EM, and TE). Eight markers were used for Thy: frequencies of CD45, CD3/CD45, CD4/CD45, CD8/CD45, $CD4^-/CD8^-$ (double negative, DN), $CD4^+/CD8^+$ (double positive, DP), $TCR\alpha\beta^+/CD3$, and CD4 to CD8 ratio values.

Step 9: PCA

Principal component analysis (31) was used to recognize clusters of interrelated markers for control and iDCpp65 mice in the different tissues. PCA constructs specific directions, which are called principal components, along which the data are most dispersed and thus best distinguishable. In this way, a data set can be represented by the principal components, which incorporate a specific amount of the variance (or dispersion). Since the components are uncorrelated of each other, the markers, which are strongly correlated with a component, compose a cluster of markers, which vary together. Here, we created these clusters by selecting the phenotypic markers that were strongly correlated or anti-correlated (more than 80%) with any component for each group. The first four components were considered for analysis since they were able to incorporate more than 80% of the total variance in both control and iDCpp65 mice in all tissues. These components were the basis of variance-distribution comparisons and correlation heat-maps for both mouse groups. The markers that were strongly correlated or anti-correlated with the first governing component were used for correlation comparisons between the control and iDCpp65 mice. The data for control and iDCpp65 mice from BM and SPL were represented by 30 variables (percentages and counts for each of the 15 markers); from combined PLN, PB, and MLN by 15 variables (only percentages); from Thy by 14 variables (percentages and counts). As in the training of ANN, the data were first standardized (i.e., each marker was normalized to 0 mean value and unit variance) in order renormalize all markers to the same scale.

RESULTS

Cryopreserved iDCpp65 Remained Viability and Characteristics after Thawing

We have shown before that human T cell responses against HCMV-pp65 were consistently stimulated in humanized NRG mice immunized with iDCpp65 (19, 20, 24). Here, iDCpp65 were generated and cryopreserved immediately after transduction, and subsequently used for prime-boost immunizations of female and male mice (**Figure 1A**). Effects of immunizations in lymphatic tissues were analyzed 20 weeks after HSCT corresponding to 9 weeks after the last immunization. The cell vaccine, iDCpp65, showed high viability directly after thawing (66–88%) and *in vitro* culture for 7 days (42–63%) relative to starting number of cells (**Figure 1B**). Efficient transduction with IDLV and persistency of episomal viral copies were confirmed for cells maintained in culture for 7 days and showing in average five lentiviral copies/cell (**Figure 1C**). Transgenic cytokines that accumulated on the cell supernatant of iDCpp65 derived from CB1 and CB3 for 7 days were detected in the range of 500–1,000 pg/ml for IFN-α and 50–100 pg/ml for GM-CSF (**Figure 1D**). The viable cells showed a typical DC immunophenotype with co-expression of HLA-DR (61.60–91.85%), CD86 (93.20–98.97%), and CD80 (29.1–97.7%) surface markers (**Figure 1E**, representative data of a batch of iDCpp65, Figure S1A in Supplementary Material). Intracellular immunostaining for detection of pp65-positive iDCpp65 cells by flow cytometry assay showed variable results among different CB donors (CB1: 49.20%, CB2: 2.49%, CB3: 16.40% when calculated for total viable cells in suspension 7 days after *in vitro* culture, Figure S1B in Supplementary Material).

iDCpp65 Immunizations Affected Lymphocytes Counts in PB, Plasma Cytokines Profiles, and Lymph Node Development

Three independent cohorts of NRG mice after $CD34^+$ HSCT were generated. 5.0×10^5 thawed and viable autologous iDCpp65 were injected at weeks 6, 7, 10, and 11 after HSCT. Body-weight and general health conditions were monitored weekly. Although females from both control and iDCpp65-immunized cohorts were lighter than males, mice of both genders gained weight normally for the 20 weeks after HSCT (**Figure 2A**) and showed no signs of graft-versus-host disease or organ pathologies at sacrifice (data not shown). The frequencies of human $CD45^+$ cells detected in PB at weeks 10, 16, and 20 post-HSCT were consistently higher in females, particularly for females immunized with iDCpp65 (**Figure 2B**). The expansion of human $CD8^+$ and $CD4^+$ T cell detectable in PB was superior in the iDCpp65 cohort compared to controls, especially in the male group (**Figure 2B**; Table S1 in Supplementary Material). Analyses of human cells in PB 20 weeks after HSCT by assessment of the

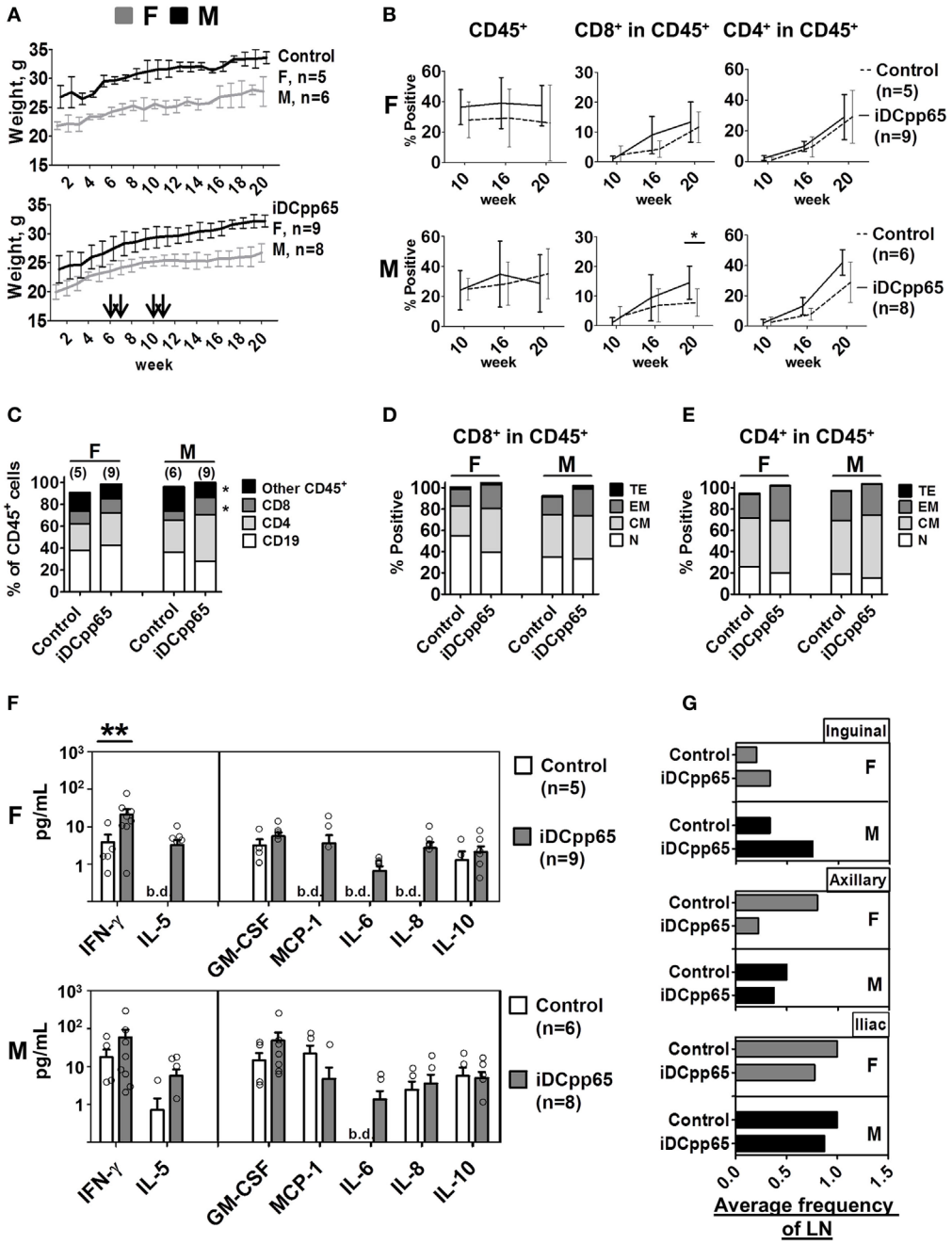

FIGURE 2 | Longitudinal analyses of female and male humanized mice. **(A)** Weight monitoring of control (n = 11, upper panel) and immunized mice (n = 17, lower panel). Arrows indicate the weeks of induced dendritic cells expressing pp65 (iDCpp65) immunizations after hematopoietic stem cell transplantation. Bi-weekly weight (g) determined for females (F) indicated in gray and for males (M) in black. The number of F and M mice per group is indicated. **(B)** Mean relative frequencies of human CD45$^+$, CD8$^+$ in CD45$^+$, and CD4$^+$ in CD45$^+$ cells determined in blood by flow cytometry of control (dashed line) and iDCpp65-immunized (solid line) F (upper panel) and M (lower panel) at weeks 10, 16, and 20 posttransplantation. Error bars represent SEs. *$p < 0.05$ are indicated on the graph. **(C)** Relative frequencies of human cell types measured by flow cytometry in PBL of female (F) and male (M) mice at week 20 posttransplantation. Mean relative frequencies of CD19$^+$ (white), CD4$^+$ (light gray), CD8$^+$ (dark gray), and other CD45$^+$ cells (black) were measured in control and iDCpp65-immunized mice, *$p < 0.05$ are indicated on the graph. **(D)** Phenotypes of distinct CD8$^+$ and **(E)** CD4$^+$ T cells were determined as naïve (N, white, CD45RA$^+$/CD62L$^+$), central memory (CM, light gray, CD45RA$^-$/CD62L$^+$), effector memory (EM, dark gray, CD45RA$^-$/CD62L$^-$) and terminal effector (TE, black, CD45RA$^+$/CD62L$^-$). Mean relative frequencies are shown for control and iDCpp65-immunized mice. **(F)** Concentration of human cytokines measured in plasma of F (upper panel) and M (lower panel) mice 20 weeks posttransplantation. Mean concentrations of cytokines were determined for iDCpp65-immunized (gray) and control (white) groups. Bars and circles reflect the SE of the estimated mean concentrations and the observed concentrations of individual samples, respectively. Concentration values below the detection limit of the assay are indicated (b.d.), *$p < 0.05$, **$p < 0.01$ indicated on the graph. **(G)** The average frequency of lymph nodes found in F (top panel) and in M (bottom panel) mice for iDCpp65-immunized and control groups. Values for inguinal (upper-), axillary (middle-), and iliac (lower panel) lymph nodes found 20 weeks after hematopoietic stem cell transplantation. Number of samples: female, n = 5/9; male, n = 6/8, control/immunized, respectively.

mean relative frequencies showed that CD8+ T cells were higher in the immunized cohort ($p = 0.03$) (Table S1 in Supplementary Material), with high significance for the male group ($p = 0.01$ CD8+; $p = 0.09$ CD4+) (**Figure 2C**; Table S1 in Supplementary Material). This was associated with a higher accumulation of EM and TE CD8+ cells in the group of iDCpp65-immunized males whereas the group of females showed higher accumulation of CM CD8+ cells in immunized versus control group (**Figure 2D**; Table S1 in Supplementary Material). The relative frequencies of CD4+ T cell subtypes were only slightly altered, showing an increase in the relative frequencies of CM cells for males and EM cells for females (**Figure 2E**; Table S1 in Supplementary Material). A fluorescent-based bead assay was used to measure the concentration of 12 human cytokines in mouse plasma (GM-CSF, MCP-1, IFN-γ, TNF-α, IL-1β, IL-2, IL-4, IL-5, IL-6, IL-8, IL-10, and IL-12p70). IL-1β, IL-2, IL-4, and IL-12p70 were below the detection limit. For the group of non-immunized mice, the baseline concentrations of human cytokines in the plasma were consistently higher for males. Remarkably, IL-5, MCP-1, and IL-8 were only detectable in non-immunized males. Upon immunizations, both genders showed increased IFN-γ (rate ratio 2.74, $p = 0.15$) and GM-CSF concentrations (rate ratio 2.96, $p = 0.092$) (Table S2 in Supplementary Material). The increase of IFN-γ concentration after immunization was particularly high for immunized females ($p = 0.003$) (**Figure 2F**). Detection of IL-5, MCP-1, IL-6, and IL-8, in plasma of females was only possible after iDCpp65 immunization. Therefore, overall, iDCpp65 immunization harnessed the maturation of human T cells in PB, which was in general associated with an increase of human cytokines in plasma (in particular for females). The undersized and incompletely developed lymph nodes in humanized mice are difficult to be detected. They can be, nonetheless, detected as quite small "fatty" structures in the expected anatomical regions (inguinal, axillary, iliac). Upon immunization with iDCpp65, these draining LNs become macroscopically more noticeable. Although these regenerated LNs are not fully "normal" in relationship to lymph nodes found in immune competent mice, they contain a high density of human T cells (19). In this current study, we confirmed a higher frequency of developed draining lymph nodes (near the immunization sites) in the immunized cohorts, which was more evident for males (**Figure 2G**). Remarkably, this observation was inverted for the axillary lymph nodes, which were more prominent in females. On the other hand, the average frequency of detectable iliac nodes was lower in the immunized cohort (**Figure 2G**). Small MLNs developed in most mice, regardless of gender or immunizations (data not shown), indicating the possibility that the development of MLNs may be induced differently.

iDCpp65-Immunized Mice Demonstrated Functional pp65-Specific Memory T Cell Responses

Lymph nodes of immunized mice were a valuable compartment for the detection of high frequencies of human T cells. Lymphocytes recovered from lymph nodes of three immunized mice were pooled and maintained *in vitro* for 48 h for homeostatic activation by beads and cytokines. Lymphocytes from non-immunized mice were not used since, from previous experience, we were not able to expand them successfully *in vitro* (19, 20). Microcultures of cell suspensions were incubated with autologous "empty" iDCs or with iDCpp65 at 10:1 T to DC ratio for 1 week to promote further expansion of T cells. The expansion was more pronounced for T cells cultured in the presence of iDCpp65 stimulation than "empty" iDCs (fold expansion relative the population before stimulation): 10.9 (iDCpp65) and 9.1 (iDCs) (**Figures 3A,B**). Activated CD8+ and CD4+ T cells were analyzed by flow cytometry for detection of intracellular IFN-γ. T cells expanded in the presence of empty iDC and re-stimulated with WT1 or pp65-peptide pools showed similar baseline frequencies of CD8+ IFN-γ+ and CD4+ IFN-γ+ T cells. In contrast, T cells expanded in the presence of iDCpp65 and then re-stimulated with the pp65-peptide pool showed variable but in average much higher relative frequencies of CD8+ IFN-γ+

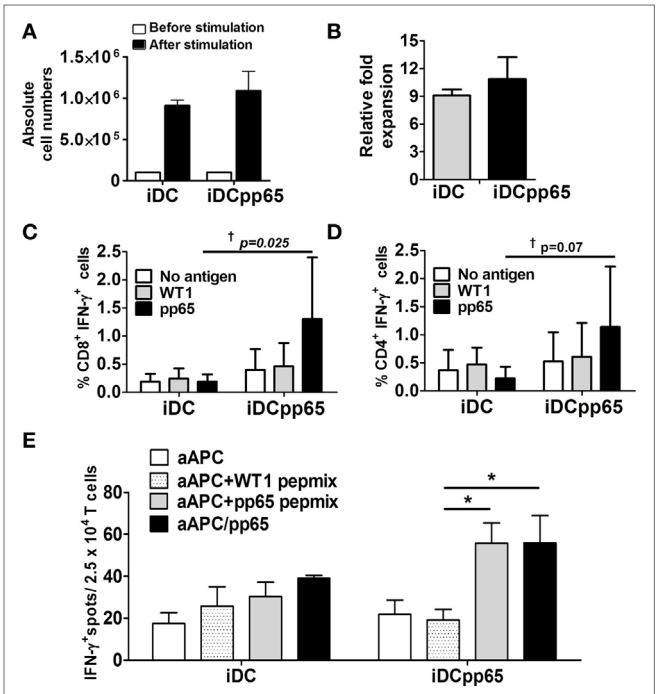

FIGURE 3 | Functional memory T responses against pp65 after induced dendritic cells expressing pp65 (iDCpp65) immunization. **(A)** T cells isolated from lymph nodes of immunized mice ($n = 3$) were re-stimulated *in vitro* with either induced DC (iDC) or iDCpp65. Absolute T cell numbers before (white bars) and 7 days after (black bars) stimulation are shown. **(B)** Relative fold increase of cells populations before and 7 days after coculture with iDC (gray bars) and iDCpp65 group (black bar). **(C)** CD8+ and **(D)** CD4+ T lymphocytes expanded after coculture with iDC ($n = 3$) or iDCpp65 ($n = 3$) were left unstimulated (white bars) or re-stimulated with a Wilms Tumor 1 (WT1) peptide pool (gray bars) or pp65-peptide pool (black bars). Frequency of cells producing IFN-γ is shown. **(E)** T cells expanded with iDC (four cultures per group) or iDCpp65 (six cultures per group) were cocultured with an artificial antigen-presenting cell (aAPC) on an ELISPOT plate. The aAPCs were ether not loaded (white bars), loaded with WT1 peptides (light gray bars), loaded with pp65-peptides (dark gray bars), or transduced for endogenous pp65 expression and loading (black bars). Mean absolute number of IFN-γ-spots and $^*p < 0.05$ (analysis of variance), $^\dagger p < 0.05$ (F-test) are indicated.

and CD4+ IFN-γ+ T cells (**Figures 3C,D**). The mean anti-pp65 response for CD8+ was 6.84 times higher in the iDCpp65 than in iDC re-stimulation group and for CD4+ T cells in 6.27 times, respectively. F-test comparing variances between iDC and iDCpp65 showed a strong evidence of variance difference between groups in case of re-stimulation with pp65-peptide pool ($p = 0.025$, CD8+; $p = 0.072$, CD4+) but not when groups were re-stimulated with WT1 or not stimulated at all ($p > 0.05$ for all cases) (**Figures 3C,D**).

As a complementary approach, the ability of T cells to recognize and be activated by pp65 epitopes presented by an aAPC positive for HLA-A*02.01 was tested by an IFN-γ-ELISPOT assay as previously described (32). T cells expanded after coculture with iDCs or iDCpp65 were exposed overnight to different types of aAPCs, and the numbers of reactive T cells were quantified. T cells expanded with iDCpp65 and cocultured with either aAPC loaded with pp65-peptides or transduced for pp65 expression showed on average significantly higher frequencies of activated T cells than when cocultured with aAPC loaded with control WT1 peptides ($p = 0.016$, $p = 0.026$, respectively). No significant amplification of T cell activation was observed when T cells were expanded in the presence of "empty" iDCs ($p > 0.05$ for both cases) (**Figure 3E**). These data confirmed that immunizations with iDCpp65 promoted a specific immune competence against pp65 in humanized mice which was mediated by human T cells.

Heterogeneous Patterns of Human Lymphocytes in Lymphatic Tissues after iDCpp65 Immunization

Isolated tissues [BM, SPL, lymph nodes (PLN + MLN and MLN)] were processed for flow cytometry analyses and quantification of human lymphocyte frequencies and absolute numbers. For BM, CD3+ T cells represented only a minority of huCD45+ cells, whereas B cells (CD19+) and other CD45+ cells prevailed. In terms of relative frequencies, a trend for increased frequencies of CD19+ cells was observed upon iDCpp65 immunization,

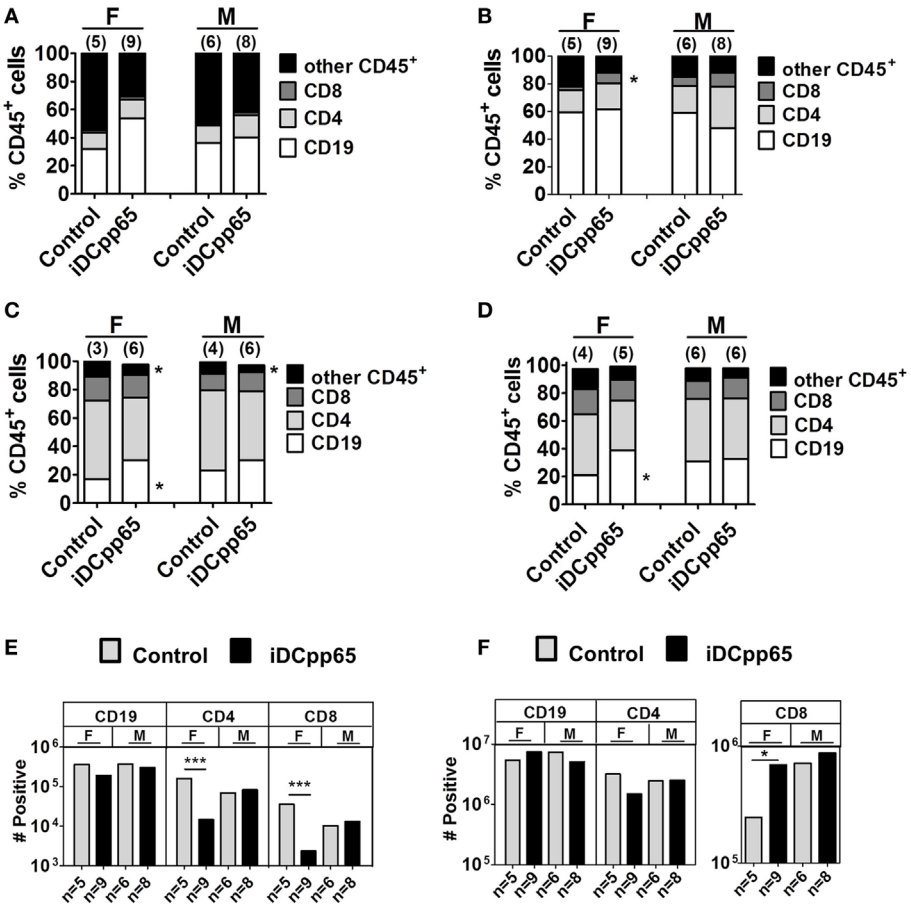

FIGURE 4 | Relative and absolute quantification of human hematopoietic lineages in lymphatic tissues. Mean relative frequency for human CD19+ (white), CD4+ (light gray), CD8+ (dark gray), and other CD45+ cells (black) detected by flow cytometry analyses of **(A)** bone marrow, **(B)** SPL, **(C)** combined peripheral lymph nodes and MLN, and **(D)** MLN. Frequencies for female (F) and male (M) mice are shown separately. **(E)** Absolute cell counts for bone marrow and **(F)** spleen were obtained. Plots represent average number of cells determined for control (gray bars) and induced dendritic cells expressing pp65 (iDCpp65)-immunized (black bars) split between female and male mice. The number of mice analyzed per group (*n*) and *$p < 0.05$ is indicated on the graph. For **(A,B,E,F)** F/control $n = 5$, F/iDCpp65 $n = 9$, M/control $n = 6$, M/iDCpp65 $n = 8$. For **(C)** F/control $n = 3$, F/iDCpp65 $n = 6$, M/control $n = 4$, M/iDCpp65 $n = 6$. For **(D)** F/control $n = 4$, F/iDCpp65 $n = 5$, M/control $n = 6$, M/iDCpp65 $n = 6$.

an effect that was more pronounced in females (**Figure 4A**; Table S3 in Supplementary Material). Remarkably, the total number of BM cells was consistently lower in the immunized group, which reflected into a noticeable lower absolute number of T cells, especially for the female group (**Figure 4E**; Table S3 in Supplementary Material). This was offset by analysis of splenocytes, showing an overall higher relative frequency and absolute counts of $CD8^+$ cells within the $huCD45^+$ population of immunized compared with control mice, especially for females (**Figures 4B,F**; Table S4 in Supplementary Material). As a consequence of the variable detection of lymph nodes in host mice, the analyses of absolute cell numbers also varied accordingly. Lymph nodes from different body parts were initially combined for CB1, but as the development and functions of PLNs (axillary, brachial, inguinal, and iliac) seemed to be distinct from that of the MLN, they were further separately analyzed into two independent groups for CB2 and CB3. Nevertheless, with either combining the lymph nodes or analyzing MLN separately, the general trend was increased frequencies of $CD19^+$ cells upon immunization and was more pronounced in females (**Figures 4C,D**). Concurrently, a relative decrease in the frequency of T cells was observed (**Figures 4C,D**; Table S5 in Supplementary Material). This data indicated that the patterns of different lymphocyte types were heterogeneous and largely influenced by the tissue analyzed, sex of the hosts, and whether they were immunized or not.

The Patterns of T Cell Maturation after iDCpp65 Immunization Varied in Lymphatic Tissues

Analysis of $CD4^+$, $CD8^+$, double positive (DP) and double negative (DN) T cells in Thy showed just a modest higher relative frequency and absolute counts of DP cells for iDCpp65-immunized mice, but only in male group (**Figure 5A**; Table S6 in Supplementary Material). Notably, females showed reduced absolute counts of single-positive $CD8^+$ cells in the immunized group (**Figure 6A**; Table S6 in Supplementary Material). For the BM, the most abundant T cell subtypes were EM (**Figures 5B** and **6B,D**). The $CD8^+$ and $CD4^+$ EM T cell frequencies were further augmented upon immunization, but only for the female group, which also resulted in the relative decrease of CM $CD8^+$ and $CD4^+$ cells (**Figure 5B**; Table S3 in Supplementary Material). For T cells in SPL, immunization with iDCpp65 resulted in a greater proportion of CD8EM and CD4EM T cell subtypes compared to control mice (Table S4 in Supplementary Material). Females demonstrated a more abundant accumulation of mature EM and TE $CD8^+$ cells (**Figures 5C** and **6C,E**; Table S4 in Supplementary Material). The analysis of T cell phenotypes in combined PLN and MLN revealed a skewing toward EM among $CD8^+$ and $CD4^+$ cells (Table S5 in Supplementary Material), notably in females for the CD8TE subtype ($p = 0.047$) upon immunization (**Figure 5D**; Table S5 in Supplementary Material). A separate analysis was performed for MLN only and similarly showed the trend toward accumulation of mature CD8TE cells upon immunization ($p = 0.06$) specifically for the female group (**Figure 5E**; Table S5 in Supplementary Material).

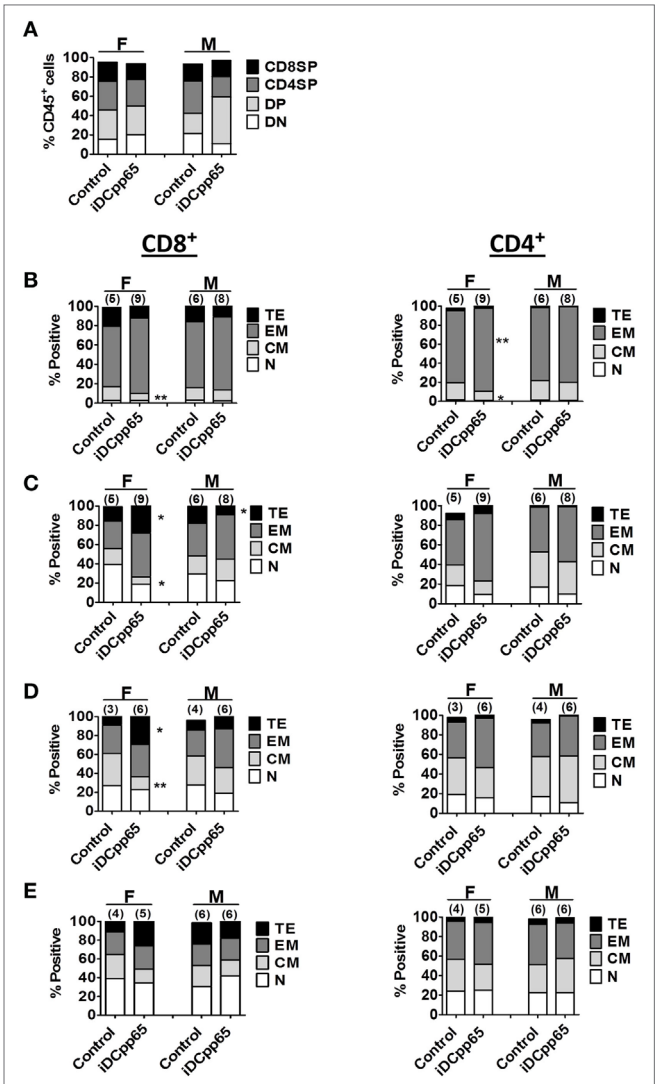

FIGURE 5 | Relative quantification of human T cell subtypes in lymphatic tissues. Mean relative frequencies of human T cell subtypes were estimated based on results of flow cytometry analyses 20 weeks posttransplantation for F and M mice. **(A)** Mean relative frequencies of thymic CD4/CD8 double negative (DN, white), CD4/CD8 double-positive (DP, light gray), $CD4^+$ single-positive (CD4SP, dark gray), and $CD8^+$ single-positive (CD8SP, black) cells within $huCD45^+$ cells in control and induced dendritic cells expressing pp65 (iDCpp65)-immunized mice. Phenotypes of distinct $CD8^+$ and $CD4^+$ T cells subtypes: **(B)** bone marrow, **(C)** SPL, **(D)** combined PLN and MLN, and **(E)** MLN. Subtypes were determined as Naïve (N, white, $CD45RA^+/CD62L^+$), central memory (CM, light gray, $CD45RA^-/CD62L^+$), effector memory (EM, dark gray, $CD45RA^-/CD62L^-$), and terminal effector (TE, black, $CD45RA^+/CD62L^-$). Mean relative frequencies are shown for control and iDCpp65-immunized mice. The sample size for female and male mice and $^*p < 0.05$, $^{**}p < 0.01$ are indicated on the graph. For **(A)** F/control $n = 5$, F/iDCpp65 $n = 9$, M/control $n = 6$, M/iDCpp65 $n = 7$. For **(B,C)** F/control $n = 6$, F/iDCpp65 $n = 9$, M/control $n = 6$, M/iDCpp65 $n = 8$. For **(D)** F/control $n = 3$, F/iDCpp65 $n = 6$, M/control $n = 4$, M/iDCpp65 $n = 6$. For **(E)** F/control $n = 4$, F/iDCpp65 $n = 5$, M/control $n = 6$, M/iDCpp65 $n = 6$.

These data confirmed that immunizations with iDCpp65 affected T cells and promoted their conversion toward more mature subtypes.

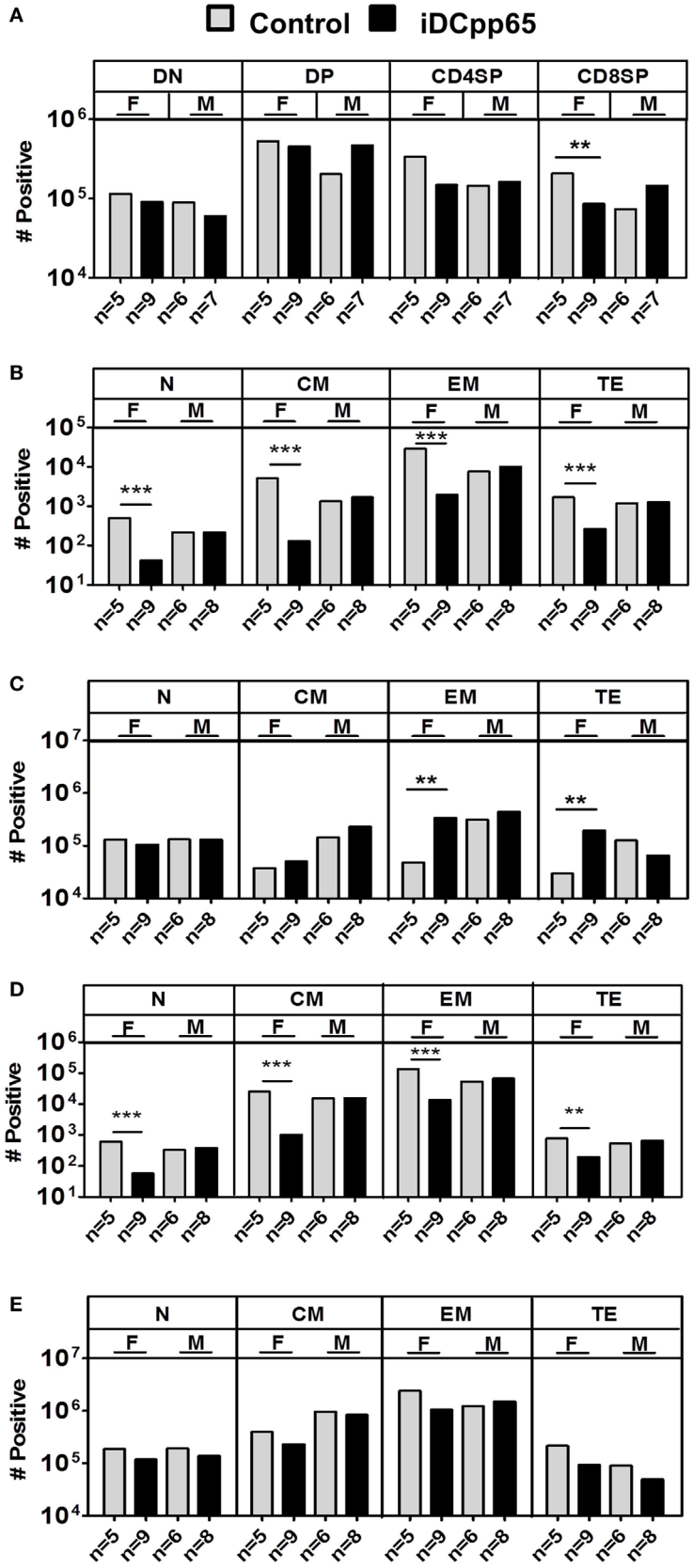

FIGURE 6 | Continued

FIGURE 6 | Continued
Absolute cell counts of T cell subtypes in different tissues. Mean cell counts determined for female (F) and male (M) mice 20 weeks posttransplantation. **(A)** Analyses of Thy showing control (gray bars) and induced dendritic cells expressing pp65 (iDCpp65)-immunized (black bars) groups. **(B)** Mean cell counts of $CD8^+$ T cell subtypes determined in bone marrow (BM) and **(C)** SPL of F and M mice for control and iDCpp65-immunized groups. **(D)** Mean cell counts of $CD4^+$ T cell subtypes determined in BM and **(E)** SPL of F and M mice for control and iDCpp65-immunized groups. Subtypes were determined as Naïve (N, $CD45RA^+/CD62L^+$), central memory (CM, $CD45RA^-/CD62L^+$), effector memory (EM, $CD45RA^-/CD62L^-$), and terminal effector (TE, $CD45RA^+/CD62L^-$). Mean relative frequencies are shown for control and iDCpp65-immunized mice. The sample size for females and males and $^{**}p < 0.01$ are indicated on the graph. **(A)** F/control $n = 5$, F/iDCpp65 $n = 9$, M/control $n = 6$, M/iDCpp65 $n = 7$. For **(B–E)** F/control $n = 5$, F/iDCpp65 $n = 9$, M/control $n = 6$, M/iDCpp65 $n = 8$.

A Machine Learning-Based Predictive Classifier of Immunized and Non-Immunized Mice

In the previous parts, the comparison of single markers to find phenotypic immunological parameters affected by immunization with iDCpp65 showed that the profile and magnitude of these immunization-influenced parameters were very heterogeneous among the analyzed tissues (**Figures 2** and **4–6**). In order to provide an integrative view on how immunizations impacted different tissues, including how the immune-phenotypic markers were correlated between the control and the immunized group, a multidimensional analysis was established.

In a first approach, and in order to understand which parts of the multidimensional immune response in different tissues contained the critical information about the responsiveness to immunization, we asked whether a classification between control and iDCpp65 samples could be achieved in each tissue by employing an ANN. We investigated whether the cellular composition of single organs would characterize the response to iDCpp65 immunization. To this end, we measured the potency of ANN to recognize any patterns associated with iDCpp65 immunization and screened for them among different tissues.

We analyzed the dataset corresponding to the raw percentages of the measured human cell lineages in different tissues: BM, PB, Thy, SPL, PLN/MLN, and MLNs considering each tissue as an independent dataset. The scheme of the data hierarchy for the tissues is shown in **Figure 7A**. The markers from control ($n = 11$) and iDCpp65-immunized ($n = 17$) mice were used to feed 2000 ANN training-validation-test cycles per tissue. In each cycle, 70% of the samples were randomly selected and used for training, 15% of samples for validation during the training process, and 15% for testing. The output was the classification accuracy, i.e., the percentage of correct classifications (control group or iDCpp65 immunized) averaged over the 2000 ANN. Primary and secondary lymphoid tissues were ranked according to their potency to provide the correct output regarding the sample origin (**Figure 7B**). The classification of control versus iDCpp65-immunized mice for both genders was most efficient using data from PB (73.3% of all samples were classified correctly), followed by PLN merged with MLN (71.1%), and SPL (70.6%) (**Figure 7C**; Table S7 in Supplementary Material). The classification accuracy for Thy was the lowest among the tissues (**Figure 7C**). The above results depicted the heterogeneous impact of immunization in the different tissues from the perspective of the ability of ANN to distinguish control versus iDCpp65-immunized mice.

Subsequently, the mouse gender was taken into consideration. The same analysis was performed for female and male mice separately and results were provided in comparison with the full dataset of combined genders. The classification accuracy for female data was higher for all of the tissues in the combined genders analysis, with exception of analyses performed for Thy and PB. The highest classification accuracy per gender was detected in combined PLN and MLN of female mice (77.3%) (**Figure 7C**; Table S7 in Supplementary Material). Notably, classifications according to sensitivity (**Figure 7D**) were in general higher than specificity for all groups (**Figure 7E**), meaning that the ability to discriminate a mice belonging to the immunized group was higher than to classify a mice as belonging to the control group. For both classifications, the frequencies of correct classification for females were again superior compared with males, especially in combined PLN and MLN or MLN alone (F 84.5%/79.5% and M 74.2%/67.3%, respectively) (Table S7 in Supplementary Material). This gender-based classification supported the concept that lymphocyte markers of immunized female mice were more distinguishable than those of their male littermates.

Correlation and Structural Elements of Immune-Phenotypic Markers in Tissues

In order to understand better the structural relationships between the measured markers in control and iDCpp65-immunized mice, we used a PCA approach. Our rationale was that these analyses might provide us with an estimate of which markers are the best predictors of immunization. Three PCAs were performed, either separately for each group (control or immunized), or including all mice (global PCA). Interestingly, the markers composing the first governing component of the global PCA (data not shown) also appeared in the separate PCAs (**Table 1**), but the group-specific PCA revealed more markers that are suitable to characterize intra-group heterogeneity.

Initially, we tested how the variance of the data sets, obtained for the two mice groups in different tissues, could be distributed within the main components. In BM and Thy, PCA showed that the variance distributions among the first main components are similar in control and iDCpp65 mice (**Figures 8A,B**). We then proceeded to compare the correlation patterns between the two mice groups (**Figures 9A,B**; Figures S2A,B in Supplementary Material) by selecting the markers, which are highly correlated or anti-correlated with the first governing component of the control group (**Table 1**). These markers should contribute more to the total variance and thus to any dynamical changes among the control mice. The correlation patterns between control and iDCpp65 mice were similar in Thy (**Figure 9A**), meaning that the immunization did not impact the correlation between these markers. For instance,

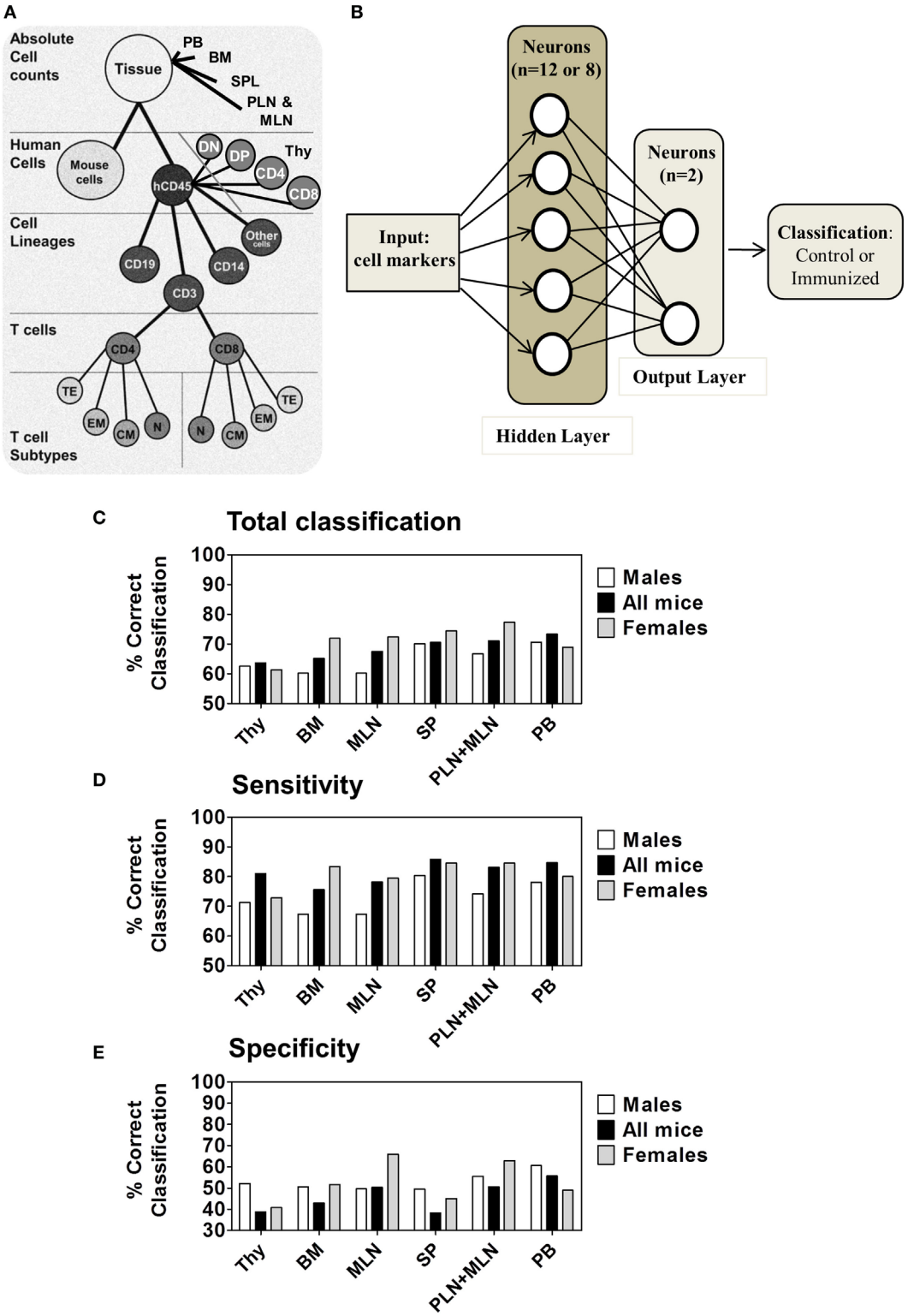

FIGURE 7 | Multilayer Neural Network for performing classification. **(A)** Hierarchy of cell subsets used for analyses of primary and secondary lymphoid organs. **(B)** Schematic representation of the artificial neural network (ANN) structure used for samples classification containing an input module, a hidden layer and an output layer for classifying mice between control (n = 11) or immunized (n = 17) mice. **(C)** ANN total classification accuracy for distinct tissues by subject factor "immunization/control" among M mice (n = 14, white), all mice (n = 28, black) and F mice (n = 14, gray) analyzed for the 20 weeks model data set. **(D)** The sensitivity and **(E)** specificity measured for each gender and for all mice together. Tissues are presented in the order of increasing total classification accuracy when all mice were used.

TABLE 1 | Immune-phenotypic markers measured in bone marrow (BM), Thy, SPL, PLN combined with MLN, MLN, and peripheral blood (PB) which are highly correlated (positive or negative correlation) with the first governing component of the principal component analysis performed in control and induced dendritic cells expressing pp65 (iDCpp65) mice.

Tissue	Control	iDCpp65
Thy	CD3%, CD4%, CD8%	CD3%, CD4%
	DP%	DP%, DN%
		DP#
BM	CD19%, CD3%, CD4%	–
	CD8%, CD8TE%	–
	CD3#, CD4#, CD4CM#, CD4EM#, CD8#, CD8CM#, CD8EM#	CD45#, CD34#, CD3#, CD4#, CD4N#, CD4CM#, CD4EM#, CD4TE#, CD8#, CD8N#, CD8CM#, CD8EM#, CD8TE#, Other CD45#
SPL	CD45%, CD19%, CD3%, CD4%	
	CD4N%, CD8N%, CD8EM%, Other CD45%	CD4N%, CD8N%
	CD45#, CD3#, CD4#, Other CD45#	CD3#, CD4EM#, CD8EM#
PLN + mesenteric lymph node (MLN)	CD4%	CD4%
	CD4N%, CD4CM%, CD4TE%	CD4N%, CD4TE%
	CD8%, CD8N%, CD8CM%	CD8EM%
MLN	CD3%, CD4%, CD8%, C4EM%, CD4TE%, CD8N%, CD8CM%	CD45%, CD19%, C14%, Other%, CD8%, CD4TE%, CD8CM%
PB	CD19%, CD3%, CD4%, CD4N%, CD4CM%, CD4EM%, CD8N%, CD8CM%, CD8EM%	CD19%, CD3%, CD8%

Color indicate the grade of correlation strength for different markers: red (correlation >80%) and blue (correlation <−80%), for frequencies (%), or absolute numbers (#). The number of samples (n) control/immunized = 11/17, respectively, except Thy (11/16), PLN + MLN (7/12), and MLN (10/11).

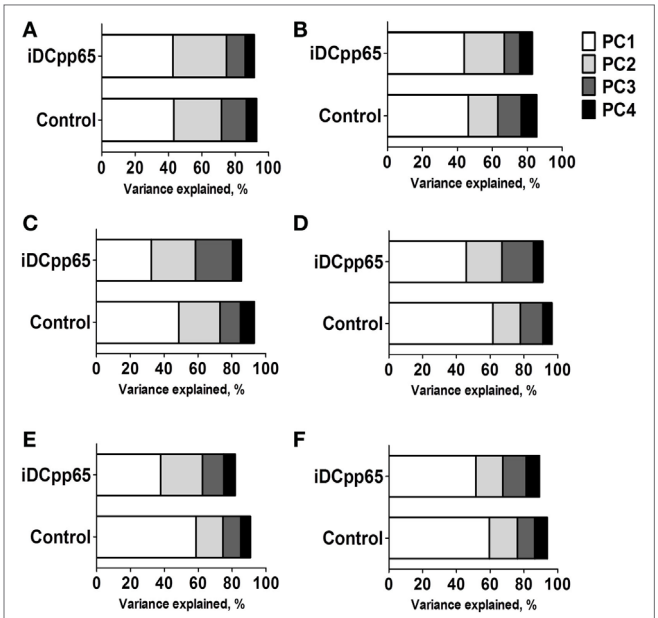

FIGURE 8 | Principal components explaining the variance in different tissues. Variance explained by using the first four components in control and induced dendritic cells expressing pp65 (iDCpp65) mice. Principal components were established based on cell counts and frequencies in thymus, bone marrow (BM), and spleen. In the case of combined peripheral and mesenteric lymph nodes (MLN), peripheral blood (PB), and MLNs only frequencies were used. The analysis showed that the variance distributions among the first main components were similar for the two data sets. The analysis indicated that the variance distributions among the first main components were similar for thymus (Thy) **(A)** and BM **(B)** but more variable for spleen (SPL) **(C)**, combined peripheral and MLNs (PLN + MLN) **(D)**, PB **(E)**, and MLN **(F)**. The number of samples (*n*) for control/immunized varied for each tissue: thymus 11/16; PLN + MLN 7/12; MLN 10/11; SP, BM, PB 11/17.

CD8SP% and CD3% cells were highly correlated in the control group, and this correlation was not altered by immunization. This result is in accordance with the classification accuracy performance where ANN could not provide a clear distinction between the control and iDCpp65 groups based on Thy specific marker analyses.

Interestingly, for BM, the correlation patterns between control and iDCpp65 mice showed differences in terms of the correlation strength that exists among specific markers (**Figure 9B**). For example, strongly positively correlated pairs of markers (CD3%, CD4CM#), (CD4%, CD8CM #), and (CD8%, CD8CM#) in the control group lost their correlation properties in the iDCpp65 group.

Noticeably, the same analysis in SPL revealed a considerable differentiation of the variance distributions in control and iDCpp65 mice (**Figure 8C**) and distinguishable correlation patterns in the heat-map analyses (**Figure 9C**; Figure S2C in Supplementary Material). An inversely correlated signature could be seen between CD45# and CD3% (positive correlation in control mice, equal to 0.6325, and negative correlation in iDCpp65 ones, equal to −0.4656) as well as between CD45# and CD4% (positive correlation in control mice, equal to 0.7179, and negative correlation in iDCpp65 ones, equal to −0.4493). The same inversely correlated signature could be also seen between CD45# and CD19% (negative correlation in control mice, equal to −0.6727, and positive correlation in iDCpp65 ones, equal to 0.5202). This indicated that the dynamics of cellular output in the spleen after iDCpp65 favored B cells and not T cells.

For combined PLN and MLN, the variance distributions and the correlative signatures between control and iDCpp65 mice showed considerable differences as well (**Figures 8D** and **9D**; Figure S2D in Supplementary Material). More specifically, the positive strong correlation between CD8% and CD8N% in control mice (equal to 0.8345) became neutral in iDCpp65 (−0.1103). The same weakening in correlation strength was observed between CD8% and CD4N% (the correlation in control mice is equal to 0.8345, while in the immunized ones is equal to 0.1944). Thus, naïve T cell activation and loss of the naïve status by immunization, as determined by the PCA analysis, is physiologically meaningful.

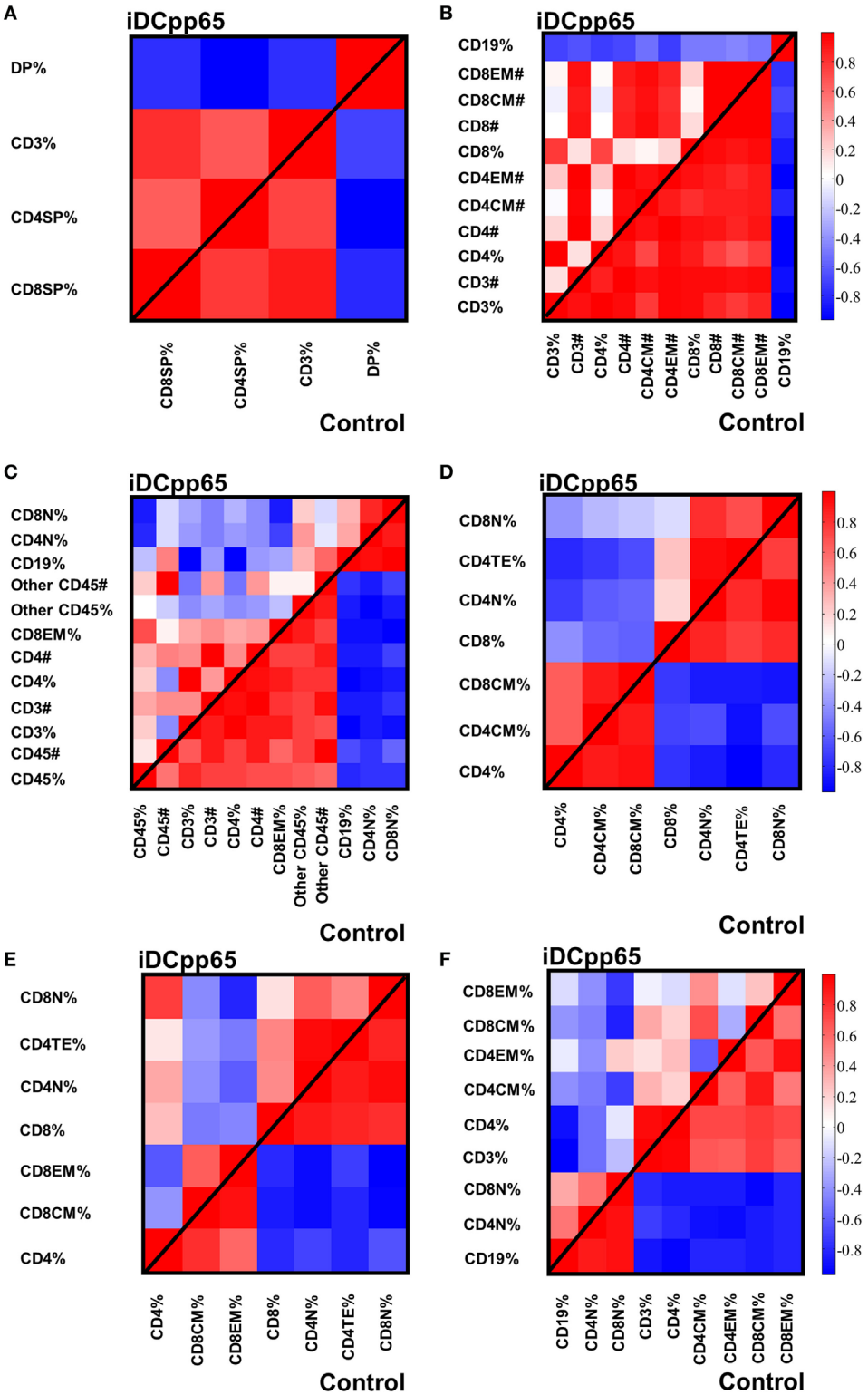

FIGURE 9 | Heat-maps showing the correlations among specifically selected markers between control and induced dendritic cells expressing pp65 (iDCpp65) groups. The markers selected are the ones which highly contribute to the first governing component of the control mice in the different tissues. Analysis was performed using frequencies for bone marrow (BM), combined PLN and mesenteric lymph node (MLN), MLN, and peripheral blood (PB). In spleen (SPL) and thymus (Thy), principal component analysis was performed using cells counts and frequencies. The correlation maps between the specific markers in control and iDCpp65-immunized groups, determined in **(A)** thymus (Thy), **(B)** BM, **(C)** spleen (SPL), **(D)** combined peripheral and MLN (PLN + MLN), **(E)** MLN, and **(F)** PB. The number of samples (*n*) for control/immunized varied for each tissue: thymus 11/16; PLN + MLN 7/12; MLN 10/11; SP, BM, PB 11/17.

The same analysis in MLN revealed important differences in the variance distribution in control and iDCpp65 mice (**Figure 8E**) and considerable correlation changes in the heat-map analysis (**Figure 9E**). Inverse correlated signatures could be seen between CD4% and CD8CM% (positive correlation in control mice, equal to 0.5969 and negative correlation in iDCpp65 ones, equal to −0.618), CD4% and CD8CM% (positive correlation in control mice, equal to 0.8102, and a weakly negative correlation in iDCpp65 ones, equal to −0.384). The same inversely correlated signature could be seen between CD4% and CD8N% (negative correlation in control mice, equal to −0.6346 and positive correlation in iDCpp65 ones, equal to 0.7513).

Finally, in PB, the same analysis revealed a striking difference in the variance distribution (**Figure 8F**) and considerable differences in the heat-map analysis (**Figure 9F**). Inversely correlated signatures could be seen between CD4CM% and CD4EM% (positive correlation in control mice, equal to 0.6414 and negative correlation in iDCpp65 ones, equal to −0.598) as well as between CD4EM% and CD8CM% (positive correlation in control mice, equal to 0.6567 and weakly negative correlation in iDCpp65 ones, equal to −0.3047). The positive strong correlation between CD4EM% and CD8EM% in control mice (equal to 0.94) became neutral in iDCpp65 (−0.09983) and the negative strong correlation between CD19% and CD4EM% in control mice (equal to −0.8088) becomes neutral in iDCpp65 (−0.06359).

The above results showed how we could exploit the intrinsic complexity and heterogeneity of the input markers to gain additional knowledge on the characteristic of an individual immunized mouse. More specifically, by checking the correlation patterns among specifically selected markers in an individual mouse, we could conclude about their immunization status. Together with the classification performance of ANN in the different tissues, these results predicted more pronounced effects of immunization in SPL and PLN combined with MLN compared with other tissues.

DISCUSSION

The use of immune deficient mice humanized with human HSCs to study and characterize the maturation of human T cells after immunizations in different lymphatic tissues generate large data sets and highly complex results. Long-term studies (20 or more weeks after transplantation) and large mouse cohorts (15 mice or more) have been commonly used (6). The initial HSC engraftment in BM, early T cell development in thymus and the egress of naïve T cells to the periphery recapitulate the general patterns found in immune competent mice and in humans (5, 33, 34) in the first 10–15 weeks after transplantation. However, analyses of the T cell maturation in secondary lymphoid organs have shown to be more heterogeneous and predictive of the quality of the immune reconstitution and development of mature T cells. This reflects the "personalized" condition of different CB donors with heterogeneous genetic backgrounds, which is amplified in a xenograft system. In addition, although the engraftment of human HSCs (35) and the higher thymic output in humanized female mice (25) had been previously reported, the relevance of the mouse sex in determining the impact of immunizations and the predictability of human T cell responses had not been presented. All these factors were taken in account when exploring humanized mice for testing a new vaccine type.

In the present work, we sought to evaluate the multidimensional spatial effects of a potent cellular vaccine against HCMV matched to the HSC donor and providing the three main relevant signals for both antigenic and homeostatic activation of T cells: an immune-dominant antigen presented *via* HLA class I and II, co-stimulatory ligands, and inflammatory cytokines. Thus, iDCpp65 which are viable for 2–3 weeks *in vivo* and effectively migrate to lymph node structures (19) were used to accelerate and potently boost the human T cell development and functional responses in humanized mice. As anticipated, improved human T cell development and maturation were longitudinally observed in PB and terminally in several lymphatic tissues in iDCpp65-immunized mice at 20-weeks after HSCT. These results complemented previous findings obtained in shorter (16 weeks) and in longer (up to 36 weeks) iDCpp65 immunization models (20, 24). Advanced statistical analyses showed that iDCpp65 immunizations promoted a typical memory T cell signature (above all for $CD8^+$ T cells) which was most prominent for T cells homing lymph nodes and spleen. As most of the studies using humanized mice have focused on analyses of human cells in blood and spleen (5, 8, 18) it is important to emphasize that, as seen from the ANN and PCA analyses, the quantity and quality of human T cell reactivity in peripheral and MLNs (even if they are small and difficult to be sampled) have to be taken in account, as lymph nodes represent the prime tissue for interactions between antigen-presenting cells with naïve $CD8^+$ and $CD4^+$ T cells. Further, the levels of human IFN-γ in plasma increased upon immunization.

In general, both cellular and cytokine immune effects were more accentuated for female mice. This confirmed and expanded our previously reported observation that humanized female mice have higher output of naïve T cells than humanized male mice until 12 weeks after HSCT (25). Around 16 weeks after HSCT, male mice showed higher development of mature T cells and by 20 weeks after HSCT, the frequencies of human $CD45^+$ cells, naïve and memory T cells in PB equalized between the sexes. Notta et al. showed that between 10 and 12 weeks after HSCT, females transplanted with limiting amounts of HSCs obtained from several CB units generally exhibited a higher frequency of $huCD45^+$ cells than male mice (35). Therefore, CB-HSCT in humanized mice could potentially mirror the effect of sex steroids on human immune reconstitution since temporarily blocking sex steroids before HSCT in patients, increased thymus function and enhanced the rate of T-cell regeneration (36). Responses to various types of vaccination are often higher among women [for a review see Ref. (37)], who are able to mount stronger humoral responses than men. A possible explanation for this phenomenon is based again on major sex steroid hormones such as the typical "female" hormone estradiol that enhances the adaptive and innate immune systems, and the "male" hormone testosterone considered immune suppressive.

Noteworthy, women display higher T helper type 2 (Th2) responses, whereas males favor Th1 responses (37). Although sex-specific responses to distinct vaccines are not usually considered and have been reported in a few clinical trials, this is an important factor also to be considered in preclinical research, when testing new vaccine types, including when humanized mice are used as a potency model. In the current model, we obtained not only higher responses, but exploring the ANN, also a better prediction of response. Thus, as a logical approach to reduce the numbers of humanized mice when testing a vaccine is initially favoring the use of female mice. In addition, from now on, studies on humanized mice should consider male and female responses as distinct responses, and should be analyzed separately and compared.

We also showed that the statistical methods can be complemented with an ANN algorithm in order to pin down the complexity of a multidimensional data sets including usual immune markers such as frequencies of the human cell phenotypes among lymphatic tissues and considering mouse sexes. As generally proposed for ANNs (38), we were able to demonstrate here that the ANN based on the humanized mouse data could "learn" to recognize the immune properties of immunized versus control mice. For studies in humans, ANNs were built with independent immunologic variables such as cell proliferation, phenotypic markers, and cytokine expression in the context of prostate cancer and in HSCT patients (39–41). To our knowledge, the application of ANNs to humanized mouse models for predicting the accuracy of immune response or defining signatures of T cell responses was not previously performed. The identification of lymph node and spleen as the most predictive organs for the immune state of control versus immunized mice might be further improved by releasing the assumption of statistically independent tissues. Along with local immune population dynamics, it would be of interest to investigate the immune cell trafficking dynamics between different tissues (42, 43). In this way, we could relax the assumption of tissue independence. However, the immune cell trafficking is an open challenge yet to be solved in future research.

Altogether, the current approach, modalities of analyses and observations give valuable information for further planning of *in vivo* testing of vaccines and immune modulators in humanized mice. The 3R principle (*R*eplace animal testing, *R*educe the number of animals, and *R*efine the analyses) can thus be advanced for Reduce and Refine: (i) by using (at least initially) female mice and (ii) exploring bio-informatics methods such as ANN to complement traditional statistical analyses in order to define the most important tissues (such as spleen and lymph nodes) and the PCA that reveal signatures and correlations of immune responses for different lymphatic tissues.

ETHICS STATEMENT

All subjects donating cord blood provided written informed consent. This study was approved by the Ethics Committee of Hannover Medical School.

AUTHOR CONTRIBUTIONS

RS planed the project, designed experiments, obtained funding and regulatory approvals, enrolled collaborators, interpreted the data, and wrote and edited the manuscript. VV conducted experiments, analyzed data, and wrote the first manuscript draft. BS, ST, AS, LG, and CR assisted in preparation and analyses of humanized mice. CF performed the human cytokine array analyses. CK assisted in the procurement and collection of HSC for the studies. LS performed the statistical analyses. AR, PR, HH, and MM-H performed the ANN and PCA analyses, interpreted the data, and wrote and edited the manuscript. SK and UK assisted in the execution of the iDCpp65 quality control analyses, and revised the manuscript.

ACKNOWLEDGMENTS

The authors thank all other current and past members of the Regenerative Immune Therapies Applied Laboratory for their valuable contributions. The authors thank Sebastian Binder for revising the manuscript.

FUNDING

This work was supported by grants of the German Research Council (DFG/SFB738 Project A6 to RS; DFG/REBIRTH Unit 6.4 to RS, Unit 6.3 to CF) and the German Center for Infections Research (DZIF-TTU07.803 to RS). VV received a DAAD/ZIB Ph.D. fellowship, ST received a RegSci Ph.D. fellowship and CDR received a CNPq "Sciences without Borders" post-doctoral fellowship. HH and AR would like to acknowledge the SYSMIFTA ERACoSysMed grant (031L0085B) for the financial support of this work. MM-H and HH were supported by the German Federal Ministry of Education and Research within the Measures for the Establishment of Systems Medicine, project SYSIMIT (BMBF eMed project SYSIMIT, FKZ: 01ZX1308B and 01ZX1608B). PR and MM-H were supported by the Human Frontier Science Program (RGP0033/2015).

SUPPLEMENTARY MATERIAL

The Supplementary Material for this article can be found online at http://www.frontiersin.org/article/10.3389/fimmu.2017.01709/full#supplementary-material.

REFERENCES

1. Kenney LL, Shultz LD, Greiner DL, Brehm MA. Humanized mouse models for transplant immunology. *Am J Transplant* (2016) 16(2):389–97. doi:10.1111/ajt.13520
2. Theocharides AP, Rongvaux A, Fritsch K, Flavell RA, Manz MG. Humanized hemato-lymphoid system mice. *Haematologica* (2016) 101(1):5–19. doi:10.3324/haematol.2014.115212
3. Walsh NC, Kenney LL, Jangalwe S, Aryee KE, Greiner DL, Brehm MA, et al. Humanized mouse models of clinical disease. *Annu Rev Pathol* (2017) 12:187–215. doi:10.1146/annurev-pathol-052016-100332
4. Brehm MA, Cuthbert A, Yang C, Miller DM, Dilorio P, Laning J, et al. Parameters for establishing humanized mouse models to study human immunity: analysis of human hematopoietic stem cell engraftment in three immunodeficient strains of mice bearing the IL2rγnull mutation. *Clin Immunol* (2010) 135:84–98. doi:10.1016/j.clim.2009.12.008

5. Harris DT, Badowski M. Long term human reconstitution and immune aging in NOD-Rag (-)-gamma chain (-) mice. *Immunobiology* (2014) 219(2):131–7. doi:10.1016/j.imbio.2013.08.013
6. Audige A, Rochat MA, Li D, Ivic S, Fahrny A, Muller CKS, et al. Long-term leukocyte reconstitution in NSG mice transplanted with human cord blood hematopoietic stem and progenitor cells. *BMC Immunol* (2017) 18(1):28. doi:10.1186/s12865-017-0209-9
7. Huntington ND, Legrand N, Alves NL, Jaron B, Weijer K, Plet A, et al. IL-15 trans-presentation promotes human NK cell development and differentiation in vivo. *J Exp Med* (2009) 206(1):25–34. doi:10.1084/jem.20082013
8. Rongvaux A, Willinger T, Martinek J, Strowig T, Gearty SV, Teichmann LL, et al. Development and function of human innate immune cells in a humanized mouse model. *Nat Biotechnol* (2014) 32(4):364–72. doi:10.1038/nbt.2858
9. Danner R, Chaudhari SN, Rosenberger J, Surls J, Richie TL, Brumeanu TD, et al. Expression of HLA class II molecules in humanized NOD.Rag1KO.IL2RgcKO mice is critical for development and function of human T and B cells. *PLoS One* (2011) 6(5):e19826. doi:10.1371/journal.pone.0019826
10. Shultz LD, Saito Y, Najima Y, Tanaka S, Ochi T, Tomizawa M, et al. Generation of functional human T-cell subsets with HLA-restricted immune responses in HLA class I expressing NOD/SCID/IL2rγnull humanized mice. *Proc Natl Acad Sci U S A* (2010) 107:13022–7. doi:10.1073/pnas.1000475107
11. Traggiai E, Chicha L, Mazzucchelli L, Bronz L, Piffaretti JC, Lanzavecchia A, et al. Development of a human adaptive immune system in cord blood cell-transplanted mice. *Science* (2004) 304(5667):104–7. doi:10.1126/science.1093933
12. Tonomura N, Habiro K, Shimizu A, Sykes M, Yang Y-G. Brief report antigen-specific human T-cell responses and T cell – dependent production of human antibodies in a humanized mouse model. *Blood* (2008) 111:4293–6. doi:10.1182/blood-2007-11-121319.The
13. Lan P, Tonomura N, Shimizu A, Wang S, Yang YG. Reconstitution of a functional human immune system in immunodeficient mice through combined human fetal thymus/liver and CD34+ cell transplantation. *Blood* (2006) 108(2):487–92. doi:10.1182/blood-2005-11-4388
14. Melkus MW, Estes JD, Padgett-Thomas A, Gatlin J, Denton PW, Othieno FA, et al. Humanized mice mount specific adaptive and innate immune responses to EBV and TSST-1. *Nat Med* (2006) 12(11):1316–22. doi:10.1038/nm1431
15. Saito Y, Ellegast JM, Manz MG. Generation of humanized mice for analysis of human dendritic cells. *Methods Mol Biol* (2016) 1423:309–20. doi:10.1007/978-1-4939-3606-9_22
16. Bol KF, Schreibelt G, Gerritsen WR, de Vries IJ, Figdor CG. Dendritic cell-based immunotherapy: state of the art and beyond. *Clin Cancer Res* (2016) 22(8):1897–906. doi:10.1158/1078-0432.CCR-15-1399
17. Lapenta C, Santini SM, Spada M, Donati S, Urbani F, Accapezzato D, et al. IFN-alpha-conditioned dendritic cells are highly efficient in inducing cross-priming CD8(+) T cells against exogenous viral antigens. *Eur J Immunol* (2006) 36(8):2046–60. doi:10.1002/eji.200535579
18. Meixlsperger S, Leung CS, Ramer PC, Pack M, Vanoaica LD, Breton G, et al. CD141+ dendritic cells produce prominent amounts of IFN-alpha after dsRNA recognition and can be targeted via DEC-205 in humanized mice. *Blood* (2013) 121(25):5034–44. doi:10.1182/blood-2012-12-473413
19. Salguero G, Daenthanasanmak A, Munz C, Raykova A, Guzman CA, Riese P, et al. Dendritic cell-mediated immune humanization of mice: implications for allogeneic and xenogeneic stem cell transplantation. *J Immunol* (2014) 192(10):4636–47. doi:10.4049/jimmunol.1302887
20. Daenthanasanmak A, Salguero G, Sundarasetty BS, Waskow C, Cosgun KN, Guzman CA, et al. Engineered dendritic cells from cord blood and adult blood accelerate effector T cell immune reconstitution against HCMV. *Mol Ther Methods Clin Dev* (2015) 1:14060. doi:10.1038/mtm.2014.60
21. Sundarasetty BS, Kloess S, Oberschmidt O, Naundorf S, Kuehlcke K, Daenthanasanmak A, et al. Generation of lentivirus-induced dendritic cells under GMP-compliant conditions for adaptive immune reconstitution against cytomegalovirus after stem cell transplantation. *J Transl Med* (2015) 13:240. doi:10.1186/s12967-015-0599-5
22. Boppana SB, Britt WJ. Recognition of human cytomegalovirus gene products by HCMV-specific cytotoxic T cells. *Virology* (1996) 222:293–6. doi:10.1006/viro.1996.0424
23. Klarenbeek PL, Remmerswaal EBM, ten Berge IJM, Doorenspleet ME, van Schaik BDC, Esveldt REE, et al. Deep sequencing of antiviral T-cell responses to HCMV and EBV in humans reveals a stable repertoire that is maintained for many years. *PLoS Pathog* (2012) 8(9):e1002889. doi:10.1371/journal.ppat.1002889
24. Sundarasetty B, Volk V, Theobald SJ, Rittinghausen S, Schaudien D, Neuhaus V, et al. Human effector memory T helper cells engage with mouse macrophages and cause graft-versus-host-like pathology in skin of humanized mice used in a nonclinical immunization study. *Am J Pathol* (2017) 187(6):1380–98. doi:10.1016/j.ajpath.2017.02.015
25. Volk V, Schneider A, Spineli LM, Grosshennig A, Stripecke R. The gender gap: discrepant human T-cell reconstitution after cord blood stem cell transplantation in humanized female and male mice. *Bone Marrow Transplant* (2016) 51(4):596–7. doi:10.1038/bmt.2015.290
26. James G, Witten D, Hastie T, Tibshirani R. *An Introduction to Statistical Learning*. New York: Springer-Verlag (2013).
27. Kooreman NG, de Almeida PE, Stack JP, Nelakanti RV, Diecke S, Shao NY, et al. Alloimmune responses of humanized mice to human pluripotent stem cell therapeutics. *Cell Rep* (2017) 20(8):1978–90. doi:10.1016/j.celrep.2017.08.003
28. Haykin S. *Neural Networks: A Comprehensive Foundation*. NY: Macmillan College Publishing (1994).
29. Kirschen RH, O'Higgins EA, Lee RT. The Royal London Space Planning: an integration of space analysis and treatment planning: part I: assessing the space required to meet treatment objectives. *Am J Orthod Dentofacial Orthop* (2000) 118(4):448–55. doi:10.1067/mod.2000.109031
30. Sharma B, Venugopalan K. Comparison of neural network training functions for hematoma classification in brain CT images. *IOSR J Comput Engin* (2014) 16(1):31–5. doi:10.9790/0661-16123135
31. Jackson JE. *A User's Guide to Principal Components*. New York: John Wiley & Sons (2004). 569 p.
32. Salguero G, Sundarasetty BS, Borchers S, Wedekind D, Eiz-Vesper B, Velaga S, et al. Preconditioning therapy with lentiviral vector-programmed dendritic cells accelerates the homeostatic expansion of antigen-reactive human T cells in NOD.Rag1-/-.IL-2rgammac-/- mice. *Hum Gene Ther* (2011) 22(10):1209–24. doi:10.1089/hum.2010.215
33. Komanduri KV, John LSS, de Lima M, McMannis J, Rosinski S, McNiece I, et al. Delayed immune reconstitution after cord blood transplantation is characterized by impaired thymopoiesis and late memory T-cell skewing. *Blood* (2007) 110(13):4543–51. doi:10.1182/blood-2007-05-092130
34. Bosch M, Khan FM, Storek J. Immune reconstitution after hematopoietic cell transplantation. *Curr Opin Hematol* (2012) 19(4):324–35. doi:10.1097/MOH.0b013e328353bc7d
35. Notta F, Doulatov S, Dick JE. Engraftment of human hematopoietic stem cells is more efficient in female NOD/SCID/IL-2Rgc-null recipients. *Blood* (2010) 115(18):3704–7. doi:10.1182/blood-2009-10-249326
36. Sutherland JS, Spyroglou L, Muirhead JL, Heng TS, Prieto-Hinojosa A, Prince HM, et al. Enhanced immune system regeneration in humans following allogeneic or autologous hemopoietic stem cell transplantation by temporary sex steroid blockade. *Clin Cancer Res* (2008) 14(4):1138–49. doi:10.1158/1078-0432.CCR-07-1784
37. Giefing-Kroll C, Berger P, Lepperdinger G, Grubeck-Loebenstein B. How sex and age affect immune responses, susceptibility to infections, and response to vaccination. *Aging Cell* (2015) 14(3):309–21. doi:10.1111/acel.12326
38. Shouval R, Bondi O, Mishan H, Shimoni A, Unger R, Nagler A. Application of machine learning algorithms for clinical predictive modeling: a data-mining approach in SCT. *Bone Marrow Transplant* (2014) 49(3):332–7. doi:10.1038/bmt.2013.146
39. Shouval R, Labopin M, Unger R, Giebel S, Ciceri F, Schmid C, et al. Prediction of hematopoietic stem cell transplantation related mortality- lessons learned from the in-silico approach: a European Society for Blood and Marrow Transplantation Acute Leukemia Working Party Data Mining Study. *PLoS One* (2016) 11(3):e0150637. doi:10.1371/journal.pone.0150637
40. Michael A, Ball G, Quatan N, Wushishi F, Russell N, Whelan J, et al. Delayed disease progression after allogeneic cell vaccination in hormone-resistant prostate cancer and correlation with immunologic variables. *Clin Cancer Res* (2005) 11(12):4469–78. doi:10.1158/1078-0432.CCR-04-2337
41. Murphy GP, Snow P, Simmons SJ, Tjoa BA, Rogers MK, Brandt J, et al. Use of artificial neural networks in evaluating prognostic factors determining the response to dendritic cells pulsed with PSMA peptides

in prostate cancer patients. *Prostate* (2000) 42(1):67–72. doi:10.1002/(Sici)1097-0045(20000101)42:1<67:Aid-Pros8>3.0.Co;2-I

42. Milanez-Almeida P, Meyer-Hermann M, Toker A, Khailaie S, Huehn J. Foxp3+ regulatory T-cell homeostasis quantitatively differs in murine peripheral lymph nodes and spleen. *Eur J Immunol* (2015) 45(1):153–66. doi:10.1002/eji.201444480
43. Marino S, El-Kebir M, Kirschner D. A hybrid multi-compartment model of granuloma formation and T cell priming in tuberculosis. *J Theor Biol* (2011) 280(1):50–62. doi:10.1016/j.jtbi.2011.03.022

Conflict of Interest Statement: One of the corresponding authors is currently applying for a patent related to the content of the manuscript: R. Stripecke, G. Salguero, A. Daenthasanmak, A. Ganser. "Induced dendritic cells and uses thereof" (PCT/EP2013/052485). All other authors declare that the research was conducted in the absence of any commercial or financial relationships that could be construed as a potential conflict of interest.

frontiers in Immunology

REVIEW
published: 15 January 2018
doi: 10.3389/fimmu.2017.01823

Type I Interferon Responses by HIV-1 Infection: Association with Disease Progression and Control

*Andrew Soper[1,2], Izumi Kimura[1,3], Shumpei Nagaoka[1,4], Yoriyuki Konno[1,4], Keisuke Yamamoto[1,2], Yoshio Koyanagi[1] and Kei Sato[1,5]**

[1] Laboratory of Systems Virology, Department of Biosystems Science, Institute for Frontier Life and Medical Sciences, Kyoto University, Kyoto, Japan, [2] Graduate School of Medicine, Kyoto University, Kyoto, Japan, [3] Graduate School of Pharmaceutical Sciences, Kyoto University, Kyoto, Japan, [4] Graduate School of Biostudies, Kyoto University, Kyoto, Japan, [5] CREST, Japan Science and Technology Agency, Kawaguchi, Japan

Human immunodeficiency virus type 1 (HIV-1) is the causative agent of acquired immunodeficiency syndrome and its infection leads to the onset of several disorders such as the depletion of peripheral CD4$^+$ T cells and immune activation. HIV-1 is recognized by innate immune sensors that then trigger the production of type I interferons (IFN-Is). IFN-Is are well-known cytokines eliciting broad anti-viral effects by inducing the expression of anti-viral genes called interferon-stimulated genes (ISGs). Extensive *in vitro* studies using cell culture systems have elucidated that certain ISGs such as APOBEC3G, tetherin, SAM domain and HD domain-containing protein 1, MX dynamin-like GTPase 2, guanylate-binding protein 5, and schlafen 11 exert robust anti-HIV-1 activity, suggesting that IFN-I responses triggered by HIV-1 infection are detrimental for viral replication and spread. However, recent studies using animal models have demonstrated that at both the acute and chronic phase of infection, the role of IFN-Is produced by HIV or SIV infection in viral replication, spread, and pathogenesis, may not be that straightforward. In this review, we describe the pluses and minuses of HIV-1 infection stimulated IFN-I responses on viral replication and pathogenesis, and further discuss the possibility for therapeutic approaches.

Keywords: type I interferon, human immunodeficiency virus type 1, innate immunity, intrinsic immunity, interferon-stimulated gene, restriction factor, humanized mouse

OPEN ACCESS

Edited by:
Moriya Tsuji,
Aaron Diamond AIDS Research Center, United States

Reviewed by:
Thorsten Demberg,
Immatics Biotechnologies, Germany
Anita S. Iyer,
Harvard Medical School, United States
Lishan Su,
University of North Carolina at Chapel Hill, United States

****Correspondence:***
Kei Sato
ksato@virus.kyoto-u.ac.jp

Specialty section:
This article was submitted to Vaccines and Molecular Therapeutics, a section of the journal Frontiers in Immunology

Received: *06 September 2017*
Accepted: *04 December 2017*
Published: *15 January 2018*

Citation:
Soper A, Kimura I, Nagaoka S, Konno Y, Yamamoto K, Koyanagi Y and Sato K (2018) Type I Interferon Responses by HIV-1 Infection: Association with Disease Progression and Control. Front. Immunol. 8:1823. doi: 10.3389/fimmu.2017.01823

HUMAN IMMUNODEFICIENCY VIRUS TYPE 1 (HIV-1) RECOGNITION FOR TYPE I INTERFERON (IFN-I) PRODUCTION

Human immunodeficiency virus type 1 infection in humans induces innate immune responses mediated mainly by IFN-I, including IFN-α and IFN-β, and the roles of IFN-I in responding to HIV-1 infection have been reviewed extensively (1–3). Upon HIV-1 infection into human immune cells, pattern recognition receptors (PRRs) and cytosolic sensors are involved in the sensing of viral cDNA or RNA, respectively. After HIV-1 infects human cells, cDNA is synthesized by RNA reverse transcription. cDNA is then recognized by either IFN-γ inducible protein 16 (IFI16) or cyclic GMP-AMP (cGAMP) synthase (cGAS) (4–9). cGAS especially recognizes cDNA and subsequently produces cGAMP. IFI16 and cGAMP both activate stimulator of interferon gene (STING; also known as transmembrane protein 173). Activated STING in turn recruits and activates TANK binding kinase 1 which phosphorylates IFN regulatory factor 3 (IRF3). Finally, IFN-I is produced by IRF3 in the pathways highlighted on the left of **Figure 1** (10–17).

IFI16 is expressed in epithelial cells, fibroblasts, and endothelial cells (4), as well as cells from hematopoietic lineages such as macrophages (5) and CD4+ T cells (6). Contrastingly, the cGAS-STING pathway is not present in T cells (6), but does play an important role in IFN-I production in myeloid lineages including macrophages (7) and monocyte-derived dendritic cells (MDDCs) (8, 9). As CD4+ T cells are more permissive to HIV-1 infection and replication than macrophages and MDDCs, this can probably be explained by the lack of cGAS expression in CD4+ T cells (5, 6).

HIV-1 single-stranded RNA can also be sensed by toll-like receptor 7 (TLR7), a PRR, when viruses are enclosed by endosomes (10, 11). Unlike IFI16 and cGAS, plasmacytoid dendritic cells (pDCs) express high levels of TLR7 (12, 13). TLR7 mediates another cascade ultimately resulting in either IRF7 homodimers translocating to the nucleus to bind to IRFBS, or the freeing of NFκB to activate the transcription of *IFN-I* genes *via* binding to the NFκB binding site (14).

IFN-STIMULATING GENES (ISGs): EFFECTOR MOLECULES EXHIBITING ANTI-VIRAL EFFECTS

Once IFN-I is produced, this protein binds to its receptor molecule that is expressed on the cell surface. IFN-I receptor (IFNAR) consists of two independent proteins, IFNAR1 (IFN-α/β receptor α chain) and IFNAR2 (IFN-α/β receptor β chain) (**Figure 2**). Binding of the ligand IFN-I to the IFN-I receptor induces the heterodimerization of IFNAR1 and IFNAR2, which leads to the autophosphorylation of Janus kinase (JAK) (**Figure 2**). The phosphorylated JAK then induces the heterodimerization of

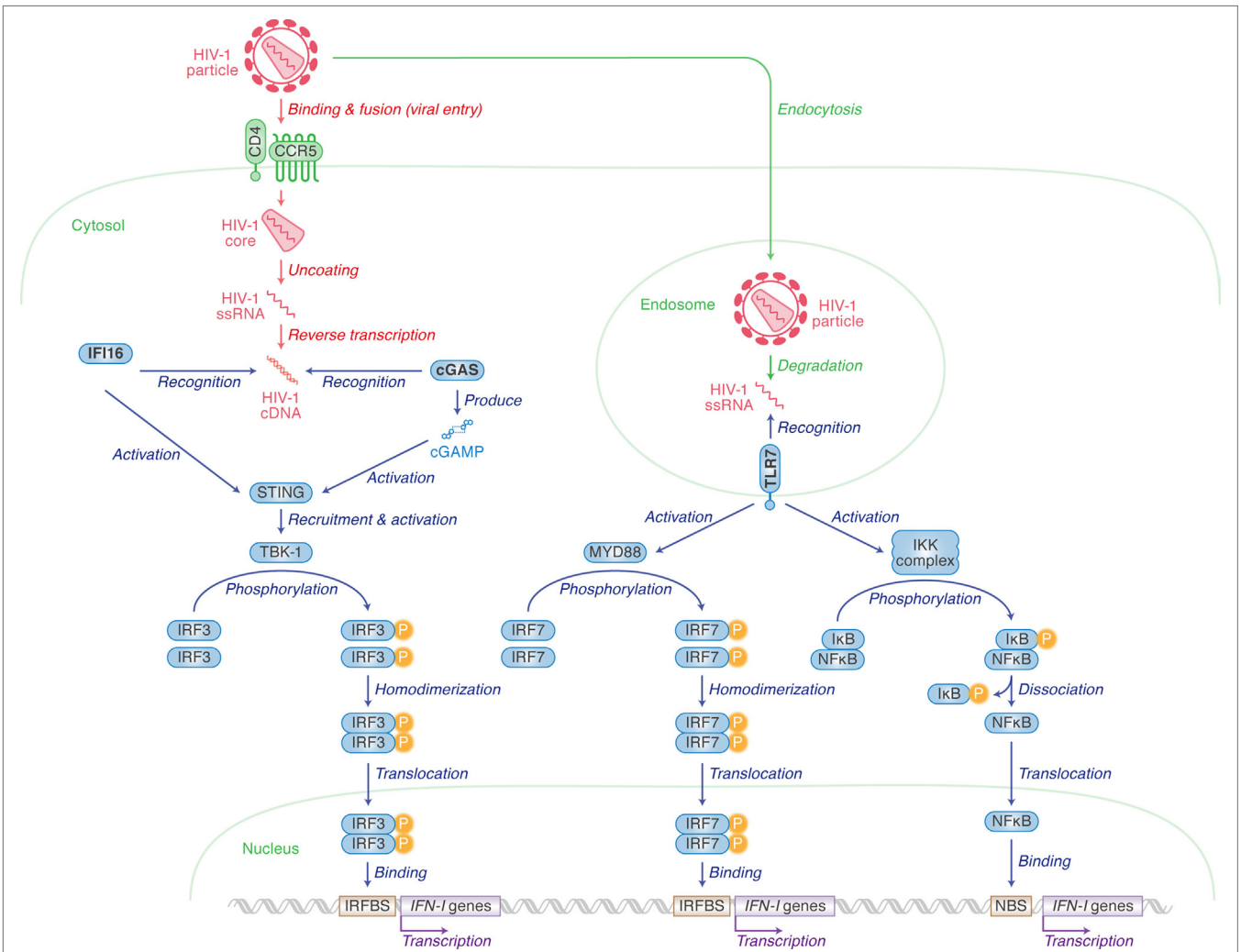

FIGURE 1 | Pattern recognition receptors (PRRs) for human immunodeficiency virus type 1 (HIV-1) recognition and the following pathway for triggering type I interferon (IFN-I) expression. Cellular actions are indicated in green (in italic) with arrows, and viral replication steps are indicated in red (in italic) with arrows. Cellular actions triggered by PRRs [IFN-γ inducible protein 16 (IFI16), cyclic GMP-AMP synthase (cGAS) and toll-like receptor 7 (TLR7)] are indicated in blue (in italic) with arrows. Cellular organelle, viral components, and sensor-related molecules are indicated in green, red, and blue, respectively. "P" with yellow circle indicates phosphorylation. The detail of each step is described in the main text.

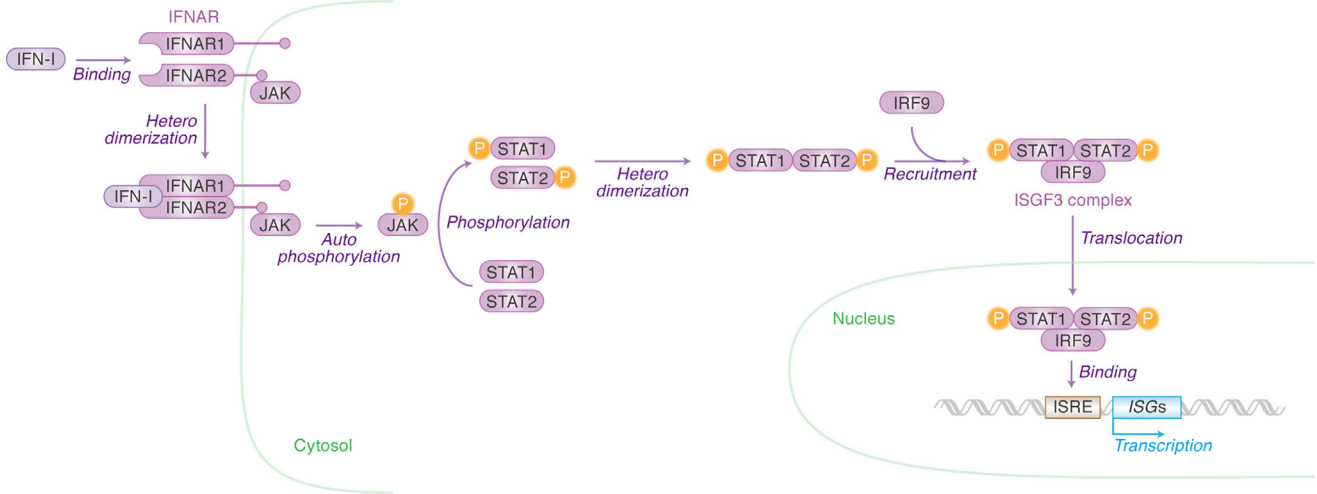

FIGURE 2 | Type I interferons (IFN-I)-initiated signaling pathway leading to interferon-stimulated gene (ISG) expression. Cellular actions triggered by IFN-I [Janus kinase (JAK)/signal transducer and activator of transcription (STAT) pathway] are indicated in purple (in italic) with arrows. Cellular organelle and the cellular molecules related to JAK/STAT pathway are indicated in green and purple, respectively. The detail of each step is described in the main text. "P" with yellow circle indicates phosphorylation.

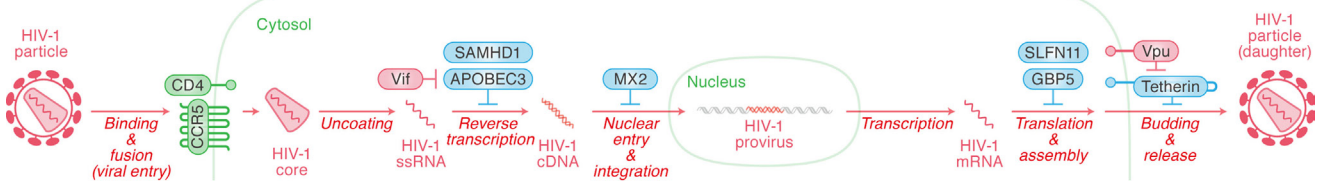

FIGURE 3 | Restriction factors (RFs) controlling human immunodeficiency virus type 1 (HIV-1) replication and viral antagonists. Viral replication steps are indicated in red (in italic) with arrows. The RFs inhibiting viral replication at respective step are indicated in cyan, while the viral accessory proteins counteracting the action of certain RFs are indicated in red. Cellular organelle and viral components are indicated in green and red, respectively. The detail of each step is described in the main text.

signal transducer and activator of transcription 1 (STAT1) and STAT2 *via* phosphorylation (**Figure 2**). This cascade is known as the JAK/STAT pathway. The STAT1–STAT2 heterodimer recruits IFN regulatory factor 9 and forms the IFN-stimulated gene factor 3 (ISGF3) complex. After the entry of ISGF3 complex into the nucleus, this complex binds to the IFN-stimulated response element located in the promoter region of ISGs and initiates their transcription (**Figure 2**) (15). There are 17 subtypes of IFN-Is (16), and there have now been over 300 ISGs identified. In humans, however, is it not known in which tissues the different INF-α isoforms are expressed upon viral infection nor which cells express them. This is an intriguing issue and will no doubt be revealed in future investigations using techniques such as next generation sequencing.

RESTRICTION FACTORS (RFs): ISGs POTENTLY CONTROL HIV-1 REPLICATION

Type I interferon treatment efficiently suppresses HIV-1 replication in *in vitro* cell cultures (17), meaning that certain ISGs potently control HIV-1 replication. Among the more than 300 known ISGs, certain ones are known to exhibit robust anti-HIV-1 activity and these ISGs are referred to as "intrinsic immunity" or "RFs." Although the types of RFs appear numerous, the most well studied to date include SAM domain and HD domain-containing protein 1 (SAMHD1) and apolipoprotein B mRNA editing enzyme catalytic-like 3 (APOBEC3) (targeting HIV-1 reverse transcription), MX dynamin-like GTPase 2 (MX2) (targeting nuclear entry), schlafen 11 (SLFN11) (targeting transcription), guanylate-binding protein 5 (GBP5) (targeting post-translational modification), and tetherin (targeting release) (**Figure 3**). In this section, we briefly summarize the restriction mechanisms employed by RFs that inhibit HIV-1 replication at multiple stages.

SAM Domain and HD Domain-Containing Protein 1

During the process of HIV-1 reverse transcription, viral reverse transcriptase requires deoxynucleoside triphosphates (dNTPs) as a substrate for the synthesis of viral cDNA (18, 19). SAMHD1 is a cytosolic enzyme with phosphohydrolase activity that enzymatically degrades ("hydrolyzes") dNTPs (18–20).

Deoxyguanosine triphosphate in particular, binds to the allosteric site of SAMHD1 and activates SAMHD1's hydrolytic activity (18).

SAM domain and HD domain-containing protein 1 is expressed in peripheral $CD4^+$ leukocytes including myeloid cells [e.g., macrophages and dendritic cells (DCs)] and $CD4^+$ T cells (19). The experiments in *in vitro* cell cultures demonstrate that SAMHD1 restricts HIV-1 infection in non-dividing cells such as macrophages (plus phorbol 12-myristate 13-acetate-stimulated macrophage-like THP-1 cell line), DCs, and resting $CD4^+$ T cells by degrading dNTPs (18, 19).

In comparison with dividing (i.e., cycling and activated/proliferating) cells, the level of intracellular dNTP is much lower in non-dividing cells (21). Previous studies have suggested that SAMHD1 plays a crucial role in maintaining a low pool of cellular dNTPs in non-dividing cells, including resting $CD4^+$ T cells, which may reduce the risk of retroviral insult without disrupting homeostasis in the non-dividing cell environment (21, 22). In dividing cells, including activated $CD4^+$ T cells, SAMHD1 is post-transcriptionally inactivated: cyclin-dependent kinases 1 (CDK1) and CDK2 phosphorylate the threonine residue at position 592 of SAMHD1 (23). This phosphorylation impairs SAMHD1's hydrolyzing activity and results in the loss of its anti-HIV-1 activity (23). CDKs, including CDK1 and CDK2, are key regulators of the cell cycle that activate cyclins during cell division (24). As dividing cells require a greater pool of dNTPs, SAMHD1's enzymatic activity is inhibited by CDK1/2-mediated phosphorylation (25).

To overcome SAMHD1-mediated restriction, an accessory protein of human lentiviruses, viral protein X (Vpx), degrades SAMHD1 *via* the ubiquitin/proteasome-dependent pathway (22). The Q76A mutation in Vpx results in the loss of SAMHD1 degradation ability suggesting that the glutamine at position 76 is critical (22). Importantly, the *vpx* gene is not encoded by HIV-1 but HIV-2, another human lentivirus and causative agent of acquired immunodeficiency syndrome (AIDS) (26).

Human immunodeficiency virus type 1 and HIV-2 are evolutionarily and phylogenetically distinct, and more intriguingly, Etienne et al. have shown evidence indicating that the lineage of primate lentiviruses, including HIV-1, lost the *vpx* gene during viral evolution (27). These observations raise an incongruous insight: although RFs such as APOBEC3 and tetherin (see below) can be degraded and antagonized by HIV-1 accessory proteins, HIV-1 does not possess any counterparts to counteract SAMHD1. Additionally, HIV-1 is able to replicate in macrophages that express SAMHD1 in its anti-viral state. Moreover, HIV-1 is more pathogenic than HIV-2 in spite of the absence of anti-SAMHD1 factor(s) (26). These insights may imply that SAMHD1 is not critical for the restriction of HIV-1 replication. In this regard, a previous paper has revealed that the concentration of dNTP required for the reverse transcriptase of HIV-1 is clearly lower than that of HIV-2, and HIV-1 can efficiently reverse transcribe a single strand template with a lower level of dNTPs (21). Therefore, HIV-1 may have evolved to overcome SAMHD1-mediated antiviral activity by decreasing the requirement for a high-dNTP concentration.

In addition to the phosphohydrolase activity, SAMHD1 possesses ribonuclease (RNase) activity. Ryoo et al. have reported that RNase activity but not phosphohydrolase is required for exhibiting an anti-HIV-1 effect (28). This is shown with the D137N mutant of SAMHD1, which possesses RNase activity but specifically loses phosphohydrolase activity and is still able to restrict HIV-1 infection. In contrast, the Q548A mutant of SAMHD1 that loses RNase activity but maintains phosphohydrolase activity is ineffective at restricting HIV-1 (28). Moreover, the phosphorylation of SAMHD1 at T592 negatively regulates its RNase activity in cells and impedes HIV-1 restriction (28), suggesting that the RNase activity of SAMHD1 is responsible for preventing HIV-1 infection by directly degrading viral RNA (28).

Apolipoprotein B mRNA Editing Enzyme Catalytic-Like 3

Apolipoprotein B mRNA editing enzyme catalytic-like 3 family proteins are cellular cytidine/cytosine deaminases and the human genome encodes seven *APOBEC3* genes: *APOBEC3A*, *B*, *C*, *D*, *F*, *G*, and *H*. Some APOBEC3 family proteins, particularly APOBEC3D, APOBEC3F, APOBEC3G, and certain haplotypes of APOBEC3H (see below), are incorporated into released viral particles and enzymatically remove the amino group ($-NH_2$) of the cytosine residue in the minus-stranded viral DNA during viral reverse transcription. This deamination converts cytosine to uracil, which results in guanine (G) to adenine (A) substitution in the plus-stranded viral DNA (this step is usually referred to as "APOBEC3-mediated G-to-A mutation"). The APOBEC3-mediated G-to-A mutations can result in the insertion of premature termination mutations [e.g., if TGG codon is converted to TGA codon by APOGEC3, the codon encoding tryptophan (TGG) is converted to a stop codon (TGA)]. Also, multiple APOBEC3-mediated G-to-A mutations can lead to the accumulation of non-synonymous mutations, which may produce defective viral proteins.

To overcome APOBEC3-mediated anti-viral action, an accessory protein of HIV-1, viral infectivity factor (Vif), degrades anti-viral APOBEC3 proteins in virus-producing cells *via* the ubiquitin/proteasome-dependent pathway. The relationship between APOBEC3 and Vif has been well studied and reviewed previously [e.g., Ref. (29, 30)].

To elucidate the roles of endogenous APOBEC3 proteins in HIV-1 infection *in vivo*, hematopoietic stem cell (HSC)-transplanted "humanized" mouse models have been utilized. First, *vif*-deficient HIV-1 was incapable of replicating in humanized mice, indicating that Vif is a prerequisite for HIV-1 infection and replication *in vivo* (31). Also, some proviral DNA in infected humanized mice exhibited G-to-A hypermutations, further suggesting that endogenous APOBEC3 protein(s) potently exhibit anti-HIV-1 activity *in vivo* (31).

Secondly, to elucidate which endogenous APOBEC3 protein(s) crucially affect HIV-1 replication *in vivo*, two *vif* mutants have been utilized: one is designated "4A," which is unable to antagonize APOBEC3D and APOBEC3F, while the other is designated "5A," which is unable to antagonize APOBEC3G (32).

As the replication efficacy of both 4A and 5A HIV-1 were significantly lower than that of wild-type (i.e., *vif*-proficient) HIV-1, endogenous APOBEC3D, APOBEC3F, and APOBEC3G are deemed to be potent intrinsic RFs in humanized mice (32). On the other hand, it is intriguing that the viral RNA in the plasma of humanized mice infected with 4A HIV-1 had greater diversity compared with 5A and wild-type HIV-1 sequences (32). This observation suggests that the G-to-A mutation caused by APOBEC3D and APOBEC3F potently contributes toward viral diversification. In this regard, APOBEC3G prefers the GG-to-AG mutation, while APOBEC3D and APOBEC3F prefer a GA-to-AA mutation (33–35). Also, an experimental-mathematical analysis has suggested that APOBEC3G-mediated substitution easily results in nonsense mutations (mainly because "TGG," a codon encoding tryptophan, is converted to "TAG," a stop codon), while the G-to-A mutations mediated by APOBEC3D and APOBEC3F (i.e., GA-to-AA mutation) lead only to missense mutations (33). Therefore, three endogenous APOBEC3 proteins, APOBEC3D, APOBEC3F, and APOBEC3G, possess the ability to suppress HIV-1 replication *in vivo*, while, at the same time, APOBEC3D and APOBEC3F may promote viral diversification.

Third, Nakano et al. have recently addressed the anti-viral effect of APOBEC3H *in vivo* (36). There are seven haplotypes within human *APOBEC3H* genes and APOBEC3H can be categorized based on the protein expression status of three phenotypes: stable (haplotypes II, V, and VII), intermediate (haplotype I), and unstable (haplotypes III, IV, and VI) (37–39). From the retrovirological point of view, only stable APOBEC3H exhibits anti-HIV-1 activity (37–39). Interestingly, although almost all of the naturally occurring HIV-1 Vif proteins can antagonize anti-viral APOBEC3 proteins including APOBEC3D, APOBEC3F, and APOBEC3G, certain Vif proteins are incapable of counteracting stable (i.e., anti-viral) APOBEC3H and are called "hypo" Vif (37). On the other hand, the Vif proteins that can antagonize stable APOBEC3H are called "hyper" Vif (37). To investigate the impact of endogenous APOBEC3H *in vivo*, an "*in vivo* competition assay" was conducted: hyper and hypo HIV-1s were co-inoculated into humanized mice encoding stable or unstable APOBEC3H and the most efficiently replicating virus was determined by RT-PCR (36). In the humanized mice encoding stable APOBEC3H, hyper HIV-1 predominantly replicated, suggesting that Vif's ability to antagonize stable APOBEC3H is a prerequisite when the host is expressing stable APOBEC3H (36). On the other hand, since the type of virus that efficiently replicated in the humanized mice encoding unstable APOBEC3H (i.e., "hyper" or "hypo") was stochastic, the selection pressure mediated by unstable APOBEC3H is relaxed (36). Moreover, hyper HIV-1 has emerged in the mice encoding stable APOBEC3H, originally infected with hypo HIV-1 (36). Altogether, these findings suggest that stable variants of APOBEC3H impose selective pressure on HIV-1. More importantly, the expression levels of these *APOBEC3* genes are upregulated in the $CD4^+$ T cells of humanized mice infected with HIV-1 (32, 36). As global transcriptome analyses have also indicated the upregulation of ISG expression levels (36), it can be said; IFN-I responses can be triggered by HIV-1 infection in humanized mice.

MX Dynamin-Like GTPase 2

The human genome encodes two IFN-inducible MX dynamin-like guanosine triphosphate hydrolases (GTPases), MX1 and MX2 (also known as MXA and MXB, respectively), which are presumably created by gene duplication over the course of evolution (40, 41). In addition to MX2's strong anti-HIV-1 activity (42–44), it has also been shown that MX1 can suppress a wide range of other pathogenic DNA and RNA viruses, not including HIV-1 (42, 44, 45).

It is well known that IFN-I stimulation strongly inhibits HIV-1 infection during the early stages of viral replication (i.e., from entry to integration process) (46). To determine the IFN-I-responsive RF(s) restricting HIV-1 replication, comparative gene expression profiling (i.e., mRNA microarray) was conducted using human cells in the presence and the absence of IFN-I, and identified MX2 as the determining factor (42, 44). Subsequent investigations revealed that MX2 participates in blocking HIV-1 infection after reverse transcription (42–44). Since MX2 overexpression reduces the levels of nuclear viral DNA (e.g., 2-LTR circles) and more efficiently suppresses HIV-1 infection in non-dividing cells when compared with dividing cells (42, 44), MX2 presumably inhibits nuclear import of the viral complex. Moreover, MX2-mediated anti-viral potency is dependent on the viral capsid protein, as N57S and G89V mutants in the HIV-1 capsid render resistance to MX2 (42). Furthermore, a previous study has suggested that MX2-mediated restriction can be overcome by the depletion of cyclophilin A (CYPA), a peptidylprolyl isomerase (officially designated PPIA), and the treatment of cyclosporin A, a compound inhibiting CYPA (43). These findings suggest that CYPA is required for MX2-mediated anti-viral activity. CYPA is a well-known interaction partner of the HIV-1 capsid protein [reviewed in Ref. (47)]. Therefore, it is plausible that MX2 is closely associated with the viral complex composed of HIV-1 capsid and lines of cellular proteins.

Guanosine triphosphate hydrolase activity is required for the anti-viral effect of MX1 (48). In contrast, the K131A and T151A mutants of MX2, which lose the ability of GTP binding and hydrolysis, respectively, still exhibit anti-HIV-1 activity that is comparable with wild-type MX2 (42), suggesting that the MX2's enzymatic activity appears to be dispensable for its anti-viral effect. On the other hand, the deletion of the nuclear localization signal at the N-terminus of MX2 results in the loss of anti-viral activity (42). These observations suggest the importance of the nuclear localization signal for MX2 to exhibit anti-HIV-1 activity, although the functional importance of the subcellular localization of MX2 remains unclear.

Schlafen 11

Schlafen 11 is also an ISG and potently inhibits HIV-1 production (49). Since SLFN11 overexpression suppresses viral protein expression but not viral transcription, this RF restricts viral replication at a post-transcriptional stage (49). Interestingly, the protein expression of codon-optimized HIV-1 Gag as well as GFP does not affect SLFN11 overexpression or knockdown. Moreover, SLFN11 binds to tRNA and impairs protein expression based on codon usage (49). Altogether, SLFN11 restricts

HIV-1-biased translation in a codon-usage-dependent manner (49). Furthermore, a subsequent study has revealed that primate *SLFN11* genes are under evolutionarily positive selection pressure and commonly possess the ability to impair viral production regardless of the virus or host target (50). However, it remains unclear how SLFN11 influences HIV-1 replication *in vivo*.

Guanylate-Binding Protein 5

Guanylate-binding protein 5 belongs to an IFN-inducible subfamily of GTPases with host defense activity against intracellular bacteria and parasites (51). Krapp et al. have recently demonstrated that GBP5 suppresses HIV-1 infectivity by interfering with *N*-linked glycosylation of the viral envelope glycoprotein (Env) (52). The cysteine residue at position 583 is critical for its anti-viral activity; however, catalytically inactive mutants still demonstrate anti-viral activity, suggesting GBP5 exhibits an anti-viral effect independent of its enzymatic activity (52).

Intriguingly, the nonsense mutations in the HIV-1 *vpu* gene (i.e., the deletion of initiation codon or the insertion of premature stop codons) increase Env expression and confer resistance to GBP5-mediated anti-viral activity (52). As described below, viral protein U (Vpu) is a crucial factor for the counteraction of tetherin-mediated restriction (53, 54). However, it should be noted that the initiation codons of the *vpu* gene in certain clinical HIV-1 isolates including HXB2 (55), BH8 (56), MAL (57), and Zr6 (58) are primarily deleted. Additionally, the expression of *GBP5* gene is upregulated by HIV-1 replication in infected individuals (52). Therefore, it might be plausible to assume that conferring resistance to GBP5 is important for HIV-1 dissemination in certain tissues or organs in infected individuals, and that there is a "trade-off" relationship between anti-tetherin activity (presence of Vpu) and GBP5 resistance (absence of Vpu).

Tetherin

The observation that the HIV-1 accessory protein, Vpu, is required for the efficient release of HIV-1 particles depending on cell type indicated the existence of an RF counteracted by Vpu (59–64). In 2008, Neil et al. and Van Damme et al. identified tetherin (also known as bone marrow stromal antigen 2, CD317, and HM1.24) (53, 54). Tetherin is an IFN-I-inducible type II membrane protein that consists of an *N*-terminal cytoplasmic tail, a transmembrane domain, and an extracellular domain with a glycosylphosphatidylinositol (GPI) modification at the C-terminus (65). Due to GPI anchoring, tetherin is mainly localized in cholesterol-enriched lipid rafts (65), where HIV-1 viruses bud from, and retains budding virions on the plasma membrane of virus-producing cells (66). To antagonize the tetherin-mediated anti-viral action, Vpu down-regulates tetherin from the surface of HIV-1-producing cells (54, 67). Vpu is a multifunctional type I transmembrane protein [reviewed in Ref. (68)] and sequesters tetherin molecules from the cell surface to endosomal compartments through transmembrane domain-mediated interaction (69–72). Additionally, the DSGXXS motif in the cytoplasmic tail of Vpu interacts with BTRC1 (beta-transducin repeat containing E3 ubiquitin protein ligase; also known as β-TrCP1 and Fbxw1), a subunit of E3 ubiquitin ligase. In this way, Vpu induces tetherin ubiquitination and enhances subcellular sorting of tetherin mediated by endosomal sorting complexes required for transport machinery into lysosomal compartments for degradation (72). The requirement of BTRC1 for tetherin antagonization, however, remains controversial.

To reveal the importance of Vpu in the dynamics of HIV-1 replication *in vivo*, Sato et al. (73) and Dave et al. (74) utilized HSC-transplanted humanized mouse models and demonstrated that Vpu strongly downregulates the expression level of tetherin on the surface of virus-producing cell *in vivo*. The replication kinetics of *vpu*-deficient HIV-1 during the early phase of infection is clearly lower than that of wild-type HIV-1 in humanized mice (73, 74), suggesting that Vpu augments HIV-1 replication during the acute phase of infection.

In addition to the tetherin's ability to impair viral release, it can also be an inducer of NFκB activation (75, 76). The molecular mechanism of tetherin-mediated NFκB activation has been well investigated in *in vitro* cell cultures (75–77). However, the importance of NFκB signaling triggered by tetherin in HIV-1 replication *in vivo* remains unknown and needs to be addressed in future investigations.

IFN-I RESPONSES AND IMMUNITY AGAINST HIV-1 INFECTION

Acquired immunodeficiency syndrome is one of many sexually transmitted diseases and HIV-1 infection is accomplished *via* mucosal transmission (78). Notably, transmitter/founder viruses that are transferred from infected patients to nascent individuals are apparently resistant to IFN-I-mediated anti-HIV-1 effects (79–81). These insights strongly suggest that RFs induced by IFN-I are involved in protecting infected individuals at many stages, from HIV-1 acquisition at the mucosal level (i.e., vagina and rectum), right through to limiting virus replication once infection has occurred. However, it remains unclear how transmitted/founder viruses exhibit such resistance to IFN-I (and presumably to the RFs induced by IFN-I).

The source of IFN-I in the acute phase of infection is thought to primarily be pDCs that reside in the mucosa (82, 83). In contrast, it is still unclear which cells are the primary sources of IFN-I during chronic infection. Almost all nucleated cells can produce IFN-Is in times of viral infection (84), pDCs being the largest producers (85, 86). IFN-Is can then act upon NK cells in an autocrine fashion (87–90) or else on macrophages (91). pDCs are found in the circulation but are also capable of dispersing into both lymphoid and most frequently, gut mucosal tissues (92–94). Similar to the other types of leukocytes, NK cells are activated by IFN-I and exhibit high cytotoxic activity (95). The NK cells activated by both IFN-α and TNF-α can suppress HIV-1 viral replication *via* the secretion of CCL3/4/5, IFN-γ, TNF-α, and GM-CSF (96–99). It is also known that IL-12 secreted by DCs and/or macrophages in combination with IFN-, stimulates NK cells to secrete higher amounts of IFN-γ (90).

As described above, the IFN-I responses induced by HIV-1 infection are assumed to contribute to the building up of an anti-viral environment in infected patients. However, it remains controversial as to whether or not IFN-I responses are beneficial for infected patients. For instance, with increased IFN-I production in pDCs, there is an increase in RANTES (regulated on activation, normal T cell expressed and secreted; also known as MIP-1α), a CCR5 ligand, aiding in the recruitment of further target cells, which probably contributes to enhanced viral expansion (82). Additionally, the IFN-α produced by pDCs is both capable of inhibiting the proliferation of bystander $CD4^+$ T cells (100), and promoting the apoptosis of uninfected bystander $CD4^+$ T cells residing in the lymphoid tissue of HIV-1-infected patients (101).

While IFN-β, a subtype of IFN-I, administered *via* the vagina was shown to protect against systemic infection of simian/HIV, a chimeric virus of SIV and HIV in rhesus macaque monkeys (102); the treatment of IFN-I for HIV-1-infected individuals was not successful [reviewed in Ref. (103)]. However, elite controllers, who are able to control HIV-1 infection without any treatment maintain higher pDC counts and IFN-α production compared with viremic patients and infected patients on combination anti-retroviral therapy (cART; previously called highly active anti-retroviral therapy) (104), suggesting that IFN-Is play pivotal roles in controlling HIV-1 infection in elite controllers. In consideration of why IFN-I treatment was not successful, most prior studies have used IFN-I subtype, IFN-α2, as standalone treatments, putative vaccine, or adjuvants for cART in patients (3). However, it has been recently suggested that IFN-α8 and IFN-α14, alternative types of IFN-I, may be better suited as these possess a higher affinity for the IFNAR and consequently result in a greater expression of certain RFs such as MX2, tetherin, and APOBEC3 (105, 106). The complicated effect of IFN-I responses subsequent to HIV-1 infection and recent observations in *in vivo* animal models are described in the following section.

EFFECT OF IFN-I ON HIV-1 INFECTION *IN VIVO*

Investigations using HSC-transplanted humanized mouse models have recently suggested that the initial burst of IFN-I is extremely important in controlling the acute phase of HIV-1 infection to limit reservoir size and disease course (105, 107). However, a sustained IFN-I response is detrimental as it contributes to increased systemic inflammation (108). It has also been shown in humanized mice that NK cells possess the ability to inhibit HIV-1 replication (109, 110).

This "phase out" concept is further supported by the natural hosts of SIV (i.e., non-pathogenic infection); African green monkeys and sooty mangabeys, that demonstrate a decrease in the expression of ISGs and systemic activation just weeks after SIV infection (111, 112). These natural hosts of SIV also differ from HIV infection in humans (as well as pathogenic SIV infection in rhesus macaque monkeys) in that they have a lack of microbial translocation from the gut and very few memory $CD4^+$ T cells are infected [reviewed in Ref. (113)]. Therefore, the IFN-I response in humans is most likely also beneficial in the early stages of infection and would be of greater benefit if it remained confined to mucosal barriers and viral reservoirs. However, if the infection is never cleared, inflammation becomes systemic and the ongoing production of IFN-Is becomes detrimental to the host (i.e., human) in the chronic phase.

Regarding this issue, Dallari et al. identified two SRC family kinases, FYN and LYN, that were constitutively activated in pDCs, potentially providing a useful target, as pDCs are deemed to be the most important IFN-I-producing cell in chronic infection (114). But are there other producer cells that also need to be targeted? And even if pDCs do turn out to be the primary producers during chronic infection, their scarcity and distribution in tissues makes them to difficult to access for *ex vivo* analyses. There is a real possibility that different cell subset(s) are producing IFN-I after peak viral load has been reached. It is also still unclear if pDCs are producing too much or too little IFN-I in HIV-1 patients in chronic infection. Certainly pDCs decrease from acute to chronic infection (in the non-pathogenic models of SIV) (115–118). It is also known that pDCs migrate from the blood to draining lymph nodes before apoptosis (119, 120), however, it is still unknown if the pDCs that migrate from the blood to the rectum or vagina continue to produce IFN-Is or also undergo apoptosis.

In addition to pDCs, DCs and macrophages potently produce IFN-Is after HIV-1 infection as described above. These cells reside at common sites of infection, such as the vagina and rectum (121, 122) and IFN-I expression is increased at these sites after SIV infection in rhesus macaques (123). Therefore, it is likely that not only pDCs but also myeloid cells such as DCs and macrophages contribute to IFN-I secretion at the port of viral entry (e.g., vaginal and rectal tissues).

To further reveal the significance of IFN-I responses in pathogenic HIV/SIV infection *in vivo*, Sandler et al. showed that by blocking IFNAR using an IFN-I antagonist immediately after SIV infection in rhesus macaque monkeys, SIV reservoir size was increased, anti-viral gene expression was decreased, and $CD4^+$ T cell depletion was accelerated leading to a progression to AIDS (124). This study highlighted the importance of IFN-I responses and how crucial they are for control of SIV infection in the acute phase. Additionally in this study, IFN-α2a, a subtype of IFN-I, was administered from 1 week prior to infection in a different cohort of macaque monkeys resulting in the initial upregulation of ISGs and prevention of systemic infection (124). However, prolonged administration resulted in IFN-I desensitization, decreased anti-viral ISG expression, increased SIV reservoir size, and the loss of $CD4^+$ T cell loss (124), suggesting IFN-I somewhat has the properties of a double-edged sword for/against pathogenic HIV/SIV infection *in vivo.*

To directly elucidate the impact of IFN-I in HIV-1 infection *in vivo*, certain groups have utilized HSC-transplanted humanized mouse models. First, Zhen et al. showed that in a humanized mouse model of chronic HIV-1 infection, blocking IFNAR in combination with cART could accelerate viral suppression, reduce the viral reservoir, and further decrease T cell exhaustion and HIV-1-driven immune activation while also restoring HIV-1-specific $CD8^+$ T cell functions (125). Secondly, because the IFN-I response perseveres even under cART, Cheng et al. attempted to combine IFNAR blockade with cART, showing a

reduction in the HIV-1 reservoir in lymphoid tissues, demonstrated by a delay in viral replication rebound following cART cessation (126). Thirdly, in another study by Cheng et al., IFNAR was blocked from weeks 6–10 post-infection (i.e., the chronic phase of infection) (127) resulting in increased viral replication correlating with elevated T cell activation, suggesting that IFN-Is suppress HIV-1 replication during the chronic phase but are not essential for HIV-1-induced aberrant immune activation (127). This study demonstrated that persistent IFN-I signaling during the chronic phase of infection may help to dampen HIV-1 viral replication although it also contributes to the depletion of $CD4^+$ T cells (127).

FUTURE DIRECTION

Here, we have described the positive and negative aspects of IFN-I responses once HIV-1 infection has occurred. Based on *in vitro* investigations using cell cultures, IFN-I quite efficiently suppresses HIV-1 replication (presumably inducing robust RFs) (**Figure 3**). In sharp contrast, the effect of IFN-I in the *in vivo* environment seems much more complicated than expected from previous knowledge around *in vitro* analyses using cell cultures. Future deep and comprehensive investigations using animal models, particularly monkey models for SIV infection and humanized mouse models for HIV-1 infection, will be important to shed light on the true behavior of IFN-I for/against viral infections.

AUTHOR CONTRIBUTIONS

KS conceived the outline of the manuscript; all authors contributed to writing the manuscript.

ACKNOWLEDGMENTS

We appreciate Ms. Naoko Misawa and Ms. Kotubu Misawa for their dedicated support.

FUNDING

This study was supported in part by CREST, JST (to KS); Japanese Initiative for Progress of Research on Infectious Disease for global Epidemic (J-PRIDE) 17fm0208006h0001, AMED (to KS), JSPS KAKENHI Grants-in-Aid for Scientific Research C 15K07166 (to KS), Scientific Research B (Generative Research Fields) 16KT0111 (to KS), and Scientific Research on Innovative Areas 16H06429 (to KS), 16K21723 (to KS) and 17H05813 (to KS); Takeda Science Foundation (to KS); Salt Science Research Foundation (to KS); Smoking Research Foundation (to KS); Chube Ito Foundation (to KS); Fordays Self-Reliance Support in Japan (to KS); Mishima Kaiun Memorial Foundation (to KS); Tobemaki Foundation (to KS); Food Science Institute Foundation (Ryoushoku-kenkyukai) (to KS); JSPS Core-to-Core program, A. Advanced Research Networks (to YK); and Research on HIV/AIDS 16fk0410203h002, AMED (to YK).

REFERENCES

1. Bosinger SE, Utay NS. Type I interferon: understanding its role in HIV pathogenesis and therapy. *Curr HIV/AIDS Rep* (2015) 12(1):41–53. doi:10.1007/s11904-014-0244-6
2. Doyle T, Goujon C, Malim MH. HIV-1 and interferons: who's interfering with whom? *Nat Rev Microbiol* (2015) 13(7):403–13. doi:10.1038/nrmicro3449
3. Utay NS, Douek DC. Interferons and HIV infection: the good, the bad, and the ugly. *Pathog Immun* (2016) 1(1):107–16. doi:10.20411/pai.v1i1.125
4. Wei W, Clarke CJ, Somers GR, Cresswell KS, Loveland KA, Trapani JA, et al. Expression of IFI 16 in epithelial cells and lymphoid tissues. *Histochem Cell Biol* (2003) 119(1):45–54. doi:10.1007/s00418-002-0485-0
5. Jakobsen MR, Bak RO, Andersen A, Berg RK, Jensen SB, Tengchuan J, et al. IFI16 senses DNA forms of the lentiviral replication cycle and controls HIV-1 replication. *Proc Natl Acad Sci U S A* (2013) 110(48):E4571–80. doi:10.1073/pnas.1311669110
6. Berg RK, Rahbek SH, Kofod-Olsen E, Holm CK, Melchjorsen J, Jensen DG, et al. T cells detect intracellular DNA but fail to induce type I IFN responses: implications for restriction of HIV replication. *PLoS One* (2014) 9(1):e84513. doi:10.1371/journal.pone.0084513
7. Ma F, Li B, Liu SY, Iyer SS, Yu Y, Wu A, et al. Positive feedback regulation of type I IFN production by the IFN-inducible DNA sensor cGAS. *J Immunol* (2015) 194(4):1545–54. doi:10.4049/jimmunol.1402066
8. Lahaye X, Satoh T, Gentili M, Cerboni S, Conrad C, Hurbain I, et al. The capsids of HIV-1 and HIV-2 determine immune detection of the viral cDNA by the innate sensor cGAS in dendritic cells. *Immunity* (2013) 39(6):1132–42. doi:10.1016/j.immuni.2013.11.002
9. Gao D, Wu J, Wu YT, Du F, Aroh C, Yan N, et al. Cyclic GMP-AMP synthase is an innate immune sensor of HIV and other retroviruses. *Science* (2013) 341(6148):903–6. doi:10.1126/science.1240933
10. Cohen KW, Dugast AS, Alter G, McElrath MJ, Stamatatos L. HIV-1 single-stranded RNA induces CXCL13 secretion in human monocytes via TLR7 activation and plasmacytoid dendritic cell-derived type I IFN. *J Immunol* (2015) 194(6):2769–75. doi:10.4049/jimmunol.1400952
11. Di Domizio J, Blum A, Gallagher-Gambarelli M, Molens JP, Chaperot L, Plumas J. TLR7 stimulation in human plasmacytoid dendritic cells leads to the induction of early IFN-inducible genes in the absence of type I IFN. *Blood* (2009) 114(9):1794–802. doi:10.1182/blood-2009-04-216770
12. Lepelley A, Louis S, Sourisseau M, Law HK, Pothlichet J, Schilte C, et al. Innate sensing of HIV-infected cells. *PLoS Pathog* (2011) 7(2):e1001284. doi:10.1371/journal.ppat.1001284
13. Beignon AS, McKenna K, Skoberne M, Manches O, DaSilva I, Kavanagh DG, et al. Endocytosis of HIV-1 activates plasmacytoid dendritic cells via toll-like receptor-viral RNA interactions. *J Clin Invest* (2005) 115(11):3265–75. doi:10.1172/JCI26032
14. Yang CH, Murti A, Pfeffer SR, Basu L, Kim JG, Pfeffer LM. IFNalpha/beta promotes cell survival by activating NF-kappa B. *Proc Natl Acad Sci U S A* (2000) 97(25):13631–6. doi:10.1073/pnas.250477397
15. Darnell JE Jr, Kerr IM, Stark GR. JAK-STAT pathways and transcriptional activation in response to IFNs and other extracellular signaling proteins. *Science* (1994) 264(5164):1415–21. doi:10.1126/science.8197455
16. Chelbi-Alix MK, Wietzerbin J. Interferon, a growing cytokine family: 50 years of interferon research. *Biochimie* (2007) 89(6–7):713–8. doi:10.1016/j.biochi.2007.05.001
17. Poli G, Orenstein JM, Kinter A, Folks TM, Fauci AS. Interferon-alpha but not AZT suppresses HIV expression in chronically infected cell lines. *Science* (1989) 244(4904):575–7. doi:10.1126/science.2470148
18. Goldstone DC, Ennis-Adeniran V, Hedden JJ, Groom HC, Rice GI, Christodoulou E, et al. HIV-1 restriction factor SAMHD1 is a deoxynucleoside triphosphate triphosphohydrolase. *Nature* (2011) 480(7377):379–82. doi:10.1038/nature10623
19. Laguette N, Sobhian B, Casartelli N, Ringeard M, Chable-Bessia C, Segeral E, et al. SAMHD1 is the dendritic- and myeloid-cell-specific HIV-1 restriction factor counteracted by Vpx. *Nature* (2011) 474(7353):654–7. doi:10.1038/nature10117
20. Hrecka K, Hao C, Gierszewska M, Swanson SK, Kesik-Brodacka M, Srivastava S, et al. Vpx relieves inhibition of HIV-1 infection of macrophages mediated by the SAMHD1 protein. *Nature* (2011) 474(7353):658–61. doi:10.1038/nature10195

21. Amie SM, Noble E, Kim B. Intracellular nucleotide levels and the control of retroviral infections. *Virology* (2013) 436(2):247–54. doi:10.1016/j.virol.2012.11.010
22. Baldauf HM, Pan X, Erikson E, Schmidt S, Daddacha W, Burggraf M, et al. SAMHD1 restricts HIV-1 infection in resting CD4(+) T cells. *Nat Med* (2012) 18(11):1682–7. doi:10.1038/nm.2964
23. Mlcochova P, Sutherland KA, Watters SA, Bertoli C, de Bruin RA, Rehwinkel J, et al. G1-like state allows HIV-1 to bypass SAMHD1 restriction in macrophages. *EMBO J* (2017) 36(5):604–16. doi:10.15252/embj.201696025
24. Satyanarayana A, Kaldis P. Mammalian cell-cycle regulation: several CDKs, numerous cyclins and diverse compensatory mechanisms. *Oncogene* (2009) 28(33):2925–39. doi:10.1038/onc.2009.170
25. Rice AP, Kimata JT. Subversion of cell cycle regulatory mechanisms by HIV. *Cell Host Microbe* (2015) 17(6):736–40. doi:10.1016/j.chom.2015.05.010
26. Nyamweya S, Hegedus A, Jaye A, Rowland-Jones S, Flanagan KL, Macallan DC. Comparing HIV-1 and HIV-2 infection: lessons for viral immunopathogenesis. *Rev Med Virol* (2013) 23(4):221–40. doi:10.1002/rmv.1739
27. Etienne L, Hahn BH, Sharp PM, Matsen FA, Emerman M. Gene loss and adaptation to hominids underlie the ancient origin of HIV-1. *Cell Host Microbe* (2013) 14(1):85–92. doi:10.1016/j.chom.2013.06.002
28. Ryoo J, Choi J, Oh C, Kim S, Seo M, Kim SY, et al. The ribonuclease activity of SAMHD1 is required for HIV-1 restriction. *Nat Med* (2014) 20(8):936–41. doi:10.1038/nm.3626
29. Harris RS, Dudley JP. APOBECs and virus restriction. *Virology* (2015) 47(9–480):131–45. doi:10.1016/j.virol.2015.03.012
30. LaRue RS, Andresdottir V, Blanchard Y, Conticello SG, Derse D, Emerman M, et al. Guidelines for naming nonprimate APOBEC3 genes and proteins. *J Virol* (2009) 83(2):494–7. doi:10.1128/JVI.01976-08
31. Sato K, Izumi T, Misawa N, Kobayashi T, Yamashita Y, Ohmichi M, et al. Remarkable lethal G-to-A mutations in Vif-proficient HIV-1 provirus by individual APOBEC3 proteins in humanized mice. *J Virol* (2010) 84(18):9546–56. doi:10.1128/JVI.00823-10
32. Sato K, Takeuchi JS, Misawa N, Izumi T, Kobayashi T, Kimura Y, et al. APOBEC3D and APOBEC3F potently promote HIV-1 diversification and evolution in humanized mouse model. *PLoS Pathog* (2014) 10(10):e1004453. doi:10.1371/journal.ppat.1004453
33. Kobayashi T, Koizumi Y, Takeuchi JS, Misawa N, Kimura Y, Morita S, et al. Quantification of deaminase activity-dependent and -independent restriction of HIV-1 replication mediated by APOBEC3F and APOBEC3G through experimental-mathematical investigation. *J Virol* (2014) 88(10):5881–7. doi:10.1128/JVI.00062-14
34. Refsland EW, Hultquist JF, Harris RS. Endogenous origins of HIV-1 G-to-A hypermutation and restriction in the nonpermissive T cell line CEM2n. *PLoS Pathog* (2012) 8(7):e1002800. doi:10.1371/journal.ppat.1002800
35. Liddament MT, Brown WL, Schumacher AJ, Harris RS. APOBEC3F properties and hypermutation preferences indicate activity against HIV-1 in vivo. *Curr Biol* (2004) 14(15):1385–91. doi:10.1016/j.cub.2004.06.050
36. Nakano Y, Misawa N, Juarez-Fernandez G, Moriwaki M, Nakaoka S, Funo T, et al. HIV-1 competition experiments in humanized mice show that APOBEC3H imposes selective pressure and promotes virus adaptation. *PLoS Pathog* (2017) 13(5):e1006348. doi:10.1371/journal.ppat.1006348
37. Refsland EW, Hultquist JF, Luengas EM, Ikeda T, Shaban NM, Law EK, et al. Natural polymorphisms in human APOBEC3H and HIV-1 Vif combine in primary T lymphocytes to affect viral G-to-A mutation levels and infectivity. *PLoS Genet* (2014) 10(11):e1004761. doi:10.1371/journal.pgen.1004761
38. Wang X, Abudu A, Son S, Dang Y, Venta PJ, Zheng YH. Analysis of human APOBEC3H haplotypes and anti-human immunodeficiency virus type 1 activity. *J Virol* (2011) 85(7):3142–52. doi:10.1128/JVI.02049-10
39. OhAinle M, Kerns JA, Li MM, Malik HS, Emerman M. Antiretroelement activity of APOBEC3H was lost twice in recent human evolution. *Cell Host Microbe* (2008) 4(3):249–59. doi:10.1016/j.chom.2008.07.005
40. Aebi M, Fah J, Hurt N, Samuel CE, Thomis D, Bazzigher L, et al. cDNA structures and regulation of two interferon-induced human Mx proteins. *Mol Cell Biol* (1989) 9(11):5062–72. doi:10.1128/MCB.9.11.5062
41. Horisberger MA, Hochkeppel HK. An interferon-induced mouse protein involved in the mechanism of resistance to influenza viruses. Its purification to homogeneity and characterization by polyclonal antibodies. *J Biol Chem* (1985) 260(3):1730–3.
42. Kane M, Yadav SS, Bitzegeio J, Kutluay SB, Zang T, Wilson SJ, et al. MX2 is an interferon-induced inhibitor of HIV-1 infection. *Nature* (2013) 502(7472):563–6. doi:10.1038/nature12653
43. Liu Z, Pan Q, Ding S, Qian J, Xu F, Zhou J, et al. The interferon-inducible MxB protein inhibits HIV-1 infection. *Cell Host Microbe* (2013) 14(4):398–410. doi:10.1016/j.chom.2013.08.015
44. Goujon C, Moncorge O, Bauby H, Doyle T, Ward CC, Schaller T, et al. Human MX2 is an interferon-induced post-entry inhibitor of HIV-1 infection. *Nature* (2013) 502(7472):559–62. doi:10.1038/nature12542
45. Gordien E, Rosmorduc O, Peltekian C, Garreau F, Brechot C, Kremsdorf D. Inhibition of hepatitis B virus replication by the interferon-inducible MxA protein. *J Virol* (2001) 75(6):2684–91. doi:10.1128/JVI.75.6.2684-2691.2001
46. Goujon C, Malim MH. Characterization of the alpha interferon-induced postentry block to HIV-1 infection in primary human macrophages and T cells. *J Virol* (2010) 84(18):9254–66. doi:10.1128/JVI.00854-10
47. Hilditch L, Towers GJ. A model for cofactor use during HIV-1 reverse transcription and nuclear entry. *Curr Opin Virol* (2014) 4:32–6. doi:10.1016/j.coviro.2013.11.003
48. Dick A, Graf L, Olal D, von der Malsburg A, Gao S, Kochs G, et al. Role of nucleotide binding and GTPase domain dimerization in dynamin-like myxovirus resistance protein A for GTPase activation and antiviral activity. *J Biol Chem* (2015) 290(20):12779–92. doi:10.1074/jbc.M115.650325
49. Li M, Kao E, Gao X, Sandig H, Limmer K, Pavon-Eternod M, et al. Codon-usage-based inhibition of HIV protein synthesis by human schlafen 11. *Nature* (2012) 491(7422):125–8. doi:10.1038/nature11433
50. Stabell AC, Hawkins J, Li M, Gao X, David M, Press WH, et al. Non-human primate schlafen11 inhibits production of both host and viral proteins. *PLoS Pathog* (2016) 12(12):e1006066. doi:10.1371/journal.ppat.1006066
51. Kim BH, Shenoy AR, Kumar P, Bradfield CJ, MacMicking JD. IFN-inducible GTPases in host cell defense. *Cell Host Microbe* (2012) 12(4):432–44. doi:10.1016/j.chom.2012.09.007
52. Krapp C, Hotter D, Gawanbacht A, McLaren PJ, Kluge SF, Sturzel CM, et al. Guanylate binding protein (GBP) 5 is an interferon-inducible inhibitor of HIV-1 infectivity. *Cell Host Microbe* (2016) 19(4):504–14. doi:10.1016/j.chom.2016.02.019
53. Neil SJ, Zang T, Bieniasz PD. Tetherin inhibits retrovirus release and is antagonized by HIV-1 Vpu. *Nature* (2008) 451(7177):425–30. doi:10.1038/nature06553
54. Van Damme N, Goff D, Katsura C, Jorgenson RL, Mitchell R, Johnson MC, et al. The interferon-induced protein BST-2 restricts HIV-1 release and is downregulated from the cell surface by the viral Vpu protein. *Cell Host Microbe* (2008) 3(4):245–52. doi:10.1016/j.chom.2008.03.001
55. Ratner L, Haseltine W, Patarca R, Livak KJ, Starcich B, Josephs SF, et al. Complete nucleotide sequence of the AIDS virus, HTLV-III. *Nature* (1985) 313(6000):277–84. doi:10.1038/313277a0
56. Ratner L, Fisher A, Jagodzinski LL, Mitsuya H, Liou RS, Gallo RC, et al. Complete nucleotide sequences of functional clones of the AIDS virus. *AIDS Res Hum Retroviruses* (1987) 3(1):57–69. doi:10.1089/aid.1987.3.57
57. Alizon M, Wain-Hobson S, Montagnier L, Sonigo P. Genetic variability of the AIDS virus: nucleotide sequence analysis of two isolates from African patients. *Cell* (1986) 46(1):63–74. doi:10.1016/0092-8674(86)90860-3
58. Srinivasan A, Anand R, York D, Ranganathan P, Feorino P, Schochetman G, et al. Molecular characterization of human immunodeficiency virus from Zaire: nucleotide sequence analysis identifies conserved and variable domains in the envelope gene. *Gene* (1987) 52(1):71–82. doi:10.1016/0378-1119(87)90396-9
59. Neil SJ, Eastman SW, Jouvenet N, Bieniasz PD. HIV-1 Vpu promotes release and prevents endocytosis of nascent retrovirus particles from the plasma membrane. *PLoS Pathog* (2006) 2(5):e39. doi:10.1371/journal.ppat.0020039
60. Varthakavi V, Smith RM, Bour SP, Strebel K, Spearman P. Viral protein U counteracts a human host cell restriction that inhibits HIV-1 particle production. *Proc Natl Acad Sci U S A* (2003) 100(25):15154–9. doi:10.1073/pnas.2433165100
61. Gottlinger HG, Dorfman T, Cohen EA, Haseltine WA. Vpu protein of human immunodeficiency virus type 1 enhances the release of capsids produced

by gag gene constructs of widely divergent retroviruses. *Proc Natl Acad Sci U S A* (1993) 90(15):7381–5. doi:10.1073/pnas.90.15.7381
62. Klimkait T, Strebel K, Hoggan MD, Martin MA, Orenstein JM. The human immunodeficiency virus type 1-specific protein Vpu is required for efficient virus maturation and release. *J Virol* (1990) 64(2):621–9.
63. Strebel K, Klimkait T, Maldarelli F, Martin MA. Molecular and biochemical analyses of human immunodeficiency virus type 1 Vpu protein. *J Virol* (1989) 63(9):3784–91.
64. Terwilliger EF, Cohen EA, Lu YC, Sodroski JG, Haseltine WA. Functional role of human immunodeficiency virus type 1 Vpu. *Proc Natl Acad Sci U S A* (1989) 86(13):5163–7. doi:10.1073/pnas.86.13.5163
65. Kupzig S, Korolchuk V, Rollason R, Sugden A, Wilde A, Banting G. BST-2/HM1.24 is a raft-associated apical membrane protein with an unusual topology. *Traffic* (2003) 4(10):694–709. doi:10.1034/j.1600-0854.2003.00129.x
66. Perez-Caballero D, Zang T, Ebrahimi A, McNatt MW, Gregory DA, Johnson MC, et al. Tetherin inhibits HIV-1 release by directly tethering virions to cells. *Cell* (2009) 139(3):499–511. doi:10.1016/j.cell.2009.08.039
67. Sato K, Yamamoto SP, Misawa N, Yoshida T, Miyazawa T, Koyanagi Y. Comparative study on the effect of human BST-2/tetherin on HIV-1 release in cells of various species. *Retrovirology* (2009) 6:53. doi:10.1186/1742-4690-6-53
68. Soper A, Juarez-Fernandez G, Aso H, Moriwaki M, Yamada E, Nakano Y, et al. Various plus unique: viral protein U as a plurifunctional protein for HIV-1 replication. *Exp Biol Med (Maywood)* (2017) 242(8):850–8. doi:10.1177/1535370217697384
69. Kobayashi T, Ode H, Yoshida T, Sato K, Gee P, Yamamoto SP, et al. Identification of amino acids in the human tetherin transmembrane domain responsible for HIV-1 Vpu interaction and susceptibility. *J Virol* (2011) 85(2):932–45. doi:10.1128/JVI.01668-10
70. Vigan R, Neil SJ. Determinants of tetherin antagonism in the transmembrane domain of the human immunodeficiency virus type 1 Vpu protein. *J Virol* (2010) 84(24):12958–70. doi:10.1128/JVI.01699-10
71. Iwabu Y, Fujita H, Kinomoto M, Kaneko K, Ishizaka Y, Tanaka Y, et al. HIV-1 accessory protein Vpu internalizes cell-surface BST-2/tetherin through transmembrane interactions leading to lysosomes. *J Biol Chem* (2009) 284(50):35060–72. doi:10.1074/jbc.M109.058305
72. Janvier K, Pelchen-Matthews A, Renaud JB, Caillet M, Marsh M, Berlioz-Torrent C. The ESCRT-0 component HRS is required for HIV-1 Vpu-mediated BST-2/tetherin down-regulation. *PLoS Pathog* (2011) 7(2):e1001265. doi:10.1371/journal.ppat.1001265
73. Sato K, Misawa N, Fukuhara M, Iwami S, An DS, Ito M, et al. Vpu augments the initial burst phase of HIV-1 propagation and downregulates BST2 and CD4 in humanized mice. *J Virol* (2012) 86(9):5000–13. doi:10.1128/JVI.07062-11
74. Dave VP, Hajjar F, Dieng MM, Haddad E, Cohen EA. Efficient BST2 antagonism by Vpu is critical for early HIV-1 dissemination in humanized mice. *Retrovirology* (2013) 10:128. doi:10.1186/1742-4690-10-128
75. Galao RP, Le Tortorec A, Pickering S, Kueck T, Neil SJ. Innate sensing of HIV-1 assembly by tetherin induces NFκB-dependent proinflammatory responses. *Cell Host Microbe* (2012) 12(5):633–44. doi:10.1016/j.chom.2012.10.007
76. Sauter D, Hotter D, Van Driessche B, Sturzel CM, Kluge SF, Wildum S, et al. Differential regulation of NF-κB-mediated proviral and antiviral host gene expression by primate lentiviral Nef and Vpu proteins. *Cell Rep* (2015) 10(4):586–99. doi:10.1016/j.celrep.2014.12.047
77. Tokarev A, Suarez M, Kwan W, Fitzpatrick K, Singh R, Guatelli J. Stimulation of NF-kappaB activity by the HIV restriction factor BST2. *J Virol* (2013) 87(4):2046–57. doi:10.1128/JVI.02272-12
78. Morrow G, Vachot L, Vagenas P, Robbiani M. Current concepts of HIV transmission. *Curr HIV/AIDS Rep* (2007) 4(1):29–35. doi:10.1007/s11904-007-0005-x
79. Iyer SS, Bibollet-Ruche F, Sherrill-Mix S, Learn GH, Plenderleith L, Smith AG, et al. Resistance to type 1 interferons is a major determinant of HIV-1 transmission fitness. *Proc Natl Acad Sci U S A* (2017) 114(4):E590–9. doi:10.1073/pnas.1620144114
80. Fenton-May AE, Dibben O, Emmerich T, Ding H, Pfafferott K, Aasa-Chapman MM, et al. Relative resistance of HIV-1 founder viruses to control by interferon-alpha. *Retrovirology* (2013) 10:146. doi:10.1186/1742-4690-10-146
81. Parrish NF, Gao F, Li H, Giorgi EE, Barbian HJ, Parrish EH, et al. Phenotypic properties of transmitted founder HIV-1. *Proc Natl Acad Sci U S A* (2013) 110(17):6626–33. doi:10.1073/pnas.1304288110
82. O'Brien M, Manches O, Bhardwaj N. Plasmacytoid dendritic cells in HIV infection. *Adv Exp Med Biol* (2013) 762:71–107. doi:10.1007/978-1-4614-4433-6_3
83. O'Brien M, Manches O, Sabado RL, Baranda SJ, Wang Y, Marie I, et al. Spatiotemporal trafficking of HIV in human plasmacytoid dendritic cells defines a persistently IFN-alpha-producing and partially matured phenotype. *J Clin Invest* (2011) 121(3):1088–101. doi:10.1172/JCI44960
84. Goodbourn S, Didcock L, Randall RE. Interferons: cell signalling, immune modulation, antiviral response and virus countermeasures. *J Gen Virol* (2000) 81(Pt 10):2341–64. doi:10.1099/0022-1317-81-10-2341
85. Siegal FP, Kadowaki N, Shodell M, Fitzgerald-Bocarsly PA, Shah K, Ho S, et al. The nature of the principal type 1 interferon-producing cells in human blood. *Science* (1999) 284(5421):1835–7. doi:10.1126/science.284.5421.1835
86. Fitzgerald-Bocarsly P. Human natural interferon-alpha producing cells. *Pharmacol Ther* (1993) 60(1):39–62. doi:10.1016/0163-7258(93)90021-5
87. Tomescu C, Tebas P, Montaner LJ. IFN-alpha augments natural killer-mediated antibody-dependent cellular cytotoxicity of HIV-1-infected autologous CD4+ T cells regardless of major histocompatibility complex class 1 down-regulation. *AIDS* (2017) 31(5):613–22. doi:10.1097/QAD.0000000000001380
88. Tomescu C, Mavilio D, Montaner LJ. Lysis of HIV-1-infected autologous CD4+ primary T cells by interferon-alpha-activated NK cells requires NKp46 and NKG2D. *AIDS* (2015) 29(14):1767–73. doi:10.1097/QAD.0000000000000777
89. Portales P, Reynes J, Pinet V, Rouzier-Panis R, Baillat V, Clot J, et al. Interferon-alpha restores HIV-induced alteration of natural killer cell perforin expression in vivo. *AIDS* (2003) 17(4):495–504. doi:10.1097/01.aids.0000050816.06065.b1
90. Hunter CA, Gabriel KE, Radzanowski T, Neyer LE, Remington JS. Type I interferons enhance production of IFN-gamma by NK cells. *Immunol Lett* (1997) 59(1):1–5. doi:10.1016/S0165-2478(97)00091-6
91. Akiyama H, Ramirez NP, Gibson G, Kline C, Watkins S, Ambrose Z, et al. Interferon-inducible CD169/Siglec1 attenuates anti-HIV-1 effects of IFN-alpha. *J Virol* (2017) 91(21):e00972-17. doi:10.1128/JVI.00972-17
92. Lehmann C, Jung N, Forster K, Koch N, Leifeld L, Fischer J, et al. Longitudinal analysis of distribution and function of plasmacytoid dendritic cells in peripheral blood and gut mucosa of HIV infected patients. *J Infect Dis* (2014) 209(6):940–9. doi:10.1093/infdis/jit612
93. Li H, Gillis J, Johnson RP, Reeves RK. Multi-functional plasmacytoid dendritic cells redistribute to gut tissues during simian immunodeficiency virus infection. *Immunology* (2013) 140(2):244–9. doi:10.1111/imm.12132
94. Barratt-Boyes SM, Wijewardana V, Brown KN. In acute pathogenic SIV infection plasmacytoid dendritic cells are depleted from blood and lymph nodes despite mobilization. *J Med Primatol* (2010) 39(4):235–42. doi:10.1111/j.1600-0684.2010.00428.x
95. Markova AA, Mihm U, Schlaphoff V, Lunemann S, Filmann N, Bremer B, et al. PEG-IFN alpha but not ribavirin alters NK cell phenotype and function in patients with chronic hepatitis C. *PLoS One* (2014) 9(4):e94512. doi:10.1371/journal.pone.0094512
96. Cooper MA, Fehniger TA, Fuchs A, Colonna M, Caligiuri MA. NK cell and DC interactions. *Trends Immunol* (2004) 25(1):47–52. doi:10.1016/j.it.2003.10.012
97. Cerwenka A, Lanier LL. Natural killer cells, viruses and cancer. *Nat Rev Immunol* (2001) 1(1):41–9. doi:10.1038/35095564
98. Cooper MA, Fehniger TA, Turner SC, Chen KS, Ghaheri BA, Ghayur T, et al. Human natural killer cells: a unique innate immunoregulatory role for the CD56(bright) subset. *Blood* (2001) 97(10):3146–51. doi:10.1182/blood.V97.10.3146
99. Trinchieri G. Biology of natural killer cells. *Adv Immunol* (1989) 47:187–376. doi:10.1016/S0065-2776(08)60664-1
100. Lehmann C, Lafferty M, Garzino-Demo A, Jung N, Hartmann P, Fatkenheuer G, et al. Plasmacytoid dendritic cells accumulate and secrete interferon alpha in lymph nodes of HIV-1 patients. *PLoS One* (2010) 5(6):e11110. doi:10.1371/journal.pone.0011110
101. Herbeuval JP, Nilsson J, Boasso A, Hardy AW, Kruhlak MJ, Anderson SA, et al. Differential expression of IFN-alpha and TRAIL/DR5 in lymphoid tissue of progressor versus nonprogressor HIV-1-infected patients. *Proc Natl Acad Sci U S A* (2006) 103(18):7000–5. doi:10.1073/pnas.0600363103
102. Veazey RS, Pilch-Cooper HA, Hope TJ, Alter G, Carias AM, Sips M, et al. Prevention of SHIV transmission by topical IFN-beta treatment. *Mucosal Immunol* (2016) 9(6):1528–36. doi:10.1038/mi.2015.146

103. Longo DL, Steis RG, Lane HC, Lotze MT, Rosenberg SA, Preble O, et al. Malignancies in the AIDS patient: natural history, treatment strategies, and preliminary results. *Ann N Y Acad Sci* (1984) 437:421–30. doi:10.1111/j.1749-6632.1984.tb37163.x
104. Machmach K, Leal M, Gras C, Viciana P, Genebat M, Franco E, et al. Plasmacytoid dendritic cells reduce HIV production in elite controllers. *J Virol* (2012) 86(8):4245–52. doi:10.1128/JVI.07114-11
105. Lavender KJ, Gibbert K, Peterson KE, Van Dis E, Francois S, Woods T, et al. Interferon alpha subtype-specific suppression of HIV-1 infection in vivo. *J Virol* (2016) 90(13):6001–13. doi:10.1128/JVI.00451-16
106. Harper MS, Guo K, Gibbert K, Lee EJ, Dillon SM, Barrett BS, et al. Interferon-alpha subtypes in an ex vivo model of acute HIV-1 infection: expression, potency and effector mechanisms. *PLoS Pathog* (2015) 11(11):e1005254. doi:10.1371/journal.ppat.1005254
107. Abraham S, Choi JG, Ortega NM, Zhang J, Shankar P, Swamy NM. Gene therapy with plasmids encoding IFN-beta or IFN-alpha14 confers long-term resistance to HIV-1 in humanized mice. *Oncotarget* (2016) 7(48):78412–20. doi:10.18632/oncotarget.12512
108. Harris LD, Tabb B, Sodora DL, Paiardini M, Klatt NR, Douek DC, et al. Downregulation of robust acute type I interferon responses distinguishes nonpathogenic simian immunodeficiency virus (SIV) infection of natural hosts from pathogenic SIV infection of rhesus macaques. *J Virol* (2010) 84(15):7886–91. doi:10.1128/JVI.02612-09
109. Seay K, Church C, Zheng JH, Deneroff K, Ochsenbauer C, Kappes JC, et al. In vivo activation of human NK cells by treatment with an interleukin-15 superagonist potently inhibits acute in vivo HIV-1 infection in humanized mice. *J Virol* (2015) 89(12):6264–74. doi:10.1128/JVI.00563-15
110. Johansson SE, Brauner H, Hinkula J, Wahren B, Berg L, Johansson MH. Accumulation and activation of natural killer cells in local intraperitoneal HIV-1/MuLV infection results in early control of virus infected cells. *Cell Immunol* (2011) 272(1):71–8. doi:10.1016/j.cellimm.2011.09.005
111. Vanderford TH, Slichter C, Rogers KA, Lawson BO, Obaede R, Else J, et al. Treatment of SIV-infected sooty mangabeys with a type-I IFN agonist results in decreased virus replication without inducing hyperimmune activation. *Blood* (2012) 119(24):5750–7. doi:10.1182/blood-2012-02-411496
112. Jacquelin B, Mayau V, Targat B, Liovat AS, Kunkel D, Petitjean G, et al. Nonpathogenic SIV infection of African green monkeys induces a strong but rapidly controlled type I IFN response. *J Clin Invest* (2009) 119(12):3544–55. doi:10.1172/JCI40093
113. Klatt NR, Silvestri G, Hirsch V. Nonpathogenic simian immunodeficiency virus infections. *Cold Spring Harb Perspect Med* (2012) 2(1):a007153. doi:10.1101/cshperspect.a007153
114. Dallari S, Macal M, Loureiro ME, Jo Y, Swanson L, Hesser C, et al. SRC family kinases FYN and LYN are constitutively activated and mediate plasmacytoid dendritic cell responses. *Nat Commun* (2017) 8:14830. doi:10.1038/ncomms14830
115. Diop OM, Ploquin MJ, Mortara L, Faye A, Jacquelin B, Kunkel D, et al. Plasmacytoid dendritic cell dynamics and alpha interferon production during simian immunodeficiency virus infection with a nonpathogenic outcome. *J Virol* (2008) 82(11):5145–52. doi:10.1128/JVI.02433-07
116. Malleret B, Karlsson I, Maneglier B, Brochard P, Delache B, Andrieu T, et al. Effect of SIVmac infection on plasmacytoid and CD1c+ myeloid dendritic cells in cynomolgus macaques. *Immunology* (2008) 124(2):223–33. doi:10.1111/j.1365-2567.2007.02758.x
117. Brown KN, Trichel A, Barratt-Boyes SM. Parallel loss of myeloid and plasmacytoid dendritic cells from blood and lymphoid tissue in simian AIDS. *J Immunol* (2007) 178(11):6958–67. doi:10.4049/jimmunol.178.11.6958
118. Reeves RK, Fultz PN. Disparate effects of acute and chronic infection with SIVmac239 or SHIV-89.6P on macaque plasmacytoid dendritic cells. *Virology* (2007) 365(2):356–68. doi:10.1016/j.virol.2007.03.055
119. Brown KN, Wijewardana V, Liu X, Barratt-Boyes SM. Rapid influx and death of plasmacytoid dendritic cells in lymph nodes mediate depletion in acute simian immunodeficiency virus infection. *PLoS Pathog* (2009) 5(5):e1000413. doi:10.1371/journal.ppat.1000413
120. Malleret B, Maneglier B, Karlsson I, Lebon P, Nascimbeni M, Perie L, et al. Primary infection with simian immunodeficiency virus: plasmacytoid dendritic cell homing to lymph nodes, type I interferon, and immune suppression. *Blood* (2008) 112(12):4598–608. doi:10.1182/blood-2008-06-162651
121. Wang Y, Abel K, Lantz K, Krieg AM, McChesney MB, Miller CJ. The toll-like receptor 7 (TLR7) agonist, imiquimod, and the TLR9 agonist, CpG ODN, induce antiviral cytokines and chemokines but do not prevent vaginal transmission of simian immunodeficiency virus when applied intravaginally to rhesus macaques. *J Virol* (2005) 79(22):14355–70. doi:10.1128/JVI.79.22.14355-14370.2005
122. Miller CJ, Li Q, Abel K, Kim EY, Ma ZM, Wietgrefe S, et al. Propagation and dissemination of infection after vaginal transmission of simian immunodeficiency virus. *J Virol* (2005) 79(14):9217–27. doi:10.1128/JVI.79.14.9217-9227.2005
123. Abel K, Rocke DM, Chohan B, Fritts L, Miller CJ. Temporal and anatomic relationship between virus replication and cytokine gene expression after vaginal simian immunodeficiency virus infection. *J Virol* (2005) 79(19):12164–72. doi:10.1128/JVI.79.19.12164-12172.2005
124. Sandler NG, Bosinger SE, Estes JD, Zhu RT, Tharp GK, Boritz E, et al. Type I interferon responses in rhesus macaques prevent SIV infection and slow disease progression. *Nature* (2014) 511(7511):601–5. doi:10.1038/nature13554
125. Zhen A, Rezek V, Youn C, Lam B, Chang N, Rick J, et al. Targeting type I interferon-mediated activation restores immune function in chronic HIV infection. *J Clin Invest* (2017) 127(1):260–8. doi:10.1172/JCI89488
126. Cheng L, Ma J, Li J, Li D, Li G, Li F, et al. Blocking type I interferon signaling enhances T cell recovery and reduces HIV-1 reservoirs. *J Clin Invest* (2017) 127(1):269–79. doi:10.1172/JCI90745
127. Cheng L, Yu H, Li G, Li F, Ma J, Li J, et al. Type I interferons suppress viral replication but contribute to T cell depletion and dysfunction during chronic HIV-1 infection. *JCI Insight* (2017) 2(12):94366. doi:10.1172/jci.insight.94366

Conflict of Interest Statement: The authors declare that the research was conducted in the absence of any commercial or financial relationships that could be construed as a potential conflict of interest.

frontiers in Immunology

ORIGINAL RESEARCH
published: 17 January 2018
doi: 10.3389/fimmu.2017.02017

Enhanced Antibody Responses in a Novel NOG Transgenic Mouse with Restored Lymph Node Organogenesis

Takeshi Takahashi[1], Ikumi Katano[1], Ryoji Ito[1], Motohito Goto[1], Hayato Abe[1], Seiya Mizuno[2], Kenji Kawai[1], Fumihiro Sugiyama[2] and Mamoru Ito[1]*

[1] Central Institute for Experimental Animals, Kawasaki, Japan, [2] Laboratory Animal Resource Center, University of Tsukuba, Tsukuba, Japan

OPEN ACCESS

Edited by:
Moriya Tsuji,
Aaron Diamond AIDS Research Center, United States

Reviewed by:
Daniel Olive,
Institut National de la Santé et de la Recherche Médicale, France
Xin M. Luo,
Virginia Tech, United States
Ping Chen,
Georgetown University School of Medicine, United States
Hergen Spits,
University of Amsterdam, Netherlands

***Correspondence:**
Takeshi Takahashi
takeshi-takahashi@ciea.or.jp

Specialty section:
This article was submitted to Vaccines and Molecular Therapeutics, a section of the journal Frontiers in Immunology

Received: 04 October 2017
Accepted: 29 December 2017
Published: 17 January 2018

Citation:
Takahashi T, Katano I, Ito R, Goto M, Abe H, Mizuno S, Kawai K, Sugiyama F and Ito M (2018) Enhanced Antibody Responses in a Novel NOG Transgenic Mouse with Restored Lymph Node Organogenesis. Front. Immunol. 8:2017. doi: 10.3389/fimmu.2017.02017

Lymph nodes (LNs) are at the center of adaptive immune responses. Various exogenous substances are transported into LNs and a series of immune responses ensue after recognition by antigen–specific lymphocytes. Although humanized mice have been used to reconstitute the human immune system, most lack LNs due to deficiency of the interleukin (IL)-2Rγ gene (cytokine common γ chain, γc). In this study, we established a transgenic strain, NOG-pRORγt-γc, in the NOD/shi-*scid*-IL-2Rγ^{null} (NOG) background, in which the γc gene was expressed in a lymph-tissue inducer (LTi) lineage by the endogenous promoter of RORγt. In this strain, LN organogenesis was normalized and the number of human T cells substantially increased in the periphery after reconstitution of the human immune system by human hematopoietic stem cell transplantation. The distribution of human T cells differed between NOG-pRORγt-γc Tg and NOG-non Tg mice. About 40% of human T cells resided in LNs, primarily the mesenteric LNs. The LN-complemented humanized mice exhibited antigen-specific immunoglobulin G responses together and an increased number of IL-21^{+}–producing CD4^{+} T cells in LNs. This novel mouse strain will facilitate recapitulation of human immune responses.

Keywords: humanized mice, NOG, lymph node, T cell, homeostasis

INTRODUCTION

Reconstitution of the human immune system in immunodeficient mice enables investigation of human immunology and facilitates drug discovery (1–3). Progress in humanized mouse technology relies on extremely immunodeficient mouse strains; e.g., NOD-*scid* (4), NOD/Shi-*scid* IL2rγ^{null} (NOG) (5), NOD/LtSz-*scid* IL2rγ^{null} (NSG) (6), and BALB/c Rag2^{null}IL2rγ^{null} (BRG) (7). These platform strains are characterized by a severe deficiency in the murine immune system. In addition to deficiency of B and T lymphocytes due to *scid* gene mutation or disruption of the RAG-2 gene, especially, it is deletion of the interleukin (IL)-2 receptor γ (γc) gene that compromises the entire murine immune system. Because γc is a subunit for the receptors for six cytokines (IL-2, IL-4, IL-7, IL-9, IL-15, and IL-21) (8, 9), all biological pathways dependent on these cytokines are affected. In many cases, the primary consequences of the lack of γc are abnormal development and differentiation of lymphocytes; e.g., blocking of B-cell differentiation at the pre-proB cell stage (10), severe reduction in the number of T cells, and total loss of natural killer cells (11–13). There are also indirect secondary effects; e.g., impaired development of lymph nodes (LNs) in γc-deficient mice (11).

The organogenesis of LNs is complex and involves many cell types (14). One important cell type is the lymphoid tissue inducer (LTi) cell, which is a subpopulation in innate lymphoid cell 3 (15). During embryo development, LTi cells migrate toward lymphoid tissue stromal organizer (LTo) cells *via* a CXCL13-CXCR5–dependent mechanism (16–18). The critical molecule in the interaction between LTi and LTo cells is lymphotoxin (LT), which triggers LN formation (14). Differentiation of LTi cells requires expression of the master transcription factor, RORγt (19). IL-7 is necessary for their survival, as the number of LTi cells is reduced in γc-deficient mice; this reduction in numbers is responsible for the poor LN development (20). The transgenic expression of mouse thymic stromal lymphopoietin (TSLP), an IL-7 family molecule, restores the number of LTi in γc-deficient mice, and such TSLP transgenic (Tg) mice in a γc-deficient background showed normal LN development (20). These results suggest the importance of interactions between LTi cells and cytokines in LN organogenesis.

Because LNs are the primary sites of induction of immune responses; i.e., influx of antigen–loaded dendritic cells and subsequent activation of antigen-specific T- and B-cells resulting in germinal center formation, the absence of LNs could result in an immunodeficient status. Indeed, various mouse strains with no LNs—such as LTα$^{-/-}$ mice (21), LTβ$^{-/-}$ mice (22), or alymphoplasia mutant mice (*aly/aly*) (23), caused by a mutation in the NIK gene—show impaired or delayed immune responses. In addition, LNs are important for maintaining lymphocyte homeostasis (24).

Humanized NOG mice, which are produced by transplanting human CD34$^+$ hematopoietic stem cells (HSCs), exhibit impaired LN development. In many cases, they have few small LNs even after full development of human B and T lymphocytes. Thus, it is plausible that the immune responses in humanized mice are insufficient due to their poor LN organogenesis. Indeed, such mice are deficient in antigen-specific responses, especially antigen-specific antibody responses (25–27).

In this study, we developed a novel NOG strain with LNs. We used a bacterial artificial chromosome (BAC) clone containing the entire RORγt locus in which the first exon of RORγt was replaced with the murine γc gene. The transgenic mice showed normal LN development in the NOG genetic background. After transplantation of human HSCs, these mice showed a significant increase in the total number of human T cells, body-wide redistribution of lymphocytes, and enhanced antibody production.

MATERIALS AND METHODS

BAC Engineering

A BAC clone, RP23-263K17, containing the entire genomic region of the RORγ gene, was purchased from Advanced GenoTechs Co. (Tsukuba, Japan). BAC clone DNA was transfected into *Escherichia coli* EL250 by electroporation followed by homologous recombination (28). The whole cDNA of mouse γc and the polyA signal was introduced into the PL451 shuttle vector (28). The DNA fragment consisting of the murine γc and the neomycin resistance gene under the control of the PGK/EM7 promoter was amplified by Primestar GXL (Takara Bio Inc., Otsu, Japan). The PCR primer sequences are as follows: forward 5′-tgtgtgctgtcctgggctaccctactgaggaggacagggagccaagttctcagtcatgttgaaactattattgtcacc-3′, and reverse 5′-cctaggaatggtgacaggacccaggctcccccatgaccggatgccccccatt cacttacgctctagaactagtggatcc-3′.

The PCR products were introduced into EL250 with RP23-263K17 to induce homologous recombination. After selecting chloramphenicol- and kanamycin-resistant colonies, we confirmed correct homologous recombination between the targeting vector and BAC DNA by sequencing and southern-blot analysis. The neomycin gene, which was flanked by flippase (FLP) recombinase target sequences, was removed by FLP-mediated site-specific recombination by arabinose treatment. As a result, the murine γc gene was inserted into exon 1 of the RORγt gene. BAC DNA was purified using NucleoBond BAC100 (Macherey-Nagel, Dueren, Germany).

Mice and Reconstitution with Human Stem Cells

Mice were maintained in the animal facility at the Central Institute for Experimental Animals under specific-pathogen-free conditions. All animal experiments were approved by the Institutional Animal Care and Use Committee (certification number 11004A) and were conducted according to the institutional guidelines.

All of the experiments using human cells were approved by the Institutional Ethical Committee and conducted according to the guide lines.

Bacterial artificial chromosome transgenic B6 mice, which express murine γc under the control of RORγt regulatory elements, were generated in the C57/BL6 (B6) background. The BAC DNA described above was digested with PI-*Sce*I and purified. The linearized DNA was microinjected into B6 fertilized eggs by the standard protocol. The obtained mice were genotyped by PCR and a founder mouse was used for backcross mating. After seven-time backcross mating to the NOG strain, we confirmed the replacement of the genetic background from B6 to NOD using microsatellite markers. NOG-GM-CSF/IL-3 transgenic mice (NOG-GM3 Tg) were described elsewhere (29).

For reconstitution of the human immune system, 6-week-old male NOG or NOG-pRORγt-γc mice were irradiated with 180 cGy of X-rays (MBR-1520R-4, Hitachi, Hitachi, Japan) and 5×10^4 umbilical cord blood CD34$^+$ cells (StemExpress, Folsom, CA, USA) were transplanted by intravenous injection the next day (hereafter, hu-HSC-NOG or hu-HSC NOG-pRORγt-γc, respectively).

Antibodies and Flow Cytometry

The following monoclonal antibodies (mAbs) were purchased from BioLegend (San Jose, CA, USA): anti-CD4-fluorescein isothiocyanate (FITC), anti-CD8a-FITC, anti-CD20-FITC, anti-CD33-FITC, anti-CD19-phycoerythrin (PE), anti-CD21-PE, anti-CD3-PECy7, anti-IgD-PECy7, anti-CD8a-allophycocyanin (APC), antimouse CD45-APC, anti-CD4-APCCy7, anti-CD19 APCCy7, and antihuman CD45-APCCy7.

To analyze human lymphocytes in mice reconstituted with the human immune system, multicolor cytometric analysis was

performed using a fluorescence-activated cell sorter (FACS) Canto (BD Biosciences). Peripheral blood (PB) was collected from the retro-orbital venous plexus using heparinized pipettes periodically under anesthesia with isoflurane to monitor the development of human cells. PB was also assessed using a blood analyzer (XT-2000i, SYSMEX, Kobe, Japan) to enumerate total white blood cells. Red blood cells were eliminated using ACK solution (150 mM NH_4Cl, 10 mM $KHCO_3$, 1 mM EDTA-Na_2) and mononuclear cells (MNCs) were stained with fluorescent marker-conjugated antibodies for flow cytometry.

At the time of euthanasia, MNCs were prepared from the thymus, spleen, LNs, or bone marrow (BM) by smashing with frosted slide glasses, or by flushing the femurs with FACS medium [phosphate-buffered saline (PBS) containing 2% fetal calf serum (FCS) with 0.1% NaN_3] using a 27-gage needle. The cells were stained with the relevant mAb cocktails for 20 min on ice, and washed with cold FACS medium. The proportion of each lineage was calculated using FACS Diva software (BD Biosciences) and the absolute number of each fraction was determined by multiplying the frequency by the total cell number.

For intracellular staining, cells were suspended in Roswell Park Memorial Institute (RPMI) medium (RPMI + 2% FCS) and stimulated with phorbol myristate acetate (50 ng/ml) and ionomycin (1 μg/ml) in the presence of Brefeldin A (BioLegend) for 4 h at 37°C, then fixed with fixation buffer (eBioscience, San Diego, CA, USA). After permeabilization with Cytofix/Cytoperm solution (BD Biosciences), cells were stained with mAbs for anti-IFNγ-FITC, anti-IL-4-PE, and anti-IL-21-APC (BioLegend), together with antibodies for surface markers, for 20 min on ice. After the final wash, the cells were subjected to flow cytometry.

Macroscopic Analysis of LNs

To visualize popliteal, inguinal, and sacral LNs, 1% Evans Blue dye (Sigma-Aldrich, St. Louis, MO, USA) was subcutaneously injected into the footpad or tail base. The mice were analyzed 1 h after injection; LNs were evidenced by accumulation of Evans Blue. In some cases, LNs were detected by stereoscopic microscopy.

Immunohistochemistry

Mouse tissues were fixed in Mildform (Wako, Osaka, Japan), embedded in paraffin and sectioned using a microtome. We used a mouse antihuman CD3 (PS1, Nichirei, Tokyo, Japan) or anti-CD20 (L26, Leica Microsystems, Tokyo, Japan) antibody for human T or B cells, respectively. The specimens were stained using a Leica BOND-MAX automated immunohistochemistry stainer (Leica Microsystems, Tokyo, Japan).

Enzyme-Linked Immunosorbent Assay (ELISA)

The total plasma human immunoglobulin (Ig) M and IgG levels in reconstituted NOG or NOG-pRORγt-γc mice were measured by ELISA using a human Ig assay kit (Bethyl, Denver, CO, USA).

To assay ovalbumin (OVA)-specific IgG antibodies, hu-HSC-NOG-GM-CSF/IL-3 Tg (NOG-GM3 Tg) or hu-HSC NOG-pRORγt-γc/GM-CSF/IL-3 Tg (NOG-pRORγt-γc/GM3 Tg) mice were immunized at 12 weeks following HSC transplantation three times every 10 days with mixture of 10 μg OVA (Sigma-Aldrich) with 2 mg Alum (Cosmo Bio, Tokyo, Japan) by intraperitoneal injection. Plasma from the immunized mice was harvested 4 days after the final immunization. Specific antibodies against OVA were measured by a standard method. Briefly, 96-well plates were coated with 5 μg/ml OVA at 4°C overnight. They were subsequently washed and blocked with PBS containing 1% bovine serum albumin. The collected plasma samples were loaded after threefold serial dilution to 1:6,561 in blocking solution. An HRP-conjugated antihuman Ig antibody was used as the secondary antibody. Anti-IgG- and -IgM-specific Abs were purchased from Bethyl. 3,3′,5,5′-Tetramethylbenzidine was used as a substrate for detection. The absorbance at 450 nm was measured using a microplate reader. The titer was defined as the dilution at which the absorbance of the sample became equivalent to that of non-immunized mice.

RESULTS

Restoration of Mouse LN Organogenesis in NOG-pRORγt-γc Tg Mice

To restore mouse LNs in the γc-deficient background, we attempted to express the mouse γc gene in an LTi-lineage-specific manner. Because RORγt is the critical master transcription factor for lineage specification, we generated a BAC transgenic strain in which expression of the γc gene was regulated by the endogenous control elements of the RORγt locus (Figure S1 in Supplementary Material). First, we investigated whether B6-pRORγt-γc Tg mice exhibited rescued normal LN development in the absence of the endogenous mouse γc gene. The Tg mice were crossed with γc-gene deficient mice (γc KO) to obtain the pRORγt-γc Tg in γc KO mice. Transgenic expression of the γc gene in the LTi-lineage restored LN development, which was absent in γc KO mice (**Figure 1**). After confirming the ability to stimulate LN organogenesis, we subsequently produced NOG-pRORγt-γc Tg mice (NOG-pRORγt-γc Tg) by backcrossing, and LN development in the NOG background was assessed (**Figures 2A,B**).

Macroscopic analysis revealed that most LNs were restored, although there were variances in the degree depending on the location. For example, restoration of cervical, mediastinal, and pyloric/pancreatic LNs was evident in almost 100% of NOG-pRORγt-γc Tg mice. The frequencies in NOG-non Tg mice of the same LNs were 30, 0, and 40%, respectively (**Figure 2B**). More than 80% of NOG-pRORγt-γc Tg mice had brachial, inguinal, and lumbar LNs, compared to 40, 0, and 5%, respectively, in NOG-non Tg mice. Axillary, sacral, and popliteal LNs were detected in about 50% of Tg mice, compared to 10, 0, and 0%, respectively, in NOG-non Tg mice. Renal LN development was not evident even in the Tg mice (**Figure 2B**). Another distinct feature of the Tg mice was enlargement of the mesenteric LNs (mLNs; **Figure 2A**).

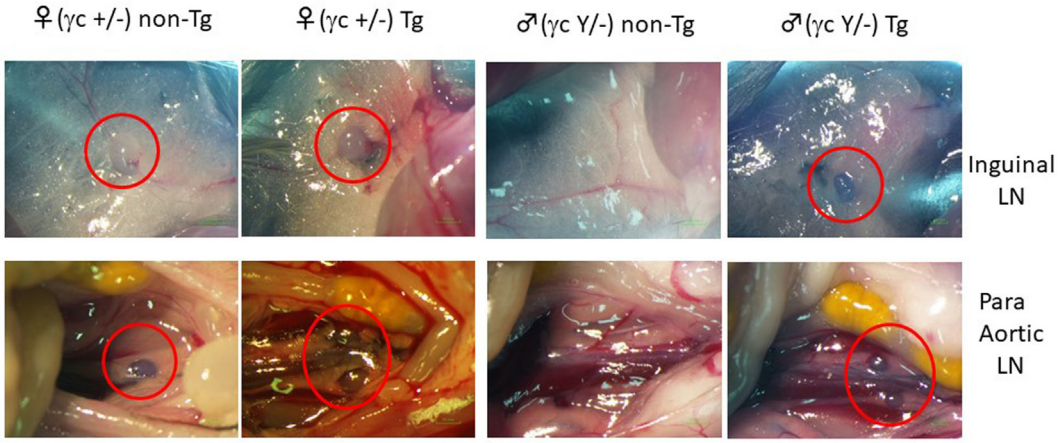

FIGURE 1 | Induction of lymph node (LN) organogenesis in γc-deficient mice using the pRORγt-γc transgene. A bacterial artificial chromosome (BAC)-transgenic (Tg) male founder mouse was crossed with female NOD/shi-*scid*-IL-2Rγ^{null} (NOG) mice. The presence of LNs in the F1 mice was macroscopically confirmed. Red circles indicate inguinal LNs (top panels) and para-aortic LNs in the abdomen (bottom panels).

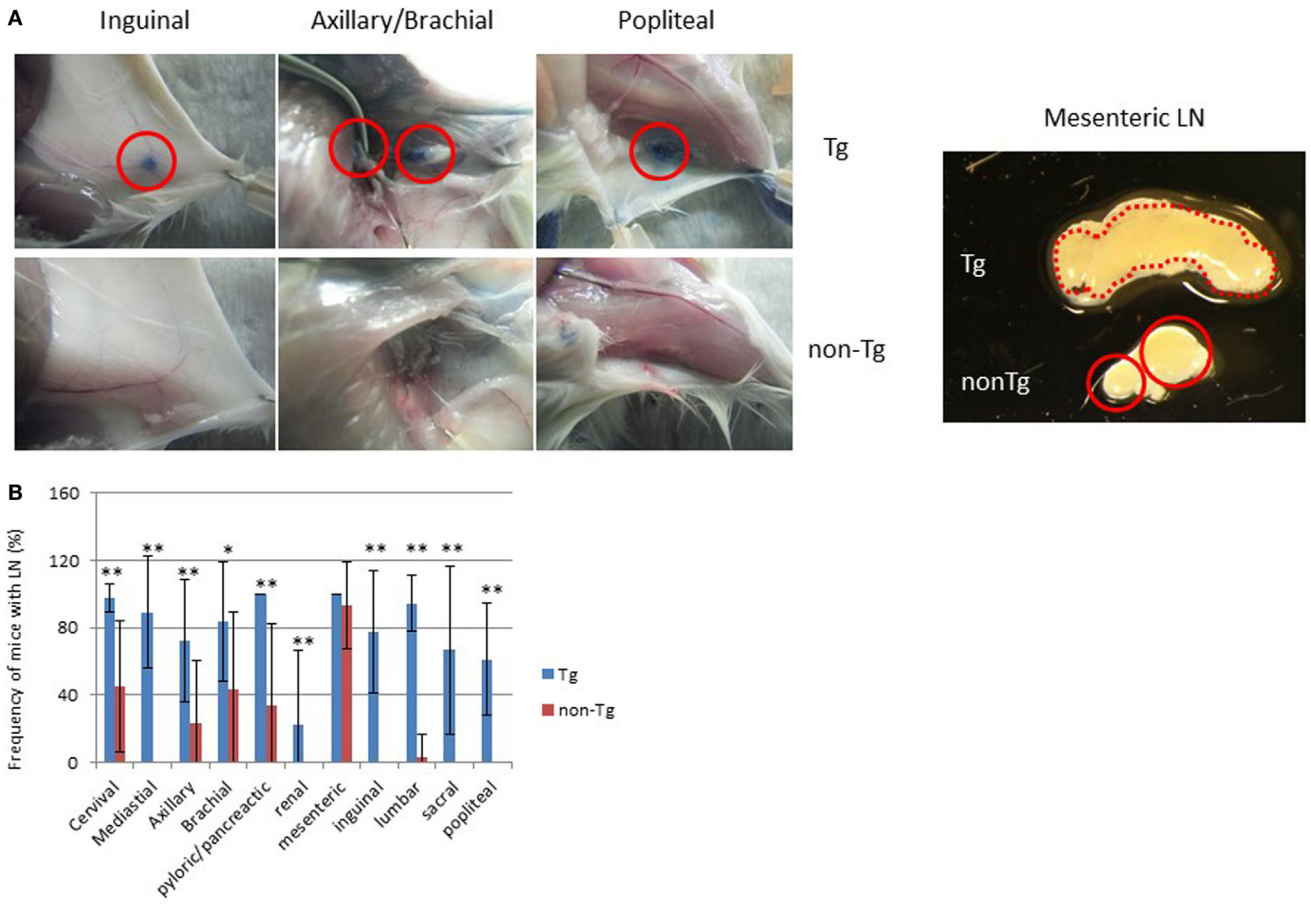

FIGURE 2 | Restored lymph nodes (LNs) in NOG mice. **(A)** LNs in NOG-pRORγt-γc Tg and NOG non-Tg mice. Evans Blue was subcutaneously administered into the tail base or foot pad for visualization of draining LNs (left panels). Red circles indicate inguinal, axillary/brachial, and popliteal LNs. Representative mesenteric LNs (mLNs) from NOG-pRORγt-γc Tg and NOG non-Tg mice are shown in the right panel. Two distinct LNs from NOG mice are circled in red. **(B)** Efficiency of LN restoration in NOG–pRORγt-γc Tg mice. NOG-pRORγt-γc Tg or NOG non-Tg mice were examined for the presence of tissue-associated LNs. For scoring, the number of LNs in each tissue from individual mice was counted and the ratio to the number of the corresponding tissue-associated LNs in wild-type NOD mice was calculated. Mean ± SD from NOG-pRORγt-γc Tg ($n = 9$) and NOG non-Tg mice ($n = 15$). Student's *t*-test was performed to assess statistical significance (*$p < 0.05$ and **$p < 0.01$).

Whereas NOG-non Tg mice had two small distinct mLNs, Tg mice had a consecutive form of mLNs similar to those in WT mice (**Figure 2A**). However, we did not detect Peyer's Patches (data not shown).

To examine whether human lymphocytes could migrate and colonize the restored LNs of NOG-pRORγt-γc Tg mice, Tg mice were X-irradiated and transplanted with HSCs. After confirming development of human T cells in PB at 20 weeks post-HSC transplantation, we isolated LNs and analyzed the MNCs in the LNs by flow cytometry. Human lymphocytes were detected in all LNs. The subsets of human lymphocytes differed depending on the LN location. Although a considerable number of human B cells were detected in most of the LNs, the brachial, axillary, and popliteal LNs contained a few human B cells, 0–5% in human CD45$^+$ cells. All LNs contained both human CD4$^+$ and CD8$^+$ T cells (**Figure 3**). Histological analysis of LNs showed a disorganized structure with a diffuse T-cell distribution rather than clear segregation of the B- and T-cell zones (**Figure 3B**). The disorganized structure was similar to that in NOG-non Tg mice (Figure S2 in Supplementary Material). We could not isolate a measurable number of human cells from the intestinal lamina propria in spite of the enlarged mLN in NOG-pRORγt-γc Tg mice (data not shown).

Development of Human Lymphocytes in NOG-pRORγt-γc Tg Mice

Human hematopoiesis was compared between NOG-non Tg and NOG-pRORγt-γc Tg mice. PB MNCs were analyzed 8–16 weeks after HSC transplantation (**Figure 4**). The frequency and number of human CD45$^+$ cells did not differ between the two strains (**Figure 4A**). The development and differentiation of human CD33$^+$ CD45$^+$ myeloid cells were also comparable between non-Tg and pRORγt-γc Tg mice (data not shown). With respect to human lymphocytes, the development of human CD45$^+$ leukocytes was not different at 8 weeks post-HSC transplantation. However, the frequency and absolute number of human T cells was significantly higher in pRORγt-γc Tg mice than in non-Tg mice at 12 weeks after HSC transplantation (**Figure 4C**). Although the frequency of human B cells was lower in Tg mice than in non-Tg mice, the absolute number of human B cells was not different (**Figure 4B**). Reflecting the increase in human

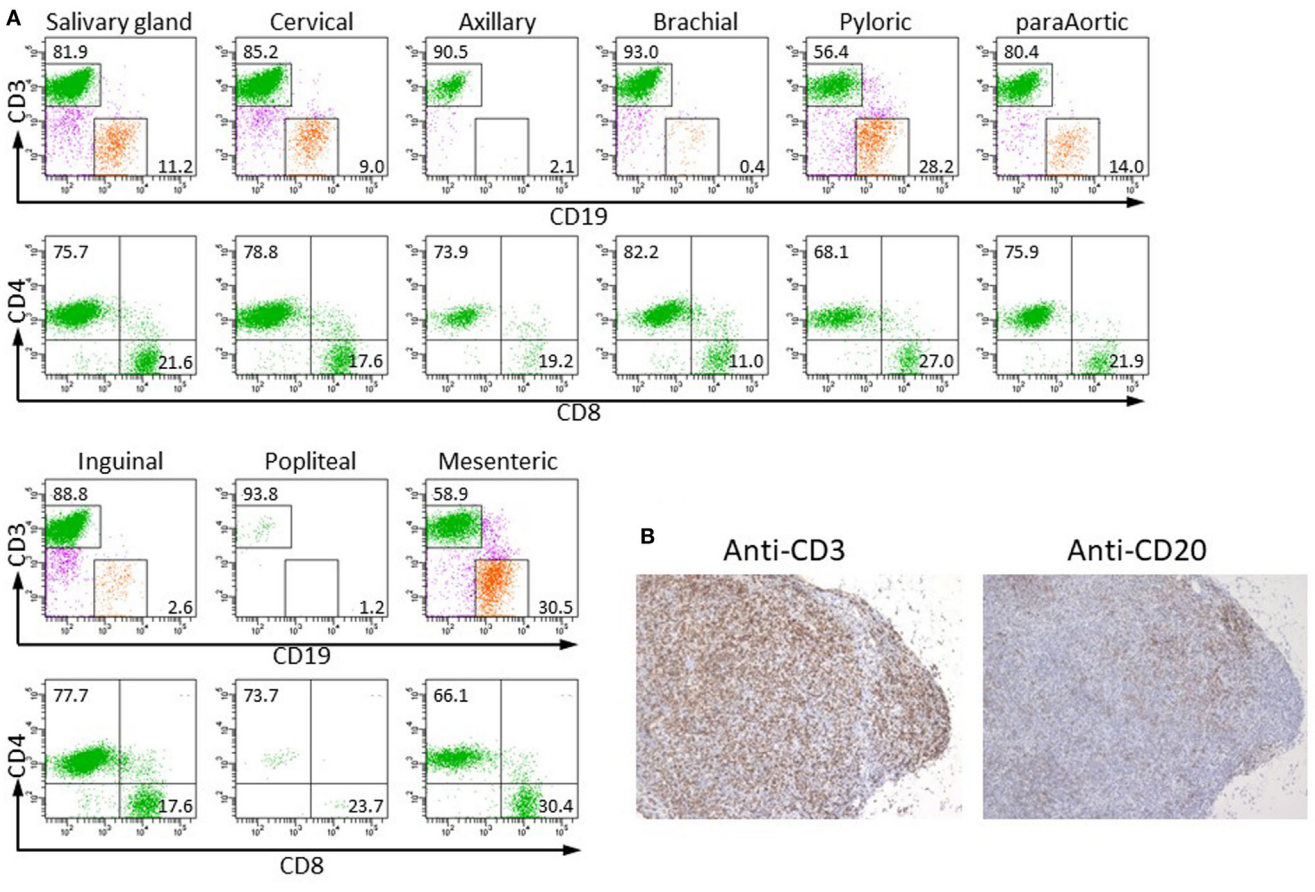

FIGURE 3 | Colonization of restored lymph nodes (LNs) by human lymphocytes. **(A)** The indicated LNs were isolated from NOG-pRORγt-γc Tg mice at 20 weeks after hematopoietic stem cell transfer, and human lymphocytes were analyzed by fluorescence-activated cell sorting (FACS). A representative result from three different mice is shown. **(B)** Immunohistochemistry of mLNs. mLNs from the same mice used in **(A)** were fixed in formalin and sectioned after embedding in paraffin. Sections were stained with antihuman CD3 (left) and CD20 (right) antibodies.

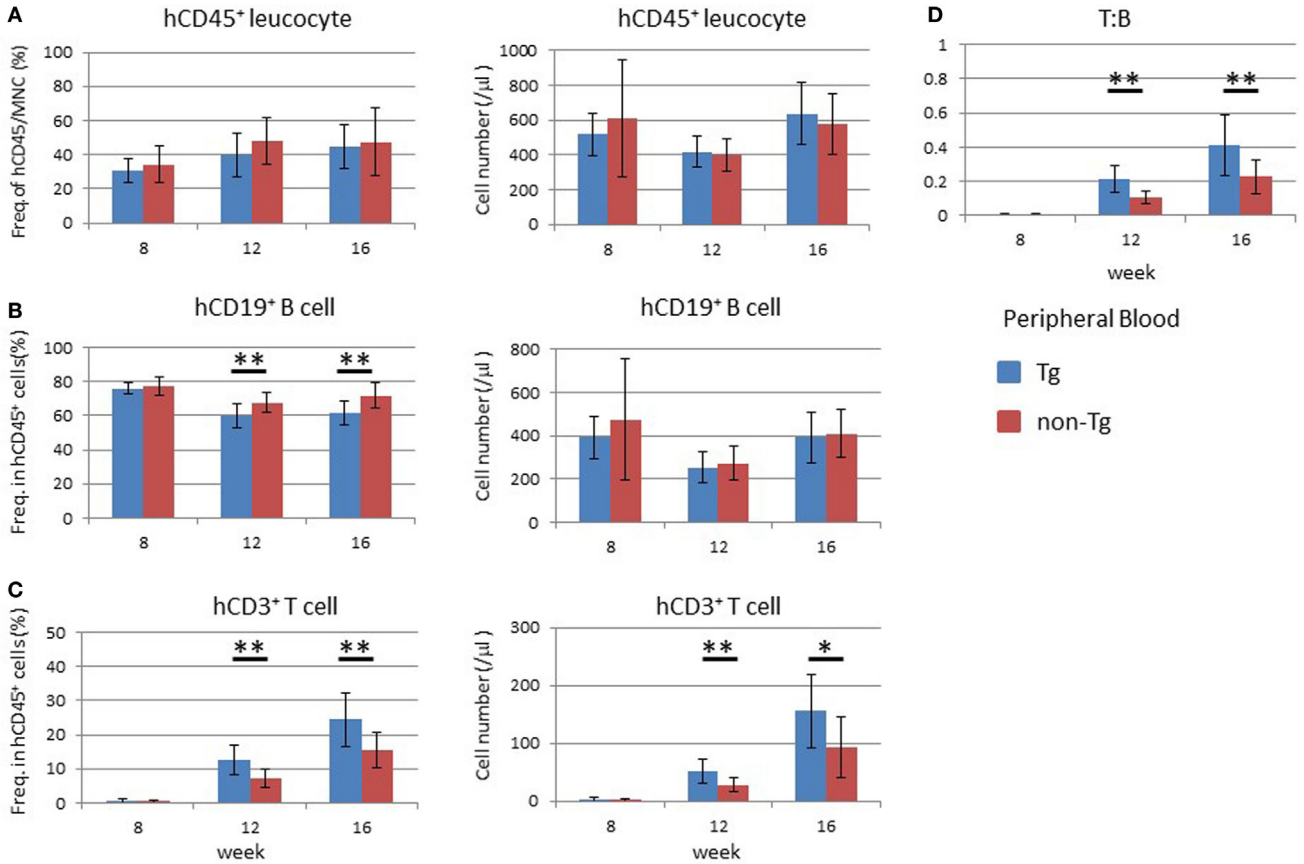

FIGURE 4 | Development of human leukocytes in NOG-pRORγt-γc Tg mice. Peripheral blood (PB) was collected at the indicated time points after hematopoietic stem cell transfer. A portion was used for enumeration of total mononuclear cells. The remaining blood was subjected to fluorescence-activated cell sorter (FACS) for human leukocytes. **(A)** Frequency and absolute number of human CD45+ cells in total mononuclear cells. **(B,C)** Frequencies and absolute numbers of human B **(B)** and human T **(C)** cells among human CD45+ cells. Cellularity was calculated by multiplying the number of total mononuclear cells by the frequencies of each human subpopulation determined by FACS. **(D)** Kinetic change of the human T to B cell ratio. Mean ± SD from NOG-pRORγt-γc Tg (n = 12) and NOG non-Tg mice (n = 11). Student's t-test was performed to assess statistical significance (*p < 0.05 and **p < 0.01). A representative result from three independent experiments is shown.

T cells, the T:B ratio was higher in Tg mice than in non-Tg mice at 12 and 16 weeks after HSC transfer (**Figure 4D**).

Analysis of the BM at 16 weeks after HSC transplantation demonstrated that the frequency and absolute number of human CD45+ leukocytes were higher in non-Tg mice than in Tg mice (Figure S3 in Supplementary Material). There were no significant differences in the frequencies and numbers of human CD19+ cells, which include human immature and mature B lineage cells, and human CD3+ T cells (Figure S3 in Supplementary Material). In the thymus, there was no significant difference in the cellularity of human thymocytes (**Figure 5A**). Analysis of subpopulations showed a significant reduction in the frequency of CD4+CD8+ thymocytes in NOG-pRORγt-γc Tg mice compared with non-Tg mice. In contrast, the frequencies of CD4+CD8− and CD4−CD8+ thymocytes were higher in NOG-pRORγt-γc Tg mice than in NOG-non-Tg mice (**Figure 5B**). However, the absolute numbers of these subpopulations were not significantly different due to the large variances in the total number of thymocytes (**Figure 5C**). FACS analysis of splenocytes demonstrated that the frequency and absolute number of human CD45+ cells were not different irrespective of LN restoration (**Figure 6A**). A considerable portion of human CD19+ cells in hu-HSC NOG mice are immature B cells, including transitional B cells, and they do not express CD20 or CD21 (27). Thus, to examine the maturation of human B cells in NOG-pRORγt-γc Tg mice, we compared the frequency and number of the CD19+CD20+CD21+ subpopulation between NOG-pRORγt-γc Tg and NOG-non-Tg mice. While the frequency of mature human B cells was higher in non-Tg than in Tg mice, there was no significant difference in the absolute number (**Figure 6B**). In contrast, the frequency of human T cells was significantly higher in Tg than in non-Tg mice. We did not detect a significant difference in the cellularity of human T cells (**Figure 6C**). The human B to T cell ratio was comparable between Tg and non-Tg mice (**Figure 6D**). Regarding T cell subsets, the ratio of CD4+ to CD8+ T cells was not altered by the presence of LNs (**Figure 6E**).

We next examined LNs and found that pRORγt-γc Tg mice showed remarkable enlargement of mLNs. The weight of the

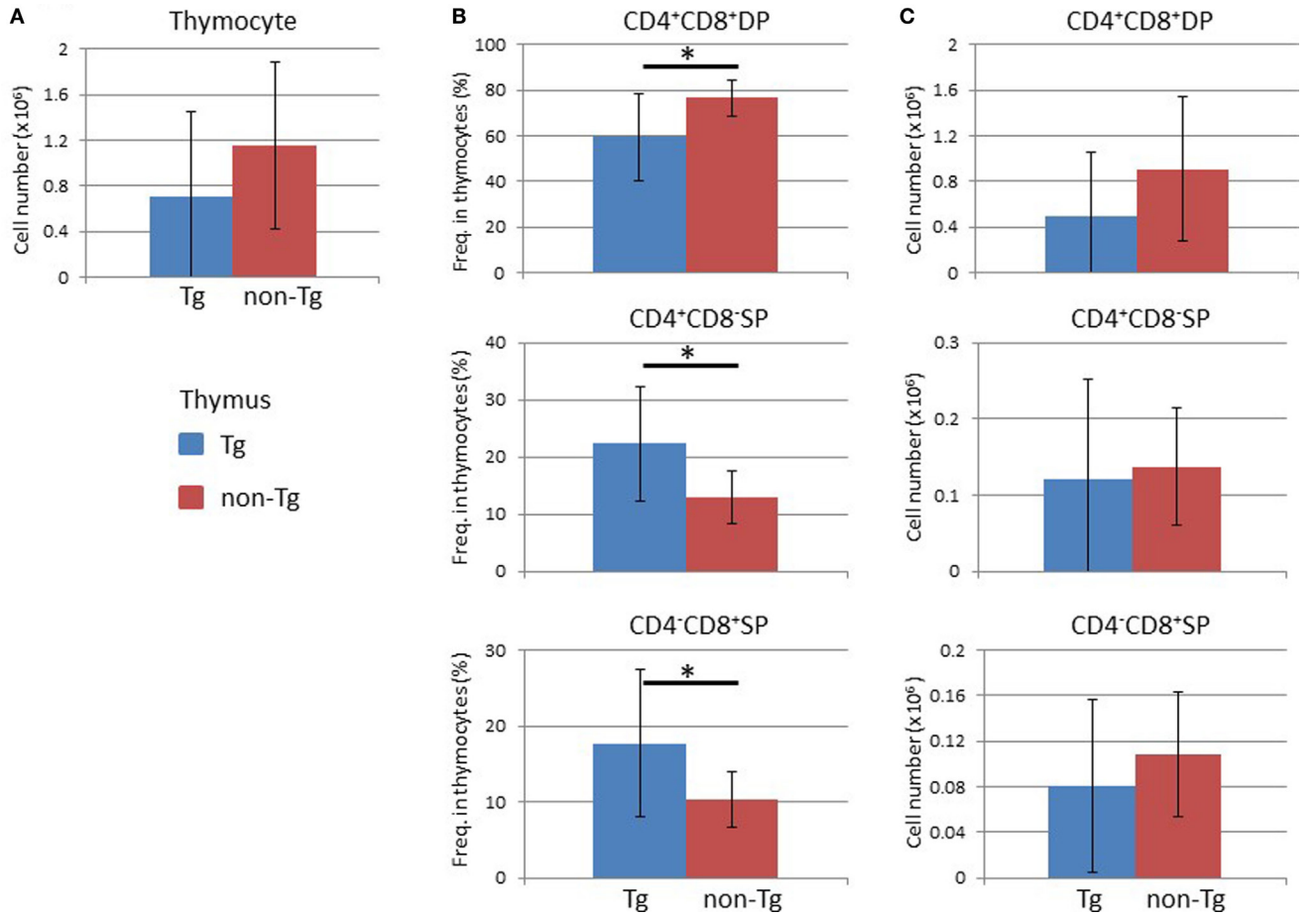

FIGURE 5 | Analysis of human cells in the thymus. Thymocytes were prepared from the thymi of NOG-pRORγt-γc Tg and NOG non-Tg mice at 24 weeks after hematopoietic stem cell transplantation and analyzed by fluorescence-activated cell sorting. **(A)** Absolute numbers of human thymocytes. **(B,C)** The frequencies of human $CD4^+CD8^+$ double positive, $CD4^+CD8^-$, and $CD4^-CD8^+$ single positive cells in human thymocytes **(B)** and the absolute numbers of each cell subpopulation **(C)**. Mean ± SD of NOG-pRORγt-γc Tg ($n = 12$) and NOG non-Tg mice ($n = 11$). Asterisk indicates statistical significance ($p < 0.05$).

mLNs in pRORγt-γc Tg mice was about eightfold higher than that in non-Tg mice (**Figure 7A**). Because other LNs were smaller than the mLNs, all LNs other than the mLNs were pooled for analysis; mLNs were analyzed separately. Reflecting the increase in weight, mLNs in NOG-pRORγt-γc Tg mice contained a significantly larger number of human leukocytes, which included both human $CD19^+$ B cells and $CD3^+$ T cells, than non-Tg mice (**Figure 7B**). The frequency of human $CD45^+$ cells in total MNCs was not influenced, suggesting that mouse $CD45^+$ cells were proportionally increased (**Figure 7B**). The T:B cell ratio was higher in Tg mice than in non-Tg mice (**Figure 7C**). As in the spleen, the CD4 to CD8 ratio was not different between Tg and non-Tg mice (**Figure 7D**).

An increased number of human leukocytes, including human $CD19^+$ B and $CD3^+$ T cells, in NOG-pRORγt-γc Tg mice was also observed in other tissue-associated LNs (**Figure 8A**). The frequency of human $CD45^+$ cells was not influenced in tissue-associated LNs as in mLNs (data not shown). The ratio of these two populations remained unchanged between non-Tg and Tg mice (**Figure 8A**). The proportions of $CD4^+$ and $CD8^+$ T cells in $CD3^+$ T cells also did not differ between non-Tg and Tg mice (**Figure 8A**).

After determining the absolute number of human lymphocytes in secondary lymphoid organs (spleen, LNs, and mLNs), the total number of human cells in the whole mouse was calculated. There was no significant difference in the human $CD45^+$ cell number between non-Tg and Tg mice (**Figure 8B**). Interestingly, the total number of human $CD3^+$ T cells increased about threefold in Tg mice compared to non-Tg mice (**Figure 8B**), while the number of human $CD19^+CD20^+CD21^+$ mature B cells was not significantly different (**Figure 8B**). Accordingly, the T to B cell ratio was higher in NOG-pRORγt-γc Tg mice than in NOG-non-Tg mice. Due to the migration of human lymphocytes into LNs, the lymphocyte tissue distribution differed markedly between NOG-pRORγt-γc Tg mice and non-Tg mice. In normal NOG non-Tg mice, almost 90% of human T cells resided in the spleen. In contrast, ≤60% of human T cells were present in the spleen in Tg mice, and ~30 and 10% of human T cells migrated into mLNs or other tissue-associated LNs, respectively (**Figure 8C**). Mature human B cells were also distributed primarily in LNs (data not shown).

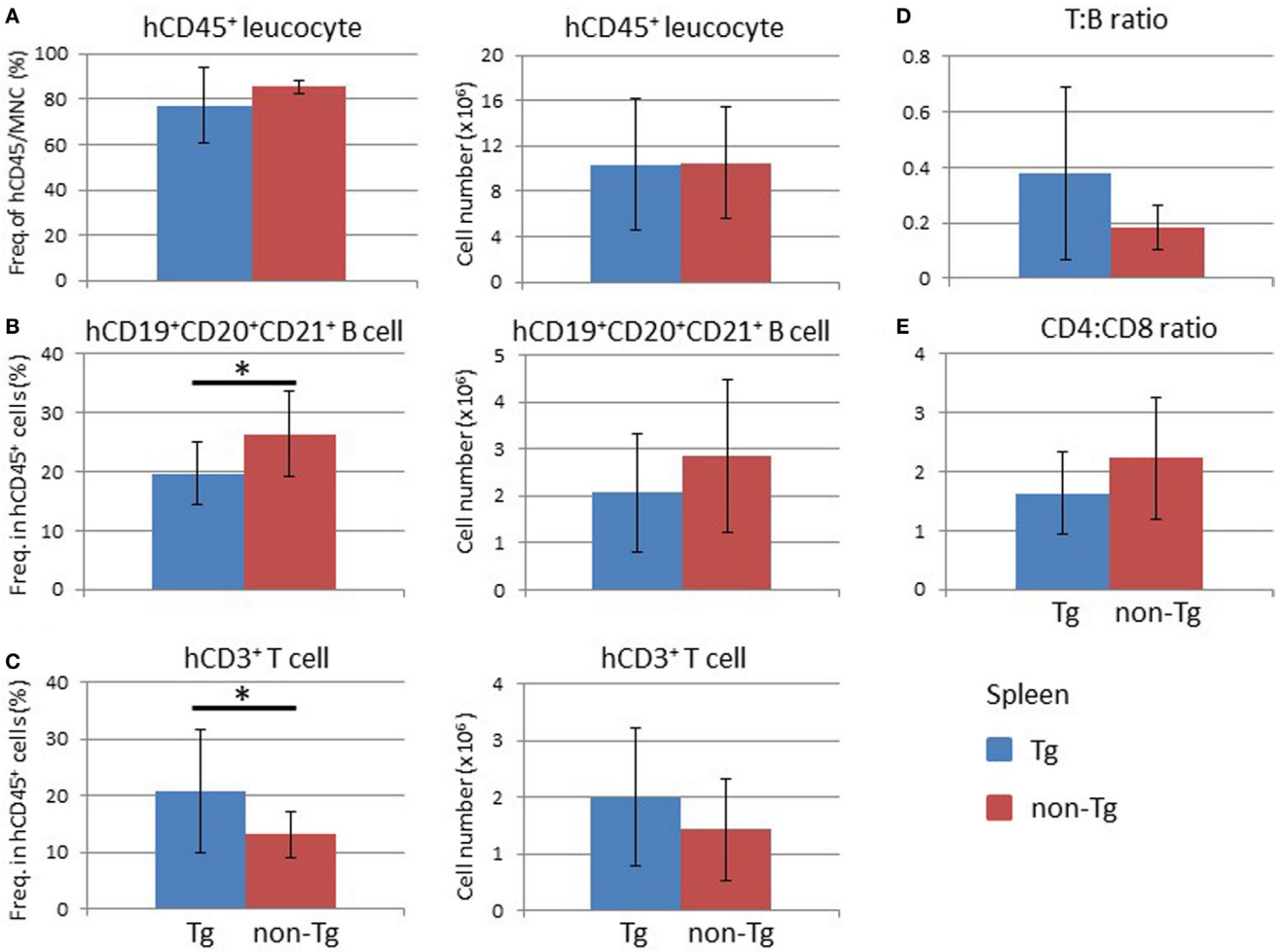

FIGURE 6 | Analysis of human cells in the mouse spleen. Splenocytes were prepared from the spleens of NOG-pRORγt-γc Tg and NOG non-Tg mice for fluorescence-activated cell sorting analysis at 24 weeks after HSC transplantation. **(A)** Frequency and absolute number of human CD45+ cells in total mononuclear cells. **(B,C)** Frequencies and absolute numbers of human CD19+ B cells **(B)** and human CD3+ T cells **(C)** among human CD45+ cells. **(D)** Human T to B cell ratio in human CD45+ cells. **(E)** The CD4+ T cell to CD8+ T cell ratio in human T cells. Mean ± SD from NOG-pRORγt-γc Tg (n = 12) and NOG non-Tg mice (n = 11). Asterisk indicates statistical significance (*$p < 0.05$).

Augmentation of Humoral Immune Responses in NOG-pRORγt-γc Tg Mice

To examine the immunological features of hu-HSC NOG-pRORγt-γc Tg mice, serum total human IgM and IgG levels were quantified by ELISA. The IgM level was equivalent in non-Tg and Tg mice, whereas the IgG level was significantly higher in Tg mice than in non-Tg mice (**Figure 9A**). Next, we investigated whether LN-sufficient humanized mice could induce antigen-specific humoral immune responses. Impaired production of antigen-specific IgG responses in humanized mice has been reported, likely due to the lack of cognate interactions between mouse major histocompatibility complex (MHC)-restricted human T cells and human leukocyte antigen (HLA) on human B cells (30, 31). However, antigen-specific IgG responses could be facilitated by crosstalk between antigen-specific B and T cells in LNs. To further improve the probability of human immune responses, we used transgenic mice the GM-CSF/IL-3 transgenic NOG (NOG-GM3 Tg). This strain allowed the development of various lineages of human cells, including lymphoid and myeloid cells, from HSCs (29). Those human cells could facilitate induction of immune responses. After reconstitution of NOG-pRORγt-γc/GM3 Tg or NOG-GM3 Tg mice with the human immune system, we immunized the animals with OVA/Alum complex. The OVA-specific human IgG titer was significantly higher in NOG-pRORγt-γc/GM3 Tg than in NOG-GM3 Tg mice (**Figure 9B**), and was ~250-fold higher than that in non-immunized mice. Although we expected that improved human hematopoiesis enhanced antigen-specific antibody responses in NOG-GM3 Tg mice, the induction of OVA-specific IgG was modest. Next, we investigated the production of IL-4 and IL-21 by CD4+ T cells, because these cytokines are important for promoting class switching and plasma cell differentiation (32, 33). The frequency of IL-21+ CD4+ T cells was significantly higher in mLNs from NOG-pRORγt-γc/GM3 Tg than NOG-GM3 Tg mice

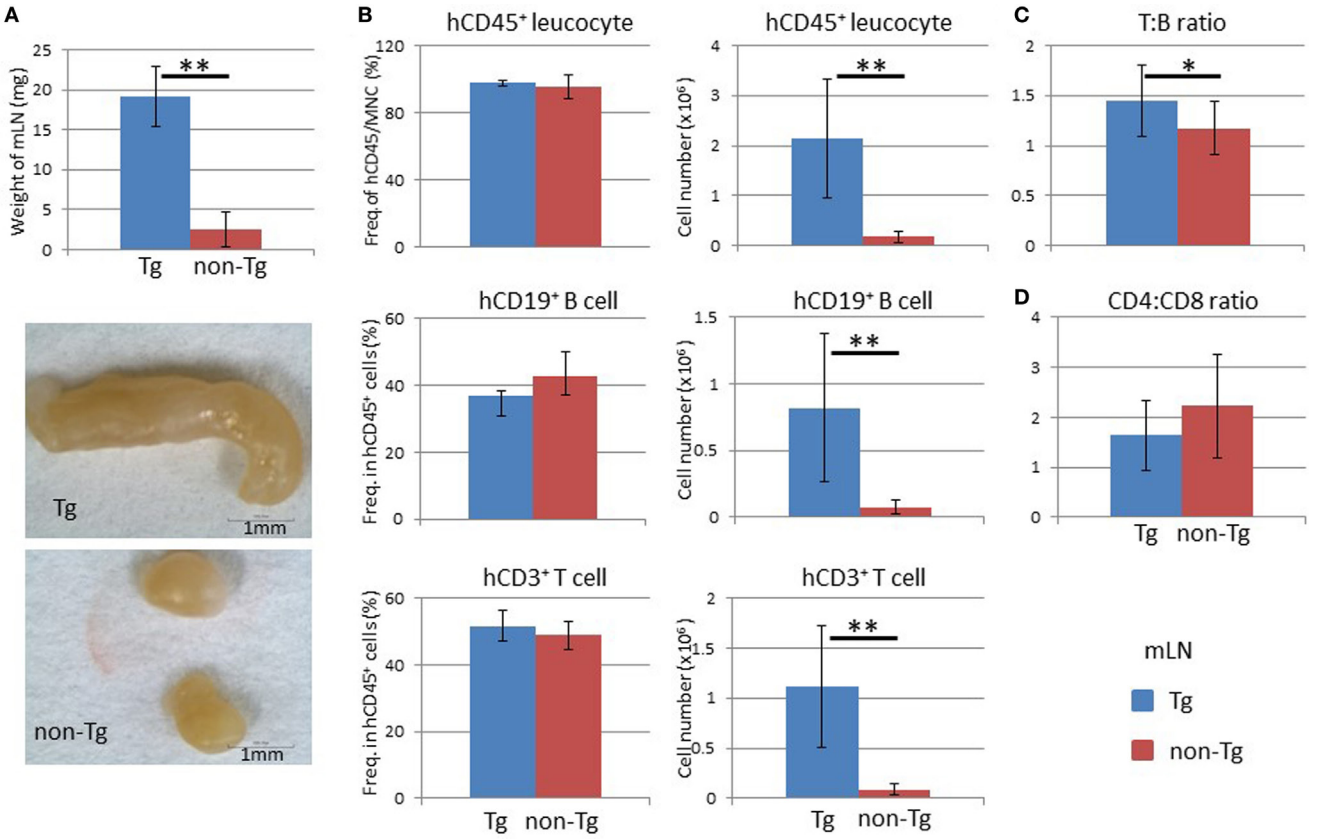

FIGURE 7 | Analysis of mesenteric lymph nodes (mLNs). **(A)** Weight of mLNs. mLNs were isolated at 24 weeks after hematopoietic stem cell transplantation. Representative photographs of mLNs from human HSC-engrafted NOG-pRORγt-γc Tg and non-Tg mice. **(B)** Frequency and absolute number of human leukocytes. Human mononuclear cells were isolated from mLNs and analyzed by fluorescence-activated cell sorting. The number of human CD45+ leukocytes was obtained by multiplying the total number of mononuclear cells by the frequency of human CD45-positive cells. **(C)** Human T to B cell ratio. **(D)** Human CD4+ T cell to CD8+ T cell ratio. Mean ± SD from NOG-pRORγt-γc Tg ($n = 12$) and NOG non-Tg mice ($n = 11$). Student's *t*-test was performed to assess statistical significance (*$p < 0.05$ and **$p < 0.01$).

(**Figure 9C**), but this was not the case in splenic CD4+ T cells from the same animals. There were no differences in the frequency of IFNγ-, IFN-17-, and IL-4–producing CD4+ T cells between NOG-pRORγt-γc/GM3 Tg and NOG-GM3 Tg mice (Figure S4 in Supplementary Material). A standard immunophenotyping protocol using chemokine receptor expression also confirmed the increase of $CD3^+CD4^+CD5RA^-CXCR5^+$ follicular helper T cells (Tfh) in frequency (34) and there was no difference in the frequency of FOXP3+ CXCR4+CD25+ CD4+ human regulatory T cells (Treg) in CD4+ T cells between NOG-pRORγt-γc Tg and non-Tg mice (Figure S5 in Supplementary Material) (35). These results suggest that the composition of T cell subsets was generally maintained in NOG-pRORγt-γc Tg mice except the increase of IL-21+ producing Tfh cells. It should be noted, however, that the absolute cell number of each subset significantly increased reflecting the increase of total CD4+ T cells.

DISCUSSION

In this study, we demonstrated that LN organogenesis could be restored in NOG mice by expressing the mouse γc gene under the control of the RORγt promoter, and that these LNs function as a reservoir for human lymphocytes after reconstitution of the human immune system. Furthermore, our results showed that restored LNs could confer immunological competence on humanized NOG mice.

To restore LN development in NOG mice, we generated a NOG transgenic strain expressing human TSLP. This approach was not successful, however, in the NOG background, as our NOG transgenic strain expressing the human TSLP gene, which possesses about 42% homology with the mouse TSLP gene, developed severe thymoma, which resembled the disease frequently seen in NOD-*scid* mice (data not shown) (36). It is possible that cytokine signaling through mouse IL-7Rα or mouse TSLP receptor stimulated oncogenic mechanisms intrinsic to mice with the NOD background. The efficiency of LN restoration was greater in TSLP Tg γc-KO mice than in NOG-pRORγt-γc Tg mice. Indeed, some NOG-pRORγt-γc Tg mice showed unilateral development of axillary, brachial, inguinal, or popliteal LNs, while the TSLP Tg γc-KO mice showed almost 100% LN organogenesis (20). It is possible that the expression level of γc in LTi cells was not sufficient for full recovery of this lineage, resulting in partial

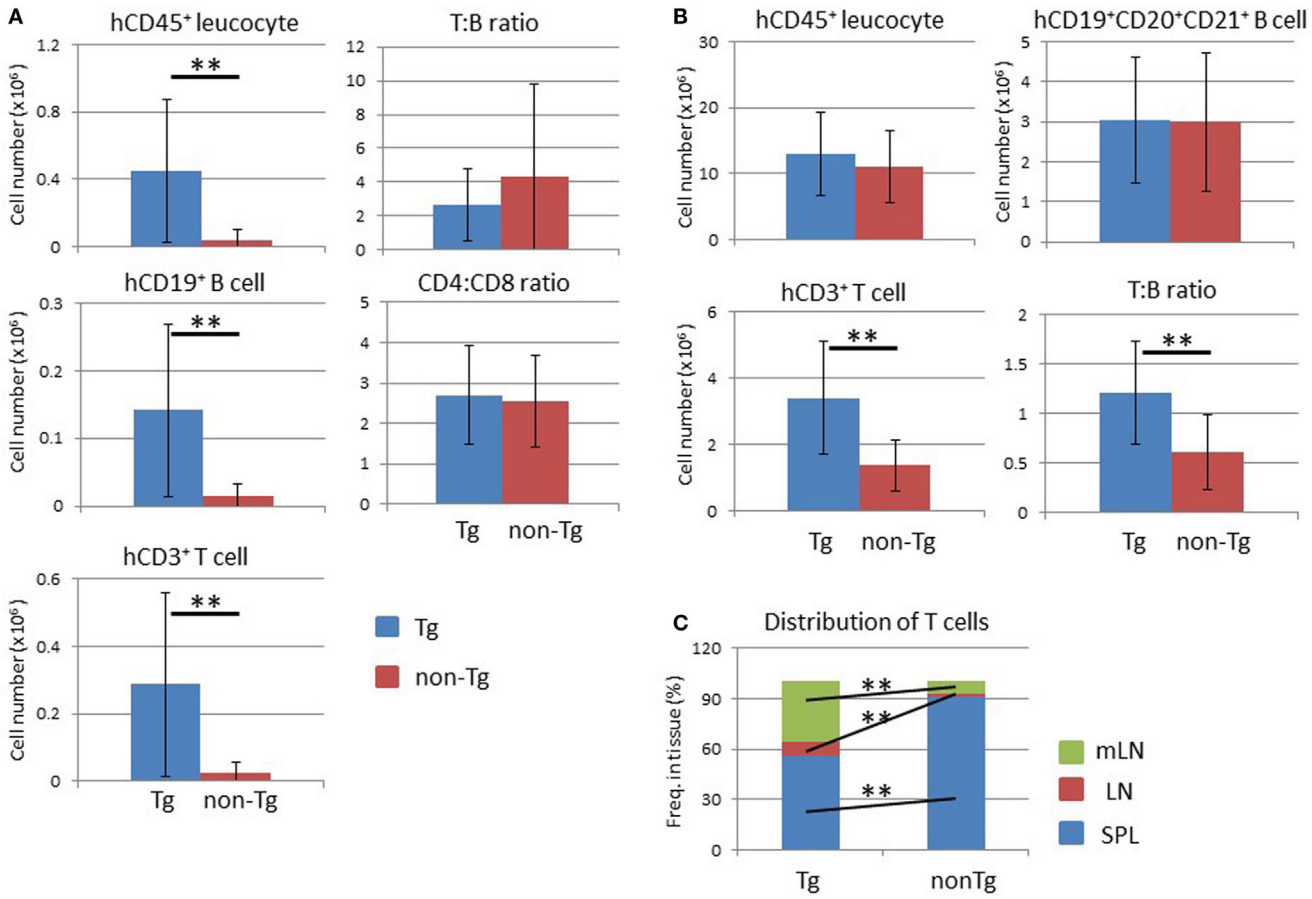

FIGURE 8 | Analysis of lymph nodes (LNs) and distribution of human T lymphocytes. **(A)** Absolute number of human leukocytes in tissue-associated LNs. Human mononuclear cells were prepared from pooled LNs from NOG-pRORγt-γc Tg and NOG non-Tg mice at 24 weeks after hematopoietic stem cell transplantation. (Left panels) Numbers of human CD45$^+$ leukocytes (upper), human B cells (middle), and human T cells (bottom) were calculated by multiplying the total number of mononuclear cells by the frequency of each fraction. (Right panels) The human T to B cell ratio (upper panel) and human CD4$^+$ T cell to CD8$^+$ T cell ratio (bottom panel). **(B)** Total number of human leukocytes in secondary lymphoid organs. Data from the spleen, LNs, and mesenteric LNs were summed for human CD45$^+$ leukocytes (upper left), human B cells (upper right), and human T cells (bottom left). The human T to B cell ratio in all lymphoid organs is also shown (bottom right). **(C)** Distribution of human T cells. The proportion of human T cells in each secondary lymphoid organ was calculated. Mean ± SD from NOG-pRORγt-γc Tg (n = 12) and NOG non-Tg mice (n = 11). Statistical significance was evaluated by Student's t-test (**$p < 0.01$).

development of LNs in NOG-pRORγt-γc Tg mice. Supporting this hypothesis, although we detected significant increase of the frequency and number of LTi cells in NOG-pRORγt-γc Tg mice compared with NOG-non-Tg mice. However, the increase was not more than twofold in number (Figure S6 in Supplementary Material). This may also explain the lack of Peyer's patches. Mice with constitutive expression of the mouse γc gene with strong promoters could results in the better restoration of LN development and Peyer's patches. As a result, such strains, an equivalent strain to NOD-*scid* mice, may have better organized LN structures and elicit better immune responses like in NOD-*scid* mice (37). However, at the expense of the benefit, such strains may develop thymoma (36). In addition, they may have various lymphoid lineages which reduce the efficiency of engraftment of human hematopoietic cells (38).

Humanized mice generated by simple transfer of human cord blood-derived HSCs exhibit suboptimal immune responses (1). These weak immune reactions can be in part explained by inefficient development of human T cells by the atrophic mouse thymus, lack of HLA-restriction of human T cells (27), incomplete maturation of human B cells (27), or accumulation of human T cells susceptible to cell death by antigen stimulation (27). These problems have been addressed by various approaches. For example, administration of recombinant human Fc-IL-7 protein (39) or lentiviral delivery of human IL-7 increased T-cell numbers (40). HLA-matching between HSC donor and recipient mice by introducing HLA transgenes into mice induced HLA-restricted human immune responses (30, 31, 41, 42). As an alternative approach to overcome the limitations inherent to humanized mice, we examined whether restoration of LNs would improve human lymphocyte homeostasis and human adaptive immune responses.

Preferential expansion of human T cells was evident in NOG-pRORγt-γc Tg mice. In addition, restoration of LNs induced a

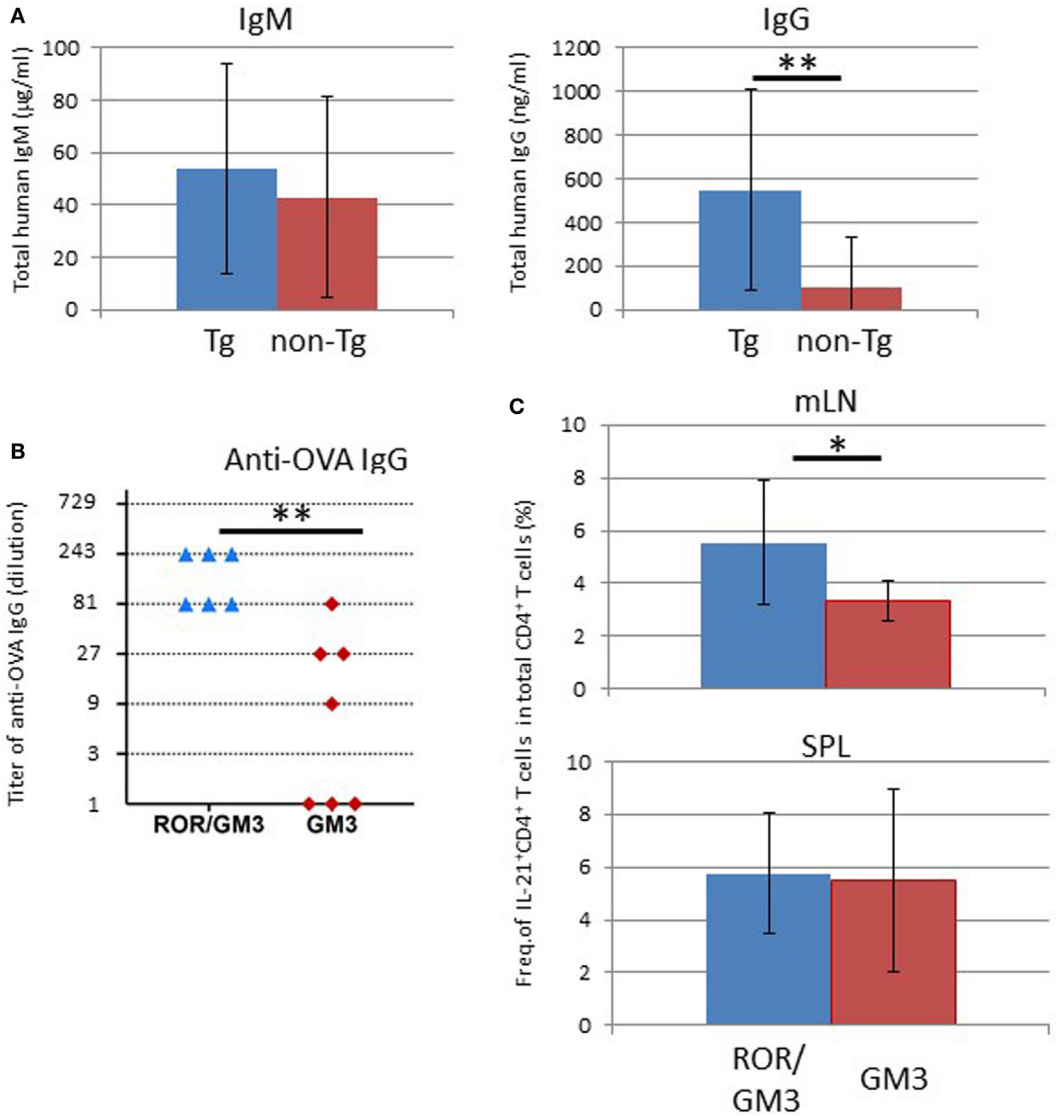

FIGURE 9 | Enhanced humoral responses in NOG-pRORγt-γc Tg mice. **(A)** Total IgM and IgG levels in plasma. Plasma was prepared 24 weeks after hematopoietic stem cell (HSC) transplantation and total IgM and IgG levels were quantified by enzyme-linked immunosorbent assay (ELISA). Mean ± SD from NOG-pRORγt-γc Tg (n = 12) and NOG non-Tg mice (n = 11). Statistical significance was evaluated by Student's t-test (**$p < 0.01$). **(B)** ELISA results for ovalbumin (OVA)-specific human IgG. NOG-pRORγt-γc/GM-CSF/IL-3 Tg (ROR/GM3) (n = 6) or NOG-GM-CSF/IL-3 Tg (GM3) (n = 7) mice were transplanted with HSCs. After confirming T-cell differentiation in the peripheral blood at 12 weeks post-HSC engraftment, mice were immunized three times with OVA/Alum. Plasma was collected 4 days after the final boost. Titers of individual mice are shown. Statistical significance was evaluated by Student's t-test (**$p < 0.01$). **(C)** Increase in the number of IL-21-producing CD4+ T cells in lymph nodes (LNs). Spleen and mesenteric LNs from OVA-immunized NOG-ROR/GM3 or NOG-GM3 mice were stimulated with phorbol myristate acetate/ionomycin for 4 h in the presence of Brefeldin A. Cytokines were stained after fixation and permeabilization. Mean ± SD frequencies of IL-21+ CD4+ T cells among total CD4+ T cells. Statistical significance was evaluated by Student's t-test (*$p < 0.05$).

significant redistribution of human lymphocytes from the spleen to the LNs. Indeed, almost 40% of total human T cells were mobilized into LNs in NOG-pRORγt-γc Tg mice, mostly to the mLNs. The macroscopic analysis demonstrated that the weight of the mLNs in NOG-pRORγt-γc Tg mice was eightfold higher than that in NOG non-Tg mice, and they harbored ~35% of the total human T cells. Although the reason for the preferred residence of human T cells in mLNs is unclear, not only simple migration but also homeostatic proliferation may be strongly induced in the enlarged mLNs in NOG–pRORγt-γc Tg mice. This seems to be mediated by thymus-independent mechanisms, as the numbers of thymocytes were not different between Tg and non-Tg mice. By draining the small intestine and colon, mLNs provide human T cells with abundant and non-competitive signals, which include pMHC, cytokines, and physical space. Thus, mLNs may have a marked impact on the homeostasis of human T cells. In contrast to the increase in the number of human T cells, the effect on human B cells was unremarkable. The absolute number of

human mature B cells was not significantly different between NOG-pRORγt-γc Tg and NOG non-Tg mice. Although the development of human T cells and the maturation of human B cells is reportedly correlated in humanized mice, the robust increase in human T cell number did not result in an increase in that of human mature B cells in NOG-pRORγt-γc Tg mice (43). Furthermore, histological analysis showed incomplete architecture of LNs, which lacked B-cell follicles and germinal centers. The persistent blockage of B cell maturation suggests that LNs do not provide an environment conducive to full maturation of human B cells. Considering the abundant T cells in LNs, T cell-independent factors may be necessary for B cell maturation. Our immunohistochemistry showed that mouse follicular dendritic cells (FDCs) were not induced in mLNs (data not shown). This may be due to the absence of interaction between mature human B cells and mouse FDC progenitor cells. Alternatively, human FDCs, which were of non-hematopoietic origin, may be necessary for inducing maturation of human B cells and thus organizing LN structures.

The serological analysis demonstrated induction of a partial human humoral immune response in the LN-sufficient humanized mice, despite the lack of HLA-II molecules. Introduction of HLA-DR molecules in recipient mice and matching of the HLA-DR haplotype between the recipient mice and HSC donors are essential for induction of antigen-specific IgG responses in humanized mice (30, 31). The importance of HLA-II in recipient mice was also confirmed in this study using NOG-GM/3 Tg mice, which did not show antigen-specific IgG responses despite differentiation of multiple types of human antigen-presenting cells, including dendritic cells, macrophages/monocytes, and B cells, in the spleen. Although the mechanisms for the induction of antigen-specific IgG responses in LN-restored humanized mice are unclear, the increases in the frequency of IL-21 producing $CD4^+$ T cells and the total number of $CD4^+$ T cells in LNs suggest that an IL-21-rich milieu is generated in LNs, which induces IgG class switch recombination in B cells in the vicinity, even in the absence of cognate interactions with T cells with the same antigen specificity. Introduction of HLA-II molecules may further enhance antibody production.

In this study, we developed a novel NOG substrain with immunologically competent LNs. The enhanced immune responses of NOG-pRORγt-γc Tg mice will be useful, particularly in combination with HLA Tg or human cytokine-gene introduced mouse strains. This would synergistically enhance the quasihuman immune response and facilitate development of novel vaccines against infectious diseases and immunotherapies for tumors.

AUTHOR CONTRIBUTIONS

TT designed the study, performed the data analysis, and wrote the manuscript. IK and TT conducted all of the experiments. MG, SM, and FS performed the embryo manipulation. HA maintained the NOG-pROPγt-γc Tg strains. KK was responsible for the pathological analysis. MI, RI, and TT organized the project.

ACKNOWLEDGMENTS

The authors would like to thank Takahiro Kagawa and Emika Sugiura for animal production and care. We thank Iyo Otsuka for performing the ELISAs and Dr. Masafumi Yamamoto for the genome-wide DNA analysis using microsatellite markers. This project was supported by a Grant in Aid (B) (26290034 to TT) from the Japanese Society for the Promotion of Science (JSPS). This project was commissioned by a Grant-in-Aid for Research on Hepatitis from the Japan Agency for Medical Research and Development.

SUPPLEMENTARY MATERIAL

The Supplementary Material for this article can be found online at http://www.frontiersin.org/articles/10.3389/fimmu.2017.02017/full#supplementary-material.

FIGURE S1 | Schematic of bacterial artificial chromosome recombination for expression of mouse interleukin 2Rγ under the control of the regulatory elements of mouse RORγt.

FIGURE S2 | Immunohistochemistry of mesenteric lymph node in hu-HSC NOG-non Tg mice.

FIGURE S3 | Analysis of human cells in the bone marrow (BM). BM from NOG-pRORγt-γc Tg and NOG non-Tg mice were isolated from the tibiae and analyzed by fluorescence-activated cell sorting (FACS). **(A)** Frequency and absolute number of human $CD45^+$ cells among total mononuclear cells. **(B,C)** Frequencies and absolute numbers of human $CD19^+$ B cells **(B)** and human $CD3^+$ T cells **(C)** among human $CD45^+$ cells. Mean ± SD from NOG-pRORγt-γc Tg (n = 12) and NOG non-Tg mice (n = 11).

FIGURE S4 | Frequency of human Th1, Th2, and Th17 cells in hu-HSC NOG-pRORγt-γc Tg. The mesenteric lymph node cells used in **Figure 9** were stained for human IFN-γ (Th1 cells), IL-4 (Th2 cells), and IL-17 (Th17 cells).

FIGURE S5 | Subpopulation in $CD4^+$ T cells. Spleen and mesenteric lymph node in NOG-pRORγt-γc Tg and NOG-non-Tg mice were analyzed at 16weeks after hematopoietic stem cell transplantation (n = 4). Th1 cells, Th17, or Tfh cells were defined as $CD3^+CD4^+CD45RA^-CXCR5^-CXCR3^+CCR6^-$, $CD3^+CD4^+CD45RA^-CXCR5^-CXCR3^-CCR6^+$, or $CD3^+CD4^+CD45RA^-CXCR5^-$ cells. Human regulatory T cells were defined as $FOXP3^+CCR4^+CD25^+CD4^+$ T cells. For immunophenotyping, following antibodies were used for staining and analyzed by a BD LSR Fortessa X-20 cell analyzer (BD Biosciences). Anti-CCR7-Brilliant Violet 421, anti-CD45-BV510, anti-CXCR3-APC, anti-CD4-APC, anti-CD45RA-APCCy7, anti-CCR6-PE, anti-CD4-PECy7, anti-CCR4-PECy7, and antimouse CD45-PerCP-Cy5.5 were from BioLegend. Anti-CXCR5-Brilliant Blue 515, anti-CD25-BB515, and anti-CD3-Brilliant Ultraviolet 737 were from BD Biosciences. Dead cells were excluded by 7-AAD (Beckman Coulter). Intracellular staining of FOXP3 was conducted using Anti-Human Foxp3 staining Set phycoerythrin from eBioscience according to the manufacturer's instruction. Student's t-test was performed to assess statistical significance ($^*p < 0.05$).

FIGURE S6 | Increase of LTi cells in NOG-pRORγt-γc Tg. The presence of LTi was examined in embryo of NOG-pRORγt-γc Tg and NOG-non-Tg mice at E15. The fetal intestine was smashed with a pestle and mononuclear cells were stained with a cocktail of antibodies; antimouse CD3-FITC, antimouse CD4-PE, antimouse B220, antimouse CD127 (IL-7Rα)-APC, and antimouse CD45-APC-Cy7. LTi cells were defined as $CD4^+CD127^+$ cells in $CD45^+CD3^-B220^-$ cells. A part of embryo was used for genotyping by PCR. Mean ± SD from NOG-pRORγt-γc Tg (n = 12) and NOG non-Tg mice (n = 14). Student's t-test was performed to assess statistical significance ($^*p < 0.05$).

REFERENCES

1. Shultz LD, Brehm MA, Garcia-Martinez JV, Greiner DL. Humanized mice for immune system investigation: progress, promise and challenges. *Nat Rev Immunol* (2012) 12:786–98. doi:10.1038/nri3311
2. Theocharides AP, Rongvaux A, Fritsch K, Flavell RA, Manz MG. Humanized hemato-lymphoid system mice. *Haematologica* (2016) 101:5–19. doi:10.3324/haematol.2014.115212
3. Ito R, Takahashi T, Ito M. Humanized mouse models: application to human diseases. *J Cell Physiol* (2017). doi:10.1002/jcp.26045
4. Hogan CJ, Shpall EJ, Mcnulty O, Mcniece I, Dick JE, Shultz LD, et al. Engraftment and development of human CD34(+)-enriched cells from umbilical cord blood in NOD/LtSz-scid/scid mice. *Blood* (1997) 90:85–96.
5. Ito M, Hiramatsu H, Kobayashi K, Suzue K, Kawahata M, Hioki K, et al. NOD/SCID/gamma(c)(null) mouse: an excellent recipient mouse model for engraftment of human cells. *Blood* (2002) 100:3175–82. doi:10.1182/blood-2001-12-0207
6. Ishikawa F, Yasukawa M, Lyons B, Yoshida S, Miyamoto T, Yoshimoto G, et al. Development of functional human blood and immune systems in NOD/SCID/IL2 receptor {gamma} chain(null) mice. *Blood* (2005) 106:1565–73. doi:10.1182/blood-2005-02-0516
7. Traggiai E, Chicha L, Mazzucchelli L, Bronz L, Piffaretti JC, Lanzavecchia A, et al. Development of a human adaptive immune system in cord blood cell-transplanted mice. *Science* (2004) 304:104–7. doi:10.1126/science.1093933
8. Sugamura K, Asao H, Kondo M, Tanaka N, Ishii N, Ohbo K, et al. The interleukin-2 receptor gamma chain: its role in the multiple cytokine receptor complexes and T cell development in XSCID. *Annu Rev Immunol* (1996) 14:179–205. doi:10.1146/annurev.immunol.14.1.179
9. Rochman Y, Spolski R, Leonard WJ. New insights into the regulation of T cells by gamma(c) family cytokines. *Nat Rev Immunol* (2009) 9:480–90. doi:10.1038/nri2580
10. Kikuchi K, Lai AY, Hsu CL, Kondo M. IL-7 receptor signaling is necessary for stage transition in adult B cell development through up-regulation of EBF. *J Exp Med* (2005) 201:1197–203. doi:10.1084/jem.20050158
11. Cao X, Shores EW, Hu-Li J, Anver MR, Kelsall BL, Russell SM, et al. Defective lymphoid development in mice lacking expression of the common cytokine receptor gamma chain. *Immunity* (1995) 2:223–38. doi:10.1016/1074-7613(95)90047-0
12. Disanto JP, Muller W, Guy-Grand D, Fischer A, Rajewsky K. Lymphoid development in mice with a targeted deletion of the interleukin 2 receptor gamma chain. *Proc Natl Acad Sci U S A* (1995) 92:377–81. doi:10.1073/pnas.92.2.377
13. Ohbo K, Suda T, Hashiyama M, Mantani A, Ikebe M, Miyakawa K, et al. Modulation of hematopoiesis in mice with a truncated mutant of the interleukin-2 receptor gamma chain. *Blood* (1996) 87:956–67.
14. Mebius RE. Organogenesis of lymphoid tissues. *Nat Rev Immunol* (2003) 3:292–303. doi:10.1038/nri1054
15. Spits H, Di Santo JP. The expanding family of innate lymphoid cells: regulators and effectors of immunity and tissue remodeling. *Nat Immunol* (2011) 12:21–7. doi:10.1038/ni.1962
16. Forster R, Mattis AE, Kremmer E, Wolf E, Brem G, Lipp M. A putative chemokine receptor, BLR1, directs B cell migration to defined lymphoid organs and specific anatomic compartments of the spleen. *Cell* (1996) 87:1037–47. doi:10.1016/S0092-8674(00)81798-5
17. Ansel KM, Ngo VN, Hyman PL, Luther SA, Forster R, Sedgwick JD, et al. A chemokine-driven positive feedback loop organizes lymphoid follicles. *Nature* (2000) 406:309–14. doi:10.1038/35018581
18. Van De Pavert SA, Olivier BJ, Goverse G, Vondenhoff MF, Greuter M, Beke P, et al. Chemokine CXCL13 is essential for lymph node initiation and is induced by retinoic acid and neuronal stimulation. *Nat Immunol* (2009) 10:1193–9. doi:10.1038/ni.1789
19. Eberl G, Marmon S, Sunshine MJ, Rennert PD, Choi Y, Littman DR. An essential function for the nuclear receptor RORgamma(t) in the generation of fetal lymphoid tissue inducer cells. *Nat Immunol* (2004) 5:64–73. doi:10.1038/ni1022
20. Chappaz S, Finke D. The IL-7 signaling pathway regulates lymph node development independent of peripheral lymphocytes. *J Immunol* (2010) 184:3562–9. doi:10.4049/jimmunol.0901647
21. Banks TA, Rouse BT, Kerley MK, Blair PJ, Godfrey VL, Kuklin NA, et al. Lymphotoxin-alpha-deficient mice. Effects on secondary lymphoid organ development and humoral immune responsiveness. *J Immunol* (1995) 155:1685–93.
22. Koni PA, Sacca R, Lawton P, Browning JL, Ruddle NH, Flavell RA. Distinct roles in lymphoid organogenesis for lymphotoxins alpha and beta revealed in lymphotoxin beta-deficient mice. *Immunity* (1997) 6:491–500. doi:10.1016/S1074-7613(00)80292-7
23. Shinkura R, Kitada K, Matsuda F, Tashiro K, Ikuta K, Suzuki M, et al. Alymphoplasia is caused by a point mutation in the mouse gene encoding Nf-kappa b-inducing kinase. *Nat Genet* (1999) 22:74–7. doi:10.1038/8780
24. Dai Z, Lakkis FG. Cutting edge: Secondary lymphoid organs are essential for maintaining the CD4, but not CD8, naive T cell pool. *J Immunol* (2001) 167:6711–5. doi:10.4049/jimmunol.167.12.6711
25. Matsumura T, Kametani Y, Ando K, Hirano Y, Katano I, Ito R, et al. Functional CD5+ B cells develop predominantly in the spleen of NOD/SCID/gammac(null) (NOG) mice transplanted either with human umbilical cord blood, bone marrow, or mobilized peripheral blood CD34+ cells. *Exp Hematol* (2003) 31:789–97. doi:10.1016/S0301-472X(03)00193-0
26. Baenziger S, Tussiwand R, Schlaepfer E, Mazzucchelli L, Heikenwalder M, Kurrer MO, et al. Disseminated and sustained HIV infection in CD34+ cord blood cell-transplanted Rag2-/-gamma c-/- mice. *Proc Natl Acad Sci U S A* (2006) 103:15951–6. doi:10.1073/pnas.0604493103
27. Watanabe Y, Takahashi T, Okajima A, Shiokawa M, Ishii N, Katano I, et al. The analysis of the functions of human B and T cells in humanized NOD/shi-scid/gammac(null) (NOG) mice (hu-HSC NOG mice). *Int Immunol* (2009) 21:843–58. doi:10.1093/intimm/dxp050
28. Liu P, Jenkins NA, Copeland NG. A highly efficient recombineering-based method for generating conditional knockout mutations. *Genome Res* (2003) 13:476–84. doi:10.1101/gr.749203
29. Ito R, Takahashi T, Katano I, Kawai K, Kamisako T, Ogura T, et al. Establishment of a human allergy model using human IL-3/GM-CSF-transgenic NOG mice. *J Immunol* (2013) 191:2890–9. doi:10.4049/jimmunol.1203543
30. Danner R, Chaudhari SN, Rosenberger J, Surls J, Richie TL, Brumeanu TD, et al. Expression of HLA class II molecules in humanized NOD.Rag1KO.IL2RgcKO mice is critical for development and function of human T and B cells. *PLoS One* (2011) 6:e19826. doi:10.1371/journal.pone.0019826
31. Suzuki M, Takahashi T, Katano I, Ito R, Ito M, Harigae H, et al. Induction of human humoral immune responses in a novel HLA-DR-expressing transgenic NOD/Shi-scid/gammacnull mouse. *Int Immunol* (2012) 24:243–52. doi:10.1093/intimm/dxs045
32. Crotty S. Follicular helper CD4 T cells (TFH). *Annu Rev Immunol* (2011) 29:621–63. doi:10.1146/annurev-immunol-031210-101400
33. Paul WE. History of interleukin-4. *Cytokine* (2015) 75:3–7. doi:10.1016/j.cyto.2015.01.038
34. Maecker HT, Mccoy JP, Nussenblatt R. Standardizing immunophenotyping for the human immunology project. *Nat Rev Immunol* (2012) 12:191–200. doi:10.1038/nri3158
35. Sugiyama D, Nishikawa H, Maeda Y, Nishioka M, Tanemura A, Katayama I, et al. Anti-CCR4 mAb selectively depletes effector-type FoxP3+CD4+ regulatory T cells, evoking antitumor immune responses in humans. *Proc Natl Acad Sci U S A* (2013) 110:17945–50. doi:10.1073/pnas.1316796110
36. Prochazka M, Gaskins HR, Shultz LD, Leiter EH. The nonobese diabetic scid mouse: model for spontaneous thymomagenesis associated with immunodeficiency. *Proc Natl Acad Sci U S A* (1992) 89:3290–4. doi:10.1073/pnas.89.8.3290
37. Denton PW, Nochi T, Lim A, Krisko JF, Martinez-Torres F, Choudhary SK, et al. IL-2 receptor gamma-chain molecule is critical for intestinal T-cell reconstitution in humanized mice. *Mucosal Immunol* (2012) 5:555–66. doi:10.1038/mi.2012.31
38. Ito R, Katano I, Ida-Tanaka M, Kamisako T, Kawai K, Suemizu H, et al. Efficient xenoengraftment in severe immunodeficient NOD/Shi-scid IL2rgammanull mice is attributed to a lack of CD11c+B220+CD122+ cells. *J Immunol* (2012) 189:4313–20. doi:10.4049/jimmunol.1200820
39. Shultz LD, Lyons BL, Burzenski LM, Gott B, Chen X, Chaleff S, et al. Human lymphoid and myeloid cell development in NOD/LtSz-scid IL2R gamma null mice engrafted with mobilized human hemopoietic stem cells. *J Immunol* (2005) 174:6477–89. doi:10.4049/jimmunol.174.10.6477

40. O'Connell RM, Balazs AB, Rao DS, Kivork C, Yang L, Baltimore D. Lentiviral vector delivery of human interleukin-7 (hIL-7) to human immune system (HIS) mice expands T lymphocyte populations. *PLoS One* (2010) 5:e12009. doi:10.1371/journal.pone.0012009
41. Strowig T, Gurer C, Ploss A, Liu YF, Arrey F, Sashihara J, et al. Priming of protective T cell responses against virus-induced tumors in mice with human immune system components. *J Exp Med* (2009) 206:1423–34. doi:10.1084/jem.20081720
42. Shultz LD, Saito Y, Najima Y, Tanaka S, Ochi T, Tomizawa M, et al. Generation of functional human T-cell subsets with HLA-restricted immune responses in HLA class I expressing NOD/SCID/IL2r gamma(null) humanized mice. *Proc Natl Acad Sci U S A* (2010) 107:13022–7. doi:10.1073/pnas.1000475107
43. Lang J, Kelly M, Freed BM, Mccarter MD, Kedl RM, Torres RM, et al. Studies of lymphocyte reconstitution in a humanized mouse model reveal a requirement of T cells for human B cell maturation. *J Immunol* (2013) 190:2090–101. doi:10.4049/jimmunol.1202810

Conflict of Interest Statement: The authors declare that the research was conducted in the absence of any commercial or financial relationships that could be construed as a potential conflict of interest.

frontiers in Immunology

MINI REVIEW
published: 26 January 2018
doi: 10.3389/fimmu.2018.00054

Modeling Human Antitumor Responses *In Vivo* Using Umbilical Cord Blood-Engrafted Mice

*Nicholas A. Zumwalde and Jenny E. Gumperz**

Department of Medical Microbiology and Immunology, University of Wisconsin School of Medicine and Public Health, Madison, WI, United States

Mice engrafted with human immune cells offer powerful *in vivo* model systems to investigate molecular and cellular processes of tumorigenesis, as well as to test therapeutic approaches to treat the resulting cancer. The use of umbilical cord blood mononuclear cells as a source of human immune cells for engraftment is technically straightforward, and provides T lymphocytes and autologous antigen-presenting cells (including B cells, monocytes, and DCs) that bear cognate antigen presenting molecules. By using a human-specific oncogenic virus, such as Epstein-Barr virus, *de novo* neoplastic transformation of the human B cells can be induced *in vivo* in a manner that models progressive stages of tumorigenesis from nascent neoplasia to the establishment of vascularized tumor masses with an immunosuppressive environment. Moreover, since tumorigenesis occurs in the presence of autologous T cells, this type of system can be used to investigate how T cells become suppressed during tumorigenesis, and how immunotherapies counteract immunosuppression. This minireview will provide a brief overview of the use of human umbilical cord blood transplanted into immunodeficient murine hosts to model antitumor responses.

Keywords: humanized mice, umbilical cord blood, tumor immunotherapy, homeostatic proliferation, xenogeneic activation

OPEN ACCESS

Edited by:
Moriya Tsuji, Aaron Diamond AIDS Research Center, United States

Reviewed by:
Wenwei Tu, University of Hong Kong, Hong Kong
María Marcela Barrio, Fundación Cáncer, Argentina

***Correspondence:**
Jenny E. Gumperz
jegumperz@wisc.edu

Specialty section:
This article was submitted to Vaccines and Molecular Therapeutics, a section of the journal Frontiers in Immunology

Received: *31 October 2017*
Accepted: *09 January 2018*
Published: *26 January 2018*

Citation:
Zumwalde NA and Gumperz JE (2018) Modeling Human Antitumor Responses In Vivo Using Umbilical Cord Blood-Engrafted Mice. Front. Immunol. 9:54. doi: 10.3389/fimmu.2018.00054

INTRODUCTION

While animal model systems, and particularly laboratory mouse strains, are absolutely indispensible for understanding the basic biology of both cancers and the immune system, preclinical analyses of tumor immunotherapy are also likely to benefit from experimental systems that utilize primary human cells obtained from genetically diverse individuals. In this minireview, we will discuss the use of immune-deficient mice engrafted with human umbilical cord blood cells for studying human T cell biology and tumor immunotherapy *in vivo*.

Clinical applications of tumor immunotherapy currently center on two main approaches. The first is the use of "checkpoint" blockade antibodies to relieve PD-1 and CTLA-4 mediated immunosuppression of endogenous T cells. When these inhibitory pathways are disabled by blocking antibodies, a patient's existing T cells can often induce tumor regression (1, 2). The second approach, cellular immunotherapy, involves administering cytolytic lymphocytes that have been expanded *in vitro*, and act as direct antitumor effectors within the patient. Most prominent in this category is the use of chimeric antigen receptor (CAR) T cells that have been genetically modified to specifically target the patient's tumor (3). Refining and further developing tumor immunotherapeutic approaches will require experimental model systems that allow us to better understand interactions between human

immune effectors and human tumors *in vivo*. In particular, it would be helpful to be able to model human T cell functions during progressive stages of tumorigenesis, from nascent neoplasia to the establishment of tumors with an immunosuppressive environment. Also key is to be able to assess *in vivo* responses of human T cells that are autologous to the tumor (e.g., those targeted by checkpoint blockade), as well as to test the impact of exogenously administered effectors (e.g., CAR-T cells) on established tumors. These elements are provided by new experimental models in which immunodeficient mice are engrafted with human immune cells, and human tumor formation is induced *in vivo via* infection with an oncogenic virus.

ENGRAFTMENT OF MICE WITH HUMAN IMMUNE CELLS

Mouse Strains

Adoptive transfer of human immune cells into murine hosts is most successful in mouse strains lacking adaptive immune cells that also have impairments in innate cell types, such as NK cells, that would otherwise kill engrafted human cells. One strain that is now commonly used for human cell engraftment is the NOD-SCID-Gamma or "NSG" mouse (NOD.Cg-Prkdc^{scid}Il2rg^{tm1Wjl}/SzJ). NSG mice fail to develop T and B cells due to the *Prkdc^{scid}* mutation, are defective in multiple innate immune functions because they are bred onto a NOD background and are also knocked out for the common γ chain of the IL-2 receptor, which is required for proper development of multiple lineages, including NK cells (4). The NSG strain shows little or no evidence of "leakiness" in regards to development of murine T cells, has highly deficient murine NK cells, and has been found to provide an excellent environment for the survival of human cells *in vivo* (5). Building on the utility of the NSG strain, strains with further genetic modifications have been generated that show additional improvements in human cell engraftment. These include strains that are transgenic for key human cytokines that promote hematopoiesis (e.g., TPO, CSF1, IL3, CSF2), and a strain lacking c-Kit that supports high levels of human hematopoietic engraftment without irradiation or myeloablative conditioning (6–10).

Hematopoietic Stem Cell (HSC) Engraftment

Engraftment of human immune cells into mice can be successfully accomplished through a variety of different protocols. However, different approaches entail key differences in the selection and specificity of the human T cell compartment that is then present in the engrafted mice. A central distinction is whether human HSCs are used to give rise to T cells that develop within the murine host, or whether T cells that have already undergone selection in the human donor are transferred into the mice (**Figure 1**). NSG mice possess thymic tissue at birth, but this tissue normally atrophies due to the absence of murine T cells, and becomes essentially undetectable within 6 weeks after birth. Engraftment protocols that transfer human HSCs into neonatal mice result in colonization of the murine thymus by human pre-T cells, which promotes the survival of the thymic tissue, and provides an environment for selection of the human T cells (11). Because the human T cells develop within the murine thymus, they undergo positive and negative selection on murine antigen presenting molecules. As a result, tolerance to murine tissues is established, but the T cells are not optimized for interactions with human antigen-presenting cells

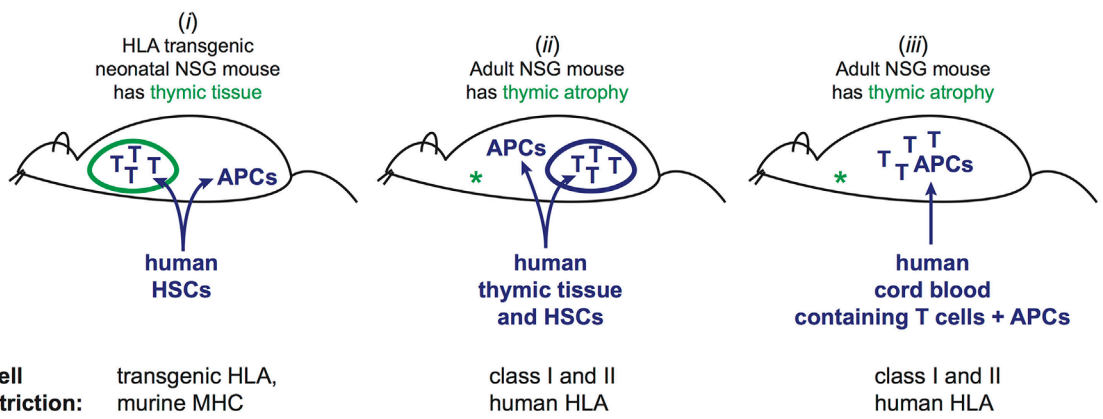

FIGURE 1 | Three different approaches to generate mice engrafted with human T cells and cognate human antigen-presenting cells (APCs). (i) Injection of human hematopoietic stem cells (HSCs) into neonatal mice. Human T cells and APCs develop from the HSCs. T cells undergo selection in murine thymus based on interactions with murine cells. By using mice that are transgenic for one or more HLA molecules, and HSCs bearing HLA alleles that match the transgenes, a fraction of the mature human T cells in the periphery will be able to recognize the human APCs, while others are restricted by murine antigen presenting molecules that are also present in the thymic environment. This method does not recapitulate the full repertoire of T cell restriction for human antigen presenting and may not produce tolerance to human peptides presented by the restricting HLA molecules, but is associated with little or no graft-versus-host disease (GVHD). (ii) Adult NSG mice, which lack murine thymic tissue due to atrophy, are injected with human HSCs. Concurrently, a fragment of human thymic tissue is surgically implanted. Human T cells and APCs develop from the HSCs, and the thymic fragment develops into a viable organoid. T cells undergo selection in the human thymic organoid based on interactions with human thymic cells. The resulting T cell repertoire includes restriction for the full panoply of autologous HLA molecules. However, signs of chronic GVHD typically manifest within 4–6 months. (iii) Human umbilical cord blood engraftment of adult NSG mice. Mature T cells (selected in the baby's thymus) are transplanted along with autologous APCs. Human T cells typically persist for at least 3 months, but signs of GVHD may become apparent after about 2 months.

(APCs) that also develop from the engrafted HSCs. However, by instead using mice that are transgenic for one or more human HLA molecules, some of the human T cells that are generated are able to interact productively with human APCs (12). Nevertheless, a potential drawback is that many of the human T cells will be developmentally selected on murine antigen presenting molecules (**Figure 1**, part *i*), and thus the human T cell compartment probably does not fully recapitulate the specificities and lineages of human T cells.

Human Thymic Engraftment

An alternative method is to transfer human HSCs into mice at 6–8 weeks of age (when the murine thymus is gone), and to cotransplant fragments of human thymic tissue, which are typically surgically implanted under the kidney capsule. This results in the growth of a human thymic organoid within the mice that allows for T cell selection by human thymic epithelial cells, and generates a T cell repertoire specific for the full complement of human HLA molecules (**Figure 1**, part *ii*). This approach has been shown to enable productive interactions of human T cells with autologous human APCs that also develop in the murine host from human HSCs (13–15). We have shown that this approach results in the generation of human T cells that recognize human non-classical antigen presenting molecules, such as CD1 molecules, and thus enables modeling of select T cell populations that are present in humans but not found in mice (16). Central disadvantages of this type of approach are the challenges associated with implanting human thymic tissue in the mice, and the length of time required for full establishment of the human immune compartment in the periphery, which typically requires about 3 months after tissue engraftment. An additional concern is that signs of graft-versus-host disease (GVHD) often become apparent within about 4–5 months after tissue engraftment (17).

Engraftment of Mature Lymphocytes

An alternative that addresses some of the challenges of the above approaches is to transfer mature human immune cells into NSG mice. While transferring adult human PBMCs into immune-deficient mice typically results in acute GVHD pathology that manifests within 3–6 weeks (17), it is nevertheless possible to model functional interactions amongst populations of human immune cells in a short-term manner using cells from adults. For example, inflammatory responses induced by interactions among human immune cells can be read-out after 24–48 h using a vascularized peripheral tissue of the mouse, such as the footpad (18, 19). Alternatively, adult human PBMCs can be systemically transferred into immune-deficient mice for short periods to investigate functional capabilities of specific populations of human lymphocytes. For example, studies of this type have demonstrated that human $V\gamma9^+V\delta2^+$ T cells can be sufficient to control the outgrowth of xenografted human tumors (20–25). Nevertheless, while adoptive transfer of immune cells from human adults into NSG mice provides an important means of investigating functional interactions of human cells *in vivo*, the GVHD responses associated with this approach significantly limit investigation of longer-term immunological processes.

In contrast, adoptive transfer of NSG mice with human umbilical cord blood mononuclear cells (CBMCs) provides a means of modeling human immune interactions *in vivo* over a longer period of time. CBMCs contain mature human T cells that were selected in a fully human environment (i.e., the baby), and that are appropriately restricted for the accompanying human APCs (e.g., B cells, monocytes, DCs), but that are as yet in a highly naive state. By removing the $CD34^+$ HSCs prior to transplantation, new human T cells will not develop after transfer, and thus the mice contain only the T cells that were selected in a human thymus and that are restricted by the antigen presenting molecules expressed on the autologous APCs that were cotransferred in the CBMC sample (**Figure 1**, part *iii*). The adoptively transferred human T cells typically expand and persist in the mice for at least 2 months without evidence of significant GVHD pathology, which provides an experimental window that is adequate for many types of analyses. As discussed below, the central concern about this approach relates to the functional competence of the cord blood T cells after engraftment.

FUNCTIONAL CHARACTERISTICS OF HUMAN CORD BLOOD T CELLS

As evidenced by their expression of CD45RA and not CD45RO, cord blood T cells are naive (26), and thus they would be expected to show less efficient cytokine production compared to previously activated T cells. However, a number of observations suggest that cord T cells may also be less functionally competent than naive peripheral blood T cells that are found later in life. Exposure to IL-10 produced by trophoblasts suppresses placental T cell activity, and the hormonal environment of pregnancy may also dampen T cell activity (27–29). It is not clear how long after birth these suppressive effects last, however, cord blood has been found to contain only very low percentages of T cells capable of producing IL-2, IFNγ, TNFα, and IL-4 (30, 31). Cord T cells also lack the constitutive expression of perforin seen in adult $CD8^+$ T cells (32). The inefficient effector cytokine production of cord T cells may be due to epigenetic alterations, since cord blood $CD4^+$ T cells were found to have hypermethylation of the IFNγ promoter (33). Additionally, PKCζ expression levels appeared to be reduced in neonatal T cells, which correlated with a deficiency in IFNγ production and affected their ability to mature into effector cytokine producing cells (34, 35). Perhaps as a result of these features, cord blood T cells are associated with substantially reduced incidence of GVHD following hematopoietic transplantation (31, 36).

Nevertheless, effector T cell responses to pathogens do occur early in life (29), indicating that cord blood T cells are capable of becoming functionally activated. Moreover, it has recently been shown that the gene expression differences that distinguish specific-pathogen-free mice from "wild" mice (i.e., those that have experienced microbial exposure found in the natural world) closely resembled the differences between human umbilical cord blood and adult peripheral blood cells (37). Thus, many of the functional characteristics of cord blood T cells may be due to a lack of immunological experience, rather than to features that

have a lasting effect on gene expression. Consistent with this, it is now clear that cord blood T cells, like naive T cells from adults, can readily be activated to undergo expansion, maturation, and polarization.

POLARIZATION OF CORD T CELLS INTO EFFECTORS

T cells derived from cord blood can be expanded *in vitro* by anti-CD3 and anti-CD28 antibody stimulation in the presence of IL-2 (38). While such antibody-driven expansion of cord T cells *in vitro* is associated with significant apoptosis, this is mitigated in the presence of IL-7, which also aids in maintaining higher T cell receptor (TCR) Vβ diversity (39). When IL-12 is present during CD3/CD28 stimulation, the cord T cells rapidly acquire Th1-polarization features such as the ability to produce IFNγ, TNFα, and granzyme A (38), and subsequently show enhanced IFNγ production after TCR stimulation suggesting a lasting polarization toward a Th1 phenotype (40). Conversely, exposing cord T cells to IL-4 during CD3/CD28 stimulation leads to Th2-skewing (40). However, this occurs more slowly and requires repeated TCR stimulation in the presence of IL-4 in order to maintain production of IL-10, IL-4, IL-5, and IL-13. Hence, cord cells that have been Th2-skewed by short-term IL-4 exposure maintain the plasticity to revert back to a Th0 phenotype, and can even convert to a Th1 profile with the addition of IL-12, suggesting that they are not intrinsically biased toward a Th2 phenotype (40). These results illustrate that, despite their initial functional reticence, the effector capabilities of cord-derived T lymphocytes do not remain suppressed in the long-term.

EVENTS AFTER TRANSFER INTO IMMUNE-DEFICIENT MICE

Since transfer of human cord T cells into murine hosts is likely to be associated with exposure to stimulating factors, it is important to consider the impact this might have on the subsequent functionality of the T cells. Major factors that might cause T cell activation after transfer include the lymphopenic environment of the host and exposure to xenogeneic antigens (see **Figure 2**). Whereas activation resulting from xenoantigenic stimulation might be an artifact of transferring human T cells into a murine host, T cell activation that is due to a lymphopenic environment is a process that occurs physiologically (41). Thus, changes in the human cord T cell population following transplantation into mice are not necessarily an indication of aberrant activation due to the use of a xenogeneic model system. Indeed, cord blood transplantation in human patients also results in thymic independent expansion of the transplanted T cells that is associated with a rapid shift from a naïve to memory phenotype (42). Hence, the lymphopenic environment of NSG mice might be expected to similarly induce a proliferative response from adoptively transferred cord T cells and might affect the nature of the TCR repertoire.

The spontaneous cellular division induced in a lymphopenic environment is broadly delineated into two major varieties: slow and fast. Slow homeostatic proliferation is driven by T cell recognition of low affinity peptides (e.g., self peptides) bound to MHC in the presence of IL-7 (43, 44). This slow spontaneous division proceeds in the absence of costimulation by CD28, CD40, or LFA-1, and appears to largely occur within T cell zones in secondary lymphoid organs (44). In contrast, fast homeostatic proliferation is an antigen driven response from a smaller subset of T cells and is IL-7 independent (44). This pathway requires costimulatory signals and leads to swift upregulation of memory markers and acquisition of effector functions such as the production of IL-2 and IFNγ. Since fast homeostatic proliferation is greatly reduced when recipient mice are housed in germ-free conditions, it has been proposed that peptides from gut microbes are a major driver of this response (44).

By engrafting NSG mice with total CBMCs, APCs bearing cognate antigen presenting molecules are present that could activate either fast or slow homeostatic proliferation by the cord T cells. However, since NSG mice are typically housed in aseptic conditions, the supply of microbial peptides required for fast homeostatic proliferation might be limited. In contrast, since murine IL-7 is highly cross-reactive with the IL-7 receptors of

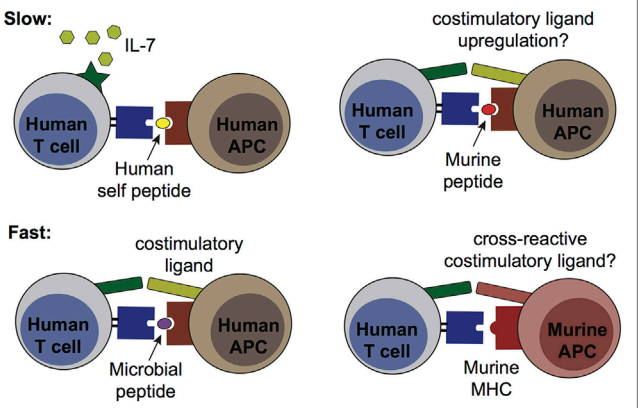

FIGURE 2 | Pathways of human T cell activation in murine engraftment models. **(A)** Homeostatic proliferation occurs via two distinct processes, termed "slow" and "fast." Slow proliferation (top panel) results from TCR stimulation by a weak agonist [e.g., autologous antigen-presenting cells (APCs) bearing self peptides] in the presence of IL-7, and does not require co-stimulatory ligands. Since murine IL-7 is recognized by human IL-7 receptors, this cytokine is likely to have high availability after transplantation into NSG mice. This pathway likely affects most of the transplanted human T cells. Fast proliferation (bottom panel) is driven by T cell receptor (TCR) recognition of high affinity antigens (e.g., microbial peptides from commensal species) in the presence of co-stimulatory ligands, and does not require IL-7. This process would likely only affect a subset of the transplanted T cells. **(B)** Xenogeneic activation may result from T cell recognition of murine peptides presented by self HLA molecules on human APCs (top panel), or by cross-reactivity of human TCRs for murine MHC molecules on murine APCs (bottom panel). Upregulation of co-stimulatory ligands by the human APCs or expression of cross-reactive co-stimulatory ligands by the murine APCs might be required for this pathway to induce productive activation, rather than anergy (which would be expected from TCR stimulation in the absence of co-stimulation). Xenogeneic activation pathways would be expected to affect only a subset of the transplanted human T cells.

human cells (45), the conditions for slow homeostatic proliferation are likely to be present (**Figure 2A**). Thus, most or all human cord T cells are expected to proliferate homeostatically after transplantation into NSG mice, although it remains unclear whether this process substantially alters their functional state.

The second major factor that might affect the functional status of transplanted cord T cells is xenoantigenic stimulation. This might occur either *via* TCR binding to murine MHC molecules or *via* recognition of murine peptides presented by self HLA molecules on other human cells (**Figure 2B**). In either case, such xenoantigenic activation would be predicted to affect only the subset of the cord T cells bearing a cross-reactive TCR. The strength of TCR signaling delivered by these recognition events is difficult to predict, and it is also not clear whether TCR signals of this type are typically accompanied by costimulatory signals that are required for a productive antigen-driven response. In the absence of appropriate costimulation xenoantigen-associated TCR signals would be expected to induce anergy, whereas if costimulation is present a classic antigen-driven expansion of the responding T cells would be expected. Importantly, productive xenoantigenic activation of cord T cells within murine hosts would be expected to result in GVHD. However, there is typically little evidence of GVHD within the first 2 months after administering cord T cells (Zumwalde and Gumperz unpublished data). Thus, xenoantigenic activation may not play a major role for a period of weeks or months after the adoptive transfer of human cord blood T cells into NSG mice.

MODELING TUMOR IMMUNITY

Perhaps surprisingly, given the evidence suggesting their effector functions are limited, cord T cells have been found to be capable of mediating efficient antitumor responses. Analyses of cord T cells exposed to tumor cells *in vitro* have unambiguously established that they can mount both cytotoxic and cytokine responses (46–49). Moreover, the ability of cord T cells to carry out antitumor effects *in vivo* has been clearly demonstrated in recent studies (47, 50). In a particularly revealing analysis, T cells purified from cord or adult blood were compared in a head-to-head manner for their ability to limit the growth of allogeneic EBV-transformed B cells (EBV-LCLs) in NSG mice (51). The EBV-LCLs were injected subcutaneously into NSG mice, leading to the formation of a solid mass at the site of injection resembling a tumor. Equivalent doses of primary cord or adult T cells were injected intravenously, and growth of the EBV-LCL mass was monitored. Administration of cord T cells was associated with significantly less growth of the implanted EBV-LCLs compared to adult T cells, and the EBV-LCL masses also showed substantially more evidence of T cell infiltration in the cord T cell treatment group (51). Studies such as these demonstrate that cord T cells are capable of promoting tumor rejection *in vivo*. However, such experimental systems, where *in vitro*-derived tumor cells are administered to immunodeficient mice and cytolytic lymphocytes are then added to test for tumor rejection, do not clearly model the impact of immunosuppressive tumor environments that must be overcome by successful immunotherapeutic strategies.

To address this need, we have developed an experimental model in which neoplastic transformation of human B cells occurs *in vivo* and is associated with suppression of the endogenous T cells. Briefly, NSG mice are injected with CD34-depleted CBMCs in the presence of a lytic strain of EBV, called M81, that was recently isolated from a patient (52). The virus induces *de novo* neoplastic transformation of the initially healthy B cells, and within approximately 4 weeks nearly all of the mice typically develop large tumors (53). The lymphomas are located in the peritoneal cavity adjacent to pancreas, liver, or bile ducts, and ultimately end up invading nearby organ tissue and causing mortality. The lymphomas in this model are heavily infiltrated by autologous $CD4^+$ and $CD8^+$ T cells, but the tumor B cells express elevated levels of the inhibitory ligands PD-L1 and PD-L2 (54). Antibody-mediated blockade of PD-1 and CTLA-4 results in reduced tumor burden, prolongs survival, and reveals EBV peptide-specific T cell responses by the autologous T cells (54). Thus, lymphoma-specific T cells are generated in this model, but are usually held in check by suppressive pathways.

We have recently shown that cellular immunotherapy using human γδ T cells has potent antitumor immune effects in this model both at early stages of nascent neoplasia (immunosurveillance) and at later stages after solid tumors containing immunosuppressive ligands have become established (55). Hence, even in the absence of checkpoint blockade, the immunotherapeutic γδ T cells are apparently able to overcome the immunosuppressive environment that stymies the responses of the endogenous T cells. We expect that preclinical models of this type will provide a valuable tool to investigate molecular and cellular mechanisms by which successful immunotherapeutic strategies overcome or avoid suppressive environments created by tumors.

AUTHOR CONTRIBUTIONS

NZ reviewed literature and cowrote manuscript; JG generated figures and cowrote the manuscript.

FUNDING

Primary funding provided by a grant from the Wisconsin Partnership Project to JG; JG also supported by NIH R21AI11 6007; NZ also supported by NIH T32 CA157322.

REFERENCES

1. Pardoll DM. The blockade of immune checkpoints in cancer immunotherapy. *Nat Rev Cancer* (2012) 12(4):252–64. doi:10.1038/nrc3239
2. Grosso JF, Jure-Kunkel MN. CTLA-4 blockade in tumor models: an overview of preclinical and translational research. *Cancer Immun* (2013) 13:5.
3. Chang ZL, Chen YY. CARs: synthetic immunoreceptors for cancer therapy and beyond. *Trends Mol Med* (2017) 23(5):430–50. doi:10.1016/j.molmed.2017.03.002
4. Shultz LD, Schweitzer PA, Christianson SW, Gott B, Schweitzer IB, Tennent B, et al. Multiple defects in innate and adaptive immunologic function in NOD/LtSz-scid mice. *J Immunol* (1995) 154(1):180–91.

5. Shultz LD, Lyons BL, Burzenski LM, Gott B, Chen X, Chaleff S, et al. Human lymphoid and myeloid cell development in NOD/LtSz-scid IL2R gamma null mice engrafted with mobilized human hemopoietic stem cells. *J Immunol* (2005) 174(10):6477–89. doi:10.4049/jimmunol.174.10.6477
6. Rongvaux A, Willinger T, Takizawa H, Rathinam C, Auerbach W, Murphy AJ, et al. Human thrombopoietin knockin mice efficiently support human hematopoiesis in vivo. *Proc Natl Acad Sci U S A* (2011) 108(6):2378–83. doi:10.1073/pnas.1019524108
7. Willinger T, Rongvaux A, Strowig T, Manz MG, Flavell RA. Improving human hemato-lymphoid-system mice by cytokine knock-in gene replacement. *Trends Immunol* (2011) 32(7):321–7. doi:10.1016/j.it.2011.04.005
8. Willinger T, Rongvaux A, Takizawa H, Yancopoulos GD, Valenzuela DM, Murphy AJ, et al. Human IL-3/GM-CSF knock-in mice support human alveolar macrophage development and human immune responses in the lung. *Proc Natl Acad Sci U S A* (2011) 108(6):2390–5. doi:10.1073/pnas.1019682108
9. Rongvaux A, Willinger T, Martinek J, Strowig T, Gearty SV, Teichmann LL, et al. Development and function of human innate immune cells in a humanized mouse model. *Nat Biotechnol* (2014) 32(4):364–72. doi:10.1038/nbt.2858
10. McIntosh BE, Brown ME, Duffin BM, Maufort JP, Vereide DT, Slukvin II, et al. Nonirradiated NOD,B6.SCID Il2rgamma-/- Kit(W41/W41) (NBSGW) mice support multilineage engraftment of human hematopoietic cells. *Stem Cell Reports* (2015) 4(2):171–80. doi:10.1016/j.stemcr.2014.12.005
11. Lepus CM, Gibson TF, Gerber SA, Kawikova I, Szczepanik M, Hossain J, et al. Comparison of human fetal liver, umbilical cord blood, and adult blood hematopoietic stem cell engraftment in NOD-scid/gammac-/-, Balb/c-Rag1-/-gammac-/-, and C.B-17-scid/bg immunodeficient mice. *Hum Immunol* (2009) 70(10):790–802. doi:10.1016/j.humimm.2009.06.005
12. Shultz LD, Saito Y, Najima Y, Tanaka S, Ochi T, Tomizawa M, et al. Generation of functional human T-cell subsets with HLA-restricted immune responses in HLA class I expressing NOD/SCID/IL2r gamma(null) humanized mice. *Proc Natl Acad Sci U S A* (2010) 107(29):13022–7. doi:10.1073/pnas.1000475107
13. Lan P, Tonomura N, Shimizu A, Wang S, Yang YG. Reconstitution of a functional human immune system in immunodeficient mice through combined human fetal thymus/liver and CD34+ cell transplantation. *Blood* (2006) 108(2):487–92. doi:10.1182/blood-2005-11-4388
14. Melkus MW, Estes JD, Padgett-Thomas A, Gatlin J, Denton PW, Othieno FA, et al. Humanized mice mount specific adaptive and innate immune responses to EBV and TSST-1. *Nat Med* (2006) 12(11):1316–22. doi:10.1038/nm1431
15. Rajesh D, Zhou Y, Jankowska-Gan E, Roenneburg DA, Dart ML, Torrealba J, et al. Th1 and Th17 immunocompetence in humanized NOD/SCID/IL2rgammanull mice. *Hum Immunol* (2010) 71(6):551–9. doi:10.1016/j.humimm.2010.02.019
16. Lockridge JL, Chen X, Zhou Y, Rajesh D, Roenneburg DA, Hegde S, et al. Analysis of the CD1 antigen presenting system in humanized SCID mice. *PLoS One* (2011) 6(6):e21701. doi:10.1371/journal.pone.0021701
17. Lockridge JL, Zhou Y, Becker YA, Ma S, Kenney SC, Hematti P, et al. Mice engrafted with human fetal thymic tissue and hematopoietic stem cells develop pathology resembling chronic graft-versus-host disease. *Biol Blood Marrow Transplant* (2013) 19(9):1310–22. doi:10.1016/j.bbmt.2013.06.007
18. Derks RA, Jankowska-Gan E, Xu Q, Burlingham WJ. Dendritic cell type determines the mechanism of bystander suppression by adaptive T regulatory cells specific for the minor antigen HA-1. *J Immunol* (2007) 179(6):3443–51. doi:10.4049/jimmunol.179.6.3443
19. Jankowska-Gan E, Hegde S, Burlingham WJ. Trans-vivo delayed type hypersensitivity assay for antigen specific regulation. *J Vis Exp* (2013) 75:e4454. doi:10.3791/4454
20. Malkovska V, Cigel FK, Armstrong N, Storer BE, Hong R. Antilymphoma activity of human gamma delta T-cells in mice with severe combined immune deficiency. *Cancer Res* (1992) 52(20):5610–6.
21. Chen J, Niu H, He W, Ba D. Antitumor activity of expanded human tumor-infiltrating gammadelta T lymphocytes. *Int Arch Allergy Immunol* (2001) 125(3):256–63. doi:10.1159/000053824
22. Zheng BJ, Chan KW, Im S, Chua D, Sham JS, Tin PC, et al. Anti-tumor effects of human peripheral gammadelta T cells in a mouse tumor model. *Int J Cancer* (2001) 92(3):421–5. doi:10.1002/ijc.1198
23. Kabelitz D, Wesch D, Pitters E, Zoller M. Characterization of tumor reactivity of human V gamma 9V delta 2 gamma delta T cells in vitro and in SCID mice in vivo. *J Immunol* (2004) 173(11):6767–76. doi:10.4049/jimmunol.173.11.6767
24. Lozupone F, Pende D, Burgio VL, Castelli C, Spada M, Venditti M, et al. Effect of human natural killer and gammadelta T cells on the growth of human autologous melanoma xenografts in SCID mice. *Cancer Res* (2004) 64(1):378–85. doi:10.1158/0008-5472.CAN-03-1501
25. Xiang Z, Liu Y, Zheng J, Liu M, Lv A, Gao Y, et al. Targeted activation of human Vgamma9Vdelta2-T cells controls Epstein-Barr virus-induced B cell lymphoproliferative disease. *Cancer Cell* (2014) 26(4):565–76. doi:10.1016/j.ccr.2014.07.026
26. D'Arena G, Musto P, Cascavilla N, Di Giorgio G, Fusilli S, Zendoli F, et al. Flow cytometric characterization of human umbilical cord blood lymphocytes: immunophenotypic features. *Haematologica* (1998) 83(3):197–203.
27. Roth I, Corry DB, Locksley RM, Abrams JS, Litton MJ, Fisher SJ. Human placental cytotrophoblasts produce the immunosuppressive cytokine interleukin 10. *J Exp Med* (1996) 184(2):539–48. doi:10.1084/jem.184.2.539
28. Szekeres-Bartho J, Faust Z, Varga P, Szereday L, Kelemen K. The immunological pregnancy protective effect of progesterone is manifested via controlling cytokine production. *Am J Reprod Immunol* (1996) 35(4):348–51. doi:10.1111/j.1600-0897.1996.tb00492.x
29. Marchant A, Goldman M. T cell-mediated immune responses in human newborns: ready to learn? *Clin Exp Immunol* (2005) 141(1):10–8. doi:10.1111/j.1365-2249.2005.02799.x
30. Wilson CB, Westall J, Johnston L, Lewis DB, Dower SK, Alpert AR. Decreased production of interferon-gamma by human neonatal cells. Intrinsic and regulatory deficiencies. *J Clin Invest* (1986) 77(3):860–7. doi:10.1172/JCI112383
31. Chalmers IM, Janossy G, Contreras M, Navarrete C. Intracellular cytokine profile of cord and adult blood lymphocytes. *Blood* (1998) 92(1):11–8.
32. Berthou C, Legros-Maida S, Soulie A, Wargnier A, Guillet J, Rabian C, et al. Cord blood T lymphocytes lack constitutive perforin expression in contrast to adult peripheral blood T lymphocytes. *Blood* (1995) 85(6):1540–6.
33. White GP, Watt PM, Holt BJ, Holt PG. Differential patterns of methylation of the IFN-gamma promoter at CpG and non-CpG sites underlie differences in IFN-gamma gene expression between human neonatal and adult CD45RO T cells. *J Immunol* (2002) 168(6):2820–7. doi:10.4049/jimmunol.168.6.2820
34. D'Vaz N, Ma Y, Dunstan JA, Lee-Pullen TF, Hii C, Meldrum S, et al. Neonatal protein kinase C zeta expression determines the neonatal T-cell cytokine phenotype and predicts the development and severity of infant allergic disease. *Allergy* (2012) 67(12):1511–8. doi:10.1111/all.12027
35. Harb H, Irvine J, Amarasekera M, Hii CS, Kesper DA, Ma Y, et al. The role of PKCzeta in cord blood T-cell maturation towards Th1 cytokine profile and its epigenetic regulation by fish oil. *Biosci Rep* (2017) 37(2):BSR20160485. doi:10.1042/BSR20160485
36. Wagner JE, Kernan NA, Steinbuch M, Broxmeyer HE, Gluckman E. Allogeneic sibling umbilical-cord-blood transplantation in children with malignant and non-malignant disease. *Lancet* (1995) 346(8969):214–9. doi:10.1016/S0140-6736(95)91268-1
37. Beura LK, Hamilton SE, Bi K, Schenkel JM, Odumade OA, Casey KA, et al. Normalizing the environment recapitulates adult human immune traits in laboratory mice. *Nature* (2016) 532(7600):512–6. doi:10.1038/nature17655
38. Mazur MA, Davis CC, Szabolcs P. Ex vivo expansion and Th1/Tc1 maturation of umbilical cord blood T cells by CD3/CD28 costimulation. *Biol Blood Marrow Transplant* (2008) 14(10):1190–6. doi:10.1016/j.bbmt.2008.07.016
39. Davis CC, Marti LC, Sempowski GD, Jeyaraj DA, Szabolcs P. Interleukin-7 permits Th1/Tc1 maturation and promotes ex vivo expansion of cord blood T cells: a critical step toward adoptive immunotherapy after cord blood transplantation. *Cancer Res* (2010) 70(13):5249–58. doi:10.1158/0008-5472.CAN-09-2860
40. Sornasse T, Larenas PV, Davis KA, de Vries JE, Yssel H. Differentiation and stability of T helper 1 and 2 cells derived from naive human neonatal CD4+ T cells, analyzed at the single-cell level. *J Exp Med* (1996) 184(2):473–83. doi:10.1084/jem.184.2.473

41. Stockinger B, Kassiotis G, Bourgeois C. Homeostasis and T cell regulation. *Curr Opin Immunol* (2004) 16(6):775–9. doi:10.1016/j.coi.2004.09.003
42. Chiesa R, Gilmour K, Qasim W, Adams S, Worth AJ, Zhan H, et al. Omission of in vivo T-cell depletion promotes rapid expansion of naive CD4+ cord blood lymphocytes and restores adaptive immunity within 2 months after unrelated cord blood transplant. *Br J Haematol* (2012) 156(5):656–66. doi:10.1111/j.1365-2141.2011.08994.x
43. Goldrath AW, Bevan MJ. Low-affinity ligands for the TCR drive proliferation of mature CD8+ T cells in lymphopenic hosts. *Immunity* (1999) 11(2):183–90. doi:10.1016/S1074-7613(00)80093-X
44. Tchao NK, Turka LA. Lymphodepletion and homeostatic proliferation: implications for transplantation. *Am J Transplant* (2012) 12(5):1079–90. doi:10.1111/j.1600-6143.2012.04008.x
45. Barata JT, Silva A, Abecasis M, Carlesso N, Cumano A, Cardoso AA. Molecular and functional evidence for activity of murine IL-7 on human lymphocytes. *Exp Hematol* (2006) 34(9):1133–42. doi:10.1016/j.exphem.2006.05.001
46. Wilson AD, Morgan AJ. Primary immune responses by cord blood CD4(+) T cells and NK cells inhibit Epstein-Barr virus B-cell transformation in vitro. *J Virol* (2002) 76(10):5071–81. doi:10.1128/JVI.76.10.5071-5081.2002
47. Wang P, Munger CM, Joshi AD, Pirruccello SJ, Joshi SS. Cytotoxicity of cord blood derived Her2/neu-specific cytotoxic T lymphocytes against human breast cancer in vitro and in vivo. *Breast Cancer Res Treat* (2004) 83(1):15–23. doi:10.1023/B:BREA.0000010688.55353.a8
48. Liu A, Claesson HE, Mahshid Y, Klein G, Klein E. Leukotriene B4 activates T cells that inhibit B-cell proliferation in EBV-infected cord blood-derived mononuclear cell cultures. *Blood* (2008) 111(5):2693–703. doi:10.1182/blood-2007-08-102319
49. Merindol N, Grenier AJ, Caty M, Charrier E, Duval A, Duval M, et al. Umbilical cord blood T cells respond against the Melan-A/MART-1 tumor antigen and exhibit reduced alloreactivity as compared with adult blood-derived T cells. *J Immunol* (2010) 185(2):856–66. doi:10.4049/jimmunol.0902613
50. Lee YS, Kim TS, Kim DK. T lymphocytes derived from human cord blood provide effective antitumor immunotherapy against a human tumor. *BMC Cancer* (2011) 11:225. doi:10.1186/1471-2407-11-225
51. Hiwarkar P, Qasim W, Ricciardelli I, Gilmour K, Quezada S, Saudemont A, et al. Cord blood T cells mediate enhanced antitumor effects compared with adult peripheral blood T cells. *Blood* (2015) 126(26):2882–91. doi:10.1182/blood-2015-06-654780
52. Tsai MH, Raykova A, Klinke O, Bernhardt K, Gartner K, Leung CS, et al. Spontaneous lytic replication and epitheliotropism define an Epstein-Barr virus strain found in carcinomas. *Cell Rep* (2013) 5(2):458–70. doi:10.1016/j.celrep.2013.09.012
53. Ma SD, Xu X, Plowshay J, Ranheim EA, Burlingham WJ, Jensen JL, et al. LMP1-deficient Epstein-Barr virus mutant requires T cells for lymphomagenesis. *J Clin Invest* (2015) 125(1):304–15. doi:10.1172/JCI76357
54. Ma SD, Xu X, Jones R, Delecluse HJ, Zumwalde NA, Sharma A, et al. PD-1/CTLA-4 blockade inhibits Epstein-Barr virus-induced lymphoma growth in a cord blood humanized-mouse model. *PLoS Pathog* (2016) 12(5):e1005642. doi:10.1371/journal.ppat.1005642
55. Zumwalde NA, Sharma A, Xu X, Ma S, Schneider CL, Romero-Masters JC, et al. Adoptively transferred Vgamma9Vdelta2 T cells show potent antitumor effects in a preclinical B cell lymphomagenesis model. *JCI Insight* (2017) 2(13):93179. doi:10.1172/jci.insight.93179

Conflict of Interest Statement: The authors declare that the research was conducted in the absence of any commercial or financial relationships that could be construed as a potential conflict of interest.

frontiers in Immunology

ORIGINAL RESEARCH
published: 02 February 2018
doi: 10.3389/fimmu.2018.00152

Generation of Human Immunosuppressive Myeloid Cell Populations in Human Interleukin-6 Transgenic NOG Mice

*Asami Hanazawa[1], Ryoji Ito[1], Ikumi Katano[1], Kenji Kawai[2], Motohito Goto[3], Hiroshi Suemizu[1], Yutaka Kawakami[4], Mamoru Ito[1] and Takeshi Takahashi[1]**

[1] Laboratory Animal Research Department, Central Institute for Experimental Animals (CIEA), Kawasaki, Japan, [2] Pathological Analysis Center, Central Institute for Experimental Animals (CIEA), Kawasaki, Japan, [3] Animal Resources Center, Central Institute for Experimental Animals (CIEA), Kawasaki, Japan, [4] Division of Cellular Signaling, Institute for Advanced Medical Research, Keio University School of Medicine, Tokyo, Japan

The tumor microenvironment contains unique immune cells, termed myeloid-derived suppressor cells (MDSCs), and tumor-associated macrophages (TAMs) that suppress host anti-tumor immunity and promote tumor angiogenesis and metastasis. Although these cells are considered a key target of cancer immune therapy, *in vivo* animal models allowing differentiation of human immunosuppressive myeloid cells have yet to be established, hampering the development of novel cancer therapies. In this study, we established a novel humanized transgenic (Tg) mouse strain, human interleukin (hIL)-6-expressing NOG mice (NOG-hIL-6 transgenic mice). After transplantation of human hematopoietic stem cells (HSCs), the HSC-transplanted NOG-hIL-6 Tg mice (HSC-NOG-hIL-6 Tg mice) showed enhanced human monocyte/macrophage differentiation. A significant number of human monocytes were negative for HLA-DR expression and resembled immature myeloid cells in the spleen and peripheral blood from HSC-NOG-hIL-6 Tg mice, but not from HSC-NOG non-Tg mice. Engraftment of HSC4 cells, a human head and neck squamous cell carcinoma-derived cell line producing various factors including IL-6, IL-1β, macrophage colony-stimulating factor (M-CSF), and vascular endothelial growth factor (VEGF), into HSC-NOG-hIL-6 Tg mice induced a significant number of TAM-like cells, but few were induced in HSC-NOG non-Tg mice. The tumor-infiltrating macrophages in HSC-NOG-hIL-6 Tg mice expressed a high level of CD163, a marker of immunoregulatory myeloid cells, and produced immunosuppressive molecules such as arginase-1 (Arg-1), IL-10, and VEGF. Such cells from HSC-NOG-hIL-6 Tg mice, but not HSC-NOG non-Tg mice, suppressed human T cell proliferation in response to antigen stimulation in *in vitro* cultures. These results suggest that functional human TAMs can be developed in NOG-hIL-6 Tg mice. This mouse model will contribute to the development of novel cancer immune therapies targeting immunoregulatory/immunosuppressive myeloid cells.

Keywords: humanized mice, MDSCs, NOG-hIL-6 Tg mice, TAMs, tumor microenvironment

Abbreviations: IL-6, interleukin-6; NOG, NOD/ShiJic/scid/IL-2Rγ^{null} mice; NOG-hIL-6 Tg, NOG mouse substrain expressing transgenic human IL-6; non-Tg, nontransgenic; HSC, hematopoietic stem cell; CB, cord blood; HSC-NOG, human hematopoietic stem cell-transplanted NOG mouse; PB, peripheral blood; BM, bone marrow; MNC, mononuclear cell; RT-PCR, reverse transcription polymerase chain reaction.

OPEN ACCESS

Edited by:
Moriya Tsuji, Aaron Diamond AIDS Research Center, United States

Reviewed by:
Anna Karolina Kozlowska, Poznan University of Medical Sciences, Poland
Amorette Barber, Longwood University, United States
Karin Schilbach, Universität Tübingen, Germany

****Correspondence:***
Takeshi Takahashi
takeshi-takahashi@ciea.or.jp

Specialty section:
This article was submitted to Cancer Immunity and Immunotherapy, a section of the journal Frontiers in Immunology

Received: *26 October 2017*
Accepted: *17 January 2018*
Published: *02 February 2018*

Citation:
Hanazawa A, Ito R, Katano I, Kawai K, Goto M, Suemizu H, Kawakami Y, Ito M and Takahashi T (2018) Generation of Human Immunosuppressive Myeloid Cell Populations in Human Interleukin-6 Transgenic NOG Mice. Front. Immunol. 9:152. doi: 10.3389/fimmu.2018.00152

INTRODUCTION

Humanized mouse technology has enabled reconstitution of human hematopoietic and immune systems in immunodeficient mice (1, 2). Accumulating evidence suggests that this novel technology is suitable for studying several infectious diseases including human immunodeficiency virus (HIV), Epstein-Barr virus, and malaria (3–6). These studies have revealed that replication of pathogens is possible *in vivo*, and that immune responses against these pathogens are elicited, even if in a limited manner. Thus, humanized mice are useful instruments for studying *in vivo* human physiology and conducting preclinical studies for novel drugs. In this context, the use of humanized mice has been applied in immuno-oncological studies to evaluate drug efficiencies (7, 8). Considering the complex pathology of tumors, it is important to clarify which cellular lineages contribute to tumor formation and disease progression, and whether those cells are present in humanized mice (9).

Humanized mice are usually produced using extremely severe immunodeficient mouse strains including, NOD/shi-scid/IL-2Rγ^{null} (NOG), NOD/LtSz-scid/IL-2Rγ^{null} (NSG), or BALB/c-Rag2^{null}/IL-2Rγ^{null} (BRG). Human immune systems can be reconstituted in these mice by transplanting human CD34$^+$ hematopoietic stem cells (HSCs) (10–12). Humanized mice based on these platform strains harbor limited human myeloid cell lineages including granulocytes, monocytes, macrophages, and their progenitors. As several of these cell lineages are relevant to disease development, our group and others have genetically modified these platform strains by introducing human cytokine genes to improve myeloid differentiation. For example, myelopoiesis was markedly enhanced in NOG-human (h) granulocyte macrophage colony-stimulating factor (GM-CSF)/interleukin (IL)-3 Tg mice (NOG-hGM/3 Tg) compared to parental NOG mice, and mast cells that developed in this strain were fully functional in mediating passive cutaneous anaphylaxis (PCA) (13). Similar results were obtained in NSG mice with human GM-CSF/IL-3/stem cell factor transgenes (NSG-SGM3). NSG-SGM3 mice showed enhanced differentiation of human myeloid lineage cells (14). BLT (bone marrow–liver–thymus) mice on the NSG-SGM3 background, a type of humanized mice generated by engrafting human fetal-derived thymus and liver in renal capsule and subsequent HSC transplantation, induced human PCA and passive systemic anaphylaxis mediated by human mast cells (15). BRG mice have been modified to generate MITRG mice, in which the murine macrophage colony-stimulating factor (M-CSF), IL-3, GM-CSF, and thrombopoietin genes were replaced by the human homologs, and MISTRG mice, which also contain the human signal-regulatory protein alpha gene (16). The development of functional human monocytes, macrophages, and natural killer (NK) cells has been promoted in these mice. For example, ~3-fold high number of CD33$^+$ total myeloid cells developed in NOG-hGM/3 Tg compared to NOG mice (13), ~3-fold increase of CD33$^+$ cells in frequency in NSG-SGM3 (15), and ~10-fold CD33$^+$ cells in MITRG compared to NSG mice (16). In addition, human NK cells consisted of 10–20% of mononuclear cells (MNCs) in peripheral blood in MISTRG mice (16). Furthermore, human macrophages infiltrate a human tumor xenograft in MITRG or MISTRG mice (16). These results suggest that human myeloid cell development can be induced in humanized mice by introducing the appropriate human cytokines.

The tumor microenvironment consists of an unusual variety of cell types that include not only cancer cells but also fibroblasts, endothelial cells in blood vessels and lymph ducts, and immune cells such as lymphocytes and myeloid cells. Patients with cancer and tumor masses have increased numbers of cells that phenotypically resemble immature myeloid cells, and the prognosis of these patients is inversely correlated with the number of these immature myeloid cells. Thus, immunoregulatory activity can facilitate tumor progression by preventing host immune systems from attacking a tumor and by inducing factors that promote angiogenesis (17). Tumor-associated macrophages (TAMs) and myeloid-derived supressor cells (MDSCs), especially, are two representatives of such immunosuppressive myeloid cells. TAMs produce various types of immunosuppressive molecules including arginase-1 (Arg-1), IL-10, tumor growth factor-β, or prostaglandin E_2 (PGE_2); and factors related to angiogenesis or cell proliferation such as vascular endothelial growth factor (VEGF), IL-8, basic fibroblast growth factor (bFGF), hepatocyte growth factor, epidermal growth factor, or platelet-derived growth factor (18, 19). MDSCs also produce Arg-1, inducible nitric oxide synthase, reactive oxygen species, and peroxynitrite for immunosuppression (20). Studies investigating the molecular mechanisms in the induction of TAMs and MDSCs revealed the critical role of inflammatory cytokines. IL-6, in particular, plays an essential role in the induction, as IL-4 receptor alpha chain (IL-4Rα)$^+$ MDSCs are produced in *in vitro* cultures of mouse bone marrow (BM) cells incubated with IL-6, granulocyte colony-stimulating factor (G-CSF), and GM-CSF (21). In addition, IL-6 promotes differentiation of granulocytic MDSCs (22, 23), and the number of monocytic MDSCs increases when IL-6 production is enhanced due to infection by hepatitis B virus (24). These studies suggest that human IL-6 (hIL-6) is an indispensable requirement for recapitulating the human tumor microenvironment in humanized mice.

In this study, we established a novel NOG sub-strain, NOG-hIL-6 Tg mice. We demonstrated that after transplantation of human HSCs, a significantly higher numbers of human monocytes and macrophages were induced in NOG-hIL-6 Tg mice than in NOG non-Tg mice. We further demonstrated that after tumor engraftment, significant numbers of immature myeloid cells, phenotypically resembling TAMs in clinical patients, differentiated in HSC transplanted NOG-hIL-6 Tg mice (HSC-NOG-hIL-6 Tg mice), whereas few myeloid cells were observed in HSC-NOG non-Tg mice. This novel mouse model is a unique tool for studying the pathology of tumor formation and will facilitate drug discovery targeting TAMs.

MATERIALS AND METHODS

Mice

NOD/ShiJic/scid/IL-2Rγ^{null} (NOG) mice and NOD/ShiJic (NOD) mice were used in this study. To generate hIL-6-expressing Tg

NOG mice, a DNA fragment containing hIL-6 cDNA, under the control of the cytomegalovirus (CMV) promoter, was microinjected into female NOD mouse eggs fertilized by male NOG mice. A founder mouse was backcrossed with NOG mice to obtain NOG-hIL-6 Tg mice (NOD.Cg-*prkdc*^{scid}*il2rγ*^{tm1Sug}/ShiJic CMV-IL-6 Tg). Serum levels of hIL-6 were measured using hIL-6 Quantikine enzyme-linked immunosorbent assay (ELISA) kits (R&D systems, Minneapolis, MN, USA). All of the mice were maintained in the Central Institute for Experimental Animals (CIEA) under specific pathogen-free conditions.

Transplantation of Human HSCs

Human umbilical-cord-blood-derived CD34$^+$ HSCs were purchased from Allcells (Alameda, CA, USA). For transplantation, 6–12-week-old adult mice were irradiated (2.5 Gy) (MBR-1505R; Hitachi Medical, Tokyo, Japan), and 5×10^4 HSCs were injected intravenously within 24 h. To monitor human hematopoiesis, the mice were bled every 3 weeks over a total of 3 months, and the MNCs were analyzed by flow cytometry.

Cell Lines

A human tumor cell line, HSC4, derived from human head and neck squamous cell carcinoma, was provided by Y. Kawakami (Keio University School of Medicine, Tokyo, Japan). HSC4s were cultured in complete RPMI-1640 medium (Life Technologies, Grand Island, NY, USA) supplemented with 10% fetal calf serum (FCS) and antibiotics, penicillin, and streptomycin. Other human tumor cell lines, L428 (Hodgkin's lymphoma), Daudi (Burkitt lymphoma), HeLaS3 (cervical epithelioid carcinoma), SAS (tongue squamous carcinoma) (25), SK-BR3 (breast adenocarcinoma) (26) and RMG1 (ovarian clear cell carcinoma) (27) were also provided by Keio University. L428, Daudi, HeLaS3, and SAS cells were cultured in complete RPMI-1640 medium with 10% FCS and antibiotics, and SK-BR3 cells were cultured in complete Dulbecco's Modified Eagle's Medium with 10% FCS and antibiotics.

In Vivo Human Tumor Transplantation Model

HSC4 cells (1.5×10^6, 100 μL PBS) were inoculated subcutaneously into HSC-NOG hIL-6 Tg mice or HSC-NOG non-Tg mice at 12–14 weeks after HSC transplantation. Solid tumor size was measured twice a week using a caliper and calculated using the following formula: tumor volume (mm^3) = 1/2 × length (mm) × [width (mm)]^2. Human MNCs in the tumor, spleen, and peripheral blood (PB) in the mice were analyzed 30–51 days post-tumor inoculation when the tumor volume reached 2000 mm^3.

Preparation of Human Immune Cells from Human Tumors Engrafted in HSC-NOG Mice

Peripheral blood was collected from the abdominal vein of HSC-NOG-hIL-6 Tg or HSC-NOG non-Tg mice under anesthesia at the time of sacrifice. Blood plasma was separated by centrifugation. BM cells were obtained by flushing femurs with 3 mL PBS with 0.1% bovine serum albumin (BSA). Splenic cells were prepared by crushing the tissues between two frosted slides, and the tissue debris was removed using a 100-μm nylon mesh. Solid tumors were dissociated using a gentleMACS™ dissociator (Miltenyi Biotec, Bergisch Gladbach, Germany) in RPMI-1640 medium with collagenase IV (1 mg/mL; Sigma-Aldrich, St. Louis, MO, USA) and DNase I (0.1 mg/mL; Sigma-Aldrich), and subsequently incubated for 30 min at 37°C under gentle rotation. These steps were repeated twice. After dissociation, cells were filtered through a 70-μm mesh filter (BD Bioscience, Franklin Lakes, NJ, USA) to remove the debris. Mouse red blood cells (RBCs) were eliminated with RBC lysis buffer (stock solution contained 155 mM NH_4Cl, 10 mM $KHCO_3$ and 0.1 mM EDTA. This solution was diluted 4:1 with Dulbecco's PBS before use). After washing, cell pellets were resuspended with PBS containing 0.1% BSA.

Flow Cytometry

Cell viability was assessed by Trypan blue exclusion. Numbers of total leukocytes in PB were counted using a blood analyzer, Sysmex XT-2000i (Sysmex, Kobe, Japan), and the total blood volume was calculated from the body weight, assuming that mice contain 72 mL blood per kg body weight (28). The number of leukocytes in the total BM was calculated as 16 × the number of leukocytes in one femur (28). Single MNC suspensions were stained with the appropriate antibodies for 20 min at 4°C in the dark. After washing with fluorescence-activated cell sorting (FACS) buffer (PBS, 0.1% BSA, 0.1% NaN_3), the cells were resusupended in FACS buffer containing propidium iodide (1 μg/mL; Dojindo Molecular Technologies, Inc., Kumamoto, Japan) to exclude dead cells. We used a BD FACSCanto™ (BD Biosciences) and a BD FACSAriaII™ (BD Biosciences) for multicolor flow cytometric analysis with FACSDiva™ software (BD Biosciences); the data were analyzed using the FlowJo® software program (ver. 7.6.1; Tree Star, Inc., Ashland, OR, USA). The following antibodies were used: anti-human CD33 -phycoerythrin (PE)-Cy7(WM-53) was purchased from eBioscience (San Diego, CA, USA); anti-human CD11b-FITC (ICRF44), anti-human CD14-FITC (HCD14), anti-human CD33-FITC (HIM3–4), anti-human CD66b-FITC (G10F5), anti-mouse CD45-FITC (30-F11), anti-HLA-DR-Alexa Flour-488 (L243), anti-human CD19-PE (G077F6), anti-human CD66b-PE (G10F5), anti-human CD124-PE (IL-4Rα), anti-human CD163-PE (GHI/61), anti-human CD335 (NKp46)-PE (9E2), anti-mouse CD45-PerCP-Cy5.5 (30-F11), anti-human CD3-PE-Cy7 (UCHT1), anti-human CD14-PE-Cy7 (HCD14), anti-human CD56-PE-Cy7 (HCD56), anti-human CD68-PE-Cy7 (Y1/82A), anti-human CD16 –allophycocyanin (APC) (3G8), anti-human CD56-APC (HCD56), anti-HLA-DR-APC (L243), anti-human CD14-APC-Cy7 (HCD14), anti-human CD45-APC-Cy7 (HI30), anti-mouse CD45-APC-Cy7 (30-F11), anti-human CD3-Brilliant Violet 421 (UCHT1), anti-human CD11b-Brilliant Violet 421 (ICRF44), anti-human CD163-Brilliant Violet 421 (GHI/61), and anti-human CD45-Brilliant Violet 510 (HI30) were purchased from BioLegend (San Diego, CA, USA).

Intracellular Staining

To investigate the expression of Arg-1 in human monocytes and macrophages, human MNCs from tumor, spleen, and PB of

HSC-NOG-hIL-6 Tg mice or HSC-NOG non-Tg mice were fixed in 2% formaldehyde (Nacalai Tesque, Kyoto, Japan) for 15 min at room temperature, and subsequently stained with anti-human CD68-PE-Cy7 (Y1/82A) and anti-human Arg-1-APC (Clone # 658922; R&D Systems) or APC-conjugated mouse IgG2b isotype control (MPC-11; BioLegend) in the presence of 0.5% saponin (Nacalai Tesque) for permeabilization. Stained samples were analyzed using a BD FACSAriaII™ flow cytometer (BD Biosciences).

Histology and Immunohistochemistry

For immunohistochemical studies, the tumor, spleen, liver, BM, lung, skin, gut, and kidney of HSC-NOG-hIL-6 Tg mice or HSC-NOG non-Tg mice were fixed in Mildform 10MN formaldehyde solution (Wako Pure Chemical, Osaka, Japan) and embedded in paraffin. The samples were serially sectioned into 3-μm thicknesses using a microtome, and placed on silane-coated slides (Muto Pure Chemicals, Tokyo, Japan). Immunostaining was performed using a Leica Bond-Max automatic immunostainer (Leica Biosystems, Mount Waverley, VIC, Australia). Paraffin sections were dewaxed in a Bond Dewax solution and rehydrated in alcohol and Bond Wash solution (Leica Biosystems). Antigen retrieval was performed using a retrieval solution (ER1, 10 mM citrate buffer, pH 6), followed by endogenous peroxidase blocking. Detection was performed using a Bond Polymer Refine Detection system. Then, the sections were counterstained with hematoxylin. We used monoclonal anti-human CD68 (clone: PG-M1, DakoCytomation, Glostrup, Denmark) and monoclonal anti-human CD163 (clone: 10D6, Leica Biosystems Newcastle Ltd., Newcastle, UK) antibodies for immunohistochemical analyses (National Institutes of Health, Bethesda, MD, USA).

Detection of mRNA

Total RNA was isolated using Isogen reagent (Nippon Gene, Tokyo, Japan). The first strand cDNA was synthesized using oligo (dT) primers and the Superscript III First-Strand Synthesis System (Thermo Fisher Scientific, Waltham, MA, USA). For semi-quantitive polymerase chain reaction (PCR) analysis, the following primers were used: *gapdh*, 5′-TTAAAAGCAGCCCTGGTGAC-3′ (sense) and 5′-CTCTGCTCCTCCTGTTCGAC-3′ (antisense) (29); *il-10*, 5′-GGGTTGCCAAGCCTTGTCTG-3′ and 5′-CGCCGTAGCCTCAGCCTG-3′ (30); *vegf*, 5′-CACACAGGATGGCTTGAAGA-3′ and 5′-AGGGCAGAATCATCACGAAG-3′ (29). Each mRNA was amplified with EX-Taq (Takara Bio, Inc., Kusatsu, Japan). The intensity of each band was measured using ImageJ software.

In Vitro Carboxyfluorescein Succinimidyl Ester (CFSE) Proliferation Assay

For CFSE prolifration assays, human CD3$^+$ T cells were purified from the spleen of HSC-NOG non-Tg mice at 16–24 weeks after HSC transplantation by MACS (Miltenyi Biotec). Human CD11b$^+$ cells were sorted from tumor or spleen of HSC-NOG-hIL-6 Tg mice or NOG non-Tg mice using a BD FACSAriaII™ (BD Biosciences). CFSE proliferation analyses were performed using a CellTrace™ CFSE Cell Proliferation Kit (Thermo Fisher Scientific) according to the manufacturer's instructions. Human CD3$^+$ T cells were sorted from tumor-free HSC-NOG non-Tg mice, which were transplanted with HSCs from a different donor from those of CD11b$^+$ human myeloid cells. Briefly, human CD3$^+$ T cells were labeled with 1 μM CellTrace™ CFSE in PBS for 5 min at 37°C and washed three times with 0.1% BSA/PBS to remove excess CFSE. CFSE-labeled human CD3$^+$ T cells (1×10^5) were stimulated with immobilized anti-hCD3 (OKT3, 20 μg/mL) and anti-hCD28 (CD28.2, 2 μg/mL)antibodies (BioLegend) at 37°C in the presence or absence of 5×10^4 human CD11b$^+$ cells. On day 7, dilutions of CFSE in human CD3$^+$ T cells were analyzed.

BD™ Cytometric Beads Array (CBA)

To measure the human cytokines produced by human tumor cell lines, we used a CBA kit (BD Biosciences). Standards (2,500–10 pg/mL and blank) and 50 μL culture supernatant from each cell line were added to 50 μL capture beads and incubated for 1 h at room temperature in the dark. After incubation, 50 μL PE detection reagents were added and incubated for 2 h at room temperature in the dark. After washing, test samples and standards were resuspended in 300 μL wash buffer and analyzed using a BD FACSCanto™ flow cytometer (BD Biosciences). The data were analyzed using FCAP Array™ v3.0 software (BD Biosciences).

RESULTS

Enhancement of Human Monocyte/Macrophage Development in HSC-NOG-hIL-6 Tg Mice

The establishment of NOG-hIL-6 Tg mice was confirmed by measuring the production of hIL-6. Quantification by ELISA demonstrated that significant amounts of hIL-6 protein were present in plasma from both homozygous and heterozygous NOG-hIL-6 Tg, but not in NOG non-Tg mice. Homozygous NOG-hIL-6 Tg mice showed significantly higher IL-6 expression levels than heterozygous NOG-hIL-6 Tg mice (**Figure 1A**).

To investigate hematopoiesis of human cells in NOG-hIL-6 Tg mice, human CD34$^+$ HSCs from umbilical CB were transferred into irradiated NOG-hIL-6 Tg mice and NOG non-Tg mice. The mice were bled for FACS analysis every 3 weeks from 6 weeks until 15 weeks after HSC transplantation (**Figure 1B**). The frequency of hCD45$^+$ leukocytes in the total leukocyte population was slightly higher in HSC-NOG-hIL-6 Tg mice than in HSC-NOG non-Tg mice, but this difference did not reach significance (**Figure 1C**). There were no significant differences in human CD3$^+$ T cells or CD19$^+$ B cells (**Figure 1C**). The frequency of CD3$^-$CD56$^+$ NK cells increased in HSC-NOG-hIL-6 Tg mice at 8–9 weeks after HSC transplantation compared to that in HSC-NOG non-Tg mice; however, this increase did not reach statistical significance. This human CD45$^+$CD3$^-$NKp46$^+$CD56$^+$ NK cells in HSC-NOG-hIL-6 Tg mice consisted of three populations, CD56^{dim}CD16^{bright} cytotoxic NK cells, cytokine producing

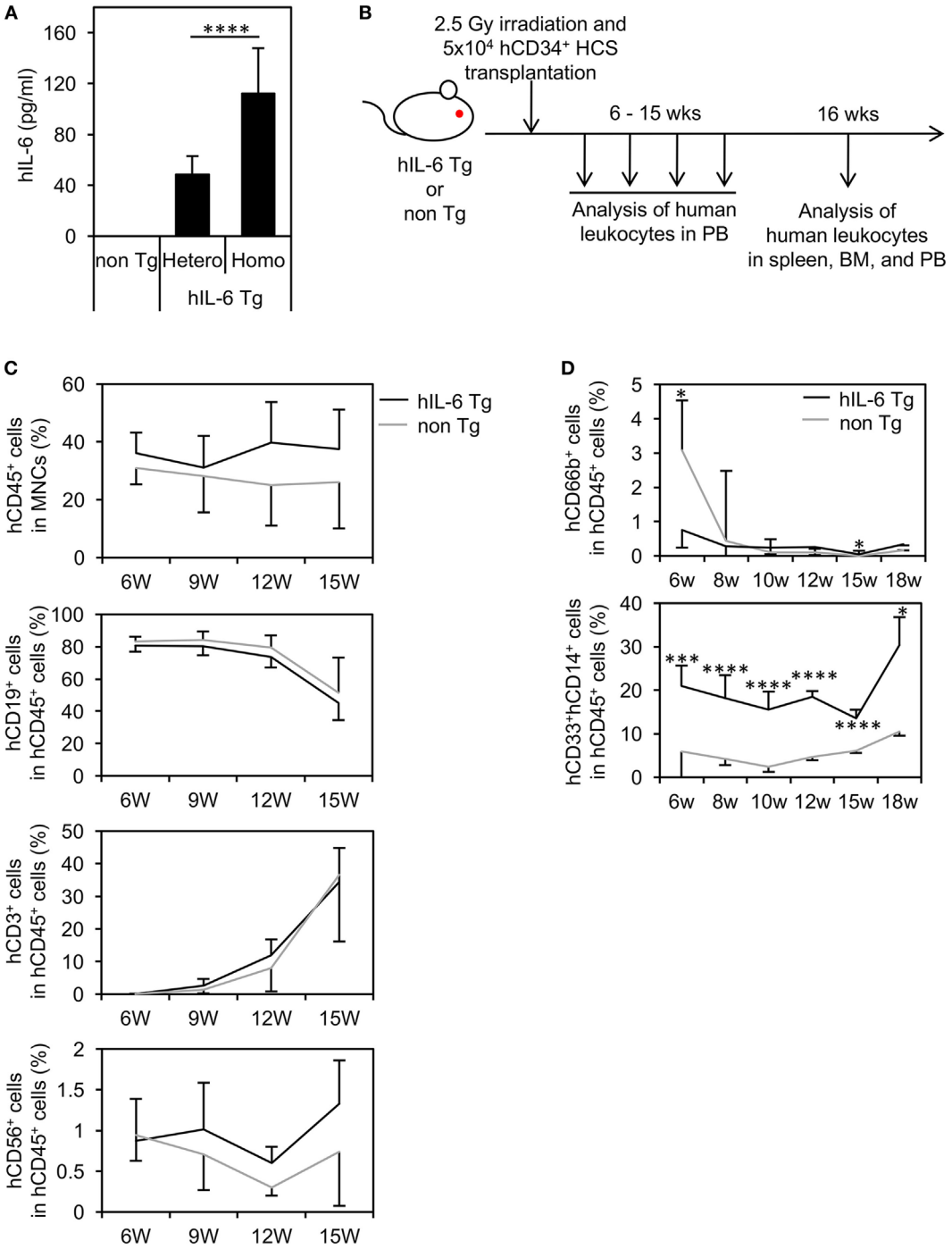

FIGURE 1 | Human cell hematopoiesis in hematopoietic stem cell (HSC)-transplanted NOD/Shi-scid-IL-2Rγ^{null} (NOG) substrain mice expressing transgenic (Tg) human interleukin 6 (hIL-6) (HSC-NOG-hIL-6 Tg). **(A)** Level of hIL-6. The levels of hIL-6 in the serum of NOG-hIL-6 homozygous Tg, heterozygous Tg, or NOG non-Tg mice were measured using enzyme-linked immunosorbent assay. The means ± SDs are shown ($n = 25$). Asterisks indicate statistical significance (****$p < 0.0001$). **(B)** NOG-hIL-6 Tg mice or NOG non-Tg mice were transplanted with 5×10^4 cord blood human CD34$^+$ HSCs 1 day after irradiation (2.5 Gy). Human leukocytes in peripheral blood (PB) were analyzed at the indicated time points. **(C)** The PB of HSC-NOG-hIL-6 Tg mice (black line, $n = 6$) and HSC-NOG non-Tg mice (gray line, $n = 4$) were analyzed by fluorescence-activated cell sorting (FACS) at 6–15 weeks after HSC transplantation. The frequencies of engrafted hCD45$^+$ cells in all of the leukocytes and frequencies of each hematopoietic lineage in the hCD45$^+$ cell population are shown. **(D)** The PB of HSC-NOG-hIL-6 Tg mice (black line, $n = 5$) and HSC-NOG non-Tg mice (gray line, $n = 5$) were FACS analyzed at 6–18 weeks after HSC transplantation. The frequencies of CD33$^+$CD14$^+$ monocytes/macrophages or hCD66b$^+$ granulocytes in the hCD45$^+$ cell population are shown (****$p < 0.0001$, *$p < 0.05$). The figures show representative data from three independent experiments. Student's t-test was performed to analyze statistical significance.

$CD56^+CD16^-$ NK cells, and $CD56^+CD16^+$ NK cells. There were no significant differences between HSC-NOG-hIL-6 Tg mice and HSC-NOG non-Tg mice in frequencies and cellularties in those $CD56^{dim}CD16^{bright}$ and $CD56^+CD16^-$ NK cell fractions (Figure S1 in Supplementary Material) (31). Myeloid cells are generally classified into monocytes/macrophages and granulocytes. In the $CD33^+$ myeloid cell fraction in the PB of HSC-NOG-hIL-6 Tg mice, $CD33^+CD14^+$ monocytes were markedly increased in HSC-NOG-hIL-6 Tg mice compared to NOG non-Tg mice, whereas $CD66b^+$ granulocytes were barely detected in HSC-NOG-hIL-6 Tg mice, in a manner similar to HSC-NOG non-Tg mice (**Figure 1D**).

Flow cytometric analysis revealed that ~five or three-fold increases in the numbers of total human $CD45^+$ cells in the spleen or BM of HSC-NOG-hIL-6 Tg mice, respectively (Figure S2 in Supplementary Material). The increase of monocytes/macrophages from HSC-NOG-hIL-6 Tg mice was more profound in the spleen and PB than in the BM (**Figure 2A**). The total cell number of $CD33^+CD14^+CD66b^-$ monocytes was ~15.4-fold (spleen, PB) or 2.4-fold (BM) higher in HSC-NOG-hIL-6 Tg mice than in HSC-NOG non-Tg mice (**Figure 2B**). These results suggest that development of human monocytes/macrophages was enhanced in NOG-hIL-6 Tg mice. To analyze the distribution of human macrophages in various tissues, tissue sections of lung, liver, spleen, and BM from HSC-NOG-hIL-6 Tg or HSC-NOG non-Tg mice were stained with peroxdase-conjugated antibody against human CD68 (**Figure 2C**). The densities of $CD68^+$ macrophages were higher in lung and liver from HSC-NOG-hIL-6 Tg mice than in those from HSC-NOG non-Tg mice, whereas the cell density in the spleen and BM of HSC-NOG non-Tg mice were comparable with those in HSC-NOG-hIL-6 Tg mice (**Figure 2C**). There were few $CD68^+$ cells in the gut, skin, and brain from HSC-NOG-hIL-6 Tg and NOG non-Tg mice (data not shown). Hence, the increase of the cellularity of human monocytes/macrophages in the spleen (**Figure 2A**) is due to the increase of the absolute number of total $CD45^+$ human cells.

Characterization of Differentiated Human Monocytes and Macrophages in NOG-hIL-6 Tg Mice

Based on expression of CD14 and CD16 (FcγRIII), human monocytes are classified into three subpopulations: $CD14^{++}CD16^-$ classical monocytes, $CD14^+CD16^{++}$ non-classical monocytes, and $CD14^{++}CD16^+$ intermediate monocytes (32, 33). In normal human PB, up to 90% of blood monocytes are $CD14^{++}CD16^-$ classical monocytes, and these cells can differentiate into $CD14^+CD16^{++}$ non-classical monocytes. We investigated the composition of human monocytes in PB from HSC-NOG-hIL-6 Tg and HSC-NOG non-Tg mice (**Figure 3A**). Nearly 80% of human monocytes were $CD14^{++}CD16^-$ classical monocytes at 6 weeks after HSC transplantation both in HSC-NOG-hIL-6 Tg and HSC-NOG non-Tg mice (**Figure 3B**). However, the populations decreased to 60% in HSC-NOG-hIL-6 Tg at 16 weeks after HSC transplantation in HSC-NOG-hIL-6 Tg (**Figures 3B,C**). The $CD14^{++}CD16^+$ intermediate monocytes increased and constituted about 30% in HSC-NOG-hIL-6 Tg mice at 16 weeks. In some individual mice in HSC-NOG-hIL-6 Tg mice, ~10% of monocytes were non-classical monocytes at 16 weeks. These monocyte populations were relatively stable in HSC-NOG non-Tg mice (**Figures 3B,C**).

Next, we analyzed the spleen of HSC-NOG-hIL-6 Tg mice and confirmed that development of human $CD33^+CD14^+$ monocytes was promoted in the spleen (**Figure 4A**). Next, we investigated expression of several molecules, including the Fc receptors. Expression of Fc receptors represents the functionality of monocytes/macrophages to mediate phagocytosis. In HSC-NOG non-Tg mice, the frequencies of $CD33^+CD14^+$ monocytes/macrophages expressing FcγRI and FcγRIII were about 20 and 0%, respectively, in the total population of $CD33^+CD14^+$ human cells. By contrast, 60 and 20% of human monocytes/macrophages expressed FcγRI and FcγRIII, respectively, in HSC-NOG-hIL-6 Tg mice (**Figure 4B**). Macrophages consist of heterogeneous functional subpopulations, which are characterized by different cytokine production patterns and different expression profiles of various surface molecules. Nevertheless, they are roughly classified into inflammatory (classically activated) M1 macrophages and immunosuppresive (alternatively activated) M2 macrophages (35). As IL-6 is an essential factor for the generation of M2 macrophages (36, 37), we investigated whether the NOG-hIL-6 Tg or NOG non-Tg mice could develop differentiated monocytes/macrophages that resemble M2 macrophages. CD163 is a scavenger receptor that is thought to be a specific marker for delineating immunoregulatory M2 macrophages and immunosuppressive MDSCs and TAMs (38–41). We detected no significant differences in levels of CD163 in monocytes/macrophages from spleen, BM, or PB from HSC-NOG-hIL-6 Tg and NOG non-Tg mice (**Figure 4C**). A different M2 macrophage marker, IL-4Rα, was not expressed in human monocytes/macrophages in any of the tissues from either HSC-NOG-hIL-6 Tg or HSC-NOG non-Tg mice (Figure S3 in Supplementary Material). Next, we examined expression levels of HLA-DR (a class II HLA molecule), as HLA-DR expression is low or lost in immature human monocytes/macrophages such as MDSCs and TAMs. The frequencies (**Figure 4D**) and absolute cell numbers (**Figure 4E**) of HLA-DR-expressing or non-expressing monocytes/macrophages were compared in the spleen, BM, and PB from HSC-NOG-hIL-6 Tg and HSC-NOG non-Tg mice. Flow cytometoric analysis of spleen and PB demonstrated that $HLA\text{-}DR^{lo/-}$ monocytes/macrophages constituted a significant subfraction of cells from the HSC-NOG-hIL-6 Tg mice, but not from the HSC-NOG non-Tg mice. In HSC-NOG-hIL-6 Tg mice, about $15.0 \pm 0.46\%$ or $26.9 \pm 9.46\%$ in $CD33^+CD14^+CD66b^-$ human monocytes/macrophages were $HLA\text{-}DR^{lo/-}$ cells in spleen or PB, respectively. Accordingly, the frequency of $HLA\text{-}DR^+$ cells was lower in HSC-NOG-hIL-6 Tg mice than in HSC-NOG non-Tg mice (**Figure 4D**). Enumeration of $HLA\text{-}DR^+$ and $HLA\text{-}DR^{lo/-}$ human monocytes/macrophages showed significant increases in the numbers of $HLA\text{-}DR^{lo/-}$ cells in the spleen and PB in HSC-NOG-hIL-6 Tg mice (**Figure 4E**). By contrast, the numbers of these cells in the HSC-NOG non-Tg mice were negligible. Both $HLA\text{-}DR^+$ and $HLA\text{-}DR^-$ populations were detected in the BM irrespective

of the transgene. Neither the cell numbers nor frequencies of these fractions significantly differed between HSC-NOG-hIL-6 Tg and HSC-NOG non-Tg mice (**Figures 4D,E**). Collectively, these results imply that a portion of the human monocytes/macrophages that developed in NOG-hIL-6 Tg mice gained the unique HLA-DR$^{lo/-}$ phenotype like MDSCs and TAMs.

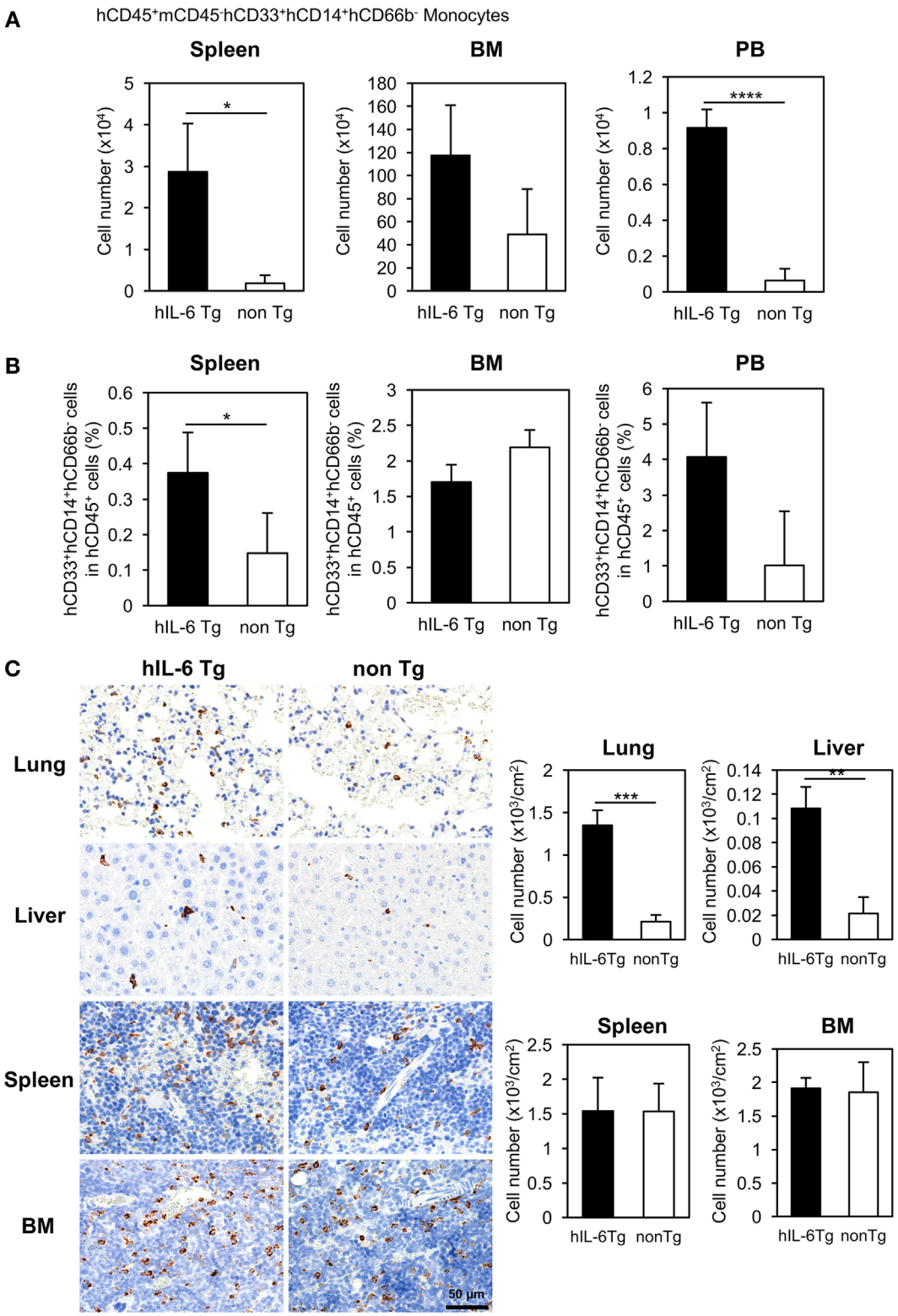

FIGURE 2 | Continued

FIGURE 2 | Development of human monocytes/macrophages in HSC-NOG-hIL-6 Tg mice. Mononuclear cells (MNCs) were prepared from the spleen, bone marrow (BM), and peripheral blood in HSC-NOG-hIL-6 Tg mice (filled column) and HSC-NOG non-Tg mice (open column) at 14 weeks after HSC transfer. The frequency of $CD33^+CD14^+$ monocytes/macrophages in $hCD45^+$ leukocytes was obtained by flow cytometry **(A)**. The absolute number of $CD33^+CD14^+$ monocytes/macrophages was calculated by multiplying the number of total MNCs by the frequencies of each human subpopulation determined by fluorescence-activated cell sorting (FACS) **(B)**. The means ± SDs are shown ($n = 3$). Student's *t*-test was performed to analyze the statistical significance. Asterisks indicate the statistical significance ($^*p < 0.05$, $^{****}p < 0.0001$). **(C)** The distributions of human macrophages in HSC-NOG-hIL-6 Tg mice were assessed in paraffin-embedded lung, liver, spleen, and BM of HSC-NOG-hIL-6 Tg mice and HSC-NOG non-Tg mice; the tissues were sliced, mounted on slides, and stained with peroxidase-conjugated anti-human CD68 antibody. For enumeration of $CD68^+$ macrophages in lung, liver, spleen, and BM, the number of signals in three different view fields in a representative tissue section was counted and divided by the area of the section using a BZ-9000 microscope (Keyence, Tokyo, Japan). The average number per unit area (cm^2) is shown. An asterisk indicates statistical significance based on Student's *t*-test ($^{**}p < 0.01$, $^{***}p < 0.001$).

Generation of Human TAMs in Tumor-Engrafted HSC-NOG-hIL-6 Tg Mice

The detection of HLA-$DR^{lo/-}$ myeloid cells in the spleen and PB in HSC-NOG-hIL-6 Tg mice prompted us to investigate the possibility that human immunosuppressive myeloid cells such as TAMs or MDSCs can be induced in NOG-hIL-6 Tg mice by the presence of transplanted human tumor cells. We analyzed the cytokine expression patterns in six different human tumor cell lines to identify the most suitable line for our experiments and found that HSC4, which is derived from human head and neck squamous cell carcinoma, exhibited high expression of IL-6, M-CSF, IL-8, and VEGF, and was the only line that produced IL-1β (Figure S4 in Supplementary Material).

HSC4 cells were subcutaneously implanted into HSC-NOG-hIL-6 Tg or HSC-NOG non-Tg mice at 12–14 weeks after $CD34^+$ HSC transplantation, a time point when human monocytes, macrophages, T cells, B cells, and NK cells were detected in the PB. Infiltration of human macrophages into HSC4 tumor was analyzed at 30–51 days after HSC4 engraftment (**Figure 5A**). We conducted immunohistochemical analysis to detect human macrophages in HSC4-tumor using anti-CD68 or anti-CD163 antibodies, which are markers of macrophages or immunoregulatory macrophages, respectively. We detected a number of $CD68^+$ macrophages in the spleen of both tumor-bearing HSC-NOG-hIL-6 Tg and HSC-NOG non-Tg mice, with greater numbers detected in HSC-NOG-hIL-6 Tg mice than in HSC-NOG non-Tg mice (**Figures 5B,C**). By contrast, analysis of tumor from the same mice demonstrated that a significant number of $CD68^+$ macrophages infiltrated into the tumor in HSC-NOG-hIL-6 Tg mice, whereas few infiltrates were detected in HSC-NOG non-Tg mice (**Figures 5B,C**). Staining of serial sections with anti-CD163 antibody revealed that the majority of the tumor-infiltrating human macrophages in HSC-NOG-hIL-6 Tg mice were strongly positive for CD163 (**Figures 5B,C**). Indeed, enumeration of the positive signals in the sections revealed a much lower frequency of CD163-positive cells in human macrophages from HSC-NOG non-Tg mice (27.8 ± 0.28%) than in those from HSC-NOG-hIL-6 Tg mice (98.2 ± 0.12%) (**Figure 5C**). In the spleen, a large proportion of human macrophages had negative or weak CD163 expression (**Figures 5B,C**).

To characterize the human macrophages in HSC-NOG-hIL-6 Tg mice further, we examined the expression of IL-4Rα in human macrophages, as IL-4 is one of the factors supporting the differentiation of TAMs and expression of the IL-4 receptor is a marker for delineating TAMs in tumor (42, 43). Human macrophages in tumor, but not in the spleen or PB, expressed a significant amount of IL-4Rα (**Figure 5D**). This expression was detected in both HSC-NOG-hIL-6 Tg and HSC-NOG non-Tg mice.

The results imply that the human macrophages that developed in the NOG-hIL-6 Tg mice preferentially gained immunosuppressive phenotypes in the tumor.

Functions of Immunosuppressive Myeloids in HSC-NOG-hIL-6 Tg Mice

Host immune reactions against tumors, particularly T cell activation and proliferation, are suppressed by multiple mechanisms in patients with cancer. Several immunosuppressive factors, including Arg-1 or IL-10 produced from MDSCs and TAMs, are responsible for this suppression (20, 35). To investigate whether TAM-like cells differentiated in humanized mice have similar immunosuppressive functions to those in cancer patients, Arg-1 expression in $CD14^+CD68^+$ monocytes/macrophages was analyzed in the tumor, spleen, and PB of HSC-NOG-hIL-6 Tg mice or HSC-NOG non-Tg mice. Significant expression of human Arg-1 was detected in the tumor-infiltrating human monocytes/macrophages, whereas monocytes/macrophages in the spleen and PB showed modest expression (**Figure 6A**). Furthermore, reverse transcription polymerase chain reaction analysis showed hIL-10 or VEGF transcripts in human $CD11b^+$ myeloid cells, which were sorted from the HSC4 tumor in HSC-NOG-hIL-6 Tg mice (**Figure 6B**). $CD11b^+$ cells in the spleen from the same mice had no detectable amounts of IL-10 and VEGF transcripts (**Figure 6B**). Finally, to examine whether these human TAM-like cells have immunosuppressive function, the TAM-like cells were cultured with T cells *in vitro*, and the proliferation of T cells was assessed using CFSE assays. Total human $CD11b^+$ myeloid cells were purified from the tumor or spleen of HSC-NOG-hIL-6 Tg mice or HSC-NOG non-Tg mice, as we could not obtain sufficient numbers of TAM-like cells when we gated HLA-$DR^{lo/-}$ IL-$4R\alpha^+$ $CD163^+$ $CD68^+$ cells. The cells were cultured with CFSE-labeled human T cells, which were purified from the spleen from different HSC-NOG non-Tg mice in the presence of immobilized anti-CD3/CD28 antibodies. The proliferation of T cells was analyzed by flow cytometry on day 7. Proliferation of $CD8^+$ T cells was reduced in the groups that were cultured with human $CD11b^+$ cells isolated from tumors of HSC-NOG-hIL-6 Tg mice. By contrast, $CD11b^+$ cells from tumors of HSC-NOG non-Tg mice showed modest suppression. $CD11b^+$ cells from spleen of HSC-NOG-hIL-6 Tg mice or HSC-NOG non-Tg mice had no suppressive activity on human T cells, rather enhanced proliferation (**Figure 6C**).

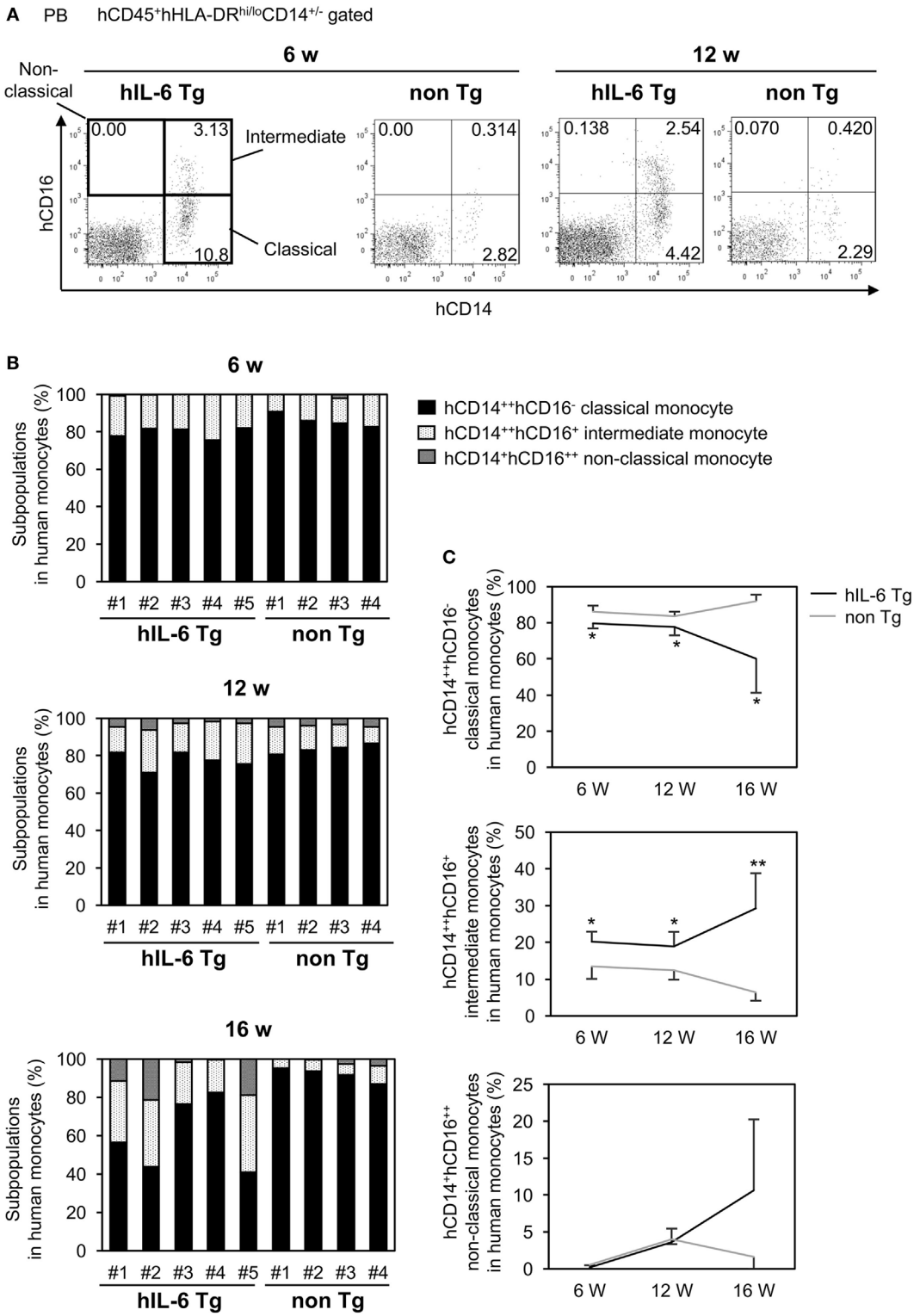

FIGURE 3 | Subpopulations in peripheral blood (PB) monocytes in HSC-NOG mice. HSC-NOG-hIL-6 Tg ($n = 6$) and HSC-NOG non-Tg mice ($n = 5$) were bled at 6, 12, and 16 weeks after HSC transplantation, and numbers of mononuclear cells (MNCs) in PB were analyzed by FACS. **(A)** FACS plots of human monocyte subpopulations. Representative data from three independent experiments are shown. **(B)** The frequencies of subpopulations ($CD14^{++}CD16^{-}$ classical monocytes, $CD14^{++}CD16^{+}$ intermediate monocytes, and $CD14^{+}CD16^{++}$ non-classical monocytes) in the human monocytes of individual mice are shown. Human monocytes were defined as previously described (32, 34). **(C)** The kinetics of classical monocytes and intermediate monocytes in HSC-NOG-hIL-6 Tg mice (black line) and HSC-NOG mice (gray line). Student's *t*-test was performed to assess statistical significance. Asterisks indicate statistical significance (**$p < 0.01$, *$p < 0.05$).

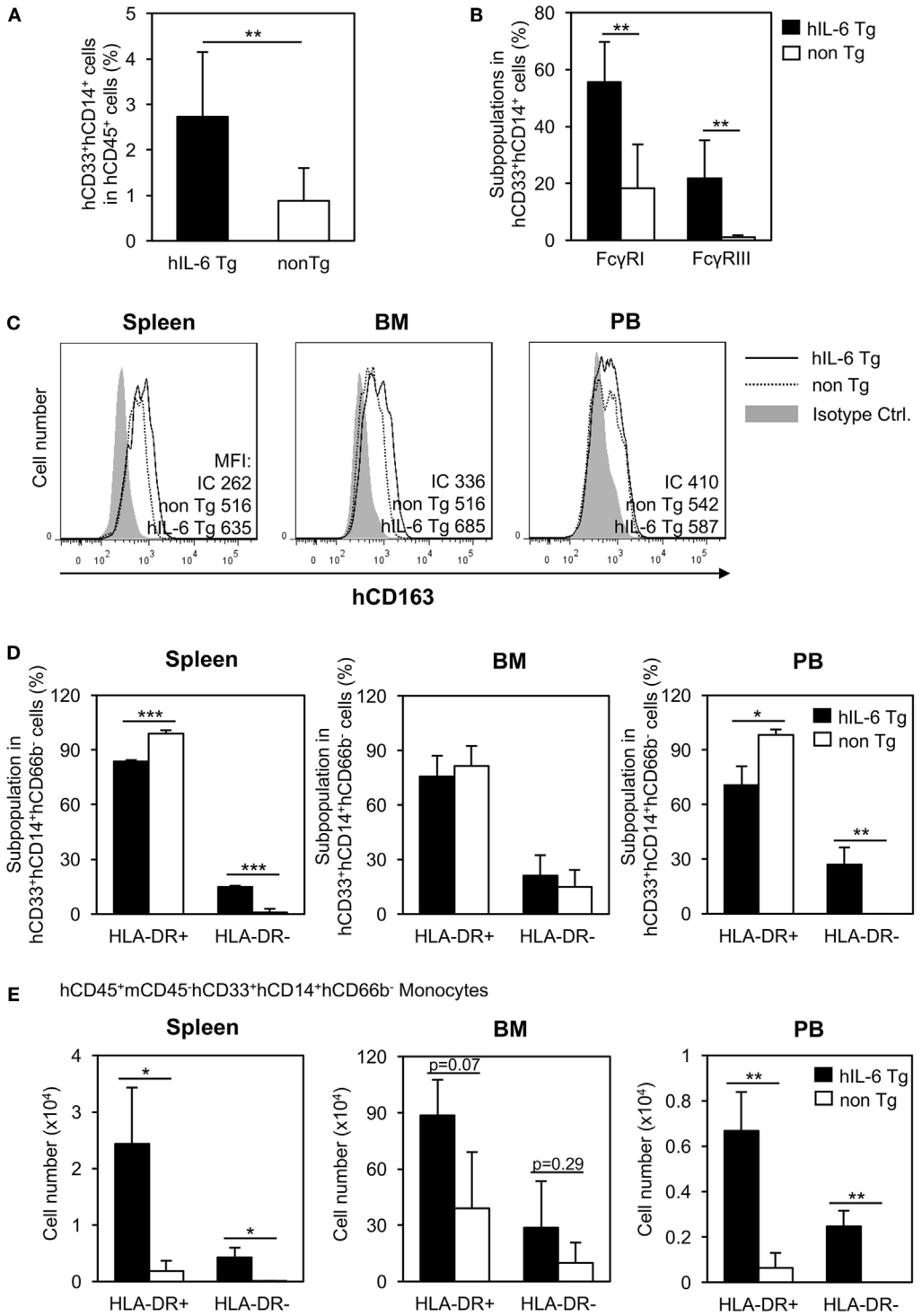

FIGURE 4 | Characterization of human monocytes/macrophages in HSC-NOG-hIL-6 Tg mice. $CD33^+CD14^+$ cells in NOG-hIL-6 Tg mice ($n = 6$) or HSC-NOG non-Tg mice ($n = 5$) were FACS analyzed at 16 to 18 weeks after HSC transplantation. **(A)** The frequency of $CD33^+CD14^+$ monocytes/macrophages in the $hCD45^+$ leukocytes is shown. An asterisk indicates the statistical significance according to the Student's *t*-test (**$p < 0.01$). **(B)** Expression of Fcγ receptors on human monocytes/macrophages. Frequencies of hFcγRI- and hFcγRIII-expressing cells in splenic $CD33^+CD14^+$ monocytes/macrophages are shown (**$p < 0.01$). **(C)** Expression of hCD163 in human monocytes/macrophages. $CD33^+CD14^+$ cells in spleen, bone marrow (BM), and peripheral blood (PB) from HSC-NOG-hIL-6 Tg mice or HSC-NOG non-Tg mice were FACS analyzed for CD163 expression at 20 weeks after HSC transfer. (Bold line: HSC-NOG-hIL-6 Tg, broken line: HSC-NOG non-Tg). **(D,E)** Development of $HLA\text{-}DR^+$ and $HLA\text{-}DR^-$ human monocytes/macrophages in HSC-NOG-hIL-6 Tg mice. HLA-DR expression in $CD33^+CD14^+$ cells in spleen, BM, and PB in HSC-NOG-hIL-6 Tg mice ($n = 3$) or HSC-NOG non-Tg mice ($n = 3$) was analyzed at 14 weeks after HSC transplantation. The frequencies **(D)** and the absolute cell number **(E)** are shown (*$p < 0.05$, **$p < 0.01$, ***$p < 0.001$).

To demonstrate their suppressive function *in vivo*, tumor progression was compared between HSC-NOG-hIL-6 Tg and HSC-NOG non-Tg mice using HSC4 cells. The tumor size was measured from days 0 to 36 after tumor engraftment. Tumor progression was enhanced in HSC-NOG-hIL-6 Tg mice compared to that in HSC-NOG non-Tg mice (**Figure 6D**).

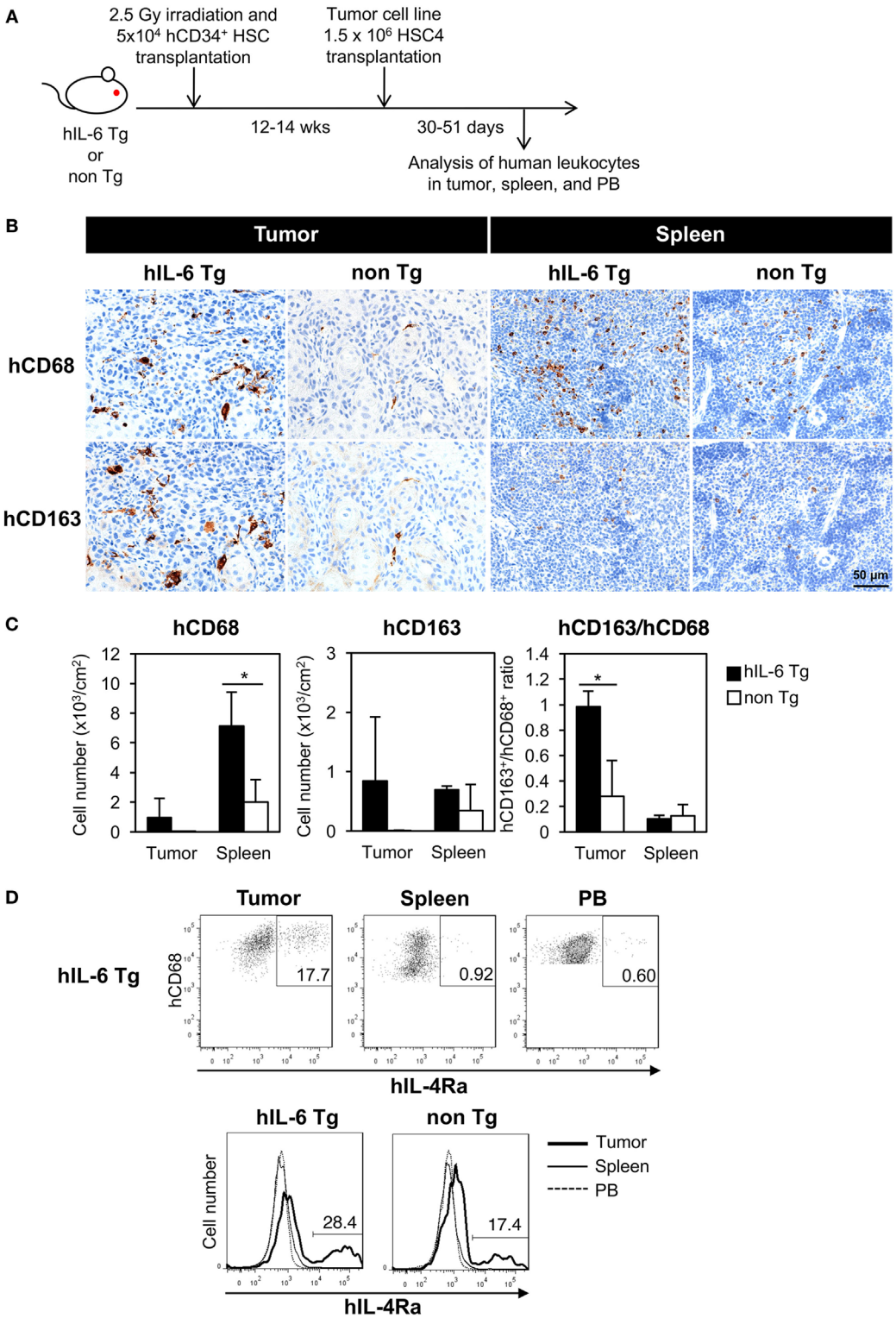

FIGURE 5 | Continued

FIGURE 5 | Development of human tumor-associated macrophages (TAMs) in tumor-engrafted HSC-NOG-hIL-6 Tg mice. **(A)** Schema of generation of tumor-bearing humanized mice. HSC-NOG-hIL-6 Tg or HSC-NOG non-Tg mice were inoculated with HSC4 (1.5×10^6) at 12–14 weeks after HSC transplantation. Human leukocytes in tumor, spleen and peripheral blood (PB) were analyzed at 30–51 days after HSC4 engraftment. **(B)** Immunohistochemistry of human macrophages in tumor and spleen. Tumor-engrafted HSC-NOG-hIL-6 Tg or HSC-NOG non-Tg mice were analyzed at 36–51 days after tumor transplantation when the tumor size reached 2,000 mm^3. Serial sections from tumor or spleen were stained with peroxidase-conjugated anti-CD68 or anti-CD163 antibodies. Each panel shows a representative image from three independent sections. **(C)** Enumeration of $CD68^+$ or $CD163^+$ macrophages. The number of signals in a whole tissue section was counted and divided by the area of the section using a BZ-9000 microscope (Keyence, Tokyo, Japan). Three independent sections were used, and the average number per unit area (cm^2) is shown. The ratio of $CD163^+$ to $CD68^+$ cells was calculated using the average numbers. An asterisk indicates statistical significance based on Student's *t*-test (*$p < 0.05$). **(D)** Expression of IL-4Rα in human macrophages. (Upper panels) FACS plots of IL-4Rα in $hCD45^+CD14^+CD68^+$ macrophages in tumor, spleen, and PB of HSC4-engrafted HSC-NOG-hIL-6 Tg. (Bottom panel) Histogram of hIL-4Rα expression in $hCD68^+$ macrophages in various tissues in HSC4-engrafted HSC-NOG-hIL-6 Tg and HSC-NOG non-Tg mice. Representative data from three experiments are shown.

DISCUSSION

We generated a novel NOG substrain, which expresses hIL-6 in a constitutive manner. We demonstrated that this strain has several intriguing features compared to the parental NOG mice, particularly under tumor-engrafted pathological conditions.

Enhanced differentiation of human monocytes/macrophages in NOG-hIL-6 Tg mice after human HSC transplantation is in line with one major activity of the IL-6 cytokine. Previous *in vitro* studies have demonstrated that the addition of anti-IL-6 receptor (IL-6R) antibody inhibits monocytic colony formation; conversely, exogenous IL-6 stimulates monocytic colony formation together with GM-CSF (44). Thus, it is probable that IL-6 in NOG-hIL-6 Tg mice stimulates monocyte differentiation in the BM. However, considering that the increase in monocytes/macrophages was greater in the periphery than in the BM in HSC-NOG-hIL-6 Tg mice (**Figure 2**), it is more likely that exogenous IL-6 promoted accumulation of human monocytes/macrophages in the periphery in HSC-NOG-hIL-6 Tg mice. Indeed, a recent study demonstrated that IL-6 and M-CSF coordinatedly promote macrophage differentiation from monocytes by regulating the expression of M-CSF receptors in the monocytes (45). Exogenous IL-6 likely regulates development of monocytes/macrophages at both the BM and peripheral levels.

Recent studies have implied a role for IL-6 in the differentiation of M1/M2 macrophages. Mauer et al. reported that IL-6 induces IL-4Rα in mouse macrophages, augmenting the IL-4-induced polarization of M2 macophages (46). However, the absence of IL-4Rα expression and the modest expression of CD163 in human monocytes/macrophages in HSC-NOG-hIL-6 Tg mice suggests that they are not always differentiated into M2 macrophages. Other cytokines such as human M-CSF might be indispensable for the polarization toward M2 lineage in humanized mouse models. Indeed, the study of Mauer et al. used bone marrow-derived macrophages, which were induced by M-CSF *in vitro* for 8–10 days. Since mouse M-CSF does not cross-react efficiently on human macrophages (data not shown), the differentiation of human macrophages in HSC-NOG-hIL-6 Tg mice may be still incomplete and fail to express IL-4Rα in response to IL-6.

An interesting phenotype of human monocytes/macrophages in NOG-hIL-6 Tg mice is that they contain a significant number of $HLA\text{-}DR^{lo/-}$ cells. Such $HLA\text{-}DR^{lo/-}$ cells were detected in the BM of both HSC-NOG-hIL-6 Tg and HSC-NOG non-Tg mice, but not in the periphery in HSC-NOG non-Tg mice. This result suggests that $HLA\text{-}DR^{lo/-}$ cells in the BM are normal immature monocytes/macrophages, whereas those in the periphery in HSC-NOG-hIL-6 Tg mice represent an unusual population. There would be two different mechanisms for the induction of $HLA\text{-}DR^{lo/-}$ cells. One is that $HLA\text{-}DR^{lo/-}$ cells in BM retained the phenotype even after migrating to the periphery. Another possibility is that $HLA\text{-}DR^+$ cells lost the expression of HLA-DR. Absence of HLA-DR is considered a marker for defining immunosuppressive myeloid cells such as TAMs or MDSCs (35). Therefore, NOG-hIL-6 Tg mice provide a unique environment that allows the spontaneous development and maintenance of immunosuppressive myeloid cells or their precursor cells, unlike mice from other strains. We previously established NOG-hGM-CSF/IL-3 Tg mice, which showed enhanced human myelopoiesis including monocytes/macrophages (13). In this model, the $HLA\text{-}DR^{lo/-}$ population was not evident (data not shown), which suggests the unique role of IL-6 in inducing $HLA\text{-}DR^{lo/-}$ monocytes/macrophages.

Tumor engraftment experiments further demonstrated distinctions between NOG-hIL-6 Tg mice and NOG non-Tg mice. Few $CD68^+$ macrophages infiltrated the tumor in HSC-NOG non-Tg mice, whereas an abundance of $CD68^+$ macrophages infiltrated the tumor in HSC-NOG-hIL-6 Tg mice. This result was likely due to the poor development of human monocytes/macrophages in HSC-NOG non-Tg mice. Our immunohistochemical analysis demonstrated that almost all of the intratumoral macrophages expressed CD163 in HSC-NOG-hIL-6 Tg mice. The strong intensity of CD163 in intratumoral macrophages compared to splenic macrophages indicates that TAM-like cells with immunosuppressive activity differentiated in the tumors of HSC-NOG-hIL-6 Tg mice. As the increase in CD163 was intratumor specific, tumor-derived stimuli were necessary for inducing the differentiation into TAM-like cells. In contrast to the prevalence of $CD163^+$ macrophages in tumor-bearing HSC-NOG-hIL-6 Tg mice, the frequency of $CD163^+$ cells in intratumoral $CD68^+$ cells was low in HSC-NOG non-Tg mice despite the small numbers of infiltrating human macrophages. This suggests that the local cytokine milieu in tumor alone is not always sufficient to induce differentiation of human macrophages into TAM-like cells. One explanation for this result is that the level of IL-6 in this tumor might be too low to induce TAM-like cells in HSC-NOG non-Tg mice. Another possibility is that systemic IL-6 in NOG-hIL-6 Tg mice predisposes human macrophages to differentiate into TAM-like cells upon exposure to stimuli from the tumor microenvironment. This notion is consistent with the accumulation of $HLA\text{-}DR^{lo/-}$ cells in tumor-free HSC-NOG-hIL-6 Tg mice. Tumor inoculation and formation of microenvironment may further induce alternations

of immunological characters in local human macrophages, resulting in the accumulation of CD163^{hi}IL-4Rα^{+} TAM-like cells in an intratumor specific manner, but not in spleen or PB.

The increase in CD163 expression levels in intratumoral TAM-like cells in HSC-NOG-hIL-6 Tg mice implies that this model is relevant to the clinical course of cancer. Accumulating evidence has suggested that not only a high frequency of CD163^{+}CD68^{+} TAMs, but also a high amount of CD163 in serum or in tumor are correlated with a poor prognosis in patients with cancer (47–49). Thus, the upregulation of CD163 in intratumoral TAM-like cells in NOG-hIL-6 Tg mice indicates that the tumor microenvironment in progressive cancer was recapitulated in this mouse model, at least in part. Importantly, induction of TAM-like cells was not HSC4-cell line specific. We have engrafted SAS and L428 with different

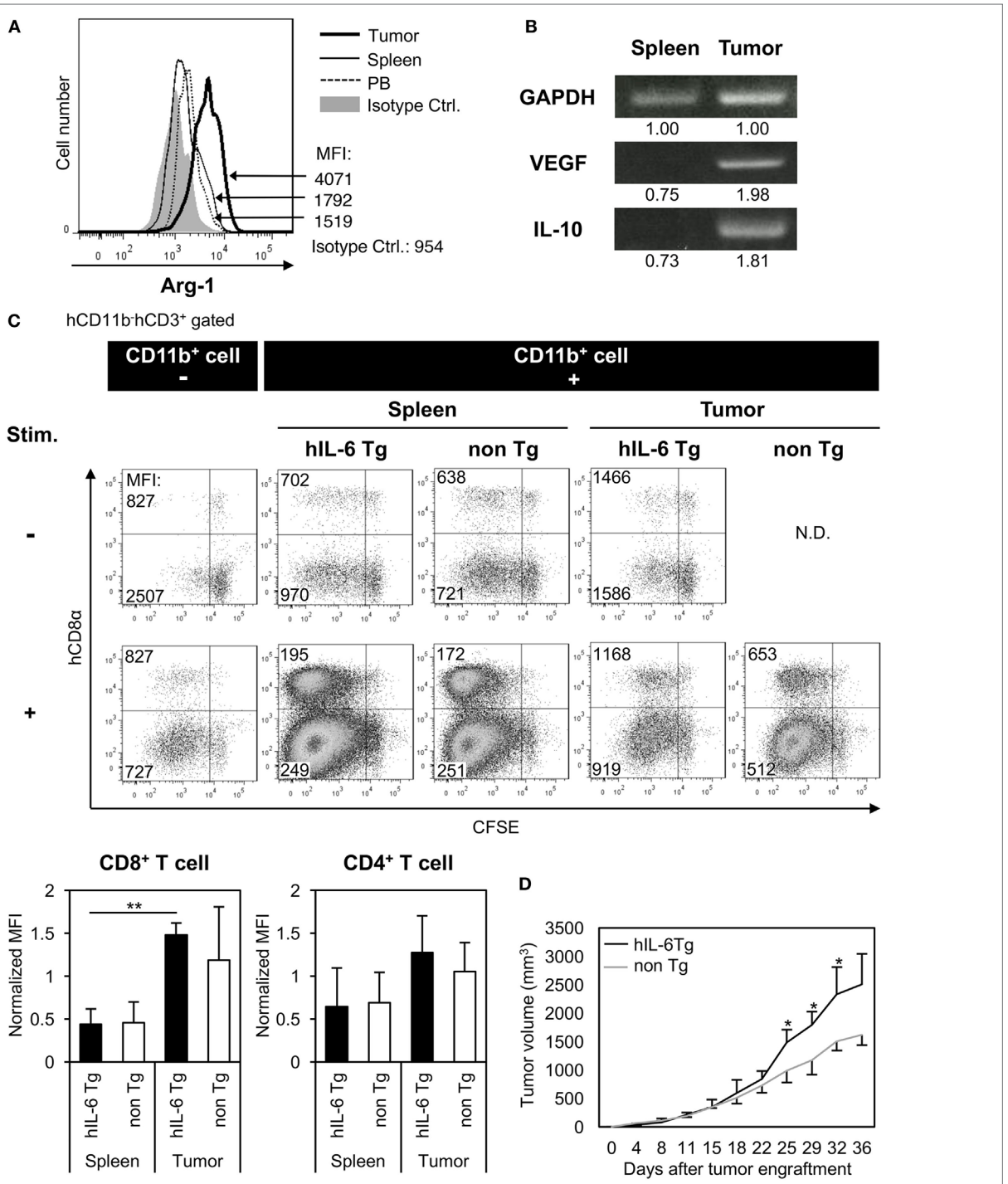

FIGURE 6 | Continued

FIGURE 6 | Immunosuppressive function of human tumor-associated macrophages (TAMs) in tumor-engrafted HSC-NOG-hIL-6 Tg mice. **(A)** Expression of human arginase-1 (Arg-1) in TAMs. Tumor-infiltrating cells and mononuclear cells (MNCs) from spleen and peripheral blood (PB), prepared from HSC4-engrafted HSC-NOG-hIL-6 Tg mice, were analyzed by intracellular staining with anti-hARG1 or isotype control. The expression of Arg-1 in $CD14^+CD68^+$ cells in tumor, spleen, and PB is shown. A representative fluorescence-activated cell sorting (FACS) plot from three independent experiments is shown. **(B)** Reverse transcription polymerase chain reaction (RT-PCR) for vascular endothelial growth factor (VEGF) and interleukin (IL)-10. $hCD45^+CD11b^+$ myeloid cells were purified from tumor and spleen in tumor-engrafted HSC-NOG-hIL-6 Tg or HSC-NOG non-Tg mice. After isolation of total RNA and synthesis of cDNA, VEGF and IL-10 were detected by PCR. The intensity of each band was measured using ImageJ software; normalized values are shown. Representative data from two independent experiments are shown. **(C)** Suppression of T cell activation by TAMs *in vitro*. $hCD45^+CD11b^+$ myeloid cells were sorted from tumor or spleen in tumor-engrafted HSC-NOG-hIL-6 Tg or HSC-NOG non-Tg mice. The cells were cultured with carboxyfluorescein succinimidyl ester (CFSE)-labeled $CD3^+$ T cells from another non-tumor engrafted HSC-NOG non-Tg mouse in a 96-well plate followed by stimulation with or without immobilized anti-CD3 and anti-CD28 antibodies. T cell proliferation was analyzed by FACS on day 7 after staining with anti-CD3 and CD8. The number in each quadrant shows the mean fluorescence intensity (MFI) value. Representative data from three independent experiments are shown. To determine the degree of suppression, the MFI value of $CD8^+$ T cells or $CD4^+$ T cells, which at least proliferated one time, in the first quadrant (left top quadrant) or in the third quadrant (left bottom quadrant), respectively, was normalized by those of T cells in a control group, which were stimulated with anti-CD3/CD28 antibodies alone without $CD11b^+$ cells. The mean ± SDs from three independent experiments are shown. Student's *t*-test was performed to analyze the statistical significance ($^{**}p < 0.01$). **(D)** Tumor growth in HSC-NOG-hIL-6 Tg or HSC-NOG non-Tg mice. HSC4 were transplanted into HSC-NOG-hIL-6 Tg mice (black, $n = 3$) or HSC-NOG non-Tg mice (gray, $n = 3$) at 14 weeks after HSC transplantation. Tumor growth was monitored over 36 days after tumor engraftment. The human $CD34^+$ HSC cells came from different donor from Figure S3 in Supplementary Material. An asterisk indicates statistical significance based on Student's *t*-test ($^*p < 0.05$).

cytokine profiles (Figure S4). An ovarian clear cell carcinoma cell line, RMG-I, was also tested. RMG-I and SAS formed tumor in NOG-hIL-6 Tg mice and flowcytometric analysis demonstrated the induction of $CD163^+$IL-4Rα^+TAM-like human myeloid cells as in HSC4-tumor (Figure S5 in Supplementary Material).

Myeloid-derived suppressor cells, another type of immunosuppressive myeloid cells, are distributed systemically in cancer patients, unlike TAMs, which localize in tumors. We examined whether MDSCs, defined as HLA-$DR^{lo/-}$ cells in monocytes gated by $CD33^+CD11b^+CD14^+CD66b^-$ (35, 50), were expanded in tumor-bearing HSC-NOG-hIL-6 Tg mice; however, we failed to detect increased numbers of HLA-$DR^{lo/-}$ cells in spleen and PB. In addition, CD163 expression was not elevated in tumor-bearing HSC-NOG-hIL-6 Tg mice (data not shown), and there were no transcripts of VEGF and IL-10 in splenic monocytes in HSC-NOG-hIL-6 Tg mice. Thus, induction of MDSC-like cells was not efficiently induced in HSC-NOG-hIL-6 Tg mice, although tumor-free HSC-NOG-hIL-6 Tg mice contained a significant number of HLA-$DR^{lo/-}$ cells. Mounting evidence has suggested that many molecules are involved in the induction of MDSCs. Although IL-6 is one of the key molecules, exogenous supplementation of other cytokines such as GM-CSF and G-CSF, or pro-imflammatory molecules like IL-1β, S100A8, and S100A9, remains necessary for efficient induction and accumulation of human MDSCs (21–24, 51). Although HSC4 produces a part of these cytokines, the amounts may be insufficient.

The expression of Arg-1, IL-10, and VEGF in intratumoral macrophages in HSC-NOG-hIL-6 Tg mice suggests similarities with TAMs in cancer patients, and that they mediate immunosuppression in tumors. *In vitro* coculture with human T cells demonstrated that they have inhibitory activity against proliferation of human T cells, especially $CD8^+$ T cells. In our experiments, we used total $CD11b^+$ cells instead of purified TAMs, as the purification of TAMs did not yield a sufficient number for the assays. Nevertheless, the inhibition of T cell activation suggests that TAM-like cells with immunosuppressive functions can be induced in tumor in HSC-NOG-hIL-6 Tg mice, even if they are not completely identical to TAMs in cancer patients. Similarities between TAM-like cells in HSC-NOG-hIL-6 Tg mice and *bona fide* TAMs should be examined in the future by gene profiling or immunophenotyping.

Given the suppression of T cell activation *in vitro* by intratumoral macrophages in HSC-NOG-hIL-6 Tg mice, we suspect that they also have suppressive activity on human T cells in tumor to prevent anti-tumor immunity. Indeed, our tumor inoculation experiments showed that tumor growth was enhanced in HSC-NOG-hIL-6 Tg mice compared to that in HSC-NOG non-Tg mice. However, this result cannot be attributed solely to the generation of human TAM-like cells in HSC-NOG-hIL-6 Tg mice. First, the number of human TAMs was not sufficient, as mentioned above. Second, many mouse myeloid cells infiltrated into the human tumor. These cells contained murine TAMs and MDSCs to support tumor growth (data not shown). Thus, elimination of tumor-infiltraing mouse cells is indispensable. Furthermore, even without human HSC transplantation, HSC4 cells grew better in NOG-hIL-6 Tg mice than in NOG non-Tg mice (Figure S6 in Supplementary Material), which was most likely due to the direct effects of hIL-6 on HSC4 cells. Hence, the use of IL-6-independent tumor cells is necessary to clarify the immunosuppressive role of TAM-like cells *in vivo*. Although we screened several human cell lines without IL-6R and gp130, all of the cell lines were positive for their expression. Developing strategies to overcome these problems will facilitate reconstitution of the tumor microenvironment with minimum interference from mouse cells.

Immunosuppressive myeloid cells have been targets for cancer immune therapy. Our NOG-hIL-6 Tg mice partly enabled reconstitution of the tumor microenvironment, which included human TAMs. Sophistication of humanized mouse technology by development of new strains with other human cytokines will recapitulate the human tumor microenvironment, not only with TAMs but also with MDSCs, in combination with NOG-hIL-6 Tg mice. These mice provide a promising tool for drug development.

ETHICS STATEMENT

All of the animal experiments were approved by the institutional animal care and use committee of the CIEA and were performed

in accordance with guidelines set forth by the CIEA (11004, 14038R). All of the experiments using human cells were approved by the institutional ethical committee of the CIEA.

AUTHOR CONTRIBUTIONS

RI established a NOG-hIL-6 Tg mouse strain. AH conducted the experiments and analysis. IK helped with the HSC transfer. KK performed the histological analysis. MG operated the embryo manipulation. YK provided the human tumor cell lines and supervised the project. HS, MI, TT, and AH designed the experiments and completed the manuscript.

ACKNOWLEDGMENTS

We thank Mika Yagoto for contributing her histology expertise, Kayo Tomiyama and Yasuhiko Ando for their work in animal production and care, and Dr. Masafumi Yamamoto for genotyping the mice. We also acknowledge our colleagues at CIEA for their suggestions and helpful discussion.

FUNDING

This project was supported by a Grant-in-Aid for Scientific Research (S) (22220007 to MI), a Grant in Aid (B) (26290034 to TT), and a Grant-in-Aid for Young Scientists (B) (JP16K18404 to AH) from the Japanese Society for the Promotion of Science (JSPS).

SUPPLEMENTARY MATERIAL

The Supplementary Material for this article can be found online at http://www.frontiersin.org/articles/10.3389/fimmu.2018.00152/full#supplementary-material.

REFERENCES

1. Ito R, Takahashi T, Katano I, Ito M. Current advances in humanized mouse models. *Cell Mol Immunol* (2012) 9:208–14. doi:10.1038/cmi.2012.2
2. Shultz LD, Brehm MA, Garcia-Martinez JV, Greiner DL. Humanized mice for immune system investigation: progress, promise and challenges. *Nat Rev Immunol* (2012) 12:786–98. doi:10.1038/nri3311
3. Denton PW, Garcia JV. Humanized mouse models of HIV infection. *AIDS Rev* (2011) 13:135–48.
4. Brehm MA, Jouvet N, Greiner DL, Shultz LD. Humanized mice for the study of infectious diseases. *Curr Opin Immunol* (2013) 25:428–35. doi:10.1016/j.coi.2013.05.012
5. Walsh NC, Kenney LL, Jangalwe S, Aryee KE, Greiner DL, Brehm MA, et al. Humanized mouse models of clinical disease. *Annu Rev Pathol* (2017) 12:187–215. doi:10.1146/annurev-pathol-052016-100332
6. Kaushansky A, Mikolajczak SA, Vignali M, Kappe SH. Of men in mice: the success and promise of humanized mouse models for human malaria parasite infections. *Cell Microbiol* (2014) 16:602–11. doi:10.1111/cmi.12277
7. Katano I, Takahashi T, Ito R, Kamisako T, Mizusawa T, Ka Y, et al. Predominant development of mature and functional human NK cells in a novel human IL-2-producing transgenic NOG mouse. *J Immunol* (2015) 194:3513–25. doi:10.4049/jimmunol.1401323
8. Sanmamed MF, Rodriguez I, Schalper KA, Onate C, Azpilikueta A, Rodriguez-Ruiz ME, et al. Nivolumab and urelumab enhance antitumor activity of human T lymphocytes engrafted in Rag2-/-IL2Rgammanull immunodeficient mice. *Cancer Res* (2015) 75:3466–78. doi:10.1158/0008-5472.CAN-14-3510
9. Holzapfel BM, Wagner F, Thibaudeau L, Levesque JP, Hutmacher DW. Concise review: humanized models of tumor immunology in the 21st century: convergence of cancer research and tissue engineering. *Stem Cells* (2015) 33:1696–704. doi:10.1002/stem.1978
10. Ito M, Hiramatsu H, Kobayashi K, Suzue K, Kawahata M, Hioki K, et al. NOD/SCID/gamma(c)(null) mouse: an excellent recipient mouse model for engraftment of human cells. *Blood* (2002) 100:3175–82. doi:10.1182/blood-2001-12-0207
11. Shultz LD, Lyons BL, Burzenski LM, Gott B, Chen X, Chaleff S, et al. Human lymphoid and myeloid cell development in NOD/LtSz-scid IL2R gamma null mice engrafted with mobilized human hemopoietic stem cells. *J Immunol* (2005) 174:6477–89. doi:10.4049/jimmunol.174.10.6477
12. Traggiai E, Chicha L, Mazzucchelli L, Bronz L, Piffaretti JC, Lanzavecchia A, et al. Development of a human adaptive immune system in cord blood cell-transplanted mice. *Science* (2004) 304:104–7. doi:10.1126/science.1093933
13. Ito R, Takahashi T, Katano I, Kawai K, Kamisako T, Ogura T, et al. Establishment of a human allergy model using human IL-3/GM-CSF-transgenic NOG mice. *J Immunol* (2013) 191:2890–9. doi:10.4049/jimmunol.1203543
14. Billerbeck E, Barry WT, Mu K, Dorner M, Rice CM, Ploss A. Development of human CD4+FoxP3+ regulatory T cells in human stem cell factor-, granulocyte-macrophage colony-stimulating factor-, and interleukin-3-expressing NOD-SCID IL2Rgamma(null) humanized mice. *Blood* (2011) 117:3076–86. doi:10.1182/blood-2010-08-301507
15. Bryce PJ, Falahati R, Kenney LL, Leung J, Bebbington C, Tomasevic N, et al. Humanized mouse model of mast cell-mediated passive cutaneous anaphylaxis and passive systemic anaphylaxis. *J Allergy Clin Immunol* (2016) 138:769–79. doi:10.1016/j.jaci.2016.01.049
16. Rongvaux A, Willinger T, Martinek J, Strowig T, Gearty SV, Teichmann LL, et al. Development and function of human innate immune cells in a humanized mouse model. *Nat Biotechnol* (2014) 32:364–72. doi:10.1038/nbt.2858
17. Kusmartsev S, Gabrilovich DI. Immature myeloid cells and cancer-associated immune suppression. *Cancer Immunol Immunother* (2002) 51:293–8. doi:10.1007/s00262-002-0280-8
18. Riabov V, Gudima A, Wang N, Mickley A, Orekhov A, Kzhyshkowska J. Role of tumor associated macrophages in tumor angiogenesis and lymphangiogenesis. *Front Physiol* (2014) 5:75. doi:10.3389/fphys.2014.00075
19. Noy R, Pollard JW. Tumor-associated macrophages: from mechanisms to therapy. *Immunity* (2014) 41:49–61. doi:10.1016/j.immuni.2014.06.010
20. Gabrilovich DI, Nagaraj S. Myeloid-derived suppressor cells as regulators of the immune system. *Nat Rev Immunol* (2009) 9:162–74. doi:10.1038/nri2506
21. Marigo I, Bosio E, Solito S, Mesa C, Fernandez A, Dolcetti L, et al. Tumor-induced tolerance and immune suppression depend on the C/EBPbeta transcription factor. *Immunity* (2010) 32:790–802. doi:10.1016/j.immuni.2010.05.010
22. Mundy-Bosse BL, Young GS, Bauer T, Binkley E, Bloomston M, Bill MA, et al. Distinct myeloid suppressor cell subsets correlate with plasma IL-6 and IL-10 and reduced interferon-alpha signaling in CD4(+) T cells from patients with GI malignancy. *Cancer Immunol Immunother* (2011) 60:1269–79. doi:10.1007/s00262-011-1029-z
23. Tsukamoto H, Nishikata R, Senju S, Nishimura Y. Myeloid-derived suppressor cells attenuate TH1 development through IL-6 production to promote tumor progression. *Cancer Immunol Res* (2013) 1:64–76. doi:10.1158/2326-6066.CIR-13-0030
24. Fang Z, Li J, Yu X, Zhang D, Ren G, Shi B, et al. Polarization of monocytic myeloid-derived suppressor cells by hepatitis B surface antigen is mediated via ERK/IL-6/STAT3 signaling feedback and restrains the activation of T cells in chronic hepatitis B virus infection. *J Immunol* (2015) 195:4873–83. doi:10.4049/jimmunol.1501362
25. Endo H, Noda H, Kinoshita N, Inui N, Nishi Y. Formation of a transplacental mutagen, 1,3-Di(4-sulfamoylphenyl)triazene, from sodium nitrite and sulfanilamide in human gastric juice and in the stomachs of hamsters. *J Natl Cancer Inst* (1980) 65:547–51.

26. Trempe GL. Human breast cancer in culture. *Recent Results Cancer Res* (1976) 57:33–41.
27. Nozawa S, Tsukazaki K, Sakayori M, Jeng CH, Iizuka R. Establishment of a human ovarian clear cell carcinoma cell line (RMG-I) and its single cell cloning – with special reference to the stem cell of the tumor. *Hum Cell* (1988) 1:426–35.
28. Tokoyoda K, Zehentmeier S, Hegazy AN, Albrecht I, Grun JR, Lohning M, et al. Professional memory CD4+ T lymphocytes preferentially reside and rest in the bone marrow. *Immunity* (2009) 30:721–30. doi:10.1016/j.immuni.2009.03.015
29. Lechner MG, Liebertz DJ, Epstein AL. Characterization of cytokine-induced myeloid-derived suppressor cells from normal human peripheral blood mononuclear cells. *J Immunol* (2010) 185:2273–84. doi:10.4049/jimmunol.1000901
30. Nakagawa M, Coleman HN, Wang X, Daniels J, Sikes J, Nagarajan UM. IL-12 secretion by Langerhans cells stimulated with *Candida* skin test reagent is mediated by dectin-1 in some healthy individuals. *Cytokine* (2014) 65:202–9. doi:10.1016/j.cyto.2013.11.002
31. Cooper MA, Fehniger TA, Caligiuri MA. The biology of human natural killer-cell subsets. *Trends Immunol* (2001) 22:633–40. doi:10.1016/S1471-4906(01)02060-9
32. Ziegler-Heitbrock L. Blood monocytes and their subsets: established features and open questions. *Front Immunol* (2015) 6:423. doi:10.3389/fimmu.2015.00423
33. Stansfield BK, Ingram DA. Clinical significance of monocyte heterogeneity. *Clin Transl Med* (2015) 4:5. doi:10.1186/s40169-014-0040-3
34. Heimbeck I, Hofer TP, Eder C, Wright AK, Frankenberger M, Marei A, et al. Standardized single-platform assay for human monocyte subpopulations: lower CD14+CD16++ monocytes in females. *Cytometry A* (2010) 77:823–30. doi:10.1002/cyto.a.20942
35. Gabrilovich DI, Ostrand-Rosenberg S, Bronte V. Coordinated regulation of myeloid cells by tumours. *Nat Rev Immunol* (2012) 12:253–68. doi:10.1038/nri3175
36. Roca H, Varsos ZS, Sud S, Craig MJ, Ying C, Pienta KJ. CCL2 and interleukin-6 promote survival of human CD11b+ peripheral blood mononuclear cells and induce M2-type macrophage polarization. *J Biol Chem* (2009) 284:34342–54. doi:10.1074/jbc.M109.042671
37. Heusinkveld M, de Vos van Steenwijk PJ, Goedemans R, Ramwadhdoebe TH, Gorter A, Welters MJ, et al. M2 macrophages induced by prostaglandin E2 and IL-6 from cervical carcinoma are switched to activated M1 macrophages by CD4+ Th1 cells. *J Immunol* (2011) 187:1157–65. doi:10.4049/jimmunol.1100889
38. Sica A, Mantovani A. Macrophage plasticity and polarization: in vivo veritas. *J Clin Invest* (2012) 122:787–95. doi:10.1172/JCI59643
39. Buechler C, Ritter M, Orso E, Langmann T, Klucken J, Schmitz G. Regulation of scavenger receptor CD163 expression in human monocytes and macrophages by pro- and antiinflammatory stimuli. *J Leukoc Biol* (2000) 67:97–103. doi:10.1002/jlb.67.1.97
40. Hogger P, Dreier J, Droste A, Buck F, Sorg C. Identification of the integral membrane protein RM3/1 on human monocytes as a glucocorticoid-inducible member of the scavenger receptor cysteine-rich family (CD163). *J Immunol* (1998) 161:1883–90.
41. Sulahian TH, Hogger P, Wahner AE, Wardwell K, Goulding NJ, Sorg C, et al. Human monocytes express CD163, which is upregulated by IL-10 and identical to p155. *Cytokine* (2000) 12:1312–21. doi:10.1006/cyto.2000.0720
42. Biswas SK, Mantovani A. Macrophage plasticity and interaction with lymphocyte subsets: cancer as a paradigm. *Nat Immunol* (2010) 11:889–96. doi:10.1038/ni.1937
43. Lacey DC, Achuthan A, Fleetwood AJ, Dinh H, Roiniotis J, Scholz GM, et al. Defining GM-CSF- and macrophage-CSF-dependent macrophage responses by in vitro models. *J Immunol* (2012) 188:5752–65. doi:10.4049/jimmunol.1103426
44. Jansen JH, Kluin-Nelemans JC, Van Damme J, Wientjens GJ, Willemze R, Fibbe WE. Interleukin 6 is a permissive factor for monocytic colony formation by human hematopoietic progenitor cells. *J Exp Med* (1992) 175:1151–4. doi:10.1084/jem.175.4.1151
45. Chomarat P, Banchereau J, Davoust J, Palucka AK. IL-6 switches the differentiation of monocytes from dendritic cells to macrophages. *Nat Immunol* (2000) 1:510–4. doi:10.1038/82763
46. Mauer J, Chaurasia B, Goldau J, Vogt MC, Ruud J, Nguyen KD, et al. Signaling by IL-6 promotes alternative activation of macrophages to limit endotoxemia and obesity-associated resistance to insulin. *Nat Immunol* (2014) 15:423–30. doi:10.1038/ni.2865
47. Fujita Y, Okamoto M, Goda H, Tano T, Nakashiro K, Sugita A, et al. Prognostic significance of interleukin-8 and CD163-positive cell-infiltration in tumor tissues in patients with oral squamous cell carcinoma. *PLoS One* (2014) 9:e110378. doi:10.1371/journal.pone.0110378
48. Yang L, Wang F, Wang L, Huang L, Wang J, Zhang B, et al. CD163+ tumor-associated macrophage is a prognostic biomarker and is associated with therapeutic effect on malignant pleural effusion of lung cancer patients. *Oncotarget* (2015) 6:10592–603. doi:10.18632/oncotarget.3547
49. Komohara Y, Niino D, Saito Y, Ohnishi K, Horlad H, Ohshima K, et al. Clinical significance of CD163(+) tumor-associated macrophages in patients with adult T-cell leukemia/lymphoma. *Cancer Sci* (2013) 104:945–51. doi:10.1111/cas.12167
50. Kotsakis A, Harasymczuk M, Schilling B, Georgoulias V, Argiris A, Whiteside TL. Myeloid-derived suppressor cell measurements in fresh and cryopreserved blood samples. *J Immunol Methods* (2012) 381:14–22. doi:10.1016/j.jim.2012.04.004
51. Condamine T, Ramachandran I, Youn JI, Gabrilovich DI. Regulation of tumor metastasis by myeloid-derived suppressor cells. *Annu Rev Med* (2015) 66:97–110. doi:10.1146/annurev-med-051013-052304

Conflict of Interest Statement: The authors declare that the research was conducted in the absence of any commercial or financial relationships that could be construed as a potential conflict of interest.

frontiers in Immunology

MINI REVIEW
published: 12 February 2018
doi: 10.3389/fimmu.2018.00238

Human γ-Herpesvirus Infection, Tumorigenesis, and Immune Control in Mice with Reconstituted Human Immune System Components

*Christian Münz**

Viral Immunobiology, Institute of Experimental Immunology, University of Zürich, Zürich, Switzerland

The human γ-herpesviruses Epstein–Barr virus (EBV or HHV4) and Kaposi sarcoma-associated herpesvirus (KSHV or HHV8) are each associated with around 2% of all tumors in humans worldwide. However, investigations into their infection, oncogenesis, and immune responses that protect from the associated tumors have been hampered by the exclusive tropism of these pathogens for humans. Mice with reconstituted human immune system components (HIS mice) provide the unique opportunity to study persistent infection, virus associated lymphoma formation, and cell-mediated immune control of EBV and KSHV. Moreover, since these pathogens are unique stimuli for cytotoxic human lymphocyte responses, they also allow us to characterize long-lasting cell-mediated immune control and the requirements for its initiation, which would also be desirable to achieve during antitumor vaccination in general. Thus, human γ-herpesvirus infection of HIS mice provides unique insights into the biology of these important human pathogens and human cell-mediated immune responses that are considered to be the main protective entity against tumors.

Keywords: Epstein–Barr virus, Kaposi sarcoma-associated herpesvirus, natural killer cells, T cells, primary effusion lymphoma, lymphoproliferative disease

OPEN ACCESS

Edited by:
Ramesh Akkina, Colorado State University, United States

Reviewed by:
Sofia A. Casares, Naval Medical Research Center, United States
Johannes S. Gach, University of California, Irvine, United States

***Correspondence:**
Christian Münz
christian.muenz@uzh.ch

Specialty section:
This article was submitted to Vaccines and Molecular Therapeutics, a section of the journal Frontiers in Immunology

Received: *21 November 2017*
Accepted: *29 January 2018*
Published: *12 February 2018*

Citation:
Münz C (2018) Human γ-Herpesvirus Infection, Tumorigenesis, and Immune Control in Mice with Reconstituted Human Immune System Components. Front. Immunol. 9:238. doi: 10.3389/fimmu.2018.00238

INTRODUCTION

The two human γ-herpesviruses Epstein–Barr virus (EBV or HHV4) and Kaposi sarcoma-associated herpesvirus (KSHV or HHV8) are WHO class I carcinogens and responsible for around 10% of the infection-associated tumors in humans (1, 2). Even so they belong to the same subfamily of herpesviruses, their penetration of the human population, oncogenicity, and tissue tropism is quite different. While EBV persistently infects more than 90% of the human adult population, KSHV seropositivity is quite rare in Europe and the USA (<10%), but approaches 50% in Africa (3). The endothelial cell-derived Kaposi sarcoma is the only malignancy that is consistently associated with KSHV alone. In addition, KSHV is found in the lymphoproliferation multicentric Castleman's disease, which can progress to non-Hodgkin's lymphoma in the minority of cases (4), and primary effusion lymphoma (PEL) which in 90% of cases also harbors EBV (5). In addition to PELs, EBV is also found in various lymphocyte and epithelial cell malignancies, including Burkitt's lymphoma, Hodgkin's lymphoma, diffuse large B cell lymphoma (DLBCL), natural killer (NK)/T cell lymphoma, nasopharyngeal carcinoma, and gastric carcinoma (5). As already suggested by the breadth of tumors that it is associated with, EBV is also the much more growth-transforming virus of the two, readily immortalizing human B cells into lymphoblastoid cell lines (LCLs) upon infection *in vitro*. Furthermore, EBV is

associated with so many different malignancies, because it adjusts its gene expression pattern to the differentiation stages of its main host cell, the human B cell, and thereby contributes to various degrees to the transformation in these different malignancies (6). The latent infection program with the largest number of expressed proteins is called latency III and is found in naïve B cells of healthy EBV carriers and DLBCL as well as LCL (7). During latency III, six nuclear proteins (EBNAs), two latent membrane proteins (LMPs), and non-translated miRNAs as well as EBERs are expressed. In latency II of Hodgkin's lymphoma and germinal center B cells of healthy EBV carriers only EBNA1, the two LMPs and the non-translated RNAs are expressed. Finally, in latency I of Burkitt's lymphoma and homeostatically dividing memory B cells, only EBNA1 and the non-translated RNAs are expressed. EBV is thought to persist in resting memory B cells without latent protein expression, only transcribing the non-translated RNAs from episomal viral DNA (8). Cognate antigen recognition by the B cell receptor is then able to reactivate EBV from this memory pool, and plasma cell differentiation is associated with lytic infectious virus production (9). Such lytic EBV infection in mucosal epithelia amplifies viral titers once more for shedding into saliva and transmission (10). In contrast to these distinct EBV infection programs, KSHV gene expression does not seem to be primarily restricted to the latency gene products latency-associated nuclear antigen, viral FLICE inhibitory protein (vFLIP), and viral D-type cyclin (vCyclin) in tumor tissues (5). Instead, expression of the lytic gene products K1, K2, and K15 seem to support the anti-apoptotic function of vFLIP to ensure survival of KSHV-associated tumor cells, which proliferate in part due to vCyclin expression (11). KSHV is thought to persist in long-lived plasma cells (12). How these patterns of viral oncogene expression are coordinated to cause KSHV- and EBV-associated pathogenesis and which immune compartments prevent them in healthy carriers of these human γ-herpesviruses has been difficult to study due to the exclusive tropism of these viruses for humans. With the advent of mice with reconstituted human immune system components (HIS mice), some of these questions can be addressed, and this review summarizes the insights into the fascinating biology of these human tumor viruses that could be gained so far.

EBV AND KSHV INFECTION

Epstein–Barr virus was one of the first pathogens that HIS mice were challenged with (13–17). All programs of EBV infection in B cells were found after intraperitoneal infection of reconstituted NOD-*scid* $\gamma_c^{-/-}$ (NSG), NOD-*scid* $\gamma_c^{truncated}$ (NOG), BALB/c Rag2$^{-/-}$ $\gamma_c^{-/-}$ (BRG), and human fetal liver plus human fetal thymus transplanted NOD-*scid* (BLT) mice, but latency III predominates (18, 19). Most of these studies found persistence of EBV in HIS mice for several months with circulating total viral loads in the blood of 10^4 and 10^3/ml in the serum after 4–5 weeks of infection with 10^5 viral particles (20, 21). At this time point, total viral loads reach 10^7 viral DNA copies/g in secondary lymphoid tissues like spleen and lymph nodes. These viral loads are comparable to blood viral loads in patients with symptomatic primary EBV infection, called infectious mononucleosis (IM) (22) that surprisingly do not differ very much from overall blood viral loads of asymptomatic primary infection (23, 24). In most of these studies, the B95-8 EBV strain was used, which reactivates only very weakly into lytic replication and was originally isolated from an American IM patient (25, 26). Indeed, in a direct comparison of wild-type (wt) and BZLF1-deficient (ZKO) EBV viruses on the B95-8 background viral titer differences were only observed at week three after infection (20). At this time point, some wt EBV-infected HIS mice reached already 10^4 DNA copies/ml in the blood, while ZKO EBV-infected mice have 10^3. These characteristics can be altered by using different viral strains for HIS mouse infection. Infection with 10^5 B cell infectious particles of the M81 EBV strain, which was isolated from a Chinese nasopharyngeal carcinoma patient, leads to 10^5–10^6 DNA copies/ml in the peripheral blood of HIS mice after 4–5 weeks of infection (27), and other EBV strains fall in between the two extremes of B95-8 and M81 (28). Thus, EBV infection with 10^5 infectious viral particles causes a primary EBV infection in HIS mice with similar viral loads that have been reported in human symptomatic and asymptomatic primary infections that can persist for months, even so many HIS mice with such high-persistent viral loads succumb to EBV-induced lymphoproliferations, as discussed below.

Kaposi sarcoma-associated herpesvirus infection of HIS mice on its own is a transient phenomenon with less than 20% of mice maintaining KSHV after infection with 10^5–10^7 infectious particles at 5 weeks post infection (29). However, repeated infections can maintain KSHV for several months in BLT mice on the NSG mouse background, as assessed by expression of KSHV gene products and KSHV-encoded GFP 2 weeks after the final inoculation (30). However, co-infection with EBV maintains KSHV in the majority of infected HIS mice of the NSG mouse background after single infection (29). During both transient and persistent KSHV infections, the virus can be found in human B cells (29, 30), and after 5 weeks of double-infection of KSHV with EBV, KSHV is primarily observed in EBV-infected B cells (29). Double-infection leads to 25% mortality of HIS mice after 5 weeks of infection, while single EBV infection causes much less pathology (29). These findings suggest that HIS mice can serve as *in vivo* infection models for both of these oncogenic γ-herpesviruses and that KSHV, surprisingly, relies on EBV for persistence in this model.

EBV AND KSHV TUMORIGENESIS

The above-discussed mortality is probably in part connected to the lymphomagenesis that can be observed in HIS mice after single EBV and EBV plus KSHV co-infection. After 5–6 weeks of infection with 10^5 infectious particles of the B95-8 EBV, 20–30% of mice develop macroscopically visible tumors in various organs, including spleen, pancreas, kidney, liver, and lymph nodes (16, 20, 21). Tumor incidence does not seem to be significantly different in EBV-infected BLT mice (18). These are EBV latency III B cell tumors, which can be grown as EBV-transformed B cell lines *in vitro* after dissociation of the visible tumors (**Figure 1**) (16, 29, 31). The ability of HIS mice to develop B cell lymphomas has been used to query the role of different latent EBV antigens and lytic EBV replication in EBV-associated lymphomagenesis. Along these lines, the nuclear antigen 3B of EBV (EBNA3B) has

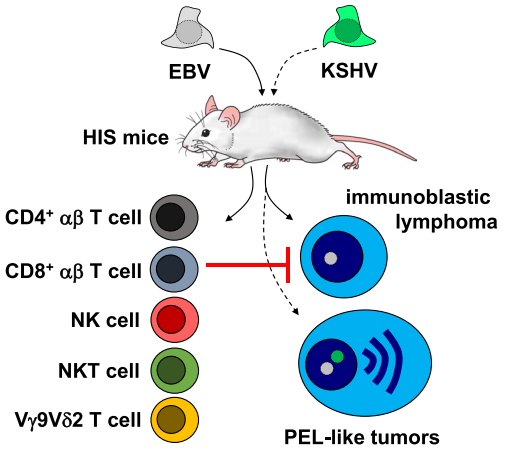

FIGURE 1 | Tumorigenesis and immune control of Epstein–Barr virus (EBV) with and without Kaposi sarcoma-associated herpesvirus (KSHV) co-infection in mice with human immune system components (HIS mice). KSHV co-infection converts EBV-induced immunoblastic lymphoma into primary effusion lymphoma (PEL)-like tumors. EBV-associated immunoblastic lymphomas are restricted by cytotoxic lymphocytes in humanized mice, including CD4⁺ and CD8⁺ T cells, natural killer (NK) cells, NKT cells, and Vγ9Vδ2 T cells.

been found to be deleted in a subset of EBV-associated DLBCLs in patients (31, 32). Accordingly, EBNA3B-deficient B95-8 EBV causes macroscopically visible tumors in 50% of HIS mice after 4 weeks of infection (31). These tumors are, interestingly, devoid of T cell infiltrates and transcriptome analysis of EBNA3B-deficient EBV-transformed B cell lines that were derived from tumors in HIS mice, and DLBCL patients demonstrated a loss of pro-inflammatory chemokine production (31). Restoration of CXCL10 expression in EBNA3A-deficient tumor cell lines resulted in T cell-mediated immune control *in vivo*. In addition, the transcriptome analysis revealed that EBNA3B-deficient EBV-transformed B cells of HIS mice were more similar to patient-derived DLBCL cell lines in their gene expression than LCLs that had been transformed with EBNA3B-deficient EBV *in vitro* (31). These findings established EBNA3B as a viral tumor suppressor by its control over pro-inflammatory chemokines.

Furthermore, it was noted that loss of lytic EBV replication decreased the ability of infection to cause lymphomagenesis (18). This at first sight counterintuitive behavior, namely that cell-destructive lytic EBV infection should benefit B cell transformation and lymphoma growth, was suggested to result from a pro-inflammatory environment upon early, possibly abortive lytic EBV replication, but the responsible pro-inflammatory components have not been identified so far. Nevertheless, decreased lymphomagenesis by the B95-8 EBV virus that lacks the immediate early lytic transactivator BZLF1 was also observed in a second study (20), and the BZLF1 overexpressing virus induced the same amount of lymphomas, but these contained up to 30% of early, but not late lytic EBV antigen expression (33), confirming a possible role of abortive lytic replication in lymphomagenesis by EBV.

In the same way, KSHV co-infection with EBV increases lytic EBV replication and EBV-associated tumorigenesis (29). Interestingly, in this first small animal *in vivo* model of KSHV persistence, the developing tumors carry KSHV in one-third of EBV-infected lymphoma cells. This leads to an upregulation of gene expression that is associated with plasma cell differentiation, including the plasma cell fingerprint that is characteristic for PELs (**Figure 1**) (34). About 39% of KSHV and EBV double-infected mice with PEL-like tumors succumb to their disease after 1 month (29), while 25% of patients with PEL succumb to tumor progression within 4 months (35). Therefore, KSHV and EBV double-infection that leads to PEL formation causes significant mortality. Interestingly, double-infection of KSHV with the lytic EBV replication-deficient BZLF1 knockout strain of B95-8 abolishes the gain of lymphomagenesis upon infection with both viruses (29). Furthermore, early and late lytic EBV gene expression were observed at higher frequencies in KSHV and EBV double-infected lymphomas of patients than in a heterogenous groups of EBV single-infected lymphomas. In good agreement, lytic EBV replication inhibition with ganciclovir caused complete sustained PEL remission in a patient with EBV and KSHV double-positive lymphoma (36), but only transient improvement in a patient with KSHV single-positive PEL (37). Thus, HIS mice infections with EBV alone and KSHV co-infection have revealed an unexpected role for lytic EBV replication during virus-associated lymphomagenesis, which might be even diagnostically useful to predict the risk of EBV-associated malignancy development during immune suppression (38).

EBV- AND KSHV-SPECIFIC IMMUNE CONTROL

Primary immunodeficiencies that predispose for EBV-associated pathologies point toward an essential role for cytotoxic lymphocytes in the immune control of this oncogenic γ-herpesvirus (39, 40). The respective mutations affect the perforin degranulation machinery, co-stimulatory receptors on cytotoxic lymphocytes and DNA binding proteins that are required for the differentiation of NK, NKT, γδT, and CD8⁺ αβ T cells. Much less is known about the protective immune responses against KSHV in humans, but the available information points to similar requirements as in the immune control of EBV (41).

Some of these cytotoxic lymphocyte compartments have been interrogated during EBV infection of HIS mice. These studies initially focused on T cell responses. In loss-of-function experiments, antibody-mediated depletion of all T cells or CD8⁺ and CD4⁺ T cells was found individually to increase EBV viral loads and associated lymphomagenesis upon infection (**Figure 1**) (16, 33, 42). Blocking of the co-stimulatory 2B4 receptor, which is compromised in one primary immunodeficiency (Duncan disease or XLP1) that predisposes for uncontrolled EBV infection, resulted in the loss of CD8⁺ T cell-mediated immune control and elevated viral loads as well as increased tumor frequency (43). In gain-of-function experiments, adoptive transfer of lytic EBV antigen-specific CD8⁺ T cells was able to further reduce the low level of lytic EBV replication upon B95-8 infection of HIS mice (20). Furthermore, late lytic EBV antigen and LCL differentiation-specific CD4⁺ T cells were able to lower viral loads in EBV-infected HIS mice (44). If human immune

system reconstitution is performed by unseparated cord blood injection rather than differentiation from human hematopoietic progenitor cells, the established T cell compartment rather supports EBV-associated lymphomagenesis, even in the absence of viral oncogenes (45, 46). These cord blood T cells provide $CD4^+$ T cell help for EBV-associated lymphomas (45). This T cell help can, however, be converted into immune control by antibody-mediated blocking of the inhibitory receptors PD-1 and CTLA-4 (47), presumably mimicking a T cell compartment that might resemble EBV-associated Hodgkin's lymphoma, a tumor entity that can be efficiently treated by check-point blockade immunotherapy (48). Thus, T cell-mediated immune control of EBV can be interrogated in HIS mice, and depending on the method of immune compartment reconstitution, immune compartments of healthy EBV carriers or patients with EBV-associated malignancies can be modeled.

In addition, innate lymphocyte compartments have also been interrogated for their contribution to immune control of EBV. NK cell depletion leads to elevated viral loads and tumor formation in EBV-infected HIS mice (**Figure 1**) (21, 49). Lytic EBV infection is primarily controlled by the early-differentiated NK cells of HIS mice, because infection with BZLF1 knockout EBV is not affected by NK cell depletion. These early-differentiated NK cells also expand in children with IM (22). It seems that further differentiated NK cells with HLA-haplotype-specific inhibitory receptors can be recruited to this response in mixed HLA-mismatched hematopoietic progenitor cell reconstitutions, which presumably allow allogeneic recognition of EBV-infected B cells of one donor by the further differentiation NK cells of the other donor (49). In addition to NK cells, adoptive transfer of $CD8^+$ NKT and Vγ9Vδ2 T cells restricts EBV-associated lymphomas in HIS mice (**Figure 1**) (50, 51). Furthermore, Vγ9Vδ2 T cell activation with phosphoantigens results in improved immune control of successive EBV infection in HIS mice (52). Interestingly, innate and adaptive lymphocyte compartments seem to compensate each other, because loss of NK cell-mediated immune control leads to enhanced $CD8^+$ T cell expansion during EBV infection of HIS mice. It will be interesting to elucidate which EBV infection programs are controlled by these different lymphocyte populations and which receptors on NK, NKT, and γδ T cells mediate EBV restriction *in vivo*. Stimulation of these cytotoxic lymphocyte compartments by vaccination could correct loss of EBV-specific immune control in patients with EBV-associated malignancies, but also teach us how to induce comprehensive cell-mediated immune control against tumors in general.

CONCLUSION AND OUTLOOK

While we are beginning to understand the protective lymphocyte compartments during EBV infection, their characterization for KSHV infection is in its infancy. Furthermore, we still have an incomplete understanding of how the comprehensive immune control by cytotoxic lymphocytes against EBV is initiated; even so, EBV is the prototypic viral pathogen that elicits $CD8^+$ T cell lymphocytosis during symptomatic infection in IM patients. A detailed understanding of the characteristics of a comprehensive immune control by cytotoxic lymphocytes and the mechanisms that lead to its priming should guide us to develop vaccines to elicit such immune control, not only against EBV in patients with associated malignancies, but also tumors or badly controlled viral infections in general.

AUTHOR CONTRIBUTIONS

The author has no financial conflicts of interest with the subject discussed in the manuscript. He has planned and written the paper.

FUNDING

The research in my laboratory is supported by Cancer Research Switzerland (KFS-4091-02-2017), SPARKS (15UOZ01), $KFSP^{MS}$, and $KFSP^{HHLD}$ of the University of Zurich, the Sobek Foundation, the Swiss Multiple Sclerosis Society, and the Swiss National Science Foundation (310030_162560 and CRSII3_160708).

REFERENCES

1. Bouvard V, Baan R, Straif K, Grosse Y, Secretan B, El Ghissassi F, et al. A review of human carcinogens – part B: biological agents. *Lancet Oncol* (2009) 10(4):321–2. doi:10.1016/S1470-2045(09)70096-8
2. Parkin DM. The global health burden of infection-associated cancers in the year 2002. *Int J Cancer* (2006) 118(12):3030–44. doi:10.1002/ijc.21731
3. Mesri EA, Cesarman E, Boshoff C. Kaposi's sarcoma and its associated herpesvirus. *Nat Rev Cancer* (2010) 10(10):707–19. doi:10.1038/nrc2888
4. Oksenhendler E, Boulanger E, Galicier L, Du MQ, Dupin N, Diss TC, et al. High incidence of Kaposi sarcoma-associated herpesvirus-related non-Hodgkin lymphoma in patients with HIV infection and multicentric Castleman disease. *Blood* (2002) 99(7):2331–6. doi:10.1182/blood.V99.7.2331
5. Cesarman E. Gammaherpesviruses and lymphoproliferative disorders. *Annu Rev Pathol* (2014) 9:349–72. doi:10.1146/annurev-pathol-012513-104656
6. Thorley-Lawson DA, Gross A. Persistence of the Epstein-Barr virus and the origins of associated lymphomas. *N Engl J Med* (2004) 350(13):1328–37. doi:10.1056/NEJMra032015
7. Babcock JG, Hochberg D, Thorley-Lawson AD. The expression pattern of Epstein-Barr virus latent genes in vivo is dependent upon the differentiation stage of the infected B cell. *Immunity* (2000) 13(4):497–506. doi:10.1016/S1074-7613(00)00049-2
8. Babcock GJ, Decker LL, Volk M, Thorley-Lawson DA. EBV persistence in memory B cells in vivo. *Immunity* (1998) 9(3):395–404. doi:10.1016/S1074-7613(00)80622-6
9. Laichalk LL, Thorley-Lawson DA. Terminal differentiation into plasma cells initiates the replicative cycle of Epstein-Barr virus in vivo. *J Virol* (2005) 79(2):1296–307. doi:10.1128/JVI.79.2.1296-1307.2005
10. Hutt-Fletcher LM. The long and complicated relationship between Epstein-Barr virus and epithelial cells. *J Virol* (2017) 91(1):e01677-16. doi:10.1128/JVI.01677-16
11. Martin DF, Kuppermann BD, Wolitz RA, Palestine AG, Li H, Robinson CA. Oral ganciclovir for patients with cytomegalovirus retinitis treated with a ganciclovir implant. Roche Ganciclovir Study Group. *N Engl J Med* (1999) 340(14):1063–70. doi:10.1056/NEJM199904083401402
12. Ganem D. KSHV infection and the pathogenesis of Kaposi's sarcoma. *Annu Rev Pathol* (2006) 1:273–96. doi:10.1146/annurev.pathol.1.110304.100133
13. Traggiai E, Chicha L, Mazzucchelli L, Bronz L, Piffaretti JC, Lanzavecchia A, et al. Development of a human adaptive immune system in cord blood cell-transplanted mice. *Science* (2004) 304(5667):104–7. doi:10.1126/science.1093933

14. Melkus MW, Estes JD, Padgett-Thomas A, Gatlin J, Denton PW, Othieno FA, et al. Humanized mice mount specific adaptive and innate immune responses to EBV and TSST-1. *Nat Med* (2006) 12(11):1316–22. doi:10.1038/nm1431
15. Yajima M, Imadome K, Nakagawa A, Watanabe S, Terashima K, Nakamura H, et al. A new humanized mouse model of Epstein-Barr virus infection that reproduces persistent infection, lymphoproliferative disorder, and cell-mediated and humoral immune responses. *J Infect Dis* (2008) 198(5): 673–82. doi:10.1086/590502
16. Strowig T, Gurer C, Ploss A, Liu YF, Arrey F, Sashihara J, et al. Priming of protective T cell responses against virus-induced tumors in mice with human immune system components. *J Exp Med* (2009) 206(6):1423–34. doi:10.1084/jem.20081720
17. Shultz LD, Saito Y, Najima Y, Tanaka S, Ochi T, Tomizawa M, et al. Generation of functional human T-cell subsets with HLA-restricted immune responses in HLA class I expressing NOD/SCID/IL2r gamma^{null} humanized mice. *Proc Natl Acad Sci U S A* (2010) 107(29):13022–7. doi:10.1073/pnas.1000475107
18. Ma SD, Hegde S, Young KH, Sullivan R, Rajesh D, Zhou Y, et al. A new model of Epstein-Barr virus infection reveals an important role for early lytic viral protein expression in the development of lymphomas. *J Virol* (2011) 85(1):165–77. doi:10.1128/JVI.01512-10
19. Cocco M, Bellan C, Tussiwand R, Corti D, Traggiai E, Lazzi S, et al. CD34$^+$ cord blood cell-transplanted Rag2$^{-/-}$ gamma$_c^{-/-}$ mice as a model for Epstein-Barr virus infection. *Am J Pathol* (2008) 173(5):1369–78. doi:10.2353/ajpath.2008.071186
20. Antsiferova O, Müller A, Rämer P, Chijioke O, Chatterjee B, Raykova A, et al. Adoptive transfer of EBV specific CD8$^+$ T cell clones can transiently control EBV infection in humanized mice. *PLoS Pathog* (2014) 10(8):e1004333. doi:10.1371/journal.ppat.1004333
21. Chijioke O, Muller A, Feederle R, Barros MH, Krieg C, Emmel V, et al. Human natural killer cells prevent infectious mononucleosis features by targeting lytic Epstein-Barr virus infection. *Cell Rep* (2013) 5(6):1489–98. doi:10.1016/j.celrep.2013.11.041
22. Azzi T, Lunemann A, Murer A, Ueda S, Beziat V, Malmberg KJ, et al. Role for early-differentiated natural killer cells in infectious mononucleosis. *Blood* (2014) 124(16):2533–43. doi:10.1182/blood-2014-01-553024
23. Jayasooriya S, de Silva TI, Njie-jobe J, Sanyang C, Leese AM, Bell AI, et al. Early virological and immunological events in asymptomatic Epstein-Barr virus infection in African children. *PLoS Pathog* (2015) 11(3):e1004746. doi:10.1371/journal.ppat.1004746
24. Abbott RJ, Pachnio A, Pedroza-Pacheco I, Leese AM, Begum J, Long HM, et al. Asymptomatic primary infection with Epstein-Barr virus: observations on young adult cases. *J Virol* (2017) 91(21):e00382-17. doi:10.1128/JVI.00382-17.
25. Miller G, Lipman M. Release of infectious Epstein-Barr virus by transformed marmoset leukocytes. *Proc Natl Acad Sci U S A* (1973) 70(1):190–4. doi:10.1073/pnas.70.1.190
26. Miller G, Lipman M. Comparison of the yield of infectious virus from clones of human and simian lymphoblastoid lines transformed by Epstein-Barr virus. *J Exp Med* (1973) 138(6):1398–412. doi:10.1084/jem.138.6.1398
27. Tsai MH, Raykova A, Klinke O, Bernhardt K, Gartner K, Leung CS, et al. Spontaneous lytic replication and epitheliotropism define an Epstein-Barr virus strain found in carcinomas. *Cell Rep* (2013) 5(2):458–70. doi:10.1016/j.celrep.2013.09.012
28. Tsai MH, Lin X, Shumilov A, Bernhardt K, Feederle R, Poirey R, et al. The biological properties of different Epstein-Barr virus strains explain their association with various types of cancers. *Oncotarget* (2017) 8(6):10238–54. doi:10.18632/oncotarget.14380
29. McHugh D, Caduff N, Barros MHM, Rämer P, Raykova A, Murer A, et al. Persistent KSHV infection increases EBV-associated tumor formation in vivo via enhanced EBV lytic gene expression. *Cell Host Microbe* (2017) 22(1):61–73. doi:10.1016/j.chom.2017.06.009
30. Wang LX, Kang G, Kumar P, Lu W, Li Y, Zhou Y, et al. Humanized-BLT mouse model of Kaposi's sarcoma-associated herpesvirus infection. *Proc Natl Acad Sci U S A* (2014) 111(8):3146–51. doi:10.1073/pnas.1318175111
31. White RE, Ramer PC, Naresh KN, Meixlsperger S, Pinaud L, Rooney C, et al. EBNA3B-deficient EBV promotes B cell lymphomagenesis in humanized mice and is found in human tumors. *J Clin Invest* (2012) 122(4):1487–502. doi:10.1172/JCI58092
32. Gottschalk S, Ng CY, Perez M, Smith CA, Sample C, Brenner MK, et al. An Epstein-Barr virus deletion mutant associated with fatal lymphoproliferative disease unresponsive to therapy with virus-specific CTLs. *Blood* (2001) 97(4):835–43. doi:10.1182/blood.V97.4.835
33. Ma SD, Yu X, Mertz JE, Gumperz JE, Reinheim E, Zhou Y, et al. An Epstein-Barr virus (EBV) mutant with enhanced BZLF1 expression causes lymphomas with abortive lytic EBV infection in a humanized mouse model. *J Virol* (2012) 86(15):7976–87. doi:10.1128/JVI.00770-12
34. Klein U, Gloghini A, Gaidano G, Chadburn A, Cesarman E, Dalla-Favera R, et al. Gene expression profile analysis of AIDS-related primary effusion lymphoma (PEL) suggests a plasmablastic derivation and identifies PEL-specific transcripts. *Blood* (2003) 101(10):4115–21. doi:10.1182/blood-2002-10-3090
35. El-Fattah MA. Clinical characteristics and survival outcome of primary effusion lymphoma: a review of 105 patients. *Hematol Oncol* (2017) 35(4):878–83. doi:10.1002/hon.2372
36. Pereira R, Carvalho J, Patricio C, Farinha P. Sustained complete remission of primary effusion lymphoma with adjunctive ganciclovir treatment in an HIV-positive patient. *BMJ Case Rep* (2014) 2014:bcr2014204533. doi:10.1136/bcr-2014-204533
37. Ozbalak M, Tokatli I, Ozdemirli M, Tecimer T, Ar MC, Ornek S, et al. Is valganciclovir really effective in primary effusion lymphoma: case report of an HIV$^-$ EBV$^-$ HHV8$^+$ patient. *Eur J Haematol* (2013) 91(5):467–9. doi:10.1111/ejh.12174
38. Kanakry J, Ambinder R. The biology and clinical utility of EBV monitoring in blood. *Curr Top Microbiol Immunol* (2015) 391:475–99. doi:10.1007/978-3-319-22834-1_17
39. Cohen JI. Primary immunodeficiencies associated with EBV disease. *Curr Top Microbiol Immunol* (2015) 390(Pt 1):241–65. doi:10.1007/978-3-319-22822-8_10
40. Tangye SG, Palendira U, Edwards ES. Human immunity against EBV-lessons from the clinic. *J Exp Med* (2017) 214(2):269–83. doi:10.1084/jem.20161846
41. Pasic S, Cupic M, Lazarevic I. HHV-8-related hemophagocytic lymphohistiocytosis in a boy with XLP phenotype. *J Pediatr Hematol Oncol* (2012) 34(6):467–71. doi:10.1097/MPH.0b013e3182375372
42. Yajima M, Imadome K, Nakagawa A, Watanabe S, Terashima K, Nakamura H, et al. T cell-mediated control of Epstein-Barr virus infection in humanized mice. *J Infect Dis* (2009) 200(10):1611–5. doi:10.1086/644644
43. Chijioke O, Marcenaro E, Moretta A, Capaul R, Munz C. The SAP-dependent 2B4 receptor mediates CD8$^+$ T cell dependent immune control of Epstein Barr virus infection in mice with reconstituted human immune system components. *J Infect Dis* (2015) 212(5):803–7. doi:10.1093/infdis/jiv114
44. Linnerbauer S, Behrends U, Adhikary D, Witter K, Bornkamm GW, Mautner J. Virus and autoantigen-specific CD4$^+$ T cells are key effectors in a SCID mouse model of EBV-associated post-transplant lymphoproliferative disorders. *PLoS Pathog* (2014) 10(5):e1004068. doi:10.1371/journal.ppat.1004068
45. Ma SD, Xu X, Plowshay J, Ranheim EA, Burlingham WJ, Jensen JL, et al. LMP1-deficient Epstein-Barr virus mutant requires T cells for lymphomagenesis. *J Clin Invest* (2015) 125(1):304–15. doi:10.1172/JCI76357
46. Ma SD, Tsai MH, Romero-Masters JC, Ranheim EA, Huebner SM, Bristol J, et al. LMP1 and LMP2A collaborate to promote Epstein-Barr virus (EBV)-induced B cell lymphomas in a cord blood-humanized mouse model but are not essential. *J Virol* (2017) 91(7):e01928-16. doi:10.1128/JVI.01928-16
47. Ma SD, Xu X, Jones R, Delecluse HJ, Zumwalde NA, Sharma A, et al. PD-1/CTLA-4 blockade inhibits Epstein-Barr virus-induced lymphoma growth in a cord blood humanized-mouse model. *PLoS Pathog* (2016) 12(5):e1005642. doi:10.1371/journal.ppat.1005642
48. Ansell SM, Lesokhin AM, Borrello I, Halwani A, Scott EC, Gutierrez M, et al. PD-1 blockade with nivolumab in relapsed or refractory Hodgkin's lymphoma. *N Engl J Med* (2015) 372(4):311–9. doi:10.1056/NEJMoa1411087
49. Landtwing V, Raykova A, Pezzino G, Beziat V, Marcenaro E, Graf C, et al. Cognate HLA absence in trans diminishes human NK cell education. *J Clin Invest* (2016) 126(10):3772–82. doi:10.1172/JCI86923
50. Yuling H, Ruijing X, Li L, Xiang J, Rui Z, Yujuan W, et al. EBV-induced human CD8$^+$ NKT cells suppress tumorigenesis by EBV-associated malignancies. *Cancer Res* (2009) 69(20):7935–44. doi:10.1158/0008-5472.CAN-09-0828
51. Zumwalde NA, Sharma A, Xu X, Ma S, Schneider CL, Romero-Masters JC, et al. Adoptively transferred Vgamma9Vdelta2 T cells show potent antitumor effects in a preclinical B cell lymphomagenesis model. *JCI Insight* (2017) 2(13): e93179. doi:10.1172/jci.insight.93179
52. Xiang Z, Liu Y, Zheng J, Liu M, Lv A, Gao Y, et al. Targeted activation of human Vgamma9Vdelta2-T cells controls Epstein-Barr virus-induced B cell

lymphoproliferative disease. *Cancer Cell* (2014) 26(4):565–76. doi:10.1016/j.ccr.2014.07.026

Conflict of Interest Statement: The author declares that the research was conducted in the absence of any commercial or financial relationships that could be construed as a potential conflict of interest.

frontiers in Immunology

MINI REVIEW
published: 05 March 2018
doi: 10.3389/fimmu.2018.00344

Ultra-Sensitive HIV-1 Latency Viral Outgrowth Assays Using Humanized Mice

*Kimberly Schmitt and Ramesh Akkina**

Department of Microbiology, Immunology and Pathology, Colorado State University, Fort Collins, CO, United States

In the current quest for a complete cure for HIV/AIDS, highly sensitive HIV-1 latency detection methods are critical to verify full viral eradication. Until now, the *in vitro* quantitative viral outgrowth assays (qVOA) have been the gold standard for assessing latent HIV-1 viral burden. However, these assays have been inadequate in detecting the presence of ultralow levels of latent virus in a number of patients who were initially thought to have been cured, but eventually showed viral rebound. In this context, new approaches utilizing *in vivo* mouse-based VOAs are promising. In the murine VOA (mVOA), large numbers of $CD4^+$ T cells or PBMC from aviremic subjects are xenografted into immunodeficient NSG mice, whereas in the humanized mouse-based VOA (hmVOA) patient $CD4^+$ T cell samples are injected into BLT or hu-hematopoetic stem cells (hu-HSC) humanized mice. While latent virus could be recovered in both of these systems, the hmVOA provides higher sensitivity than the mVOA using a fewer number of input cells. In contrast to the mVOA, the hmVOA provides a broader spectrum of highly susceptible HIV-1 target cells and enables newly engrafted cells to home into preformed human lymphoid organs where they can infect cells *in situ* after viral activation. Hu-mice also allow for both xenograft- and allograft-driven cell expansions with less severe GvH providing a longer time frame for potential viral outgrowth from cells with a delayed latent viral activation. Based on these advantages, the hmVOA has great potential in playing an important role in HIV-1 latency and cure research.

Keywords: HIV-1 latent viral outgrowth assay using humanized mice, humanized mouse-based HIV-1 latency outgrowth assay, comparison of quantitative viral outgrowth assays with humanized mouse-based viral outgrowth assay, comparison of mVOA with humanized mouse-based viral outgrowth assay, non-human primate-based latent simian immunodeficiency viral outgrowth assay, sensitivity of humanized mouse-based viral outgrowth assay over mVOA, ultra-sensitive HIV-1 latent viral outgrowth assay in hu-mice, mouse-based HIV-1 viral outgrowth assays

OPEN ACCESS

Edited by:
Jeffrey K. Actor, University of Texas Health Science Center at Houston, United States

Reviewed by:
Mangala Rao, United States Military HIV Research Program, United States
James Di Santo, Institut Pasteur, France

***Correspondence:**
Ramesh Akkina
akkina@colostate.edu

Specialty section:
This article was submitted to Vaccines and Molecular Therapeutics, a section of the journal Frontiers in Immunology

Received: *14 December 2017*
Accepted: *07 February 2018*
Published: *05 March 2018*

Citation:
Schmitt K and Akkina R (2018) Ultra-Sensitive HIV-1 Latency Viral Outgrowth Assays Using Humanized Mice. Front. Immunol. 9:344. doi: 10.3389/fimmu.2018.00344

INTRODUCTION

Since the beginning of the deadly HIV/AIDS epidemic, major research emphasis has been placed on developing effective vaccines for prevention and potent drugs to control the infection. Since HIV-1 is a retrovirus which integrates into the host cell genome and can establish viral latency, a complete cure was thought not to be possible until the case of the "Berlin patient" (1, 2). This HIV-1+ patient had undergone allogenic bone marrow (BM) transplantation from a homozygous *CCR5Δ32* donor to treat acute myeloid leukemia. No HIV-1 could be detected during later years in this individual even after extensive testing thus confirming his HIV-1 negative status and a complete cure. Following this example additional cases of possible HIV-1 cure generated excitement.

Two individuals known as the "Boston patients," (A and B) underwent allogeneic hematopoietic stem cell transplant (HSCT), in this case with wild-type CCR5+ donor cells to treat lymphoma (3). For 4.3 years after the transplant both patients were treated with ART (4). During this time no proviral DNA or replication-competent virus could be detected in PBMC, plasma or rectal tissues by using the most sensitive methods including the gold standard quantitative viral outgrowth assays (qVOA)(3, 4). After the cessation of ART however, virus rebounded within patient A by 12 weeks and patient B by 32 weeks (5). In the case of the "Mississippi baby," ART was started 30 h after birth and continued for the first 18 months of life (6). After the cessation of ART, the "Mississippi baby" controlled viremia for 2 years and was antibody negative (7). No HIV-1 could be detected with PCR tests or qVOA using 22 million resting $CD4^+$ T cells (6, 7), which led to the speculation that she could be another example of a complete HIV-1 cure. However, the virus eventually rebounded. Both of these cases exemplified "potential cures," wherein all the tests including the gold standard qVOA (see below) could not detect the ultralow levels of latently infected cells thus necessitating the search for more sensitive HIV-1 latency detection methods.

Current Assays for Measuring the Latent Viral Reservoir and Limitations

Since the latent HIV-1 is transcriptionally silent and the minuscule number of latently infected cells (0.1–10 infectious units per million (IUPM) resting $CD4^+$ T cells) are distributed over difficult to reach anatomical sites measuring the quiescent viral reservoir poses challenges (8–12). Many sensitive viral DNA, RNA or protein detection methods are currently employed to determine the viral burden (13). However, they overestimate the reservoir size as they cannot distinguish between the defective viral genomes and replication-competent virus. More recent advanced assays could simultaneously assess viral RNA, proteins and cell markers enabling the detection of viral induced cells (14–18). However, limitations remain to distinguish and accurately measure the true replication-competent latent virus.

The most accurate approach in determining the full efficacy of HIV-1 cure strategies is analytic treatment interruption (ATI) also known as monitored antiretroviral pause. However, this is impractical for routine application and poses unnecessary risk. The long-standing qVOA is considered as the "gold standard" in the HIV-1 latency field to measure the replication-competent virus and employs a co-culturing method to amplify the induced virus from rare latent cells (19–21). Serial dilution of test cells allows for quantitation, expressed as IUPM (22). Besides being time-consuming, a major drawback with this method is its tendency to underestimate the viral reservoir size since not all latent cells are induced during the assay period (23). New versions of the qVOA have been developed that use reporter cells and/or cell lines to amplify the virus with significantly increased sensitivity in a shorter time-span (13–17, 24, 25). Importantly, the stochastic aspect observed during *in vitro* viral activation wherein repeated stimulation of cells over time results in release of virus from previously non-responding cells (23) suggesting that approaches such as the *in vivo* methods described below that allow for long-term viral outgrowth may capture these late responder cells.

Non-Human Primate (NHP) Models of Latency Detection

Many aspects of HIV-1 pathogenesis and latent reservoirs distributed in different anatomical sites are difficult to directly assess if not impossible to study in a human subject. In this context, the simian immunodeficiency (SIV)-macaque model of AIDS has been extremely useful in gathering relevant data on viral persistence and latency (26–28). In NHP studies, latent virus was successfully recovered from naïve macaques that underwent adoptive transfer of resting $CD4^+$ T cells obtained from virally suppressed SIV-infected macaques (as determined by all standard tests) undergoing intensive ART (29). These findings showed that ultralow levels of otherwise undetectable latently infected cells could be induced and detected with an *in vivo* system using adoptive transfer of test cells. More recently, Avalos et al. assessed viral persistence in brain macrophages of five ART-suppressed SIV-infected pig-tailed macaques using a newly developed macrophage quantitative viral outgrowth assay (Mϕ-VOA) (30). In one macaque, latency reversing agents (LRAs) ingenol-B (protein kinase C agonist) and vorinostat (HDAC inhibitor) reactivated latent viral genomes that were genetically distinct from virus circulating in the plasma. This data demonstrated the utility of the Mϕ-VOA for latency detection in macrophages.

Non-Humanized Mouse Models for Latent Viral Outgrowth (mVOA)

Immunodeficient mice permit the transplantation of human cells such as PBMCs without rejection which led to the development of the hu-PBL-SCID mouse model (31, 32). Infection of these mice with HIV-1 gives rise to viremia and the engraftment of PBMC from HIV-1+ subjects resulted in viral outgrowth. With this as a background, Metcaf Pate et al. recently developed a latent HIV-1 murine viral out growth assay (mVOA) (**Figure 1**) (33). The mVOA assay is based on the principle that engrafted human cells undergo xenograft-mediated expansion leading to consequent latent viral induction. Immunodeficient NSG mice were injected with large number of cells (66 million PBMC or 10–26 million resting $CD4^+$ T cells) from 11 HIV-1+ subjects, including six elite controllers. All of these samples had undetectable viral loads by qRT-PCR (<50 copies/mL) but were positive for viral outgrowth by qVOA except for one elite controller. The engrafted mice were treated with anti-CD8 antibody to deplete the human $CD8^+$ T cells and with anti-CD3/CD28 antibodies for the activation of T cells. Viral outgrowth was detected in all 11 patient samples in these mice, including the one elite controller negative for viral outgrowth in the qVOA. This study also evaluated latent cells from ART-suppressed SIV-infected pig-tailed macaques. NSG mice were injected with 40 million PBMC or 6.8 million resting $CD4^+$ T cells. All inoculated mice had detectable SIV RNA in the plasma after 7 days.

Another recent mVOA study evaluated cells from two HIV-1 infected subjects enrolled in a PrEP program who were treated soon after infection (participants A and B treated within 10 and

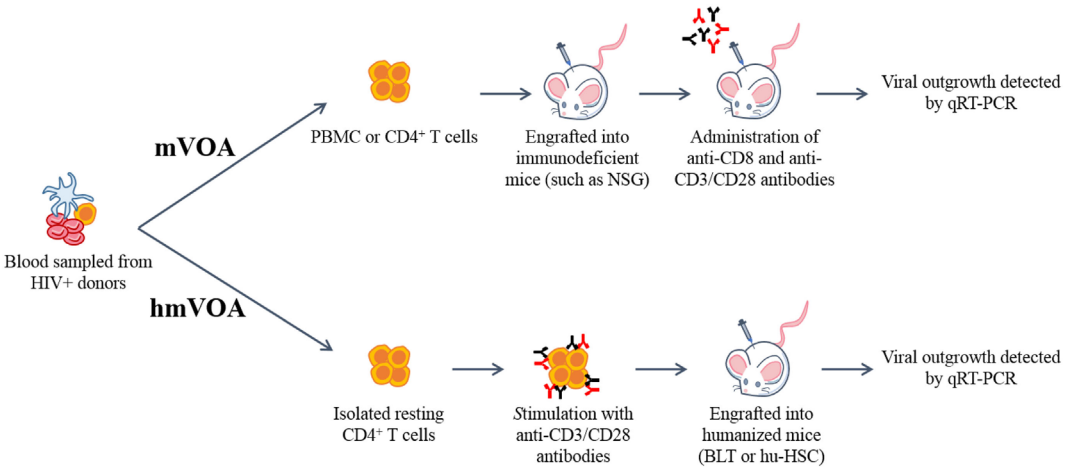

FIGURE 1 | Schematic representation of the murine (mVOA) and humanized mouse-based viral outgrowth assay (hmVOA) for HIV-1. Previously frozen unfractionated PBMC or isolated resting CD4+ T cells obtained from HIV-1 infected donors on ART with undetectable viral loads were used for both the mVOA and hmVOA. In the mVOA, cells were either clonally expanded or directly xenografted into immunodeficient mice (such as NSG). CD8+ T cells were depleted and T cell activation was prolonged using anti-CD3/CD28 antibodies *in vivo*. In the hmVOA, resting CD4+ T cells were purified using PBMC and stimulated with anti-CD3/CD28 antibodies. Stimulated cells were xenografted into either hu-HSC or BLT mice. Viral outgrowth was detected by qRT-PCR.

12 days, respectively) (34). During the following 2-year period, participant A had undetectable HIV RNA and/or DNA in both the blood and tissue whereas participant B showed a low level of intermittent HIV RNA and/or DNA in various CD4+ T cell subsets, but not in tissue samples. The qVOA results were negative. To test these patients' cells for latent viral detection by mVOA, 530 million peripheral CD4+ T cells from participant A (53 million per mouse, 10 mice total) and 379 million cells from participant B (50 million per mouse, eight mice total), were injected intraperitoneally into NSG mice. Approximately 5.5 weeks post-inoculation, mice were treated with anti-CD3 antibody to stimulate T cells *in vivo* and reactivate latent virus. One out of ten mice injected with CD4+ T cells from participant A became borderline positive (201 copies per ml) at only one time point. Terminal mouse spleen tissue sample was negative for viral detection and both RNA and DNA sequencing efforts for viral identification by an independent laboratory were unsuccessful. In contrast, three out of eight mice injected with CD4+ T cells from participant B became strongly virus positive with high viral loads (1,000, 5,000 and 11,000 copies per ml). While the sample sizes of the qVOA negative subjects are small in the above two studies, it is apparent that the mVOA could recover latent virus to a certain extent (2 out of 3 samples).

In a different twist to the mVOA, Yuan et al. utilized cells from a single aviremic subject which were positive for viral outgrowth by *in vitro* qVOA (0.518 IUPM) (35). First, the subject's CD4+ T cells were clonally expanded *in vitro* and then split into two groups: qVOA negative or positive. NSG mice were then injected with resting or clonally expanded CD4+ T cells from each group. The clonally expanded cells that appeared qVOA positive and used to inoculate mice displayed detectable HIV-1 within 4 weeks while the qVOA negative cells used to inject mice became positive by week 10. Utilization of split portions of clonally expanded cells with a potentially uneven distribution of qVOA positive cells in the test samples, sample size of a single patient and lack of details on how many mice were used are limitations of this study.

In a recent report by Salgado et al., CD4+ T cells isolated from four HIV-1+ subjects that underwent allogenic BM stem cell transplantation to treat hematalogic malignancies were evaluated for the presence of any residual latent virus (36). Five immunodeficient NSG mice per each donor were xenografted with 10–50 million cells to detect possible viral outgrowth. However, none of these xenografted mice showed positive viral outgrowth by week 13. Since it is unlikely that these four individuals are fully cured based on previous examples like the "Boston patients," and mVOA was not able to recover any latent virus from these, caution needs to be exercised about the reliability of mVOA for ultra-sensitive latency detection.

Several other limitations also exist for mVOA in its current form (**Table 1**). These include variable levels of donor cell engraftment, the need for CD8+ T cell depletion through injection of anti-CD8 antibodies and the administration of anti-CD3/CD28 antibodies for prolonged T cell activation. Most importantly, since a very large number of donor cells are xenografted, rapid GvH is a major drawback often resulting in untimely/unpredictable loss of engrafted mice thus not permitting longer assay periods to allow for the detection of delayed latent virus outgrowth.

Humanized Mouse Model-Based Latent Viral Outgrowth Assay (hmVOA)

New generation humanized mouse models have now become integral tools in many aspects of HIV research. The advent of highly immunodeficient mice incorporating the IL-2 receptor common gamma chain (IL2Rγc) mutation together with others, such as SCID, NOD, RAG1, or RAG2 gene mutations permitted far superior human tissue/cell engraftment (31, 37). Among these are the Rag1 $^{-/-}\gamma c^{-/-}$, Rag2$^{-/-}\gamma c^{-/-}$, NOD/Shi-scid/$\gamma c^{-/-}$ null (NOG),

TABLE 1 | The advantages and disadvantages of the mVOA and humanized mouse VOA (hmVOA) for HIV-1 latency detection.

Model	Methods	Advantages	Disadvantages
mVOA	Large number of human PBMC or CD4+ T cells are xenografted into NSG mice followed by the administration of anti-CD8 and anti-CD3/CD28 antibodies	• Straightforward inoculation of donor cells into NSG mice • Larger number of cells can be assayed compared to the *in vitro* quantitative viral outgrowth assays (qVOA) • Can be used to assess either HIV-1+ or SIV+ donor samples	• Rapid onset of GvH, thus limiting the assay's time table • Variable levels of donor cell engraftment • Additional anti-CD8 and anti-CD3/CD28 antibody injections are needed
hmVOA	Resting CD4+ T cells are xenografted into humanized mice	• Broader spectrum of HIV-1 target cells are available • Engrafted cells home into a preexisting lymphoid system • Allows for both xeno- and allograft-mediated stimulation and cell expansion • Less severe (BLT mice) or no GvH (hu-HSC mice) • No additional antibody (anti-CD8 and anti-CD3/CD28 antibody) injections required • Larger number of cells than the qVOA can be assayed and fewer number of cells required than the mVOA	• Human hematopoetic stem cells (HSC) and tissues are required to prepare the humanized mice • More expensive

NOD/SCIDγc$^{-/-}$ (NSG), NOD.Rag1KO.IL2RγcKO (DRAG), and NOD.HLA-A2.HLA-DR4.RagKO.IL2RγcKO (DRAGA) (38, 39). Two current leading hu-mouse models are the hu-HSC and BLT mice. Hu-HSC mice are prepared by intrahepatic injection of CD34+ HSC into irradiated newborn RAG1, RAG2, NSG or NOG mice (40–43). Engraftment of these mice seeds the BM and gives rise to *de novo* multilineage human hematopoiesis. BLT mice are prepared by surgical implantation of human fetal liver and thymic tissue under the kidney capsule in addition to reconstitution with autologous HSC (40, 42, 44, 45). In both these models, there is *de novo* production of human T cells, B cells, monocytes/macrophages, dendritic cells and NK cells, as well as successful mucosal compartment engraftment (40–42, 45). While both the models permit human immune responses, the presence of an autologous human thymus in BLT mice allows for human T cell education and HLA restricted responses (40, 42–47). Thus, these hu-mice offer an excellent *in vivo* system for the engraftment and long-term maintenance of exogenous latently infected cells and potential outgrowth of the latent virus from these. Another potentially suitable hu-mouse model currently available employs HLA class II (DR4) transgenic mice (DRAG mice) reconstituted with HLA-matched HSC (38, 39).

In a recent study, we systematically evaluated humanized mice for developing an ultra-sensitive latent viral detection system (**Figure 1**) (48). First, resting CD4+ T cells from HIV-1+ subjects on ART with low, but detectable plasma HIV-1 RNA levels were tested by *in vitro* qVOA to measure the extent of the latent viral reservoir. These samples were positive for viral outgrowth showing a broad range of IUPM levels from 0.102 to 4.468. The CD4+ T cells either unstimulated or stimulated *in vitro* with PHA or anti-CD3/CD28 antibodies were injected into humanized mice. Positive viral outgrowth was observed in all of these samples within 1–3 weeks demonstrating the capacity of hu-mice to detect latently infected cells. In some of the patient samples, viral outgrowth was seen with a lesser number of input cells than in the standard qVOA. Stimulation of cells was found to give better viral outgrowth than no stimulation and anti-CD3/CD28 antibody stimulation yielded higher numbers of viable cells for testing compared to that of PHA. To determine if the hmVOA is more sensitive than conventional qVOA, five patient samples that were qVOA negative were tested using a range of CD4+ T cells (2–10 million cells/mouse) injected into mice. Of the five qVOA negative patient samples evaluated, four yielded unequivocal positive viral outgrowth in the hmVOA. The earliest time point of viral detection was 2 weeks, whereas the latest time point was 6 weeks. The negative sample did not show any viral outgrowth by 8 weeks, the last time point tested. These observations showed that the hmVOA can detect replication-competent latent HIV-1 when the standard qVOA is unable to do so thus demonstrating the higher sensitivity of this assay. The higher sensitivity of hmVOA over than the *in vitro* qVOA could be attributed to the provision of a more physiological *in vivo* setting for long-term maintenance and expansion of the engrafted cells permitting latency reactivation when compared to the short-term culture of 2 weeks employed *in vitro*.

Advantages of the hmVOA over the mVOA for Detecting Latent HIV-1

The hmVOA is endowed with higher sensitivity over the mVOA since it was able to detect latent HIV-1 from a higher number of qVOA negative samples and with a fewer number of input cells based on the data published so far (33–36, 48) (**Table 1**). The higher sensitivity of the hmVOA is likely due to the humanized mice being able to provide more optimal conditions for latent viral outgrowth for several reasons. First, hu-mice generate fresh human HIV-1 targets cells *de novo* (CD4+ T cells, monocytes/macrophages, and dendritic cells), including the highly susceptible immature thymocytes thus providing a much broader spectrum of susceptible cells conducive for virus outgrowth. Second, the latently infected cells have the opportunity to home into preformed human lymphoid organs where they can infect cells *in situ* after activation and amplifying the viral signal. Third, hu-mice provide an environment for both xenograft- and allograft-driven cell expansions. Fourth, GvH is almost non-existent in hu-HSC mice and less severe, occurring later in onset, with the BLT mice thus providing a longer time frame (2–3 months) for viral outgrowth. Furthermore, compared to mVOA, no expensive

anti-CD8 or anti-CD3 antibody injections are needed after donor cell engraftment.

Limitations of mVOA and hmVOA and Future Prospects

As discussed above, the *in vivo* mouse-based VOA assays are more sensitive than *in vitro* qVOAs in detecting low levels of HIV-1 latent cells with the hmVOA being the most sensitive. However, these are limitations for these assays to be of wider use. They are not capable of a high-throughput screening, require special animal facilities and are expensive. Nevertheless, due to their higher sensitivity than any *in vitro* tests, they will play an important role in viral latency studies and in "kick/shock and kill" approaches toward a complete cure for HIV/AIDS. These tests will be of utmost benefit *in lieu* of ATI in guiding future curative drug development. Further improvements can be foreseen in the hmVOA and mVOA models with additional research. One approach would be to increase the sensitivity by using HIV-1 LRAs either alone or in various combinations. Thus far, the hmVOA has primarily focused on HIV-1 latency in $CD4^+$ T cells. With the recent attention on viral latency in other cell types such as macrophages and work done with SIV latency detection, it is apparent that hmVOA can also be put to good use in evaluating viral outgrowth from HIV-1 latent macrophages as well. Streamlining the hu-mouse generation on a larger scale with increased efficiency should help reduce the overall costs of hmVOA permitting its wider application.

AUTHOR CONTRIBUTIONS

Both KS and RA contributed equally in writing and editing this manuscript.

ACKNOWLEDGMENTS

We would like to thank Laurén Kinner-Bibeau for generating artwork in **Figure 1**.

FUNDING

Work on hmVOA research in RA's laboratory is supported by NIH, USA grant RO1 AI120021.

REFERENCES

1. Archin NM, Liberty AL, Kashuba AD, Choudhary SK, Kuruc JD, Crooks AM, et al. Administration of vorinostat disrupts HIV-1 latency in patients on antiretroviral therapy. *Nature* (2012) 487:482–5. doi:10.1038/nature11286
2. Krim M, Johnston R. AIDS: the final chapter? *AIDS Res Hum Retroviruses* (2014) 30:5–7. doi:10.1089/aid.2013.1503
3. Henrich TJ, Hu Z, Li JZ, Sciaranghella G, Busch MP, Keating SM, et al. Long-term reduction in peripheral blood HIV type 1 reservoirs following reduced-intensity conditioning allogeneic stem cell transplantation. *J Infect Dis* (2013) 207:1694–702. doi:10.1093/infdis/jit086
4. Henrich TJ, Hanhauser E, Sirignano M, Davis B, Lee TH, Keating S, et al. In depth investigation of peripheral and gut HIV-1 reservoirs, HIV-1 specific cellular immunity, and host microchimerism following allogeneic hematopoetic stem cell transplantation. *7th IAS Conference on HIV Pathogenesis, Treatment and Prevention*. Kuala Lumpur, Malaysia (2013).
5. Hyden EC. Hopes for HIV cure in 'Boston patients' dashed. *Nat News* (2013). doi:10.1038/nature.2013.14324
6. Persaud D, Gay H, Ziemniak C, Chen YH, Piatak M Jr, Chun TW, et al. Absence of detectable HIV-1 viremia after treatment cessation in an infant. *N Engl J Med* (2013) 369:1828–35. doi:10.1056/NEJMoa1302976
7. Shah SK, Persaud D, Wendler DS, Taylor HA, Gay H, Kruger M, et al. Research on very early ART in neonates at risk of HIV infection. *Lancet Infect Dis* (2014) 14:797. doi:10.1016/S1473-3099(14)70893-X
8. Bailey JR, Sedaghat AR, Kieffer T, Brennan T, Lee PK, Wind-Rotolo M, et al. Residual human immunodeficiency virus type 1 viremia in some patients on antiretroviral therapy is dominated by a small number of invariant clones rarely found in circulating CD4+ T cells. *J Virol* (2006) 80:6441–57. doi:10.1128/JVI.00591-06
9. Finzi D, Blankson J, Siliciano JD, Margolick JB, Chadwick K, Pierson T, et al. Latent infection of CD4+ T cells provides a mechanism for lifelong persistence of HIV-1, even in patients on effective combination therapy. *Nat Med* (1999) 5:512–7. doi:10.1038/8394
10. Siliciano JD, Kajdas J, Finzi D, Quinn TC, Chadwick K, Margolick JB, et al. Long-term follow-up studies confirm the stability of the latent reservoir for HIV-1 in resting CD4+ T cells. *Nat Med* (2003) 9:727–8. doi:10.1038/nm880
11. Bruner KM, Hosmane NN, Siliciano RF. Towards an HIV-1 cure: measuring the latent reservoir. *Trends Microbiol* (2015) 23:192–203. doi:10.1016/j.tim.2015.01.013
12. Eriksson S, Graf EH, Dahl V, Strain MC, Yukl SA, Lysenko ES, et al. Comparative analysis of measures of viral reservoirs in HIV-1 eradication studies. *PLoS Pathog* (2013) 9:e1003174. doi:10.1371/journal.ppat.1003174
13. Henrich TJ, Deeks SG, Pillai SK. Measuring the size of the latent human immunodeficiency virus reservoir: the present and future of evaluating eradication strategies. *J Infect Dis* (2017) 215:S134–41. doi:10.1093/infdis/jiw648
14. Prasad VR, Kalpana GV. FISHing out the hidden enemy: advances in detecting and measuring latent HIV-infected cells. *MBio* (2017) 8:e1433–1417. doi:10.1128/mBio.01433-17
15. Baxter AE, Niessl J, Fromentin R, Richard J, Porichis F, Charlebois R, et al. Single-cell characterization of viral translation-competent reservoirs in HIV-infected individuals. *Cell Host Microbe* (2016) 20:368–80. doi:10.1016/j.chom.2016.07.015
16. Martrus G, Niehrs A, Cornelis R, Rechtien A, Garcia-Beltran W, Lutgehetmann M, et al. Kinetics of HIV-1 latency reversal quantified on the single-cell level using a novel flow-based technique. *J Virol* (2016) 90:9018–28. doi:10.1128/JVI.01448-16
17. Grau-Exposito J, Serra-Peinado C, Miguel L, Navarro J, Curran A, Burgos J, et al. A novel single-cell FISH-flow assay identifies effector memory CD4(+) T cells as a Major Niche for HIV-1 transcription in HIV-infected patients. *MBio* (2017) 8:e01433-17. doi:10.1128/mBio.00876-17
18. Descours B, Petitjean G, Lopez-Zaragoza JL, Bruel T, Raffel R, Psomas C, et al. CD32a is a marker of a CD4 T-cell HIV reservoir harbouring replication-competent proviruses. *Nature* (2017) 543:564–7. doi:10.1038/nature21710
19. Chun TW, Carruth L, Finzi D, Shen X, DiGiuseppe JA, Taylor H, et al. Quantification of latent tissue reservoirs and total body viral load in HIV-1 infection. *Nature* (1997) 387:183–8. doi:10.1038/387183a0
20. Siliciano JD, Siliciano RF. Enhanced culture assay for detection and quantitation of latently infected, resting CD4+ T-cells carrying replication-competent virus in HIV-1-infected individuals. *Methods Mol Biol* (2005) 304:3–15. doi:10.1385/1-59259-907-9:003
21. Laird GM, Eisele EE, Rabi SA, Lai J, Chioma S, Blankson JN, et al. Rapid quantification of the latent reservoir for HIV-1 using a viral outgrowth assay. *PLoS Pathog* (2013) 9:e1003398. doi:10.1371/journal.ppat.1003398
22. Rosenbloom DI, Elliott O, Hill AL, Henrich TJ, Siliciano JM, Siliciano RF. Designing and interpreting limiting dilution assays: general principles and applications to the latent reservoir for human immunodeficiency virus-1. *Open Forum Infect Dis* (2015) 2:ofv123. doi:10.1093/ofid/ofv123

23. Ho YC, Shan L, Hosmane NN, Wang J, Laskey SB, Rosenbloom DI, et al. Replication-competent noninduced proviruses in the latent reservoir increase barrier to HIV-1 cure. *Cell* (2013) 155:540–51. doi:10.1016/j.cell.2013.09.020
24. Sanyal A, Mailliard RB, Rinaldo CR, Ratner D, Ding M, Chen Y, et al. Novel assay reveals a large, inducible, replication-competent HIV-1 reservoir in resting CD4(+) T cells. *Nat Med* (2017) 23:885–9. doi:10.1038/nm.4347
25. Fun A, Mok HP, Wills MR, Lever AM. A highly reproducible quantitative viral outgrowth assay for the measurement of the replication-competent latent HIV-1 reservoir. *Sci Rep* (2017) 7:43231. doi:10.1038/srep43231
26. Whitney JB, Hill AL, Sanisetty S, Penaloza-MacMaster P, Liu J, Shetty M, et al. Rapid seeding of the viral reservoir prior to SIV viraemia in rhesus monkeys. *Nature* (2014) 512:74–7. doi:10.1038/nature13594
27. Dinoso JB, Rabi SA, Blankson JN, Gama L, JL Mankowski, Siliciano RF, et al. A simian immunodeficiency virus-infected macaque model to study viral reservoirs that persist during highly active antiretroviral therapy. *J Virol* (2009) 83:9247–57. doi:10.1128/JVI.00840-09
28. Policicchio BB, Pandrea I, Apetrei C. Animal models for HIV cure research. *Front Immunol* (2016) 7:12. doi:10.3389/fimmu.2016.00012
29. Okoye A. *Early Antiretroviral Therapy Limits Viral Reservoir in SIV-Infected Macaques, in NIH Meeting: Strategies for an HIV Cure*. Besthesda, MD (2014).
30. Avalos CR, Abreu CM, Queen SE, Li M, Price S, Shirk EN, et al. Brain macrophages in simian immunodeficiency virus-infected, antiretroviral-suppressed macaques: a functional latent reservoir. *MBio* (2017) 8(4):e1186–1117. doi:10.1128/mBio.01186-17
31. Shultz LD, Brehm MA, Bavari S, Greiner DL. Humanized mice as a preclinical tool for infectious disease and biomedical research. *Ann N Y Acad Sci* (2011) 1245:50–4. doi:10.1111/j.1749-6632.2011.06310.x
32. Mosier DE. Viral pathogenesis in hu-PBL-SCID mice. *Semin Immunol* (1996) 8:255–62. doi:10.1006/smim.1996.0032
33. Metcalf Pate KA, Pohlmeyer CW, Walker-Sperling VE, Foote JB, Najarro KM, Cryer CG, et al. A murine viral outgrowth assay to detect residual HIV type 1 in patients with undetectable viral loads. *J Infect Dis* (2015) 212:1387–96. doi:10.1093/infdis/jiv230
34. Henrich TJ, Hatano H, Bacon O, Hogan LE, Rutishauser R, Hill A, et al. HIV-1 persistence following extremely early initiation of antiretroviral therapy (ART) during acute HIV-1 infection: an observational study. *PLoS Med* (2017) 14:e1002417. doi:10.1371/journal.pmed.1002417
35. Yuan Z, Kang G, Lu W, Li Q. Reactivation of HIV-1 proviruses in immune-compromised mice engrafted with human VOA-negative CD4+ T cells. *J Virus Erad* (2017) 3:61–5.
36. Salgado M, Kwon M, Galvez C, Nijuis M, Vilaplana C, Bandera A, et al., editors. Murine model to predict viral rebound in HIV-1+ allotransplanted subjects. *Conference on Retroviruses and Opportunistic Infections (CROI)*. Seattle, WA (2017).
37. Berges BK, Rowan MR. The utility of the new generation of humanized mice to study HIV-1 infection: transmission, prevention, pathogenesis, and treatment. *Retrovirology* (2011) 8:65. doi:10.1186/1742-4690-8-65
38. Akkina R, Allam A, Balazs AB, Blankson JN, Burnett JC, Casares S, et al. Improvements and limitations of humanized mouse models for HIV research: NIH/NIAID "Meet the Experts" 2015 Workshop Summary. *AIDS Res Hum Retroviruses* (2016) 32(2):109–19. doi:10.1089/AID.2015.0258
39. Allam A, Majji S, Peachman K, Jagodzinski L, Kim J, Ratto-Kim S, et al. TFH cells accumulate in mucosal tissues of humanized-DRAG mice and are highly permissive to HIV-1. *Sci Rep* (2015) 5:10443. doi:10.1038/srep10443
40. Akkina R. New generation humanized mice for virus research: comparative aspects and future prospects. *Virology* (2013) 435:14–28. doi:10.1016/j.virol.2012.10.007
41. Ito R, Takahashi T, Katano I, Ito M. Current advances in humanized mouse models. *Cell Mol Immunol* (2012) 9:208–14. doi:10.1038/cmi.2012.2
42. Traggiai E, Chicha L, Mazzucchelli L, Bronz L, Piffaretti JC, Lanzavecchia A, et al. Development of a human adaptive immune system in cord blood cell-transplanted mice. *Science* (2004) 304:104–7. doi:10.1126/science.1093933
43. Lan P, Tonomura N, Shimizu A, Wang S, Yang YG. Reconstitution of a functional human immune system in immunodeficient mice through combined human fetal thymus/liver and CD34+ cell transplantation. *Blood* (2006) 108:487–92. doi:10.1182/blood-2005-11-4388
44. Shultz LD, Brehm MA, Garcia-Martinez JV, Greiner DL. Humanized mice for immune system investigation: progress, promise and challenges. *Nat Rev Immunol* (2012) 12:786–98. doi:10.1038/nri3311
45. Wege AK, Melkus MW, Denton PW, Estes JD, Garcia JV. Functional and phenotypic characterization of the humanized BLT mouse model. *Curr Top Microbiol Immunol* (2008) 324:149–65. doi:10.1007/978-3-540-75647-7
46. Melkus MW, Estes JD, Padgett-Thomas A, Gatlin J, Denton PW, Othieno FA, et al. Humanized mice mount specific adaptive and innate immune responses to EBV and TSST-1. *Nat Med* (2006) 12:1316–22. doi:10.1038/nm1431
47. Seung E, Tager AM. Humoral immunity in humanized mice: a work in progress. *J Infect Dis* (2013) 208(Suppl 2):S155–9. doi:10.1093/infdis/jit448
48. Charlins P, Schmitt K, Remling-Mulder L, Hogan LE, Hanhauser E, Hobbs KS, et al. A humanized mouse-based HIV-1 viral outgrowth assay with higher sensitivity than in vitro qVOA in detecting latently infected cells from individuals on ART with undetectable viral loads. *Virology* (2017) 507:135–9. doi:10.1016/j.virol.2017.04.011

Conflict of Interest Statement: The authors declare that the research was conducted in the absence of any commercial or financial relationships that could be construed as a potential conflict of interest.

frontiers in Immunology

METHODS
published: 14 March 2018
doi: 10.3389/fimmu.2018.00524

Plasmodium falciparum Liver Stage Infection and Transition to Stable Blood Stage Infection in Liver-Humanized and Blood-Humanized FRGN KO Mice Enables Testing of Blood Stage Inhibitory Antibodies (Reticulocyte-Binding Protein Homolog 5) *In Vivo*

Lander Foquet[1†], Carola Schafer[1†], Nana K. Minkah[1], Daniel G. W. Alanine[2], Erika L. Flannery[1], Ryan W. J. Steel[1], Brandon K. Sack[1], Nelly Camargo[1], Matthew Fishbaugher[1], Will Betz[1], Thao Nguyen[1], Zachary P. Billman[3,4], Elizabeth M. Wilson[5], John Bial[5], Sean C. Murphy[3,4], Simon J. Draper[2], Sebastian A. Mikolajczak[1] and Stefan H. I. Kappe[1,6]*

[1] Center for Infectious Disease Research, Seattle, WA, United States, [2] Jenner Institute, University of Oxford, Oxford, United Kingdom, [3] Department of Laboratory Medicine, University of Washington, Seattle, WA, United States, [4] Department of Microbiology, University of Washington, Seattle, WA, United States, [5] Yecuris Corporation, Tualatin, OR, United States, [6] Department of Global Health, University of Washington, Seattle, WA, United States

The invention of liver-humanized mouse models has made it possible to directly study the preerythrocytic stages of *Plasmodium falciparum.* In contrast, the current models to directly study blood stage infection *in vivo* are extremely limited. Humanization of the mouse blood stream is achievable by frequent injections of human red blood cells (hRBCs) and is currently the only system with which to study human malaria blood stage infections in a small animal model. Infections have been primarily achieved by direct injection of *P. falciparum*-infected RBCs but as such, this modality of infection does not model the natural route of infection by mosquito bite and lacks the transition of parasites from liver stage infection to blood stage infection. Including these life cycle transition points in a small animal model is of relevance for testing therapeutic interventions. To this end, we used FRGN KO mice that were engrafted with human hepatocytes and performed a blood exchange under immune modulation to engraft the animals with more than 50% hRBCs. These mice were infected by mosquito bite with sporozoite stages of a luciferase-expressing *P. falciparum* parasite, resulting in noninvasively measurable liver stage burden by *in vivo* bioluminescent imaging (IVIS) at days 5–7 postinfection. Transition to blood stage infection was observed by IVIS from day 8 onward and then blood stage parasitemia increased with a kinetic similar to that observed in controlled human malaria infection. To assess the utility of this model, we tested whether a monoclonal antibody targeting the erythrocyte invasion ligand reticulocyte-binding protein homolog 5 (with known growth inhibitory activity *in vitro*) was capable of blocking blood stage infection *in vivo* when parasites emerge from the liver and found it highly effective.

OPEN ACCESS

Edited by:
Moriya Tsuji, Aaron Diamond AIDS Research Center, United States

Reviewed by:
Scherf Artur, Institut Pasteur, France
James B. Burns Jr., Drexel University, United States

***Correspondence:**
Stefan H. I. Kappe
stefan.kappe@cidresearch.org

[†]These authors have contributed equally to this work.

Specialty section:
This article was submitted to Vaccines and Molecular Therapeutics, a section of the journal Frontiers in Immunology

Received: *11 January 2018*
Accepted: *28 February 2018*
Published: *14 March 2018*

Citation:
Foquet L, Schafer C, Minkah NK, Alanine DGW, Flannery EL, Steel RWJ, Sack BK, Camargo N, Fishbaugher M, Betz W, Nguyen T, Billman ZP, Wilson EM, Bial J, Murphy SC, Draper SJ, Mikolajczak SA and Kappe SHI (2018) Plasmodium falciparum Liver Stage Infection and Transition to Stable Blood Stage Infection in Liver-Humanized and Blood-Humanized FRGN KO Mice Enables Testing of Blood Stage Inhibitory Antibodies (Reticulocyte-Binding Protein Homolog 5) In Vivo. Front. Immunol. 9:524. doi: 10.3389/fimmu.2018.00524

Together, these results show that a combined liver-humanized and blood-humanized FRGN mouse model infected with luciferase-expressing *P. falciparum* will be a useful tool to study *P. falciparum* preerythrocytic and erythrocytic stages and enables the testing of interventions that target either one or both stages of parasite infection.

Keywords: *Plasmodium falciparum*, humanized mouse model, *Plasmodium falciparum* blood stages, reticulocyte-binding protein homolog 5, clodronate liposomes, cyclophosphamide

INTRODUCTION

More than 200 million clinical cases of malaria are reported each year, with children under the age of 5 being particularly susceptible to illness and death. *Plasmodium falciparum* is the most lethal human malaria parasite (WHO World Malaria Report 2016) and continued discovery and development of interventions against it is necessitated by the occurrence of drug resistance and the lack of an effective vaccine. Transmission of *Plasmodium* parasites occurs by the bite of infected female *Anopheles* mosquitoes, which inject motile sporozoites into the skin where they traverse endothelial cells to enter the bloodstream and travel to the liver. In the liver, sporozoites infect hepatocytes, which marks the beginning of the asymptomatic liver stage infection. Within a time period of 6–7 days, parasites mature inside hepatocytes and eventually form tens of thousands of merozoites, which are released into the bloodstream where they invade red blood cells (RBCs). Blood stage infection becomes symptomatic and the cyclic infection and destruction of RBCs by the parasite as well as the adhesion of infected RBCs to the vascular endothelium, causes the morbidity and mortality associated with infection.

Although *P. falciparum* can be cultured *in vitro*, several aspects of malaria infections can only be addressed by *in vivo* research. The complex mechanisms of malaria transmission through mosquito bites, the multiple tissue barriers crossed by the parasite, and the different cell types that are infected during its life cycle make it impossible to study all aspects in one *in vitro* system. Also, drug studies will require an *in vivo* system for PK/PD analysis and for prodrugs, which will not be metabolized *in vitro* and therefore their potential antimalarial activity cannot be assessed (1). The standardization of controlled human malaria infections (CHMI) has made it possible to study the efficacy of novel drugs and vaccines in the human system (2). However, the high cost and ethical considerations involved with CHMI necessitate the testing of new compounds in relevant animal models prior to moving them forward in clinical trials.

The recent development of liver-humanized mouse models has made it possible to study *P. falciparum* liver stage infection *in vivo*. One of these mouse models is the FRG KO mouse which was developed by adding $Rag2^{-/-}$ and $IL2rg^{-/-}$ immunodeficiency backgrounds to the C57BL/6 fumarylacetoacetate hydrolase (FAH) knock-out mouse developed by Grompe et al. (3). The FAH KO results in a defect in the tyrosine catabolic pathway, which leads to the accumulation of maleylacetoacetate and fumarylacetoacetate, upstream of the FAH blockade. These metabolites are highly reactive and unstable, and upon breakdown cause hepatocellular injury (3). This toxicity can be prevented by oral administration of 2-(2-nitro-4-trifluoro-methylbenzoyl)-1,3-cyclohexanedione (NTBC), which blocks the tyrosine catabolism pathway upstream of the toxic metabolites (4). Liver injury can be induced by withdrawing mice from NTBC, thereby allowing repopulation of the diseased mouse liver with human hepatocytes (5).

The $Rag2^{-/-}$ and $IL2rg^{-/-}$ mutations prevent the development of B cells, T cells, and NK cells. Backcrossing of the FRG mouse onto the non-obese diabetic (NOD) background enables additional repopulation of the resulting NOD $Fah^{-/-}Rag2^{-/-}IL2rg^{-/-}$ (FRGN KO) mice with hematopoietic stem cells (HSCs). The NOD background has various intrinsic immune deficiencies, most importantly, it carries a polymorphism in the SIRPα gene that improves crosstalk between CD47 on human cells and the SIRPα receptor on mouse phagocytes, thereby preventing NOD macrophages from engulfing human grafts (6).

The transplantation of immunodeficient mice with CD34 + HSCs leads to the development of most human blood cell lineages. Unfortunately, human erythropoiesis is not sufficient in these mice, therefore, only very low amounts of human red blood cells (hRBCs) can be detected in the periphery (7–9). The only current method to achieve high amounts of hRBCs in mice is the frequent injection of large volumes of hRBCs. One option to study *P. falciparum* blood stages *in vivo* is the injection of *in vitro* cultured asexual stage parasites into immunodeficient mice that have been preloaded with hRBCs (10, 11). By combining this approach with the injection of macrophage and neutrophil-depleting chemicals, the development of gametocytes that sequester in spleen and bone marrow could be observed, therefore somewhat mimicking human infection (12). A disadvantage of this system is that it does not model the natural route of infection by mosquito bite and it lacks liver to blood stage transition. These life cycle transition stages are important to include in a mouse system that will serve as a model for the complete *P. falciparum* life cycle. Especially the transition from liver to blood stage is a critical step in the parasite life cycle and provides a target for intervention with drugs and vaccines in order to prevent the establishment of a blood stage infection. Therefore, it should be included in a mouse model for malaria drug and vaccine testing.

Liver to blood stage transition has been reported previously in the liver humanized TK-NOG mouse. Similar to other NSG models, the blood stream of these mice can be reconstituted with hRBCs by daily intraperitoneal (i.p.) injections of 1 ml hRBCs starting 6 days before i.v. injection of a large number of *P. falciparum* sporozoites, thereby allowing liver stage to blood stage transition and subsequent blood stage infection. The numbers of sexual and asexual stages were highly variable in these mice and *in vivo* solely detected by thin blood smears (13). The liver humanized FRGN KO (FRGN huHep) mouse can also be reconstituted with human erythrocytes, thus allowing the transition of *P. falciparum* liver

to blood stage infection, which can be further propagated in an *in vitro* culture after exsanguinating the mice (14).

Here, we report the development of a protocol for the long-term engraftment of hRBCs in *P. falciparum* sporozoite-infected FRGN huHep mice. As mosquito bite is the natural route of infection, we have included this modality of *P. falciparum* sporozoite transmission. Following our protocol for hRBC engraftment, we achieve liver to blood stage transition followed by the stable maintenance of a *P. falciparum* blood stage infection with increasing parasitemia. The transition from liver stage to blood stage is visualized by *in vivo* bioluminescent imaging (IVIS), allowing the discrimination of treatment efficacy against either one or both stages. We assessed the utility of this model by showing that blood stage infection emerging from the liver can be blocked successfully by a monoclonal antibody (mAb) recognizing *P. falciparum* reticulocyte-binding protein homolog 5 (RH5). RH5 is an essential merozoite invasion ligand that interacts with the basigin receptor on hRBCs. This interaction is a prerequisite for infection throughout all parasite strains tested to date (15, 16). Recently, the first clinical study assessing RH5 as a vaccine candidate was conducted. Substantial RH5-specific immune responses could be induced by immunization of malaria-naïve individuals with viral vectors encoding PfRH5 (17). The RH5–basigin interaction therefore constitutes an important potential vaccine target. The inhibition of *P. falciparum* blood stage infection by an anti-RH5 mAb in our mouse model underlines its utility for the study of potential antibody-based malaria intervention strategies.

RESULTS AND DISCUSSION

Plasmodium falciparum liver infection can be studied *in vivo* using liver humanized FRG KO or FRGN KO mice. Infection with sporozoites of luciferase-expressing parasites made it possible to follow the progression of infection by *in vivo* bioluminescent imaging (IVIS), without sacrificing the animal. Liver infection was detected until day 7 postinfection. One injection of hRBCs on day 6 postinfection allowed parasites to transition from liver stage to blood stage infection. The parasitemia was detectable by quantitative PCR and the infection can be propagated *in vitro* after exsanguinating the mice (14). Unfortunately, this method does not allow a stable blood stage infection *in vivo* due to rapid clearance of infected hRBCs (iRBC) by mouse phagocytes.

Here, we addressed this issue and developed an immune modulation protocol that allows the iRBCs to remain in the circulation without being phagocytosed. The efficient engraftment of sporozoite infected mice with high amounts of hRBCs leads to expansion of the infection and thereby increasing parasitemia over time.

DEVELOPMENT OF AN IMMUNE MODULATION PROTOCOL TO PREVENT PHAGOCYTOSIS OF iRBCs

To prevent phagocytosis of iRBCs, we optimized an immune modulation protocol to specifically eliminate mouse phagocytes, namely macrophages and neutrophils. As previously described, mouse macrophages can be eliminated by the administration of clodronate-containing liposomes, which are phagocytosed by macrophages and subsequently induce apoptosis (18). Experimental neutropenia is commonly induced either by administration of antibodies targeting neutrophil-specific receptors such as Ly6G (19) or by the cytotoxic chemotherapy agent cyclophosphamide (20). Compared to antibodies, which are highly specific, cyclophosphamide has a broader immunosuppressive effect, as it targets all dividing cells. Therefore, we decided to utilize this method to deplete neutrophils, as any further immune suppression could aid in preventing phagocytosis of iRBCs.

To assess the effect of clodronate-containing liposomes (CloLip; Clophosome®-A, FormuMax) alone and in combination with cyclophosphamide (Sigma Aldrich, St. Louis, MO, USA), six liver humanized FRGN KO mice received an injection of 50 µl CloLip i.v. + 50 µl CloLip i.p. on day −2 before infection to remove macrophages and monocytes from both the circulation and the peritoneal cavity. Three mice additionally received 150 mg/kg cyclophosphamide i.p. All animals were bled 200 µl, and received an i.v. injection of 500 µl hRBCs [70% O + human erythrocytes in RPMI 1640 (25 mM HEPES, 2 mM L-glutamine) supplemented with 50 µM hypoxanthine plus 10% human

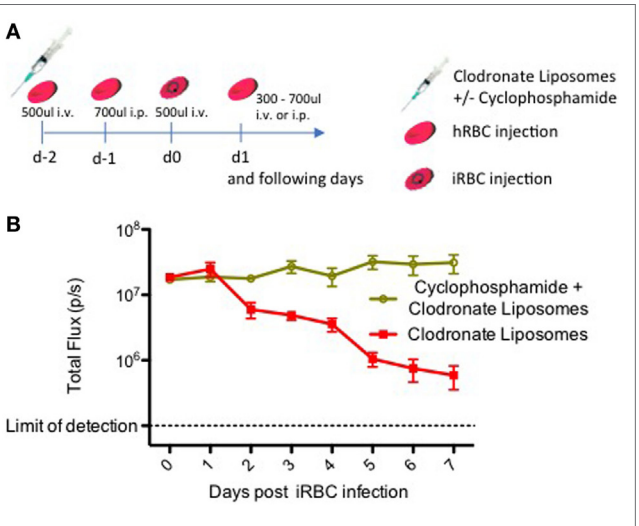

FIGURE 1 | Immune modulation with clodronate liposomes and cyclophosphamide leads to a stable *Plasmodium falciparum* blood stage infection. **(A)** Timeline showing the protocol for the repopulation of liver-humanized FRGN KO mice with human red blood cells (hRBCs) and subsequent infection with blood stage parasites. This protocol was utilized here to assess the effect of cyclophosphamide on a *P. falciparum* blood stage infection in FRGN huHep mice. Six mice received an injection of 50 µl CloLip i.v. + 50 µl CloLip i.p. on day −2 and three mice additionally received 150 mg/kg (approximately 150 µl per mouse) cyclophosphamide i.p. All animals were bled 200 µl, and received one i.v. injection of 500 µl hRBCs. On day −1, the animals were bled 100 µl and received an i.p. injection of 700 µl hRBCs. On day 0, the animals were bled 100 µl and received an i.v. injection of 500 µl hRBCs containing 1×10^7 iRBCs. The following days, all mice received an individually determined amount of hRBCs. Parasitemia was followed by daily intravital imaging **(B)**. The IVIS signal of mice treated only with CloLip started decreasing on day 2 postinfection. Only the mice which received both CloLip and cyclophosphamide, showed a stable *P. falciparum* blood stage infection throughout the 7-day observation period.

serum and 5 µl penicillin–streptomycin (Gibco™, 10,000 U/ml penicillin, 10,000 µg/ml streptomycin)] to preload the mice with a pool of hRBCs. On day −1, the animals were bled 100 µl and received an i.p. injection of 700 µl hRBCs. On day 0, the animals were bled 100 µl and received an i.v. injection of 500 µl hRBCs containing 1×10^7 *P. falciparum* NF54 GFP-Luc iRBCs from an *in vitro* blood culture. On the day of infection, the animals were reconstituted with approximately 20–30% hRBCs independent of the immune modulation protocol. The animals received an individually determined amount of hRBCs each day to stabilize the percentage between 50 and 70%. This protocol is depicted in **Figure 1A**.

Our results in **Figure 1B** show that elimination of monocytes with CloLip is beneficial, but not yet sufficient to enable a stable blood stage infection, as the parasitemia starts to decline as early as 2 days postinfection. Only the additional elimination of neutrophils with cyclophosphamide results in a stable blood stage infection quantifiable by IVIS (**Figure 1B**). In contrast to mice treated with CloLip alone, the IVIS signal of macrophage and neutrophil depleted mice remained stable over the 7-day observation period, indicating that the iRBCs are not being cleared. Notably, this immunomodulation protocol did not lead to any loss of mice throughout the experiment.

REPOPULATION OF SPOROZOITE-INFECTED FRGN huHEP MICE WITH hRBCs

The immune modulation protocol described above had to be refined for the setting of mice infected with sporozoites by mosquito bite, as it is known that *Plasmodium* skin and liver stages

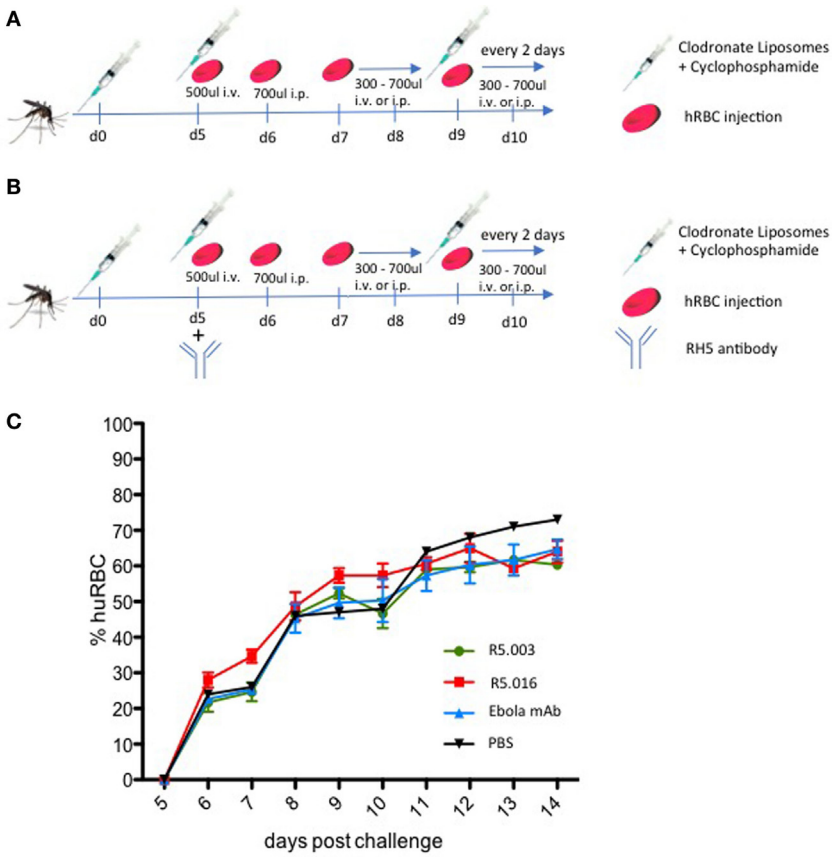

FIGURE 2 | Protocol for the repopulation of sporozoite-infected FRGN mice with human red blood cells (hRBCs). **(A)** Mice are infected by mosquito bite with *Plasmodium falciparum* NF54 GFP-Luc sporozoites ($n = 50$ mosquitoes per mouse; 20 min). On the day of infection, mice are injected with 50 µl CloLip i.v. + 50 µl CloLip intraperitoneal (i.p.) and 150 mg/kg cyclophosphamide i.p. These injections are repeated on days 5, 9, 11, and 13 postinfection. On day 5 postinfection, 200 µl blood is drawn and the mice receive one injection of 500 µl hRBCs i.v. On day 6 postinfection, 100 µl blood is drawn and 700 µl hRBCs are injected i.p. The volumes of hRBCs injected the following days are determined individually in order to stabilize the percentages of hRBCs between 50 and 70%. **(B)** In order to assess the effect of antireticulocyte-binding protein homolog 5 antibody on transition and maintenance of a *P. falciparum* blood stage infection, blood humanization was achieved as described in **(A)**. On day 5 postmosquito-bite infection, all mice received one i.p. injection of 100 mg/kg of R5.003, R5.016, or control anti-Ebola monoclonal antibody (mAb) (EBL040). All three mAbs were human IgG1. One mouse received PBS as a control. **(C)** The percentages of hRBCs were assessed by FACS analysis using a CD235ab antibody. All mice show similar percentages of hRBCs throughout the 14-day observation period, independent of the treatment regimen, demonstrating that the differences observed in blood stage infection were not due to varying amounts of hRBCs. The mean ± SD is shown for each treatment group.

induce an innate immune response in the host (21). In order to reduce this initial immune response, on the day of mosquito bite challenge mice were injected both in the retro-orbital plexus and the peritoneal cavity with 50 µl CloLip and 150 mg/kg cyclophosphamide i.p. The CloLip (50 µl i.v. and i.p.) and cyclophosphamide (following doses are 100 mg/kg i.p.) injections were repeated on days 5, 9, 11, and 13 postinfection, thereby preventing the iRBCs from being cleared from the circulation.

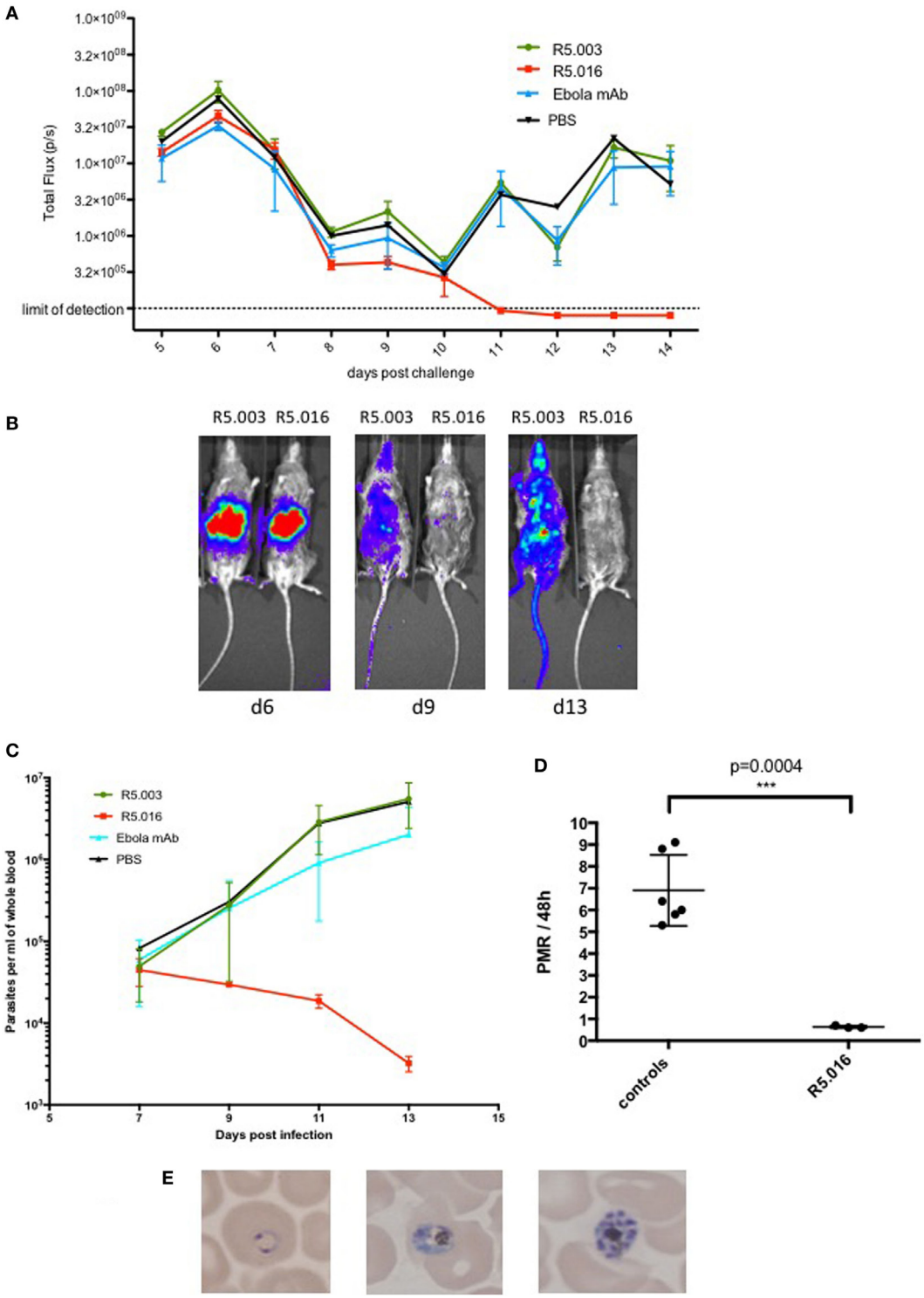

FIGURE 3 | Continued

FIGURE 3 | Inhibition of *Plasmodium falciparum* blood stage infection by anti-reticulocyte-binding protein homolog 5 (anti-RH5) antibody. 10 mice were challenged with *P. falciparum* NF54 GFP-Luc infected mosquitoes ($n = 50$ per mouse; 20 min). Blood humanization and passive transfer of RH5 and control monoclonal antibodies (mAbs) was achieved using the protocol as depicted in **Figure 2B**. **(A)** Mice were imaged daily by IVIS starting 5 days postinfection. They were intraperitoneally injected with 100 µl of Rediject D-luciferin (Perkin Elmer) and imaged after 5 min for a 5-min exposure. Liver and blood-stage burden was assessed by placing an identical region of interest around each mouse and measuring total flux in pixels/second (p/s). The liver-derived IVIS signal peaks on day 6 postinfection and declines thereafter until day 10 due to the transition of the parasite from liver to blood stage infection. After day 10, the blood stage infection increases in all mice except for the ones treated with R5.016. In these mice, the infection decreases further and is undetectable by IVIS by day 11 postinfection. The mean ± SD is shown for each treatment group. **(B)** Representative IVIS images of R5.003 and R5.016 treated animals from days 6, 9, and 13. The liver-derived IVIS signal on day 6 is comparable for both mice. On days 9 and 13, the mouse treated with R5.003 shows a strong IVIS signal distributed throughout the body due to the increasing parasitemia, whereas the mouse treated with R5.016 shows only a very weak signal on day 9 and no signal is detectable on day 13, indicating that blood stage infection was potently inhibited. **(C)** *P. falciparum* parasites per ml of whole blood measured by quantitative reverse transcription (qRT-PCR) targeting *P. falciparum* 18S RNA as described previously (22) showing a dramatic decrease of infection levels only in the mice treated with R5.016. The mean ± SD is shown for each treatment group. **(D)** The parasite multiplication rate per 48 h was calculated for days 9–11 from the qRT-PCR data shown in **Figure 3C**. Controls refer to the mice treated with R5.003, Ebola mAb, or PBS. One control mouse showed low parasitemia on day 9 but reached levels comparable to the other mice on day 11, therefore the PMR is not comparable to the other mice and this data had to be excluded from the analysis. Each dot represents one mouse and the mean ± SD is shown. **(E)** Giemsa stained thin blood smears were analyzed daily by microscopy. Starting on day 8 postinfection, different developmental stages of asexual parasites could be detected in all animals except for the ones who received R5.016, where no parasites could be detected by microscopy at any time point.

In order to rapidly repopulate mice with high amounts of hRBCs using a limited amount of injections, we optimized a blood exchange method where blood was drawn from the animals daily during the final days of the liver stage development while concurrently receiving large volumes of hRBCs. The first injection of 500 µl hRBCs is administered on day 5 postsporozoite challenge, 1 day before exoerythrocytic merozoites start emerging from the liver. To prevent overloading the animals with erythrocytes, this is accompanied by a 200 µl blood draw. Human RBC counts are quantified daily by FACS analysis using a CD235ab antibody, as described before (11). The following day, day 6 postinfection, mice are bled 200 µl and injected 700 µl hRBCs i.p. Following this procedure, already on day 7 the percentage of hRBCs reaches 20–30%, thereby providing a large pool of target cells for the emerging parasites. By day 8, the percentage of hRBCs reaches 50% and in order to keep the percentage stable between 50 and 70% mice are injected daily with 300–700 µl hRBCs. Higher percentages are achievable however this does not increase the success rate of transition, but can increase mortality due to elevated hematocrit. The described protocol is depicted in **Figure 2**. This protocol allows the maintenance of a stable *P. falciparum* blood stage infection with increasing parasitemia over time.

INHIBITION OF BLOOD STAGE INFECTION BY AN ANTIBODY TARGETING RH5

To assess the utility of our model, we measured for the first time the *in vivo* efficacy of two anti-RH5 human monoclonal antibodies on the transition and establishment of blood stage infection.

To this end, we infected 10 FRGN huHep mice by *P. falciparum* NF54 GFP-Luc infected mosquito bites ($n = 50$ mosquitoes per mouse; 20 min). Starting 5 days postinfection, mice were imaged daily by IVIS to measure the liver infection level. Based on initial liver stage parasite burden on day 5, the mice were randomized into four groups and received an i.p. injection of vehicle control (PBS, $n = 1$), antibody control (Ebola mAb EBL040, $n = 3$) (Rijal P. et al., in preparation), or anti-RH5 mAb R5.003 ($n = 3$) or R5.016 ($n = 3$) at a dose of 100 mg/kg. *In vitro* assays of growth inhibition activity (GIA) have shown R5.016 is a potent inhibitor of parasite growth, whereas R5.003 does not show any GIA (Alanine et al., in preparation). Confirming these results *in vivo* is of great importance, since it remains highly debated as to whether vaccines or antibodies prioritized on the basis of *in vitro* GIA would subsequently confer *in vivo* efficacy (15). Following our protocol as described above and outlined in **Figure 2B**, all mice showed similar repopulation levels with hRBCs ranging from 20 to 35% on day 7 and steadily increasing afterward (**Figure 2C**). Blood stage parasitemia was detectable by quantitative reverse transcription PCR (qRT-PCR) starting on day 7 (**Figure 3C**), and by IVIS (**Figure 3A**) and microscopy of thin blood smears (**Figure 3E**) on day 8. The serum antibody concentrations were similar for all treatment groups throughout the experiment (Figure S1 in Supplementary Material). In animals passively transferred with R5.003 (GIA-negative mAb) the parasitemia increased over time in a manner indistinguishable from the vehicle or antibody control mice. In contrast, the mice passively transferred with R5.016 (GIA-positive mAb) showed no IVIS signal on day 13 postinfection (**Figures 3A,B**) and no detectable parasites by microscopy of thin blood smears. The infection level by qRT-PCR remained above the limit of detection of 20 parasites/ml for all mice during the 13-day observation period, but a dramatic decrease was seen in the mice passively transferred with R5.016 (**Figure 3C**).

In addition, we calculated the parasite multiplication rates (PMRs) per 48 h between days 9 and 11 for the mice treated with R5.003, Ebola mAb, or PBS, combined as the control group, and the mice passively transferred with R5.016 (**Figure 3D**). The PMR per 48 h for the control group is approximately 7-fold, which is similar to the kinetics seen in CHMI studies, where the PMR was shown to be about 10-fold per 48 h (16). The slight difference in PMR between our murine model and CHMI might be due to the fact that in the murine model not all RBCs are of human origin. The mice passively transferred with R5.016 show a PMR of 0.5-fold, indicating that the parasites cannot multiply, most likely due to the invasion-inhibitory effect of R5.016. These passive transfer results confirm that *in vivo* efficacy of the antibodies tested here aligns with their ability to show GIA *in vitro*, and underline the utility of our liver stage/blood stage model to test anti-malarial blood stage interventions.

It has been shown previously that human monocytes act synergistically with antibodies directed against the merozoite surface (23). Since no human monocytes are present in our mouse model and mouse monocytes have been depleted by CloLip treatment, the inhibitory effect of the anti-RH5 mAb R0.016 cannot be attributed to monocyte activity, but likely to direct inhibition of merozoite entry into the RBC. It may be speculated that the presence of human monocytes might increase this inhibitory effect even further.

CONCLUSION

In conclusion, we show the establishment of a *in vivo* FRGN huHep/hRBC model to study *P. falciparum* liver stages, the transition to blood stage infection and the development of blood stage parasitemia. As shown by inhibition studies using a mAb targeting RH5, this combined model will be useful to study the effect of novel therapeutics on the different life cycle stages of human *Plasmodium* parasites as well as stage transitions *in vivo*. Because both liver and blood stage infection can be measured separately by intravital imaging, this model will allow us to distinguish the effects on either stages and determine the combined efficacy on the human host cycle of malaria *in vivo*.

Additionally, this improved mouse model will be of great value for the recovery of progeny from genetic crosses. Genetic crosses between phenotypically distinct parasite strains allow the identification of genes controlling drug resistance and other key phenotypes. Previously, *P. falciparum* genetic crosses had to be carried out in splenectomized chimpanzees, but it was recently reported that recombinant progeny can also be recovered from FRG huHep mice that had been injected with hRBCs (24). Parasitemia is low though (typically <0.1%) so that the recovered parasites have to be expanded *ex vivo* before initiating cloning. This may bias the results toward parasites that can replicate better in culture conditions. With our improved protocol which leads to 20–30% hRBCs on day 7 postinfection, when transition from liver to blood stage occurs, higher parasitemias could potentially be achieved, leading to the recovery of a larger population of progeny. Recovery of more clones would lead to a wider variation of progeny and cloning could be initiated directly out of the mouse.

Although this mouse model provides the opportunity to study most aspects of *P. falciparum* infection as well as the effects of novel drug and vaccine candidates, it does require an experienced researcher in order to reproducibly achieve high levels of hRBCs as the volumes of hRBCs injected after day 6 have to be adjusted on a day-to-day basis. To circumvent these issues, the ideal *in vivo* model for malaria research would be a mouse which intrinsically promotes human erythropoiesis. A first step in this direction is the DRAG (HLA-DR4.RagKO.IL2RγcKO.NOD) mouse model, an immune deficient mouse expressing human HLA class II genes (25). These mice can be reconstituted with human hepatocytes, Kupffer cells, liver endothelial cells, and erythrocytes by infusing HLA-matched HSC's (26). Although the resulting liver (only 0.023 versus 90% for FRG mice) (27) and blood (0.2–1%) humanization was extremely low, injected sporozoites were still able to infect human hepatocytes, leading to a low, but detectable blood stage infection after 10–28 days (3–5 parasites/μl of blood) (26). These low repopulation efficiencies limit the use of DRAG mice, nevertheless raise hope that in the future a human liver chimeric mouse will be developed that additionally promotes human erythropoiesis. Until this is the case, the model we present here will be an extremely useful tool for the *in vivo* study of human *Plasmodium* parasites and the evaluation of novel antimalaria drug and vaccine candidates.

ETHICS STATEMENT

This study was carried out in accordance with the recommendations of the NIH Office of Laboratory Animal Welfare standards (OLAW welfare assurance # A3640-01). The protocol was approved by the Center for Infectious Disease Research Institutional Animal Care and Use Committee (IACUC) under protocol SK-16.

AUTHOR CONTRIBUTIONS

LF, CS, NM, DA, EF, RS, BS, and ZB carried out laboratory work and collected and analyzed data. LF and CS drafted the manuscript. NC, MF, WB, and TN produced gametocytes and sporozoite-infected mosquitoes. DA and SD provided the RH5 and Ebola mAbs. JB and EW provided FRGN huHep mice. SM, SD, SM, and SK analyzed data, supervised the work, and contributed to discussion. All authors read and edited the final manuscript.

ACKNOWLEDGMENTS

We would like to thank the insectary team at the Center for Infectious Disease Research for production of sporozoite-infected mosquitoes and Yecuris Corporation (Tualatin, OR, USA) for providing liver humanized FRGN mice. We thank Dr. Ashley Vaughan for helpful discussions and critical reading of this manuscript. This work was funded by a fellowship of the Belgian American Educational Foundation (to LF); a fellowship of the German Research Association (grant SCHA 2047/1-1) (to CS); a UK MRC iCASE PhD Studentship (grant MR/K017632/1) (to DA); a Wellcome Trust Senior Fellowship (grant 106917/Z/15/Z); and a Lister Institute Research Prize Fellowship to SD who is also a Jenner Investigator; and the Center for Infectious Disease Research internal funding sources.

SUPPLEMENTARY MATERIAL

The Supplementary Material for this article can be found online at https://www.frontiersin.org/articles/10.3389/fimmu.2018.00524/full#supplementary-material.

FIGURE S1 | The amount of hIgG1 present in the mouse serum was measured by standardized ELISA, as previously described (28, 29), except that the plates were coated with full-length reticulocyte-binding protein homolog protein expressed in *Drosophila* S2 cells. All mice show similar antibody levels throughout the experiment. Each sample was measured as quadruplicate and the mean ± SD is plotted for each mouse.

REFERENCES

1. Moreno A, Badell E, Van Rooijen N, Druilhe P. Human malaria in immunocompromised mice: new in vivo model for chemotherapy studies. *Antimicrob Agents Chemother* (2001) 45(6):1847–53. doi:10.1128/AAC.45.6.1847-1853.2001
2. Roestenberg M, Bijker EM, Sim BK, Billingsley PF, James ER, Bastiaens GJ, et al. Controlled human malaria infections by intradermal injection of cryopreserved *Plasmodium falciparum* sporozoites. *Am J Trop Med Hyg* (2013) 88(1):5–13. doi:10.4269/ajtmh.2012.12-0613
3. Grompe M, al-Dhalimy M, Finegold M, Ou CN, Burlingame T, Kennaway NG, et al. Loss of fumarylacetoacetate hydrolase is responsible for the neonatal hepatic dysfunction phenotype of lethal albino mice. *Genes Dev* (1993) 7(12A):2298–307. doi:10.1101/gad.7.12a.2298
4. Overturf K, Al-Dhalimy M, Tanguay R, Brantly M, Ou CN, Finegold M, et al. Hepatocytes corrected by gene therapy are selected in vivo in a murine model of hereditary tyrosinaemia type I. *Nat Genet* (1996) 12(3):266–73. doi:10.1038/ng0396-266
5. Azuma H, Paulk N, Ranade A, Dorrell C, Al-Dhalimy M, Ellis E, et al. Robust expansion of human hepatocytes in Fah-/-/Rag2-/-/Il2rg-/- mice. *Nat Biotechnol* (2007) 25(8):903–10. doi:10.1038/nbt1326
6. Takenaka K, Prasolava TK, Wang JC, Mortin-Toth SM, Khalouei S, Gan OI, et al. Polymorphism in Sirpa modulates engraftment of human hematopoietic stem cells. *Nat Immunol* (2007) 8(12):1313–23. doi:10.1038/ni1527
7. Rongvaux A, Willinger T, Martinek J, Strowig T, Gearty SV, Teichmann LL, et al. Development and function of human innate immune cells in a humanized mouse model. *Nat Biotechnol* (2014) 32(4):364–72. doi:10.1038/nbt.2858
8. Amaladoss A, Chen Q, Liu M, Dummler SK, Dao M, Suresh S, et al. De novo generated human red blood cells in humanized mice support *Plasmodium falciparum* infection. *PLoS One* (2015) 10(6):e0129825. doi:10.1371/journal.pone.0129825
9. Rahmig S, Kronstein-Wiedemann R, Fohgrub J, Kronstein N, Nevmerzhitskaya A, Bornhäuser M, et al. Improved human erythropoiesis and platelet formation in humanized NSGW41 mice. *Stem Cell Reports* (2016) 7(4):591–601. doi:10.1016/j.stemcr.2016.08.005
10. Jiménez-Díaz MB, Mulet T, Viera S, Gómez V, Garuti H, Ibáñez J, et al. Improved murine model of malaria using *Plasmodium falciparum* competent strains and non-myelodepleted NOD-scid IL2Rgammanull mice engrafted with human erythrocytes. *Antimicrob Agents Chemother* (2009) 53(10):4533–6. doi:10.1128/AAC.00519-09
11. Angulo-Barturen I, Jiménez-Díaz MB, Mulet T, Rullas J, Herreros E, Ferrer S, et al. A murine model of falciparum-malaria by in vivo selection of competent strains in non-myelodepleted mice engrafted with human erythrocytes. *PLoS One* (2008) 3(5):e2252. doi:10.1371/journal.pone.0002252
12. Duffier Y, Lorthiois A, Cisteró P, Dupuy F, Jouvion G, Fiette L, et al. A humanized mouse model for sequestration of *Plasmodium falciparum* sexual stages and in vivo evaluation of gametocytidal drugs. *Sci Rep* (2016) 6:35025. doi:10.1038/srep35025
13. Soulard V, Bosson-Vanga H, Lorthiois A, Roucher C, Franetich JF, Zanghi G, et al. *Plasmodium falciparum* full life cycle and *Plasmodium ovale* liver stages in humanized mice. *Nat Commun* (2015) 6:7690. doi:10.1038/ncomms8690
14. Vaughan AM, Mikolajczak SA, Wilson EM, Grompe M, Kaushansky A, Camargo N, et al. Complete *Plasmodium falciparum* liver-stage development in liver-chimeric mice. *J Clin Invest* (2012) 122(10):3618–28. doi:10.1172/JCI62684
15. Duncan CJ, Hill AV, Ellis RD. Can growth inhibition assays (GIA) predict blood-stage malaria vaccine efficacy? *Hum Vaccin Immunother* (2012) 8(6):706–14. doi:10.4161/hv.19712
16. Payne RO, Milne KH, Elias SC, Edwards NJ, Douglas AD, Brown RE, et al. Demonstration of the blood-stage *Plasmodium falciparum* controlled human malaria infection model to assess efficacy of the *P. falciparum* apical membrane antigen 1 vaccine, FMP2.1/AS01. *J Infect Dis* (2016) 213(11):1743–51. doi:10.1093/infdis/jiw039
17. Payne RO, Silk SE, Elias SC, Miura K, Diouf A, Galaway F, et al. Human vaccination against RH5 induces neutralizing antimalarial antibodies that inhibit RH5 invasion complex interactions. *JCI Insight* (2017) 2(21). doi:10.1172/jci.insight.96381
18. van Rooijen N, van Kesteren-Hendrikx E. "In vivo" depletion of macrophages by liposome-mediated "suicide". *Methods Enzymol* (2003) 373:3–16. doi:10.1016/S0076-6879(03)73001-8
19. Bruhn KW, Dekitani K, Nielsen TB, Pantapalangkoor P, Spellberg B. Ly6G-mediated depletion of neutrophils is dependent on macrophages. *Results Immunol* (2016) 6:5–7. doi:10.1016/j.rinim.2015.12.001
20. Hirsh M, Carmel J, Kaplan V, Livne E, Krausz MM. Activity of lung neutrophils and matrix metalloproteinases in cyclophosphamide-treated mice with experimental sepsis. *Int J Exp Pathol* (2004) 85(3):147–57. doi:10.1111/j.0959-9673.2004.00385.x
21. Lindner SE, Miller JL, Kappe SH. Malaria parasite pre-erythrocytic infection: preparation meets opportunity. *Cell Microbiol* (2012) 14(3):316–24. doi:10.1111/j.1462-5822.2011.01734.x
22. Sack BK, Mikolajczak SA, Fishbaugher M, Vaughan AM, Flannery EL, Nguyen T, et al. Humoral protection against mosquito bite-transmitted *Plasmodium falciparum* infection in humanized mice. *NPJ Vaccines* (2017) 2:27. doi:10.1038/s41541-017-0028-2
23. Galamo CD, Ali J, Blanc C, Druilhe P. Anti-MSP1 block 2 antibodies are effective at parasite killing in an allele-specific manner by monocyte-mediated antibody-dependent cellular inhibition. *J Infect Dis* (2009) 199(8):1151–4. doi:10.1086/597426
24. Vaughan AM, Pinapati RS, Cheeseman IH, Camargo N, Fishbaugher M, Checkley LA, et al. *Plasmodium falciparum* genetic crosses in a humanized mouse model. *Nat Methods* (2015) 12(7):631–3. doi:10.1038/nmeth.3432
25. Danner R, Chaudhari SN, Rosenberger J, Surls J, Richie TL, Brumeanu TD, et al. Expression of HLA class II molecules in humanized NOD.Rag1KO.IL2RgcKO mice is critical for development and function of human T and B cells. *PLoS One* (2011) 6(5):e19826. doi:10.1371/journal.pone.0019826
26. Wijayalath W, Majji S, Villasante EF, Brumeanu TD, Richie TL, Casares S. Humanized HLA-DR4.RagKO.IL2RγcKO.NOD (DRAG) mice sustain the complex vertebrate life cycle of *Plasmodium falciparum* malaria. *Malar J* (2014) 13:386. doi:10.1186/1475-2875-13-386
27. Foquet L, Hermsen CC, van Gemert GJ, Libbrecht L, Sauerwein R, Meuleman P, et al. Molecular detection and quantification of *Plasmodium falciparum*-infected human hepatocytes in chimeric immune-deficient mice. *Malar J* (2013) 12:430. doi:10.1186/1475-2875-12-430
28. Sheehy SH, Duncan CJ, Elias SC, Collins KA, Ewer KJ, Spencer AJ, et al. Phase Ia clinical evaluation of the *Plasmodium falciparum* blood-stage antigen MSP1 in ChAd63 and MVA vaccine vectors. *Mol Ther* (2011) 19(12):2269–76. doi:10.1038/mt.2011.176
29. Sheehy SH, Duncan CJ, Elias SC, Biswas S, Collins KA, O'Hara GA, et al. Phase Ia clinical evaluation of the safety and immunogenicity of the *Plasmodium falciparum* blood-stage antigen AMA1 in ChAd63 and MVA vaccine vectors. *PLoS One* (2012) 7(2):e31208. doi:10.1371/journal.pone.0031208

Conflict of Interest Statement: JB and EW work for Yecuris Corp., the company that sells FRGN huHep mice. All other authors declare that the research was conducted in the absence of any commercial or financial relationships that could be construed as a potential conflict of interest.

frontiers in Immunology

MINI REVIEW
published: 04 April 2018
doi: 10.3389/fimmu.2018.00649

Human Immune System Mice for the Study of Human Immunodeficiency Virus-Type 1 Infection of the Central Nervous System

Teresa H. Evering and Moriya Tsuji*

Aaron Diamond AIDS Research Center, An Affiliate of the Rockefeller University, New York, NY, United States

Immunodeficient mice transplanted with human cell populations or tissues, also known as human immune system (HIS) mice, have emerged as an important and versatile tool for the *in vivo* study of human immunodeficiency virus-type 1 (HIV-1) pathogenesis, treatment, and persistence in various biological compartments. Recent work in HIS mice has demonstrated their ability to recapitulate critical aspects of human immune responses to HIV-1 infection, and such studies have informed our knowledge of HIV-1 persistence and latency in the context of combination antiretroviral therapy. The central nervous system (CNS) is a unique, immunologically privileged compartment susceptible to HIV-1 infection, replication, and immune-mediated damage. The unique, neural, and glia-rich cellular composition of this compartment, as well as the important role of infiltrating cells of the myeloid lineage in HIV-1 seeding and replication makes its study of paramount importance, particularly in the context of HIV-1 cure research. Current work on the replication and persistence of HIV-1 in the CNS, as well as cells of the myeloid lineage thought to be important in HIV-1 infection of this compartment, has been aided by the expanded use of these HIS mouse models. In this review, we describe the major HIS mouse models currently in use for the study of HIV-1 neuropathogenesis, recent insights from the field, limitations of the available models, and promising advances in HIS mouse model development.

Keywords: human immunodeficiency virus, central nervous system, human immune system mice, myeloid cells, HIV-associated neurocognitive disorders

OPEN ACCESS

Edited by:
Urszula Krzych, Walter Reed Army Institute of Research, United States

Reviewed by:
Johannes S. Gach, University of California, Irvine, United States
Ji Wang, Harvard Medical School, United States

****Correspondence:***
Teresa H. Evering
tevering@adarc.org

Specialty section:
This article was submitted to Vaccines and Molecular Therapeutics, a section of the journal Frontiers in Immunology

Received: *20 January 2018*
Accepted: *16 March 2018*
Published: *04 April 2018*

Citation:
Evering TH and Tsuji M (2018) Human Immune System Mice for the Study of Human Immunodeficiency Virus-Type 1 Infection of the Central Nervous System. Front. Immunol. 9:649. doi: 10.3389/fimmu.2018.00649

INTRODUCTION

Infection with human immunodeficiency virus-type 1 (HIV-1) results in CD4+ T cell destruction and progressive debilitation of the immune system (1). Although combination antiretroviral therapy (cART) can effectively suppress HIV-1 RNA to undetectable levels in the peripheral blood (2), the ability of replication-competent HIV-1 to persist in cellular and tissue reservoirs despite suppressive therapy is a barrier to cure (3–5). Penetration of the central nervous system (CNS) by HIV-1 occurs early in infection (6, 7). HIV is postulated to cross the blood–brain barrier (BBB) *via* the infiltration of infected monocytes, CD4+ T lymphocytes (8, 9), or as cell-free virus (10, 11). Resulting CNS immune activation; the infection and activation of monocytes, perivascular macrophages, and resident microglia; and indirect mechanisms are all thought to play a critical role in the pathogenesis of HIV-1 in the CNS (12–16). Early neuropathological characterization of the CNS

in those with advanced untreated HIV-1 and HIV-associated dementia (HAD) revealed encephalitis marked by inflammation, microglial activation, astrogliosis, and neuronal loss (17, 18). Use of highly effective cART has significantly reduced the incidence of HAD (19). Nonetheless, HIV-1-associated neurocognitive disorders (HANDs) persist as an important clinical complication of HIV-1 infection in the cART era and can result in an array of cognitive, behavioral, and motor deficits (20). Murine models that mimic human immune systems (HIS) have been extremely valuable tools for the elucidation of a number of pathophysiological mechanisms responsible for HIV-1 CNS pathogenesis. However, no adjunctive therapies for HAND exist beyond cART, and a combination of novel and more physiologically relevant HIS mouse models is now being evaluated to advance our knowledge of the complex immunological and pathological features of HIV-1 neuropathogenesis in the cART era (21, 22).

ANIMAL MODELS FOR STUDIES OF HIV-1 CNS PATHOGENESIS

Animal models provide an important complementary approach to the study of HIV-1 pathogenesis (23). To varying degrees, these *in vivo* models replicate the intricacies of complex immunological interactions between multiple cell types to an extent not possible *in vitro*. In addition, they are free from many of the experimental constraints imposed by the inaccessibility/limited availability of human tissue (24). Commonly used non-human primate (NHP) animal models include rhesus, pigtail, and cynomolgus macaques that can be infected with a simian or chimeric simian/human immunodeficiency virus. NHP models have provided great insight into HIV-1 neuropathogenesis. In particular, rhesus macaques have been shown to develop HIV encephalitis (HIVE) and microglial infection (25), and a highly neurovirulent (although not physiologic) challenge model has been developed in pigtail macaques (26). However, studies using NHPs are limited by high cost, special housing requirements, and small experimental groups. In response to these constraints, small animal models of human disease have been developed and widely employed (27). However, their ability to recapitulate human disease can be limited as some important human pathogens (including HIV) display tropism unique to humans (28, 29). The transgenic expression of select HIV-1 proteins such as HIV-1 envelope and trans-activator of transcription, human receptors and co-receptors in mice result in animals with a broad range of HIV-1-related pathologies (30–34). These include a spectrum of neurotoxicity, defective neurogenesis, and glial abnormalities in mouse CNS that resemble those seen in the brains of HIV-1-infected humans (35–39). Although these transgenic models mirror specific components of the pathophysiological effects of select HIV-1 proteins on the CNS (40), as well as some of the cognitive and behavioral features of HAND (41), they are unable to model critical aspects of HIV-1 CNS infection in the human host, such as viral CNS invasion (42). For these reasons, the use of small animal models that can more accurately mimic the HIS is of great value.

HUMAN IMMUNE SYSTEM (HIS) MOUSE MODELS FOR THE STUDY OF HIV-1

In contrast to transgenic or chimeric mice, the creation of mice with human immune system components (HIS mice) provide an *in vivo* environment that allows for the study of HIV-1 and its interaction with cells of the human immune system (24). HIS mouse production initiates with the choice of an immunodeficient mouse strain that can accommodate the engraftment of human cells and tissues without rejection (43). Early immunodeficient mice used for human tissue or cell xenografts included "nude" mice, which lack mature CD4+ and CD8+ T cells (44) and severe combined immunodeficiency (SCID) mice, which harbor a mutation in the protein kinase, DNA-activated, catalytic polypeptide gene (Prkdcscid) and lack mature T and B cells (45). The ability of these strains to support long-term, systemic reconstitution with human cells were, however, limited by relatively high residual levels of innate immune responses, such as those mediated by natural killer (NK) cells resulting in the rejection of human bone-marrow allographs (46). Improved levels of immunodeficiency were found in strains lacking mature B and T lymphocytes due to disruptions in the recombination-activating genes Rag1 and Rag2 (47, 48), that were further augmented in mice also harboring a complete null mutation of the common cytokine receptor γ chain (IL2Rγ, or γc), resulting in the absence of mouse NK cells (49–51). As a result, modern HIS mouse models are typically produced by engrafting human hematopoietic stem cells (hHSCs), human peripheral mononuclear cells, and/or human tissues into these highly immunodeficient strains following their preconditioning with sublethal irradiation or chemotherapy. The main platforms in use include NSG (NOD-scid IL2Rγnull and NOD.Cg-PrkdcscidIL-2Rγtm1Wjll/Sz) (52), NRG (NOD-Rag1−/−IL2RγC-null), NOG (NOD.Cg-Prkdcscid IL-2Rγtm1Sug), and BRG (BALB/c-Rag2null IL-2Rγnull) strains (24, 53). Although important differences in the extent of humanization and functional quality of the populating human cells exist between models, multilineage reconstitution with hHSCs can include all major human lymphocyte classes (CD4+ and CD8+ T cells, B cells, and NK cells) as well as various myeloid cells (monocytes, macrophages, and dendritic cells). In those strains of mice that support human T-cell development when transplanted with human CD34+ hHSCs, T cell maturation occurs in the murine thymus (52, 54, 55). When humanized mice are engineered by implanting human thymus and liver tissue, developing T cells are educated on human thymic epithelial cells, allowing for restriction by human leukocyte antigens (HLAs) I and II (56, 57). The bone marrow–liver–thymus (BLT) mouse model, which combines the implantation of fetal liver and thymus under the kidney capsule of NOD/SCID, NSG, or C57BL/6 Rag2−/− IL2γ−/− mice, along with the transplant of autologous CD34+ hHSCs is the most complete and well explored (58–60). The technical demands of this system are associated with considerable expense, and the need to surgically implant each mouse can result in significant variation in HIS repopulation (61). However, with their strong lymph node and intestinal reconstitution, BLT mice are particularly useful for the study of HIV-1 infection at mucosal surfaces (62–64). Modern HIS mouse models provide stable

human cellular reconstitution that can support HIV-1 replication in the peripheral blood and multiple organs (27), allowing them to provide insights into many aspects of HIV-1 biology including viral life cycle and innate and adaptive immune responses to HIV-1 (59, 62, 65–68). Viral suppression with clinically relevant cART (69–73) has been demonstrated in HIS mice, and they have proven effective for the investigation of multiple immune-based approaches for the *in vivo* control of viral replication and elimination of HIV-infected cells (74–78).

HIS MODELS FOR THE STUDY OF HIV-1 NEUROPATHOGENESIS AND RESPONSE TO TREATMENT

Early neuroAIDS mouse models involved the generation of HIVE through the direct injection of human microglia or macrophages into the brain of SCID mice (79, 80). While the resultant SCID-HIVE model recapitulates some of the neuropathological features of human HIVE, these approaches are traumatic and result in xenoreactivity induced-inflammation through the artificial insertion of human cells into a foreign mouse cellular environment (81). Despite these caveats, studies investigating the impact of cART in this model have demonstrated reductions in neuropathological features of HIVE including decreased astro- and micro-gliosis and reductions in HIV-1 brain viral loads (82–84). Subsequent development of the humanized mouse model, in which NSG mice are engrafted with CD34+ hHSCs (CD34+-NSG mice), has allowed for more detailed, prolonged studies of HIV-1 CNS infection and neurodegeneration in the context of unchecked HIV-1 replication (85). Systemic HIV-1 infection in this model is characterized by low CNS viral burdens and the transmigration of HIV-infected human monocytes and macrophages into the mouse CNS. These human cells localize predominantly to the meninges, perivascular spaces, and, to a lesser extent, brain parenchyma (85–88). Regional activation of resident murine microglia and astrocytes, neuroinflammation, and neurodegeneration are also among the salient findings in this model (85, 86, 89). Some of these changes were reversible by long-acting nanoparticle-based cART (90). More recently, pre- and post-infection dosing with a novel sonic hedgehog mimetic was found to increase BBB integrity in acutely infected CD34+-NSG mice, resulting in decreased leukocyte extravasation into CNS during and pathologic evidence of neuroprotection (91). Finally, a simplified HIS model generated by the intraperitoneal (IP) injection of human PBMCs into non-irradiated NSG mice (NSG-huPBL) has recently been described (92). In this model, IP challenge with HIV-1 resulted in systemic viral infection and CNS invasion with infected CD4+ T cells. The presence of neuropathology—characterized by neurodegeneration, activated microglia, and astrocytes—was found to be dependent on the infecting viral strain (93). A brief summary of currently available HIS mouse models with published data on HIV-1 CNS infection can be found in **Table 1**.

HIS MODELS IN ELUCIDATING THE ROLE OF MYELOID CELLS IN HIV-1 CNS PERSISTENCE

Monocytes and macrophages can be infected with HIV-1 both *in vitro* and *in vivo* (94–96). However, the question of whether cells of myeloid lineage serve as true HIV-1 reservoirs in the context of suppressive cART remains of great interest (97). This

TABLE 1 | HIS mouse models with published studies of human immunodeficiency virus-type 1 (HIV-1) infection of the central nervous system (CNS).

HIS mouse model (reference)	Method of generation	Salient CNS findings in response to HIV-1 infection
Severe combined immunodeficiency (SCID)–HIV encephalitis (HIVE) (79–84)	Direct injection of HIV-1-infected human microglia or macrophages into the brain of SCID mice	Measurable HIV-1 brain viral load and neuropathological features of HIVE including astrogliosis and microgliosis. Reduction in CNS pathology in response to combination antiretroviral therapy (cART).
NSG-huPBL (93)	Intraperitoneal injection of human donor PBMCs into non-irradiated NSG mice	HIV-1-infected human CD4+ T cells present in meninges and cortex of infected animals. Appearance of neurodegeneration, microgliosis, and astrogliosis dependent on infecting viral strain.
CD34+-NSG (85, 86, 89–91, 105)	NSG mice transplanted with human CD34+ hematopoietic stem cells (hCD34+)	Low CNS viral burdens, transmigration of HIV-infected human monocytes and macrophages into the mouse CNS, regional activation of resident murine microglia and astrocytes, neuroinflammation, and neurodegeneration. Reduction in CNS pathology with long-acting nanoparticle-based cART. Increased blood–brain barrier integrity in acutely infected CD34+-NSG mice and decreased leukocyte extravasation into CNS following treatment with a novel sonic hedgehog mimetic.
CD34+-NSG (+hNPC) (133)	NSG mice transplanted with hCD34+ combined with intraventricular injection of neural progenitor cells	Detection of human glia in diverse brain regions of HIS mice including periventricular areas, white matter tracts and brain stem. Mice infected with HIV-1 display glial transcriptional signatures and viral defense signaling pathways that mirror human disease.
Myeloid-only mice (60)	NOD/SCID mice transplanted with hCD34+	HIV-1 DNA and RNA as well as macrophages expressing HIV-1 p24 detected in the brains of infected animals.
DRAG (121)	NRG mice expressing human leukocyte antigen (HLA) class II (DR4) transplanted with HLA-matched hHSC	HIV-1 replication in brain following mucosal infection.

question is central to the study of HIV-1 persistence in the CNS as perivascular monocyte-derived macrophages and parenchymal microglia are the most important cellular targets of HIV-1 in the CNS (98), and infection of these cell types is critical to HIV-1 CNS pathogenesis and HAND (99). Recent evidence suggesting that macrophages may become positive for viral DNA through the capture and phagocytosis of infected CD4+ T cells implies a mechanism of infection distinct from virological synapse formation and furthers the debate (100, 101). Recent study in the T cell only mouse in which implantation of autologous human fetal liver and thymus under the kidney capsule of an NSG mouse results in systemic reconstitution almost exclusively with human T cells predictably demonstrates the development of latent T cell reservoirs of HIV-1 (102). Complementary studies by Honeycutt et al. in myeloid-only mice (MoM) in which NOD/SCID mice transplanted with CD34+ hHSCs are reconstituted with human myeloid and B cells in the absence of human T cells have proven informative. Using this novel HIS model, Honeycutt et al. demonstrated that macrophages can support efficient HIV-1 replication *in vivo* in multiple compartments in the absence of T cells following infection with certain macrophage-tropic (M-tropic) HIV-1 strains such as HIV-1 ADA. HIV-1 DNA and RNA as well as macrophages expressing HIV-1 p24 were detected in the brains of infected MoM (60). In addition, cessation of suppressive cART in MoM resulted in measurable *in vivo* viral rebound after 7 weeks (103) supporting infection of long-lived tissue macrophage populations (104). Another recent study in CD34+-NSG mice infected with M-tropic HIV-1 found evidence for CD14+CD16+ monocyte/macrophage cells with HIV-1 RNA and integrated proviral DNA in the spleen and bone marrow. Consistent with previous reports in this model, viral RNA was detected in the brains in a few animals at low copy numbers (105). As a result, HIS mouse models have proven utility in defining cellular sites for HIV-1 infection and hold promise for further elucidating the viral dynamics of the establishment and recrudescence of potential CNS-based HIV-1 reservoirs.

CURRENT CHALLENGES AND ADVANCES IN HIS MODELS FOR THE STUDY OF HIV-1 IN THE CNS

Although they represent powerful research tools, limitations to the use of HIS mice for the *in vivo* study of HIV-1 exist. HIS models do not perfectly recapitulate human hematopoiesis and can display a relatively short lifespan, particularly after the approximately 8- to 18-week period needed for appropriate engraftment (43). Variability in the efficiency of human cell engraftment is an important challenge to robust experimentation. In addition, despite the fact that most HIS mouse models have demonstrated highly effective adaptive T-cell immune responses, the majority of models display an absence of species-specific human cytokines and impaired B-cell function and humoral immune responses (55, 106–108). This is important, as one proposed mechanism for the pathology induced in the CNS in response to HIV-1 infection is an abnormal cytokine/chemokine response (16). Another important limitation of currently available HIS mouse models is the frequent development of graft-versus-host disease (GVHD), characterized by multiorgan lymphocytic infiltration and sclerosis in the weeks following hHSC transplant (109). This is an important limitation to the study of HIV-1 in the CNS in particular, as longer-term experiments are necessary to demonstrate productive infection of the CNS by HIV-1 and CNS pathology in animals naïve to and under cART and/or putative adjunct therapeutics. Several research groups are working to improve the functionality of HIS mouse models in response to these limitations. Lavender et al. have described the evaluation of GVHD-resistant triple knockout (TKO) mice, which lack CD47 in addition to Rag 1 and IL2rg. These TKO-BLT mice reportedly remained healthy for 45 weeks post-humanization and could be virally suppressed on cART (110). Additional efforts to improve HIS mouse platforms have included the depletion of endogenous mouse macrophages (111) and the development of strains expressing human cytokines for improved human NK-cell development (112, 113). HIS models with improved development of HLA-restricted human T cells have been achieved through engraftment of HLA-matched hHSC into immunodeficient mice with transgenic expression of human HLA molecules (114). Huang et al. have reported the development of a novel HIS mouse model utilizing recombinant adeno-associated virus-based gene transfer technologies (115) to introduce genes encoding HLA-A2/DR and selected human cytokines into NSG mice. The ability of this resultant HIS mouse model to endogenously encode for human MHC constitutively during its lifespan and key human cytokines during development of lymphoid and myeloid progenitor cells allows for an accurate recapitulation of many aspects of the human immune system. This is reflected in highly functional human CD4+ and CD8+T-cell and B-cell responses (116, 117) as well as the successful reconstitution of human monocytes (CD14+) and macrophages (CD14+/CD11b+) (117). These HIS mice can be productively infected with HIV-1 (118) and have the ability to secrete measurable human IFN-γ, IL-2, CCL3, and IL-1β *in vivo* in response to parasitic and viral pathogens (117–120). With high rates of engraftment and low rates of GVHD, this model can be a useful tool for the study of potentially important viral reservoirs of HIV-1 in the CNS. In a similar vein, Kim et al. have recently reported the use of immunodeficient mice expressing HLA class II (DR4) (DRAG mice) engrafted with HLA-matched hHSCs to study early HIV-1 infection. The authors report HIV-1 replication in various tissues, including bone marrow, lymph nodes, and the brain, which on day 21 following mucosal infection, was the last tissue examined to become HIV-1 viral RNA positive (121). Finally, infiltrating human myeloid cells and lymphocytes have been demonstrated in the brains of HIV-1 infected HIS mice (85). However, the generation of models harboring functional human myeloid cells in percentages approximating those seen in humans has been challenging. In several HIS platforms, strategies to improve human myeloid cell reconstitution include the administration of exogenous human Flt3 ligand (122), exogenous delivery of human granulocyte-macrophage colony-stimulating factor (GM-CSF) and IL-4 (123, 124), and human GM-CSF and IL-3 knock-in (125, 126).

Limitations of HIS mouse models that are of unique interest to the study of HIV-1 in the CNS exist as well. Common to all

HIS mouse models is the absence of human microglia in the CNS (127)—a major deficiency as microglia represent one of the most important cellular targets of HIV-1 in the brain (98). Unfortunately, engrafted CD34+ hHSCs are unlikely to repopulate human microglial cells within the brains of HIS mice, as microglial cells are derived early during development from yolk sack precursors (127). Additionally, human glia (astrocytes and oligodendrocytes)—the most abundant cell types in the human CNS—are absent in the majority of HIS mouse models (128). As a result, these platforms are unable to recapitulate innate glial cell responses resulting from the complex interactions between human glia and infected mononuclear phagocytes during progressive HIV-1 infection (129, 130). In response, several groups have attempted to reconstitute HIS mouse brain with neonatally transplanted human glial progenitor cells (131, 132). Following such interventions, Li et al. reported the detection of human glia in diverse brain regions of HIS mice including periventricular areas, white matter tracts, and brain stem. RNA-sequencing in the selected brain regions of such mice infected with M-tropic HIV-1 reportedly display glial transcriptional signatures and viral defense signaling pathways that mirror human disease (133–136). Although this approach does not repopulate the brain with human microglia, such experimental improvements are welcome and will allow for the improved modeling of human HIV-1 CNS neuropathological disease.

CONCLUSION

Human immune system (HIS) mouse models have proven to be extremely valuable tools for the study of HIV-1 infection of the CNS, its resulting neuropathology and the potential for HIV-1 persistence in this immunologically privileged compartment. As with all model systems, experimental and biologic limitations exist. These include the absence of human CNS cell types that in response to HIV-1 invasion play key roles in the development of the neuroinflammatory milieu and impaired immune, glial, and neural cell functions leading to HAND. However, model improvements are ongoing, with the general aims of preventing GVHD and enhancing the levels, reproducibility, and quality of human immune cell reconstitution. The rational evolution of these models will continue to foster authentic human immune responses in HIS mouse models and will further facilitate development of diagnostic, novel therapeutic, and viral eradication strategies for HIV-1 in the CNS.

AUTHOR CONTRIBUTIONS

TE and MT contributed to the conception, writing, and discussion of this review manuscript. TE wrote the initial draft of the manuscript. The final version of the manuscript was approved by both authors.

FUNDING

This work was supported by the Mark S. Bertuch AIDS Research Fund (#554400), Leidos, Inc. (P010148091 and P010173450) and The Rockefeller University Bernard L. Schwartz Program for Physician Scientists.

REFERENCES

1. Gottlieb MS, Schroff R, Schanker HM, Weisman JD, Fan PT, Wolf RA, et al. *Pneumocystis carinii* pneumonia and mucosal candidiasis in previously healthy homosexual men: evidence of a new acquired cellular immunodeficiency. *N Engl J Med* (1981) 305(24):1425–31. doi:10.1056/NEJM198112103052401
2. UNAIDS. *UNAIDS Fact Sheet November 2016. Global HIV Statistics*. Geneva: UNAIDS (2016).
3. Chun TW, Stuyver L, Mizell SB, Ehler LA, Mican JA, Baseler M, et al. Presence of an inducible HIV-1 latent reservoir during highly active antiretroviral therapy. *Proc Natl Acad Sci U S A* (1997) 94(24):13193–7. doi:10.1073/pnas.94.24.13193
4. Finzi D, Hermankova M, Pierson T, Carruth LM, Buck C, Chaisson RE, et al. Identification of a reservoir for HIV-1 in patients on highly active antiretroviral therapy. *Science* (1997) 278(5341):1295–300. doi:10.1126/science.278.5341.1295
5. Wong JK, Hezareh M, Gunthard HF, Havlir DV, Ignacio CC, Spina CA, et al. Recovery of replication-competent HIV despite prolonged suppression of plasma viremia. *Science* (1997) 278(5341):1291–5. doi:10.1126/science.278.5341.1291
6. Pilcher CD, Shugars DC, Fiscus SA, Miller WC, Menezes P, Giner J, et al. HIV in body fluids during primary HIV infection: implications for pathogenesis, treatment and public health. *AIDS* (2001) 15(7):837–45. doi:10.1097/00002030-200105040-00004
7. Schacker T, Collier AC, Hughes J, Shea T, Corey L. Clinical and epidemiologic features of primary HIV infection. *Ann Intern Med* (1996) 125(4):257–64. doi:10.7326/0003-4819-125-4-199608150-00001
8. Haase AT. Pathogenesis of lentivirus infections. *Nature* (1986) 322(6075):130–6. doi:10.1038/322130a0
9. Dahiya S, Irish BP, Nonnemacher MR, Wigdahl B. Genetic variation and HIV-associated neurologic disease. *Adv Virus Res* (2013) 87:183–240. doi:10.1016/B978-0-12-407698-3.00006-5
10. Collman R, Balliet JW, Gregory SA, Friedman H, Kolson DL, Nathanson N, et al. An infectious molecular clone of an unusual macrophage-tropic and highly cytopathic strain of human immunodeficiency virus type 1. *J Virol* (1992) 66(12):7517–21.
11. Spudich S, Gonzalez-Scarano F. HIV-1-related central nervous system disease: current issues in pathogenesis, diagnosis, and treatment. *Cold Spring Harb Perspect Med* (2012) 2(6):a007120. doi:10.1101/cshperspect.a007120
12. Koenig S, Gendelman HE, Orenstein JM, Dal Canto MC, Pezeshkpour GH, Yungbluth M, et al. Detection of AIDS virus in macrophages in brain tissue from AIDS patients with encephalopathy. *Science* (1986) 233(4768):1089–93. doi:10.1126/science.3016903
13. Hagberg L, Fuchs D, Rosengren L, Gisslen M. Intrathecal immune activation is associated with cerebrospinal fluid markers of neuronal destruction in AIDS patients. *J Neuroimmunol* (2000) 102(1):51–5. doi:10.1016/S0165-5728(99)00150-2
14. Williams KC, Hickey WF. Central nervous system damage, monocytes and macrophages, and neurological disorders in AIDS. *Annu Rev Neurosci* (2002) 25:537–62. doi:10.1146/annurev.neuro.25.112701.142822
15. Garden GA. Microglia in human immunodeficiency virus-associated neurodegeneration. *Glia* (2002) 40(2):240–51. doi:10.1002/glia.10155
16. Kaul M, Garden GA, Lipton SA. Pathways to neuronal injury and apoptosis in HIV-associated dementia. *Nature* (2001) 410(6831):988–94. doi:10.1038/35073667
17. Budka H. Multinucleated giant cells in brain: a hallmark of the acquired immune deficiency syndrome (AIDS). *Acta Neuropathol* (1986) 69(3–4):253–8. doi:10.1007/BF00688301

18. Petito CK, Cho ES, Lemann W, Navia BA, Price RW. Neuropathology of acquired immunodeficiency syndrome (AIDS): an autopsy review. *J Neuropathol zExp Neurol* (1986) 45(6):635–46. doi:10.1097/00005072-198611000-00003
19. McArthur JC. HIV dementia: an evolving disease. *J Neuroimmunol* (2004) 157(1–2):3–10. doi:10.1016/j.jneuroim.2004.08.042
20. Heaton RK, Franklin DR, Ellis RJ, McCutchan JA, Letendre SL, Leblanc S, et al. HIV-associated neurocognitive disorders before and during the era of combination antiretroviral therapy: differences in rates, nature, and predictors. *J Neurovirol* (2011) 17(1):3–16. doi:10.1007/s13365-010-0006-1
21. Jaeger LB, Nath A. Modeling HIV-associated neurocognitive disorders in mice: new approaches in the changing face of HIV neuropathogenesis. *Dis Model Mech* (2012) 5(3):313–22. doi:10.1242/dmm.008763
22. Gelman BB, Endsley J, Kolson D. When do models of NeuroAIDS faithfully imitate "the real thing"? *J Neurovirol* (2017). doi:10.1007/s13365-017-0601-5
23. Hatziioannou T, Evans DT. Animal models for HIV/AIDS research. *Nat Rev Microbiol* (2012) 10(12):852–67. doi:10.1038/nrmicro2911
24. Marsden MD, Zack JA. Humanized mouse models for human immunodeficiency virus infection. *Annu Rev Virol* (2017) 4(1):393–412. doi:10.1146/annurev-virology-101416-041703
25. Harbison C, Zhuang K, Gettie A, Blanchard J, Knight H, Didier P, et al. Giant cell encephalitis and microglial infection with mucosally transmitted simian-human immunodeficiency virus SHIVSF162P3N in rhesus macaques. *J Neurovirol* (2014) 20(1):62–72. doi:10.1007/s13365-013-0229-z
26. Zink MC, Amedee AM, Mankowski JL, Craig L, Didier P, Carter DL, et al. Pathogenesis of SIV encephalitis. Selection and replication of neurovirulent SIV. *Am J Pathol* (1997) 151(3):793–803.
27. Masse-Ranson G, Mouquet H, Di Santo JP. Humanized mouse models to study pathophysiology and treatment of HIV infection. *Curr Opin HIV AIDS* (2018) 13(2):143–51. doi:10.1097/COH.0000000000000440
28. Shibata R, Kawamura M, Sakai H, Hayami M, Ishimoto A, Adachi A. Generation of a chimeric human and simian immunodeficiency virus infectious to monkey peripheral blood mononuclear cells. *J Virol* (1991) 65(7):3514–20.
29. Morrow WJ, Wharton M, Lau D, Levy JA. Small animals are not susceptible to human immunodeficiency virus infection. *J Gen Virol* (1987) 68(Pt 8):2253–7. doi:10.1099/0022-1317-68-8-2253
30. Kopp JB, Klotman ME, Adler SH, Bruggeman LA, Dickie P, Marinos NJ, et al. Progressive glomerulosclerosis and enhanced renal accumulation of basement membrane components in mice transgenic for human immunodeficiency virus type 1 genes. *Proc Natl Acad Sci U S A* (1992) 89(5):1577–81. doi:10.1073/pnas.89.5.1577
31. Browning J, Horner JW, Pettoello-Mantovani M, Raker C, Yurasov S, DePinho RA, et al. Mice transgenic for human CD4 and CCR5 are susceptible to HIV infection. *Proc Natl Acad Sci U S A* (1997) 94(26):14637–41. doi:10.1073/pnas.94.26.14637
32. Hanna Z, Kay DG, Rebai N, Guimond A, Jothy S, Jolicoeur P. Nef harbors a major determinant of pathogenicity for an AIDS-like disease induced by HIV-1 in transgenic mice. *Cell* (1998) 95(2):163–75. doi:10.1016/S0092-8674(00)81748-1
33. Leonard JM, Abramczuk JW, Pezen DS, Rutledge R, Belcher JH, Hakim F, et al. Development of disease and virus recovery in transgenic mice containing HIV proviral DNA. *Science* (1988) 242(4886):1665–70. doi:10.1126/science.3201255
34. Seay K, Qi X, Zheng JH, Zhang C, Chen K, Dutta M, et al. Mice transgenic for CD4-specific human CD4, CCR5 and cyclin T1 expression: a new model for investigating HIV-1 transmission and treatment efficacy. *PLoS One* (2013) 8(5):e63537. doi:10.1371/journal.pone.0063537
35. Toggas SM, Masliah E, Rockenstein EM, Rall GF, Abraham CR, Mucke L. Central nervous system damage produced by expression of the HIV-1 coat protein gp120 in transgenic mice. *Nature* (1994) 367(6459):188–93. doi:10.1038/367188a0
36. Kim BO, Liu Y, Ruan Y, Xu ZC, Schantz L, He JJ. Neuropathologies in transgenic mice expressing human immunodeficiency virus type 1 Tat protein under the regulation of the astrocyte-specific glial fibrillary acidic protein promoter and doxycycline. *Am J Pathol* (2003) 162(5):1693–707. doi:10.1016/S0002-9440(10)64304-0
37. Potash MJ, Chao W, Bentsman G, Paris N, Saini M, Nitkiewicz J, et al. A mouse model for study of systemic HIV-1 infection, antiviral immune responses, and neuroinvasiveness. *Proc Natl Acad Sci U S A* (2005) 102(10):3760–5. doi:10.1073/pnas.0500649102
38. Okamoto S, Kang YJ, Brechtel CW, Siviglia E, Russo R, Clemente A, et al. HIV/gp120 decreases adult neural progenitor cell proliferation via checkpoint kinase-mediated cell-cycle withdrawal and G1 arrest. *Cell Stem Cell* (2007) 1(2):230–6. doi:10.1016/j.stem.2007.07.010
39. Lee MH, Wang T, Jang MH, Steiner J, Haughey N, Ming GL, et al. Rescue of adult hippocampal neurogenesis in a mouse model of HIV neurologic disease. *Neurobiol Dis* (2011) 41(3):678–87. doi:10.1016/j.nbd.2010.12.002
40. Mucke L, Masliah E, Campbell IL. Transgenic models to assess the neuropathogenic potential of HIV-1 proteins and cytokines. *Curr Top Microbiol Immunol* (1995) 202:187–205.
41. Fitting S, Ignatowska-Jankowska BM, Bull C, Skoff RP, Lichtman AH, Wise LE, et al. Synaptic dysfunction in the hippocampus accompanies learning and memory deficits in human immunodeficiency virus type-1 Tat transgenic mice. *Biol Psychiatry* (2013) 73(5):443–53. doi:10.1016/j.biopsych.2012.09.026
42. Saylor D, Dickens AM, Sacktor N, Haughey N, Slusher B, Pletnikov M, et al. HIV-associated neurocognitive disorder – pathogenesis and prospects for treatment. *Nat Rev Neurol* (2016) 12(4):234–48. doi:10.1038/nrneurol.2016.27
43. Denton PW, Sogaard OS, Tolstrup M. Using animal models to overcome temporal, spatial and combinatorial challenges in HIV persistence research. *J Transl Med* (2016) 14:44. doi:10.1186/s12967-016-0807-y
44. Flanagan SP. 'Nude', a new hairless gene with pleiotropic effects in the mouse. *Genet Res* (1966) 8(3):295–309. doi:10.1017/S0016672300010168
45. Bosma GC, Custer RP, Bosma MJ. A severe combined immunodeficiency mutation in the mouse. *Nature* (1983) 301(5900):527–30. doi:10.1038/301527a0
46. Murphy WJ, Kumar V, Bennett M. Rejection of bone marrow allografts by mice with severe combined immune deficiency (SCID). Evidence that natural killer cells can mediate the specificity of marrow graft rejection. *J Exp Med* (1987) 165(4):1212–7. doi:10.1084/jem.165.4.1212
47. Mombaerts P, Iacomini J, Johnson RS, Herrup K, Tonegawa S, Papaioannou VE. RAG-1-deficient mice have no mature B and T lymphocytes. *Cell* (1992) 68(5):869–77. doi:10.1016/0092-8674(92)90030-G
48. Shinkai Y, Rathbun G, Lam KP, Oltz EM, Stewart V, Mendelsohn M, et al. RAG-2-deficient mice lack mature lymphocytes owing to inability to initiate V(D)J rearrangement. *Cell* (1992) 68(5):855–67. doi:10.1016/0092-8674(92)90029-C
49. Cao X, Shores EW, Hu-Li J, Anver MR, Kelsall BL, Russell SM, et al. Defective lymphoid development in mice lacking expression of the common cytokine receptor gamma chain. *Immunity* (1995) 2(3):223–38. doi:10.1016/1074-7613(95)90047-0
50. DiSanto JP, Muller W, Guy-Grand D, Fischer A, Rajewsky K. Lymphoid development in mice with a targeted deletion of the interleukin 2 receptor gamma chain. *Proc Natl Acad Sci U S A* (1995) 92(2):377–81. doi:10.1073/pnas.92.2.377
51. Ohbo K, Suda T, Hashiyama M, Mantani A, Ikebe M, Miyakawa K, et al. Modulation of hematopoiesis in mice with a truncated mutant of the interleukin-2 receptor gamma chain. *Blood* (1996) 87(3):956–67.
52. Ishikawa F, Yasukawa M, Lyons B, Yoshida S, Miyamoto T, Yoshimoto G, et al. Development of functional human blood and immune systems in NOD/SCID/IL2 receptor {gamma} chain(null) mice. *Blood* (2005) 106(5):1565–73. doi:10.1182/blood-2005-02-0516
53. Shultz LD, Brehm MA, Garcia-Martinez JV, Greiner DL. Humanized mice for immune system investigation: progress, promise and challenges. *Nat Rev Immunol* (2012) 12(11):786–98. doi:10.1038/nri3311
54. Shultz LD, Lyons BL, Burzenski LM, Gott B, Chen X, Chaleff S, et al. Human lymphoid and myeloid cell development in NOD/LtSz-scid IL2R gamma null mice engrafted with mobilized human hemopoietic stem cells. *J Immunol* (2005) 174(10):6477–89. doi:10.4049/jimmunol.174.10.6477
55. Traggiai E, Chicha L, Mazzucchelli L, Bronz L, Piffaretti JC, Lanzavecchia A, et al. Development of a human adaptive immune system in cord blood cell-transplanted mice. *Science* (2004) 304(5667):104–7. doi:10.1126/science.1093933
56. Olesen R, Wahl A, Denton PW, Garcia JV. Immune reconstitution of the female reproductive tract of humanized BLT mice and their susceptibility to human immunodeficiency virus infection. *J Reprod Immunol* (2011) 88(2):195–203. doi:10.1016/j.jri.2010.11.005

57. Wege AK, Melkus MW, Denton PW, Estes JD, Garcia JV. Functional and phenotypic characterization of the humanized BLT mouse model. *Curr Top Microbiol Immunol* (2008) 324:149–65. doi:10.1007/978-3-540-75647-7_10
58. Lan P, Tonomura N, Shimizu A, Wang S, Yang YG. Reconstitution of a functional human immune system in immunodeficient mice through combined human fetal thymus/liver and CD34+ cell transplantation. *Blood* (2006) 108(2):487–92. doi:10.1182/blood-2005-11-4388
59. Melkus MW, Estes JD, Padgett-Thomas A, Gatlin J, Denton PW, Othieno FA, et al. Humanized mice mount specific adaptive and innate immune responses to EBV and TSST-1. *Nat Med* (2006) 12(11):1316–22. doi:10.1038/nm1431
60. Honeycutt JB, Wahl A, Baker C, Spagnuolo RA, Foster J, Zakharova O, et al. Macrophages sustain HIV replication in vivo independently of T cells. *J Clin Invest* (2016) 126(4):1353–66. doi:10.1172/JCI84456
61. Nixon CC, Mavigner M, Silvestri G, Garcia JV. In vivo models of human immunodeficiency virus persistence and cure strategies. *J Infect Dis* (2017) 215(Suppl_3):S142–51. doi:10.1093/infdis/jiw637
62. Sun Z, Denton PW, Estes JD, Othieno FA, Wei BL, Wege AK, et al. Intrarectal transmission, systemic infection, and CD4+ T cell depletion in humanized mice infected with HIV-1. *J Exp Med* (2007) 204(4):705–14. doi:10.1084/jem.20062411
63. Denton PW, Estes JD, Sun Z, Othieno FA, Wei BL, Wege AK, et al. Antiretroviral pre-exposure prophylaxis prevents vaginal transmission of HIV-1 in humanized BLT mice. *PLoS Med* (2008) 5(1):e16. doi:10.1371/journal.pmed.0050016
64. Wahl A, Swanson MD, Nochi T, Olesen R, Denton PW, Chateau M, et al. Human breast milk and antiretrovirals dramatically reduce oral HIV-1 transmission in BLT humanized mice. *PLoS Pathog* (2012) 8(6):e1002732. doi:10.1371/journal.ppat.1002732
65. Gorantla S, Sneller H, Walters L, Sharp JG, Pirruccello SJ, West JT, et al. Human immunodeficiency virus type 1 pathobiology studied in humanized BALB/c-Rag2-/-gammac-/- mice. *J Virol* (2007) 81(6):2700–12. doi:10.1128/JVI.02010-06
66. Brainard DM, Seung E, Frahm N, Cariappa A, Bailey CC, Hart WK, et al. Induction of robust cellular and humoral virus-specific adaptive immune responses in human immunodeficiency virus-infected humanized BLT mice. *J Virol* (2009) 83(14):7305–21. doi:10.1128/JVI.02207-08
67. Dudek TE, No DC, Seung E, Vrbanac VD, Fadda L, Bhoumik P, et al. Rapid evolution of HIV-1 to functional CD8(+) T cell responses in humanized BLT mice. *Sci Transl Med* (2012) 4(143):143ra98. doi:10.1126/scitranslmed.3003984
68. Rongvaux A, Takizawa H, Strowig T, Willinger T, Eynon EE, Flavell RA, et al. Human hemato-lymphoid system mice: current use and future potential for medicine. *Annu Rev Immunol* (2013) 31:635–74. doi:10.1146/annurev-immunol-032712-095921
69. Denton PW, Krisko JF, Powell DA, Mathias M, Kwak YT, Martinez-Torres F, et al. Systemic administration of antiretrovirals prior to exposure prevents rectal and intravenous HIV-1 transmission in humanized BLT mice. *PLoS One* (2010) 5(1):e8829. doi:10.1371/journal.pone.0008829
70. Denton PW, Olesen R, Choudhary SK, Archin NM, Wahl A, Swanson MD, et al. Generation of HIV latency in humanized BLT mice. *J Virol* (2012) 86(1):630–4. doi:10.1128/JVI.06120-11
71. Horwitz JA, Halper-Stromberg A, Mouquet H, Gitlin AD, Tretiakova A, Eisenreich TR, et al. HIV-1 suppression and durable control by combining single broadly neutralizing antibodies and antiretroviral drugs in humanized mice. *Proc Natl Acad Sci U S A* (2013) 110(41):16538–43. doi:10.1073/pnas.1315295110
72. Kovarova M, Council OD, Date AA, Long JM, Nochi T, Belshan M, et al. Nanoformulations of rilpivirine for topical pericoital and systemic coitus-independent administration efficiently prevent HIV transmission. *PLoS Pathog* (2015) 11(8):e1005075. doi:10.1371/journal.ppat.1005075
73. Nischang M, Sutmuller R, Gers-Huber G, Audige A, Li D, Rochat MA, et al. Humanized mice recapitulate key features of HIV-1 infection: a novel concept using long-acting anti-retroviral drugs for treating HIV-1. *PLoS One* (2012) 7(6):e38853. doi:10.1371/journal.pone.0038853
74. Sango K, Joseph A, Patel M, Osiecki K, Dutta M, Goldstein H. Highly active antiretroviral therapy potently suppresses HIV infection in humanized Rag2-/-gammac-/- mice. *AIDS Res Hum Retroviruses* (2010) 26(7):735–46. doi:10.1089/aid.2009.0136
75. Diskin R, Klein F, Horwitz JA, Halper-Stromberg A, Sather DN, Marcovecchio PM, et al. Restricting HIV-1 pathways for escape using rationally designed anti-HIV-1 antibodies. *J Exp Med* (2013) 210(6):1235–49. doi:10.1084/jem.20130221
76. Denton PW, Long JM, Wietgrefe SW, Sykes C, Spagnuolo RA, Snyder OD, et al. Targeted cytotoxic therapy kills persisting HIV infected cells during ART. *PLoS Pathog* (2014) 10(1):e1003872. doi:10.1371/journal.ppat.1003872
77. Halper-Stromberg A, Lu CL, Klein F, Horwitz JA, Bournazos S, Nogueira L, et al. Broadly neutralizing antibodies and viral inducers decrease rebound from HIV-1 latent reservoirs in humanized mice. *Cell* (2014) 158(5):989–99. doi:10.1016/j.cell.2014.07.043
78. Klein F, Halper-Stromberg A, Horwitz JA, Gruell H, Scheid JF, Bournazos S, et al. HIV therapy by a combination of broadly neutralizing antibodies in humanized mice. *Nature* (2012) 492(7427):118–22. doi:10.1038/nature11604
79. Persidsky Y, Limoges J, McComb R, Bock P, Baldwin T, Tyor W, et al. Human immunodeficiency virus encephalitis in SCID mice. *Am J Pathol* (1996) 149(3):1027–53.
80. Poluektova LY, Munn DH, Persidsky Y, Gendelman HE. Generation of cytotoxic T cells against virus-infected human brain macrophages in a murine model of HIV-1 encephalitis. *J Immunol* (2002) 168(8):3941–9. doi:10.4049/jimmunol.168.8.3941
81. Persidsky Y, Buttini M, Limoges J, Bock P, Gendelman HE. An analysis of HIV-1-associated inflammatory products in brain tissue of humans and SCID mice with HIV-1 encephalitis. *J Neurovirol* (1997) 3(6):401–16. doi:10.3109/13550289709031186
82. Cook JE, Dasgupta S, Middaugh LD, Terry EC, Gorry PR, Wesselingh SL, et al. Highly active antiretroviral therapy and human immunodeficiency virus encephalitis. *Ann Neurol* (2005) 57(6):795–803. doi:10.1002/ana.20479
83. Cook-Easterwood J, Middaugh LD, Griffin WC III, Khan I, Tyor WR. Highly active antiretroviral therapy of cognitive dysfunction and neuronal abnormalities in SCID mice with HIV encephalitis. *Exp Neurol* (2007) 205(2):506–12. doi:10.1016/j.expneurol.2007.03.007
84. Koneru R, Olive MF, Tyor WR. Combined antiretroviral therapy reduces brain viral load and pathological features of HIV encephalitis in a mouse model. *J Neurovirol* (2014) 20(1):9–17. doi:10.1007/s13365-013-0223-5
85. Gorantla S, Makarov E, Finke-Dwyer J, Castanedo A, Holguin A, Gebhart CL, et al. Links between progressive HIV-1 infection of humanized mice and viral neuropathogenesis. *Am J Pathol* (2010) 177(6):2938–49. doi:10.2353/ajpath.2010.100536
86. Boska MD, Dash PK, Knibbe J, Epstein AA, Akhter SP, Fields N, et al. Associations between brain microstructures, metabolites, and cognitive deficits during chronic HIV-1 infection of humanized mice. *Mol Neurodegener* (2014) 9:58. doi:10.1186/1750-1326-9-58
87. Marsden MD, Zack JA. Studies of retroviral infection in humanized mice. *Virology* (2015) 479-480:297–309. doi:10.1016/j.virol.2015.01.017
88. Akkina R, Allam A, Balazs AB, Blankson JN, Burnett JC, Casares S, et al. Improvements and limitations of humanized mouse models for HIV research: NIH/NIAID "meet the experts" 2015 workshop summary. *AIDS Res Hum Retroviruses* (2016) 32(2):109–19. doi:10.1089/AID.2015.0258
89. Dash PK, Gorantla S, Gendelman HE, Knibbe J, Casale GP, Makarov E, et al. Loss of neuronal integrity during progressive HIV-1 infection of humanized mice. *J Neurosci* (2011) 31(9):3148–57. doi:10.1523/JNEUROSCI.5473-10.2011
90. Dash PK, Gendelman HE, Roy U, Balkundi S, Alnouti Y, Mosley RL, et al. Long-acting nanoformulated antiretroviral therapy elicits potent antiretroviral and neuroprotective responses in HIV-1-infected humanized mice. *AIDS* (2012) 26(17):2135–44. doi:10.1097/QAD.0b013e328357f5ad
91. Singh VB, Singh MV, Piekna-Przybylska D, Gorantla S, Poluektova LY, Maggirwar SB. Sonic hedgehog mimetic prevents leukocyte infiltration into the CNS during acute HIV infection. *Sci Rep* (2017) 7(1):9578. doi:10.1038/s41598-017-10241-0
92. Kim KC, Choi BS, Kim KC, Park KH, Lee HJ, Cho YK, et al. A simple mouse model for the study of human immunodeficiency virus. *AIDS Res Hum Retroviruses* (2016) 32(2):194–202. doi:10.1089/AID.2015.0211
93. Wu X, Liu L, Cheung KW, Wang H, Lu X, Cheung AK, et al. Brain invasion by CD4(+) T cells infected with a transmitted/founder HIV-1BJZS7 during acute stage in humanized mice. *J Neuroimmune Pharmacol* (2016) 11(3):572–83. doi:10.1007/s11481-016-9654-0

94. Embretson J, Zupancic M, Ribas JL, Burke A, Racz P, Tenner-Racz K, et al. Massive covert infection of helper T lymphocytes and macrophages by HIV during the incubation period of AIDS. *Nature* (1993) 362(6418):359–62. doi:10.1038/362359a0
95. Gendelman HE, Orenstein JM, Martin MA, Ferrua C, Mitra R, Phipps T, et al. Efficient isolation and propagation of human immunodeficiency virus on recombinant colony-stimulating factor 1-treated monocytes. *J Exp Med* (1988) 167(4):1428–41. doi:10.1084/jem.167.4.1428
96. Ho DD, Rota TR, Hirsch MS. Infection of monocyte/macrophages by human T lymphotropic virus type III. *J Clin Invest* (1986) 77(5):1712–5. doi:10.1172/JCI112491
97. Merino KM, Allers C, Didier ES, Kuroda MJ. Role of monocyte/macrophages during HIV/SIV infection in adult and pediatric acquired immune deficiency syndrome. *Front Immunol* (2017) 8:1693. doi:10.3389/fimmu.2017.01693
98. Persidsky Y, Poluektova L. Immune privilege and HIV-1 persistence in the CNS. *Immunol Rev* (2006) 213:180–94. doi:10.1111/j.1600-065X.2006.00440.x
99. Joseph SB, Arrildt KT, Sturdevant CB, Swanstrom R. HIV-1 target cells in the CNS. *J Neurovirol* (2015) 21(3):276–89. doi:10.1007/s13365-014-0287-x
100. Baxter AE, Russell RA, Duncan CJ, Moore MD, Willberg CB, Pablos JL, et al. Macrophage infection via selective capture of HIV-1-infected CD4+ T cells. *Cell Host Microbe* (2014) 16(6):711–21. doi:10.1016/j.chom.2014.10.010
101. Calantone N, Wu F, Klase Z, Deleage C, Perkins M, Matsuda K, et al. Tissue myeloid cells in SIV-infected primates acquire viral DNA through phagocytosis of infected T cells. *Immunity* (2014) 41(3):493–502. doi:10.1016/j.immuni.2014.08.014
102. Honeycutt JB, Wahl A, Archin N, Choudhary S, Margolis D, Garcia JV. HIV-1 infection, response to treatment and establishment of viral latency in a novel humanized T cell-only mouse (TOM) model. *Retrovirology* (2013) 10:121. doi:10.1186/1742-4690-10-121
103. Honeycutt JB, Thayer WO, Baker CE, Ribeiro RM, Lada SM, Cao Y, et al. HIV persistence in tissue macrophages of humanized myeloid-only mice during antiretroviral therapy. *Nat Med* (2017) 23(5):638–43. doi:10.1038/nm.4319
104. Stevenson M. HIV persistence in macrophages. *Nat Med* (2017) 23(5):538–9. doi:10.1038/nm.4337
105. Arainga M, Su H, Poluektova LY, Gorantla S, Gendelman HE. HIV-1 cellular and tissue replication patterns in infected humanized mice. *Sci Rep* (2016) 6:23513. doi:10.1038/srep23513
106. Brehm MA, Shultz LD, Luban J, Greiner DL. Overcoming current limitations in humanized mouse research. *J Infect Dis* (2013) 208(Suppl 2):S125–30. doi:10.1093/infdis/jit319
107. Karpel ME, Boutwell CL, Allen TM. BLT humanized mice as a small animal model of HIV infection. *Curr Opin Virol* (2015) 13:75–80. doi:10.1016/j.coviro.2015.05.002
108. Martinez-Torres F, Nochi T, Wahl A, Garcia JV, Denton PW. Hypogammaglobulinemia in BLT humanized mice – an animal model of primary antibody deficiency. *PLoS One* (2014) 9(10):e108663. doi:10.1371/journal.pone.0108663
109. Greenblatt MB, Vrbanac V, Tivey T, Tsang K, Tager AM, Aliprantis AO. Graft versus host disease in the bone marrow, liver and thymus humanized mouse model. *PLoS One* (2012) 7(9):e44664. doi:10.1371/journal.pone.0044664
110. Lavender KJ, Pace C, Sutter K, Messer RJ, Pouncey DL, Cummins NW, et al. An advanced BLT-humanized mouse model for extended HIV-1 cure studies. *AIDS* (2018) 32(1):1–10. doi:10.1097/QAD.0000000000001674
111. Hu Z, Van Rooijen N, Yang YG. Macrophages prevent human red blood cell reconstitution in immunodeficient mice. *Blood* (2011) 118(22):5938–46. doi:10.1182/blood-2010-11-321414
112. Huntington ND, Alves NL, Legrand N, Lim A, Strick-Marchand H, Mention JJ, et al. IL-15 transpresentation promotes both human T-cell reconstitution and T-cell-dependent antibody responses in vivo. *Proc Natl Acad Sci U S A* (2011) 108(15):6217–22. doi:10.1073/pnas.1019167108
113. Huntington ND, Legrand N, Alves NL, Jaron B, Weijer K, Plet A, et al. IL-15 trans-presentation promotes human NK cell development and differentiation in vivo. *J Exp Med* (2009) 206(1):25–34. doi:10.1084/jem.20082013
114. Shultz LD, Saito Y, Najima Y, Tanaka S, Ochi T, Tomizawa M, et al. Generation of functional human T-cell subsets with HLA-restricted immune responses in HLA class I expressing NOD/SCID/IL2r gamma(null) humanized mice. *Proc Natl Acad Sci U S A* (2010) 107(29):13022–7. doi:10.1073/pnas.1000475107
115. Flotte TR, Carter BJ. Adeno-associated virus vectors for gene therapy. *Gene Ther* (1995) 2(6):357–62.
116. Huang J, Li X, Coelho-dos-Reis JG, Wilson JM, Tsuji M. An AAV vector-mediated gene delivery approach facilitates reconstitution of functional human CD8+ T cells in mice. *PLoS One* (2014) 9(2):e88205. doi:10.1371/journal.pone.0088205
117. Huang J, Li X, Coelho-dos-Reis JG, Zhang M, Mitchell R, Nogueira RT, et al. Human immune system mice immunized with *Plasmodium falciparum* circumsporozoite protein induce protective human humoral immunity against malaria. *J Immunol Methods* (2015) 427:42–50. doi:10.1016/j.jim.2015.09.005
118. Saito A, Henning MS, Serrao E, Dubose BN, Teng S, Huang J, et al. Capsid-CPSF6 interaction is dispensable for HIV-1 replication in primary cells but is selected during virus passage in vivo. *J Virol* (2016) 90(15):6918–35. doi:10.1128/JVI.00019-16
119. Li X, Huang J, Zhang M, Funakoshi R, Sheetij D, Spaccapelo R, et al. Human CD8+ T cells mediate protective immunity induced by a human malaria vaccine in human immune system mice. *Vaccine* (2016) 34(38):4501–6. doi:10.1016/j.vaccine.2016.08.006
120. Sharma A, Wu W, Sung B, Huang J, Tsao T, Li X, et al. Respiratory syncytial virus (RSV) pulmonary infection in humanized mice induces human anti-RSV immune responses and pathology. *J Virol* (2016) 90(10):5068–74. doi:10.1128/JVI.00259-16
121. Kim J, Peachman KK, Jobe O, Morrison EB, Allam A, Jagodzinski L, et al. Tracking human immunodeficiency virus-1 infection in the humanized DRAG mouse model. *Front Immunol* (2017) 8:1405. doi:10.3389/fimmu.2017.01405
122. Li Y, Mention JJ, Court N, Masse-Ranson G, Toubert A, Spits H, et al. A novel Flt3-deficient HIS mouse model with selective enhancement of human DC development. *Eur J Immunol* (2016) 46(5):1291–9. doi:10.1002/eji.201546132
123. Chen Q, Khoury M, Chen J. Expression of human cytokines dramatically improves reconstitution of specific human-blood lineage cells in humanized mice. *Proc Natl Acad Sci U S A* (2009) 106(51):21783–8. doi:10.1073/pnas.0912274106
124. Chen Q, He F, Kwang J, Chan JK, Chen J. GM-CSF and IL-4 stimulate antibody responses in humanized mice by promoting T, B, and dendritic cell maturation. *J Immunol* (2012) 189(11):5223–9. doi:10.4049/jimmunol.1201789
125. Willinger T, Rongvaux A, Takizawa H, Yancopoulos GD, Valenzuela DM, Murphy AJ, et al. Human IL-3/GM-CSF knock-in mice support human alveolar macrophage development and human immune responses in the lung. *Proc Natl Acad Sci U S A* (2011) 108(6):2390–5. doi:10.1073/pnas.1019682108
126. Saito Y, Ellegast JM, Rafiei A, Song Y, Kull D, Heikenwalder M, et al. Peripheral blood CD34(+) cells efficiently engraft human cytokine knock-in mice. *Blood* (2016) 128(14):1829–33. doi:10.1182/blood-2015-10-676452
127. Ginhoux F, Lim S, Hoeffel G, Low D, Huber T. Origin and differentiation of microglia. *Front Cell Neurosci* (2013) 7:45. doi:10.3389/fncel.2013.00045
128. Windrem MS, Schanz SJ, Morrow C, Munir J, Chandler-Militello D, Wang S, et al. A competitive advantage by neonatally engrafted human glial progenitors yields mice whose brains are chimeric for human glia. *J Neurosci* (2014) 34(48):16153–61. doi:10.1523/JNEUROSCI.1510-14.2014
129. Gorantla S, Poluektova L, Gendelman HE. Rodent models for HIV-associated neurocognitive disorders. *Trends Neurosci* (2012) 35(3):197–208. doi:10.1016/j.tins.2011.12.006
130. Oberheim NA, Takano T, Han X, He W, Lin JH, Wang F, et al. Uniquely hominid features of adult human astrocytes. *J Neurosci* (2009) 29(10):3276–87. doi:10.1523/JNEUROSCI.4707-08.2009
131. Han X, Chen M, Wang F, Windrem M, Wang S, Shanz S, et al. Forebrain engraftment by human glial progenitor cells enhances synaptic plasticity and learning in adult mice. *Cell Stem Cell* (2013) 12(3):342–53. doi:10.1016/j.stem.2012.12.015
132. Uchida N, Buck DW, He D, Reitsma MJ, Masek M, Phan TV, et al. Direct isolation of human central nervous system stem cells. *Proc Natl Acad Sci U S A* (2000) 97(26):14720–5. doi:10.1073/pnas.97.26.14720
133. Li W, Gorantla S, Gendelman HE, Poluektova LY. Systemic HIV-1 infection produces a unique glial footprint in humanized mouse brains. *Dis Model Mech* (2017) 10(12):1489–502. doi:10.1242/dmm.031773

134. Gelman BB, Chen T, Lisinicchia JG, Soukup VM, Carmical JR, Starkey JM, et al. The national NeuroAIDS tissue consortium brain gene array: two types of HIV-associated neurocognitive impairment. *PLoS One* (2012) 7(9):e46178. doi:10.1371/journal.pone.0046178
135. Sanfilippo C, Pinzone MR, Cambria D, Longo A, Palumbo M, Di Marco R, et al. OAS gene family expression is associated with HIV-related neurocognitive disorders. *Mol Neurobiol* (2018) 55(3):1905–14. doi:10.1007/s12035-017-0460-3
136. Sanna PP, Repunte-Canonigo V, Masliah E, Lefebvre C. Gene expression patterns associated with neurological disease in human HIV infection. *PLoS One* (2017) 12(4):e0175316. doi:10.1371/journal.pone.0175316

Conflict of Interest Statement: The authors declare that the research was conducted in the absence of any commercial or financial relationships that could be construed as a potential conflict of interest.

frontiers in Immunology

REVIEW
published: 19 April 2018
doi: 10.3389/fimmu.2018.00807

Humanized Mouse Models for the Study of Human Malaria Parasite Biology, Pathogenesis, and Immunity

*Nana K. Minkah[1], Carola Schafer[1] and Stefan H. I. Kappe[1,2]**

[1] Center for Infectious Disease Research, Seattle, WA, United States, [2] Department of Global Health, University of Washington, Seattle, WA, United States

Malaria parasite infection continues to inflict extensive morbidity and mortality in resource-poor countries. The insufficiently understood parasite biology, continuously evolving drug resistance and the lack of an effective vaccine necessitate intensive research on human malaria parasites that can inform the development of new intervention tools. Humanized mouse models have been greatly improved over the last decade and enable the direct study of human malaria parasites *in vivo* in the laboratory. Nevertheless, no small animal model developed so far is capable of maintaining the complete life cycle of *Plasmodium* parasites that infect humans. The ultimate goal is to develop humanized mouse systems in which a *Plasmodium* infection closely reproduces all stages of a parasite infection in humans, including pre-erythrocytic infection, blood stage infection and its associated pathology, transmission as well as the human immune response to infection. Here, we discuss current humanized mouse models and the future directions that should be taken to develop next-generation models for human malaria parasite research.

Keywords: *Plasmodium falciparum*, humanized mouse models, FRG human hepatocyte, human immune system mice, malaria vaccines

OPEN ACCESS

Edited by:
Ramesh Akkina, Colorado State University, United States

Reviewed by:
Richard Culleton, Nagasaki University, Japan
Stasya Zarling, Walter Reed Army Institute of Research, United States

****Correspondence:***
Stefan H. I. Kappe
stefan.kappe@cidresearch.org

Specialty section:
This article was submitted to Vaccines and Molecular Therapeutics, a section of the journal Frontiers in Immunology

Received: *15 December 2017*
Accepted: *03 April 2018*
Published: *19 April 2018*

Citation:
Minkah NK, Schafer C and Kappe SHI (2018) Humanized Mouse Models for the Study of Human Malaria Parasite Biology, Pathogenesis, and Immunity. Front. Immunol. 9:807. doi: 10.3389/fimmu.2018.00807

MALARIA: DISEASE BURDEN, PARASITE LIFE CYCLE, NATURAL IMMUNITY, AND THE DEVELOPMENT OF A MALARIA VACCINE

Malaria, a disease caused by protozoan *Plasmodium* parasites, causes more than 200 million clinical cases annually and is responsible for more than 400,000 deaths each year, mainly in children under the age of 5 and pregnant women living in the resource-poor countries of sub-Saharan Africa. In humans, the majority of malaria infections are caused by *Plasmodium falciparum* and *Plasmodium vivax*. In more temperate regions of the world, socioeconomic development, vector control programs, and the use of antimalarial chemotherapeutics have driven successful malaria elimination. However, declines in malaria infections have been slowest in tropical, resource-poor countries with a high malaria burden necessitating the development of new effective antimalaria therapeutics and vaccines that will prevent infection, disease, and onward transmission.

Transmission of malaria parasites to the mammalian host begins with the deposition of the infectious, motile sporozoite stages into the skin via the bite of infected mosquitoes (1–3). Sporozoites initially traverse multiple cell types in the skin in search of capillaries to gain access to the bloodstream within which they are transported to the liver (3). Each sporozoite infects a hepatocyte, then transforms into a liver stage that undergoes growth, genome replication, and differentiation into tens of thousands of red blood cell (RBC) infectious exo-erythrocytic merozoites. In humans,

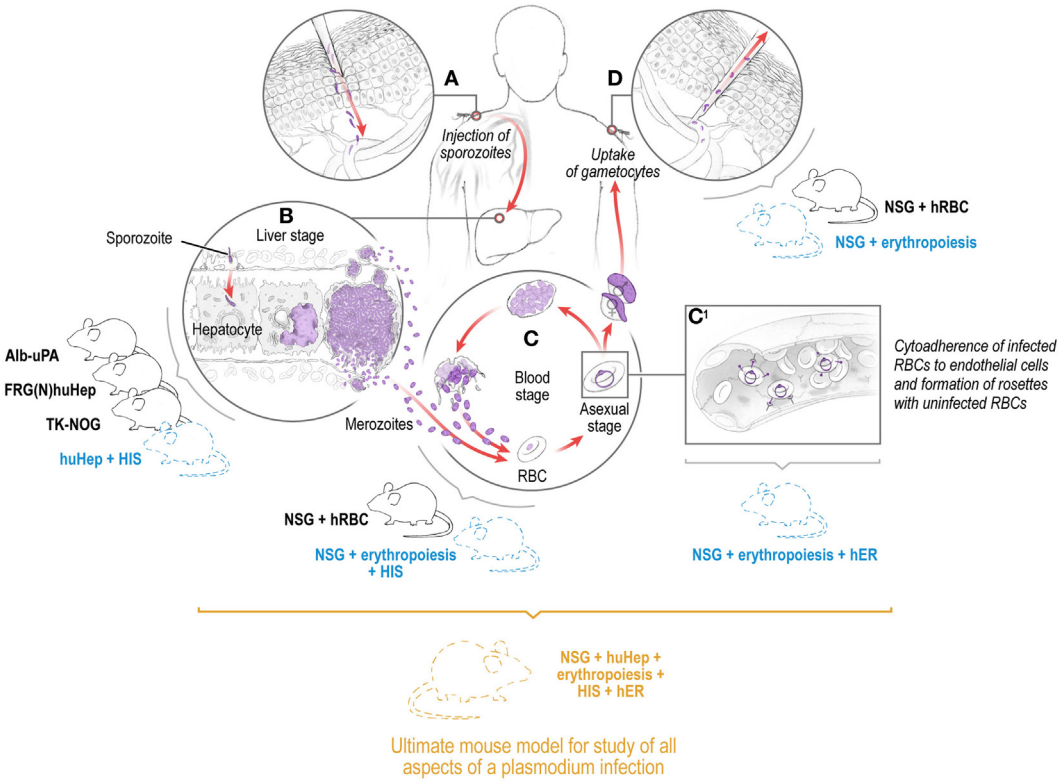

FIGURE 1 | Depiction of the *Plasmodium* life cycle in humans showing the skin, liver, and blood stages with the corresponding existing (solid lines) and future (dashed lines) humanized mouse systems to model each of the individual stages and eventually the full *Plasmodium* life cycle including pathology and transmission. Infection is initiated when a female *Anopheles* mosquito injects saliva-containing sporozoites into the skin. Sporozoites traverse dermal cells and gain access to the blood **(A)**. The highly motile sporozoites transit to the liver where each sporozoite infects a single hepatocyte **(B)**. One to two weeks after hepatocyte invasion, merozoites exit the liver and begin a 48-h cycle of red blood cell (RBC) invasion, replication, RBC rupture, and new merozoite release **(C)**. During RBC infection, the parasite expresses variant surface antigens on the surface of the infected red blood cell, which interacts with human endothelial receptors (hER), thus mediating the binding of infected RBCs to the microvascular endothelium of various organs **(C[1])**. A small number of blood-stage parasites differentiate into sexual gametocytes, which are taken up by mosquitoes in blood meals to continue the transmission to new human hosts **(D)**.

merozoites are released from the liver into the bloodstream 7–10 days after initial transmission where they infect RBCs, replicate within, and are released to undergo continuous cycles of infection, replication, and release, allowing parasite numbers to reach billions within weeks (**Figure 1**). In *P. vivax* infection, a subset of sporozoites form persistent liver stages (hypnozoites) that activate at later time points to cause relapsing blood stage (BS) infections (4, 5). All symptoms associated with malaria are caused by BS infection, and this is in large part due to the massive destruction of RBCs but also the sequestration of infected RBCs in the microvasculature (6). This sequestration can occur in a tissue-specific manner, leading, for example, to cerebral malaria pathology through sequestration of infected RBCs in the brain or pregnancy associated malaria due to sequestration of infected RBCs in the placenta. Uptake of parasite sexual forms in a blood meal leads to infection of the mosquito, sporogonic development, and colonization of salivary glands by sporozoites, which ensures transmission to new human hosts (7, 8) (**Figure 1**).

Repeated *Plasmodium* infection does not result in complete immunity, rendering populations in endemic regions continuously susceptible to infection, malaria-associated morbidity and mortality as well as transmission. A fully protective malaria vaccine has yet to be developed (9). Moreover, evolution of parasite resistance to frontline antimalarial drugs necessitates continuous research and development of next-generation antimalarials (10). These efforts require robust experimental systems that accurately model human malaria parasite biology, immunology, and pathogenesis. Given the tropism of the human *Plasmodium* species for human hepatocytes (huHeps) and RBCs, researchers have relied on *in vitro* infection models for human parasites to query malaria biology and identify targets of intervention. In this review, we will discuss how blood, tissue, and immune system-humanized mouse models can provide novel avenues to examine human malaria parasites. Humanized mice and their past use in malaria research have been reviewed recently (11, 12). Therefore, in this review, we will focus more on critical research gaps in our understanding of human malaria parasite biology, pathology, and immunology that might be addressed in humanized mouse models and improvements to these models that are needed to achieve this. We will also reflect on the role of next-generation multi-compartment-humanized mice in the modeling of the complete *Plasmodium* life cycle in physiologically relevant human cells and tissues.

PRE-ERYTHROCYTIC (PE) *Plasmodium* INFECTION: BIOLOGY OF TRANSMISSION - THE SKIN AND LIVER STAGES

The sporozoite and liver stages comprise the PE stage of infection. Unlike the BSs, the PE stages are asymptomatic, are small in numbers during natural infection, and are not as antigenically variant. These characteristics render them extremely attractive targets for malaria intervention (13). Dissimilar to the BSs, the PE stages of *P. falciparum* cannot be easily generated in the laboratory and although some aspects of human infection can be modeled *in vitro*, these systems have limitations. Therefore, most of our knowledge on PE biology has been derived from studies of rodent malaria parasites, which were originally isolated from wild African rodents and subsequently adapted to laboratory mice (14–16). For transmission research, the biology of skin infection between different rodent parasite species (*Plasmodium yoelii* and *Plasmodium berghei*) made it attractive to speculate that parasite behavior in the skin should be similar in *Plasmodium* species that infected humans. However, the recent identification of the development of exo-erythrocytic merozoites in the skin of *P. berghei*-infected mice (17) but not in *P. yoelii*-infected mice (18) identified one point of divergence even within these two closely allied parasite species. Thus, whether the development of skin exo-erythrocytic merozoites occurs in human *Plasmodium* parasites remains an open question, as preventive therapeutics targeted to the liver stage might be ineffective in the skin. Given that this skin stage of infection can only be adequately modeled within the three-dimensional architecture of the skin tissue, recent advances in the engraftment of human skin into immunodeficient mice (19) represent an exciting opportunity to examine interaction of human parasites with human skin components *in vivo* and an opportunity to explore the occurrence and relevance of "skin exo-erythrocytic merozoites" in *Plasmodium* parasites that infect humans.

Each sporozoite that reaches the liver invades a single hepatocyte, transforms into a trophic stage, and then commences liver stage development (also called exo-erythrocytic development). Traditional rodent malaria models have been critical to the identification of host hepatocyte surface factors necessary for sporozoite invasion (7, 20). Recently, human liver-chimeric mice have been employed to examine the contribution of these invasion factors in human malaria parasite liver infection (21). The efficient engraftment of huHeps into mice is dependent on an environment of severe immunodeficiency to limit huHep rejection coupled with the elimination of mouse hepatocytes to provide the huHep a niche in the liver parenchyma. Three different mouse models have been utilized for huHep engraftment and have been used to assess liver stage infection by *Plasmodium* parasites infecting humans. The SCID Alb-uPA model expresses the toxic urokinase plasminogen activator (uPA) under the control of an albumin promoter in the livers of the highly immunodeficient *S*evere *C*ombined *I*mmune *D*eficiency mice (SCID Alb-uPA). Upon engraftment with huHeps, these mice become susceptible to infection with *P. falciparum* sporozoites and support complete liver stage development including the release of exo-erythrocytic merozoites that egress and invade human RBCs (huRBCs) *ex vivo* (22, 23). An alternate to the induction of hepatotoxicity by uPA transgene expression is genetic ablation of *fumarylacetoacetate hydrolase* (FAH) in mice resulting in acute liver failure which can be rescued by administration of the drug, 2-(2-nitro-4-fluoromethlbenzoyl)-1,-3-cyclohexanedione (NTBC). Crossing these FAH$^{-/-}$ mice onto the severely immunocompromised C57BL/6 Rag2$^{-/-}$IL2r$\gamma^{-/-}$ mouse generated FAH$^{-/-}$Rag2$^{-/-}$IL2rg$^{-/-}$ (FRG) mice. These mice have also been backcrossed onto the non-obese diabetic (NOD) background (FRGN), which additionally renders them hospitable to transplantation with CD34^{+} hematopoietic stem cells (HSCs) (24). Using NTBC cycling during engraftment, these mice can exhibit over 90% engraftment with huHeps (FRG huHep) (25), are susceptible to infection with both *P. falciparum* and *P. vivax* sporozoites (26, 27) and support full liver stage development, including the release of exo-erythrocytic merozoites capable of invading huRBCs that were infused into the mice. When infected with *P. vivax*, FRG huHep mice also harbor non-replicating hypnozoites (27). More recently, the TK-NOG (NOD/Shi-scid/IL2rg$^{-/-}$) mouse has been developed as yet another model for *P. falciparum* PE infection (28). These mice express the herpes simplex virus thymidine kinase transgene under the control of the albumin promoter on the NOD SCID IL2r$\gamma^{-/-}$ background. Destruction of mouse hepatocytes is achieved by treatment with ganciclovir, allowing repopulation of the liver with huHeps. TK-NOG mice support *P. falciparum* and *Plasmodium ovale* sporozoite infection and liver stage development (28).

Anti-PE *Plasmodium* IMMUNITY AND VACCINE DEVELOPMENT: FROM TRADITIONAL MOUSE MODELS TO HUMAN CLINICAL TRIAL

The pronounced human host cell tropism of malaria parasites that infect humans precludes infection of the traditional immunology workhorse, the in-bred mouse. Thus, the rodent malaria parasites, *P. yoelii* and *P. berghei* have been extensively utilized because they allow a careful examination of PE immunity. Perhaps the greatest contribution of the rodent malaria models is in the examination of immunity and protection against an infectious sporozoite challenge after vaccination with whole, attenuated sporozoites. Attenuation was originally generated by gamma irradiation (29) but can now be achieved by genetic engineering with the precise removal of genes from the parasite genome (30, 31) or by treatment of an infectious sporozoite immunization with drugs that prevent BS infection (32, 33). Over the last decade, studies utilizing whole sporozoite infection of mice have identified roles for humoral immunity (3, 34–37) and both peripheral and tissue-resident memory CD8 T cells in the protective response to immunization (13, 38–41). Previously thought to be immunologically silent, liver stage *Plasmodium* infection also induces an innate immune response (42–45). The pathways by which this innate immune response is induced and the influence it has on the ensuing adaptive immune response are areas of active investigation.

Although traditional rodent models of PE infection have been useful, differences in rodent and human *Plasmodium* species (46)

compounded with significant divergence in rodent and human hosts presents significant implications for the extrapolation of results achieved with the former to the latter, particularly with regard to host–parasite interactions and immunity. Also, while the liver stages of rodent *Plasmodium* species develop fully within 2–3 days, the human *Plasmodium* parasites undergo 7–10 days of liver stage development before exiting the liver to infect erythrocytes. In addition, none of the rodent parasites form persistent liver stages that could model those found in *P. vivax* infection, affirming that PE biology in the rodent is not an ideal model for human malaria infection. Human clinical trials have identified robust induction of both humoral and cellular immune responses after whole sporozoite immunization yet unequivocal identification of correlates of protection from these studies has proven to be challenging. To reconcile divergent observations, functional *in vitro* assays have been developed such as the examination of immune sera and its inhibitory activity on infection of cultured hepatoma cell lines with sporozoites (47–49). Yet, *in vitro* cultured cells do not accurately model the complex architecture of the liver tissue, rendering them only partially physiologically relevant as infection assays. In addition, tissue-resident memory T cells, which have been shown to be critical in the control of liver stages in rodent malaria infection, do not recirculate into the blood stream (40), impeding the examination of their contribution to PE immunity after *P. falciparum* immunization of humans. Peripheral T cell populations that correlate with protection have been identified in rodent *Plasmodium* models (50). However, no *ex vivo* assays exist to robustly quantify CD8 T cell killing of hepatocytes or the augmentation of humoral and cellular immune responses by CD4 T cells. Thus, many questions remain regarding the relevance of these cell populations for protection in humans.

HUMANIZED MICE TO MODEL PE IMMUNITY

Given the lack of robust *ex vivo* and *in vitro* assays to functionally examine human immune responses to *Plasmodium* infection and immunization with candidate vaccines, the identification of true correlates of protection will require the development of animal models that better mimic human *Plasmodium* infection. Traditionally, this role has been occupied by non-human primates (NHP) where *Plasmodium* infection better mirrors observations made in humans. Numerous NHP species support infection by *Plasmodium* species that occur in simians and some NHP support direct infection with *P. falciparum* and *P. vivax* (51). Moreover, the immune response in NHP is similar to humans and tissue-resident immune populations can be sampled to query their importance to vaccine-engendered protection (52). However, NHP systems are still not a perfect model for human *Plasmodium* infection, and in addition to ethical and financial barriers, logistical concerns regarding housing requirements for NHPs have curtailed their use in malaria research. Thus, the development of immunodeficient mice that have been engrafted with functional human immune cells and human tissues will enable the examination of infection in human cells and tissues in the context of human immune responses *in vivo* within a small animal model.

Human liver-chimeric mice can play important roles to study functionality of human immune responses. They might serve as an important and cheaper alternative to NHP models in the final down-selection of antibody-based vaccine antigens. For example, we and others have utilized these mice to demonstrate that the passive transfer of human monoclonal antibodies or polyclonal sera from humans immunized with whole *P. falciparum* sporozoites, blocks liver infection (53–55). Of note, mosquito bite challenge of FRG huHep mice after passive transfer allowed superior discrimination of antibody-mediated protection as compared to established *in vitro* assays. However, given the absence of an adaptive immune response in these mice, active immunization experiments cannot be carried out.

To analyze intrinsic human immune responses, human immune system (HIS) mice have been developed that enable the direct analysis of the HIS responses *in vivo* after infection with human pathogens or after vaccination. HIS mice are generated by the transplantation of human $CD34^+$ cells containing HSCs into immunodeficient NOG or NSG mice, to model relatively normal human immune responses (56). Huang and colleagues have recently pioneered the generation of HIS mice that possess functional human CD4, human CD8, and human B cell responses (57, 58) for the study of PE immunity. To generate humanized mice with a competent human humoral response (referred to as HIS-CD4/B mice), immunocompromised NSG mice were transduced with recombinant adeno-associated virus (AAV) vectors encoding human HLA class II (HLA DR1 or HLA DR4) and a cocktail of human cytokines followed by engraftment with human $CD34^+$ cells (58). To examine the ability of these HIS-CD4/B mice to mount a protective humoral response, HIS-CD4/B mice were first immunized with recombinant *P. falciparum* circumsporozoite protein (CSP) and then subsequently challenged with a transgenic *P. berghei* parasite encoding the repeat regions of *P. falciparum* CSP. Immunized HIS-CD4/B mice exhibited high titers of circulating *P. falciparum* CSP antibodies and showed reduced parasite liver burden after challenge as compared with naïve controls (58).

Given the importance of CD8 T cells in PE-engendered protection in rodent models of *Plasmodium* infection, Huang and colleagues also generated a humanized CD8 T cell mice referred to as HIS-CD8 (57) by transducing NSG mice with AAV vectors encoding functional HLA-A*0201 and a cocktail of human cytokines. Immunization of HIS-CD8 mice with AAV vectors bearing *P. falciparum* CSP resulted in an induction of HLA-restricted human CD8 T cells. These immunized HIS-CD8 mice greatly reduced parasite burden in the liver after challenge with transgenic *P. berghei* parasites encoding full length *P. falciparum* CSP (59). Importantly, *in vivo* depletion of human CD8 T cells completely abolished the reduction in liver burden in immunized HIS-CD8 mice (60).

These HIS studies, however, only support challenge with transgenic rodent malaria parasites expressing selected *P. falciparum* proteins. Thus, there is a need to combine humanized liver-chimeric mice with the HIS models to generate dual-chimeric mice (HIS huHep) susceptible to human *Plasmodium* liver infection and

capable of driving functional human immune responses. However, such a model will not yet completely replicate human immunity because although liver-chimeric mice can be repopulated with high levels of huHeps, their liver sinusoidal endothelial cells, Kupffer cells, hepatic stellate cells, and cells of the myeloid lineage all remain of mouse origin. In rodent malaria systems, $CD8^+$ dendritic cells have been shown to be critical to the generation of an effective immune response after whole sporozoite immunization (61, 62). In addition, in *P. berghei*-infected mice, IFNAR expression on myeloid cells is critical for the propagation of the innate immune response to whole parasite infection (42). What roles these cells play in the effective PE immune response to human whole sporozoite immunization remains unknown. Finally, given the importance of liver-resident memory CD8 T cells in PE immunity (38–40), it will be important to examine whether HIS-CD8 mice recapitulate the critical roles of tissue-resident cells observed in rodent malaria studies.

HUMANIZED MICE TO MODEL MALARIA BS INFECTION

Although *P. falciparum* BSs can be cultured *in vitro*, a small animal model of human BS malaria would offer great advantages, as it would allow the preclinical testing of drugs and vaccine candidates in an *in vivo* setting against the human pathogen. The liver-chimeric mice described above support liver infection and liver stage-to-BS transition after injection of target huRBCs (27, 63). The presence of huRBCs on the day of exo-erythrocytic merozoite egress from the liver leads to a short period of low parasitemia, and these parasites can then be removed and maintained in huRBC culture. However, BS infection cannot be maintained in the mice as huRBCs are rapidly cleared. Fortunately, different immune-modulation protocols combined with daily injections of huRBCs can support high engraftment levels and promote a continuous *P. falciparum* BS infection in NSG mice (64). These mice show sequestration of the parasite in bone marrow and spleen, suggesting it might resemble the behavior of the parasite in humans. One drawback is that in this study the mice were directly infected with BS parasites, as they are not human liver-chimeric. Moreover, as *P. falciparum* gametocytes take 10–14 days to mature, this is the time span the infected RBC has to be maintained to allow transmission back to the mosquito. If this is achieved, the model might enable the study of transmission in an *in vivo* setting and might allow the testing of transmission blocking drugs and vaccines before moving on to clinical trials. Our laboratory has recently developed a robust protocol to engraft and maintain huRBCs in human liver-chimeric mice to better assess the efficacy of transmission blocking small molecules, antibodies and vaccines (65). Another promising application for combined huHep/huRBC mice is the preclinical evaluation of safety of attenuated *P. falciparum* whole sporozoite vaccine candidates, allowing for exquisite sensitivity in detecting potential breakthrough infection into the blood before testing of new attenuated strains in human trials (66). Furthermore, combined huHep/huRBC mice have been successfully used for the recovery of recombinant parasite progeny from *P. falciparum* genetic crosses. Previously, such genetic crosses had to be carried out in splenectomized chimpanzees, but it was recently reported that recombinant progeny can also be recovered from FRG huHep mice that had been injected with huRBCs at the time point of merozoite egress from the liver (67). The option to perform genetic crosses in a small animal model provides a robust avenue for forward genetics research and a new avenue to determine the underlying traits of *P. falciparum* drug resistance and other phenotypes of clinical importance.

Whereas *P. falciparum* BSs can be easily cultured *in vitro*, all efforts to establish a long-term *in vitro* culture for *P. vivax* have so far met with limited success. Therefore, research on this widespread parasite would especially benefit from a small animal infection model. The distinct feature of *P. vivax* BS parasites is the strong preference for $CD71^+$ reticulocytes (68). These are highly immature erythrocytes that are mainly found in the bone marrow. Consequently, high amounts of *P. vivax* ring stage infected cells are also found in the bone marrow (69). To establish a humanized mouse model that will propagate *P. vivax* BS infection, mice will have to be engrafted with these rare cells. Reticulocytes account for only 0.5–2% of peripheral blood, of which only a very small fraction are $CD71^+$. Higher numbers of $CD71^+$ cells are found in umbilical cord blood (UCB) and enriched reticulocytes from UCB have been successfully used for in *P. vivax in vitro* BS invasion assays (70). It remains to be determined whether the amount of target cells in mice engrafted with the enriched reticulocyte fraction from UCB would be sufficient to propagate a *P. vivax* infection. One avenue to achieve high numbers of $CD71^+$ reticulocytes is to differentiate human HSCs into erythroid precursor cells. These cells should closely resemble *P. vivax* target cells and therefore might support a *P. vivax* BS infection *in vivo*. Encouragingly, infection of FRG huHep mice with *P. vivax* sporozoites leads to development of liver stages that undergo full schizogony and release exo-erythrocytic merozoites. When provided with reticulocyte target cells at the time points of release, infection of and development of asexual BSs was observed (27). FRG huHep mice also support hypnozoite persistence, giving hope that a combined liver and blood model for *P. vivax* could one day enable the routine study of relapsing infection (27).

The repeated injection of huRBCs, combined with different immunomodulatory protocols, is a cumbersome process, necessitating an experienced researcher and often leading to losses of mice. An elegant alternative to repeated huRBC reconstitution would be a mouse that intrinsically sustains human erythropoiesis after HSC transplantation. Especially regarding the cell tropism of *P. vivax* described above, a model in which human erythropoiesis takes place in the bone marrow would hopefully provide a setting in which *P. vivax* BSs can develop. Unfortunately, in the humanized mouse models published to date, human erythropoiesis is severely impaired (71). The injection of human cytokines important for human erythropoiesis only leads to a small increase in huRBCs in the periphery (72). A mouse in which human $CD34^+$ HSC transplantation leads to robust human erythropoiesis combined with an HIS, and which in addition harbors a human-chimeric liver, would ultimately enable the production of reproducible data on the developmental life cycle of human malaria parasites. Therefore, it is a high priority goal for malaria research to develop a humanized mouse model, which intrinsically

promotes human erythropoiesis and can then be combined with one of the human liver-chimeric models described above. Such an advanced humanized mouse model would open up completely unexplored avenues of research. For example, despite its obvious importance, there is an enormous lack of knowledge in the area of *Plasmodium* coinfections with other pathogens. Malaria and HIV/AIDS especially have a wide geographical overlap, particularly in sub-Saharan Africa, and epidemiological studies have shown cross-contribution to each other's pathogenicity (73), potential antimalarial treatment failure in HIV^+ patients (74) as well as potential drug–drug interactions (75). Very little is known about the underlying molecular mechanisms of these observations, as we lack a model system to investigate them. Currently, the questions of drug–drug interactions or vaccine safety in co-infected individuals can solely be addressed in clinical trials, as carried out previously for the malaria vaccine candidate RTS, S (76). However, the advanced mouse model described above, with a human-chimeric liver, human erythropoiesis and HIS, could potentially fill this gap.

BS MALARIA PATHOLOGY IN HUMANIZED MICE

The question of whether a humanized mouse model might enable the study of *P. falciparum* malaria-associated pathophysiology remains largely unexplored. The pathology of severe malaria is mainly determined by adhesion interactions between infected erythrocytes and human endothelial cells. These adhesion interactions lead to the sequestration of infected erythrocytes in the microvasculature, which benefit the parasite by avoiding clearance in the spleen. Unfortunately, this sequestration also leads to vascular occlusion and inflammation, which are important contributors to severe malaria pathology. Three forms of adhesive interactions have been described: the cytoadherence of infected erythrocytes to endothelial cells, formation of rosettes with uninfected erythrocytes and platelet-mediated clumping of infected cells (77). These interactions are mediated by the *P. falciparum* erythrocyte membrane protein 1 (PfEMP1) family, variant antigens expressed on the surface of infected RBCs that interact with multiple host receptors, including ICAM1, CD36, E-selectin, and endothelial protein C receptor (EPCR) (78). There are approximately 60 different variants of PfEMP1, which are encoded by genes of the *var* family but only expressed one at a time. Depending on which *var* gene is expressed, the parasite modifies the antigenic properties of infected erythrocytes, which allows it to evade the host immune system but also changes the binding specificity for host receptors. *Var* gene switching is currently under extensive investigation and a small animal model allowing the controlled *in vivo* evaluation of this phenomenon would be of great benefit to this important field of research.

The most lethal complication of a *P. falciparum* infection is cerebral malaria. It has been speculated that the targeting of different receptors via the expression of different PfEMP1 variants leads to tissue-specific sequestration of the parasites. In the brain microvasculature, the EPCR has been shown to play an important role in the sequestration of parasites (79). To date, we lack any knowledge of whether infected RBCs sequester in the brain of *P. falciparum*-infected humanized mice. It is thus highly relevant to investigate whether the described pathologies of human malaria are recapitulated in any of the humanized mouse models described above. If high huRBC reconstitution and high parasitemia can be achieved in humanized mice it is likely that rosetting of infected erythrocytes will take place in a mouse model. Whether PfEMP1 molecules on infected erythrocytes interact with mouse receptors on endothelial cells remains an unanswered question, however. If this is not the case, a mouse model must be developed in which human receptors are expressed on mouse endothelial cells. If this could be achieved it would open up new possibilities for exploring the potential of anti-adhesion drugs or antibodies as novel malaria therapies.

BS MALARIA IMMUNITY IN HUMANIZED MICE

Animal models of malaria continue to provide important insights into the immune response to *Plasmodium* BS infection in general. However, the development of novel immunotherapeutic strategies against BS parasites requires a thorough investigation of the human immune response, particularly to *P. falciparum* BS infection. Our understanding of the human immune response to early BS infection, vaccination, and natural infection has been gleaned from longitudinal studies on subjects enrolled in controlled human malaria infection trials (80–82). Together with the rodent *Plasmodium* studies, two immunological processes critical for the control of BS malaria infection have been identified, namely, the inflammatory response from innate immune sensing of *Plasmodium* infections and the humoral response. *Plasmodium* pathogen-associated molecular patterns engage pattern recognition receptors on innate immune cells and trigger an inflammatory response critical for early parasite control (83, 84). However, this inflammatory response can also be pathogenic to the host. Indeed, *Plasmodium*-engendered type I IFN signaling impairs dendritic cell function in *Plasmodium chabaudi* (85) and *P. berghei*-infected mice (86) and promotes the production of the immunosuppressive cytokine, IL-10 by Tr1 cells in a human CHMI trial (87). Antibodies have long been known to play a central role in BS malaria immunity (88). Yet, over half a century later, our understanding of the parasite proteins that induce protective antibody responses, the mechanisms of *Plasmodium*-engendered humoral protection and why protective antibodies only develop after years of repeated exposure is finally maturing. Mounting evidence in rodent models and correlative data in humans from endemic regions have established that *Plasmodium* evades humoral immunity through dysregulation of $CD4^+$ T cell (89) and B cell dysfunction (90–95). Although the mechanisms behind the roles of inflammation on dendritic cell function and B cell dysfunction have been well studied in rodent models of malaria, a mouse model with a humanized immune system will be critical to confirming whether the mechanisms outlined in the rodent malaria models apply to infection with the human *P. falciparum* parasite. However, as described in preceding sections, the existing humanized mouse models will not accurately mimic a complete HIS as they still contain murine antigen presenting cells, or other murine myeloid cells. Mice that retain human

antigen presentation and human myeloid cell function will need to be developed to measure these effects.

CONCLUSION

Conventional mouse model infections with rodent malaria parasites have critically contributed to our understanding of malaria parasite biology, pathogenesis, and immunology and have been important in malaria vaccine and drug discovery. However, differences between the genomes of the human-infective and rodent-infective *Plasmodium* species as well as significant divergence between mouse and human biology might preclude facile application of knowledge gleaned from traditional rodent systems to the design of effective interventions in humans. Humanized mouse models have emerged as a critical link between traditional rodent models and humans. huHep mice will enable better examination of the factors critical for hepatocyte infection and liver stage development and the understanding of liver stage-directed, infection-preventing interventions. HIS mice are poised to greatly accelerate our understanding of the immune response to human *Plasmodium* parasites and vaccine candidates as the data gleaned from these studies will more closely represent the immune response in humans. However, current iterations of these HIS mice retain mouse myeloid compartments likely influencing antigen presentation and immune cell residency. Next-generation HIS mice for malaria research will likely require humanization of the liver, bone marrow, lymphoid compartments, and human erythrocytes. BLT (bone marrow, liver, and thymus) mice, where human fetal thymus and liver tissues as well as autologous HSCs are engrafted into the same mouse represent the most complete humanized mouse system to date (96). Combining this with huHep mice would generate the triple-humanized mouse sorely needed for the study of human malaria parasite infection and immunology. However, the high costs and technical demands of such a system will likely preclude it from being widely employed. Ultimately, future humanized mouse models for *Plasmodium* research will utilize the transplantation of $CD34^+$ HSC cells to develop robust human immune and erythropoietic compartments and hepatocyte transplantation to ensure human liver chimerism. Ideally, this mouse will in addition harbor human receptors on endothelial cells so that the pathobiology of malaria BS infection can also be modeled. As it will take great effort to create such a complete and complex mouse model, a continued iterative cycle of basic parasitological discovery and immunology in rodent malaria models combined with studies in currently available, albeit imperfect huHep, HIS, and huRBC mice will further increase the predictive value of animal models for human clinical intervention.

AUTHOR CONTRIBUTIONS

NM and CS prepared the original drafts of this manuscript with subsequent revision by SK.

ACKNOWLEDGMENTS

Work by the authors is supported by the NIH (SK: R01 AI 114699-01), the German Research Foundation (SCHA 2047/1-1), and the Bill and Melinda Gates Foundation. We thank Dr. Ashley Vaughan and Dr. Brandon Sack for helpful discussions and critical reading of this manuscript.

REFERENCES

1. Matsuoka H, Yoshida S, Hirai M, Ishii A. A rodent malaria, *Plasmodium berghei*, is experimentally transmitted to mice by merely probing of infective mosquito, *Anopheles stephensi*. *Parasitol Int* (2002) 51:17–23. doi:10.1016/S1383-5769(01)00095-2
2. Sidjanski S, Vanderberg JP. Delayed migration of *Plasmodium* sporozoites from the mosquito bite site to the blood. *Am J Trop Med Hyg* (1997) 57:426–9. doi:10.4269/ajtmh.1997.57.426
3. Vanderberg JP, Frevert U. Intravital microscopy demonstrating antibody-mediated immobilisation of *Plasmodium berghei* sporozoites injected into skin by mosquitoes. *Int J Parasitol* (2004) 34:991–6. doi:10.1016/j.ijpara.2004.05.005
4. Mendis K, Sina BJ, Marchesini P, Carter R. The neglected burden of *Plasmodium vivax* malaria. *Am J Trop Med Hyg* (2001) 64:97–106. doi:10.4269/ajtmh.2001.64.97
5. Mueller I, Galinski MR, Baird JK, Carlton JM, Kochar DK, Alonso PL, et al. Key gaps in the knowledge of *Plasmodium vivax*, a neglected human malaria parasite. *Lancet Infect Dis* (2009) 9:555–6. doi:10.1016/S1473-3099(09)70177-X
6. Miller LH, Baruch DI, Marsh K, Doumbo OK. The pathogenic basis of malaria. *Nature* (2002) 415:673–9. doi:10.1038/415673a
7. Kaushansky A, Kappe SH. Selection and refinement: the malaria parasite's infection and exploitation of host hepatocytes. *Curr Opin Microbiol* (2015) 26:71–8. doi:10.1016/j.mib.2015.05.013
8. Prudencio M, Mota MM, Mendes AM. A toolbox to study liver stage malaria. *Trends Parasitol* (2011) 27:565–74. doi:10.1016/j.pt.2011.09.004
9. Matuschewski K. Vaccines against malaria—still a long way to go. *FEBS J* (2017) 284:2560–8. doi:10.1111/febs.14107
10. Flannery EL, Chatterjee AK, Winzeler EA. Antimalarial drug discovery-approaches and progress towards new medicines. *Nat Rev Microbiol* (2013) 11:849–62. doi:10.1038/nrmicro3138
11. Kaushansky A, Mikolajczak SA, Vignali M, Kappe SH. Of mice in men: the success and promise of humanized mouse models for human malaria parasite infections. *Cell Microbiol* (2014) 16:602–11. doi:10.1111/cmi.12277
12. Siu E, Ploss A. Modeling malaria in humanized mice: opportunities and challenges. *Ann N Y Acad Sci* (2015) 1342:29–36. doi:10.1111/nyas.12618
13. Butler NS, Vaughan AM, Harty JT, Kappe SH. Whole parasite vaccination approaches for prevention of malaria infection. *Trends Immunol* (2012) 33:247–54. doi:10.1016/j.it.2012.02.001
14. Menard R, Tavares J, Cockburn I, Markus M, Zavala F, Amino R. Looking under the skin: the first steps in malarial infection and immunity. *Nat Rev Microbiol* (2013) 11:701–12. doi:10.1038/nrmicro3111
15. Mota MM, Rodriguez A. Migration through host cells by apicomplexan parasites. *Microbes Infect* (2001) 3:1123–8. doi:10.1016/S1286-4579(01)01473-3
16. Risco-Castillo V, Topcu S, Marinach C, Manzoni G, Bigorgne AE, Briquet S, et al. Malaria sporozoites traverse host cells within transient vacuoles. *Cell Host Microbe* (2015) 18:593–603. doi:10.1016/j.chom.2015.10.006
17. Gueirard P, Tavares J, Thiberge S, Bernex F, Ishino T, Milon G, et al. Development of the malaria parasite in the skin of the mammalian host. *Proc Natl Acad Sci U S A* (2010) 107:18640–5. doi:10.1073/pnas.1009346107
18. Voza T, Miller JL, Kappe SH, Sinnis P. Extrahepatic exoerythrocytic forms of rodent malaria parasites at the site of inoculation: clearance after immunization, susceptibility to primaquine, and contribution to blood-stage infection. *Infect Immun* (2012) 80:2158–64. doi:10.1128/IAI.00246-12
19. Guerrero-Aspizua S, Garcia M, Murillas R, Retamosa L, Illera N, Duarte B, et al. Development of a bioengineered skin-humanized mouse model for

psoriasis: dissecting epidermal-lymphocyte interacting pathways. *Am J Pathol* (2010) 177:3112–24. doi:10.2353/ajpath.2010.100078
20. Kaushansky A, Douglass AN, Arang N, Vigdorovich V, Dambrauskas N, Kain HS, et al. Malaria parasites target the hepatocyte receptor EphA2 for successful host infection. *Science* (2015) 350:1089–92. doi:10.1126/science.aad3318
21. Foquet L, Meuleman P, Hermsen CC, Sauerwein R, Leroux-Roels G. Assessment of parasite liver-stage burden in human-liver chimeric mice. *Methods Mol Biol* (2015) 1325:59–68. doi:10.1007/978-1-4939-2815-6_5
22. Sacci JB Jr, Alam U, Douglas D, Lewis J, Tyrrell DL, Azad AF, et al. *Plasmodium falciparum* infection and exoerythrocytic development in mice with chimeric human livers. *Int J Parasitol* (2006) 36:353–60. doi:10.1016/j.ijpara.2005.10.014
23. Morosan S, Hez-Deroubaix S, Lunel F, Renia L, Giannini C, Van Rooijen N, et al. Liver-stage development of *Plasmodium falciparum*, in a humanized mouse model. *J Infect Dis* (2006) 193:996–1004. doi:10.1086/500840
24. Wilson EM, Bial J, Tarlow B, Bial G, Jensen B, Greiner DL, et al. Extensive double humanization of both liver and hematopoiesis in FRGN mice. *Stem Cell Res* (2014) 13:404–12. doi:10.1016/j.scr.2014.08.006
25. Bissig KD, Wieland SF, Tran P, Isogawa M, Le TT, Chisari FV, et al. Human liver chimeric mice provide a model for hepatitis B and C virus infection and treatment. *J Clin Invest* (2010) 120:924–30. doi:10.1172/JCI40094
26. Vaughan AM, Mikolajczak SA, Wilson EM, Grompe M, Kaushansky A, Camargo N, et al. Complete *Plasmodium falciparum* liver-stage development in liver-chimeric mice. *J Clin Invest* (2012) 122:3618–28. doi:10.1172/JCI62684
27. Mikolajczak SA, Vaughan AM, Kangwanrangsan N, Roobsoong W, Fishbaugher M, Yimamnuaychok N, et al. *Plasmodium vivax* liver stage development and hypnozoite persistence in human liver-chimeric mice. *Cell Host Microbe* (2015) 17:526–35. doi:10.1016/j.chom.2015.02.011
28. Soulard V, Bosson-Vanga H, Lorthiois A, Roucher C, Franetich JF, Zanghi G, et al. *Plasmodium falciparum* full life cycle and *Plasmodium ovale* liver stages in humanized mice. *Nat Commun* (2015) 6:7690. doi:10.1038/ncomms8690
29. Nussenzweig RS, Vanderberg J, Most H, Orton C. Protective immunity produced by the injection of x-irradiated sporozoites of *Plasmodium berghei*. *Nature* (1967) 216:160–2. doi:10.1038/216160a0
30. Mueller AK, Camargo N, Kaiser K, Andorfer C, Frevert U, Matuschewski K, et al. *Plasmodium* liver stage developmental arrest by depletion of a protein at the parasite-host interface. *Proc Natl Acad Sci U S A* (2005) 102:3022–7. doi:10.1073/pnas.0408442102
31. Doll KL, Butler NS, Harty JT. CD8 T cell independent immunity after single dose infection-treatment-vaccination (ITV) against *Plasmodium yoelii*. *Vaccine* (2014) 32:483–91. doi:10.1016/j.vaccine.2013.11.058
32. Beaudoin RL. Should cultivated exoerythrocytic parasites be considered as a source of antigen for a malaria vaccine? *Bull World Health Organ* (1977) 55:373–6.
33. Steel RW, Kappe SH, Sack BK. An expanding toolkit for preclinical preerythrocytic malaria vaccine development: bridging traditional mouse malaria models and human trials. *Future Microbiol* (2016) 11:1563–79. doi:10.2217/fmb-2016-0077
34. Potocnjak P, Yoshida N, Nussenzweig RS, Nussenzweig V. Monovalent fragments (Fab) of monoclonal antibodies to a sporozoite surface antigen (Pb44) protect mice against malarial infection. *J Exp Med* (1980) 151:1504–13. doi:10.1084/jem.151.6.1504
35. Charoenvit Y, Mellouk S, Cole C, Bechara R, Leef MF, Sedegah M, et al. Monoclonal, but not polyclonal, antibodies protect against *Plasmodium yoelii* sporozoites. *J Immunol* (1991) 146:1020–5.
36. Sack BK, Kappe SH. A novel immune regulator links malaria and inflammatory bowel disease. *J Exp Med* (2014) 211. doi:10.1084/jem.21113insight1
37. Keitany GJ, Sack B, Smithers H, Chen L, Jang IK, Sebastian L, et al. Immunization of mice with live-attenuated late liver stage-arresting *Plasmodium yoelii* parasites generates protective antibody responses to preerythrocytic stages of malaria. *Infect Immun* (2014) 82:5143–53. doi:10.1128/IAI.02320-14
38. Tse SW, Radtke AJ, Espinosa DA, Cockburn IA, Zavala F. The chemokine receptor CXCR6 is required for the maintenance of liver memory CD8(+) T cells specific for infectious pathogens. *J Infect Dis* (2014) 210:1508–16. doi:10.1093/infdis/jiu281
39. Tse SW, Cockburn IA, Zhang H, Scott AL, Zavala F. Unique transcriptional profile of liver-resident memory CD8+ T cells induced by immunization with malaria sporozoites. *Genes Immun* (2013) 14:302–9. doi:10.1038/gene.2013.20
40. Fernandez-Ruiz D, Ng WY, Holz LE, Ma JZ, Zaid A, Wong YC, et al. Liver-resident memory CD8(+) T cells form a front-line defense against malaria liver-stage infection. *Immunity* (2016) 45:889–902. doi:10.1016/j.immuni.2016.08.011
41. McNamara HA, Cai Y, Wagle MV, Sontani Y, Roots CM, Miosge LA, et al. Up-regulation of LFA-1 allows liver-resident memory T cells to patrol and remain in the hepatic sinusoids. *Sci Immunol* (2017) 2. doi:10.1126/sciimmunol.aaj1996
42. Liehl P, Zuzarte-Luis V, Chan J, Zillinger T, Baptista F, Carapau D, et al. Host-cell sensors for *Plasmodium* activate innate immunity against liver-stage infection. *Nat Med* (2014) 20:47–53. doi:10.1038/nm.3424
43. Liehl P, Meireles P, Albuquerque IS, Pinkevych M, Baptista F, Mota MM, et al. Innate immunity induced by *Plasmodium* liver infection inhibits malaria reinfections. *Infect Immun* (2015) 83:1172–80. doi:10.1128/IAI.02796-14
44. Miller JL, Sack BK, Baldwin M, Vaughan AM, Kappe SH. Interferon-mediated innate immune responses against malaria parasite liver stages. *Cell Rep* (2014) 7:436–47. doi:10.1016/j.celrep.2014.03.018
45. Zheng H, Tan Z, Zhou T, Zhu F, Ding Y, Liu T, et al. The TLR2 is activated by sporozoites and suppresses intrahepatic rodent malaria parasite development. *Sci Rep* (2015) 5:18239. doi:10.1038/srep18239
46. Carlton JM, Angiuoli SV, Suh BB, Kooij TW, Pertea M, Silva JC, et al. Genome sequence and comparative analysis of the model rodent malaria parasite *Plasmodium yoelii yoelii*. *Nature* (2002) 419:512–9. doi:10.1038/nature01099
47. Kaushansky A, Rezakhani N, Mann H, Kappe SH. Development of a quantitative flow cytometry-based assay to assess infection by *Plasmodium falciparum* sporozoites. *Mol Biochem Parasitol* (2012) 183:100–3. doi:10.1016/j.molbiopara.2012.01.006
48. Finney OC, Keitany GJ, Smithers H, Kaushansky A, Kappe S, Wang R. Immunization with genetically attenuated *P. falciparum* parasites induces long-lived antibodies that efficiently block hepatocyte invasion by sporozoites. *Vaccine* (2014) 32:2135–8. doi:10.1016/j.vaccine.2014.02.055
49. Seder RA, Chang LJ, Enama ME, Zephir KL, Sarwar UN, Gordon IJ, et al. Protection against malaria by intravenous immunization with a nonreplicating sporozoite vaccine. *Science* (2013) 341:1359–65. doi:10.1126/science.1241800
50. Van Braeckel-Budimir N, Harty JT. CD8 T-cell-mediated protection against liver-stage malaria: lessons from a mouse model. *Front Microbiol* (2014) 5:272. doi:10.3389/fmicb.2014.00272
51. Beignon AS, Le Grand R, Chapon C. In vivo imaging in NHP models of malaria: challenges, progress and outlooks. *Parasitol Int* (2014) 63:206–15. doi:10.1016/j.parint.2013.09.001
52. Joyner C, Barnwell JW, Galinski MR. No more monkeying around: primate malaria model systems are key to understanding *Plasmodium vivax* liver-stage biology, hypnozoites, and relapses. *Front Microbiol* (2015) 6:145. doi:10.3389/fmicb.2015.00145
53. Foquet L, Hermsen CC, van Gemert GJ, Van Braeckel E, Weening KE, Sauerwein R, et al. Vaccine-induced monoclonal antibodies targeting circumsporozoite protein prevent *Plasmodium falciparum* infection. *J Clin Invest* (2014) 124:140–4. doi:10.1172/JCI70349
54. Behet MC, Foquet L, van Gemert GJ, Bijker EM, Meuleman P, Leroux-Roels G, et al. Sporozoite immunization of human volunteers under chemoprophylaxis induces functional antibodies against pre-erythrocytic stages of *Plasmodium falciparum*. *Malar J* (2014) 13:136. doi:10.1186/1475-2875-13-136
55. Sack BK, Miller JL, Vaughan AM, Douglass A, Kaushansky A, Mikolajczak S, et al. Model for in vivo assessment of humoral protection against malaria sporozoite challenge by passive transfer of monoclonal antibodies and immune serum. *Infect Immun* (2014) 82:808–17. doi:10.1128/IAI.01249-13
56. Ishikawa F. Modeling normal and malignant human hematopoiesis in vivo through newborn NSG xenotransplantation. *Int J Hematol* (2013) 98:634–40. doi:10.1007/s12185-013-1467-9
57. Huang J, Li X, Coelho-dos-Reis JG, Wilson JM, Tsuji M. An AAV vector-mediated gene delivery approach facilitates reconstitution of functional

human CD8+ T cells in mice. *PLoS One* (2014) 9:e88205. doi:10.1371/journal.pone.0088205
58. Huang J, Li X, Coelho-dos-Reis JG, Zhang M, Mitchell R, Nogueira RT, et al. Human immune system mice immunized with *Plasmodium falciparum* circumsporozoite protein induce protective human humoral immunity against malaria. *J Immunol Methods* (2015) 427:42–50. doi:10.1016/j.jim.2015.09.005
59. Li X, Huang J, Zhang M, Funakoshi R, Sheetij D, Spaccapelo R, et al. Human CD8+ T cells mediate protective immunity induced by a human malaria vaccine in human immune system mice. *Vaccine* (2016) 34:4501–6. doi:10.1016/j.vaccine.2016.08.006
60. Li X, Huang J, Kaneko I, Zhang M, Iwanaga S, Yuda M, et al. A potent adjuvant effect of a CD1d-binding NKT cell ligand in human immune system mice. *Expert Rev Vaccines* (2017) 16:73–80. doi:10.1080/14760584.2017.1256208
61. Shortman K, Heath WR. The CD8+ dendritic cell subset. *Immunol Rev* (2010) 234:18–31. doi:10.1111/j.0105-2896.2009.00870.x
62. Cockburn IA, Zavala F. Dendritic cell function and antigen presentation in malaria. *Curr Opin Immunol* (2016) 40:1–6. doi:10.1016/j.coi.2016.01.010
63. Vaughan AM, Kappe SH, Ploss A, Mikolajczak SA. Development of humanized mouse models to study human malaria parasite infection. *Future Microbiol* (2012) 7:657–65. doi:10.2217/fmb.12.27
64. Duffier Y, Lorthiois A, Cistero P, Dupuy F, Jouvion G, Fiette L, et al. A humanized mouse model for sequestration of *Plasmodium falciparum* sexual stages and in vivo evaluation of gametocytidal drugs. *Sci Rep* (2016) 6:35025. doi:10.1038/srep35025
65. Foquet L, Schafer C, Minkah NK, Alanine DGW, Flannery El, Steel RWJ, et al. *Plasmodium falciparum* liver stage infection and transition to stable blood stage infection in liver-humanized and blood-humanized FRGN KO mice enables testing of blood stage inhibitory antibodies (reticulocyte-binding protein homolog 5) in vivo. *Front in Immunol* (2018) 9:524. doi:10.3389/fimmu.2018.00524
66. Mikolajczak SA, Lakshmanan V, Fishbaugher M, Camargo N, Harupa A, Kaushansky A, et al. A next-generation genetically attenuated *Plasmodium falciparum* parasite created by triple gene deletion. *Mol Ther* (2014) 22:1707–15. doi:10.1038/mt.2014.85
67. Vaughan AM, Pinapati RS, Cheeseman IH, Camargo N, Fishbaugher M, Checkley LA, et al. *Plasmodium falciparum* genetic crosses in a humanized mouse model. *Nat Methods* (2015) 12:631–3. doi:10.1038/nmeth.3432
68. Malleret B, Renia L, Russell B. The unhealthy attraction of *Plasmodium vivax* to reticulocytes expressing transferrin receptor 1 (CD71). *Int J Parasitol* (2017) 47:379–83. doi:10.1016/j.ijpara.2017.03.001
69. Baro B, Deroost K, Raiol T, Brito M, Almeida AC, de Menezes-Neto A, et al. *Plasmodium vivax* gametocytes in the bone marrow of an acute malaria patient and changes in the erythroid miRNA profile. *PLoS Negl Trop Dis* (2017) 11:e0005365. doi:10.1371/journal.pntd.0005365
70. Russell B, Suwanarusk R, Borlon C, Costa FT, Chu CS, Rijken MJ, et al. A reliable ex vivo invasion assay of human reticulocytes by *Plasmodium vivax*. *Blood* (2011) 118:e74–81. doi:10.1182/blood-2011-04-348748
71. Rongvaux A, Willinger T, Martinek J, Strowig T, Gearty SV, Teichmann LL, et al. Development and function of human innate immune cells in a humanized mouse model. *Nat Biotechnol* (2014) 32:364–72. doi:10.1038/nbt.2858
72. Amaladoss A, Chen Q, Liu M, Dummler SK, Dao M, Suresh S, et al. De novo generated human red blood cells in humanized mice support *Plasmodium falciparum* infection. *PLoS One* (2015) 10:e0129825. doi:10.1371/journal.pone.0129825
73. Rattanapunya S, Kuesap J, Chaijaroenkul W, Rueangweerayut R, Na-Bangchang K. Prevalence of malaria and HIV coinfection and influence of HIV infection on malaria disease severity in population residing in malaria endemic area along the Thai-Myanmar border. *Acta Trop* (2015) 145:55–60. doi:10.1016/j.actatropica.2015.02.001
74. Bukirwa H, Yeka A, Kamya MR, Talisuna A, Banek K, Bakyaita N, et al. Artemisinin combination therapies for treatment of uncomplicated malaria in Uganda. *PLoS Clin Trials* (2006) 1:e7. doi:10.1371/journal.pctr.0010007
75. Kredo T, Bernhardsson S, Machingaidze S, Young T, Louw Q, Ochodo E, et al. Guide to clinical practice guidelines: the current state of play. *Int J Qual Health Care* (2016) 28:122–8. doi:10.1093/intqhc/mzv115
76. Otieno L, Oneko M, Otieno W, Abuodha J, Owino E, Odero C, et al. Safety and immunogenicity of RTS,S/AS01 malaria vaccine in infants and children with WHO stage 1 or 2 HIV disease: a randomised, double-blind, controlled trial. *Lancet Infect Dis* (2016) 16:1134–44. doi:10.1016/S1473-3099(16)30161-X
77. Adams Y, Kuhnrae P, Higgins MK, Ghumra A, Rowe JA. Rosetting *Plasmodium falciparum*-infected erythrocytes bind to human brain microvascular endothelial cells in vitro, demonstrating a dual adhesion phenotype mediated by distinct *P. falciparum* erythrocyte membrane protein 1 domains. *Infect Immun* (2014) 82:949–59. doi:10.1128/IAI.01233-13
78. Rowe JA, Claessens A, Corrigan RA, Arman M. Adhesion of *Plasmodium falciparum*-infected erythrocytes to human cells: molecular mechanisms and therapeutic implications. *Expert Rev Mol Med* (2009) 11:e16. doi:10.1017/S1462399409001082
79. Bernabeu M, Smith JD. EPCR and malaria severity: the center of a perfect storm. *Trends Parasitol* (2017) 33:295–308. doi:10.1016/j.pt.2016.11.004
80. Sauerwein RW, Roestenberg M, Moorthy VS. Experimental human challenge infections can accelerate clinical malaria vaccine development. *Nat Rev Immunol* (2011) 11:57–64. doi:10.1038/nri2902
81. Engwerda CR, Minigo G, Amante FH, McCarthy JS. Experimentally induced blood stage malaria infection as a tool for clinical research. *Trends Parasitol* (2012) 28:515–21. doi:10.1016/j.pt.2012.09.001
82. Tran TM, Samal B, Kirkness E, Crompton PD. Systems immunology of human malaria. *Trends Parasitol* (2012) 28:248–57. doi:10.1016/j.pt.2012.03.006
83. Stevenson MM, Riley EM. Innate immunity to malaria. *Nat Rev Immunol* (2004) 4:169–80. doi:10.1038/nri1311
84. Gazzinelli RT, Kalantari P, Fitzgerald KA, Golenbock DT. Innate sensing of malaria parasites. *Nat Rev Immunol* (2014) 14:744–57. doi:10.1038/nri3742
85. Tamura T, Kimura K, Yui K, Yoshida S. Reduction of conventional dendritic cells during *Plasmodium* infection is dependent on activation induced cell death by type I and II interferons. *Exp Parasitol* (2015) 159:127–35. doi:10.1016/j.exppara.2015.09.010
86. Haque A, Best SE, de Oca M, James KR, Ammerdorffer A, Edwards CL, et al. Type I IFN signaling in CD8- DCs impairs Th1-dependent malaria immunity. *J Clin Invest* (2014) 124:2483–96. doi:10.1172/JCI70698
87. Montes, de Oca M, Kumar R, Rivera FL, Amante FH, Sheel M, et al. Type I interferons regulate immune responses in humans with blood-stage *Plasmodium falciparum* infection. *Cell Rep* (2016) 17:399–412. doi:10.1016/j.celrep.2016.09.015
88. Cohen S, Butcher GA, Mitchell GH. Mechanisms of immunity to malaria. *Bull World Health Organ* (1974) 50:251–7.
89. Butler NS, Moebius J, Pewe LL, Traore B, Doumbo OK, Tygrett LT, et al. Therapeutic blockade of PD-L1 and LAG-3 rapidly clears established blood-stage *Plasmodium* infection. *Nat Immunol* (2011) 13:188–95. doi:10.1038/ni.2180
90. Ryg-Cornejo V, Ioannidis LJ, Ly A, Chiu CY, Tellier J, Hill DL, et al. Severe malaria infections impair germinal center responses by inhibiting T follicular helper cell differentiation. *Cell Rep* (2016) 14:68–81. doi:10.1016/j.celrep.2015.12.006
91. Kurup SP, Obeng-Adjei N, Anthony SM, Traore B, Doumbo OK, Butler NS, et al. Regulatory T cells impede acute and long-term immunity to blood-stage malaria through CTLA-4. *Nat Med* (2017) 23:1220–5. doi:10.1038/nm.4395
92. Hansen DS, Obeng-Adjei N, Ly A, Ioannidis LJ, Crompton PD. Emerging concepts in T follicular helper cell responses to malaria. *Int J Parasitol* (2017) 47:105–10. doi:10.1016/j.ijpara.2016.09.004
93. Krishnamurty AT, Thouvenel CD, Portugal S, Keitany GJ, Kim KS, Holder A, et al. Somatically hypermutated *Plasmodium*-specific IgM(+) memory B cells are rapid, plastic, early responders upon malaria rechallenge. *Immunity* (2016) 45:402–14. doi:10.1016/j.immuni.2016.06.014
94. Zander RA, Obeng-Adjei N, Guthmiller JJ, Kulu DI, Li J, Ongoiba A, et al. PD-1 Co-inhibitory and OX40 Co-stimulatory crosstalk regulates helper T cell differentiation and anti-*Plasmodium* humoral immunity. *Cell Host Microbe* (2015) 17:628–41. doi:10.1016/j.chom.2015.03.007
95. Obeng-Adjei N, Portugal S, Holla P, Li S, Sohn H, Ambegaonkar A, et al. Malaria-induced interferon-gamma drives the expansion of Tbethi atypical memory B cells. *PLoS Pathog* (2017) 13:e1006576. doi:10.1371/journal.ppat.1006576

96. Wege AK, Melkus MW, Denton PW, Estes JD, Garcia JV. Functional and phenotypic characterization of the humanized BLT mouse model. *Curr Top Microbiol Immunol* (2008) 324:149–65.

Conflict of Interest Statement: The authors declare that the research was conducted in the absence of any commercial or financial relationships that could be construed as a potential conflict of interest.

frontiers in Immunology

ORIGINAL RESEARCH
published: 19 April 2018
doi: 10.3389/fimmu.2018.00817

Humanized Mice Engrafted With Human HSC Only or HSC and Thymus Support Comparable HIV-1 Replication, Immunopathology, and Responses to ART and Immune Therapy

Liang Cheng[1,2], Jianping Ma[1], Guangming Li[1] and Lishan Su[1,2]**

[1] Lineberger Comprehensive Cancer Center, University of North Carolina at Chapel Hill, Chapel Hill, NC, United States,
[2] Department of Microbiology and Immunology, University of North Carolina at Chapel Hill, Chapel Hill, NC, United States

OPEN ACCESS

Edited by:
Ramesh Akkina,
Colorado State University,
United States

Reviewed by:
Larisa Y. Poluektova,
University of Nebraska Medical Center, United States
Fatah Kashanchi,
George Mason University,
United States

***Correspondence:**
Liang Cheng
chengl84@email.unc.edu;
Lishan Su
lsu@email.unc.edu

Specialty section:
This article was submitted to Vaccines and Molecular Therapeutics, a section of the journal Frontiers in Immunology

Received: 20 December 2017
Accepted: 04 April 2018
Published: 19 April 2018

Citation:
Cheng L, Ma J, Li G and Su L (2018) Humanized Mice Engrafted With Human HSC Only or HSC and Thymus Support Comparable HIV-1 Replication, Immunopathology, and Responses to ART and Immune Therapy. Front. Immunol. 9:817. doi: 10.3389/fimmu.2018.00817

Immunodeficient mice reconstituted with human immune tissues and cells (humanized mice) are relevant and robust models for the study of HIV-1 infection, immunopathogenesis, and therapy. In this study, we performed a comprehensive comparison of human immune reconstitution and HIV-1 infection, immunopathogenesis and therapy between immunodeficient NOD/Rag2$^{-/-}$/$\gamma_c^{-/-}$ (NRG) mice transplanted with human HSCs (NRG-hu HSC) and mice transplanted with HSCs and thymus fragments (NRG-hu Thy/HSC) from the same donors. We found that similar human lymphoid and myeloid lineages were reconstituted in NRG-hu HSC and NRG-hu Thy/HSC mice, with human T cells more predominantly reconstituted in NRG-hu Thy/HSC mice, while NRG-hu HSC mice supported more human B cells and myeloid cells reconstitution. HIV-1 replicated similarly and induced similar T cell depletion, immune activation, and dysfunction in NRG-hu HSC and NRG-hu Thy/HSC mice. Moreover, combined antiretroviral therapy (cART) inhibited HIV-1 replication efficiently with similar persistent HIV-1 reservoirs in both models. Finally, we found that blocking type-I interferon signaling under cART treatment transiently activated HIV-1 reservoirs, enhanced T cell recovery and reduced HIV-1 reservoirs in both HIV-1 infected NRG-hu HSC and NRG-hu Thy/HSC mice. In summary, we report that NRG-hu Thy/HSC and NRG-hu HSC mice support similar HIV-1 infection and similar HIV-1 immunopathology; and HIV-1 replication responds similarly to cART and IFNAR blockade therapies. The NRG-hu HSC mouse model reconstituted with human HSC only is sufficient for the study of HIV-1 infection, pathogenesis, and therapy.

Keywords: humanized mice, NRG-hu HSC, NRG-hu Thy/HSC, HIV-1 replication, HIV-1 immunopathology, combined antiretroviral therapy, HIV-1 immune therapy

INTRODUCTION

Human immunodeficiency virus type 1 (HIV-1) infects and progressively depletes CD4$^+$ T cells, causing acquired immune deficiency syndrome (AIDS). Approximately 70 million people have been infected with HIV-1, and half of them have died of HIV/AIDS-related causes (1). The development of combined antiretroviral therapy (cART), which can efficiently suppress viral replication, has

significantly improved survival and life quality of HIV-1-infected patients who can both access and tolerate cART (2). However, cART is not curative and must be continued for life (3, 4). Moreover, lifelong treatment is associated with significant side effects and non-AIDS-related "end-organ disease" (5). Thus, there is a great need for the development of novel therapies that can both control the epidemic and cure those individuals who have already been infected with HIV-1.

Understanding how HIV-1 infection leads to immunodeficiency is key for the development of new treatments. After more than 30 years of research, the precise mechanism by which HIV-1 infection causes AIDS development is still poorly understood, mainly due to the lack of robust small animal models. The recent development of humanized mice with functional human immune systems offer a relevant and robust model for the study of HIV-1 infection, replication, pathogenesis, and therapies (6–8). Humanized mice were constructed by transplantation of human $CD34^+$ hematopoietic stem cells and/or implantation of human thymus tissue into immunodeficient mice, such as the NOD-scid $\gamma_c^{-/-}$ (NSG) mice and NOD-$Rag2^{-/-}\gamma_c^{-/-}$ (NRG) mice (9). Two major humanized mouse models, the NRG-hu HSC model and the hu-BLT model, are widely used for HIV-1 studies. The NRG-hu HSC model involves preconditioning neonate immunodeficient mice with radiation and then injecting them with human $CD34^+$ HSCs (10–13). In the hu-BLT model, implantation of human thymus tissue under the kidney capsule is combined with HSCs infusion into irradiated adult immunodeficient mice (14, 15). We and others have reported that all the major human lymphoid lineage including T cell, B cell, and innate immune cells including NK cell, monocytes, myeloid dendritic cells (mDC), and plasmacytoid dendritic cells (pDC) are developed in both NRG-hu HSC mice and hu-BLT mice (10–20).

Both NRG-hu HSC and hu-BLT models can develop significant levels of innate and adaptive immune responses (21–25) and can be infected by HIV-1 (7, 26–28). HIV-1 infection leads to progressive $CD4^+$ T cell depletion in both peripheral blood and lymphoid tissues (8). Moreover, like in humans, HIV-1 infection also leads to T cell activation and exhaustion in both NRG-hu HSC and hu-BLT mice (29–31). HIV-1 infection can be treated with the antiretroviral drugs that are used in infected humans (32–36). Also like in humans, antiretroviral treatment of HIV-1 infection results in systemic recovery of CD4 T cells in humanized mice. In addition, both mouse models are used for testing the effectiveness of immunotherapy to inhibit HIV-1 replication, reverse HIV-1 induced immunopathology and control HIV-1 reservoir (25, 29, 30, 34, 37–39).

The advantage of the NRG-hu HSC model is that the procedure to construct the mice is simple, only involving pre-irradiating the neonate immunodeficient mice followed by injecting human $CD34^+$ HSCs (10, 11, 13). To generate hu-BLT mice, a time consuming and technically difficult surgery procedure is needed to implant the human thymus tissue into the kidney capsule of the mice (14, 15). Another major difference between these two models is that in NRG-hu HSC mouse, the human T cells are produced in the mouse thymus and presumed to be educated in the context of mouse major histocompatibility complex (MHC) (10–13). In hu-BLT mice, human T cells can develop in the presence of human thymic epithelium, resulting in human MCH-restricted T cells (14, 15, 40). Thus, although both models are versatile tools for HIV-1 study, parallelly study to compare the human immune reconstitution, HIV-1 replication, immunopathology, and responses to therapy in both models will help to guide researchers how to balance and decide which system to use. In this study, we performed a comprehensive parallel comparison of human immune reconstitution and HIV-1 replication, immunopathogenesis and therapy between newborn immunodeficient mice transplanted with HSCs (NRG-hu HSC) and 6- to 8-week-old adult mice transplanted with HSCs and thymus (NRG-hu Thy/HSC) from same human donors into same background of immunodeficient mice. We report that both NRG-hu HSC and NRG-hu Thy/HSC mice support significant levels of human immune reconstitution and comparable levels of HIV-1 replication, immunopathology, and responses to cART and immune therapy.

MATERIALS AND METHODS

Construction of Humanized Mice

NRG (NOD-$Rag2^{-/-}\gamma c^{-/-}$) mice were obtained from the Jackson Laboratory. Human fetal liver and thymus (gestational age of 16–20 weeks) were obtained from medically or elective indicated termination of pregnancy through a non-profit intermediary working with outpatient clinics (Advanced Bioscience Resources, Alameda, CA, USA). Written informed consent of the maternal donors is obtained in all cases, under regulation governing the clinic. NRG-hu HSC mice were generated by intrahepatic injection of new born (1–5 days old) NRG mice (irradiated at 200 cGy from a 137Cs gamma radiation source) with 3×10^5 human fetal liver derived $CD34^+$ HSCs as previously reported (41). To generate NRG-hu Thy/HSC mice, 6- to 8-week-old NRG mice were sub-lethally irradiated (250 cGy) and anesthetized, and ~1-mm^3 fragments of human fetal thymus fragments were implanted under the kidney capsule. 5×10^5 $CD34^+$ HSCs purified from fetal liver of the same donor were injected i.v. within 3 h. All mice were housed and bred in a specific pathogen-free environment. All animal studies were approved by the University of North Carolina Institutional Animal Care and Use Committee.

Antibodies and Flow Cytometry

Antibodies to CD45 (HI30), CD4 (RPA-T4), CD8 (HIT8a), CD56 (5.1h11), CD123 (6H6), CD14 (63D3), CD11c (3.9), CD45RA (HI100), CCR7 (G043H7), CD10 (HI10a), IL-2 (MQ1-17H12), IFN-γ (4S.B3), HLA-DR (L243), CD38 (HIT2), and PD-1 (EH12.2H7) were purchased from BioLegend. Antibodies to CD3 (7D6), CD19 (6D5), mouse CD45 (30-F11), and LIVE/DEAD Fixable Yellow Dead Cell Stain Kit were purchased from Invitrogen. Antibody to HIV-1 p24 (KC57) were purchased from Beckman Coulter.

Total lymphocytes were isolated prepared from peripheral blood, spleen, bone marrow (BM), and mesenteric lymph nodes (mLNs) according to standard protocols; red blood cells were lysed with ACK buffer. Intrahepatic lymphocytes were prepared

as described (42). Total cell number was quantified by Guava Easycytes with Guava Express software (Guava). For surface staining, single cell suspension was stained with surface markers and analyzed on a CyAn ADP flow cytometer (Dako). For intracellular staining, cells were first stained with surface markers and then fixed and permeabilized with cytofix/cytoperm buffer (BD Bioscience), followed by intracellular staining. Data were analyzed using Summit4.3 software (Dako).

T Cell Stimulation and Intracellular Cytokine Staining

Splenocytes from humanized mice were stimulated *ex vivo* with PMA (phorbol 12-myristate 13-acetate) (50 ng/ml) and ionomycin (1 μM) (Sigma, St. Louis, MO, USA) for 4 h in the presence of brefeldin A (BioLegend). Cell were then fixed and permeabilized with cytofix/cytoperm buffer (BD Biosciences), and intracellular staining was then performed.

TLR-L Treatment *In Vivo*

CpG-B (ODN 2006), R848, and poly I:C were all purchased from InvivoGen. For *in vivo* treatment, humanized mice were treated with 50 μg/mouse of CpG-B, poly I:C or 20 μg/mouse R848 through i.p. injection.

Detection of Cytokines in Plasma

Human pan IFN-α (subtypes 1/13, 2, 4, 5, 6, 7, 8, 10, 14, 16, and 17) were detected by enzyme-linked immunosorbent assay using the human IFN-α pan ELISA kits purchased from Mabtech (Nacka Strand, Sweden). Human IL-6 in plasma of humanized mice were detected by immunology multiplex assay (Luminex) (Millipore, Billerica, MA, USA).

HIV-1 Infection of Humanized Mice

The CCR5-tropic strain of HIV-1 (JR-CSF) was generated by transfection of 293T cells (ATCC) with plasmid containing full length HIV-1 (JR-CSF) genome. Humanized mice with stable human leukocyte reconstitution were anesthetized and infected with HIV-1 (JR-CSF) (10 ng p24/mouse) through retro-orbital injection.

HIV-1 Genomic RNA Detection in Plasma

HIV-1 RNA was purified from the plasma with the QIAamp® Viral RNA Mini Kit. The RNA was then reverse transcribed and quantitatively detected by real-time PCR using the TaqMan® Fast Virus 1-Step PCR kit (ThermoFisher Scientific). The primers used for detecting the HIV Gag gene were (5′-GGTGCGAGA GCGTCAGTATTAAG-3′ and 5′-AGCTCCCTGCTTGCCCAT A-3′). The probe (FAM-AAAATTCGGTTAAGGCCAGGGGGA AAGAA-QSY7) used for detection was ordered from Applied Biosystems, and the reactions were set up following the manufacturer's guidelines and were run on the QuantStudio 6 Flex PCR system (Applied Biosystems). The detection limit of the real-time PCR reaction is four copies per reaction. Accordingly, the limit of detection of the assay with 50 μl of blood is 400 copies/ml in humanized mice.

Combination Antiretroviral Therapy

Food formulated with antiretroviral individual drug was prepared as reported with elevated dose modifications (34). In brief, tablets of emtricitabine and tenofovir disoproxil fumarate (Truvada®; Gilead Sciences) and raltegravir (Isentress®; Merck) were crushed into fine powder and manufactured with TestDiet 5B1Q feed (Modified LabDiet 5058 with 0.12% amoxicillin) into 1/2" irradiated pellets. Final concentrations of drugs in the food were 4,800 mg/kg raltegravir, 1,560 mg/kg tenofovir disoproxil, and 1,040 mg/kg emtricitabine. The estimated drug daily doses were 768 mg/kg raltegravir, 250 mg/kg tenofovir disoproxil, and 166 mg/kg emtricitabine.

In Vivo IFNAR1 Blocking Antibody Treatments

The α-IFNAR1 monoclonal antibody (mAb) was generated as previous reported (29). To block type-I interferon (IFN-I) signaling during chronic HIV-1 infection, humanized mice were treated i.p. with IFNAR1 blocking antibodies twice a week with the dose 400 μg/mouse at the first injection and 200 μg/mouse for the following treatments. Cohorts of mice were randomized into different treatment groups by level of HIV-1 RNA in plasma.

Cell-Associated HIV-1 DNA Detection

To measure total cell-associated HIV-1 DNA, nucleic acid was extracted from spleen and BM cells using the DNeasy Blood & Tissue Kit (Qiagen). HIV-1 DNA was quantified by real-time PCR. DNA from serial dilutions of ACH2 cells, which contain one copy of HIV genome in each cell, was used to generate a standard curve.

Viral Outgrowth Assay

Viral outgrowth assay was performed as reported (43). Serial dilutions of human cells from splenocytes of humanized mice (1×10^6, 2×10^5, and 4×10^4 human cells) were stimulated with PHA (2 μg/ml) and IL-2 (100 U/ml) for 24 h. MOLT4/CCR5 cells were added on day 2 to enhance the survival of the cultured cells as well as to support and facilitate further HIV-1 replication. Culture medium containing IL-2 (NIH AIDS reagents program) and T cell growth factor (homemade as describe in the standard protocol) was replaced on days 5 and 9. After 7 and 14 days of culture, supernatant from each well was harvested, and HIV-1 RT-qPCR was performed to score viral outgrowth. Estimated frequencies of cells with replication-competent HIV-1 were determined by maximum likelihood statistics (43).

Statistical Analysis

In all other experiments, significance levels of data were determined by using Prism5 (GraphPad Software). Experiments were analyzed by two-tailed Student's *t*-test, or by one-way analysis of variance (ANOVA) and Bonferroni's *post hoc* test according to the assumptions of the test, as indicated for each experiment. A *P* value less than 0.05 was considered significant. The number of animals and replicates is specified in each figure legend.

RESULTS

Human Lymphoid and Myeloid Lineage Cells Are Reconstituted in Peripheral Blood of Both NRG-hu HSC and NRG-hu Thy/HSC Mice

To compare the level of human immune reconstitution in humanized mice (hu-mice) transplanted with human HSCs only (NRG-hu HSC) or with human HSCs plus thymus tissue (NRG-hu Thy/HSC), we reconstituted newborn NRG mice with human fetal liver derived CD34$^+$ HSCs (NRG-hu HSC) or reconstituted 6- to 8-week-old NRG mice with human fetal liver derived CD34$^+$ HSCs together with fetal thymus tissue (NRG-hu Thy/HSC) from the same donor. The difference between the NRG-hu Thy/HSC model and the hu-BLT model is that we only transplant thymus tissue but not fetal liver tissue under the kidney capsule. The other difference is that we transplant human HSCs within 3 h after human thymus transplantation. As reported in hu-BLT mice (14, 15), human thymic organoid was well developed and showed long-term sustained thymopoiesis in NRG-hu Thy/HSC mice (Figure S1 in Supplementary Material). Human immune cell reconstitution in the peripheral blood was detected by flow cytometry 12 weeks after transplantation. All major human CD45$^+$ leukocyte subsets including T cells (CD3$^+$), B cells (CD19$^+$), NK cells (CD3$^-$ CD56$^+$), monocytes (CD3$^-$CD19$^-$HLA$^-$DR$^+$CD14$^+$), and pDCs (CD3$^-$CD19$^-$HLA$^-$DR$^+$CD4$^+$CD123$^+$) were detected in peripheral blood of both NRG-hu HSC and NRG-hu Thy/HSC mice (**Figure 1**; Figure S1 in Supplementary Material). Similar level of human CD45$^+$ cells was found in NRG-hu HSC (65.3 ± 5.3%) and NRG-hu Thy/HSC (68.8 ± 3.1%) mice (**Figure 1A**). The percentage of human T cells within human CD45$^+$ leukocytes was significantly higher in NRG-hu Thy/HSC mice (61.1 ± 3.2%) compared with the level in NRG-hu HSC mice (20.1 ± 3.4%) (**Figure 1B**). The result indicated that fetal liver/thymus "sandwich" structure (14, 15) is not essential for the long-term functioning human thymus development if human CD34$^+$ HSCs were transplanted immediately after thymus transplantation. Progenitor cells derived from CD34$^+$ HSCs can serve as the source of thymocyte progenitors. Both CD4 and CD8 T cells were developed in NRG-hu HSC and NRG-hu Thy/HSC mice (**Figures 1C,D**). The ratio of CD4 T cells to CD8 T cells was slightly higher in NRG-hu Thy/HSC mice compare to NRG-hu HSC mice (**Figures 1C,D**). The percentage of human B cells was 65.8 ± 3.3% in NRG-hu HSC mice and 33 ± 4.9% in NRG-hu Thy/HSC mice (**Figure 1E**). The percentages of human NK cells, pDCs, and monocytes were also lower in NRG-hu Thy/HSC mice compared with NRG-hu HSC mice (**Figures 1F–H**).

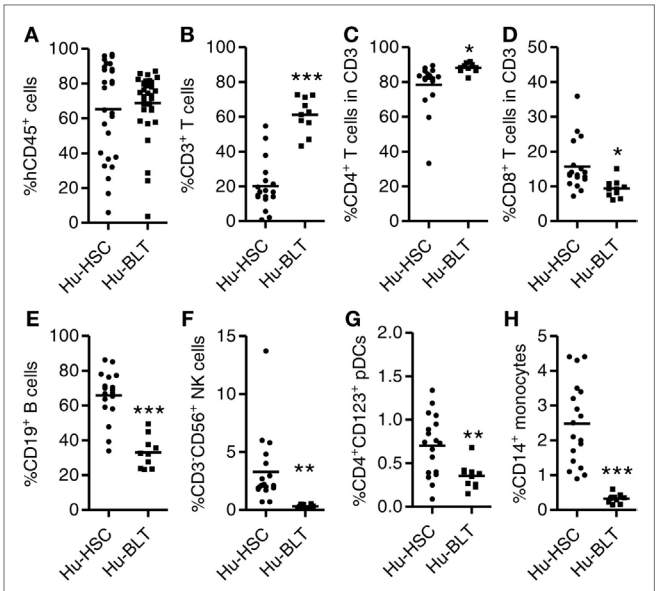

FIGURE 1 | Comparison of human immune cell reconstitution in peripheral blood of NRG-hu HSC and NRG-hu Thy/HSC mice. NRG-hu HSC and NRG-hu Thy/HSC mice were generated as indicated in Section "Materials and Methods." **(A)** Summarized data show percentage of human leukocytes (hCD45$^+$) in total peripheral blood leukocytes 12 weeks after reconstitution. Shown are combined data from two cohorts of NRG-hu HSC mice (n = 27) and NRG-hu Thy/HSC mice (n = 35) reconstituted with HSCs ± thymus from the same human donor. **(B–H)** Summarized data show percentage of human T cells (CD3$^+$), B cells (CD19$^+$), NK cells (CD3$^-$CD56$^+$), plasmacytoid dendritic cells (pDCs) (CD3$^-$CD19$^-$HLA-DR$^+$CD4$^+$CD123$^+$), and monocytes (CD3$^-$CD19$^-$HLA-DR$^+$CD14$^+$) in human CD45$^+$ cells **(B,E–H)** and percentage of human CD4 T and CD8 T cells in human CD3 T cells **(C,D)**. Shown are representative data **(B–H)** from n = 18 (NRG-hu HSC) and n = 10 (NRG-hu Thy/HSC) hu-mice reconstituted with HSCs ± thymus from same donor. Each dot represents one individual mouse; bars indicate mean (*P < 0.05, **P < 0.01, and ***P < 0.001, by unpaired, two-tailed Student's t-test).

Human Leukocytes Are Equally Reconstituted in Lymphoid Organs in Both NRG-hu HSC and NRG-hu Thy/HSC Mice

We also detected human immune reconstitution in lymphoid organs including spleen, mLNs, liver, and BM of NRG-hu HSC and NRG-hu Thy/HSC mice. The percentage of human CD45$^+$ cell and total number of human CD45$^+$ cells were comparable in spleen, mLN, and BM between NRG-hu HSC and NRG-hu Thy/HSC mice (**Figures 2A,B**). The level of human immune cells in the liver was slightly higher in NRG-hu Thy/HSC mice (95.7 ± 0.8%) compared with the NRG-hu HSC mice (85.6 ± 2.2%), consistent with the higher number of human CD45$^+$ cells in the liver in NRG-hu Thy/HSC mice (**Figures 2A,B**).

Similar Phenotype and Function of Human T and B Cells Developed in NRG-hu HSC and NRG-hu Thy/HSC Mice

We next determined the phenotype and function of human T cells and B cells from spleen of NRG-hu HSC and NRG-hu Thy/HSC mice. As in the peripheral blood, both the percentage and number of CD3$^+$ T cells were higher in the spleen of NRG-hu Thy/HSC mice (**Figures 3A,B**). The percentages of CD4 and CD8 T cells in total T cells did not show difference in the spleen between these two models (**Figure 3A**). Most of the T cells from both NRG-hu HSC (64.4 ± 3.1%) and NRG-hu Thy/HSC (64.3 ± 5.8%) showed naïve phenotype at 20 weeks posttransplantation (**Figure 3C**). The function of T cells from both humanized mouse models were equal as they produced

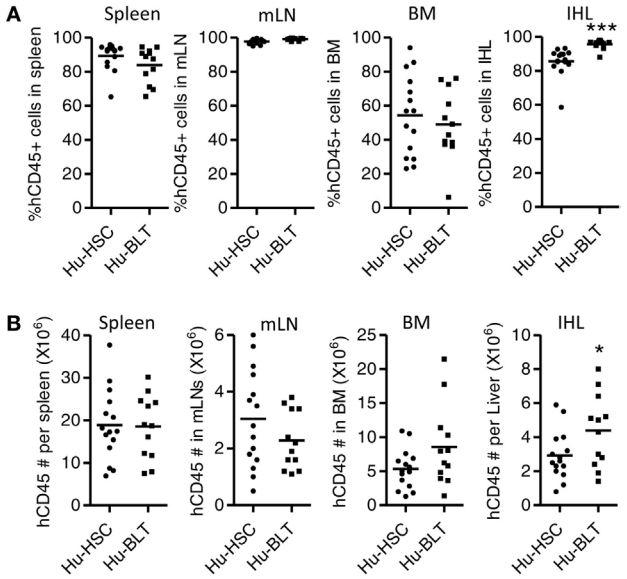

FIGURE 2 | Comparison of total human immune cell reconstitution in lymphoid organ of NRG-hu HSC and NRG-hu Thy/HSC mice. NRG-hu HSC and NRG-hu Thy/HSC mice were terminated at 20 weeks after reconstitution and human immune cells in lymphoid organs were detected by flow cytometry. Summarized data show percentage **(A)** and number **(B)** of human leukocytes (hCD45+) in spleen, mesenteric lymph nodes (mLNs), bone marrow (BM), and intrahepatic leukocytes (IHL) of NRG-hu HSC and NRG-hu Thy/HSC mice. Shown are representative data from $n = 15$ (NRG-hu HSC) and $n = 12$ (NRG-hu Thy/HSC) hu-mice per group reconstituted with HSCs ± thymus from same donor. Each dot represents one individual mouse; bars indicate mean ($^*P < 0.05$ and $^{***}P < 0.001$, by unpaired, two-tailed Student's *t*-test).

similar level of IFN-γ and IL-2 in response to mitogen stimulation *ex vivo* (**Figure 3D**). No spontaneous IFN-γ and IL-2 production by T cells was detected from either the NRG-hu HSC or NRG-hu Thy/HSC mice.

As in the peripheral blood, the percentage and number of B cells in the spleen were lower in NRG-hu Thy/HSC mice compared with the NRG-hu HSC mice (**Figure 3E**). It has been reported that human B cells developed in humanized mice were immature and cannot produce significant level of antigen-specific IgG by vaccination (44–46). We also compared the phenotype of B cells from both NRG-hu HSC and NRG-hu Thy/HSC mice and found that they both express high level of immature marker CD10 (**Figure 3F**). The expression of CD10 on B cells from NRG-hu Thy/HSC mice was slightly higher (**Figure 3F**), indicating that co-transplantation of thymus had minor effect on the maturation of B cells in NRG-hu Thy/HSC mice.

Innate Immune Cells Were Developed in Spleen of Both NRG-hu HSC and NRG-hu Thy/HSC Mice and Responded Similarly to TLR-Ls Stimulation

We compared the reconstitution of human innate immune cells including pDCs, mDCs and monocytes/macrophages in the spleen of NRG-hu HSC and NRG-hu Thy/HSC mice. The percentage and number of pDC (**Figure 4A**) and monocytes/macrophage (**Figure 4B**) were comparable, while there were more mDCs in the spleen of NRG-hu HSC mice compared with NRG-hu Thy/HSC mice (**Figure 4C**).

To detect the function of innate immune cells developed in NRG-hu HSC and NRG-hu Thy/HSC mice, we treated the mice *in vivo* with the TLR9-ligands CpG-B, the TLR7/8-L R848 and the TLR3-L poly I:C and detected cytokine production in the serum. We found that all the three TLR-Ls induced significant levels of IFN-α and IL-6 in both NRG-hu HSC and NRG-hu Thy/HSC mice (**Figure 4D**). The induction of IFN-α by poly(I:C) and R848 stimulation is slightly lower in NRG-hu Thy/HSC mice compared with NRG-hu HSC mice (**Figure 4D**) which probably due to the lower number of mDC developed in NRG-hu Thy/HSC mice compared with NRG-hu HSC mice (**Figure 4C**).

In summary, most human lymphoid and myeloid lineage cells are reconstituted in both NRG-hu HSC and NRG-hu Thy/HSC mice, with human T cells predominantly developed in NRG-hu Thy/HSC mice, while NRG-hu HSC mice support better human B cell and myeloid cell development. The phenotype and function of human immune cells developed in NRG-hu HSC mice and NRG-hu Thy/HSC mice are similar.

NRG-hu HSC and NRG-hu Thy/HSC Mice Support Similar Level of HIV-1 Replication *In Vivo*

We and others have reported that both NRG-hu HSC and NRG-hu Thy/HSC mice supported HIV-1 replication *in vivo* (7, 8, 47). Here we compared the HIV-1 replication kinetics in NRG-hu HSC mice and NRG-hu Thy/HSC mice transplanted with HSCs ± thymus from the same donor tissue. We found the viremia reached to peak level at 2 weeks postinfection (wpi) in NRG-hu HSC mice (**Figure 5A**), while in NRG-hu Thy/HSC mice, the viremia reached the peak level at 4 wpi (**Figure 5B**). At 2 wpi, NRG-hu HSC mice supported efficient HIV-1 replication in nearly all mice (98%) but NRG-hu Thy/HSC mice supported HIV-1 replication in about 73% of infected mice (**Figure 5B**). The results suggest that the immune cells in NRG-hu Thy/HSC mice may control/delay HIV-1 replication at the early stage of HIV-1 infection. At 4 wpi, all the infected BLT mice showed similar viremia as detected in NRG-hu HSC mice and sustained through 10 wpi when we terminated the mice (**Figures 5A–C**). HIV-1 p24 levels in CD4 T cells from the spleen were similar in NRG-hu HSC and NRG-hu Thy/HSC mice at 10 wpi (**Figures 5D,E**). In summary, the results indicated that both the NRG-hu HSC and NRG-hu Thy/HSC mice support similar levels of HIV-1 replication, although there was a 2 weeks delay reaching the peak viremia in NRG-hu Thy/HSC mice.

HIV-1 Infection Induces Similar Levels of T Cell Depletion, Activation, and Exhaustion in NRG-hu HSC and NRG-hu Thy/HSC Mice

We next detected HIV-1 induced immunopathology including T cell depletion, activation and dysfunction in both NRG-hu

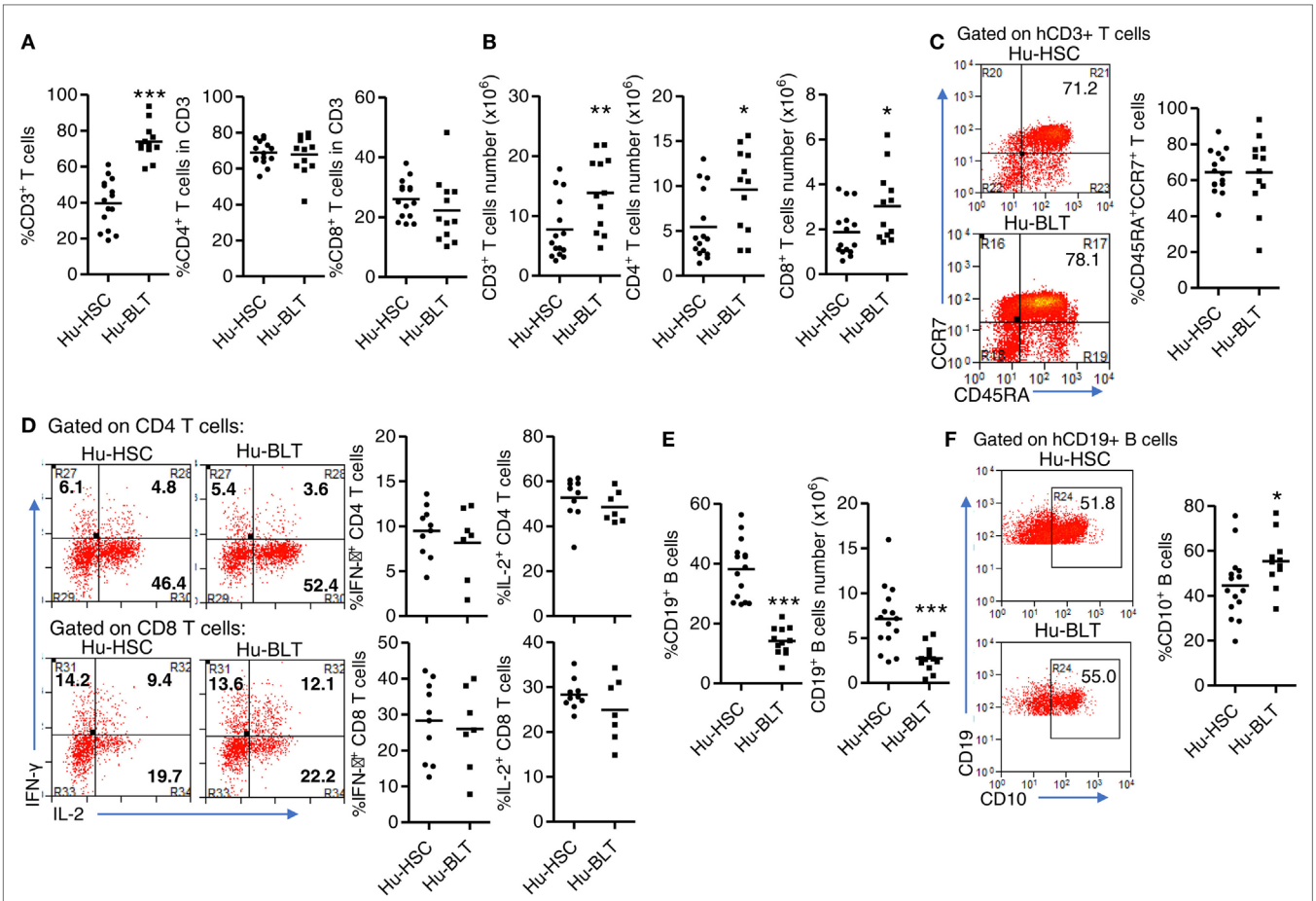

FIGURE 3 | Phenotype and function of human T and B cells from NRG-hu HSC and NRG-hu Thy/HSC mice. NRG-hu HSC and NRG-hu Thy/HSC mice were terminated at 20 weeks after reconstitution. **(A,B)** Summarized data show percentage **(A)** and number **(B)** of total human T cells, CD4 T and CD8 T cells in spleen of NRG-hu HSC and NRG-hu Thy/HSC mice. **(C)** Representative dot plots and summarized data show the expression of CD45RA and CCR7 on CD3 T cells from the spleen of NRG-hu HSC and NRG-hu Thy/HSC mice detected by flow cytometry. Shown **(A–C)** are data from $n = 15$ (NRG-hu HSC) and $n = 12$ (NRG-hu Thy/HSC) hu-mice per group reconstituted with HSCs/thymus from same donor. **(D)** Splenocytes were stimulated *ex vivo* with PMA/ionomycin for 4 h followed by intracellular cytokine staining. Representative dot plots and summarized data show percentages of IFN-γ and IL-2 producing CD4 and CD8 T cells. Shown are data from $n = 10$ (NRG-hu HSC) and $n = 7$ (NRG-hu Thy/HSC) hu-mice per group. **(E)** Summarized data showed percentage and number of total human B cells in spleen of NRG-hu HSC and NRG-hu Thy/HSC mice. **(F)** Representative dot plots and summarized data show expression of CD10 on B cells from the spleen of NRG-hu HSC and NRG-hu Thy/HSC mice. Shown **(E,F)** are data from $n = 15$ (NRG-hu HSC) and $n = 12$ (NRG-hu Thy/HSC) hu-mice per group reconstituted with HSCs ± thymus from the same donor. Each dot represents one individual mouse; bars indicate mean (*$P < 0.05$, **$P < 0.01$, and ***$P < 0.001$, by unpaired, two-tailed Student's *t*-test).

HSC and NRG-hu Thy/HSC mice. We found that HIV-1 induced similar level of total human CD45$^+$ cells and human T cells depletion in both NRG-hu HSC and NRG-hu Thy/HSC mice (**Figures 6A,B**). HIV-1 infection also induced similar level of CD38 and HLA-DR expression on CD8 T cells in both NRG-hu HSC and NRG-hu Thy/HSC mice (**Figures 6C,D**). In addition, we detected the T cells exhaustion marker PD-1 expression and found that both CD8 T cell from NRG-hu HSC and NRG-hu Thy/HSC mice expressed higher level of PD-1 than mock-infected mice, which indicated HIV-1 induced human T cell exhaustion in both humanized mouse models (**Figures 6E,F**). The results indicate that HIV-1 infection induced T cell depletion, activation and exhaustion to similar levels in both NRG-hu HSC and NRG-hu Thy/HSC mice.

cART Efficiently Inhibits HIV-1 Replication in Both NRG-hu HSC and NRG-hu Thy/HSC Mice

We and others have shown before that as in human patients, cART can efficiently inhibit HIV-1 replication in hu-mice (29, 33, 34, 38). We compared the efficacy of cART to inhibit HIV-1 replication in NRG-hu HSC mice and NRG-hu Thy/HSC mice. The results indicate that plasma viremia decreased to undetectable levels (<400 genome copies/ml) in all HIV-infected NRG-hu HSC and NRG-hu Thy/HSC mice within 3 weeks after cART treatment (**Figures 7A,B**). Similar to cART-treated patients, HIV-1 reservoirs persisted stably in both NRG-hu HSC and NRG-hu Thy/HSC mice and virus rebounded rapidly

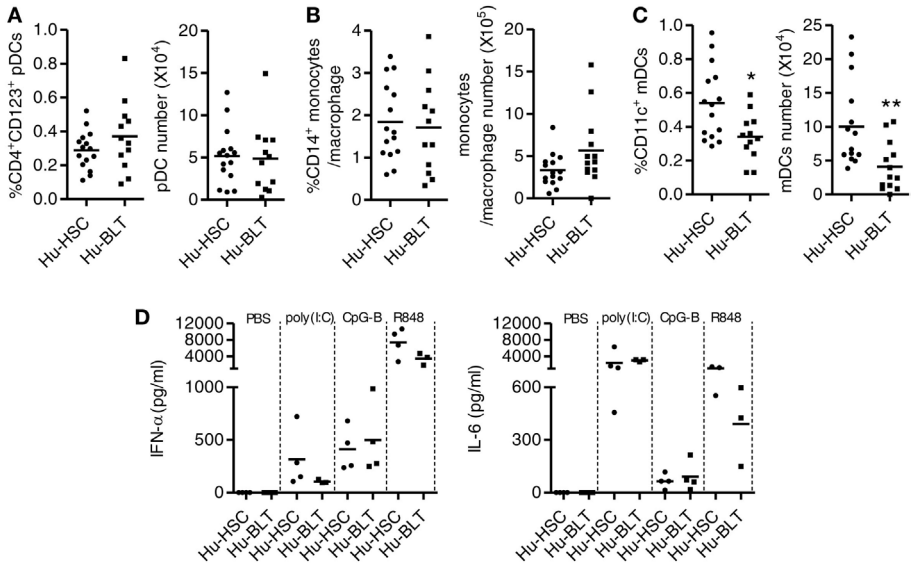

FIGURE 4 | Development and function of human innate immune cells from NRG-hu HSC and NRG-hu Thy/HSC mice. NRG-hu HSC and NRG-hu Thy/HSC mice were terminated at 20 weeks after reconstitution. **(A–C)** Summarized data show percentage and number of total human plasmacytoid dendritic cells (pDCs) ($CD3^-CD19^-HLA\text{-}DR^+CD4^+CD123^+$), monocytes or macrophage ($CD3^-CD19^-HLA\text{-}DR^+CD14^+$), and myeloid dendritic cell (mDC) ($CD3^-CD19^-HLA\text{-}DR^+CD11c^+CD14^-$) in spleen. Shown **(A–C)** are data from $n = 15$ (NRG-hu HSC) and $n = 12$ (NRG-hu Thy/HSC) hu-mice per group reconstituted with HSCs ± thymus from same donor. **(D)** NRG-hu HSC and NRG-hu Thy/HSC mice were injected intraperitoneally with CpG-B (50 μg/mouse), poly I:C (50 μg/mouse), R848 20 μg/mouse, or PBS. Plasma was collected at different time points posttreatment. IFN-α levels in plasma were detected at 24 h after treatment. IL-6 level was detected at 4 h after treatment. Shown **(D)** are data from three to four mice each group for each treatment conditions. Each dot represents one individual mouse; bars indicate mean (*$P < 0.05$ and **$P < 0.01$, by unpaired, two-tailed Student's *t*-test).

after cART cessation (**Figures 7C,D**). HIV-1 rebounded in 60% NRG-hu HSC mice at 1-week post cART cessation and in 100% NRG-hu HSC mice at 2 weeks post cART cessation (**Figure 7E**). Similarly, HIV-1 rebounded in 50% NRG-hu Thy/HSC mice at 1-week post cART cessation and in 100% NRG-hu Thy/HSC mice at 2 weeks post cART cessation (**Figure 7F**).

IFNAR Blockade During cART-Suppressed HIV-1 Infection Reverses Aberrant Immune Activation and Exhaustion Phenotype of Human T Cells

We next determined whether IFNAR blockade can reverses aberrant immune activation and exhaustion phenotype of human T cells in both NRG-hu HSC and NRG-hu Thy/HSC mice. We found that in both HIV-1 infected NRG-hu HSC and NRG-hu Thy/HSC mice, cART alone significantly rescued the number of human CD4 and CD8 T cells (**Figures 8A,B**), however, it only slightly decreased the expression level of CD38/HLA-DR (**Figures 8C,D**) and PD-1 on CD8 T cells (**Figures 8E,F**). CD8 T cells from both cART-treated NRG-hu HSC and NRG-hu Thy/HSC mice still expressed significantly higher levels of activation marker (**Figures 8C,D**) and exhaustion marker PD-1 (**Figures 8E,F**) compared with uninfected hu-mice. Interestingly, IFNAR blockade significantly reversed aberrant CD8 T-cell activation and exhaustion in the presence of cART in both NRG-hu HSC and NRG-hu Thy/HSC mice (**Figures 8C–F**).

IFNAR Blockade Reduce HIV-1 Reservoirs in Both HIV-1 Infected NRG-hu HSC and NRG-hu Thy/HSC Mice Under cART

Combined antiretroviral therapy is able to suppress HIV-1 replication but does not eradicate HIV reservoir, which cause virus rebound after cART interruption. We have reported before that during chronic phase of HIV-1 infection in humanized mice, blockade of IFN-I signaling using a mAb targeting to IFN-I receptor (IFNAR) reduces the level of T cell activation, reverses T cell exhaustion, and improves HIV-specific $CD8^+$ T cells (29). Most strikingly, we found that IFNAR blockade during cART administration markedly reduced HIV-1 reservoirs (29). Here we compared the effect of IFNAR blockade in HIV-1 reservoir reduction in NRG-hu HSC and NRG-hu Thy/HSC mice. We treated HIV-1-infected NRG-hu HSC and NRG-hu Thy/HSC mice that were fully cART-suppressed with α-IFNAR1 mAb for 3 weeks during 7–10 wpi (**Figures 9A,B**). Interestingly, IFNAR blockade led to low blips of HIV-1 replication, which returned to undetectable levels after stopping α-IFNAR1 mAb treatment, in the presence of cART in both NRG-hu HSC and NRG-hu Thy/HSC mice (**Figures 9A,B**). We next analyzed the HIV-1 reservoir size in lymphoid organs 2 weeks after IFNAR blockade in both NRG-hu HSC and NRG-hu Thy/HSC mice. We measured cell-associated HIV-1 DNA by PCR, and replication-competent HIV-1 by the quantitative virus outgrowth assay. We found that IFNAR blockade reduced cell-associated HIV-1 DNA by 10.8-fold in the spleen of NRG-hu HSC mice (**Figure 9C**) and by 7.9-fold

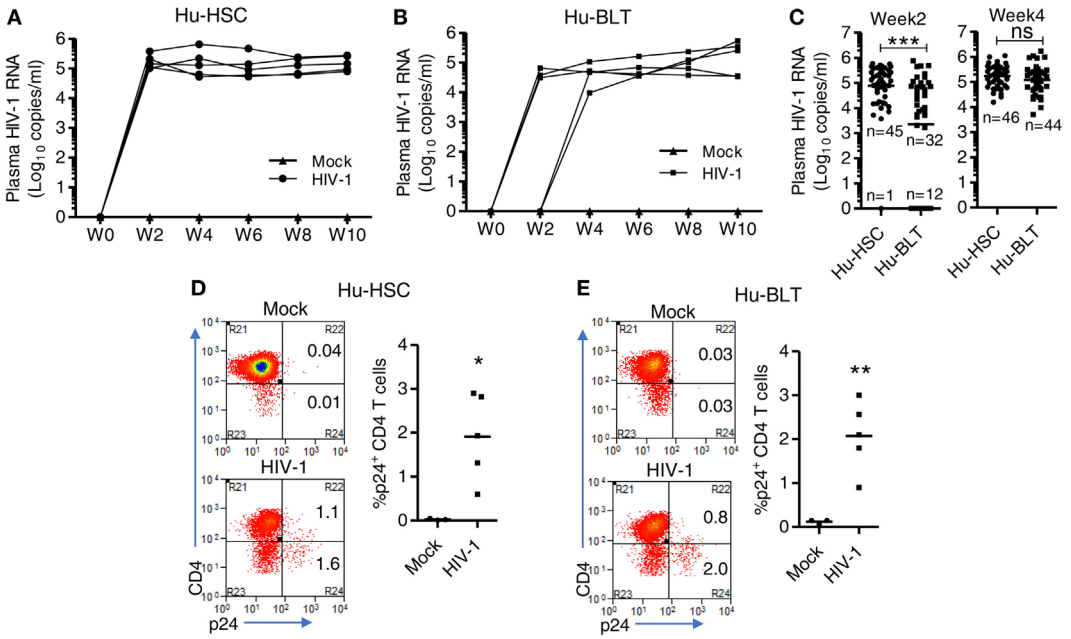

FIGURE 5 | HIV-1 replication kinetics in NRG-hu HSC and NRG-hu Thy/HSC mice *in vivo*. NRG-hu HSC and NRG-hu Thy/HSC mice were infected with HIV-1 at 12–13 weeks postinfection (wpi). **(A,B)** Plasma HIV-1 genomic RNA levels were measured at indicated time points in each NRG-hu HSC **(A)** and NRG-hu Thy/HSC **(B)** mice. Shown are representative data from $n = 3$ (NRG-hu HSC/Mock), $n = 5$ (NRG-hu HSC/HIV-1), $n = 3$ (NRG-hu Thy/HSC/Mock), and $n = 5$ (NRG-hu Thy/HSC/HIV-1) mice transplanted with HSCs ± thymus from the same donor. The broken horizontal line indicates the limit of detection (400 copies/ml). **(C)** Summary data show plasma HIV-1 genomic RNA levels at 2 and 4 wpi from NRG-hu HSC ($n = 46$) and NRG-hu Thy/HSC ($n = 44$) mice. Shown **(C)** are combined data from five cohorts of NRG-hu HSC mice and six cohorts of NRG-hu Thy/HSC mice. The viral infection data were collected previously by the laboratory. **(D,E)** Representative FACS plots and summarized data show percentages of HIV-1 p24-positive CD4 T cells ($CD3^+CD8^-$) in the spleen of NRG-hu HSC **(D)** and NRG-hu Thy/HSC **(E)** mice at 10 wpi. Shown are representative data from $n = 3$ (NRG-hu HSC/Mock), $n = 5$ (NRG-hu HSC/HIV-1), $n = 3$ (NRG-hu Thy/HSC/Mock), and $n = 5$ (NRG-hu Thy/HSC/HIV-1) mice transplanted with HSCs ± thymus from the same donor. Each dot represents one individual mouse; bars indicate mean ($^*P < 0.05$, $^{**}P < 0.01$, and $^{***}P < 0.001$, by unpaired, two-tailed Student's *t*-test).

in NRG-hu Thy/HSC mice (**Figure 9D**). More importantly and consistently, IFNAR blockade significantly reduced the size of replication-competent HIV-1 reservoirs measured by quantitative virus outgrowth assay in both NRG-hu HSC and NRG-hu Thy/HSC mice (**Figures 9E,F**).

Taken together, we conclude that both NRG-hu HSC and NRG-hu Thy/HSC mouse models are valuable tools for the study of HIV-1 replication, pathogenesis and therapeutics.

DISCUSSION

Humanized mice with human immune cells are highly relevant and robust models for HIV-1 study (6–8). The models are generated *via* transplantation of $CD34^+$ HSCs and/or implantation of human tissue into immunodeficient mice. There are different humanized mouse models available as well as different means to prepare them (6, 7, 9). The degree of human immune system reconstitution can vary between different models, and between different batches of HSCs and/or tissue donors, and non-standardized operating procedure between laboratories. Also, HIV-1 infection, replication and HIV-1 induced pathology can vary between different models and dependant on which HIV-1 virus strain is used. These factors make researchers, especially those who have limited experiences on humanized mouse models difficult to decide which model to choose for their studies. Here we performed a comprehensive parallel comparison of systemic immune reconstitution and HIV-1 replication, HIV-1 induced pathology and their response to cART and immunotherapy between two humanized mouse models, the NRG-hu HSC and NRG-hu Thy/HSC models. We used NRG-hu HSC and NRG-hu Thy/HSC mice transplanted with HSCs without or with thymus fragment from same donors into same background of immunodeficient mice in our experiment to minimize the variation factors. Our results indicate that both NRG-hu HSC and NRG-hu Thy/HSC mice support significant level of human immune reconstitution and comparable level of HIV-1 replication, immunopathology and responses to ART and immune therapy.

We and others have reported that all the major human lymphoid and myeloid lineage cells are developed in both NRG-hu HSC mice and hu-BLT mice (10–20). However, no study has performed to parallelly compare the human immune reconstitution in these two models which transplanted with HSCs ± thymus from same donor into the same background of immunodeficient mice. In the NRG-hu Thy/HSC model, we co-transplanted $CD34^+$ HSCs by intravenous injection within 3 h after thymus fragment (without fetal liver fragment) transplantation. Human thymic organoid developed under the kidney capsule in our NRG-hu Thy/HSC as well as reported in hu-BLT mice which indicated

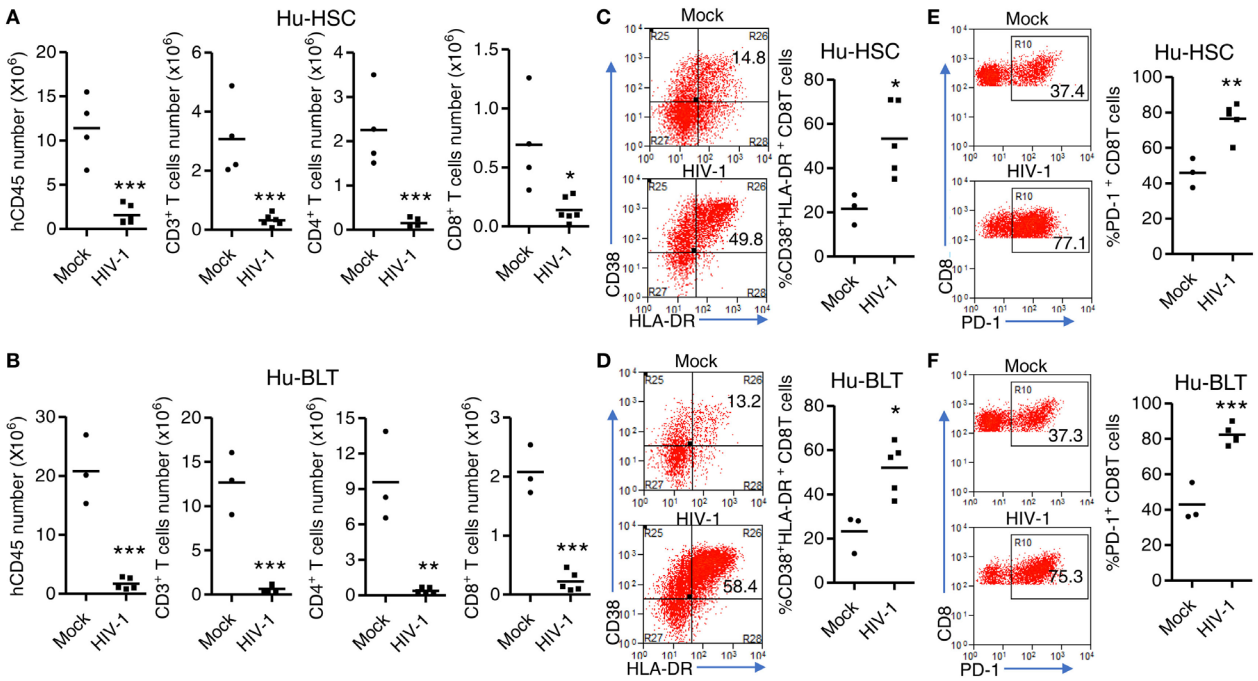

FIGURE 6 | HIV-1-induced immunopathology in NRG-hu HSC and NRG-hu Thy/HSC mice. NRG-hu HSC and NRG-hu Thy/HSC mice were infected with HIV-1. Mice were sacrificed at 10 weeks postinfection. **(A,B)** Numbers of total human leukocytes, $CD3^+$ T cells, CD4 T cells ($CD3^+CD8^-$), and CD8 T cells ($CD3^+CD8^-$) and in spleens of NRG-hu HSC **(A)** and NRG-hu Thy/HSC **(B)** mice. **(C,D)** Representative FACS plots and summarized data show the expression of CD38 and HLA-DR on CD8 T cells from spleen of NRG-hu HSC **(C)** and NRG-hu Thy/HSC **(D)** mice. **(E,F)** Representative FACS plots and summarized data show the expression of PD-1 on CD8 T cells from spleen of NRG-hu HSC **(E)** and NRG-hu Thy/HSC **(F)** mice. Shown are representative data from $n = 3$ (NRG-hu HSC/Mock), $n = 5$ (NRG-hu HSC/HIV-1), $n = 3$ (NRG-hu Thy/HSC/Mock), and $n = 5$ (NRG-hu Thy/HSC/HIV-1) mice reconstituted with HSCs/thymus from the same donor. Each dot represents one individual mouse; bars indicate mean ($^*P < 0.05$, $^{**}P < 0.01$, and $^{***}P < 0.001$, by unpaired, two-tailed Student's *t*-test).

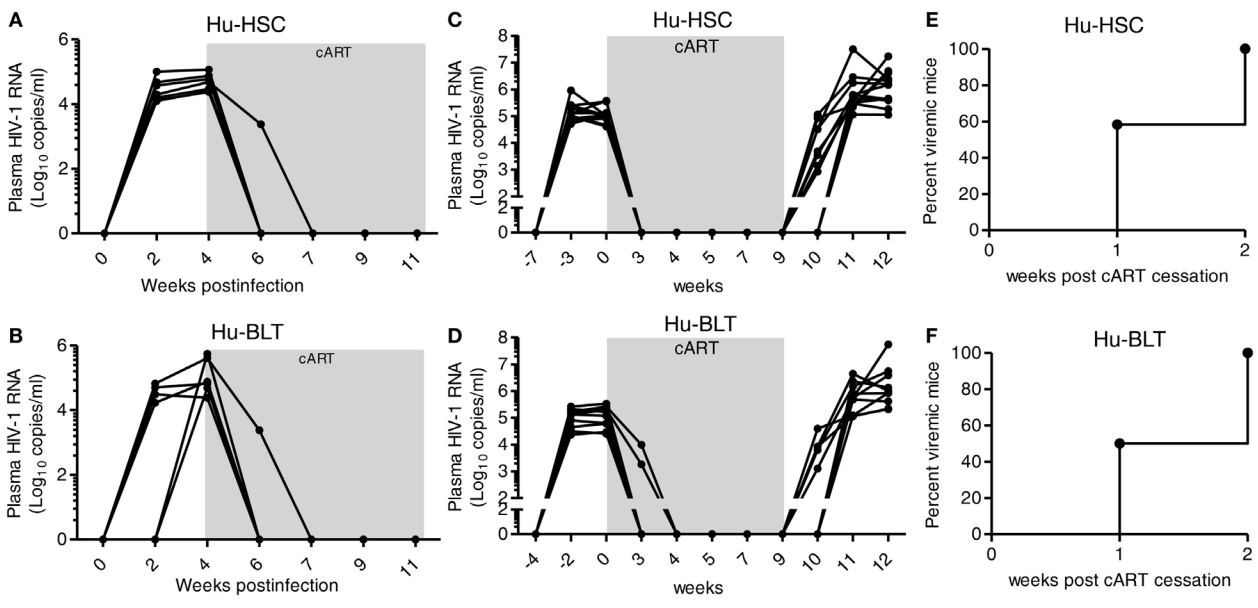

FIGURE 7 | Similar efficacy of combined antiretroviral therapy (cART) response in HIV-1-infected NRG-hu HSC and NRG-hu Thy/HSC mice. **(A,B)** NRG-hu HSC ($n = 6$) and NRG-hu Thy/HSC mice ($n = 7$) reconstituted with HSCs ± thymus from the same donor were infected with HIV-1 and treated with cART from 4 to 11 weeks postinfection. HIV-1 genomic RNA levels in the plasma were detected at indicated time points. **(C,D)** A different cohort of NRG-hu HSC ($n = 12$) and NRG-hu Thy/HSC mice ($n = 10$) were infected with HIV-1 and treated with cART for 9 weeks. HIV-1 genomic RNA levels in the plasma were detected before and after cART discontinuation at indicated time points. The broken horizontal line indicates the limit of detection (400 copies/ml). **(E,F)** Kinetic analysis of HIV-1 rebound post-cART cessation. Shown **(C–E)** are combined data from $n = 12$ (NRG-hu HSC) and $n = 10$ (NRG-hu Thy/HSC) mice.

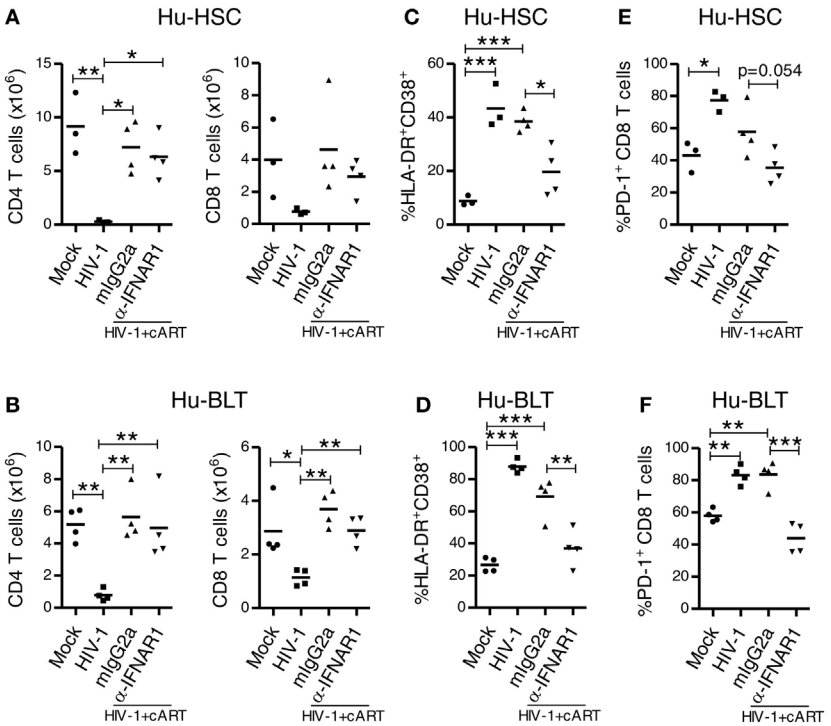

FIGURE 8 | IFNAR blockade reduces activation and PD-1 expression on CD8 T cells in both HIV-1 infected NRG-hu HSC and NRG-hu Thy/HSC mice under combined antiretroviral therapy (cART). NRG-hu HSC and NRG-hu Thy/HSC mice infected with HIV-1 were treated with cART from 4 to 12 weeks postinfection (wpi). From 7 to 10 wpi, the cART-treated mice were injected with α-IFNAR1 antibody or isotype control mIgG2a antibody. Mice were sacrificed at 12 wpi. **(A,B)** Summarized data show numbers of human CD4 and CD8 T cells from spleens of NRG-hu HSC **(A)** and NRG-hu Thy/HSC **(B)** mice. **(C,D)** Summarized data show percent HLA-DR$^+$CD38$^+$ of CD8 T cells from spleens of NRG-hu HSC **(C)** and NRG-hu Thy/HSC **(D)** mice. **(E,F)** Summarized data show percent PD-1$^+$ of CD8 T cells from spleens of NRG-hu HSC **(E)** and NRG-hu Thy/HSC **(F)** mice. Shown are representative data from $n = 3$ (NRG-hu HSC/Mock), $n = 3$ (NRG-hu HSC/HIV-1), $n = 4$ (NRG-hu HSC/HIV-1/cART/mIgG2a), $n = 4$ (NRG-hu HSC/HIV-1/cART/α-IFNAR1), $n = 4$ (NRG-hu Thy/HSC/Mock), $n = 4$ (NRG-hu Thy/HSC/HIV-1), and $n = 4$ (NRG-hu Thy/HSC/HIV-1/cART/mIgG2a), $n = 4$ (NRG-hu Thy/HSC/HIV-1/cART/α-IFNAR1) mice. Each dot represents one individual mouse; bars indicate mean (*$P < 0.05$, **$P < 0.01$, and ***$P < 0.001$, by one-way analysis of variance and Bonferroni's *post hoc* test).

that the fetal liver/thymus "sandwich" are not essential for thymic organoid development. Progenitor cells derived from CD34$^+$ HSCs can serve as the source of thymocyte progenitors. It should be noted that the fetal liver fragments co-transplanted with thymus fragments in the BLT or SCID-hu Thy/Liv (48) mice also provide mostly human HSC/progenitors and no other liver-related functions. Our results indicate that similar level of total human CD45$^+$ cells were developed in peripheral blood, spleen, mLNs, and BM of both NRG-hu HSC and NRG-hu Thy/HSC mice transplanted with HSCs ± thymus from same donor. We also found that all the major human lymphoid and myeloid lineage including T, B, NK cells, monocytes/macrophages, mDC, and pDC were developed in both NRG-hu HSC mice and NRG-hu Thy/HSC mice. The major difference between these two models is that human T cells are predominantly developed in NRG-hu Thy/HSC mice due to more efficient T cell development in human thymus tissue (or xeno-reactive T cells) in NRG-hu HSC-Thy mice. This may lead to preferential reconstitution of T cells and reduced NK/monocyte/pDC engraftment in NRG-hu HSC-Thy mice (**Figures 1** and **3**).

Our results indicated that majority of human T cells from both NRG-hu HSC and NRG-hu Thy/HSC mice were with naïve phenotype and they responded similarly to mitogen stimulation. However, it is important to point out that human T cells can develop in the presence of human thymic epithelium, resulting in human HLA class I and class II restriction in NRG-hu Thy/HSC mice (14, 15, 40). While in NRG-hu HSC mice, human T cells are produced in the mouse thymus and presumed to be educated in the context of mouse MHC (10–13). To study human HLA-restricted immune response in NRG-hu HSC mice, an immune-compromised non-obese diabetic/SCID/IL2rg$^{-/-}$ strain (NSG) with homozygous expression of HLA class I heavy chain and light chain (NSG-HLA-A2/HHD) was generated (49). Human CTLs developing in the NSG-HLA-A2/HHD mice recognized EBV-derived peptides in an HLA-restricted manner and showed HLA-restricted cytotoxicity against EBV-infected human B cells (49). We also reported that HIV-1 infection can induce HIV-1 antigen-specific, HLA-A2-restricted CD8 T cell responds in humanized NSG-HLA-A2/HHD mice (31).

Both NRG-hu HSC and NRG-hu Thy/HSC mice support HIV-1 replication *in vivo*. Our results show that plasma HIV-1 viremia reached to peak levels at 2 wpi in NRG-hu HSC mice, while the peak viremia appeared at 4 wpi in NRG-hu Thy/HSC mice. The results suggest that anti-HIV-1 immunity at the early

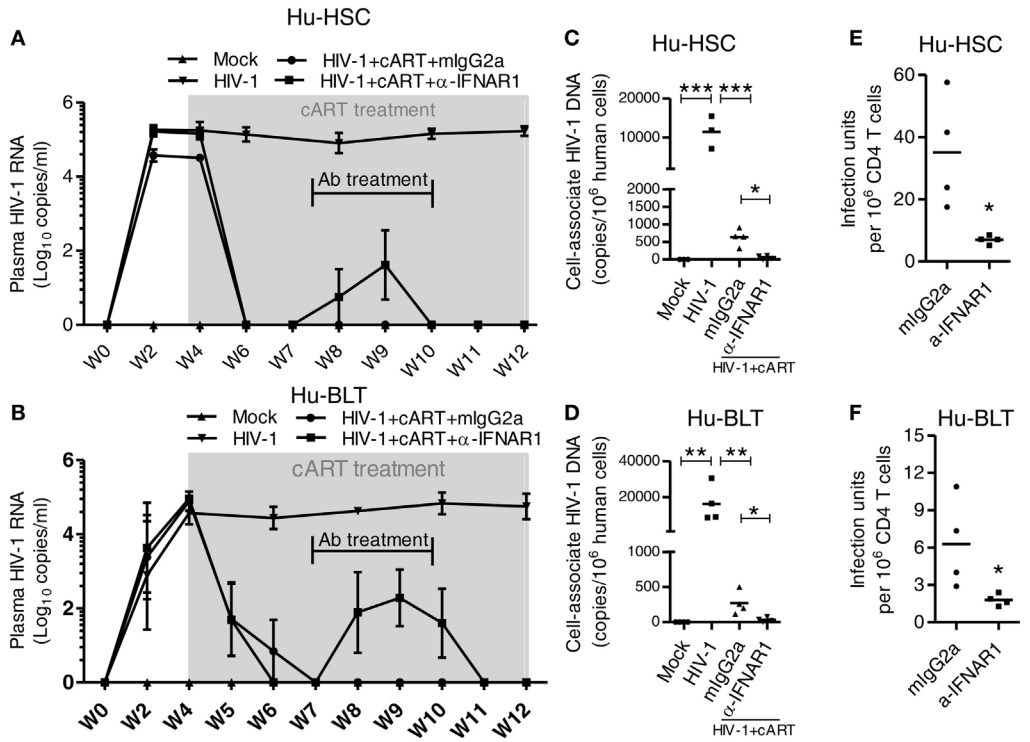

FIGURE 9 | IFNAR blockade reduce HIV-1 reservoir in both HIV-1 infected NRG-hu HSC and NRG-hu Thy/HSC mice under combined antiretroviral therapy (cART). NRG-hu HSC and NRG-hu Thy/HSC mice infected with HIV-1 were treated with cART from 4 to 12 weeks postinfection (wpi). From 7 to 10 wpi, the cART-treated mice were injected with α-IFNAR1 antibody or isotype control mIgG2a antibody. **(A,B)** HIV-1 genomic RNA levels in the plasma of NRG-hu HSC **(A)** and NRG-hu Thy/HSC **(B)** mice. **(C,D)** Cell-associated HIV-1 DNA in human cells from spleen of NRG-hu HSC **(C)** and NRG-hu Thy/HSC **(D)** mice was quantified by PCR. **(E,F)** Replication-competent HIV-1 viruses from unfractionated human CD45$^+$ cells from spleen of NRG-hu HSC **(E)** and NRG-hu Thy/HSC **(F)** mice were detected by the quantitative virus outgrowth assay. The frequency was determined by maximum likelihood statistics. The infectious units in CD4 T cells were calculated based on the percentage of CD4 T cells in total human CD45$^+$ cells. Shown are representative data from $n = 3$ (NRG-hu HSC/Mock), $n = 3$ (NRG-hu HSC/HIV-1), $n = 4$ (NRG-hu HSC/HIV-1/cART/mIgG2a), $n = 4$ (NRG-hu HSC/HIV-1/cART/α-IFNAR1), $n = 4$ (NRG-hu Thy/HSC/Mock), $n = 4$ (NRG-hu Thy/HSC/HIV-1), $n = 4$ (NRG-hu Thy/HSC/HIV-1/cART/mIgG2a), $n = 4$ (NRG-hu Thy/HSC/HIV-1/cART/α-IFNAR1) mice. Each dot represents one individual mouse; bars indicate mean (*$P < 0.05$, **$P < 0.01$, and ***$P < 0.001$, by one-way analysis of variance and Bonferroni's *post hoc* test).

stage of HIV-1 infection is better in NRG-hu Thy/HSC mice. The better HLA-restricted anti-HIV-1 T cells response in NRG-hu Thy/HSC mice (23) may contribute to the delay of peak viremia. However, other unknown factors, such as the difference in immune subset reconstitution or donor genetics, may also lead to the reduced or delayed HIV-1 infection in NRG-hu Thy/HSC mice. After 4 weeks, HIV-1 replicated to similar levels in NRG-hu HSC and NRG-hu Thy/HSC mice. Furthermore, HIV-1 infection induced similar pathology including the depletion of human T cells and activation and exhaustion of T cells.

Combined antiretroviral therapy is able to suppress HIV-1 replication but does not eradicate HIV-1 reservoir, which cause virus rebound after cART interruption. This lack of *in vivo* models of HIV-1 infection has hindered progress in finding a cure for HIV-1/AIDS. The use of both NRG-hu HSC and NRG-hu Thy/HSC models of HIV-1 infection have made significant contribution to the field of HIV cure research (6, 7). We found here that both the HIV-1 infected NRG-hu HSC and NRG-hu Thy/HSC mice responded similarly to cART. Importantly, we found that type-I IFN signaling contributed to HIV-1 induced immune activation, dysfunction and fostered viral persistence in both NRG-hu HSC and NRG-hu Thy/HSC mice. Blockade of IFNAR reduced the level of T cell activation, reversed T cell exhaustion, and reduced HIV-1 reservoirs in both models. Multiple mechanisms may lead to the reduction of HIV-1 reservoir size after IFNAR blockade. The rescued human T cells could target the HIV-1 reservoirs with elevated gene expression and clear the reservoir cells as we have reported (29, 30). Other factors, including HIV-1 induced death of reservoir cells, reduced general T cell activation after IFNAR blockade, may also contribute to the reduction of HIV-1 reservoir size (29).

Taken together, we conclude that both NRG-hu HSC and NRG-hu Thy/HSC mouse models are relevant and robust for the study of HIV-1 replication, pathogenesis and therapeutics. Each model has its own advantage and disadvantages. Compared with the NRG-hu Thy/HSC or Hu-BLT models, the advantages of the NRG-hu HSC model are as follows: (1) the procedure to construct NRG-hu HSC mice is simple, which only involving pre-irradiating the neonate immunodeficient mice followed by injecting human CD34$^+$ HSCs (10, 11, 13). To generate NRG-hu Thy/HSC or Hu-BLT mice, a time consuming and technically difficult surgery procedure is needed to implant the human thymus

tissue under the kidney capsule of the mice (14, 15); (2) the source of HSCs to construct NRG-hu HSC mice is not restricted to fetal liver derived $CD34^+$ cells. $CD34^+$ HSCs from cord blood or human BM can also support the systemic development of human immune system (10, 14); (3) the graft-versus-host disease (GVHD) rarely happens in NRG-hu HSC mice, while the incident of GVHD is high in NRG-hu Thy/HSC or BLT mice (50) probably due to the mature human thymocytes in the transplanted thymic fragments; and (4) neonate immunodeficient mice are used to generate NRG-hu HSC mice, while 6- to 8-week-old mice are used for NRG-hu Thy/HSC or BLT mice construction. As the time needed for human immune reconstitution is 12–16 weeks in both models, researchers can start their experiments with younger NRG-hu HSC mice. The hu-Thy/HSC or BLT model also has its own advantages. It was reported that NOD-SCID-BLT (not NSG-BLT) mice supported better gut-associated lymphoid tissue development (GALT) (51). The other advantage of NRG-hu Thy/HSC or BLT model or hu-BLT model is that it supports the study of human HLA class I and class II restricted T cell response because human T cells develop in the presence of human thymic epithelium (14, 15, 40). However, as discussed earlier, human MHC-restricted T cell response and therapies can be studied in NRG-hu HSC mice that transgenically express human HLA-genes (49).

ETHICS STATEMENT

The project was reviewed by the University's Office of Human Research Ethics, which has determined that this submission does not constitute human subjects research as defined under federal regulations [45 CFR 46.102 (d or f) and 21 CFR 56.102(c)(e)(l)]. All animal studies were carried out in accordance with the recommendations of NIH guidelines for housing and care of laboratory animals. The protocol and was approved by the University of North Carolina Institutional Animal Care and Use Committee (IACUC ID: 14-100).

AUTHOR CONTRIBUTIONS

LC and LS conceived the study and designed the experiments. LC, JM, and GL performed the experiments. LC performed the analyses. LC and LS interpreted the data, wrote the manuscript, and supervised the study. All the authors approved the final version.

ACKNOWLEDGMENTS

The authors thank L. Chi, Y. Wu, and A. Pons for technical support; Lineberger Comprehensive Cancer Center cores, UNC flow cytometer core, DLAM, and UNC CFAR for support.

FUNDING

This study was supported in part by NIH grants AI127346, AI109784, and AI095097 (to LS).

SUPPLEMENTARY MATERIAL

The Supplementary Material for this article can be found online at https://www.frontiersin.org/articles/10.3389/fimmu.2018.00817/full#supplementary-material.

REFERENCES

1. UNAIDS. *UNAIDS Fact Sheet November 2016. Global HIV Statistics*. Geneva: UNAIDS (2016).
2. Antiretroviral Therapy Cohort Collaboration. Life expectancy of individuals on combination antiretroviral therapy in high-income countries: a collaborative analysis of 14 cohort studies. *Lancet* (2008) 372(9635):293–9. doi:10.1016/S0140-6736(08)61113-7
3. Archin NM, Sung JM, Garrido C, Soriano-Sarabia N, Margolis DM. Eradicating HIV-1 infection: seeking to clear a persistent pathogen. *Nat Rev Microbiol* (2014) 12(11):750–64. doi:10.1038/nrmicro3352
4. Katlama C, Deeks SG, Autran B, Martinez-Picado J, van Lunzen J, Rouzioux C, et al. Barriers to a cure for HIV: new ways to target and eradicate HIV-1 reservoirs. *Lancet* (2013) 381(9883):2109–17. doi:10.1016/S0140-6736(13)60104-X
5. Deeks SG. HIV infection, inflammation, immunosenescence, and aging. *Annu Rev Med* (2011) 62:141–55. doi:10.1146/annurev-med-042909-093756
6. Victor Garcia J. Humanized mice for HIV and AIDS research. *Curr Opin Virol* (2016) 19:56–64. doi:10.1016/j.coviro.2016.06.010
7. Marsden MD, Zack JA. Humanized mouse models for human immunodeficiency virus infection. *Annu Rev Virol* (2017) 4(1):393–412. doi:10.1146/annurev-virology-101416-041703
8. Zhang L, Su L. HIV-1 immunopathogenesis in humanized mouse models. *Cell Mol Immunol* (2012) 9(3):237–44. doi:10.1038/cmi.2012.7
9. Shultz LD, Brehm MA, Garcia-Martinez JV, Greiner DL. Humanized mice for immune system investigation: progress, promise and challenges. *Nat Rev Immunol* (2012) 12(11):786–98. doi:10.1038/nri3311
10. Traggiai E, Chicha L, Mazzucchelli L, Bronz L, Piffaretti JC, Lanzavecchia A, et al. Development of a human adaptive immune system in cord blood cell-transplanted mice. *Science* (2004) 304(5667):104–7. doi:10.1126/science.1093933
11. Ishikawa F, Yasukawa M, Lyons B, Yoshida S, Miyamoto T, Yoshimoto G, et al. Development of functional human blood and immune systems in NOD/SCID/IL2 receptor {gamma} chain(null) mice. *Blood* (2005) 106(5):1565–73. doi:10.1182/blood-2005-02-0516
12. Zhang L, Kovalev GI, Su L. HIV-1 infection and pathogenesis in a novel humanized mouse model. *Blood* (2007) 109(7):2978–81. doi:10.1182/blood-2006-07-033159
13. Shultz LD, Lyons BL, Burzenski LM, Gott B, Chen X, Chaleff S, et al. Human lymphoid and myeloid cell development in NOD/LtSz-scid IL2R gamma null mice engrafted with mobilized human hemopoietic stem cells. *J Immunol* (2005) 174(10):6477–89. doi:10.4049/jimmunol.174.10.6477
14. Lan P, Tonomura N, Shimizu A, Wang S, Yang YG. Reconstitution of a functional human immune system in immunodeficient mice through combined human fetal thymus/liver and CD34+ cell transplantation. *Blood* (2006) 108(2):487–92. doi:10.1182/blood-2005-11-4388
15. Melkus MW, Estes JD, Padgett-Thomas A, Gatlin J, Denton PW, Othieno FA, et al. Humanized mice mount specific adaptive and innate immune responses to EBV and TSST-1. *Nat Med* (2006) 12(11):1316–22. doi:10.1038/nm1431
16. Jiang Q, Zhang L, Wang R, Jeffrey J, Washburn ML, Brouwer D, et al. FoxP3+CD4+ regulatory T cells play an important role in acute HIV-1 infection in humanized Rag2-/-gammaC-/- mice in vivo. *Blood* (2008) 112(7):2858–68. doi:10.1182/blood-2008-03-145946
17. Zhang L, Jiang Q, Li G, Jeffrey J, Kovalev GI, Su L. Efficient infection, activation, and impairment of pDCs in the BM and peripheral lymphoid organs during early HIV-1 infection in humanized rag2(-)/(-)gamma C(-)/(-) mice in vivo. *Blood* (2011) 117(23):6184–92. doi:10.1182/blood-2011-01-331173
18. Zhang Z, Cheng L, Zhao J, Li G, Zhang L, Chen W, et al. Plasmacytoid dendritic cells promote HIV-1-induced group 3 innate lymphoid cell depletion. *J Clin Invest* (2015) 125(9):3692–703. doi:10.1172/JCI82124

19. Meixlsperger S, Leung CS, Ramer PC, Pack M, Vanoaica LD, Breton G, et al. CD141+ dendritic cells produce prominent amounts of IFN-alpha after dsRNA recognition and can be targeted via DEC-205 in humanized mice. *Blood* (2013) 121(25):5034–44. doi:10.1182/blood-2012-12-473413
20. Cheng L, Zhang Z, Li G, Li F, Wang L, Zhang L, et al. Human innate responses and adjuvant activity of TLR ligands in vivo in mice reconstituted with a human immune system. *Vaccine* (2017) 35(45):6143–53. doi:10.1016/j.vaccine.2017.09.052
21. Gorantla S, Makarov E, Finke-Dwyer J, Gebhart CL, Domm W, Dewhurst S, et al. CD8+ cell depletion accelerates HIV-1 immunopathology in humanized mice. *J Immunol* (2010) 184(12):7082–91. doi:10.4049/jimmunol.1000438
22. Brainard DM, Seung E, Frahm N, Cariappa A, Bailey CC, Hart WK, et al. Induction of robust cellular and humoral virus-specific adaptive immune responses in human immunodeficiency virus-infected humanized BLT mice. *J Virol* (2009) 83(14):7305–21. doi:10.1128/JVI.02207-08
23. Dudek TE, No DC, Seung E, Vrbanac VD, Fadda L, Bhoumik P, et al. Rapid evolution of HIV-1 to functional CD8(+) T cell responses in humanized BLT mice. *Sci Transl Med* (2012) 4(143):143ra98. doi:10.1126/scitranslmed.3003984
24. Seung E, Dudek TE, Allen TM, Freeman GJ, Luster AD, Tager AM. PD-1 blockade in chronically HIV-1-infected humanized mice suppresses viral loads. *PLoS One* (2013) 8(10):e77780. doi:10.1371/journal.pone.0077780
25. Palmer BE, Neff CP, Lecureux J, Ehler A, Dsouza M, Remling-Mulder L, et al. In vivo blockade of the PD-1 receptor suppresses HIV-1 viral loads and improves CD4+ T cell levels in humanized mice. *J Immunol* (2013) 190(1):211–9. doi:10.4049/jimmunol.1201108
26. Berges BK, Akkina SR, Folkvord JM, Connick E, Akkina R. Mucosal transmission of R5 and X4 tropic HIV-1 via vaginal and rectal routes in humanized Rag2-/- gammac-/- (RAG-hu) mice. *Virology* (2008) 373(2):342–51. doi:10.1016/j.virol.2007.11.020
27. Denton PW, Garcia JV. Mucosal HIV-1 transmission and prevention strategies in BLT humanized mice. *Trends Microbiol* (2012) 20(6):268–74. doi:10.1016/j.tim.2012.03.007
28. Akkina R, Berges BK, Palmer BE, Remling L, Neff CP, Kuruvilla J, et al. Humanized Rag1-/- gammac-/- mice support multilineage hematopoiesis |and are susceptible to HIV-1 infection via systemic and vaginal routes. *PLoS One* (2011) 6(6):e20169. doi:10.1371/journal.pone.0020169
29. Cheng L, Ma J, Li J, Li D, Li G, Li F, et al. Blocking type I interferon signaling enhances T cell recovery and reduces HIV-1 reservoirs. *J Clin Invest* (2017) 127(1):269–79. doi:10.1172/JCI90745
30. Zhen A, Rezek V, Youn C, Lam B, Chang N, Rick J, et al. Targeting type I interferon-mediated activation restores immune function in chronic HIV infection. *J Clin Invest* (2017) 127(1):260–8. doi:10.1172/JCI89488
31. Cheng L, Yu H, Li G, Li F, Ma J, Li J, et al. Type I interferons suppress viral replication but contribute to T cell depletion and dysfunction during chronic HIV-1 infection. *JCI Insight* (2017) 2(12):1–13. doi:10.1172/jci.insight.94366
32. Denton PW, Estes JD, Sun Z, Othieno FA, Wei BL, Wege AK, et al. Antiretroviral pre-exposure prophylaxis prevents vaginal transmission of HIV-1 in humanized BLT mice. *PLoS Med* (2008) 5(1):e16. doi:10.1371/journal.pmed.0050016
33. Denton PW, Olesen R, Choudhary SK, Archin NM, Wahl A, Swanson MD, et al. Generation of HIV latency in humanized BLT mice. *J Virol* (2012) 86(1):630–4. doi:10.1128/JVI.06120-11
34. Halper-Stromberg A, Lu CL, Klein F, Horwitz JA, Bournazos S, Nogueira L, et al. Broadly neutralizing antibodies and viral inducers decrease rebound from HIV-1 latent reservoirs in humanized mice. *Cell* (2014) 158(5):989–99. doi:10.1016/j.cell.2014.07.043
35. Veselinovic M, Yang KH, LeCureux J, Sykes C, Remling-Mulder L, Kashuba ADM, et al. HIV pre-exposure prophylaxis: mucosal tissue drug distribution of RT inhibitor tenofovir and entry inhibitor maraviroc in a humanized mouse model. *Virology* (2014) 464-465:253–63. doi:10.1016/j.virol.2014.07.008
36. Hu S, Neff CP, Kumar DM, Habu Y, Akkina SR, Seki T, et al. A humanized mouse model for HIV-2 infection and efficacy testing of a single-pill triple-drug combination anti-retroviral therapy. *Virology* (2017) 501:115–8. doi:10.1016/j.virol.2016.11.013
37. Klein F, Halper-Stromberg A, Horwitz JA, Gruell H, Scheid JF, Bournazos S, et al. HIV therapy by a combination of broadly neutralizing antibodies in humanized mice. *Nature* (2012) 492(7427):118–22. doi:10.1038/nature11604
38. Horwitz JA, Halper-Stromberg A, Mouquet H, Gitlin AD, Tretiakova A, Eisenreich TR, et al. HIV-1 suppression and durable control by combining single broadly neutralizing antibodies and antiretroviral drugs in humanized mice. *Proc Natl Acad Sci U S A* (2013) 110(41):16538–43. doi:10.1073/pnas.1315295110
39. Denton PW, Long JM, Wietgrefe SW, Sykes C, Spagnuolo RA, Snyder OD, et al. Targeted cytotoxic therapy kills persisting HIV infected cells during ART. *PLoS Pathog* (2014) 10(1):e1003872. doi:10.1371/journal.ppat.1003872
40. Wege AK, Melkus MW, Denton PW, Estes JD, Garcia JV. Functional and phenotypic characterization of the humanized BLT mouse model. *Curr Top Microbiol Immunol* (2008) 324:149–65. doi:10.1007/978-3-540-75647-7_10
41. Li G, Cheng M, Nunoya J, Cheng L, Guo H, Yu H, et al. Plasmacytoid dendritic cells suppress HIV-1 replication but contribute to HIV-1 induced immunopathogenesis in humanized mice. *PLoS Pathog* (2014) 10(7):e1004291. doi:10.1371/journal.ppat.1004291
42. Chen Y, Wei H, Sun R, Dong Z, Zhang J, Tian Z. Increased susceptibility to liver injury in hepatitis B virus transgenic mice involves NKG2D-ligand interaction and natural killer cells. *Hepatology* (2007) 46(3):706–15. doi:10.1002/hep.21872
43. Laird GM, Rosenbloom DI, Lai J, Siliciano RF, Siliciano JD. Measuring the frequency of latent HIV-1 in resting CD4(+) T cells using a limiting dilution coculture assay. *Methods Mol Biol* (2016) 1354:239–53. doi:10.1007/978-1-4939-3046-3_16
44. Biswas S, Chang H, Sarkis PT, Fikrig E, Zhu Q, Marasco WA. Humoral immune responses in humanized BLT mice immunized with West Nile virus and HIV-1 envelope proteins are largely mediated via human CD5+ B cells. *Immunology* (2011) 134(4):419–33. doi:10.1111/j.1365-2567.2011.03501.x
45. Seung E, Tager AM. Humoral immunity in humanized mice: a work in progress. *J Infect Dis* (2013) 208(Suppl 2):S155–9. doi:10.1093/infdis/jit448
46. Martinez-Torres F, Nochi T, Wahl A, Garcia JV, Denton PW. Hypogammaglobulinemia in BLT humanized mice – an animal model of primary antibody deficiency. *PLoS One* (2014) 9(10):e108663. doi:10.1371/journal.pone.0108663
47. Garcia JV. In vivo platforms for analysis of HIV persistence and eradication. *J Clin Invest* (2016) 126(2):424–31. doi:10.1172/JCI80562
48. Namikawa R, Kaneshima H, Lieberman M, Weissman IL, McCune JM. Infection of the SCID-hu mouse by HIV-1. *Science* (1988) 242(4886):1684–6. doi:10.1126/science.3201256
49. Shultz LD, Saito Y, Najima Y, Tanaka S, Ochi T, Tomizawa M, et al. Generation of functional human T-cell subsets with HLA-restricted immune responses in HLA class I expressing NOD/SCID/IL2r gamma(null) humanized mice. *Proc Natl Acad Sci U S A* (2010) 107(29):13022–7. doi:10.1073/pnas.1000475107
50. Greenblatt MB, Vrbanac V, Tivey T, Tsang K, Tager AM, Aliprantis AO. Graft versus host disease in the bone marrow, liver and thymus humanized mouse model. *PLoS One* (2012) 7(9):e44664. doi:10.1371/journal.pone.0044664
51. Nochi T, Denton PW, Wahl A, Garcia JV. Cryptopatches are essential for the development of human GALT. *Cell Rep* (2013) 3(6):1874–84. doi:10.1016/j.celrep.2013.05.037

Conflict of Interest Statement: The authors declare that the research was conducted in the absence of any commercial or financial relationships that could be construed as a potential conflict of interest.

frontiers in Immunology

REVIEW
published: 20 April 2018
doi: 10.3389/fimmu.2018.00746

The Use of the Humanized Mouse Model in Gene Therapy and Immunotherapy for HIV and Cancer

*Mayra A. Carrillo, Anjie Zhen and Scott G. Kitchen**

Department of Medicine, Division of Hematology and Oncology, University of California Los Angeles, Los Angeles, CA, United States

HIV and cancer remain prevailing sources of morbidity and mortality worldwide. There are current efforts to discover novel therapeutic strategies for the treatment or cure of these diseases. Humanized mouse models provide the investigative tool to study the interaction between HIV or cancer and the human immune system *in vivo*. These humanized models consist of immunodeficient mice transplanted with human cells, tissues, or hematopoietic stem cells that result in reconstitution with a nearly full human immune system. In this review, we discuss preclinical studies evaluating therapeutic approaches in stem cell-based gene therapy and T cell-based immunotherapies for HIV and cancer using a humanized mouse model and some recent advances in using checkpoint inhibitors to improve antiviral or antitumor responses.

Keywords: HIV, cancer, humanized mice, gene therapy, immunotherapy, T cell receptor, chimeric antigen receptor, hematopoietic stem cells

OPEN ACCESS

Edited by:
Ramesh Akkina, Colorado State University, United States

Reviewed by:
James Riley, University of Pennsylvania, United States
Sylvie Fournel, Université de Strasbourg, France

***Correspondence:**
Scott G. Kitchen
skitchen@ucla.edu

Specialty section:
This article was submitted to Vaccines and Molecular Therapeutics, a section of the journal Frontiers in Immunology

Received: *23 December 2017*
Accepted: *26 March 2018*
Published: *20 April 2018*

Citation:
Carrillo MA, Zhen A and Kitchen SG (2018) The Use of the Humanized Mouse Model in Gene Therapy and Immunotherapy for HIV and Cancer. Front. Immunol. 9:746. doi: 10.3389/fimmu.2018.00746

INTRODUCTION

Humanized mice have emerged as an invaluable tool in providing a model system that enables researchers to study the human immune system and its development and function/dysfunction *in vivo* (1). The identification of the severe combined immunodeficiency (*Prkcd*^{scid} or SCID) mouse provided the cornerstone of the development of the humanized mouse model by allowing the xenoengraftment of human (hu) cells [specifically, human peripheral blood lymphocytes (PBLs)] without mouse immune system-mediated rejection (known as the hu-PBL SCID model) (2). This allowed limited examination of components of the human immune system in a manipulatable model system. Further development occurred with the engraftment of SCID mice with human fetal thymus and liver tissue, which is implanted under the kidney capsule of the animals (termed the SCID-hu mouse) (3, 4). The fetal liver tissue provided the hematopoietic cells and the thymus tissue provided the stromal elements to facilitate the engraftment and development of a functional human thymus in these animals. This allowed the closed examination and long-term engraftment of human hematopoietic tissue *in vivo*. Humanized mouse model development rapidly expanded with the identification and breeding of immunodeficient strains of mice that facilitated a greater engraftment of human cells. SCID mice have been crossed with other mouse strains, such as the nonobese diabetic (NOD) mouse to generate NOD/SCID mice that have defects in innate and adaptive immunity (5). Other mice that have been crossed to SCID mouse strains include those that have genetic mutations in the Rag1, Rag2, or the IL-2 receptor common gamma chain (IL2rγ) genes to generate new strains of immuno-incompetent mice which allow greater human cell and tissue engraftment, particularly the tissues and cells that have a high hematopoietic potential (6). The NOD/SCID and NOD/SCID/IL2rγ-knockout (NSG) strains have been used to generate one of the more recent humanized mouse

models that has shown to have the most robust human immune system engraftment, providing long-term human hematopoietic stem/progenitor cell (HSPC) engraftment and functional multilineage hematopoietic differentiation. This model facilitated the engraftment of human CD34$^+$ HSPCs in the bone marrow of the animals and subsequent multilineage hematopoiesis, including B cell production and limited T cell development [termed the CD34-humanized mouse (7)]. More robust T cell reconstitution, which provides a more relevant model for HIV infection and the study of T cell immunity (8), was subsequently developed and involved the intravenous injection of autologous CD34$^+$ human hematopoietic cells from fetal liver tissues, which engraft in the bone marrow (B), along with the transplantation of human fetal liver (L) and thymus (T) tissue under the kidney capsule of the mice, which forms a recapitulated human thymus [known as the bone marrow–liver–thymus (BLT) mouse] (9, 10). New mice strains, such as NOD-SCID IL2Rγnull/IL-3/GM-CSF(NSG-SGM3), are also being adopted for constructing BLT mice for better differentiation of myeloid cells or cancer engraftment (11, 12). Overall, immune-incompetent mouse strains can be humanized by either the transplantation of human peripheral blood mononuclear cells (PBMCs), the transplantation of human HSPCs, or the engraftment of human fetal tissue and HSPCs (**Table 1**). Among them, the humanized BLT mice are the most robust model in supporting multilineage human immune system development (13). The development of humanized mouse models has been extensively reviewed in Ref. (6, 14, 15) and been utilized in preclinical studies that revealed important discoveries in several fields of research (1).

In particular, HIV researchers have taken advantage of the humanized mouse model to better understand the pathogenesis of the infection and to examine novel therapeutic strategies to treat and possibly eradicate infection (19). Relatively early in the use of these types of humanized mice, researchers used the SCID-hu mouse as a platform to design and test a gene therapy approach for the treatment of HIV infection. Human HSPCs were transduced with a retroviral vector expressing a reporter gene and were then injected into the human thymus organoid to evaluate the differentiation and development of mature cells carrying the transgene reporter *in vivo* (20, 21). These studies formed the basis of the development of this approach to protect cells from HIV infection in what was the largest phase II gene therapy trial to that date (22). This sets the stage for the forward progression of other types of HSPC-based gene therapy research involving the development of lentiviral vectors expressing anti-HIV components that result in HIV-resistant immune cells *in vivo* in humanized mice (23–27). Results for some of these studies enabled stem cell-based gene therapy clinical trials that are currently ongoing (ClinicalTrials.gov Identifier: NCT01734850). Thus, studies such as these performed in humanized mice illustrate the utility of testing new stem cell-based gene therapy approached in humanized mice and highlight the potential therapeutic efficacy and safety of engineering such aspects as HIV resistance through the genetic modification of HSCs with anti-HIV genes (28).

Currently, humanized mouse models are being highly utilized to study human diseases and develop novel therapeutic approaches that can potentially be translated into clinical trials as described above. HIV and cancer are two research fields that have been taking advantage of the humanized mouse model to study stem cell- and T cell-based immunotherapy approaches to treat these chronic diseases. In this review, we highlight important studies using the humanized mouse model in stem cell- and T cell-based immunotherapy using highly potent transgenic T cell receptors (TCRs) and chimeric antigen receptors (CARs). We also discuss utilizing checkpoint inhibitors to overcome common immunosuppression mechanisms used by both diseases that promote disease progression and persistence.

PERIPHERAL CELL-BASED IMMUNOTHERAPY MODELING IN HUMANIZED MICE

Transgenic TCRs in Humanized Mice

One of the earliest attempts for treating HIV through an immunotherapy-based approach using peripheral T cells was to

TABLE 1 | Engraftment of human immune system in the most commonly used immunodeficient mouse models.

Common engraftment method of human cells	Common immunodeficient strains used	Characteristics of the reconstituted human immune system	Source and references
Injection of peripheral blood mononuclear cells	Nonobese diabetic (NOD).CB17-*Prkdc*^{scid} (NOD-SCID)	Engraftment of T cells, rapid GVHD development	Jackson Laboratory (2)
Injection of HSCs	NOD.Cg-*Prkdc*^{scid}*IL2rg*^{tm1Wjl}/*Sz* (NSG)	Multiple hematopoietic lineages including T and B cells, APCs, and NK cells	Jackson Laboratory (7)
Implantation of fetal liver and thymus tissue	NOD-SCID NSG	Robust thymocyte development, thymocytes educated on autologous thymic epithelium, minimal development of peripheral immune system	Jackson Laboratory (3, 4)
Implantation of fetal liver and thymus tissue and injection of autologous HSCs	NSG NOD-SCID NOD.129S7 (B6)-*Rag1*^{tm1Mom}*IL2rg*^{tm1Wjl}/*Sz* (NRG) B6.129 (Cg)-*Rag2*^{tm1Fwa}*Cd47*$^{tm1Fpl/2rgtm1Wjl/J}$ (TKO-C57BL6)	Complete human immune system, human leukocyte antigen-restricted T cells, mucosal immune system, delayed GVHD	Jackson Laboratory (14, 16–18)

isolate HIV-specific CTLs from HIV patients, expand *ex vivo*, and infuse them back into the patients (29–32). However, these studies demonstrated that this approach had very little impact on antiviral efficacy in treated individuals. There are current attempts to improve the efficiency of this approach through the "redirection" of peripheral T cells to target HIV infection through the genetic modification of cells with HIV-specific, molecularly cloned TCRs [for review on transgenic TCRs, see Ref. (33, 34)]. Proof of principle studies were conducted in the humanized mouse model wherein Joseph et al. produced a lentiviral vector encoding the TCR that recognizes the HIV-1 gag epitope SL9, which elicits a potent antiviral response by CTLs carrying the SL9-specific TCR (35). Using the SCID-hu mouse model, transduced $CD8^+$ T cells carrying the SL9-specific TCR were co-injected with human leukocyte antigen (HLA)-matched HIV-1-infected PBMCs and tested for *in vivo* suppression of HIV-1. Isolated spleens of the mice treated with transduced HIV TCR CD8 T cells showed no signs of HIV-1-infected PBMCs; thus, peripheral $CD8^+$ T cells modified with this potent anti-HIV TCR were capable of controlling and clearing HIV-1 infection *in vivo*. Although TCR-based immunotherapy has been shown to be effective in nonhumanized mouse models (36–38), there are rising safety concerns with using cloned TCRs in adoptive immunotherapy because of the possibility of exogenous TCR mispairing with an endogenous TCR chain, generating a new TCR that can have lethal off-target toxicity (39, 40). However, other studies conducted in humanized mice suggest that this may not be a significant issue (see below).

CAR-Based Immunotherapy in Humanized Mice

An ever-present issue with the use of molecularly cloned TCRs in therapy is that they have to be used in HLA-matched individuals, lessening their potential use to a limited number of people. CARs, which combine antigen-recognizing, HLA-independent extracellular domains with the TCR-zeta chain intracellular signaling domain, broaden these molecules' potential use as a T cell redirection/engineering therapeutic approach [for a review on CAR T cell design, see Ref. (41)]. There have been numerous preclinical studies and clinical trials that have tested or are currently testing the effectiveness of CAR T cell therapy against certain cancers, reviewed in Ref. (42). In many preclinical studies, humanized mice were used to test the antitumor efficacy of various CAR designs: for example, second- or third-generation CARs which contain immune-enhancing costimulatory domains (43–45). Humanized mice can also be used to study the effect of combination therapy with CAR T cells and antibody-targeting immune checkpoint inhibitors such as PD-1 and CTLA-4 (46). A combinatorial therapeutic approach using CAR T cells and an immune checkpoint inhibitor has recently been studied in a humanized mouse model of metastatic clear-cell renal cell carcinoma (47). These CAR T cells targeting human anti-carbonic anhydrase are also equipped to secrete human anti-programmed death ligand 1 (PD-L1) antibodies to overcome checkpoint inhibition mediated by PD-1 and PD-L1 interactions. This approach to immune-checkpoint blockade resulted in an enhanced antitumor efficacy compared to mice treated with CAR T cells alone. Continuous efforts to study the behavior of CAR T cells *in vivo* using humanized mice can provide important understandings into overcoming the immunosuppressive properties of the tumor microenvironment.

With the success of CAR T cell therapy against B cell malignancies, HIV researchers are revisiting the CAR T cell approach for the treatment of HIV infection (48–50). Very recently, peripheral anti-HIV CAR T cells have been tested for antiviral efficacy using a humanized mouse model of HIV infection (51). The study's approach was to redesign a CD4-based CAR vector used previously in clinical trials to augment expression and CAR T cell performance. Anti-HIV CAR T cells that contained the costimulatory 4-1BB domain outperformed those that contained the CD28 costimulatory domain in reducing viral rebound after ART treatment and prolonged persistence *in vivo* in the absence of antigen. Thus, opposed to the minimal clinical efficacy seen with the first-generation CD4-based CAR, newer generation of anti-HIV CARs can potentially have a more promising outcome in clinical trials. Future studies using humanized mouse models of HIV infection can provide more information on differences in anti-HIV responses and the clearance of HIV infection *in vivo* using anti-HIV CAR T cells containing different combinations of costimulatory domains.

STEM CELL-BASED GENE THERAPY IN HUMANIZED MICE

Recent developments of new humanized mouse models have opened opportunities in efforts to modify human stem cells to generate an immune system designed to mount a more efficient, targeted immune response against a specific pathogen or a disease. Humanized mice are being employed to test the therapeutic efficacies of stem cell-based gene therapies involving the modification of HSPCs with potent antigen-specific TCRs and CARs, and engineering a human immune system equipped to specifically target HIV or cancer antigens *in vivo*. Below, we discuss key studies that have utilized the humanized mouse model system for stem cell-based therapy for HIV and cancer.

Stem Cell-Based Gene Therapy Using TCRs Against HIV and Cancer

To enhance the immune response to HIV infection, studies have used HSPCs to introduce HIV-specific TCRs into immunodeficient mice to reconstitute a human immune system that contains a population of T cells carrying an HIV-specific TCR. The testing of this concept initially utilized the SCID-hu mouse model (52). $CD34^+$ HSPCs were isolated from a human fetal liver, transduced with a molecularly cloned anti-HIV TCR, and transplanted into irradiated HLA-matched SCID-hu mice. This resulted in the generation of mature $CD8^+$ T cells carrying the transgenic anti-HIV TCR. These anti-HIV TCR^+ T cells were functional in response to peptide stimulation *ex vivo*, differentiating into effector cells, producing interferon (IFN)-gamma, and lysing targeted cells. To test the functionality of anti-HIV TCR^+ T cells generated from transduced HSCs *in vivo*, a follow up study used the NSG strain mouse that is engrafted with human liver/thymus

and injected with transduced fetal liver CD34+ cells. Using this NSG-CTL mouse model, the injected transduced HSCs were able to differentiate into mature human CD8+ T cells carrying the transgenic anti-HIV TCR (16). More importantly, anti-HIV TCR+ CD8 T cells were found to migrate into multiple tissues including the spleen, bone marrow, and the implanted human thymus. Following an HIV-1 challenge into these mice, these anti-HIV TCR+ CD8 T cells were able to suppress viral load at 2 weeks and 6 weeks post infection in the peripheral blood. In addition, mice carrying the anti-HIV TCR T cells were protected against CD4 T cell depletion and had lower levels of infected cells by 6 weeks post infection. Other key outcomes observed in this study were the reduced viral burden in anti-HIV TCR mice in lymphoid tissues and the expansion and differentiation of anti-HIV TCR+ T cells in response to an active HIV infection. These studies using two different humanized mouse models showed the feasibility and therapeutic potential of modifying HSCs with a potent anti-HIV TCR to produce a functional antiviral immune response to HIV.

Investigators have turned to the humanized mouse model to test the proof of principle of this type of stem cell-based gene therapy against cancer. Similar to the HIV-based studies, stem cell-based gene therapy for cancer is also being examined as a potential therapeutic strategy to provide a long-lasting immune surveillance against tumor cells using human HSPCs modified with an antitumor TCR (53). Using the BLT-humanized mouse model, Vatakis et al. transplanted HSPCs modified with a HLA-A*0201-restricted anti-melanoma TCR (54, 55). The transduced HSPCs were able to differentiate and produce high levels of naïve CD8+ T cells carrying the anti-melanoma TCR. Upon challenging these mice with HLA-matched tumors, mice treated with anti-melanoma TCRs were able to control tumor growth, and in some mice, clear the tumor compared to control mice carrying nonmodified T cells. Further analysis on the functionality of these anti-melanoma-specific T cells showed that they can differentiate into different subsets of effector and memory phenotype and infiltrate into tumors. Moreover, analysis of the bone marrow of these mice carrying transgenic HSCs showed continued expression of the integrated vector in isolated bone marrow samples. Thus, transgenic HSPCs can repopulate the bone marrow and provide a long-lasting supply of modified mature immune cells, including T and natural killer (NK) cells, directed against a specific pathogen. Other studies have also utilized the CD34-humanized mouse model in examining stem cell gene therapy using candidate antitumor specific TCRs which exhibited similar and new informative outcomes (56–58). In particular, these studies found that the introduction of the TCR transgene in HSPCs could inhibit endogenous TCR rearrangement in T cells (56, 57, 59). This is an important discovery as it can overcome the potential of off-target toxicities from transgene expression and endogenous TCR chains rearrangement and alpha and beta chain receptor mixing. Hence, humanized mouse models enabled investigators to study the development and dynamics of an immune system with unlimited replenishment of immune cells carrying a disease-specific receptor which can provide key aspects of its therapeutic potential in clearing a persistent infection or a disease.

Stem Cell-Based CAR T Cell Studies in HIV and Cancer

To test the safety and efficacy of a stem cell-based CAR approach in HIV infection, Zhen et al. used the BLT-humanized mouse model and modified HSPCs with a lentiviral vector expressing an anti-HIV CD4-based CAR to determine whether this can result in the generation of mature anti-HIV CAR+ CTLs (17). This anti-HIV CAR is based on utilizing the HIV receptor CD4 molecule that is fused to an internal TCR-signaling domain (60). Stem cells from fetal liver were modified with anti-HIV CAR-expressing lentiviral vector and infused into NSG mice transplanted with fetal liver and thymus. Investigators observed subsequent maturation of CAR+ T cells, NK cells, B cells, and myeloid cells *in vivo*. In addition, cells carrying the CAR-expressing lentiviral vectors were protected from HIV infection by coexpressing protective anti-HIV shRNAs and were able to functionally suppress HIV replication *in vivo* through CTL activity. Also, similar to the TCR-modified HSPC-based studies, developing T cells carrying the anti-HIV CAR receptor can successfully go through positive selection in a human thymus, and the expression of the anti-HIV CAR resulted in the suppression of endogenous TCR rearrangement. This observation that developing T cells expressing an anti-HIV CD4-based CAR suppressed endogenous TCR rearrangement suggests that the CD4-based CAR can act as the sole natural TCR during development. This could be a beneficial trait in the long term, as emerging T cells expressing CD4-based CARs will be specific to HIV antigen and chances of off-target activation will be minimal. A similar approach was also done examining the development of CD19CAR-expressing cells in the CD34-humanized mouse model (61, 62). They found that the introduction of a lentiviral vector expressing either a CD19CAR or a second-generation CD19CD28CAR into HSPCs and engrafting into NSG mice led to the differentiation of different hematopoietic lineages expressing CAR including T cells, B cells, and myeloid cells and produced potent antitumor responses in the CD19CD28CAR-treated mice (61, 62). It remains to be seen if the therapeutic effects of stem cell-based CAR T cell therapy performed on humanized mice will be translated into human clinical trials.

PD-1 AND IFN-I BLOCKADE THERAPY FOR HIV AND CANCER

While humanized mice have been useful in the examination of human immunotherapeutic approaches involving gene therapies, their use in examining antiviral or antimalignancy responses and immunotherapies is at a relatively nascent stage. More sensitive immune-based assays and improvements in humanized mice now allow the examination of antitumor and antiviral immune responses and show great promise in the development of novel immunotherapies to treat these conditions. In recent studies, humanized mouse models were used to examine the effects of blocking key immune and antiviral factors in chronic HIV infection. Chronic viral infections can persist by upregulating immune checkpoint receptors that can functionally compromise virus-specific T cells and prevent them from clearing the infection (63). HIV infection has been shown to upregulate T cell

exhaustion markers that enable the virus to chronically persist, which includes PD-1, Tim-3, LAG-3 among others (64–69). To investigate whether T cell exhaustion can be reversed and rescue function in exhausted T cells, these recent studies closely examined immune factors in chronically HIV-infected mice and found elevated PD-1 levels on T cells, similar to that seen in infected individuals. These chronically infected mice were treated with an antibody that blocks the PD-1/PD-L1 pathway and found reduced viral loads and increased $CD4^+$ and $CD8^+$ T cell levels (70, 71). In addition, PD-L1 blockade increased the percentages of naïve and central memory T cells and increased Th1 cytokines IFN-gamma and IL-12 during treatment (70). Thus, blocking the PD-1/PL-1 pathway during chronic HIV leading to reduced viral loads has now been shown in two different humanized mouse models and supports results seen in a study applying PD-1 blockade during chronic SIV infection in a macaque model, which reduced SIV levels (72). It remains to be seen whether PD-1/PD-L1 blockade can have clinical success in antiviral therapy in chronically HIV-infected individuals as it has already been observed in individuals treated for human cancer (73–75). PD-1 blockade treatment for cancer therapy has been shown to have therapeutic benefits in patients with certain types of malignancies (76). Recently, preclinical studies have utilized humanized mice either transplanted with human $CD34^+$ HSPCs (HuNSG) or mice containing a double knockout of MHC class I or class II (NOG-dKO) to show the therapeutic potential of utilizing PD-1 blockade for cancer therapy (77, 78). These studies highlight the usefulness of humanized mice to study not only the antitumor effects of anti-PD-1 blockade but also the human immune responses to human tumors, as these studies revealed significant tumor growth suppression and antitumor $CD8^+$ T cell responses following PD-1 blockade treatment.

Hyper-immune activation is a hallmark of chronic HIV infection, and arising evidence is suggesting that chronic type I (IFN-I) is driving this continuous immune activation that may be leading to disease progression (79). To investigate the role IFN-I plays in driving chronic HIV infection, investigators have turned to BLT-humanized mouse models of HIV infection to study this (80, 81). In the study by Zhen et al., after establishing a chronic HIV infection, blocking IFN-1 signaling using an anti-interferon alpha receptor 2(IFNR2)-blocking antibody resulted in a decreased immune activation, a decreased expression of T exhaustion markers and reversal of T cell exhaustion, and reduced plasma viral loads. In addition, treatment with the anti-IFNR2-blocking antibody in combination with ART resulted in a rapid viral suppression and reduced viral reservoirs. Cheng et al. found similar results using IFNR1-blocking antibody in combination with ART treatment throughout their study (80). These results shed light on the role IFN-I signaling plays during chronic HIV infection in maintaining chronic immune activation and T cell exhaustion that leads to uncontrolled HIV infection *in vivo*. Findings from these and future studies may lead to the application of IFN-I blockade treatment in combination with ART during chronic HIV infection that could alleviate residual immune activation and reduce viral reservoirs in HIV-positive individuals. It remains to be seen whether IFN-I blockade will have a beneficial antitumor efficacy during tumor progression since IFN-I is important in inducing antitumor responses such as promoting CD8 T cell priming. However, continuous IFN-I signaling can also have immunosuppressive properties that may play a role in promoting tumor growth (82). It has been recently shown that continuous IFN signaling drives PD-L1-dependent and -independent resistance to radiation therapy and checkpoint blockade, and blocking IFN-I signaling restores tumor cell response to checkpoint blockade treatment (83). Whether IFN-I blockade treatment can restore response to treatment in tumors that are resistant to PD-1 blockade or other immune checkpoint blockade in a humanized mouse model of cancer remains to be determined.

FUTURE DIRECTIONS

Although humanized mice have been an essential tool in several fields of research to better understand the mechanisms of disease progression and develop therapeutic strategies, these mouse models do come with their own limitations that need to be addressed to create more optimized models that will fit the needs of each research field (84). Currently, SCID mice engrafted with human PBMCs develop graft-versus-host disease (GVHD) within 4 weeks of engraftment, limiting the time of experimentation to just a few short weeks. The humanized BLT mouse model also has its own limitations for use. BLT mice can have poor B cell development, limited antibody class switching following activation, and lymphocyte homing in lymph nodes and germinal centers, limiting their antibody responses. In addition, these mice also typically develop a GVHD-like condition after around 20 weeks post engraftment of fetal tissue and HSCs, putting a limitation on the duration of a given study (84, 85). Therefore, there is a pressing need to develop new mouse strains with genetic properties that will eliminate the generation of this GVHD-like condition. Recently, a new modification of the BLT mouse model was made by transplanting fetal thymus, liver, and autologous $CD34^+$ HSCs into a C57BL/6 mouse strain that contain a triple knockout of Rag2, IL-2Yc, and CD47 genes (TKO-BLT) (18). These mice were observed to be healthy with no signs of GVHD for 45 weeks post transplantation, which is months longer than that of the current BLT models. In addition, they retained high reconstitution of human cells throughout the 45 weeks. They also found this model to establish HIV latency, respond well to orally fed and subcutaneously injected ART treatment, and upon ART interruption, can generate rapid viral rebound. Thus, this new humanized TKO-BLT mouse model can provide an extended duration of a variety of studies that will be useful for addressing issues requiring longer periods of infection or disease progression.

Because of the variety of humanized mouse models currently available, it is important for investigators to be knowledgeable on the different mouse models and which one will be the more appropriate model to answer the questions they are investigating. Differences in the background mutations of the immunocompromised strains can have an impact on the engraftment of human cells and the development of peripheral lymph nodes and germinal centers (14). Therefore, results using humanized mice must be carefully interpreted. It is also important to include proper controls, particularly for immune-based studies, such as

uninfected and unmanipulated animals, to control for any potential changes/interference by GVHD or specific effects pertaining to the individual tissues.

Humanized mouse models are also currently being improved upon for cancer research (86). Cancer therapy studies evaluating the immune response to tumors would benefit from a humanized BLT model where the human reconstituted immune system is compatible with the transplanted tumor tissue. One possibility will be to acquire HSPCs from a patient and transplant autologous tumor cells or HLA-matched tumor cells into the mice. This will generate a closer representative of the patient's antitumor response without the interference of alloreactive T cells resulting from the mismatch of the reconstituted immune system and engrafted tumor cells. Further advances in generating humanized mouse models that overcome current limitations will be highly beneficial for HIV and cancer researchers to advance stem cell-based gene therapy, T cell immunotherapy, and other immunological studies such as T cell exhaustion and tumor immunosuppressive microenvironment for eradicating HIV and cancer.

AUTHOR CONTRIBUTIONS

MC, AZ, and SK contributed equally to the preparation of this manuscript.

FUNDING

This work was funded by NIH grants AI078806 and AI110306-01 (to SK); NIH/NIAID 1U19AI117941—01; AmfAR 108929-56-RGRL, 108688-54-RGRL, 109577-62-RGRL (Kitchen-PI), the UCLA Center for AIDS Research (P30AI28697); the California Institute for Regenerative Medicine (TR4-06845, DISC2-10748), and California HIV/AIDS Research Program (F12-LA-215 to AZ); NIH grant T32-AI060567 (to AZ and MC); the UCLA AIDS Institute and UCLA Center for AIDS Research (AI28697 to AZ), and the UCLA AIDS Institute and UCLA Center for AIDS Research (AI028697 to MC), and the UPLIFT: UCLA Postdocs' Longitudinal Investment in Faculty (K12 GM106996 to MC).

REFERENCES

1. Walsh NC, Kenney LL, Jangalwe S, Aryee KE, Greiner DL, Brehm MA, et al. Humanized mouse models of clinical disease. *Annu Rev Pathol* (2017) 12:187–215. doi:10.1146/annurev-pathol-052016-100332
2. Mosier DE, Gulizia RJ, Baird SM, Wilson DB. Transfer of a functional human immune system to mice with severe combined immunodeficiency. *Nature* (1988) 335:256–9. doi:10.1038/335256a0
3. McCune JM, Namikawa R, Kaneshima H, Shultz LD, Lieberman M, Weissman IL. The SCID-hu mouse: murine model for the analysis of human hematolymphoid differentiation and function. *Science* (1988) 241:1632–9. doi:10.1126/science.2971269
4. Namikawa R, Weilbaecher KN, Kaneshima H, Yee EJ, McCune JM. Long-term human hematopoiesis in the SCID-hu mouse. *J Exp Med* (1990) 172:1055–63. doi:10.1084/jem.172.4.1055
5. Shultz LD, Schweitzer PA, Christianson SW, Gott B, Schweitzer IB, Tennent B, et al. Multiple defects in innate and adaptive immunologic function in NOD/LtSz-scid mice. *J Immunol* (1995) 154:180–91.
6. Shultz LD, Brehm MA, Bavari S, Greiner DL. Humanized mice as a preclinical tool for infectious disease and biomedical research. *Ann N Y Acad Sci* (2011) 1245:50–4. doi:10.1111/j.1749-6632.2011.06310.x
7. Watanabe Y, Takahashi T, Okajima A, Shiokawa M, Ishii N, Katano I, et al. The analysis of the functions of human B and T cells in humanized NOD/shi-scid/gammac(null) (NOG) mice (hu-HSC NOG mice). *Int Immunol* (2009) 21:843–58. doi:10.1093/intimm/dxp050
8. Karpel ME, Boutwell CL, Allen TM. BLT humanized mice as a small animal model of HIV infection. *Curr Opin Virol* (2015) 13:75–80. doi:10.1016/j.coviro.2015.05.002
9. Lan P, Tonomura N, Shimizu A, Wang S, Yang YG. Reconstitution of a functional human immune system in immunodeficient mice through combined human fetal thymus/liver and CD34+ cell transplantation. *Blood* (2006) 108:487–92. doi:10.1182/blood-2005-11-4388
10. Melkus MW, Estes JD, Padgett-Thomas A, Gatlin J, Denton PW, Othieno FA, et al. Humanized mice mount specific adaptive and innate immune responses to EBV and TSST-1. *Nat Med* (2006) 12:1316–22. doi:10.1038/nm1431
11. Bryce PJ, Falahati R, Kenney LL, Leung J, Bebbington C, Tomasevic N, et al. Humanized mouse model of mast cell-mediated passive cutaneous anaphylaxis and passive systemic anaphylaxis. *J Allergy Clin Immunol* (2016) 138:769–79. doi:10.1016/j.jaci.2016.01.049
12. Jangalwe S, Shultz LD, Mathew A, Brehm MA. Improved B cell development in humanized NOD-SCID IL2Rgamma(null) mice transgenically expressing human stem cell factor, granulocyte-macrophage colony-stimulating factor and interleukin-3. *Immun Inflamm Dis* (2016) 4:427–40. doi:10.1002/iid3.124
13. Wege AK, Melkus MW, Denton PW, Estes JD, Garcia JV. Functional and phenotypic characterization of the humanized BLT mouse model. *Curr Top Microbiol Immunol* (2008) 324:149–65. doi:10.1007/978-3-540-75647-7_10
14. Shultz LD, Brehm MA, Garcia-Martinez JV, Greiner DL. Humanized mice for immune system investigation: progress, promise and challenges. *Nat Rev Immunol* (2012) 12:786–98. doi:10.1038/nri3311
15. Shultz LD, Ishikawa F, Greiner DL. Humanized mice in translational biomedical research. *Nat Rev Immunol* (2007) 7:118–30. doi:10.1038/nri2017
16. Kitchen SG, Levin BR, Bristol G, Rezek V, Kim S, Aguilera-Sandoval C, et al. *In vivo* suppression of HIV by antigen specific T cells derived from engineered hematopoietic stem cells. *PLoS Pathog* (2012) 8:e1002649. doi:10.1371/journal.ppat.1002649
17. Zhen A, Kamata M, Rezek V, Rick J, Levin B, Kasparian S, et al. HIV-specific immunity derived from chimeric antigen receptor-engineered stem cells. *Mol Ther* (2015) 23:1358–67. doi:10.1038/mt.2015.102
18. Lavender KJ, Pace C, Sutter K, Messer RJ, Pouncey DL, Cummins NW, et al. An advanced BLT-humanized mouse model for extended HIV-1 cure studies. *AIDS* (2018) 32:1–10. doi:10.1097/QAD.0000000000001674
19. Marsden MD, Zack JA. Mouse models for human immunodeficiency virus infection. *Annu Rev Virol* (2017) 4:393–412. doi:10.1146/annurev-virology-101416-041703
20. Akkina RK, Rosenblatt JD, Campbell AG, Chen IS, Zack JA. Modeling human lymphoid precursor cell gene therapy in the SCID-hu mouse. *Blood* (1994) 84:1393–8.
21. An DS, Koyanagi Y, Zhao JQ, Akkina R, Bristol G, Yamamoto N, et al. High-efficiency transduction of human lymphoid progenitor cells and expression in differentiated T cells. *J Virol* (1997) 71:1397–404.
22. Mitsuyasu RT, Merigan TC, Carr A, Zack JA, Winters MA, Workman C, et al. Phase 2 gene therapy trial of an anti-HIV ribozyme in autologous CD34+ cells. *Nat Med* (2009) 15:285–92. doi:10.1038/nm.1932
23. Burke BP, Levin BR, Zhang J, Sahakyan A, Boyer J, Carroll MV, et al. Engineering cellular resistance to HIV-1 infection *in vivo* using a dual therapeutic lentiviral vector. *Mol Ther Nucleic Acids* (2015) 4:e236. doi:10.1038/mtna.2015.10
24. Ringpis GE, Shimizu S, Arokium H, Camba-Colon J, Carroll MV, Cortado R, et al. Engineering HIV-1-resistant T-cells from short-hairpin RNA-expressing hematopoietic stem/progenitor cells in humanized BLT mice. *PLoS One* (2012) 7:e53492. doi:10.1371/journal.pone.0053492
25. Walker JE, Chen RX, McGee J, Nacey C, Pollard RB, Abedi M, et al. Generation of an HIV-1-resistant immune system with CD34(+) hematopoietic stem cells transduced with a triple-combination anti-HIV lentiviral vector. *J Virol* (2012) 86:5719–29. doi:10.1128/JVI.06300-11
26. Shimizu S, Hong P, Arumugam B, Pokomo L, Boyer J, Koizumi N, et al. A highly efficient short hairpin RNA potently down-regulates CCR5 expression

in systemic lymphoid organs in the hu-BLT mouse model. *Blood* (2010) 115:1534–44. doi:10.1182/blood-2009-04-215855
27. Shimizu S, Ringpis GE, Marsden MD, Cortado RV, Wilhalme HM, Elashoff D, et al. RNAi-mediated CCR5 knockdown provides HIV-1 resistance to memory T cells in humanized BLT mice. *Mol Ther Nucleic Acids* (2015) 4:e227. doi:10.1038/mtna.2015.3
28. Pernet O, Yadav SS, An DS. Stem cell-based therapies for HIV/AIDS. *Adv Drug Deliv Rev* (2016) 103:187–201. doi:10.1016/j.addr.2016.04.027
29. Lieberman J, Skolnik PR, Parkerson GR III, Fabry JA, Landry B, Bethel J, et al. Safety of autologous, *ex vivo*-expanded human immunodeficiency virus (HIV)-specific cytotoxic T-lymphocyte infusion in HIV-infected patients. *Blood* (1997) 90:2196–206.
30. Koenig S, Conley AJ, Brewah YA, Jones GM, Leath S, Boots LJ, et al. Transfer of HIV-1-specific cytotoxic T lymphocytes to an AIDS patient leads to selection for mutant HIV variants and subsequent disease progression. *Nat Med* (1995) 1:330–6. doi:10.1038/nm0495-330
31. Brodie SJ, Lewinsohn DA, Patterson BK, Jiyamapa D, Krieger J, Corey L, et al. *In vivo* migration and function of transferred HIV-1-specific cytotoxic T cells. *Nat Med* (1999) 5:34–41. doi:10.1038/4716
32. McKinney DM, Lewinsohn DA, Riddell SR, Greenberg PD, Mosier DE. The antiviral activity of HIV-specific CD8+ CTL clones is limited by elimination due to encounter with HIV-infected targets. *J Immunol* (1999) 163:861–7.
33. Ping Y, Liu C, Zhang Y. T-cell receptor-engineered T cells for cancer treatment: current status and future directions. *Protein Cell* (2018) 9:254–66. doi:10.1007/s13238-016-0367-1
34. Patel S, Jones RB, Nixon DF, Bollard CM. T-cell therapies for HIV: preclinical successes and current clinical strategies. *Cytotherapy* (2016) 18:931–42. doi:10.1016/j.jcyt.2016.04.007
35. Joseph A, Zheng JH, Follenzi A, Dilorenzo T, Sango K, Hyman J, et al. Lentiviral vectors encoding human immunodeficiency virus type 1 (HIV-1)-specific T-cell receptor genes efficiently convert peripheral blood CD8 T lymphocytes into cytotoxic T lymphocytes with potent *in vitro* and *in vivo* HIV-1-specific inhibitory activity. *J Virol* (2008) 82:3078–89. doi:10.1128/JVI.01812-07
36. Morris EC, Tsallios A, Bendle GM, Xue SA, Stauss HJ. A critical role of T cell antigen receptor-transduced MHC class I-restricted helper T cells in tumor protection. *Proc Natl Acad Sci U S A* (2005) 102:7934–9. doi:10.1073/pnas.0500357102
37. de Witte MA, Bendle GM, van den Boom MD, Coccoris M, Schell TD, Tevethia SS, et al. TCR gene therapy of spontaneous prostate carcinoma requires *in vivo* T cell activation. *J Immunol* (2008) 181:2563–71. doi:10.4049/jimmunol.181.4.2563
38. de Witte MA, Jorritsma A, Kaiser A, van den Boom MD, Dokter M, Bendle GM, et al. Requirements for effective antitumor responses of TCR transduced T cells. *J Immunol* (2008) 181:5128–36. doi:10.4049/jimmunol.181.7.5128
39. Bendle GM, Linnemann C, Hooijkaas AI, Bies L, de Witte MA, Jorritsma A, et al. Lethal graft-versus-host disease in mouse models of T cell receptor gene therapy. *Nat Med* (2010) 16:565–70. doi:10.1038/nm.2128
40. Cameron BJ, Gerry AB, Dukes J, Harper JV, Kannan V, Bianchi FC, et al. Identification of a Titin-derived HLA-A1-presented peptide as a cross-reactive target for engineered MAGE A3-directed T cells. *Sci Transl Med* (2013) 5:197ra03. doi:10.1126/scitranslmed.3006034
41. Oldham RAA, Medin JA. Practical considerations for chimeric antigen receptor design and delivery. *Expert Opin Biol Ther* (2017) 17:961–78. doi:10.1080/14712598.2017.1339687
42. Fesnak AD, June CH, Levine BL. Engineered T cells: the promise and challenges of cancer immunotherapy. *Nat Rev Cancer* (2016) 16:566–81. doi:10.1038/nrc.2016.97
43. Guedan S, Chen X, Madar A, Carpenito C, McGettigan SE, Frigault MJ, et al. ICOS-based chimeric antigen receptors program bipolar TH17/TH1 cells. *Blood* (2014) 124:1070–80. doi:10.1182/blood-2013-10-535245
44. Song DG, Powell DJ. Pro-survival signaling *via* CD27 costimulation drives effective CAR T-cell therapy. *Oncoimmunology* (2012) 1(4):547–9. doi:10.4161/onci.19458
45. Carpenito C, Milone MC, Hassan R, Simonet JC, Lakhal M, Suhoski MM, et al. Control of large, established tumor xenografts with genetically retargeted human T cells containing CD28 and CD137 domains. *Proc Natl Acad Sci U S A* (2009) 106(9):3360–5. doi:10.1073/pnas.0813101106
46. Gay F, D'Agostino M, Giaccone L, Genuardi M, Festuccia M, Boccadoro M, et al. Immuno-oncologic approaches: CAR-T cells and checkpoint inhibitors. *Clin Lymphoma Myeloma Leuk* (2017) 17:471–8. doi:10.1016/j.clml.2017.06.014
47. Suarez ER, Chang de K, Sun J, Sui J, Freeman GJ, Signoretti S, et al. Chimeric antigen receptor T cells secreting anti-PD-L1 antibodies more effectively regress renal cell carcinoma in a humanized mouse model. *Oncotarget* (2016) 7:34341–55. doi:10.18632/oncotarget.9114
48. Deeks SG, Wagner B, Anton PA, Mitsuyasu RT, Scadden DT, Huang C, et al. A phase II randomized study of HIV-specific T-cell gene therapy in subjects with undetectable plasma viremia on combination antiretroviral therapy. *Mol Ther* (2002) 5:788–97. doi:10.1006/mthe.2002.0611
49. Mitsuyasu RT, Anton PA, Deeks SG, Scadden DT, Connick E, Downs MT, et al. Prolonged survival and tissue trafficking following adoptive transfer of CD4zeta gene-modified autologous CD4(+) and CD8(+) T cells in human immunodeficiency virus-infected subjects. *Blood* (2000) 96:785–93.
50. Scholler J, Brady TL, Binder-Scholl G, Hwang WT, Plesa G, Hege KM, et al. Decade-long safety and function of retroviral-modified chimeric antigen receptor T cells. *Sci Transl Med* (2012) 4:132ra53. doi:10.1126/scitranslmed.3003761
51. Leibman RS, Richardson MW, Ellebrecht CT, Maldini CR, Glover JA, Secreto AJ, et al. Supraphysiologic control over HIV-1 replication mediated by CD8 T cells expressing a re-engineered CD4-based chimeric antigen receptor. *PLoS Pathog* (2017) 13:e1006613. doi:10.1371/journal.ppat.1006613
52. Kitchen SG, Bennett M, Galic Z, Kim J, Xu Q, Young A, et al. Engineering antigen-specific T cells from genetically modified human hematopoietic stem cells in immunodeficient mice. *PLoS One* (2009) 4:e8208. doi:10.1371/journal.pone.0008208
53. Gschweng E, De Oliveira S, Kohn DB. Hematopoietic stem cells for cancer immunotherapy. *Immunol Rev* (2014) 257:237–49. doi:10.1111/imr.12128
54. Vatakis DN, Koya RC, Nixon CC, Wei L, Kim SG, Avancena P, et al. Antitumor activity from antigen-specific CD8 T cells generated *in vivo* from genetically engineered human hematopoietic stem cells. *Proc Natl Acad Sci U S A* (2011) 108:E1408–16. doi:10.1073/pnas.1115050108
55. Vatakis DN, Bristol GC, Kim SG, Levin B, Liu W, Radu CG, et al. Using the BLT humanized mouse as a stem cell based gene therapy tumor model. *J Vis Exp* (2012) (70):4181. doi:10.3791/4181
56. Giannoni F, Hardee CL, Wherley J, Gschweng E, Senadheera S, Kaufman ML, et al. Allelic exclusion and peripheral reconstitution by TCR transgenic T cells arising from transduced human hematopoietic stem/progenitor cells. *Mol Ther* (2013) 21:1044–54. doi:10.1038/mt.2013.8
57. Najima Y, Tomizawa-Murasawa M, Saito Y, Watanabe T, Ono R, Ochi T, et al. Induction of WT1-specific human CD8+ T cells from human HSCs in HLA class I Tg NOD/SCID/IL2rgKO mice. *Blood* (2016) 127:722–34. doi:10.1182/blood-2014-10-604777
58. Hu Z, Xia J, Fan W, Wargo J, Yang YG. Human melanoma immunotherapy using tumor antigen-specific T cells generated in humanized mice. *Oncotarget* (2016) 7:6448–59. doi:10.18632/oncotarget.7044
59. Vatakis DN, Arumugam B, Kim SG, Bristol G, Yang O, Zack JA. Introduction of exogenous T-cell receptors into human hematopoietic progenitors results in exclusion of endogenous T-cell receptor expression. *Mol Ther* (2013) 21:1055–63. doi:10.1038/mt.2013.28
60. Kitchen SG, Zack JA. Engineering HIV-specific immunity with chimeric antigen receptors. *AIDS Patient Care STDS* (2016) 30:556–61. doi:10.1089/apc.2016.0239
61. De Oliveira SN, Ryan C, Giannoni F, Hardee CL, Tremcinska I, Katebian B, et al. Modification of hematopoietic stem/progenitor cells with CD19-specific chimeric antigen receptors as a novel approach for cancer immunotherapy. *Hum Gene Ther* (2013) 24:824–39. doi:10.1089/hum.2012.202
62. Larson SM, Truscott LC, Chiou TT, Patel A, Kao R, Tu A, et al. Pre-clinical development of gene modification of haematopoietic stem cells with chimeric antigen receptors for cancer immunotherapy. *Hum Vaccin Immunother* (2017) 13:1094–104. doi:10.1080/21645515.2016.1268745
63. Kahan SM, Wherry EJ, Zajac AJ. T cell exhaustion during persistent viral infections. *Virology* (2015) 47(9–480):180–93. doi:10.1016/j.virol.2014.12.033
64. Day CL, Kaufmann DE, Kiepiela P, Brown JA, Moodley ES, Reddy S, et al. PD-1 expression on HIV-specific T cells is associated with T-cell exhaustion and disease progression. *Nature* (2006) 443:350–4. doi:10.1038/nature05115
65. Trautmann L, Janbazian L, Chomont N, Said EA, Gimmig S, Bessette B, et al. Upregulation of PD-1 expression on HIV-specific CD8+ T cells leads to reversible immune dysfunction. *Nat Med* (2006) 12:1198–202. doi:10.1038/nm1106-1329b

66. Chew GM, Fujita T, Webb GM, Burwitz BJ, Wu HL, Reed JS, et al. TIGIT marks exhausted T cells, correlates with disease progression, and serves as a target for immune restoration in HIV and SIV infection. *PLoS Pathog* (2016) 12:e1005349. doi:10.1371/journal.ppat.1005349
67. Eichbaum Q. PD-1 signaling in HIV and chronic viral infection—potential for therapeutic intervention? *Curr Med Chem* (2011) 18:3971–80. doi:10.2174/092986711796957239
68. Hoffmann M, Pantazis N, Martin GE, Hickling S, Hurst J, Meyerowitz J, et al. Exhaustion of activated CD8 T cells predicts disease progression in primary HIV-1 infection. *PLoS Pathog* (2016) 12:e1005661. doi:10.1371/journal.ppat.1005661
69. Tian X, Zhang A, Qiu C, Wang W, Yang Y, Liu A, et al. The upregulation of LAG-3 on T cells defines a subpopulation with functional exhaustion and correlates with disease progression in HIV-infected subjects. *J Immunol* (2015) 194:3873–82. doi:10.4049/jimmunol.1402176
70. Palmer BE, Neff CP, Lecureux J, Ehler A, Dsouza M, Remling-Mulder L, et al. *In vivo* blockade of the PD-1 receptor suppresses HIV-1 viral loads and improves CD4+ T cell levels in humanized mice. *J Immunol* (2013) 190:211–9. doi:10.4049/jimmunol.1201108
71. Seung E, Dudek TE, Allen TM, Freeman GJ, Luster AD, Tager AM. PD-1 blockade in chronically HIV-1-infected humanized mice suppresses viral loads. *PLoS One* (2013) 8:e77780. doi:10.1371/journal.pone.0077780
72. Velu V, Titanji K, Zhu B, Husain S, Pladevega A, Lai L, et al. Enhancing SIV-specific immunity *in vivo* by PD-1 blockade. *Nature* (2009) 458:206–10. doi:10.1038/nature07662
73. Feng D, Hui X, Shi-Chun L, Yan-Hua B, Li C, Xiao-Hui L, et al. Initial experience of anti-PD1 therapy with nivolumab in advanced hepatocellular carcinoma. *Oncotarget* (2017) 8:96649–55. doi:10.18632/oncotarget.20029
74. Overman MJ, McDermott R, Leach JL, Lonardi S, Lenz HJ, Morse MA, et al. Nivolumab in patients with metastatic DNA mismatch repair-deficient or microsatellite instability-high colorectal cancer (CheckMate 142): an open-label, multicentre, phase 2 study. *Lancet Oncol* (2017) 18:1182–91. doi:10.1016/S1470-2045(17)30422-9
75. Guo L, Zhang H, Chen B. Nivolumab as programmed death-1 (PD-1) inhibitor for targeted immunotherapy in tumor. *J Cancer* (2017) 8:410–6. doi:10.7150/jca.17144
76. Wang Y, Wu L, Tian C, Zhang Y. PD-1–PD-L1 immune-checkpoint blockade in malignant lymphomas. *Ann Hematol* (2017) 97(2):229–37. doi:10.1007/s00277-017-3176-6
77. Wang M, Yao LC, Cheng M, Cai D, Martinek J, Pan CX, et al. Humanized mice in studying efficacy and mechanisms of PD-1-targeted cancer immunotherapy. *FASEB J* (2018) 32(3):1537–49. doi:10.1096/fj.201700740R
78. Ashizawa T, Iizuka A, Nonomura C, Kondou R, Maeda C, Miyata H, et al. Antitumor effect of programmed death-1 (PD-1) blockade in humanized the NOG-MHC double knockout mouse. *Clin Cancer Res* (2017) 23:149–58. doi:10.1158/1078-0432.CCR-16-0122
79. Snell LM, Brooks DG. New insights into type I interferon and the immunopathogenesis of persistent viral infections. *Curr Opin Immunol* (2015) 34:91–8. doi:10.1016/j.coi.2015.03.002
80. Cheng L, Ma J, Li J, Li D, Li G, Li F, et al. Blocking type I interferon signaling enhances T cell recovery and reduces HIV-1 reservoirs. *J Clin Invest* (2017) 127:269–79. doi:10.1172/JCI90745
81. Zhen A, Rezek V, Youn C, Lam B, Chang N, Rick J, et al. Targeting type I interferon-mediated activation restores immune function in chronic HIV infection. *J Clin Invest* (2017) 127:260–8. doi:10.1172/JCI89488
82. Snell LM, McGaha TL, Brooks DG. Type I interferon in chronic virus infection and cancer. *Trends Immunol* (2017) 38:542–57. doi:10.1016/j.it.2017.05.005
83. Benci JL, Xu B, Qiu Y, Wu TJ, Dada H, Twyman-Saint Victor C, et al. Tumor interferon signaling regulates a multigenic resistance program to immune checkpoint blockade. *Cell* (2016) 167:1540–54.e12. doi:10.1016/j.cell.2016.11.022
84. Brehm MA, Shultz LD, Luban J, Greiner DL. Overcoming current limitations in humanized mouse research. *J Infect Dis* (2013) 208(Suppl 2):S125–30. doi:10.1093/infdis/jit319
85. Akkina R, Allam A, Balazs AB, Blankson JN, Burnett JC, Casares S, et al. Improvements and limitations of humanized mouse models for HIV research: NIH/NIAID "Meet the Experts" 2015 Workshop Summary. *AIDS Res Hum Retroviruses* (2016) 32:109–19. doi:10.1089/aid.2015.0258
86. Morton JJ, Bird G, Refaeli Y, Jimeno A. Humanized mouse xenograft models: narrowing the tumor-microenvironment gap. *Cancer Res* (2016) 76:6153–8. doi:10.1158/0008-5472.CAN-16-1260

Conflict of Interest Statement: The authors declare that the research was conducted in the absence of any commercial or financial relationships that could be construed as a potential conflict of interest.

frontiers in Immunology

ORIGINAL RESEARCH
published: 30 April 2018
doi: 10.3389/fimmu.2018.00816

Dissemination of *Orientia tsutsugamushi*, a Causative Agent of Scrub Typhus, and Immunological Responses in the Humanized DRAGA Mouse

Le Jiang[1], Erin K. Morris[2], Rodrigo Aguilera-Olvera[3], Zhiwen Zhang[1], Teik-Chye Chan[1], Soumya Shashikumar[3], Chien-Chung Chao[1,4], Sofia A. Casares[3,4] and Wei-Mei Ching[1,4]**

[1] Viral and Rickettsial Diseases Department, Naval Medical Research Center, Silver Spring, MD, United States, [2] Veterinary Services Program, Department of Pathology Services, Walter Reed Army Institute of Research, Silver Spring, MD, United States, [3] US Military Malaria Vaccine Program, Naval Medical Research Center, Walter Reed Army Institute of Research, Silver Spring, MD, United States, [4] Uniformed Services University of the Health Sciences, Bethesda, MD, United States

OPEN ACCESS

Edited by:
Ramesh Akkina,
Colorado State University,
United States

Reviewed by:
Mamoru Ito,
Central Institute for Experimental Animals, Japan
Nianshuang Wang,
The University of Texas at Austin,
United States

***Correspondence:**
Sofia A. Casares
sofia.a.casares.civ@mail.mil;
Wei-Mei Ching
wei-mei.m.ching.civ@mail.mil

Specialty section:
This article was submitted to Vaccines and Molecular Therapeutics, a section of the journal Frontiers in Immunology

Received: 21 December 2017
Accepted: 04 April 2018
Published: 30 April 2018

Citation:
Jiang L, Morris EK, Aguilera-Olvera R, Zhang Z, Chan T-C, Shashikumar S, Chao C-C, Casares SA and Ching W-M (2018) Dissemination of Orientia tsutsugamushi, a Causative Agent of Scrub Typhus, and Immunological Responses in the Humanized DRAGA Mouse. Front. Immunol. 9:816. doi: 10.3389/fimmu.2018.00816

Scrub typhus is caused by *Orientia tsutsugamushi*, an obligated intracellular bacterium that affects over one million people per year. Several mouse models have been used to study its pathogenesis, disease immunology, and for testing vaccine candidates. However, due to the intrinsic differences between the immune systems in mouse and human, these mouse models could not faithfully mimic the pathology and immunological responses developed by human patients, limiting their value in both basic and translational studies. In this study, we have tested for the first time, a new humanized mouse model through footpad inoculation of *O. tsutsugamushi* in DRAGA (HLA-A2.HLA-DR4.Rag1KO.IL2RγcKO.NOD) mice with their human immune system reconstituted by infusion of HLA-matched human hematopoietic stem cells from umbilical cord blood. Upon infection, *Orientia* disseminated into various organs of DRAGA mice resulted in lethality in a dose-dependent manner, while all C3H/HeJ mice infected by the same route survived. Tissue-specific lesions associated with inflammation and/or necroses were observed in multiple organs of infected DRAGA mice. Consistent with the intracellular nature of *Orientia*, strong Th1, but subdued Th2 responses were elicited as reflected by the human cytokine profiles in sera from infected mice. Interestingly, the percentage of both activated and regulatory ($CD4^+FOXP3^+$) human T cells were elevated in spleen tissues of infected mice. After immunization with irradiated whole cell *Orientia*, humanized DRAGA mice showed a significant activation of human T cells as evidenced by increased number of human $CD4^+$ and $CD8^+$ T cells. Specific human IgM and IgG antibodies were developed after repetitive immunization. The humanized DRAGA mouse model represents a new pre-clinical model for studying *Orientia*-human interactions and also for testing vaccines and novel therapeutics for scrub typhus.

Keywords: scrub typhus, *Orientia*, mouse model, humanized mice, footpad inoculation

INTRODUCTION

Scrub typhus is an infectious disease, affecting over one million people per year and putting over a billion people at risk in its endemic areas (1). It is also of military significance and historically has been a leading cause of morbidity and mortality during warfare in the Asia-Pacific region. Patients with scrub typhus often display symptoms, including fever, eschar, headache, rash, pneumonitis,

and lymphadenopathy. If diagnosed early, it can be effectively treated with antibiotics, such as doxycycline, delayed treatment; however, can be lethal (2). Recent outbreaks of scrub typhus in endemic regions and emergence of this disease in non-traditional areas, such as Middle East (3), South America (4), and Africa (5) have emphasized the importance for early diagnosis, disease control, and treatment. Furthermore, no vaccine is currently available, mainly due to strain variations which lead to antigenic heterogeneity and short-term immunity (6). Insight into the pathogenesis and immunological responses upon *Orientia* infection is paramount not only in understanding its disease progression, but also for developing preventive strategies and novel therapeutics.

Scrub typhus is caused by *Orientia*, an obligate intracellular Gram-negative bacterium transmitted to human by chigger, the larval stage of *Leptotrombidium* mite (7). Due to the short length of their mouth pieces, chiggers can only reach the epidermis part of the skin (8), where *Orientia* will enter the host during feeding. In certain percentage of patients, this will elicit strong local immunological reactions leading to the formation of eschars at the bite site. Examination of the composite structure of eschar has suggested that dendritic cells and monocytes/macrophages might be the major early host cells to encounter and harbor *Orientia* (9). The intracellular bacteria appear to possess the ability to escape from host defense mechanisms and proliferate in these antigen presenting cells including macrophages (10). In a matter of days, they can disseminate to distant major organs presumably *via* both lymphatic and hematologic circulatory systems.

Numerous animal models have been developed to study scrub typhus, including mice, rats, rabbits, monkeys, etc. (11). Monkeys are probably the best model, but they are very expensive and require specialized facilities (12). Mice are most frequently used due to their low cost and ease to handle. Mouse models have been very instrumental in previous studies looking into pathogenesis (13), vaccine tests (14) and more recently, into dissecting functions and mechanisms of specific immunological events (15). However, mouse models could not faithfully mimic the immunological reactions developed by human patients. This is probably due to the fundamental differences between the two species, especially in terms of their immune system makeup (16). These differences make it difficult to apply knowledge gained with mouse model to humans. Utilizing humanized mice could probably bridge this gap and hold the promise of providing more relevant models for immunological studies and vaccine development (17).

Earlier generations of human immune system humanized mice showed poor ability to support reconstitution and development of functional human T cells or B cells that are able to secrete IgG (17). With the introduction of HLA transgenes in the Rag1KO.IL2RγcKO.NOD (NRG) background, the DRAG mice (HLA-DR4.Rag1KO.IL2RγcKO.NOD), and DRAGA mice (HLA-A2.HLA-DR4.Rag1KO.IL2RγcKO.NOD) infused with HLA-matched human hematopoietic stem cells (HSC) have been shown to repopulate the mouse thymus and to reconstitute functional human T cells that support human B cell immunoglobulin class switching and secretion of human IgG (18–24). These mice have been used successfully for supporting infection with human pathogens, such as *Plasmodium falciparum* (malaria), HIV, Zika, and influenza A virus, and for analyzing human immune responses upon infection or vaccination (20–25). In this study, we successfully established a lethal challenge mouse model in humanized DRAGA mice using footpad inoculation of *Orientia tsutsugamushi* (*O. tsutsugamushi*) (Karp strain). We showed live *Orientia* dissemination into major organs of DRAGA mice, which caused pathological changes in various tissues. More importantly, *Orientia* infection induced human immune responses, including T cell activation, cytokine secretion, and specific antibody development.

MATERIALS AND METHODS

Generation of Humanized DRAGA Mice and Ethics Statement

DRAGA mice express HLA-A2.1 and HLA-DR0401 molecules on a NRG background and they have been previously described (19, 22, 24). HLA-A2.1/HLA-DR0401 positive umbilical cord blood was obtained from the NY Blood Center, Long Island City. Four- to six-week-old DRAGA mice were irradiated (350 rads) and injected intravenously with CD3 T cell-depleted cord blood cells (EasySep Human CD3 Positive Selection Kit, Stem Cell Technologies, #18051) containing approximately 10^5 human hematopoietic stem cells (HSCs) ($CD34^+$) as measured by fluorescence-activated cell shorting using human CD34 antibodies (clone #563, BD Biosciences). The procedures for assessing human immune cell reconstitution in peripheral blood have been previously described (18, 19). DRAGA mice were used for 4 months after infusion of human HSCs. All animal procedures reported herein were conducted under IACUC protocols approved by WRAIR/NMRC in compliance with the Animal Welfare Act and in accordance with the principles set forth in the "Guide for the Care and Use of Laboratory Animals," Institute of Laboratory Animals Resources, National Research Council, National Academy Press, 2011.

Orientia Inoculum Preparation and Footpad Inoculation

All procedures involved using live *Orientia* was performed in biosafety level 3 (BSL-3) laboratories. *Orientia* (Karp strain) inoculum that was purified previously (14) was injected into peritoneal cavity of C3H/HeJ mice. Mice were euthanized 7 to 10 days post inoculation. Liver and spleen tissues were homogenized in SYN1 buffer (0.22 M sucrose, 3.6 mM KH_2PO_4, 8.6 mM Na_2HPO_4, and 4.9 mM glutamic acid) at 1:20 ratio (v/v) and then aliquoted and stored in −80°C freezer until use. Serial dilution of the inoculum were used for intraperitoneal (i.p.) inoculation in CD-1 mice to calculate mLD^{50} (26) and also quantified by quantitative PCR (qPCR). Inoculation of humanized DRAGA mice was performed by injecting 30 µL inoculum into each footpad (total 60 µL per mouse). Homogenized liver and spleen tissues from non-infected C3H/HeJ mice were injected as controls.

Quantification of *Orientia*

DNA from bone marrow and major tissues were extracted using blood/tissue DNA kit (Qiagen) and qPCR targeting 47 kDa

gene of *Orientia* were performed on a 7500 Fast Real-Time PCR System (27). Serial dilutions of plasmid containing the amplification fragment sequence (28) was used to generate standard curves for absolute copy number quantification.

Cell Culture and Bacterial Infection

L929 mouse fibroblast cells originally from ATCC were maintained in DMEM media containing 10% FBS, 100 U/mL penicillin, and 100 μg/mL streptomycin. Cells were cultured in incubator at 37°C with 5% CO_2. Antibiotics were removed from cell culture 24 h prior to infection. Two microliters of inoculum prepared from humanized DRAGA lung tissues were added to a T25 flask containing L929 cells and rocked for 1 h at room temperature and used for immunofluorescent staining on day 7 and day 14.

Immunofluorescent and Immunohistochemistry

Cultured L929 cells or frozen lung and liver sections on glass slides were fixed with 4% paraformaldehyde for 20 min and permeabilized with 0.1% Triton for 5 min at room temperature. They were then blocked in 1% BSA in PBS for 45 min before incubation with scrub typhus patient sera as primary antibody (pooled on day 11 post onset of fever and diluted at 1:1,000) at room temperature for 1 h. The slides were then washed three times (5 min each) in PBS before incubating with a goat anti-human IgG secondary antibody conjugated with Alexa Fluor 568 (Thermo Fisher Scientific). The slides were then washed three times (5 min each) in PBS before being examined under a fluorescent microscope. For immunohistochemistry, animal tissues were fixed in formalin overnight and replaced with 70% ethanol the next day. Paraffin-embedded tissue sections from humanized DRAGA mice post challenge were cut into 5 μm sections and stained with hematoxylin and eosin (H&E).

Immunization

Orientia (Karp stain) inoculum was irradiated at 200 krads for inactivation. Inoculum prepared from uninfected mouse was irradiated as well and used as the control. A total of four immunizations were performed with 2-week intervals. For each immunization, 1×10^7 irradiated bacteria were injected intraperitoneally into each humanized DRAGA mouse.

Antibody Detection and Characterization

Blood from each mouse was collected *via* tail vein. Enzyme-linked immunosorbent assay (ELISA) was used to monitor the development of IgM and IgG specific to 56 kDa recombinant protein (14). Positive sera were confirmed by immunofluorescence assay on glass slides spotted with whole cell antigen of *Orientia*.

Cytokine Profiling

Cytokines and chemokines from humanized DRAGA mouse sera were profiled using Bio-Plex Pro human cytokine 17-plex Assay (Bio-Rad) in a MAGPIX system (Luminex). To ensure mouse cytokines were not interfering with the results, sera from CD-1 mice with or without *Orientia* infection were included as negative controls.

Flow Cytometry

Blood (50 μL) from tail vein was collected using heparin-coated capillary tubes, spun down, and erythrocytes were lysed with ACK buffer for 5 min in ice followed by a washed with 1% BSA in PBS. Splenocytes were isolated as previously described (19). Cells were blocked with anti-mouse Fc block (BD Biosciences) and surface stained with antibodies against human CD3 (#HIT3a), CD4 (#SK3), CD8 (#RPA-T8), CD69 (#L78), CD62L (#DREG-56), and CCR7/CD197 (#150503) from BD Biosciences as described (18–20). To evaluate the frequency of human $CD4^+FOXP3^+$ regulatory T cells in spleens of DRAGA mice, cells were first surface stained with human CD3, CD4 antibodies, and then intracellularly stained with a antibody against human FOXP3 (#236A/E7, Thermo Fisher Scientific) following the manufacturer's instructions. Cells were analyzed in the gated mononuclear FSC/SSC as described previously (19).

Statistical Analysis

Comparison between two groups of data was performed using Welch's *t*-test in Graphpad Prism 7 software. A p value less than 0.05 was considered significant.

RESULTS

Footpad Inoculation of *O. tsutsugamushi* Causes Lethality in Humanized DRAGA Mice, But Not in C3H/HeJ Mice

Footpad inoculation has been used in recent mouse models to study inflammatory responses induced by *O. tsutsugamushi* (29). It is considered as a route that combines intradermal and subcutaneous inoculation (30), which mimics the natural way of infection *via* chigger bites. Humanized DRAGA mice were inoculated with inoculum (liver/spleen homogenate) containing various amount of *Orientia* ranging from 6×10^1 to 6×10^4 mLD^{50} *via* footpad. For the control group, liver/spleen homogenate that does not contain any bacteria were injected. As illustrated in **Figure 1A**, mice challenged with the highest dose of *Orientia* (6×10^4) group began to show signs of illness such as ruffled fur on day 11 infection and succumbed to infection starting from day 14 post infection. By day 18, all six mice in this group died. However, when inoculated into inbred C3H/HeJ mice, the same high dose did not cause any lethality. This is consistent to what has been reported in inbred BALB/c mice upon footpad inoculation, where the infected BALB/c mice did not die due to infection (29). Lower *Orientia* challenge doses in humanized DRAGA mice substantially delayed the appearance of sickness and eventual lethality (**Figure 1A**). Over the course of the infection, the body weights of DRAGA mice decreased gradually and this reduction accelerated during the last 4–5 days before death (**Figure 1B**). These data indicated that *Orientia* caused dose-dependent lethality in footpad-inoculated humanized DRAGA mice, but not in C3H/HeJ or in BALB/c mice.

Orientia Disseminates Into Major Organs of Humanized DRAGA Mice

In order to investigate tissue tropism of *Orientia*, we harvested tissues when humanized DRAGA mice became severely sick after

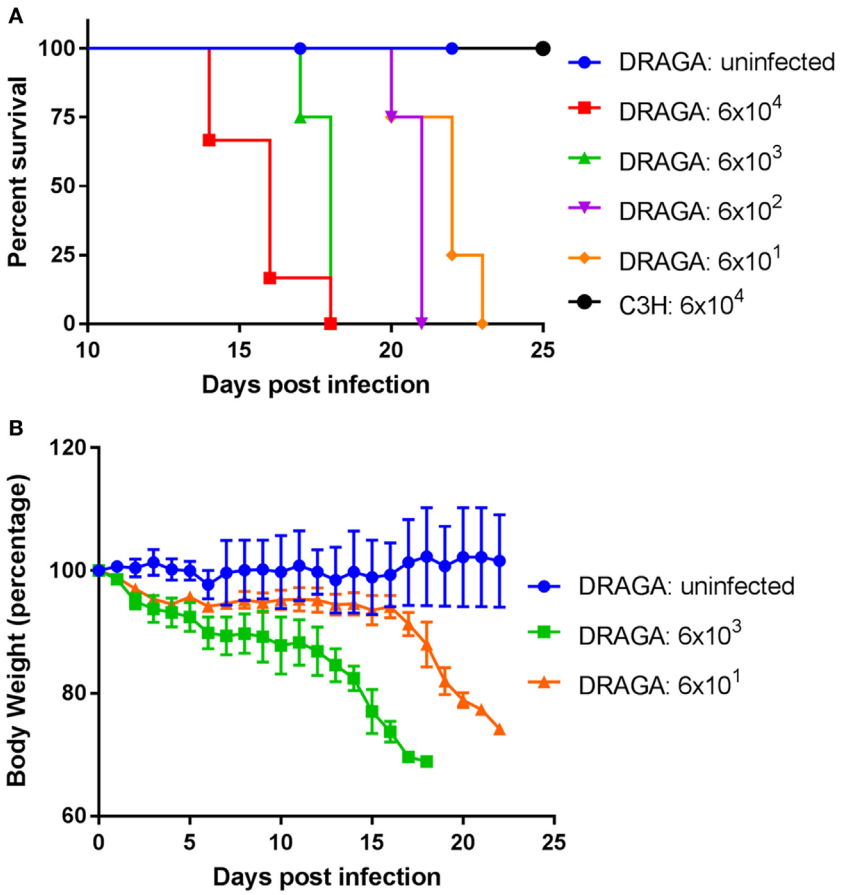

FIGURE 1 | A lethal model for scrub typhus using humanized DRAGA mice. **(A)** Survival curve of humanized DRAGA and C3H mice inoculated *via* footpad with vehicle control or *Orientia tsutsugamushi* (Karp) of various dosages (mLD^{50}): 6×10^4 (DRAGA, $n = 6$; C3H, $n = 4$), 6×10^3 ($n = 4$), 6×10^2 ($n = 4$), and 6×10^1 ($n = 4$). **(B)** The body weight was monitored daily after infection with vehicle control or *Orientia* inoculum at mLD^{50} of 6×10^3 and 6×10^1.

infection. DNA was extracted and the number of *Orientia* was quantified by qPCR. As illustrated in **Figure 2A**, lung was found to contain the most number of bacteria, followed by spleen, liver, kidney, and heart. Brain and bone marrow had the least number of bacteria among the tissues examined. Furthermore, immunofluorescent staining of *Orientia* in frozen tissue sections showed extensive proliferation of bacteria in about 50% of cells in the lung (**Figure 2B**) and to a lesser extent in liver cells (Figure S1 in Supplementary Material). To further test the infectivity of *Orientia* isolated from infected DRAGA mice, tissue homogenate from lung tissue was prepared and used to inoculate L929 cells, a common cell line for culturing *Orientia*. As illustrated in **Figures 2C,D**, L929 cells were infected with *Orientia* as indicated by specific staining (**Figure 2C**) and proliferation of *Orientia* in these cells were quantified by qPCR (**Figure 2D**). These results clearly indicated that humanized DRAGA mice sustain infection with *Orientia.*

Pathological Changes in Humanized DRAGA Mice due to *Orientia* Infection

Splenomegaly was apparent in infected mice when they became severely sick. The weight of the spleens ranged from 92 to 196 g in the infected group compared to around 80 g in the controls (**Figure 3A**). Histologic findings on tissue sections stained with H&E revealed inflammation and necrosis in the lung, liver, and spleen. Areas of pyogranulomatous and necrotizing splenitis were multifocal to coalescing (**Figure 3B**). There was mild to moderate red pulp necrosis, characterized by cellular debris, neutrophils, and multinucleated giant cells, admixed with increased extramedullary hematopoiesis (EMH) that crowded out normal lymphocytes. The EMH was characterized by abundant hematopoietic precursor cells, megakaryocytes, and intracellular hemosiderin due to increased erythrocyte breakdown (Figures S2A,B in Supplementary Material). Multifocal, miliary, and random necrosis in hepatocytes was clearly identifiable in infected liver associated with fibrinosuppurative and lymphohistiocytic inflammation. Hepatocytes within necrotic foci frequently contained intracellular bacteria, which were confirmed with Gram stains. Infected lungs in humanized DRAGA mice displayed perivasculitis, edema, fibrin, and hemorrhage, and multifocal foci of septal necrosis (**Figure 3B**; Figures S2C,D in Supplementary Material). Interestingly, no histologic changes were noted in the kidney, heart, and brain, where much less amount of bacteria were present as quantified in **Figure 2A**.

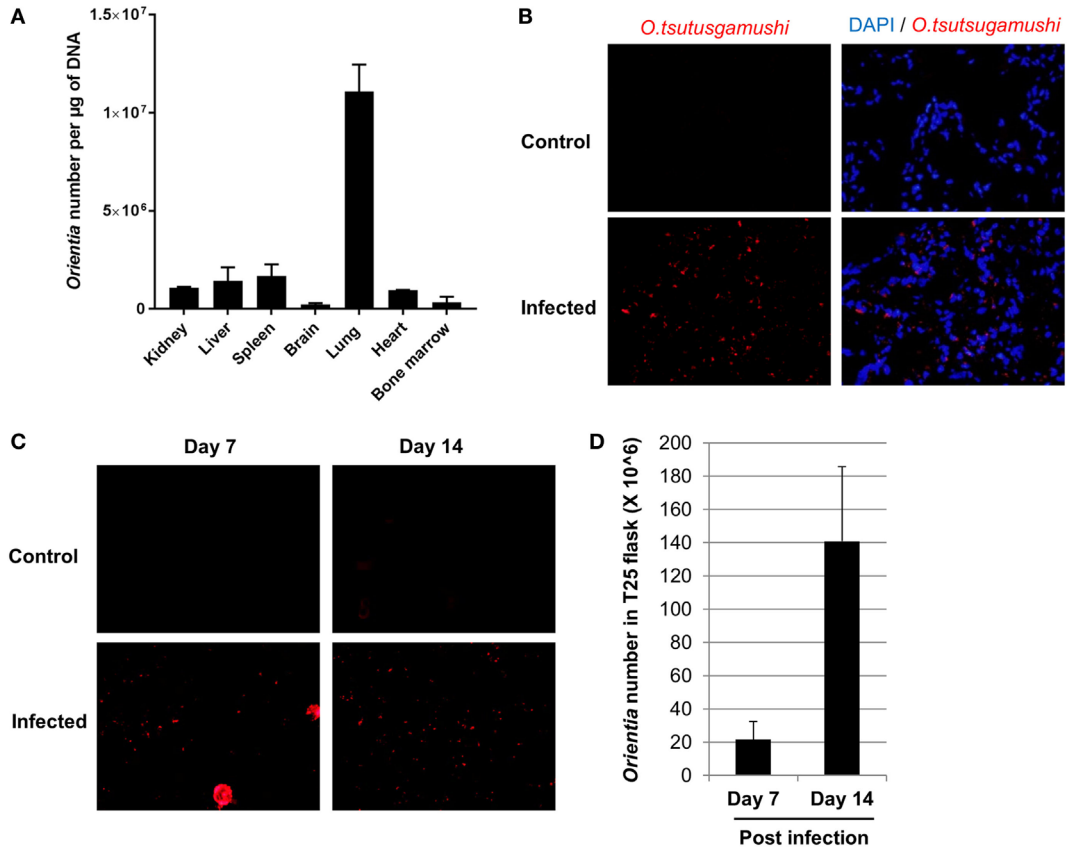

FIGURE 2 | Live *Orientia tsutsugamushi* disseminates into organs of infected humanized DRAGA mice. **(A)** DNA was extracted from various organs of humanized DRAGA mice 2 weeks post infection at 6 × 10^4 mLD_{50} and *O. tsutsugamushi* was quantified by quantitative PCR (qPCR). **(B)** Immunofluorescence staining showing *O. tsutsugamushi* (red) in lung tissue frozen sections from humanized DRAGA mice 3 weeks post infection at 6 × 10^2 mLD_{50} (cell nuclei were stained blue with DAPI, magnification, 400×). **(C)** Tissue homogenates were prepared from lung tissue and used to inoculate L929 cells. Immunofluorescence staining was performed to detect the presence of *O. tsutsugamushi* (magnification, 400×) at day 7 and day 14 post inoculation. **(D)** qPCR was used to quantify number of *Orientia* in L929 cells collected in **(C)**.

Strong Th1 but Subdued Th2 Human Cytokine Regulation in Humanized DRAGA Mice Upon *Orientia* Infection

Cytokines and chemokines are small proteins released by immune cells such as T helper cells and macrophages. They are critical in cell signaling involved in recruiting, regulating immune cells, and modulating inflammatory reactions that act upon pathogen invasions (31). Using a multiplex assay, we measured cytokine levels in sera collected from control and infected DRAGA mice. Strong Th1-cytokine responses were induced, including IL-2, IL12, IFN-γ, and TNF-α. The average levels of human IFN-γ and TNF-α were over 10-fold in the infected versus the control group. Levels of human IL-12p70 increased by 100-folds in the sera of infected mice, as compared to control (uninfected) mice. However, levels of cytokines for Th2 responses had either modest increase, such as IL-10 or were inhibited, such as IL-13 (**Figure 4**). Serum concentration of IL-4 were either below 0.6 pg/mL or mostly undetectable in the infected or control mice. Other cytokines or chemokines that had significant increase due to *Orientia* infection included IL-8, MIP-1β, MCP-1, IL-1β, IL-6, and G-CSF. An important player for pro-inflammatory Th17 cells, IL-17A, significantly decreased due to the infection. GM-CSF level remained unchanged (**Figure 4**; Figure S3 in Supplementary Material). Consistent with these cytokine profiles, the percentage of cells expressing CD69 and CD62L increased in the spleen for both $CD4^+$ and $CD8^+$ T cell subsets (Figure S4 in Supplementary Material). Intriguingly, the percentage of human T regulatory cells (Tregs) ($CD4^+FOXP3^+$) significantly increased in the spleen of infected mice as well (2.2 to 7.6%).

Antigen-Specific Humoral and Cellular Responses Are Developed in Humanized DRAGA Mice Post Immunization

Previous studies using serum or cell transfer experiments suggested that both antibody and T-cell responses were important for effective control of *Orientia* growth and provided protection in conventional mouse models by i.p. infection route (32–34). In order to evaluate these critical immune functions in humanized DRAGA mice, we immunized them with whole cell *Orientia*

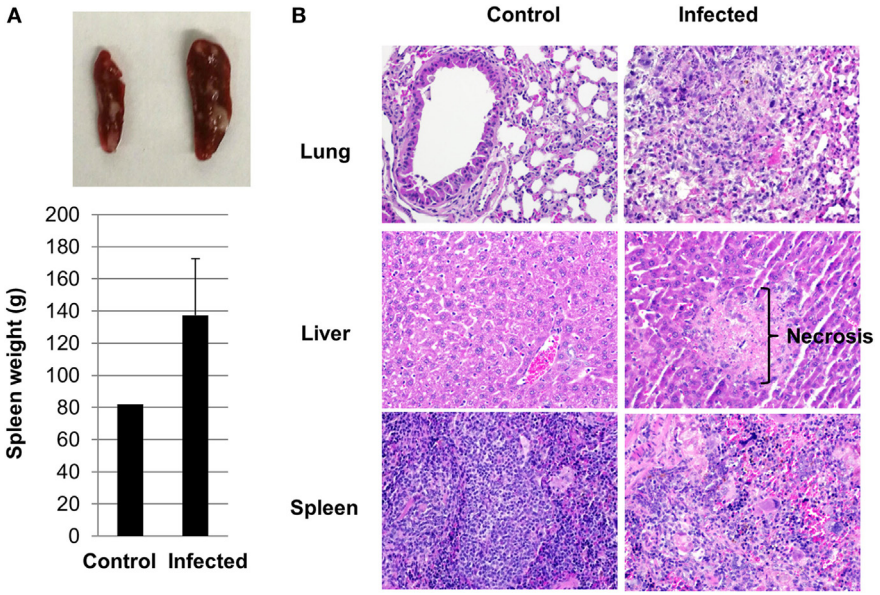

FIGURE 3 | Pathological changes in infected humanized DRAGA mice. **(A)** A representative photo of splenomegaly and average spleen organ weight from control and infected humanized DRAGA mice when they were severely sick. **(B)** Hematoxylin and eosin staining reveals pathological changes in organs of humanized DRAGA mice infected with *Orientia tsutsugamushi* (magnification, 200×).

inactivated by irradiation (200 krads), which has been shown as effective immunogens previously (35). In inbred BALB/c mice, specific antibodies were detected 3 weeks after the initial immunization using irradiated *Orientia* although antibody levels were much lower when compared to viable organisms (36). ELISA using a recombinant 56 kDa antigen, the dominant surface antigen for *Orientia*, showed that human IgM developed between 2 and 4 weeks after initial immunization and by 10 weeks, both human IgM and IgG were readily detectable in the sera of immunized DRAGA mice. The serum levels of human antibodies reactive to recombinant 56 kDa antigen were quantified based on a standard curve generated from a humanized monoclonal antibody against 56 kDa antigen with known concentrations (**Figures 5A,B**). Furthermore, significant human T cell activation was observed in the blood from immunized DRAGA mice. Percentage of human $CD3^+$ T cells more than doubled 8 weeks post initial immunization and this was accompanied with a significant increase of $CD4^+$ T cells (~3-fold) and moderate increase for cytotoxic $CD8^+$ T cells (~2-fold), although it did not reach statistical significance (**Figures 5C–E**).

DISCUSSION

Although mouse models have been extensively used for scrub typhus research for many years, there is an urgent need for the development of an animal model that represent the pathology and immune responses of human scrub typhus (6). Given the vast differences in immune system between mouse and human species (16) and recent advancements in generating human immune system humanized mice, we aimed to develop a humanized mouse model for scrub typhus. To the best of our knowledge, this is the first of such study in the field. The fact that footpad *Orientia* inoculation leads to lethality in the humanized DRAGA mice, but not in C3H or BALB/c mice (29) very likely is due to differences of their immune systems. In this study, we have shown that humanized DRAGA mice could be infected by *Orientia via* footpad followed by dissemination into major organs. This caused severe pathological changes in liver, lung, and spleen, but not in organs with less bacterium load, such as brain, heart, and kidney. Th1-dominant human cytokines were induced dramatically in response to the inoculation. Both humoral and cellular adaptive immune responses were observed when humanized DRAGA mice were immunized by irradiated whole cell antigen.

Regulation of cytokines in patient sera has been reported for scrub typhus. Consistent with the intracellular nature of *Orientia* infection, Th1 cytokines, such as IFN-γ, TNF-α, and IL-12 were significantly upregulated while cytokines in Th2 category were much less regulated (37, 38). A very similar pattern of cytokine regulation was observed in our humanized DRAGA mice upon footpad inoculation. These included marked increase of IFN-γ, TNF-α, and IL-12 (Th1 cytokines), and moderate induction of IL-10 and suppression of IL-13 (Th2 cytokines) (**Figure 4**). Serum levels of IL-4, which is responsible for triggering Th2 differentiation, were mostly below the lower detection limit of our assay and thus too low to be determined. IL-10, which is considered to be a Th2 cytokine and anti-inflammatory, was moderately elevated probably due to the fact that in humans both Th1 and Th2 cells can produce IL-10 (39). Increase of IL-10 was found previously in scrub typhus patients as well (38). IL-17A, a pro-inflammatory cytokine secreted by Th17 cells was significantly inhibited in the infected DRAGA mice. Recent profiling in scrub typhus patients' sera identified three human chemokines (MCP-1, MIP-1β, and

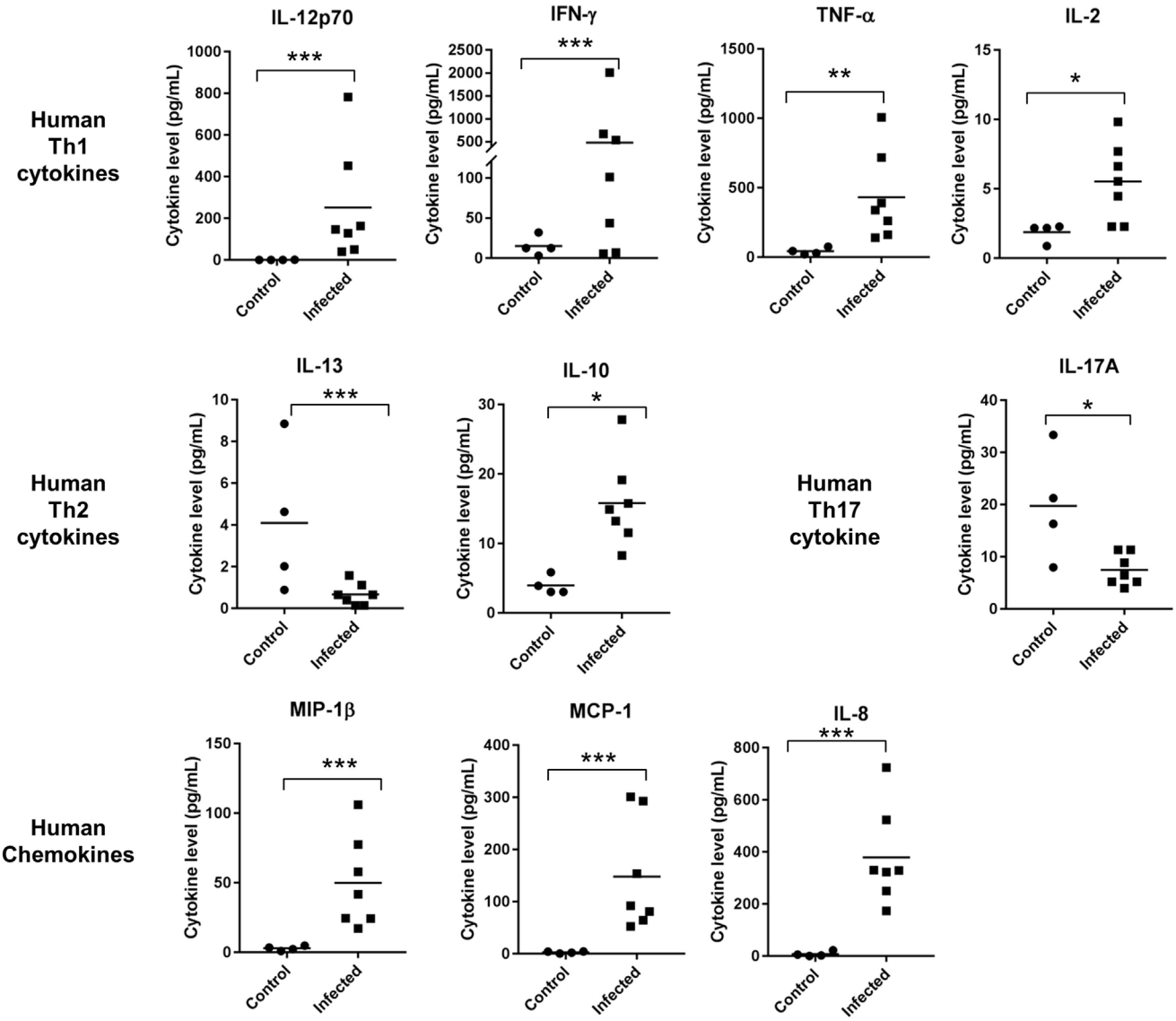

FIGURE 4 | Cytokine and chemokine levels were significantly regulated in sera collected from control ($n = 4$) and infected humanized DRAGA mice ($n = 7$) (*p value < 0.05; **p value < 0.01; ***p value < 0.001).

IL-8) that were upregulated during scrub typhus infection and associated with disease severity and mortality (40). Intriguingly, all three chemokines were dramatically upregulated in our mouse model, suggestive of severe infections in our humanized DRAGA mice. Although investigations into cytokine regulation using conventional mouse models also mimicked human situations to certain extent (41), they failed to identify important regulators, such as IL-8 (as a marker of scrub typhus disease severity) which is not present in the mouse immune system (42).

Peripheral T cells in scrub typhus patient blood have been characterized recently (43), where the percentage of both $CD4^+$ and $CD8^+$ T cells decreased due to programmed cell death (apoptosis) during the acute phase of infection. Similar reduction of $CD4^+$ and $CD8^+$ T cells occurred in the spleen of humanized DRAGA mice infected with *Orientia* (Figure S4A in Supplementary Material). More interestingly, as central mediators of immune suppression, human Tregs significantly increased in the spleen upon *Orientia* infection (Figure S4C in Supplementary Material). Stimulation of $CD4^+FOXP3^+$ Tregs upon host/pathogen interaction have been reported in many infectious diseases (44), and it could have multifold impact on protecting the human host from excessive inflammation and at the same time, serving as a mechanism for pathogens to evade human immune system, which increases the risk of pathogen persistence and chronic disease. Given the severe tissue damages in humanized DRAGA mice (**Figure 3**; Figure S2 in Supplementary Material), increase of Tregs in these tissues might have protective effect for the host. Scrub typhus patients were documented to display significant decrease of Tregs in the

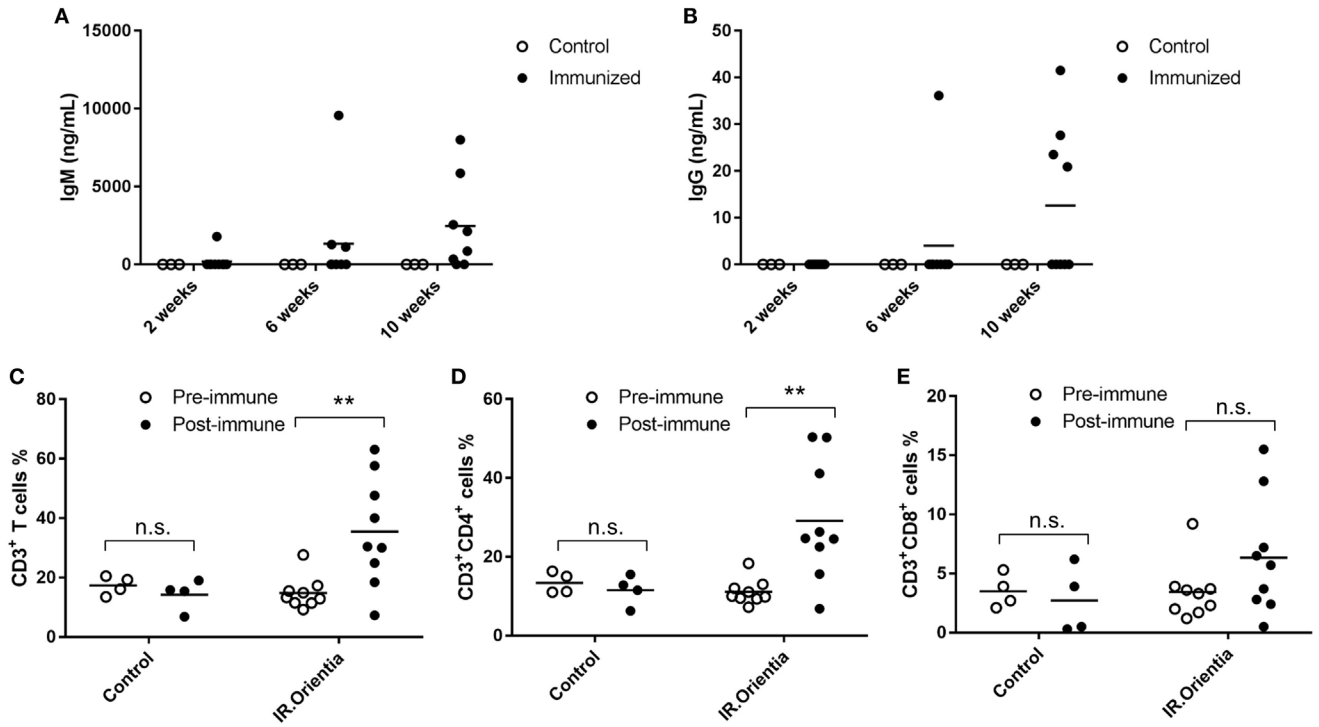

FIGURE 5 | Antibody and T cell responses after immunization with irradiated whole cell *Orientia*. Concentrations for IgM **(A)** and IgG **(B)** specifically against 56 kDa protein in serum collected at 2, 6, and 10 weeks after initial immunization. **(C–E)** Percentage of $CD3^+$, $CD4^+$, and $CD8^+$ T cells among total mononuclear cells in blood (**p value < 0.01; n.s, not significant).

peripheral blood (43) and the authors postulated that this reduction might be due to the migration of Tregs into tissues. It will be interesting to test this hypothesis in our humanized DRAGA mouse models. Functional investigations of Tregs in scrub typhus may provide further insights into its pathogenesis and immune regulation.

T cell responses have been recently shown to be critical in controlling *Orientia* growth and scrub typhus disease progression (45, 46). The marked increase of $CD3^+$ T cells, along with increases in both $CD4^+$ and $CD8^+$ cell populations upon immunization (**Figure 5**), suggests that the humanized DRAGA mice might be suitable for future vaccine or mechanistic studies. In addition, tissue damage caused by necrotic cell death was seen in multiple organs of humanized DRAGA mice post infection (**Figure 3B**; Figure S2 in Supplementary Material). It has been shown recently by Hauptmann et al. that hepatocellular injury and subcapsular necrotic lesions were caused by $CD8^+$ T cells (45). It is very likely that similar lesions observed in the liver tissues (**Figure 3B**) were triggered by $CD8^+$ T cells as well. Given the appropriate human T cell and B cell responses after immunization (**Figure 5**), it will be very intriguing to test whether they will offer protection against live *Orientia* challenge.

Through the many failures of translating knowledge gained in conventional mouse models to human clinical studies (16), the difference between mouse and human (especially with regards to their immune systems) has been increasingly appreciated. For example, formation of granulomas that resemble those observed in human mycobacteriosis was only observed in humanized mice, but not in non-humanized infected controls (47). Humanized mouse models might bridge this gap (48). We are in urgent need of mouse models that can better mimic the disease pathology and immunological responses for many human diseases, including scrub typhus. This study represents a successful attempt in this effort. *Orientia* dissemination, disease pathology, cytokine regulations, and adapted immune responses as observed in humanized DRAGA mice make it a valuable tool in future basic and preclinical research for scrub typhus.

ETHICS STATEMENT

All animal procedures reported herein were conducted under IACUC protocols approved by WRAIR/NMRC in compliance with the Animal Welfare Act and in accordance with the principles set forth in the "Guide for the Care and Use of Laboratory Animals," Institute of Laboratory Animals Resources, National Research Council, National Academy Press, 2011.

AUTHOR CONTRIBUTIONS

WMC and SC conceived the study. LJ, ZZ, TCC, and SS performed the experiments. CCC, LJ, EM, SC, and WMC analyzed and interpreted data. SC and RAO provided the humanized DRAGA mice for the study. LJ wrote the manuscript with contributions from all authors.

ACKNOWLEDGMENTS

The authors would like to thank Victor Sugiharto for technical assistance. This work was supported by work unit number A1231 with funding from the Military Infectious Diseases Research Program (MIDRP) to WMC project number WJ107_17_NM, and by work unit A1210 with funding from the Military Infectious Diseases Research Program (MIDRP) to SC project number F0552_18_WR. CCC, SC, and WMC are U.S. Government employees and EM is a military service member. The work of these individuals was prepared as part of official government duties. Title 17 U.S.C. §105 provides that "copyright protection under this title is not available for any work of the United States Government." Title 17 U.S.C. §101 defines a U.S. Government work as a work prepared by a military service member or employee of the U.S. Government as part of that person's official duties. The views expressed are those of the authors and do not necessarily reflect the official policy or position of the Department of the Navy, Department of the Army, Department of Defense, nor the U.S. Government.

SUPPLEMENTARY MATERIAL

The Supplementary Material for this article can be found online at https://www.frontiersin.org/articles/10.3389/fimmu.2018.00816/full#supplementary-material.

REFERENCES

1. Watt G, Parola P. Scrub typhus and tropical rickettsioses. *Curr Opin Infect Dis* (2003) 16:429–36. doi:10.1097/01.qco.0000092814.64370.70
2. Taylor AJ, Paris DH, Newton PN. A systematic review of mortality from untreated scrub typhus (*Orientia tsutsugamushi*). *PLoS Negl Trop Dis* (2015) 9:e0003971. doi:10.1371/journal.pntd.0003971
3. Izzard L, Fuller A, Blacksell SD, Paris DH, Richards AL, Aukkanit N, et al. Isolation of a novel *Orientia* species (O. chuto sp. nov.) from a patient infected in Dubai. *J Clin Microbiol* (2010) 48:4404–9. doi:10.1128/JCM.01526-10
4. Weitzel T, Dittrich S, López J, Phuklia W, Martinez-Valdebenito C, Velásquez K, et al. Endemic scrub typhus in South America. *N Engl J Med* (2016) 375:954–61. doi:10.1056/NEJMoa1603657
5. Horton KC, Jiang J, Maina A, Dueger E, Zayed A, Ahmed AA, et al. Evidence of *Rickettsia* and *Orientia* infections among abattoir workers in Djibouti. *Am J Trop Med Hyg* (2016) 95:462–5. doi:10.4269/ajtmh.15-0775
6. Paris DH, Shelite TR, Day NP, Walker DH. Unresolved problems related to scrub typhus: a seriously neglected life-threatening disease. *Am J Trop Med Hyg* (2013) 89:301–7. doi:10.4269/ajtmh.13-0064
7. Traub R, Wisseman CL. The ecology of chigger-borne rickettsiosis (scrub typhus). *J Med Entomol* (1974) 11:237–303. doi:10.1093/jmedent/11.3.237
8. Shatrov AB, Takahashi M, Noda S, Misumi H. Stylostome organization in feeding *Leptotrombidium larvae* (Acariformes: Trombiculidae). *Exp Appl Acarol* (2014) 64:33–47. doi:10.1007/s10493-014-9809-8
9. Paris DH, Phetsouvanh R, Tanganuchitcharnchai A, Jones M, Jenjaroen K, Vongsouvath M, et al. *Orientia* tsutsugamushi in human scrub typhus eschars shows tropism for dendritic cells and monocytes rather than endothelium. *PLoS Negl Trop Dis* (2012) 6:e1466. doi:10.1371/journal.pntd.0001466
10. Fukuhara M, Fukazawa M, Tamura A, Nakamura T, Urakami H. Survival of two *Orientia tsutsugamushi* bacterial strains that infect mouse macrophages with varying degrees of virulence. *Microb Pathog* (2005) 39:177–87. doi:10.1016/j.micpath.2005.08.004
11. Ridgway RL, Oaks SC, LaBarre DD. Laboratory animal models for human scrub typhus. *Lab Anim Sci* (1986) 36:481–5.
12. Robinson DM, Chan TC, Huxsoll DL. Clinical response of silvered leaf monkeys (*Presbytis cristatus*) to infection with strains of *Rickettsia tsutsugamushi* virulent and avirulent for mice. *J Infect Dis* (1976) 134:193–7. doi:10.1093/infdis/134.2.193
13. Shelite TR, Saito TB, Mendell NL, Gong B, Xu G, Soong L, et al. Hematogenously disseminated *Orientia tsutsugamushi*-infected murine model of scrub typhus [corrected]. *PLoS Negl Trop Dis* (2014) 8:e2966. doi:10.1371/journal.pntd.0002966
14. Ni Y-S, Chan T-C, Chao C-C, Richards AL, Dasch GA, Ching W-M. Protection against scrub typhus by a plasmid vaccine encoding the 56-KD outer membrane protein antigen gene. *Am J Trop Med Hyg* (2005) 73:936–41. doi:10.4269/ajtmh.2005.73.936
15. Shelite TR, Liang Y, Wang H, Mendell NL, Trent BJ, Sun J, et al. IL-33-dependent endothelial activation contributes to apoptosis and renal injury in *Orientia tsutsugamushi*-infected mice. *PLoS Negl Trop Dis* (2016) 10:e0004467. doi:10.1371/journal.pntd.0004467
16. Mestas J, Hughes CCW. Of mice and not men: differences between mouse and human immunology. *J Immunol* (2004) 172:2731–8. doi:10.4049/jimmunol.172.5.2731
17. Akkina R. Human immune responses and potential for vaccine assessment in humanized mice. *Curr Opin Immunol* (2013) 25:403–9. doi:10.1016/j.coi.2013.03.009
18. Danner R, Chaudhari SN, Rosenberger J, Surls J, Richie TL, Brumeanu T-D, et al. Expression of HLA class II molecules in humanized NOD.Rag1KO.IL2RgcKO mice is critical for development and function of human T and B cells. *PLoS One* (2011) 6:e19826. doi:10.1371/journal.pone.0019826
19. Majji S, Wijayalath W, Shashikumar S, Pow-Sang L, Villasante E, Brumeanu TD, et al. Differential effect of HLA class-I versus class-II transgenes on human T and B cell reconstitution and function in NRG mice. *Sci Rep* (2016) 6:28093. doi:10.1038/srep28093
20. Wijayalath W, Majji S, Kleschenko Y, Pow-Sang L, Brumeanu TD, Villasante EF, et al. Humanized HLA-DR4 mice fed with the protozoan pathogen of oysters *Perkinsus marinus* (Dermo) do not develop noticeable pathology but elicit systemic immunity. *PLoS One* (2014) 9:e87435. doi:10.1371/journal.pone.0087435
21. Allam A, Majji S, Peachman K, Jagodzinski L, Kim J, Ratto-Kim S, et al. TFH cells accumulate in mucosal tissues of humanized-DRAG mice and are highly permissive to HIV-1. *Sci Rep* (2015) 5:10443. doi:10.1038/srep10443
22. Mendoza M, Ballesteros A, Qi Q, Sang LP, Shashikumar S, Casares S, et al. Generation and testing anti-influenza human monoclonal antibodies in a new humanized mouse model (DRAGA: HLA-A2. HLA-DR4. Rag1 KO. IL-2Rγc KO. NOD). *Hum Vaccin Immunother* (2017) 14(2):345–60. doi:10.1080/21645515.2017.1403703
23. Yi G, Xu X, Abraham S, Petersen S, Guo H, Ortega N, et al. A DNA vaccine protects human immune cells against Zika virus infection in humanized mice. *EBioMedicine* (2017) 25:87–94. doi:10.1016/j.ebiom.2017.10.006
24. Majji S, Wijayalath W, Shashikumar S, Brumean TD, Casares SA. Humanized DRAGA mice immunized with *Plasmodium falciparum* sporozoites and chloroquine elicit protective pre-erythrocytic immunity. *Malar J* (2018) 17:114. doi:10.1186/s12936-018-2264-y
25. Kim J, Peachman KK, Jobe O, Morrison EB, Allam A, Jagodzinski L, et al. Tracking human immunodeficiency virus-1 infection in the humanized DRAG mouse model. *Front Immunol* (2017) 8:1405. doi:10.3389/fimmu.2017.01405
26. Chan TC, Jiang J, Temenak JJ, Richards AL. Development of a rapid method for determining the infectious dose (ID)50 of *Orientia tsutsugamushi* in a scrub typhus mouse model for the evaluation of vaccine candidates. *Vaccine* (2003) 21:4550–4. doi:10.1016/S0264-410X(03)00505-X
27. Chao C-C, Belinskaya T, Zhang Z, Ching W-M. Development of recombinase polymerase amplification assays for detection of *Orientia tsutsugamushi* or *Rickettsia typhi*. *PLoS Negl Trop Dis* (2015) 9:e0003884. doi:10.1371/journal.pntd.0003884
28. Jiang J, Chan T-C, Temenak JJ, Dasch GA, Ching W-M, Richards AL. Development of a quantitative real-time polymerase chain reaction assay specific for *Orientia tsutsugamushi*. *Am J Trop Med Hyg* (2004) 70:351–6. doi:10.4269/ajtmh.2004.70.351

29. Keller CA, Hauptmann M, Kolbaum J, Gharaibeh M, Neumann M, Glatzel M, et al. Dissemination of *Orientia tsutsugamushi* and inflammatory responses in a murine model of scrub typhus. *PLoS Negl Trop Dis* (2014) 8:e3064. doi:10.1371/journal.pntd.0003064
30. Kamala T. Hock immunization: a humane alternative to mouse footpad injections. *J Immunol Methods* (2007) 328:204–14. doi:10.1016/j.jim.2007.08.004
31. Turner MD, Nedjai B, Hurst T, Pennington DJ. Cytokines and chemokines: at the crossroads of cell signalling and inflammatory disease. *Biochim Biophys Acta* (2014) 1843:2563–82. doi:10.1016/j.bbamcr.2014.05.014
32. Robinson DM, Huxsoll DL. Protection against scrub typhus infection engendered by the passive transfer of immune sera. *Southeast Asian J Trop Med Public Health* (1975) 6:477–82.
33. Palmer BA, Hetrick FM, Jerrells TJ. Production of gamma interferon in mice immune to *Rickettsia tsutsugamushi*. *Infect Immun* (1984) 43:59–65.
34. Palmer BA, Hetrick FM, Jerrells TR. Gamma interferon production in response to homologous and heterologous strain antigens in mice chronically infected with *Rickettsia tsutsugamushi*. *Infect Immun* (1984) 46:237–44.
35. Eisenberg GH, Osterman JV. Gamma-irradiated scrub typhus immunogens: development and duration of immunity. *Infect Immun* (1978) 22:80–6.
36. Jerrells TR, Palmer BA, Osterman JV. Gamma-irradiated scrub typhus immunogens: development of cell-mediated immunity after vaccination of inbred mice. *Infect Immun* (1983) 39:262–9.
37. Iwasaki H, Mizoguchi J, Takada N, Tai K, Ikegaya S, Ueda T. Correlation between the concentrations of tumor necrosis factor-alpha and the severity of disease in patients infected with *Orientia tsutsugamushi*. *Int J Infect Dis* (2010) 14:e328–33. doi:10.1016/j.ijid.2009.06.002
38. Chung DR, Lee YS, Lee SS. Kinetics of inflammatory cytokines in patients with scrub typhus receiving doxycycline treatment. *J Infect* (2008) 56:44–50. doi:10.1016/j.jinf.2007.09.009
39. Del Prete G, De Carli M, Almerigogna F, Giudizi MG, Biagiotti R, Romagnani S. Human IL-10 is produced by both type 1 helper (Th1) and type 2 helper (Th2) T cell clones and inhibits their antigen-specific proliferation and cytokine production. *J Immunol* (1993) 150:353–60.
40. Astrup E, Janardhanan J, Otterdal K, Ueland T, Prakash JAJ, Lekva T, et al. Cytokine network in scrub typhus: high levels of interleukin-8 are associated with disease severity and mortality. *PLoS Negl Trop Dis* (2014) 8:e2648. doi:10.1371/journal.pntd.0002648
41. Soong L, Wang H, Shelite TR, Liang Y, Mendell NL, Sun J, et al. Strong type 1, but impaired type 2, immune responses contribute to *Orientia tsutsugamushi*-induced pathology in mice. *PLoS Negl Trop Dis* (2014) 8:e3191. doi:10.1371/journal.pntd.0003191
42. Zlotnik A, Yoshie O. Chemokines: a new classification system and their role in immunity. *Immunity* (2000) 12:121–7. doi:10.1016/S1074-7613(00)80165-X
43. Cho B-A, Ko Y, Kim Y-S, Kim S, Choi M-S, Kim I-S, et al. Phenotypic characterization of peripheral T cells and their dynamics in scrub typhus patients. *PLoS Negl Trop Dis* (2012) 6:e1789. doi:10.1371/journal.pntd.0001789
44. Boer MC, Joosten SA, Ottenhoff THM. Regulatory T-cells at the interface between human host and pathogens in infectious diseases and vaccination. *Front Immunol* (2015) 6:217. doi:10.3389/fimmu.2015.00217
45. Hauptmann M, Kolbaum J, Lilla S, Wozniak D, Gharaibeh M, Fleischer B, et al. Protective and pathogenic roles of CD8+ T lymphocytes in murine *Orientia tsutsugamushi* infection. *PLoS Negl Trop Dis* (2016) 10:e0004991. doi:10.1371/journal.pntd.0004991
46. Xu G, Mendell NL, Liang Y, Shelite TR, Goez-Rivillas Y, Soong L, et al. CD8+ T cells provide immune protection against murine disseminated endotheliotropic *Orientia tsutsugamushi* infection. *PLoS Negl Trop Dis* (2017) 11:e0005763. doi:10.1371/journal.pntd.0005763
47. Heuts F, Gavier-Widén D, Carow B, Juarez J, Wigzell H, Rottenberg ME. CD4+ cell-dependent granuloma formation in humanized mice infected with mycobacteria. *Proc Natl Acad Sci U S A* (2013) 110:6482–7. doi:10.1073/pnas.1219985110
48. Brehm MA, Wiles MV, Greiner DL, Shultz LD. Generation of improved humanized mouse models for human infectious diseases. *J Immunol Methods* (2014) 410:3–17. doi:10.1016/j.jim.2014.02.011

Conflict of Interest Statement: The authors declare that the research was conducted in the absence of any commercial or financial relationships that could be construed as a potential conflict of interest.

Advantages of publishing in Frontiers

OPEN ACCESS
Articles are free to read for greatest visibility and readership

FAST PUBLICATION
Around 90 days from submission to decision

HIGH QUALITY PEER-REVIEW
Rigorous, collaborative, and constructive peer-review

TRANSPARENT PEER-REVIEW
Editors and reviewers acknowledged by name on published articles

Frontiers
Avenue du Tribunal-Fédéral 34
1005 Lausanne | Switzerland

Visit us: www.frontiersin.org
Contact us: info@frontiersin.org | +41 21 510 17 00

REPRODUCIBILITY OF RESEARCH
Support open data and methods to enhance research reproducibility

DIGITAL PUBLISHING
Articles designed for optimal readership across devices

FOLLOW US
@frontiersin

IMPACT METRICS
Advanced article metrics track visibility across digital media

EXTENSIVE PROMOTION
Marketing and promotion of impactful research

LOOP RESEARCH NETWORK
Our network increases your article's readership